DISSERTATION

SUSPENDED-SEDIMENT CHARACTERISTICS IN FOUR HUMID TROPICAL WATERSHEDS OF CONTRASTING LAND USE, PUERTO RICO

Volume I
Chapters 1-12

Submitted by

Allen C Gellis

Department of Geosciences

In partial fulfillment of the requirements

For the Degree of Doctor of Philosophy

Colorado State University

Fort Collins, Colorado

Fall, 2003

Reproduced with permission of the copyright owner. Further reproduction prohibited without permission.

UMI Number: 3114676

INFORMATION TO USERS

The quality of this reproduction is dependent upon the quality of the copy submitted. Broken or indistinct print, colored or poor quality illustrations and photographs, print bleed-through, substandard margins, and improper alignment can adversely affect reproduction.

In the unlikely event that the author did not send a complete manuscript and there are missing pages, these will be noted. Also, if unauthorized copyright material had to be removed, a note will indicate the deletion.

UMI®

UMI Microform 3114676

Copyright 2004 by ProQuest Information and Learning Company.

All rights reserved. This microform edition is protected against unauthorized copying under Title 17, United States Code.

ProQuest Information and Learning Company
300 North Zeeb Road
P.O. Box 1346
Ann Arbor, MI 48106-1346

Reproduced with permission of the copyright owner. Further reproduction prohibited without permission.

COLORADO STATE UNIVERSITY

May 2, 2003

WE HEREBY RECOMMEND THAT THE DISSERTATION PREPARED UNDER OUR SUPERVISION BY ALLEN C. GELLIS ENTITLED SUSPENDED-SEDIMENT CHARACTERISTICS IN FOUR HUMID TROPICAL WATERSHEDS OF CONTRASTING LAND USE, PUERTO RICO BE ACCEPTED AS FULFILLING IN PART REQUIREMENTS FOR THE DEGREE OF DOCTOR OF PHILOSOPHY.

Committee on Graduate Work

Adviser

Department Head/Director

Reproduced with permission of the copyright owner. Further reproduction prohibited without permission.

ABSTRACT OF DISSERTATION

SUSPENDED-SEDIMENT CHARACTERISTICS IN FOUR HUMID TROPICAL WATERSHEDS OF CONTRASTING LAND USE, PUERTO RICO

A hypothetical model of sediment production, delivery, and transport in the humid-tropics of Puerto Rico was developed through statistical analysis of storm-generated sediment loads and hydrologic characteristics from three time categories: (1) the current storm-generated event, (2) previous storm-generated events, and (3) minor yet localized rainfall and runoff between the storm-generated events. The effect of previous storms in reducing sediment availability for the current event operates differently as sediment supply increases in a basin. In sediment-limited systems, such as the forested Rio Icacos basin, a dominant cycle of sediment production and delivery exists, where large previous storm events mobilize sediment on hillslopes and in low-order channels, and transport the sediment to the main channel where it is deposited. In the next event, this deposited sediment becomes the main source of sediment and clockwise hysteresis loops are more common. Small rainfall events that occur between large flow events in forested basins flush some of this deposited sediment and reduce the sediment load of the next large runoff event. Quebrada Blanca a basin with small sediment sources, pasture (54%) and cropland (8%), has a cycle of sediment production and delivery where large previous storm events and localized rainfall and runoff between major runoff events mobilize and make sediment available for the next large runoff event. Depending on the magnitude of previous events, the mobilized sediment may be transported varying distances in the basin. Larger previous storm events mobilize sediment which is deposited further along the fluvial system, making sediment available to the rising limb portion of the next runoff event. The increased availability of sediment on the rising limb leads to hydrographs where clockwise

Reproduced with permission of the copyright owner. Further reproduction prohibited without permission.

hysteresis loops dominate. As the previous events lessen in magnitude, less sediment is delivered to the main channel, and sediment in the next event is transported to the collection station after the highest peak flow; counterclockwise loops are common. In the agricultural Rio Caguitas basin, sediment supply increases and a cycle of sediment production and delivery exists where previous rainfall events supply sediment to the system which is flushed by the corresponding large previous flow event. Rainfall between large runoff events also supplies sediment to the system which is flushed by higher runoff between events. In the highly disturbed Rio Piedras, which is undergoing urbanization, sediment is so abundant that large previous runoff and rainfall events and rainfall between events act to remove sediment and reduce sediment loads of the next runoff event. As sediment supply in a basin increases, channel hysteresis loops trend from clockwise to counterclockwise. Disturbance in watersheds draining fine-grain soils will more likely exhibit counterclockwise hysteresis loops as sediment that is entrained remains in suspension longer, often peaking after the peak flow. Flushing sediment is more important as disturbance in a basin increases.

Allen Cary Gellis
Department of Geosciences
Colorado State University
Fort Collins, CO 80523
Fall 2003
Advisors: Deb Anthony and Ellen Wohl

Reproduced with permission of the copyright owner. Further reproduction prohibited without permission.

Acknowledgements

One cannot work seven years on a Ph.D. without the involvement of many persons. I would like to thank my advisors Deb Anthony and Ellen Wohl for all their help and support. Deb, your patience during this entire endeavor is more than appreciated. I wish to thank my committee, Waite Osterkamp, Stan Schumm, and Jorge Ramirez for their help and advice. I would like to thank the U.S. Geological Survey for their assistance, especially the Puerto Rico District, and notably Carlos Figueroa, Matt Larsen, Ahmed Valencia, and Rick Webb. Annette, my sister, thanks for the use of your house and asylum to complete this. I am indebted to my family for their support, Mark, Ariel, and Dylan. We will always remember many a vacation with dad on his laptop working on his Ph.D. Michelle, I could not have completed this without you, love ya.

I used to say that working on my Ph.D was my hobby. It was a challenge, creative, at times frustrating, and I'm glad its over!

Reproduced with permission of the copyright owner. Further reproduction prohibited without permission.

MOUNTAIN

River took you down the land
A beach for us to play on

A. Gellis, 1981

Reproduced with permission of the copyright owner. Further reproduction prohibited without permission.

Table of Contents

Volume I

Abstract iii
Acknowledgements v
Table of Contents vii

I. INTRODUCTION 1

II. PREVIOUS STUDIES 5
Tropical Geomorphology 5
Climatic definition 6
Climatic geomorphology 8
Recent geomorphic studies 10
Effects of land use on erosion and sediment yield in the tropics 16
Previous Studies in Puerto Rico 19
Landslidding 27
Sheetwash 31
Fluvial sediment 32
Reservoir sedimentation in Puerto Rico 34
Suspended Sediment Characteristics 39

III. SETTING 47
Geology and Soils of Puerto Rico and Study Basins 47
Rio Icacos 54
Quebrada Blanca at El Jagual 55
Rio Caguitas basin 60
Rio Piedras Basin 64
Climate and Hydrology of Puerto Rico and Study Area 69
Climate 69
Climate of the study basins 70
Human and land-use history 70

IV. METHODS 78
GIS 78
Rainfall 79
Collection 79
Rainfall event definition 79
Rainfall intensity 82
Areal distribution 82
Streamflow 83
Collection 83
Storm-generated event definition 84
Hydrograph Separation 86
Results of hydrograph separation methodologies 93
Complex Events 96
Quickflow Calculation 101
Sediment Transport and Erosion 105
Hillslope erosion 105
Fluvial sediment 108
Data Collection 109
Sediment-Transport Curves 112
Calculation of Suspended-Sediment Loads 114
Geomorphic Measurements 117
Statistical Analysis of Discharge and Sediment data 117

Reproduced with permission of the copyright owner. Further reproduction prohibited without permission.

Descriptive statistics 117
Statistical analysis of storm sediment loads 119
Dependent variables 120
Walling (1974) Sediment-Transport Curve Approach 124
Independent variables 124
Hysteresis 128
Normality 132
Multiple linear regression analysis 133
Correlation matrix 135
Principal component and factor analysis 136

V. SUSPENDED-SEDIMENT TRANSPORT AT RIO ICACOS 139
Rainfall and Discharge for the Study Period 139
Suspended-Sediment Load and Yield 140
Suspended-Sediment Analysis 141
Sediment-transport curves 142
Walling (1974) Sediment-Transport Curve Approach 149
Statistical Results at Rio Icacos 153
Entire event analysis 153
Quickflow Results (entire event) 159
Forward stepwise regression (entire event, quickflow) 160
Factor analysis - (entire event, quickflow) 161
Varimax rotation (entire event, quickflow) 162
Runoff Results (entire event) 164
Forward stepwise regression (entire event, runoff) 166
Factor analysis - (entire event, runoff) 167
Varimax rotation (entire event, runoff) 168
Discussion 169
Highest peak flow analysis 170
Quickflow Results (highest peak) 172
Forward stepwise regression (highest peak, quickflow) 173
Factor analysis - (highest peak, quickflow) 174
Varimax rotation (highest peak, quickflow) 175
Runoff Results (highest peak) 176
Forward stepwise regression (highest peak, runoff) 177
Factor analysis - (highest peak, runoff) 177
Varimax rotation (highest peak, runoff) 179
Discussion 180
Hysteresis 181
Summary of Results for Rio Icacos 185

VI. SUSPENDED-SEDIMENT TRANSPORT AT QUEBRADA BLANCA 192
Rainfall and Discharge for the Study Period 192
Suspended-Sediment Load and Yield 193
Suspended-Sediment Analysis 194
Sediment-transport curves 198
Walling (1974) Sediment-Transport Curve Approach 207
Statistical Results at Quebrada Blanca 207
Entire event analysis 207
Quickflow Results (entire event) 216
Forward stepwise regression (entire event, quickflow) 217
Factor analysis - (entire event, quickflow) 219
Varimax rotation (entire event, quickflow) 222
Runoff Results (entire event) 224
Forward stepwise regression (entire event, runoff) 224
Factor analysis - (entire event, runoff) 226

Reproduced with permission of the copyright owner. Further reproduction prohibited without permission.

Varimax rotation (entire event, runoff)....229
Discussion....230
Highest peak flow analysis....232
Quickflow Results (highest peak)....232
Forward stepwise regression (highest peak, quickflow)....234
Factor analysis - (highest peak, quickflow)....235
Varimax rotation (highest peak, quickflow)....238
Runoff Results (highest peak)....240
Forward stepwise regression (highest peak, runoff)....240
Factor analysis - (highest peak, runoff)....242
Varimax rotation (highest peak, runoff)....244
Discussion....246
Hysteresis....247
Summary of Results for Quebrada Blanca....255

VII. SUSPENDED-SEDIMENT TRANSPORT AT RIO CAGUITAS....261
Rainfall and Discharge for the Study Period....261
Suspended-Sediment Load and Yield....263
Suspended-Sediment Analysis....263
Sediment-transport curves....264
Walling (1974) Sediment-Transport Curve Approach....271
Statistical Results at Rio Caguitas....273
Entire event analysis....273
Quickflow Results (entire event)....280
Forward stepwise regression (entire event, quickflow)....281
Factor analysis - (entire event, quickflow)....282
Varimax rotation (entire event, quickflow)....286
Runoff Results (entire event)....287
Forward stepwise regression (entire event, runoff)....289
Factor analysis - (entire event, runoff)....290
Varimax rotation (entire event, runoff)....292
Discussion....293
Highest peak flow analysis....294
Quickflow Results (highest peak)....296
Forward stepwise regression (highest peak, quickflow)....297
Factor analysis - (highest peak, quickflow)....297
Varimax rotation (highest peak, quickflow)....300
Runoff Results (highest peak)....300
Forward stepwise regression (highest peak, runoff)....301
Factor analysis - (highest peak, runoff)....302
Varimax rotation (highest peak, runoff)....304
Discussion....305
Hysteresis....305
Summary of Results for Rio Caguitas....309

VIII. SUSPENDED-SEDIMENT TRANSPORT AT RIO PIEDRAS....317
Rainfall and Discharge for the Study Period....317
Suspended-Sediment Load and Yield....319
Suspended-Sediment Analysis....319
Sediment-transport curves....321
Walling (1974) Sediment-Transport Curve Approach....328
Statistical Results at Rio Piedras....331
Entire event analysis....331
Quickflow Results (entire event)....337
Forward stepwise regression (entire event, quickflow)....338
Factor analysis - (entire event, quickflow)....340

Reproduced with permission of the copyright owner. Further reproduction prohibited without permission.

Varimax rotation (entire event, quickflow) 342
Runoff Results (entire event) 343
Forward stepwise regression (entire event, runoff) 345
Factor analysis - (entire event, runoff) 346
Varimax rotation (entire event, runoff) 347
Discussion 349
Highest peak flow analysis 349
Quickflow Results (highest peak) 350
Forward stepwise regression (highest peak, quickflow) 352
Factor analysis - (highest peak, quickflow) 353
Varimax rotation (highest peak, quickflow) 355
Runoff Results (highest peak) 356
Forward stepwise regression (highest peak, runoff) 356
Factor analysis - (highest peak, runoff) 357
Varimax rotation (highest peak, runoff) 359
Discussion 360
Hysteresis 360
Summary of Results for Rio Piedras 368

IX. SHEETWASH EROSION 375

X. SUMMARY 396
Sheetwash Erosion 398
Hydrology and Sediment Characteristics at the Four Study Basins 400
Sediment Yields 402
Suspended-Sediment Transport 410
Sediment-Transport Curves 412
Results of Statistical Analysis 420
Walling (1974) Sediment-Transport Curve Approach 420
Storm-Generated Suspended-Sediment Loads and Concentrations 422
Event definition 422
Hydrograph separation 422
Multiple regression and principal components analysis 425
Rio Icacos 426
Quebrada Blanca 436
Rio Caguitas 439
Rio Piedras 440
Hysteresis Results 442
Discussion 448

XI.CONCLUSIONS 452

XII. REFERENCES 471

Volume II

Table of Contents xi

XIII. APPENDIX 490

Reproduced with permission of the copyright owner. Further reproduction prohibited without permission.

CHAPTER 1

INTRODUCTION

The humid tropics, defined by an average annual precipitation greater than 1000 mm and annual temperatures of 20-30^{0}C (68-86 ^{0}F), cover 25 percent of the world's surface area and by the year 2000 were expected to hold one-half of the world's population (UNESCO, 1990). With this growing population stresses are being placed on the environment and water resources. Problems associated with land-use changes in the tropics include deforestation, reservoir sedimentation, channel conveyance, and degradation of terrestrial and marine habitats (UNESCO, 1990; Bonell and others, 1993; World Resources Institute, 1996; Gellis and others, 1999). All of these land-use problems influence erosion and sediment characteristics of tropical watersheds. The distinction between background erosion rates, determined by natural (geologic and climatic) factors, and human-accelerated erosion has important implications for land-use planning and resource management. To successfully manage environmental problems in the humid tropics it is necessary to understand the role of land use on erosion and sediment transport.

Suspended-sediment load is the largest percentage of total sediment load in world rivers, typically accounting for greater than 90 percent of total sediment load (Meade and others, 1990). Sources of suspended sediment in most basins can be generalized into channel corridor (bed and banks) and upland sources related to land use and land cover. The availability of sediment for transport is related to natural phenomenon, such as landslides, and human accelerated erosion from land-use disturbance, such as agriculture. Erosion of

Reproduced with permission of the copyright owner. Further reproduction prohibited without permission.

the surface soil (A, B, and C, horizons) from land-use disturbance generally generates silts and clays, which become suspended sediment. During storms suspended-sediment concentrations often vary over several orders-of-magnitude for a given discharge (Walling, 1974; Walling and Webb, 1982).

Few studies have been performed in the humid tropics on the characteristics of suspended-sediment transport in tropical rivers, specifically identifying causes for the variability in storm-generated suspended sediment concentrations and loads. In part, this deficit stems from the lack of an extensive and accurate data set from a humid-tropical region (Krishnaswamy and others, 2001). The objectives of this PhD research are to:

- **Assemble a defensible suspended-sediment data set for select basins in the humid tropics, Puerto Rico.**
- **Using this data set, determine the relationships of storm-generated suspended-sediment loads and concentrations to hydrologic characteristics for 3 different time categories : the current event, the previous event(s), and minor rainfall and runoff between the current and previous event.**
- **Determine how land use in relatively undisturbed (forest, pasture) to disturbed (agriculture, and urbanizing) basins affects storm-generated suspended-sediment characteristics.**
- **Determine how the geomorphic system generates and transports sediment in these different land-use settings.**

The null hypothesis put forth in this PhD research is that land use does not affect upland erosion and suspended-sediment characteristics in a humid-tropical environment. The alternative hypothesis is that land-use changes affect upland erosion and downstream

Reproduced with permission of the copyright owner. Further reproduction prohibited without permission.

suspended-sediment characteristics. It is hypothesized that many of the rivers draining disturbed areas in Puerto Rico may show abnormally high basin-wide erosion rates and sediment yields.

Suspended-sediment characteristics that will be analyzed to accept or reject the null hypothesis include differences in sediment characteristics among instrumented basins in Puerto Rico (suspended-sediment loads, concentrations, hysteresis, and sediment flushing). Sediment flushing is the removal of sediment on hillslopes and in channels by preceding rainfall and runoff events. Sediment flushing is a particular process that is poorly understood and may be the most important original contribution from this research.

The major classes of land use (forest, agriculture, pasture, and urban) are well represented in Puerto Rico. The U.S. Geological Survey (USGS), Water Resources Division has been collecting suspended-sediment data at several sites on the Island since the 1960's. Thus, Puerto Rico provides an excellent natural laboratory to research suspended-sediment characteristics under different land use settings. For the purposes of this research, land use, erosion, and sediment transport were investigated for four watersheds in Puerto Rico: Quebrada Blanca, Rio Piedras, Rio Icacos, and Rio Caguitas (fig. 1.1). The Rio Icacos basin (fig. 1.1) is a relatively undisturbed forested basin, draining 1.26 mi^2 (3.26 km^2) in the Luquillo Experimental Forest (LEF) (Larsen, 1997). The 3.25 mi^2 (8.42 km^2) Quebrada Blanca basin drains dominantly pasture (Gellis and others, 1999). The 5.30 mi^2 (13.7 km^2). Rio Caguitas basin drains a mixture of cropland, pasture, and forest. The 7.49 mi^2 (19.4 km^2) Rio Piedras basin (fig. 1.1) is a disturbed basin undergoing rapid land-use changes in response to housing construction and is in the San Juan metropolitan area (Gellis, 1991). The 7.49 mi^2 (19.4 km^2) Quebrada Salvatierra basin was only used in the analysis of hydrograph separation (fig. 1.1).

Reproduced with permission of the copyright owner. Further reproduction prohibited without permission.

Results of this research can be used in Puerto Rico and other tropical environments facing erosion and sediment problems to help managers, planners, and government better understand the natural background rate of sediment yields and the anthropogenic effects on those yields.

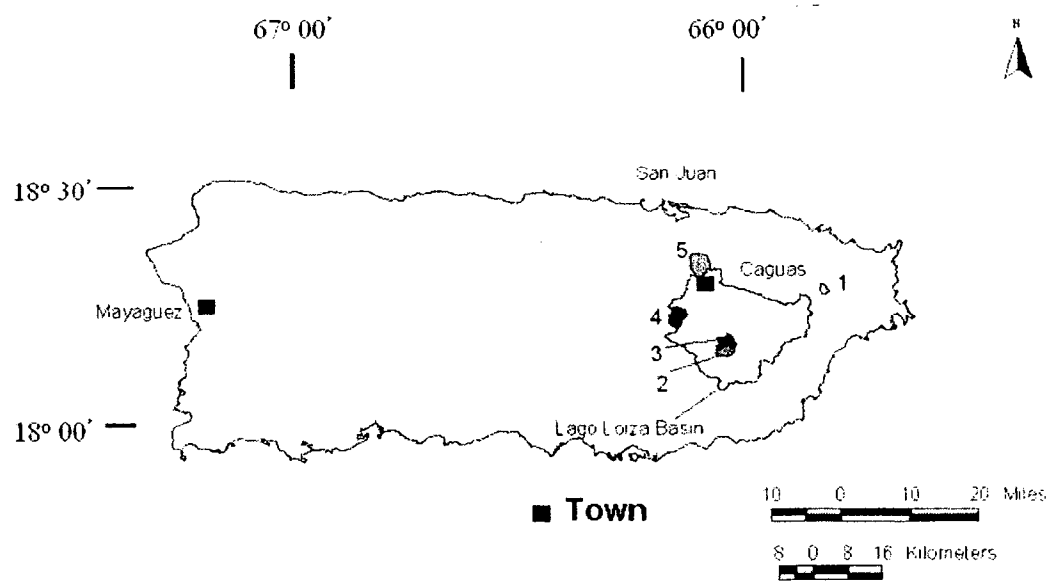

Figure 1.1. Location of study basins, (1) Rio Icacos (50075000), (2) Quebrada Blanca (50051150), (3) Quebrada Salvatierra (50051180), (4) Rio Caguitas (50055225), and (5) Rio Piedras (50048700).

Reproduced with permission of the copyright owner. Further reproduction prohibited without permission.

CHAPTER II

PREVIOUS STUDIES

This chapter will review previous geomorphic studies in the humid tropics and Puerto Rico. While not all of these studies refer directly to suspended-sediment transport, they all relate either directly or indirectly to landscape processes that affect soil erosion, sediment delivery and transport. Finally, since the objectives of this research relate primarily to suspended sediment in the tropics, a short review of suspended-sediment transport in the more well-studied humid-temperate environments is included.

Tropical Geomorphology

Tropical geomorphology is the study of weathering and landform development in warm, humid climates, such as those typical of Puerto Rico (Thomas, 1974). A review of tropical geomorphology illustrates a familiar argument in geomorphology on whether landforms are controlled by climate. Early writers on the subject, namely Europeans in the 18th and 19th century, were impressed by the differences they saw in tropical landforms. Much of their work described how tropical landforms differ from those found in semi-arid and humid-temperate climatic regions, even on the same lithology. Geologists and geographers in the early 20th century applied Davisan concepts to tropical landforms in terms of cycles of evolution and erosion surfaces. The latter half

Reproduced with permission of the copyright owner. Further reproduction prohibited without permission.

of the 20th century saw a shift to process-oriented geomorphic studies and interpretations of tropical landforms.

Climatic definition

The term "tropics" has a wide meaning, depending on the discipline providing the explanation. For geographers the area between the Tropics of Cancer and Capricorn (23 1/2^0 N and S) is the tropics. These areas are also referred to by geographers as the "low" latitudes. A conventional climatic system, the Koppen System, separates climatic areas of the Earth on the basis of temperature characteristics. In the Koppen system a tropical rainy climate is defined as one in which the average temperature of each month is above 64^{0}F (18^{0}C). The tropical climate zone of the Koppen System is subdivided into: (1) rain forest, where the driest month has 2.4 inches (60 mm) rainfall, (2) monsoon, where the driest month has less than 2.4 inches (60 mm) rainfall and the dry season is of short duration, and (3) savanna, where at least 1 month has less than 2.4 inches (60 mm) rainfall and the dry season is well developed (fig. 2.1). Rain forest together with savanna regions occupy 35 percent of the Earth's land area (Goudie, 1984).

On the basis of temperature, Goudie (1984) defined the tropics as having an annual average temperature around 77^{0}F (25^{0}C) and a small annual temperature range of less than 50^{0}F (10^{0}C). In the tropics, the lowest monthly mean temperature does not fall below 68^{0}F (20^{0}C) (Tricart, 1972; Stallard, 1988).

On the basis of rainfall, Stallard (1988) defined tropical forests and moist savannas as areas where precipitation exceeds 39 to 79 inches (1,000 to 2,000 mm) annually and temperatures are greater than 68^{0}F (20^{0}C). Goudie (1984) defined the wet tropics as areas where annual rainfall

Reproduced with permission of the copyright owner. Further reproduction prohibited without permission.

totals 60 to 98 inches (1,750 to 2,500 mm). In contrast to average daily rainfall in humid temperate stations of 0.16-0.24 inches (4-6 mm), annual rainfall per day in the tropics is 0.60

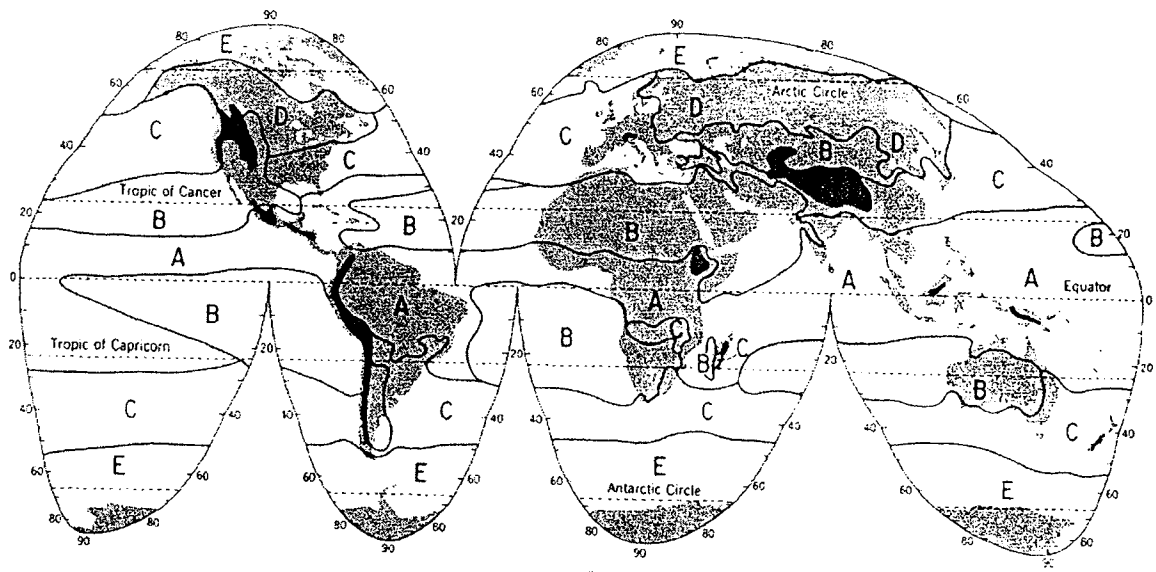

Figure 2.1. Koppen classification system of climate (Strahler and Strahler, 1976). ***A - Tropical climates, B - Dry climates, C - mesothermal climate , D - microthernal climate, E - ice climate.***

inches (15.2 mm) (Goudie, 1984). In Sharma's (1987) study of the Rajasthan Region in India, this humid tropical region was defined as having annual rainfall between 39 to 63 inches (1,000 to 1,600 mm) and weak physical weathering with chemical weathering, landslides, and dominant fluvial processes.

Many tropical areas are subject to dry seasons, monsoons, and hurricanes. Wet-dry climates in the tropics are usually associated with monsoonal activity between 35^{0}N and 25^{0}S. Annual rainfall in monsoonal regions is still more than 39 inches (1000 mm), but varies. For example, in Calcutta, India, average precipitation ranges from 0.2 to 12 inches (5 mm to 308 mm)

Reproduced with permission of the copyright owner. Further reproduction prohibited without permission.

monthly. Closed low pressure systems, tropical cyclones (hurricane, typhoon, willy willy) can produce torrential rains. For example, over 79 inches (2,000 mm) of rainfall was recorded in one day in the Philippines (Goudie, 1984). On average, 75 to 100 days in the tropics have thunderstorms (Goudie, 1984), but the number can be much higher. The number of rainy days in Belen, Brazil is 243 (66%). Therefore, although the average yearly rainfall is a defining factor to the tropics, the frequency of major meteorological events cannot be discounted nor can its effect on the geomorphic system be ignored.

Climatic geomorphology

The first geomorphic studies in the tropics were built on the work of early European naturalists and scientists visiting their country's colonies in the tropics (Dana, 1850; Douglas, 1977; Bremer, 1980). These early workers noticed significant differences in tropical landforms from their familiar European landscapes. These early studies in tropical geomorphology and those following influenced a "school of thought" in geomorphology that the main influence on landform development is climate, known as 'climatic geomorphology' (Peltier, 1950; Budel, 1957; Birot, 1960; 1966; Stoddart, 1969; Tricart, 1972; Tricart and Cailleux 1972; Douglas, 1978; Douglas and Spencer, 1985a). Landform development in the humid tropics was described by Budel (1982), Ruxton and Berry (1957, 1961), and Swan (1970, 1972). The concept of climatic- morphogenic regions has been severely challenged, mostly for its failure to incorporate tectonics and lithology into its definition, and has led to substantial arguments and controversy in the geomorphic community.

One of the main distinctions, of course, between the humid tropics and other morphoclimatic regions is vegetation. Biologically, the humid-tropical rain forest is two to three

Reproduced with permission of the copyright owner. Further reproduction prohibited without permission.

times as productive as temperate forests (Douglas, 1977). Tropics are optimum zones for the creation of organic matter (photosynthesis); for example, tropical evergreens produce 3 to 4 times as much vegetal matter per hectare as mid-latitude forests. This abundant vegetation influences chemical weathering (i.e. the exchange between soil and atmosphere of water, gases, and minerals). Decomposition produces substances active in weathering such as fluvic acids. Although litter supply is high in the tropics (4.9 tons/acre; 11 metric tons/ha), decomposition is higher and humus is less than in temperate regions. Decomposition is controlled by bacteria, which are affected by temperature, pH, and oxygen.

A factor cited in the selection of the humid tropics as a morphogenetic region is characteristic intense chemical weathering. Deep chemical weathering is related to several mechanisms such as high temperatures, high rainfall, and high biomass that promotes rapid chemical weathering of rock minerals. Van't Hoff's rule states that the speed of chemical reactions doubles with every 10^0C rise in temperature (Chang, 1981). Rates of decaying organic matter in tropical soils are five times higher than under temperate conditions, and this releases organic acids which increases chemical weathering (Douglas, 1977; Birkeland, 1984). Complete saturation of soils by slightly acidic ground water and throughflow also influences chemical weathering. The result of this chemical weathering is a thick regolith that may exceed 98 feet (30 m), and locally be as great as 410 feet (125 m).

General impressions of processes in the humid tropics that emerge from the early work up to the 1960's and 1970's are that: (1) chemical weathering is high and mechanical weathering is low, (2) formation of laterites is unique to the tropics, (3) parallel slopes retreat by basal chemical weathering and stripping by sheetwash or Budel's etchaplanation double action process, (4) mass

Reproduced with permission of the copyright owner. Further reproduction prohibited without permission.

wasting is important yet episodic, (5) because of intense chemical weathering, fluvial erosion is minimal and river gradients are low, (6) dissolved load is high and suspended load is low, (6) slopewash is minimum to moderate, (7) hydraulic geometry width changes less strikingly than in extra-tropical rivers due to lack of a coarse load, (8) the landscape is best expressed as inselbergs, flat plains (less than 0.5^0) with abrupt hills, (9) smooth flowing slopes occur in contrast to sharp ridges in arid areas, and (10) there is little talus accumulation due to lack of freeze thaw, chemical weathering, and strong vegetative hold on debris (Thornbury, 1954; Pugh, 1966).

Stoddart (1969) and Douglas and Spencer (1985a) identify key questions related to tropical geomorphology that emerged from geomorphic research in the tropics:

(a) Are there typical tropical landforms?

(b) How do climatic contrasts, especially in the amount and seasonal distribution of rainfall, affect geomorphic processes in low latitudes?

(c) Can changes in climate produce recognizable sequences of forms in the landscape?

A reaction to these questions might have been responsible for been the increase in process-based geomorphic studies beginning in the 1970's.

Recent geomorphic studies

Beginning in the 1970's process-based geomorphic studies were conducted in the tropics. Many of these studies sought to explain tropical hydrology (streamflow and sheetwash) and mass movements (Eyles and Ho, 1970; Williams, 1973; Lewis, 1974; Gupta, 1975, 1988; Walsh, 1985; Kesel, 1985; Chatterjea, 1989; Lal, 1990). Other studies sought to explain channel geometry,

Reproduced with permission of the copyright owner. Further reproduction prohibited without permission.

sediment transport , and the effects of land use on sediment yields (Dunne, 1979; Pickup and others, 1981).

Lal (1990) generalized the water balance in the tropics as: 70-90% throughflow, 10-30% stemflow, and 10-20% canopy interception. The high spatial variability of soil texture, organic litter, and antecedent conditions lead to variable infiltration rates reported for the tropics. Vegetation and thick soils can promote rapid infiltration and throughflow, and groundwater flow is important. Groundwater flow along the regolith-bedrock contact may supply most of the base flow to tropical rivers (Swan, 1970). Four important contributors to storm runoff are (1) widespread saturation overland flow, (2) localized saturation overland flow, (3) throughflow, and (4) pipeflow (Walsh, 1985). Because of the high vegetative cover, the canopy in tropical forest intercepts up to 91 percent of rainfall so that stemflow and leaf drip are important contributors in the hydrologic cycle (Chatterjea, 1989). Stemflow down tree trunks in Singapore are local point-sources for surface flow development (Chatterjea, 1989).

Studies of surface wash in the tropics have reported varied findings on the importance of overland flow. Some researchers report minimal overland flow, others report substantial overland flow (Walsh, 1985; Douglas and Spencer, 1985b) (fig. 2.2). Figure 2.2 indicates a range in overland flow from zero in Amazonas, Brazil to 95 percent in Queensland, Australia. The variations in range of overland flow is related to thickness of the humus layer and tree roots. Kesel (1977) related overland flow to laterites and their topographic expression. On ridge tops and valley bottoms well developed impermeable laterites create rapid saturation and runoff. On the valley sides, laterites are poorly developed and discontinuous, which leads to infiltration and reduced overland flow . Based on work in Dominica, West Indies, Walsh (1985) noted the

Reproduced with permission of the copyright owner. Further reproduction prohibited without permission.

variability of runoff in the tropics and depicted a simple model of runoff. Two important soil properties defining runoff were topsoil water storage capacity and subsoil permeability. Interesting to note in Walsh's (1985) findings were the lack of overland flow in extremely wet conditions and the presence of throughflow. In the remaining rainforest in Singapore, geomorphic processes are controlled by surface and subsurface waters with complementary processes such as piping and slope failures (Chatterjea, 1989).

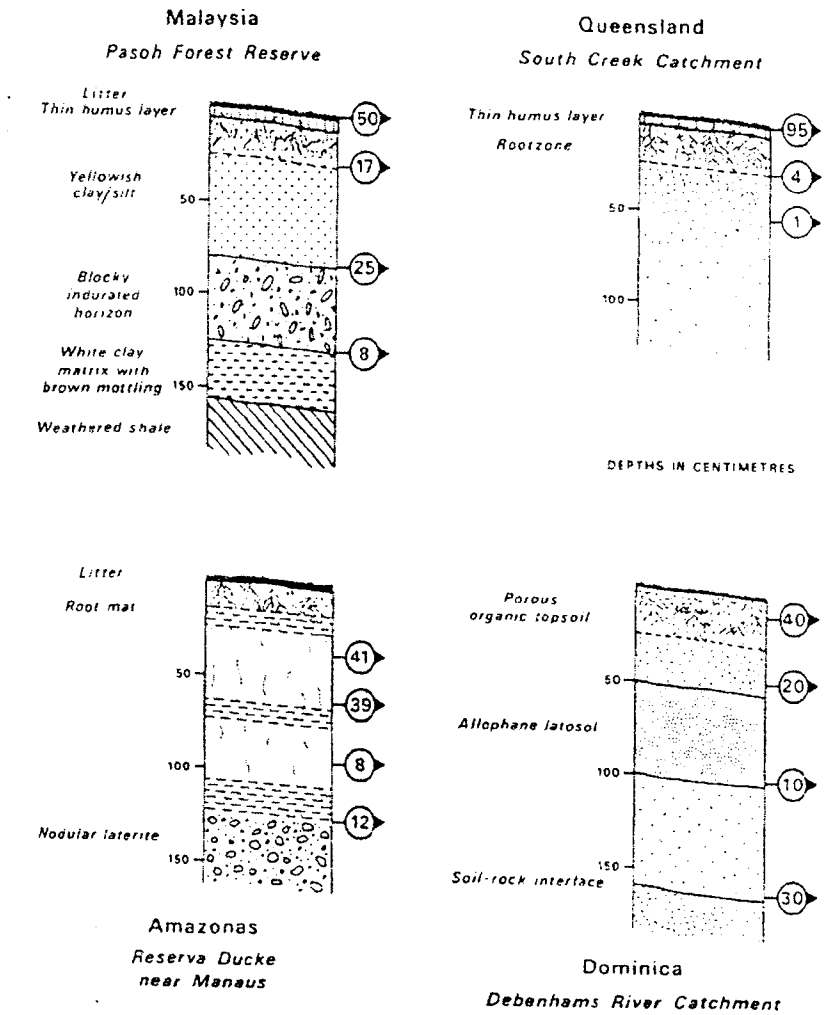

Figure. 2.2. Proportion of runoff draining different surface and soil horizons in four tropical rainforest sites (from Douglas and Spencer, 1985b).

Reproduced with permission of the copyright owner. Further reproduction prohibited without permission.

There seems to be much debate in the literature on which is the more dominant process of erosion in the tropics: sheetwash or soil creep (Eyles and Ho, 1970; Williams, 1973). Eyles and Ho (1970) in a comparison to other climatic regimes showed creep to be somewhat higher in the tropics; however, the need for more statistical tests was noted. Under tropical conditions, leaf litter is low because of high decomposition rates which may lead to high surface erosion. Williams (1973) reported that in tropical Northern Territory, Australia, sheetwash was five times more important than soil creep in hillslope denudation. Sheetwash, which works over the entire forest floor in Singapore, is the primary generator of sediment with slope failure, treefall, and piping as secondary localized generators of sediment (Chatterjea, 1989). In the Fly River basin, New Guinea, reworked stream bed and bank sediment, landslides, and sheetwash are the major contributors of sediment (Pickup and others, 1981).

Soil erosion is a major mechanism of land degradation in the tropics (El-Swaify, 1990). Mechanisms for soil detachment vary. Spencer and others (1990) concluded that in Borneo, sediment was mobilized by natural processes of fire, landslides, and treefalls. Debris trapped sediment on the forest floor until a high magnitude rainfall event released the sediment. Much of the throughflow in tropical Malaysia occurs from leaf drip and stemflow (Chatterjea, 1989). Sediment that was dislodged from leaf drip was transported by overland flow. Under forested conditions in Guyana, sediment yield may be as low as 0.09 tons/acre/yr (0.2 metric tons/ha/yr). Under deforested conditions sediment yield was as high as 268 to 535 tons/acre/yr (600 to 1,200 metric tons/ha/yr) (Brunig, 1975). In contrast, humid-temperate regions of the Pacific Northwest, sheetwash and raindrop impact are ineffective in transporting sediment (Dietrich and others, 1982).

Reproduced with permission of the copyright owner. Further reproduction prohibited without permission.

Raindrop impact is important in soil erosion and tropical rainfall intensities are higher than in temperate regions; although Sharma and Correia (1989) concluded that on the Ivory Coast, West Africa, soil was entrained by overland flow and not by raindrop impact. The kinetic energy of a raindrop is related to its terminal velocity, which increases with size. Tropical rainfall events are associated with large drop size and drop density (Thomas, 1994). Raindrop impact may not be important in a closed canopy, where up to 90% may be intercepted. Ross and others (1990) state that the amount of material impacted by leaf drip was 600% greater than by rainfall and attributed this increase to a lack of leaf litter. Spencer and others (1990) also state that tropical forest floors offer less resistance to raindrop impact than temperate regions. This is related to the rapid decomposition of litter in the tropics. In general, on cleared areas in the tropics both the increased rainfall intensity, raindrop size, and density will promote greater raindrop impact than in the temperate zones.

Landsliding may be an important form of landform development in the humid tropics (Scatena, 1995). There are four conditions in the humid tropics that make it susceptible to mass movements: (1) dense vegetation with a shallow root zone, (2) steep slopes, (3) high intensity rainfall, and (4) debris character of regolith and its moisture holding capacity (Chorley and others, 1984). Shallow root systems often promote treefalls during storm events. In Panama, tree falls affect 60-125% of a given area in 100 years (Chorley and others, 1984). In New Guinea, 2-3 landslides per year occur in a 162 mi^2 (420 km^2) basin; average landslide volume is 1.06×10^6 ft^3 (30,000 m^3), of which 40-50% enters the river; equivalent to 529,000 tons (480,000 metric tons) (Pickup and others, 1981). Most of the slides occur on weathered rock and reworked alluvium. Frequency of major failures is once in ten years (Pickup and others, 1981).

Reproduced with permission of the copyright owner. Further reproduction prohibited without permission.

Kesel (1985) contrasted alluvial fans in wet tropical climates to each other and to fans in other morphoclimatic regions. The size of alluvial fans are affected by lithology, tectonics, climate, and slope. Humid fans were thought to be convex with the proximal portions less steep than arid fans. However, with respect to drainage area, humid fans are comparable in size to arid fans (Kesel, 1985). Similarities between arid and wet-tropical fans exist, in that the rate of decrease of clast size down-gradient is the same. Gradients are just as steep and fan size is similar in both settings. However, some differences were noticed between arid and wet-tropical fans. In the wet tropics, clasts are dominantly fluvially transported, the correlation coefficient (R^2) of clast size to drainage area is better, and at the same gradient clasts sizes are larger. Differences in transport characteristics may be due to the intense discharge events experienced during tropical cyclones.

In a study on the Island of Dominica, West Indies, a humid-tropical environment with rainfall varying from 1,000 to 10,000 mm, drainage density on the island was related to climate, lithology, and age of volcanic flows (Walsh, 1985). The relation between rainfall and drainage density was not linear but rather curvilinear. This attenuation of drainage density with increased rainfall is a result of a contrast in soil and vegetation types associated with the higher rainfall. Weathering associated with an increase in precipitation changes clay mineralogy from montmorillonite to kaolinite to allophane. The change in clay mineralogy causes an increase in infiltration, decreases in sheetwash, and attenuation of drainage density (Walsh, 1985).

The humid tropics make an important contribution to the ocean's dissolved and solid load. The humid tropics occupy 25% of the Earth's surface and supply 65% of the dissolved silica, 38% of the ionic load, and 50% of the total river solid load (Stallard, 1988; Milliman and Meade 1983). In a global budget of runoff, 50% of the runoff to the world's oceans is contributed by low-latitude

Reproduced with permission of the copyright owner. Further reproduction prohibited without permission.

rivers (Lerman, 1985). It is generally thought that because of low erosion rates, dissolved load is high and sediment loads are low in tropical rivers. The Langbein and Schumm (1958) curve indicates that semi-arid regions have the highest sediment yields (fig. 2.3a). Fournier (1960) included data from monsoonal regions and reported a second spike in these areas (fig. 2.3b).

Effects of land use on erosion and sediment yield in the tropics

Human changes to the environment date back to the early Holocene. Sheep domestication in the Middle East goes back to 11ka BP and agriculture in the Near East back to 9ka BP (Williams and others, 1993). In the tropics, several ancient civilizations have accelerated soil erosion from agriculture, grazing, and timber harvesting, including the Phoenicians, Mesopotamians, and civilizations in Lebanon, Syria, and northwestern Africa (Lal, 1990).

Rates of deforestation in the tropics during the 20th century were alarming. Tropical forests make up one-half of the world's forests (World Resources Institute, 1996). UNESCO (1990) predicted that by the year 2000 one-half of the world's population will reside in the tropics. Over 42 million acres (17 million hectares) of deforestation occur annually (Rietbergen, 1993). The world's forests declined by 2% or 247 million acres (100 million hectares) between 1980 to 1990 (World Resources Institute, 1996). By the year 2000, vegetation in the Amazon Region and Africa was expected to be reduced by an estimated 50% and 28%, respectively, and between 249,000 and 1,250,000 species would become extinct (Goudie, 1984). Forests are cleared for agriculture, cattle, infrastructure, timber, and fuelwood. Associated with deforestation are geomorphological changes in rates of upland erosion and fluvial sediment transport, coupled with changes to landforms. Douglas (1967) documented a five-fold increase in sediment yield in

Reproduced with permission of the copyright owner. Further reproduction prohibited without permission.

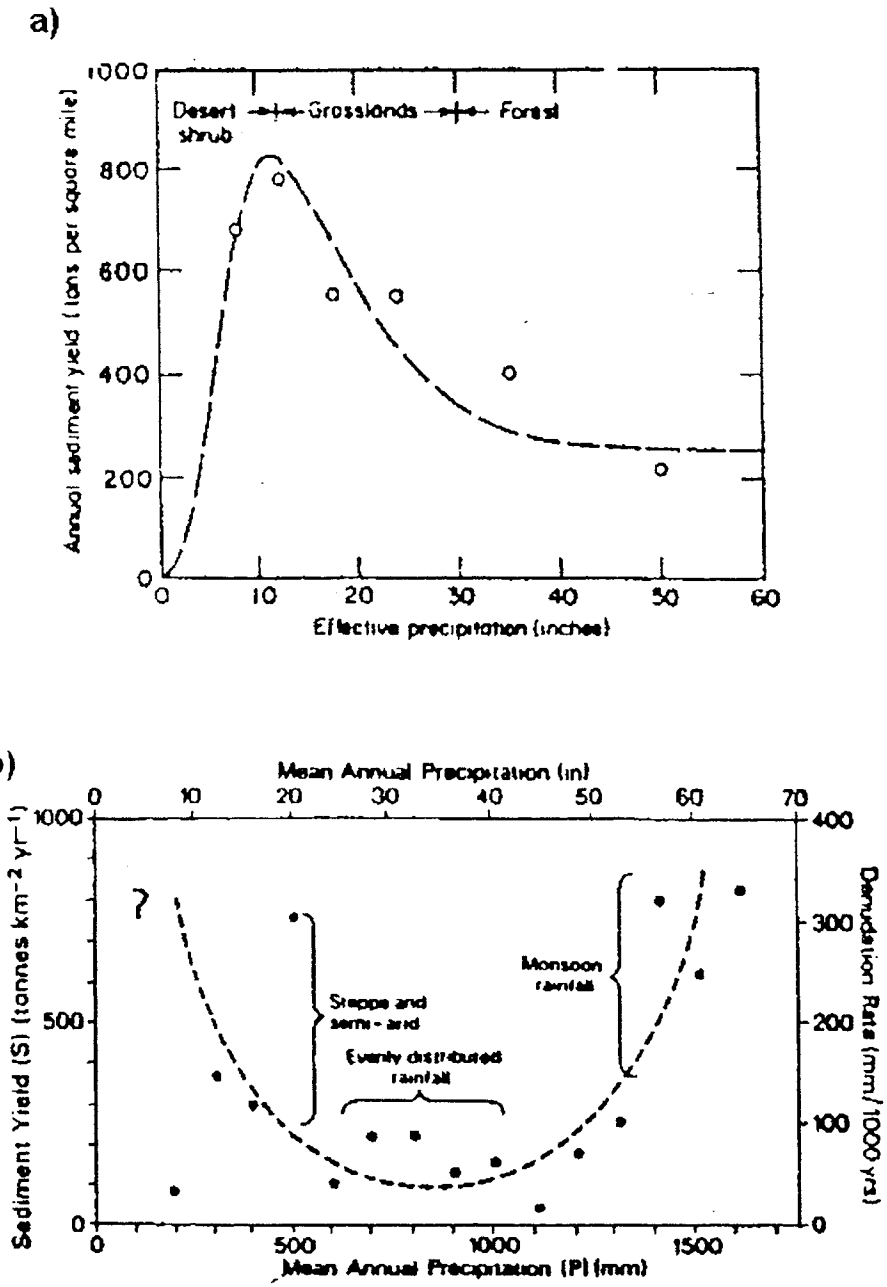

Figure 2.3. a) Variation of sediment yield with climate (Langbein and Schumm, 1958). b) Variation of sediment yield with climate (after Fournier, 1960).

Malaysia from clearcutting 64% to 100% of the watershed area. Runoff was six-times higher and sediment yield seven-times higher in deforested plots than forested plots in an experiment carried out in Brazil (Ross and others, 1990). Pasture in the tropics is often managed for improvement by

Reproduced with permission of the copyright owner. Further reproduction prohibited without permission.

burning which leads to increased soil erosion. Grassland burning in the Philippines resulted in increased peak flows, higher suspended-sediment concentrations, increased soil erosion, and increased channel sedimentation (Dano, 1990). Sediment yields were 59 and 72% less, in the non-burned grassland and reforested areas, respectively.

Data from studies performed at the plot scale on sheetwash erosion on varying land uses in the tropics were assembled for this research (Table 2.1). In these studies, plots ranged from 9.8 to 1,970 ft^2 (3 to 600 m^2), slopes ranged from 2 to 65 %, and rainfall varied from 24 to 130 inches (612 to 3,300 mm). Data from these studies indicate that sheetwash erosion is highest on bare ground, followed by land used for agriculture (fig. 2.4). In comparison to tropical forested conditions, which had an average soil erosion rate of 1.5 tons/ac/yr (3.4 metric tons/Ha/yr), under various crops the average erosion rate was 24.6 tons/acre/yr (55 metric tons/Ha/yr) (fig. 2.4, Table 2.1). El-Swaify (1990) and Wiersum (1985) argue that accumulated litter in the forest understory is particularly important in reducing erosion.

In Dunne's (1979) study of land use and sediment yield in Kenya, grazed areas showed higher sediment yield per annual runoff than agriculture and forest (fig. 2.5). Erosion rates in Nepal were highest in grazed areas: 15.5 tons/acre/yr (34.7 metric tons/ha/yr) compared to forest with 4 tons/acre/yr (8 metric tons/ha/yr) (Fleming, 1985). In temperate regions, grazing is thought to increase soil erosion through a decrease in vegetative cover, trampling, trail gullying, streambank erosion, and soil compaction leading to increased runoff (Reid, 1991). In the tropics, a similar cause and effect should ensue, although soil erosion rates may be higher because of more intense precipitation.

Reproduced with permission of the copyright owner. Further reproduction prohibited without permission.

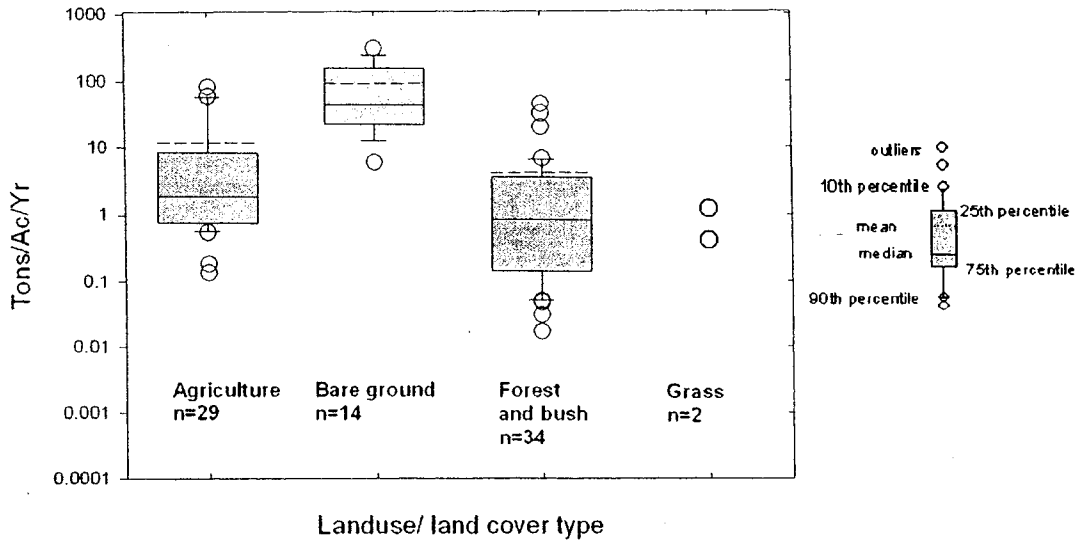

Figure 2.4. Sheetwash erosion measurements made in the tropics. See Table 2.1 for source of data.

In general, there are many studies in the tropics relating deforestation to changes in runoff, erosion, and sediment yield (Lal, 1981; Bons, 1990; Douglas and others, 1990; Malmer, 1990). However, these studies are often short term, event based, and not directed at understanding the causes of change. Based on a literature review, it appears that studies on the effects of deforestation in the tropics are not as rigorous as studies carried out in temperate regions.

Previous Studies in Puerto Rico

This section describes previous work on geomorphic research in Puerto Rico. Most of the research falls into categories of soil creep, soil erosion, mass wasting, sheetwash erosion, and fluvial sediment transport.

Reproduced with permission of the copyright owner. Further reproduction prohibited without permission.

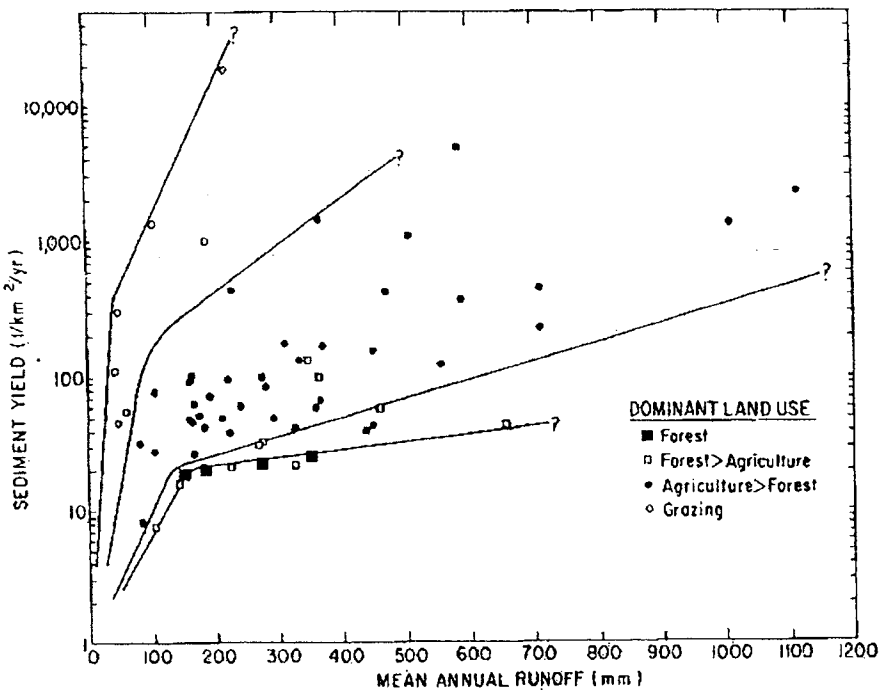

Figure 2.5. Mean annual sediment yield and mean annual runoff for catchments with indicated dominant land uses (Dunne, 1979).

Because of its thick soils and intense rainfall events, Puerto Rico is subject to a wide variety of mass movements. Soil creep was studied by Lewis (1974, 1975), who measured soil creep rates at a humid-tropical site in the Luquillo Mountains and at a semi-arid site on the southwestern coast. Soil creep rates in the humid site were 0.16 in/yr (4 mm/yr) in the upper layers of the soil profile, higher than rates reported for extra-humid tropical areas (Lewis, 1974). Two rates of soil creep were observed in the tropical rainforest, a faster shallow soil creep and a slower subsurface flow (Lewis, 1974). Volumetric soil creep over 3 years was

Reproduced with permission of the copyright owner. Further reproduction prohibited without permission.

Reproduced with permission of the copyright owner. Further reproduction prohibited without permission.

Table 2.1. Sheetwash erosion measurements in the tropics.

Land Use Specific	General land use/ land cover	Country	Plot Size (ft x ft)	Slope, in percent	Erosion (lb/Ac/Yr)	Annual rainfall (in)	Reference
Banana	Agriculture	Jamaica		30	81.7		El-Swaify, 1990
Bare Soil - Fallow	Agriculture	Java		11	191		El-Swaify, 1990
Bare Soil - Fallow	Agriculture	Java		14	229		El-Swaify, 1990
Cassava	Agriculture	Thailand	13.1x65.6	8-10	6.0	46	Thongmee and Vannapraqsert, 1990
Cassava	Agriculture	Nigeria		11	55.8		El-Swaify, 1990
Coffee, w/natural ground cover	Agriculture	Puerto Rico	13.8x51.8	62	0.79	79	Smith and Abruna, 1955
Corn	Agriculture	Trinidad		22	0.88		El-Swaify, 1990
Corn	Agriculture	Trinidad		22	1.1	24	El-Swaify, 1990
Corn	Agriculture	Jamaica		30	56.7		El-Swaify, 1990
Cowpea	Agriculture	Trinidad		22	0.74	24	El-Swaify, 1990
Cowpea no tillage	Agriculture	Trinidad	23x6.5	52	2.62		Gumbs and others, 1985
Cowpea no tillage	Agriculture	Trinidad	23x6.5	22	1.1		Gumbs and others, 1985
Cowpea tillage	Agriculture	Trinidad	23x6.5	11	0.65		Gumbs and others, 1985
Cowpea tillage	Agriculture	Trinidad	23x6.5	22	0.74		Gumbs and others, 1985
Kudzu	Agriculture	Puerto Rico	13.8x51.8	40	0.18	67	Smith and Abruna, 1955
Maize tillage	Agriculture	Trinidad	23x6.5	52	2.7		Gumbs and others, 1985
Maize tillage	Agriculture	Trinidad	23x6.5	22	0.88		Gumbs and others, 1985
Maize tillage	Agriculture	Trinidad	23x6.5	22	1.1		Gumbs and others, 1985
Maize tillage	Agriculture	Trinidad	23x6.5	11	0.60		Gumbs and others, 1985
Mixed Crops	Agriculture	Puerto Rico	13.8x51.8	40	17.7	75	Smith and Abruna, 1955
Peanut	Agriculture	Thailand	13.1x65.6	8-10	10.7	46	Thongmee and Vannapraqsert, 1990
Pineapple	Agriculture	Hawaii			4.6		El-Swaify, 1990

Reproduced with permission of the copyright owner. Further reproduction prohibited without permission.

Table 2.1 Continued.

Land Use Specific	General land use/ land cover	Country	Plot Size (ft x ft)	Slope, in percent	Erosion (lb/Ac/Yr)	Annual rainfall (in)	Reference
Pineapple	Agriculture	Hawaii			3.6		El-Swaify, 1990
Sugar Cane w/ Trash Burned	Agriculture	Puerto Rico	13.8x51.8	40	7.6	78	Smith and Abruna, 1955
Sugar Cane w/ Trash Mulch	Agriculture	Puerto Rico	13.8x51.8	40	0.69	76	Smith and Abruna, 1955
Sugarcane	Agriculture	Hawaii			0.54		El-Swaify, 1990
Sugarcane	Agriculture	Hawaii			1.9		El-Swaify, 1990
Sugarcane	Agriculture	Hawaii			3.2		El-Swaify, 1990
Tea	Agriculture	Sri Lanka			17.9		El-Swaify, 1990
Tea	Agriculture	Sri Lanka			0.13		El-Swaify, 1990
Yams	Agriculture	Jamaica		30	59.4		El-Swaify, 1990
Bare-in forest	Bare Ground	Sierra Leone		5	13.4	130	Millington, 1981
Bare no tillage	Bare Ground	Trinidad	23x6.5	22	15.5		Gumbs and others, 1985
Bare no tillage	Bare Ground	Trinidad	23x6.5	52	30.2		Gumbs and others, 1985
Bare Soil-Control, tilled	Bare Ground	Thailand	13.1x65.6	8-10	33.1	46	Thongmee and Vannapraqsert, 1990
Bare Soil - Fallow	Bare Ground	Java		4	51.3		El-Swaify, 1990
Bare tillage	Bare Ground	Trinidad	23x6.5	22	21.8		Gumbs and others, 1985
Bare tillage	Bare Ground	Trinidad	23x6.5	11	5.8		Gumbs and others, 1985
Fallow, desurfaced	Bare Ground	Puerto Rico	13.8x51.8	46-53	152	75	Smith and Abruna, 1955
Fallow, normal soil	Bare Ground	Puerto Rico	13.8x51.8	40-45	127	75	Smith and Abruna, 1955
Secondary forest	Bare Ground	Ivory coast		20	293	83	Roose, 1986
Secondary forest	Bare Ground	Ivory coast		4.5	26.8	83	Roose, 1986
Secondary forest	Bare Ground	Ivory coast		7	61.6	83	Roose, 1986
Dense bush	Bush	Bouake		4	0.04	47	Roose, 1986
Dense bush	Bush	Bouake		4	14.1	47	Roose, 1986
2ndry 'rain forest	Forest	Ivory coast	49.2x19.7	65	0.45		Leigh, 1982
2ndry 'rain forest	Forest	Ivory coast		7	0.01		Leigh, 1982

Reproduced with permission of the copyright owner. Further reproduction prohibited without permission.

Table 2.1. Continued

Land Use Specific	General land use/ land cover	Country	Plot Size (ft x ft)	Slope, in percent	Erosion (lb/Ac/Yr)	Annual rainfall (in)	Reference
2ndry 'rain forest	Forest	Ivory coast	49.2x19.7	23	0.04		Leigh, 1982
Deciduous forest	Forest	Ivory coast	49.2x19.7	8	0.22		Leigh, 1982
Dry forest	Forest	Thailand	32.8x6.5		2.3		Leigh, 1982
Eucalyptus	Forest	Thailand	13.1x65.6	8-10	0.58	46	Thongmee and Vannapraqsert, 1990
Eucalyptus	Forest	Thailand	13.1x65.6	8-10	0.19	46	Thongmee and Vannapraqsert, 1990
Eucalyptus	Forest	India			0.04		El-Swaify, 1990
Forest	Forest	Java	9.8x3.3	32	0.49		Leigh, 1982
Forest	Forest	Java			0.13		El-Swaify, 1990
Forest	Forest	Thailand	32.8x6.5		2.7		Leigh, 1982
Forest with litter	Forest	Java			19.3	130	El-Swaify, 1990
High forest	Forest	Sierra Leone		29	0.02	130	Millington, 1981
High forest	Forest	India		7.5-24	0.08	82	Sharma and Correira, 1989
Hill rain forest	Forest	Mindanao	26.2x26.2	25	0.02		Leigh, 1982
Leucaena	Forest	Thailand	13.1x65.6	8-10	0.90	46	Thongmee and Vannapraqsert, 1990
Leucaena	Forest	Thailand	13.1x65.6	8-10	1.2	46	Thongmee and Vannapraqsert, 1990
Mahogany Forest	Forest	Java	9.8x3.3	13	0.23		Leigh, 1982
Mixed deciduous	Forest	Thailand			1.3		Leigh, 1982
Montane Forest	Forest	Thailand	13.1x65.6	6-15	0.96		Leigh, 1982
Pomegrante	Forest	India			0.62		El-Swaify, 1990
Rain forest	Forest	Guyana	9.8x4	27	2.2		Leigh, 1982
Rain forest	Forest	Guyana	9.8x4	18	1.8		Leigh, 1982
Rain forest	Forest	Guyana	80x80	2	0.03		Leigh, 1982
Rain forest	Forest	Ivory coast	39.4x19.7	12-15	0.11		Leigh, 1982
Rain forest	Forest	Senegal	131x49.2	2	0.10		Leigh, 1982

Reproduced with permission of the copyright owner. Further reproduction prohibited without permission.

Table 2.1 Continued.

Land Use Specific	General land use/ land cover	Country	Plot Size (ft x ft)	Slope, in percent	Erosion (lb/Ac/Yr)	Annual rainfall (in)	Reference
Secondary forest	Forest	Ivory coast		20	0.02	83	Roose, 1986
Secondary forest	Forest	Ivory coast		7	0.01	83	Roose, 1986
Teak forest	Forest	Thailand			2.9		Leigh, 1982
Teak forest	Forest	Thailand	32.8x6.5		8.6		Leigh, 1982
Teak forest	Forest	Java	9.8x3.3	32	0.44		Leigh, 1982
Teak forest	Forest	Java	9.8x3.3	14	0.30		Leigh, 1982
Teak forest	Forest	Java	9.8x3.3	13	0.30		Leigh, 1982
Teak plantation	Forest	Thailand	32.8x6.5		2.8		Leigh, 1982
Grasses	Grass	Puerto Rico	13.8x51.8	40	1.2	81	Smith and Abruna, 1955
Grass/undergrowth	Grass	Java	9.8x3.3	32	0.40		Leigh, 1982
Euc and Cassava	Mixed Crop/ Forest	Thailand	13.1x65.6	8-10	3.5	46	Thongmee and Vannapraqsert, 1990
Euc and Cassava	Mixed Crop/ Forest	Thailand	13.1x65.6	8-10	6.3	46	Thongmee and Vannapraqsert, 1990
Euc and Euc and Peanut	Mixed Crop/ Forest	Thailand	13.1x65.6	8-10	10.5	46	Thongmee and Vannapraqsert, 1990
Euc and Euc and Peanut	Mixed Crop/ Forest	Thailand	13.1x65.6	8-10	6.1	46	Thongmee and Vannapraqsert, 1990
Leu-Cassaca	Mixed Crop/ Forest	Thailand	13.1x65.6	8-10	7.6	46	Thongmee and Vannapraqsert, 1990
Leu-Cassaca	Mixed Crop/ Forest	Thailand	13.1x65.6	8-10	8.2	46	Thongmee and Vannapraqsert, 1990
Leu-Peanut	Mixed Crop/ Forest	Thailand	13.1x65.6	8-10	13.1	46	Thongmee and Vannapraqsert, 1990
Leu-Peanut	Mixed Crop/ Forest	Thailand	13.1x65.6	8-10	11.1	46	Thongmee and Vannapraqsert, 1990

measured at 0.09 in^3/in/yr (1.52 cm^3/cm/yr) in the semiarid site (Lewis, 1975). This number was similar to rates reported in semi-arid mid-latitude sites (Lewis, 1975).

Soil erosion on Puerto Rico has been studied by Bonnet and Lugo-Lopez (1950), Smith and Abruna (1955), Lugo-Lopez (1969), and Barnett and others (1971, 1972). Ten years of runoff-erosion results using plots on different crop-management activities were presented by Smith and Abruna (1955) (Table 2.2a). Erosion plots were 12 feet wide by 52 feet long (4.2 by 15.8 m) on 40 to 62 percent slopes. Plots were in Mayaguez (fig. 1.1) on Catalina-Cialitos clay and Mucara clay. Measured crop activities included: mixed crops (sweet potatoes, beans, corn, squashes, and pigeon peas), grasses (Guinea grass, Molasses grass, and Bermuda grass), sugarcane, kudzu, mulching, and bare soil (natural and desurfaced). Cultivated crops had 7 to 8 times less erosion than fallow plots. Tropical kudzu showed the lowest soil loss (Table 2.2a).

Table 2.2. A) Results of soil erosion measurements made by A) Smith and Abruna (1955) and B) Barnett and others (1972).

A)

Ground Cover	Slope %	Soil Loss (lb/ac/yr)	Soil Loss (lb/ac/ per inch rain)
Fallow soil, normal	40-45	253,000	3,370
Fallow soil, desurfaced	46-53	303,000	4,040
Mixed Crops	40	35,390	475
Grasses	40	2,360	29
Tropical Kudzu	40	360	5.4
Sugar Cane w/ Trash Burned	40	15,240	196
Sugar Cane w/ Trash Mulch	40	1,370	18
Coffee, w/natural ground cover	62	1,573	20

Reproduced with permission of the copyright owner. Further reproduction prohibited without permission.

Table 2.2 Continued.

B)

Ground Cover	Slope %	Soil Loss	Soil Loss (lb/ac/ per inch
Fallow	35	892	117
Fallow	32	5,443	732
Fallow	26	42,387	5,465
Tobacco conventional tillage	38	11,422	1612
Tobacco conventional tillage	33	1,785	236
Tobacco conventional tillage	28	16,687	2108
Tobacco with mulch	38	1,071	151
Tobacco with mulch	34	1,160	158
Tobacco with mulch	26	535	69
Tobacco grass strips	37	3,569	467
Tobacco grass strips	32	1,695	229
Tobacco grass strips	29	714	94
Pangola Grass	39	625	85
Pangola Grass	46	9,637	1368

Barnett and others (1972) measured runoff and sediment on 5.9 by 35.1 feet (1.8 by 10.7 m) length plots under different management practices. Plots were at 3 locations in Puerto Rico: Corozal (on Humatas clay), Gurabo and Juncos (silty clay), and Yabucoa (Pandura sandy loam). Cropping practices included fallow ground, tobacco, and Pangola Grass. Rainfall simulators were used to generate two storms. One storm for 60 minutes had 2.5 inches (6.35 cm) of rain and the second storm for 120 minutes had 4.3 inches (10.9 cm). Table 2.2b shows results from summing the two rainfall events.

Using the Revised Universal Soil Loss Equation (RUSLE), Mar-Lopez and others (1998)

Reproduced with permission of the copyright owner. Further reproduction prohibited without permission.

determined soil loss on different land uses in the 4.0 mi^2 (10.3 km^2) Guadiana watershed. Soil loss on bare soil was 238 tons/ac/yr (534 metric tons/ha/yr), open canopy forest 12 tons/ac/yr (26 metric tons/ha/yr), agriculture 10 tons/ac/yr (22 metric tons/ha/yr), pasture 8 tons/ac/yr (17 metric tons/ha/yr), and closed canopy forest 3 tons/ac/yr (7 metric tons/ha/yr). If 5% of the basin was reforested, basin wide erosion would decrease by 20%. If the entire basin was reforested, erosion rates would decrease by 37% (Mar-Lopez and others, 1998).

Landsliding

Research into mechanisms of mass wasting have been extensively carried out in the Luquillo Mountains of Eastern Puerto Rico. Simon and others (1990) examined the role of soil properties on landslides of contrasting geology: quartz-diorite and volcaniclastics. Permeability and infiltration rates were highest in the quartz diorite at all levels on the slope. In the intrusive quartz-diorite rock, zones of contrasting density were found at 1.6 feet (0.5 m) and 9.8 to 23 feet (3 to 7 m) that create pathways for water. These pathways lead to excess pore pressures and determine the failure plane of slides. Soil creep influenced slope failure by reducing tensile strength of the soil. Peak excess pore pressure and the possibility of landsliding occur 12-96 hours following a major storm. Based on this study, Simon and others (1990) assert that landsliding is the main geomorphic process responsible for erosion and landform development in the Luquillo Mountains.

Intense rainfall events, especially hurricanes, cause most of the landsliding in the Luquillo Mountains. Based on 41 storms between 1959 and 1991 that produced landslides, Larsen and Simon (1993) produced a threshold equation that determined landsliding:

$$I=91.46D^{-0.82}$$

Reproduced with permission of the copyright owner. Further reproduction prohibited without permission.

where, I is the rainfall intensity in millimeters per hour and D is the duration in hours. Landslides occur at an average rate of 1.2 per year. Hurricane Hugo which struck Puerto Rico on September 18, 1989, had average rainfall intensities of 1.3- 1.5 in/hr (34-39 mm/hr) and triggered more than 400 landslides in the Luquillo Mountains (Larsen and Torres-Sanchez, 1992). Shallow soil slips 1.6-5.0 feet in length (0.5-1.5 m) and debris flows 5.0-6.5 feet in length (1.5-2 m) accounted for 91% of the slope failures. Slope angle is also important in landslide propagation. A 12^0 slope was identified as a threshold slope for landslides in 3 studied basins in Puerto Rico (Larsen and Torres-Sanchez, 1998). Human activities in the Rio Blanca watershed, which the Rio Icacos drains, significantly increased the frequency of landslides (Larsen and Torres-Sanchez, 1998). Roads and structures have 4 times more landslides (1.2/ mi^2, 3.2/km^2) than forested areas (0.3 mi^2, 0.8/km^2). One construction site had 13 times more landslides than forested areas. Agricultural areas had a landslide density of 1.0 mi^2(2.5/km^2). Landslide scars have been observed to be active sources of sediment 17 to 26 years after they formed (Larsen and others, 1999).

Jibson (1989) described landsliding as a result of the tropical storm that hit southern Puerto Rico on October 5-8, 1985. Four-day precipitation totals in southern Puerto Rico were 21.4 in (544 mm) with maximum 24-hour totals of 18.5 in (470 mm) and rainfall intensities that reached 2.76 in/hr (70 mm/hr). Debris flows ranged in volume from a few cubic feet to 3 x 10^5 ft^3 (10,000 m^3) and up to 1,970 feet (600 m) in length with 660 feet (200 m) of vertical relief. The presence of colluvium was a major factor in debris flow generation. Dating of older debris flow deposits indicated recurrence intervals of several decades to several hundred years (Jibson, 1989).

Reproduced with permission of the copyright owner. Further reproduction prohibited without permission.

Cosmogenic radionuclide (^{10}Be, ^{26}Al, ^{14}C) abundances in near-surface (<3.3 feet, <1 m) quartz provide a relation between the rate at which sediment is produced (e.g. from bedrock weathering) and transported within a drainage basin (Brown and others, 1995; Bierman and Steig, 1996; Clapp and others, 1997). In low erosion areas, sediment in the upper 50 cm accumulates a high abundance of cosmogenic radionuclides. Conversely, in high erosion areas, the abundance of radionuclides in sediment is low. Because the abundance of cosmogenic radionuclides is related to erosion rates, sediment can be used as a provenance of erosion within the basin from which it was derived. Denudation rates were examined in the Rio Icacos basin using the cosmogenic isotope ^{10}Be (Brown and others, 1995). ^{10}Be concentrations were related to grain size. Coarser material brought to the surface by deep-seated landslides contained lower concentrations of ^{10}Be (~35,000 ^{10}Be atom g^{-1}) compared to finer grained sands (~220,000 ^{10}Be atom g^{-1}), thought to be derived from stable ridge crests and hillslopes. ^{10}Be in river transported sand has concentrations of 120,000 ^{10}Be atom g^{-1}, indicating that approximately 55% of the transported sand is derived from landslides and the remaining 45% from sheetwash (Brown and others, 1995). Denudation rates reported for the Rio Icacos basin were 43 mm/1000 years (1.69 in/1000 years).

^{10}Be concentrations were measured in the agriculturally-dominated Rio Cayaguas basin, a subbasin of the Lago Loiza basin (Brown and others, 1998). Deforestation for agriculture in the Rio Cayaguas basin peaked in the 1940's. The ratio of ^{10}Be in fine sand relative to coarse sand was used to demonstrate the sources of sediment in river-borne quartz. If landsliding is an active process in the basin, large quantities of coarse material would be brought up from depths containing low ^{10}Be concentrations which would then be supplied to the system and ratios would decrease. Ratios in the Rio Icacos basin were ~5 to 6 (Brown and others, 1998). Ratios for the Cayaguas

Reproduced with permission of the copyright owner. Further reproduction prohibited without permission.

basin were ~2 to 3. The low ratios in the Cayaguas were thought to reflect accelerated soil erosion in the 20th century which removed the normally high-concentration sheetwash-dominated hillslope surface layer. Denudation rates in the Rio Cayaguas calculated using ^{10}Be were ~85mm/1000 years (3.35 in/1000 years). Assuming that denudation rates in the Rio Icacos are analogous to natural background rates, after a century of agriculture the Rio Cayaguas has denudation rates twice as high as Rio Icacos (Brown and others, 1998).

Larsen and Santiago-Roman (2001) mapped landslides, colluvium, and sediment in channel storage in the Rio Cayaguas basin using 1937, 1951, and 1995 aerial photography in conjunction with GIS analysis. Accelerated landsliding may have begun in the late 18th century when forests were cleared for agriculture. A total of 2,321 landslides were mapped at a density of 80 landslides per km^2/100 years. This rate of landsliding is twice the rate of total fluvial sediment discharge (7,140 tons/mi^2/yr; 2,500 Mg/km^2) measured over 8 years (Larsen and Santiago-Roman, 2001). Sediment yields from sheetwash estimates (28 to 246 tons/mi^2/yr; 10 to 86 Mg/km^2) account for a small percentage of the sediment discharge. A major source of fluvial sediment is the colluvial sediment in storage (425,700 tons/mi^2; 149,000 Mg/km^2). If this colluvium were mobilized, it could supply sediment at the present sediment yield rate for up to 129 years. Results from Larsen and Santiago-Roman (2001) illustrate the importance of sediment in storage. Clark and Wilcock (2000) noticed a downstream decrease in channel cross sectional area in three watershed in northeastern Puerto Rico related to an increase in channel storage in a downstream direction. Sediment in storage was from the earlier agricultural period.

A sediment budget for the Rio Icacos basin based on sheetwash erosion and fluvial sediment indicated that sheetwash erosion was 5% of the average annual basin sediment yield

Reproduced with permission of the copyright owner. Further reproduction prohibited without permission.

(2,725 tons/mi^2, 954 metric tons/km^2) (Larsen and others, 1999). Landslides accounted for 73% of basin sediment yield, 2% was attributed to treethrow, 1% to soil creep, and the remaining 19% to unmeasured processes (gullying, channel banks, and channel storage).

Sheetwash

Gellis and others (1999) during 1991 and 1992 measured sheetwash erosion on 12 slopes representing four land uses (cropland, forest, pasture, urban) in the Lago Loiza basin. Each slope had a minimum of 3 sediment traps. Erosion was reported as an average volume-weighted sediment concentration or total sediment divided by total runoff. Values for each land use were: construction sites- 61,400 ppm, cropland - 45,500 ppm, pasture - 3,430 ppm, and forest - 2,050 ppm. Sediment yields on the land uses ranged from: construction sites 0.36 to 4.05 tons/ac/yr (0.81 to 9.08 tons//ha/yr), cropland - 0.14 to 0.32 tons/ac/yr (0.31 to 0.72 tons/ha/yr), pasture - 0.005 to 0.02 tons/ac/yr (0.011 to 0.05 /tons/ha/yr), and forest - 0.01 to 0.04 tons/ac/yr (0.02 to 0.09 tons/ha/yr). Values reported by Gellis and others (1999) were lower than the USLE values calculated by Molinelli (1982) and the values reported by Smith and Abruna (1955).

In a four-year study in the Luquillo Experimental Forest from 1991 through 1995, Larsen and others (1999) studied the relation of rainfall and fine litter transport to sheetwash rates on forested slopes and in fresh landslide scars. Surface runoff in forested areas was almost non-existent and averaged 2 to 3% of rainfall. Low surface runoff was due to a highly porous root and leaf litter (Larsen and others, 1999). Sheetwash erosion averaged 0.20 tons/ac/yr (0.46 tons/ha/yr) in sandy loams underlain by quartz diorite and 0.04 tons/ac/yr (0.09 tons/ha/yr) in clay soils underlain by volcaniclastics. Fresh landslide scars with sheetwash erosion had sediment

Reproduced with permission of the copyright owner. Further reproduction prohibited without permission.

yields that ranged from 0.44 to 1.56 tons/ac/yr (1.0 to 3.48 tons/ha/yr). Erosion rates on the landslide scars decreased significantly over 4 years as vegetation became established. The mass of sediment produced from sheetwash erosion on landslide scars was 7,000 times less than that produced from the initial episode of landsliding (Larsen and others, 1999).

Fluvial sediment

Molinelli (1982) used the Universal Soil Loss Equation (USLE) to predict soil erosion, sediment sources, and sediment loadings to Lago Loiza. Total watershed soil loss was 1,289,400 tons (1,169,500 metric tons) with approximately 450,200 tons (408,300 metric tons) delivered to the reservoir. Average soil loss rates for the 4 types of land use investigated were: cropland - 34.6 tons/ac/yr (77.5 tons/ha/yr), construction Sites - 35.1 tons/ac/yr (78.7 tons/ha/yr), pasture - 11.1 tons/ac/yr (24.9 tons/ha/yr), and forest - 8.7 tons/ac/yr (19.5 tons/ha/yr). Based on his analysis, Molinelli (1982) concluded that sources of sediment to the reservoir were: pasture - 60%, forest - 25%, cropland - 14%, and construction sites - 1%. Pasture and forest together occupied 95% of the basin and contributed 85% of the sediment.

River sediments in Puerto Rico reflect the climatic aspects of their watersheds with respect to clay mineralogy and weathering (Ehlmann, 1968). In more humid portions of Puerto Rico halloysite and kaolinite form in the soil and river sediments in these drainages reflect this. In more arid regions of Puerto Rico, montmorillonite is formed and is found in the sediment of the rivers draining these areas.

Using the bed-material discharge formulas of Yang (1973, 1984) combined with measured suspended-sediment loads, Simon and Guzman-Rios (1990) calculated total sediment discharge

Reproduced with permission of the copyright owner. Further reproduction prohibited without permission.

for rivers draining to Lago Loiza. Bed material discharge, except for one station, ranged from >50% to 92% of the total sediment discharge. They attributed the high proportion of bed material available for transport in the basin to the delivery of coarse-grained saprolitic material to the streams by mass-wasting processes. Gellis and others (1999) measured bed load rates in the Rio Gurabo by surveying a dredged site over time. Calculated bed load rates were 12% of the total sediment discharge, considerably less than the 72% reported by Simon and Guzman-Rios (1990).

Average annual sediment yields, measured between 1990 and 1993, in 12 subbasins of the Lago Loiza basin ranged from 400 to 2,680 tons/mi^2/yr (140 to 940 metric tons/km^2/yr) (Gellis and others, 1999). Independent variables compiled to describe sediment yield and sediment concentration included land use (cropland, disturbed ground, pasture, urban, and forest), basin slope, and soil texture (percent sand, silt, and clay). Using best-subset regression for sediment yield against the independent variables indicated disturbed ground, cropland, and pasture as the three most significant variables. Average annual sediment concentration as a dependent variable indicated urban and disturbed ground as the most significant variables. Land use in the Lago Loiza basin has been changing since completion of the reservoir in 1953 (Gellis and others, 1999). A problem using land use as an independent variable is that it is not constant over time. Best subset-regression using 'changing land use' from 1977 through 1987, indicated that pasture best explains sediment yield and average annual sediment concentration. Pasture is the land use undergoing the most change, decreasing up to 20% of its area in some subbasins (Gellis and others, 1999).

High suspended-sediment concentrations and high sediment yields were reported by Gellis (1991) for the Rio Piedras basin, a suburban area near San Juan. The basin was undergoing

Reproduced with permission of the copyright owner. Further reproduction prohibited without permission.

urbanization in the 1980s with many construction projects exposing bare soil. Population in the suburban area increased 44% between 1970 and 1980. Suspended-sediment concentrations measured in the Rio Piedras basin were as high as 80,000 mg/L (Gellis, 1991). Sediment yields were 21,600 to 33,200 tons/mi^2/yr (7,560 to 11,600 metric tons/km^2/yr), which were 3 to 5 times higher than the largely rural Rio Cayaguas basin (Gellis, 1991).

Although hurricanes are known to produce large amounts of runoff and transport large quantities of sediment, Gellis (1993) showed that runoff during Hurricane Hugo transported less than half the suspended-sediment load that might have been expected. At the Rio Grande de Loiza near Caguas station, Hurricane Hugo had the second lowest storm-average suspended-sediment concentrations from a data set of 12 storms. Hurricane Hugo was a class IV hurricane with maximum sustained winds of 77 mi/hr (124 km/hr) and gusts up to 92 mi/hr (148 km/hr) (Gellis, 1993). Hurricane-force winds, which uprooted vegetation and led to debris dams in streams, lowered stream velocities, caused sedimentation, and may have reduced suspended-sediment concentrations (Gellis, 1993).

Reservoir sedimentation in Puerto Rico

More than thirty reservoirs have been built in Puerto Rico during this century. Reservoir sedimentation is a problem that was identified as early as the 1940's (Nevares and Dunlop, 1948). It was determined that the sedimentation rates from the three reservoirs studied in Puerto Rico, Comerio, Coamo, and Guayabal, exceeded the sedimentation rates calculated for two-thirds of the 65 reservoirs examined in the United States. High erosion rates in all three reservoir basins

Reproduced with permission of the copyright owner. Further reproduction prohibited without permission.

were attributed to geologic conditions, deforestation, and intensive cultivation of steep slopes (Nevares and Dunlop, 1948).

Most reservoirs impounded by dams are designed for a life of 50 to 100 years when they are terminated by sedimentation (Hotchkiss, 1995). Around the world there is evidence of declining trends in reservoir storage from siltation (Nordin, 1991; Palmeiri and others, 1998; Nagle and others, 1999); in Africa (Ward, 1980; Jordan, 1989; Shahin, 1993), Asia (Ongkosongo and others, 1992), Australia (Chanson, 1998), and the United Kingdom (Butcher and others, 1992). Mahmood (1987) estimated worldwide reservoir sedimentation at 1% a year. The rate of reservoir sedimentation can be accelerated by modifications to the watershed, imposed by either natural or human factors which increases the sediment load to the reservoir (Ongkosongo and others, 1992; Renwick, 1996). If management strategies to reduce sedimentation rates are to be effective, distinguishing between background erosion rates in undisturbed settings and human-accelerated erosion in disturbed setting is important (Ongkosongo and others, 1992; Palmeiri and others, 1998; Nagle and others, 1999).

The USGS has published bathymetric surveys for many of Puerto Rico's reservoirs. Annual reservoir sediment rates were compiled from these reports and are shown in Table 2.3. Reservoir sedimentation rates quantified in the earlier part of the 20th century by Navares and Dunlop (1948) do not show higher sediment yields compared to more recent rates (Table 2.3). The lowest sediment yield based on reservoir surveys is for the Lago Loiza basin which also has the largest drainage area of any surveyed reservoir (Table 2.3). Comparisons of Puerto Rico reservoir sedimentation rates to world sedimentation rates are shown in Figure 2.6.

Reproduced with permission of the copyright owner. Further reproduction prohibited without permission.

Reproduced with permission of the copyright owner. Further reproduction prohibited without permission.

Table 2.3. Compilation of reservoir sedimentation surveys for Puerto Rico.

Reservoir	Drainage Area (mi^2)	Major River Drainage	Dates between surveys	Original capacity (million ft^3)	Accumulated sediment (million ft^3)	Storage loss (%)	Average annual sedimentation rate (ft^3/yr)	Average annual sediment yield (tons/mi^2)*	Reference
Coamo	58	Coamo River	1914-1948	123	80	65	2.34E+06	1,680	Nevares and Dunlop, 1948
Comerio	135	Rio De La Plata	1914-1935	214	147	69	7.00E+06	2,160	Nevares and Dunlop, 1948
Guayabal Lago	43.4	Jacagues River	1914-1939	417	169	40	6.77E+06	6,490	Nevares and Dunlop, 1948
Caonillas	85.5	Rio Caonillas	1948-1995	1965	242	12	5.16E+06	2,500	Webb and Soler-Lopez, 1996
Lago Dos Bocas	170	Rio Grande de Arecibo	1942-1997	1324	610	46	11087340	2710	Soler-Lopez and Webb, 1998
Lago Garzas	5.87	Rio Vacas	1943-1996	205	1871	12	4.60E+05	2,440	Soler-Lopez and others, 1999a
Lago Loiza	208	Rio Grande de Loiza	1953-1994	946	445	47	1.07E+07	1,600	Webb and Soler-Lopez, 1997
Lago Patillas	25.2	Rio Grande De Patillas	1961-1997	623	134	22	3.73E+06	6,150	Soler-Lopez and others, 1999b
Lago Prieto	9.58	Rio Prieto	1955-1997	27.0	19.2	71	4.55E+05	1,980	Soler-Lopez and Webb, 1999
Lago Toa Vaca	21.9	Rio Toa Vaca	1972-1985	2204	414	16	3.18E+07	60,400	Figueroa-Alamo, 1990
Lago Yahuecas	17.4	Rio Blanco	1956-1997	62.1	50.5	81	1.23E+06	2,210	Soler-Lopez and others, 1998

* *Assuming a trap efficiency of 75% and a sediment density of 62.4 Ib/ft3*

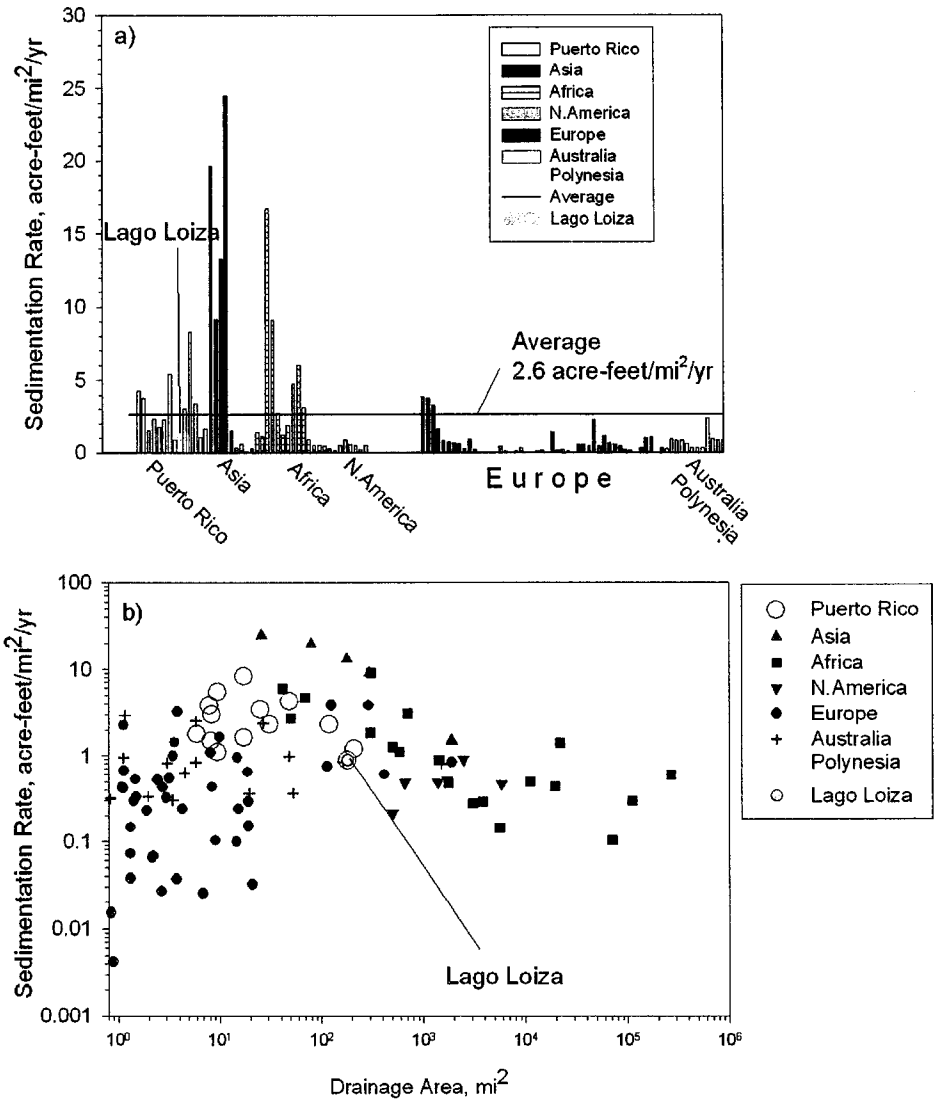

Figure 2.6. a) Puerto Rico reservoir sedimentation rates (from Soler-Lopez, 1998) compared to world sedimentation rates (from Chanson, 1998). b) Drainage area versus sedimentation rates for Puerto Rico and world reservoirs (from Chanson, 1998; from Soler-Lopez and others, 1998a,b, 1999a,b; Soler-Lopez and Webb, 1999).

Lago Loiza (also referred to as Lago Carraizo), impounded in 1953, provides San Juan with over one-half of its water supply. A bathymetric survey in 1988 by Quinones and others (1989) indicated that 58% of the capacity of the reservoir had been reduced by sedimentation.

Reproduced with permission of the copyright owner. Further reproduction prohibited without permission.

Lago Loiza (also referred to as Lago Carraizo), impounded in 1953, provides San Juan with over one-half of its water supply. A bathymetric survey in 1988 by Quinones and others (1989) indicated that 58% of the capacity of the reservoir had been reduced by sedimentation. The results of Quinones and others (1989) led to concerns in Puerto Rico about the sustainability of their water supply (Medina, 1989; De La Torre, 1990). Analysis of the Quinones and others (1989) data by Collar and Guzman-Rios (1991) indicated that there was an exponential increase in the sedimentation rate over time and that the reservoir might be rendered useless by the year 1998. In 1994, a drought occurred in northeastern Puerto Rico, including the San Juan metropolitan area (Ross, 1994; Beard, 1994). Lago Loiza water level reached a record low at that time and water rationing was started. The loss of storage capacity, resulting from sedimentation over the years, has impaired the reservoir's ability to provide water for public supply during a drought (Garcia, 1994).

Gellis and others (1999) investigated sedimentation rates of Lago Loiza over time and concluded that low resolution in data acquisition in the 1985 survey, in both the horizontal and vertical dimensions, resulted in an underestimate of the 1985 volume (12.46 Mm^3) and the interpretation by Quinones and others (1989) that 58% of the reservoir had been reduced by sedimentation may be in error. The 1994 bathymetric survey of Lago Loiza by Webb and Soler-Lopez (1997) indicated the reservoir's capacity was 11,500 acre-feet (14.2 x 10^6 m^3) and the reservoir lost 47% of its original storage capacity of 21,720 acre-feet (26.8 x 10^6 m^3). Brune-curve analysis of sedimentation in Lago Loiza projected that the reservoir will be 90% silted by the year 2044 (Gellis and others, 1999).

The review of literature on tropical geomorphology (in general) and specifically for Puerto Rico, creates an impression that the humid tropics has erosion rates and sediment yields different from other

Reproduced with permission of the copyright owner. Further reproduction prohibited without permission.

climates. Although the objective of the PhD is not to determine if climatic-geomorphic theories hold for Puerto Rico, the erosion rates and sediment yields presented in this research will be contrasted to rates from other climates to determine if differences exist.

Suspended Sediment Characteristics

This PhD research focuses on the suspended-sediment characteristics of Puerto Rican streams and a review of important properties of suspended sediment follows. Sediment transported through the fluvial system ranges in size from clay to boulders and can be separated into suspended-sediment load and bed load. Bedload is typically sand-sized and larger particles that move by sliding, rolling, and saltating. Suspended sediment is that sediment entrained by a fluid that remains in suspension for an appreciable length of time (Bhowmik, 1988). Sediment particles settle because of their weight but fluid turbulence counteracts this downward motion. Suspended sediment is typically sand sized and smaller. Wash load is the term for clay and silt-sized suspended sediment (<0.0625 mm) that is derived from non-channel sources (Knighton, 1996). There is an exchange between bedload and suspended load in the sand size fraction. Suspended sediment typically contributes over 90% of the total load of most rivers (Meade and others, 1990).

Bedload transport is governed by hydraulic factors of flow, slope, viscosity, and turbulence. Suspended-sediment transport is a function of energy conditions (flow, hydraulic conditions, sediment characteristics - size and density of material) and sediment supply (Sidle and Campbell, 1985). Because these two functions for suspended-sediment transport differ markedly, study of suspended sediment transport has taken two paths, that of (1) understanding fluid dynamics and its relation to the initiation of

Reproduced with permission of the copyright owner. Further reproduction prohibited without permission.

sediment (cohesionless and cohesive) transport and (2) a sediment supply, geomorphic-watershed approach. The fluid-dynamics approach to suspended sediment can be based on turbulent flow structures (Clifford and others, 1993), density stratification (McLean, 1992), or applied shear stress (Rooseboom and Mulke, 1982). The watershed approach seeks to understand suspended-sediment transport by examining sources of sediment and causes for variability (Walling and Webb, 1982; VanSickle and Beschta, 1983; Beschta, 1987). This study will focus on the geomorphic-watershed approach to understanding variability in suspended-sediment concentrations.

Many suspended-sediment transport approaches are based on the empirical relationships between suspended-sediment concentration and discharge, expressed as:

$$C = aQ^b$$

where C is suspended-sediment concentration, Q is stream discharge, and a and b are determined from linear regression between Log Q and Log C. The scatter of suspended-sediment concentrations at a single discharge can be over several orders of magnitude. Attempts to understand this scatter have employed multivariate statistical approaches (Guy, 1964; Walling, 1974) and transport curves (Walling and Webb, 1982) .

Walling (1974) analyzed sediment-transport curves in a 0.10 mi^2 (0.26 km^2) watershed in Devon, England. In a first approximation of the suspended-sediment discharge rating curve, scatter was obvious, and discharge only accounted for 33% of the total variance in sediment concentrations. Scatter in the sediment transport curve was due to hysteresis, decrease of sediment availability in multi-peaked events, and seasons. Walling (1974) found that using four variables to describe suspended-sediment concentration, 1) discharge minus base flow, 2) time relation of sample to major peak, 3) base flow at start of storm, and

Reproduced with permission of the copyright owner. Further reproduction prohibited without permission.

4) index of flood intensity, explained 70% of the variation; an improvement over the 33%. Flood intensity was defined as:

$$\textit{Flood intensity} = \frac{\textit{Major Peak - Base flow at start of storm } (ft^3/s)}{\textit{Time of Rise to Major Peak} \text{ (hours)}}$$

Analysis of 102 storm events with 13 independent variables reflecting rainfall and discharge parameters showed that the most significant independent variables are peak discharge, total rainfall, rainfall energy, and time of year (Walling, 1974). In general, higher loads are associated with heavy rainfall in the winter under higher soil moisture conditions that lead to increased storm runoff.

Guy (1964) analyzed the factors effecting storm-period sediment transport for seven streams in the Atlantic coast area of the United States. The mean concentration of sediment for a storm event was regarded as a better dependent variable than sediment discharge, which was a result of the intercorrelation of water discharge and sediment discharge. Water discharge proved to be the most important variable in describing sediment concentration variation. Rainfall quantity was not important in describing sediment concentration variation. Sediment in streams increases with storm intensity, measured as the peak flow divided by total runoff. Sediment concentration showed an increase with mean air temperature and a decrease with increasing base flow. These relations are both related to seasonality. Mean air temperature is highest in the summer when convective storms are common and cause large runoff events. Base flow is highest in the winter when intense rainfall events are scarce.

The scatter in the relationship of discharge to suspended-sediment concentration is thought to be due to the exhaustion of sediment during a single storm or season (VanSickle and Beschta, 1983; Sidle and Campbell, 1985; Kattan and others, 1987; Goodwin and Denton, 1991; Wang and others, 1998; Picouet

Reproduced with permission of the copyright owner. Further reproduction prohibited without permission.

and others, 2001). When plotted over a single event or a season, the resulting decrease in sediment can be shown as a clockwise pattern or hysteresis loop. Rieger and Olive (1986) described seven types of hysteresis loops for storm events developed from small forested watersheds in New South Wales, Australia (fig. 2.7a). Wood (1977) developed six hysteresis loops based on length of time between events, exhaustion of sediment, and whether the event was single or multipeaked (fig. 2.7b). VanSickle and Beschta (1983) described hysteresis patterns related to seasonality and tributary input (fig. 2.7c). Causes for the observed peak in suspended concentration before discharge have varied but have been explained

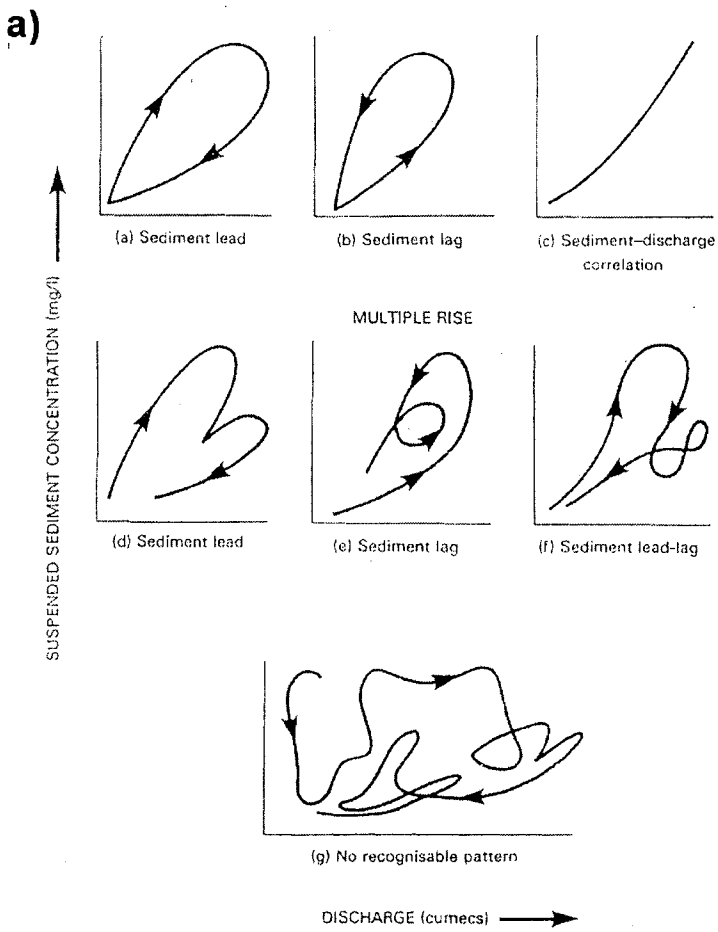

Figure 2.7. Illustration of various proposed hysteresis loops. a) Pattern related to timing of sediment concentration relative to discharge (Rieger and Olive, 1986).

Reproduced with permission of the copyright owner. Further reproduction prohibited without permission.

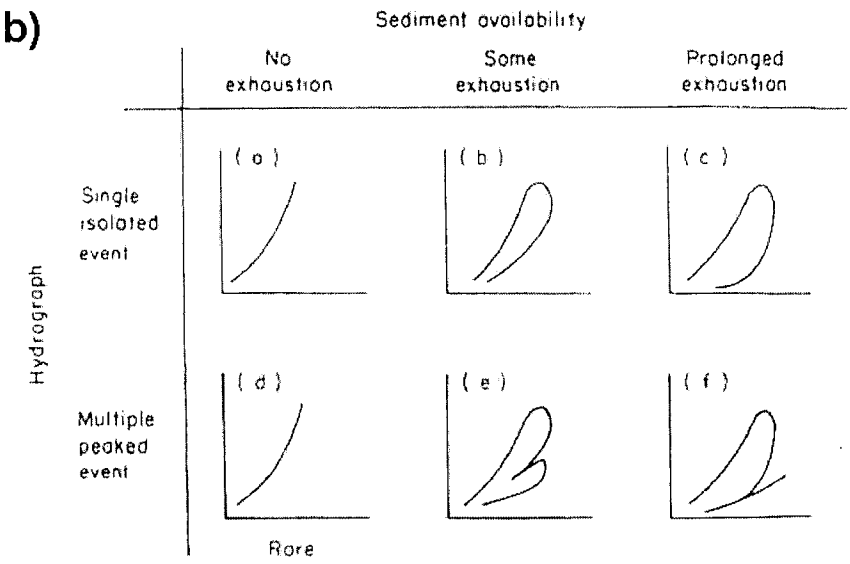

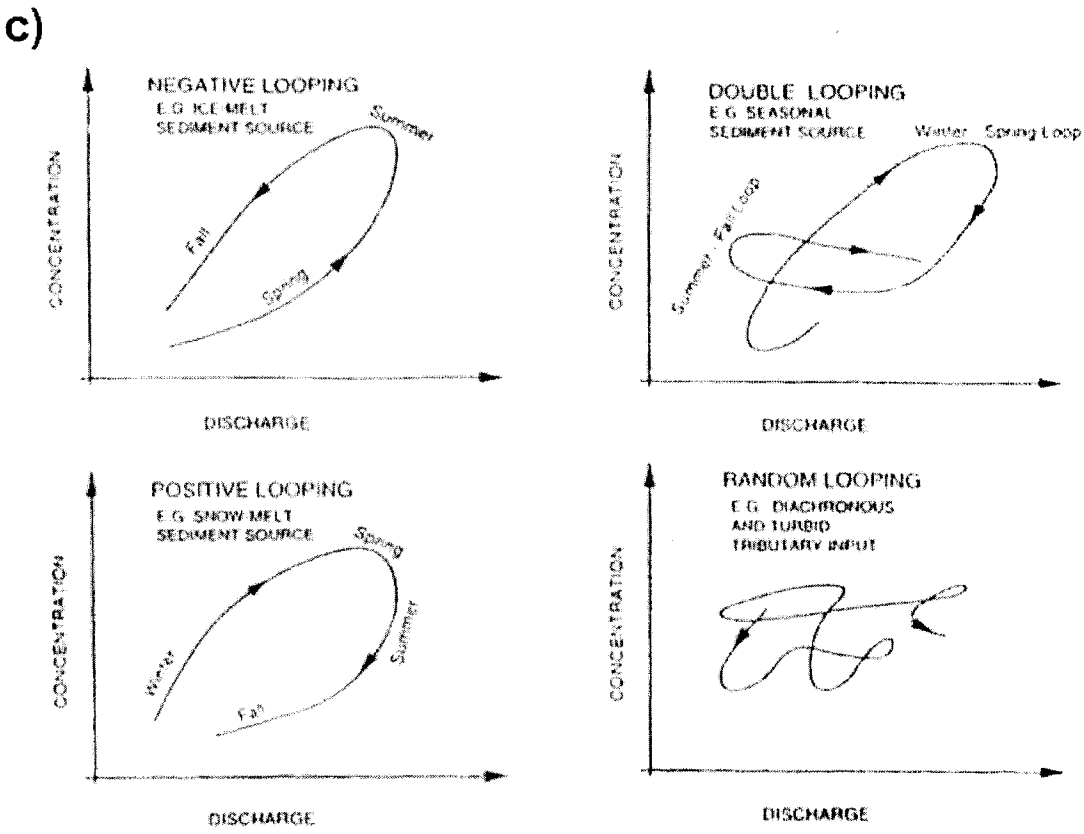

Figure 2.7. Continued. b) Pattern related to exhaustion of sediment (Wood, 1977). c) Hysteresis pattern related to seasonality and tributary input (VanSickle and Beschta, 1983).

Reproduced with permission of the copyright owner. Further reproduction prohibited without permission.

primarily by a first flush mechanism (Table 2.4). Sediment that is readily available on the bed of the channel is immediately mobilized and an immediate spike in sediment concentration is observed. Kurashige (1994) proposed that depth and hydraulic gradient increase before peak discharge and since sediment flux is

Table 2.4. Summary of hysteresis types in the literature and their causes.

Hysteresis type	Cause of hysteresis shape	Reference
Type 1 (clockwise)	Depletion of sediment source	Walling, 1974; Wood, 1977; Costa, 1977; Bull and others, 1995
	Formation of armored layer before peak discharge	Williams, 1989
	Maximum shear stress on the bed appears before the peak	Kurashige, 1994
	Water depth and water slope increases before peak discharge	Kurashige, 1994
	Increased base flow after peak discharge leading to dilution of sediment concentration	Walling, 1974; Costa, 1977
	Seasonality, higher concentration early in the year followed by flushing and depletion of sediment	Sidle and Campbell, 1985; Kattan and others, 1987; Wang and others, 1998; Asselman, 1999; Picouet and others, 2001
Type 2 (clockwise then counterclockwise)	Ice breakup	
Type 3 (counterclockwise)	Floodwave traveling faster than mean flow velocity	Marcus, 1989;Williams, 1989; Brasington and Richards, 2000
	High soil erodibility	Williams, 1989
	Distant sediment source	Williams, 1989
	Upstream tributaries	Asselman, 1999
	Seasonality, lower concentrations early in the year followed by increasing sediment concentrations	Sidle and Campbell, 1985; Wang and others, 1998
	Thin, exposed soil surfaces	Kurashige, 1994
Type 5 (stationary)	Uninterrupted supply of sediment ranging from ample to inhibited	Wood, 1977; Williams, 1989

Reproduced with permission of the copyright owner. Further reproduction prohibited without permission.

proportional to hydraulic gradient, maximum sediment concentration occurs before peak discharge. VanSickle and Beschta (1983), Asselman (1999), Picouet and others (2001) simulated exhaustion of sediment over time by adding a storage term, S(t) to equation (2) to represent sediment supply and its depletion over time.

Seasonal effects can cause both a clockwise or counterclockwise hysteresis (Wang and others, 1998). In some rivers spring snowmelt brings higher sediment concentrations which are then reduced over time. In British Columbia a delayed response of sediment sources from glacial ice melt caused higher sediment concentration later in the year (Wang and others, 1998). Counterclockwise hysteresis loops are uncommon but have been explained by a delayed source from tributaries or bank collapse on the falling limb. Heidel (1956) and Marcus (1989) explained counterclockwise hysteresis as a hydraulic phenomenon occurring in big rivers when the floodwave travels faster than the sediment wave. The sediment wave is thought to travel with mean flow velocity which lags behind the floodwave. Bull and others (1995) examined downstream changes in sediment in the River Severn, UK and found both increases and decreases in sediment concentration in a downstream direction. The velocity wave traveled at different rates depending on the type of storm.

Literature on sediment hysteresis seems to suggest that the source(s) of suspended sediment, whether channel or hillslope, may determine the type of hysteresis, clockwise or counterclockwise. To determine sediment sources during individual storm events two approaches, a provenance or 'fingerprinting' approach (Peart and Walling, 1986; Walling and Woodward, 1992) and a hydrologic approach (Kattan and others, 1987; Okunishi and others, 2000) have been used. Recent advances using multiple anthropogenic and natural radionuclides, and stable isotopes have been used to "fingerprint" sediment

Reproduced with permission of the copyright owner. Further reproduction prohibited without permission.

sources (Walling and Woodward, 1992;1995; Collins and others, 1998; Walling and others, 1999). This approach necessitates the identification and establishment of a specific physical and/or chemical property of sediment that is specific to the stream corridor (bed and banks), land use, and geology of the watershed. Fallout radionuclides, in particular radionuclides, ^{137}Cs and ^{210}Pb, appear to be valuable tracers, as they are continuously delivered to the surface as wet and dry fallout and are rapidly adsorbed on sediments. Consequently, they are expected to label surface sediments versus channel corridor derived sediment consistently over large areas within a drainage basin and independently of lithology or soil (Walling and Woodward, 1992). Using this fingerprint approach, Peart and Walling (1986) stated that in the Jackmoor River basin 70% of the suspended sediment load is derived from surface wash on cropland and 6% is contributed by channel banks and pasture.

Hydrologic approaches utilize information on discharge and rainfall to determine relative sources of suspended sediment and hence provide reasons for correlation or non-correlations to discharge. For example, in many studies it is assumed that suspended-sediment concentration is correlated to discharge. But sources of suspended sediment may be hillslopes and channel banks where the delivery of sediment to the channel does not coincide with the hydrograph. Channel sources versus upland sources have been estimated by separating out components of the hydrograph into base flow and stormflow and determining suspended-sediment relationships for both (Kattan and others, 1987; Okunishi and others, 2000). Brasington and Richards (2000) used rainfall and turbidity data to show that sediment in Nepalese rivers was derived predominately from sheetwash on hillslopes. They based this interpretation on the relation of turbidity peaks which showed a lagged dependence on rainfall intensity and not changes in flow.

Reproduced with permission of the copyright owner. Further reproduction prohibited without permission.

CHAPTER III

SETTING

This chapter describes geology, climate, and land use for Puerto Rico and the basins being investigated: Rio Icacos, Quebrada Blanca, Rio Caguitas, and Rio Piedras.

Geology and Soils of Puerto Rico and Study Basins

Puerto Rico measures 110 miles (180 km) by 40 miles (65 km) and is the smallest island in the greater Antilles (fig. 3.1). It is on the Caribbean Plate in an oceanic island arc setting that was created in the early Cretaceous (120Ma) and active through the Eocene (40 Ma), as the Caribbean Plate was being subducted below Puerto Rico in the Muertos Trough (Donnelly, 1989; Lewis and Draper, 1990) (fig. 3.2a). Puerto Rico is volcanic in origin with two main morphotectonic settings: the Central Igneous Zone composed of volcaniclastic rocks ranging from Late Jurassic to late Eocene and intruded by Upper Cretaceous and lower Tertiary granitoid rocks; and the Northern and Southern Carbonate Zones comprising middle Oligocene through middle Miocene limestones (fig. 3.2b)(Monroe, 1980a). Miocene to Holocene surficial deposits cover 15% of the Island. Two major fault zones that cross the Island are the Great North Puerto Rico Fault Zone (NFZ) and the Great South Puerto Rico Fault Zone (SFZ) (fig. 3.2b) (Lewis and Draper, 1990). Present motion of the Caribbean Plate relative to North America is strike-slip

Reproduced with permission of the copyright owner. Further reproduction prohibited without permission.

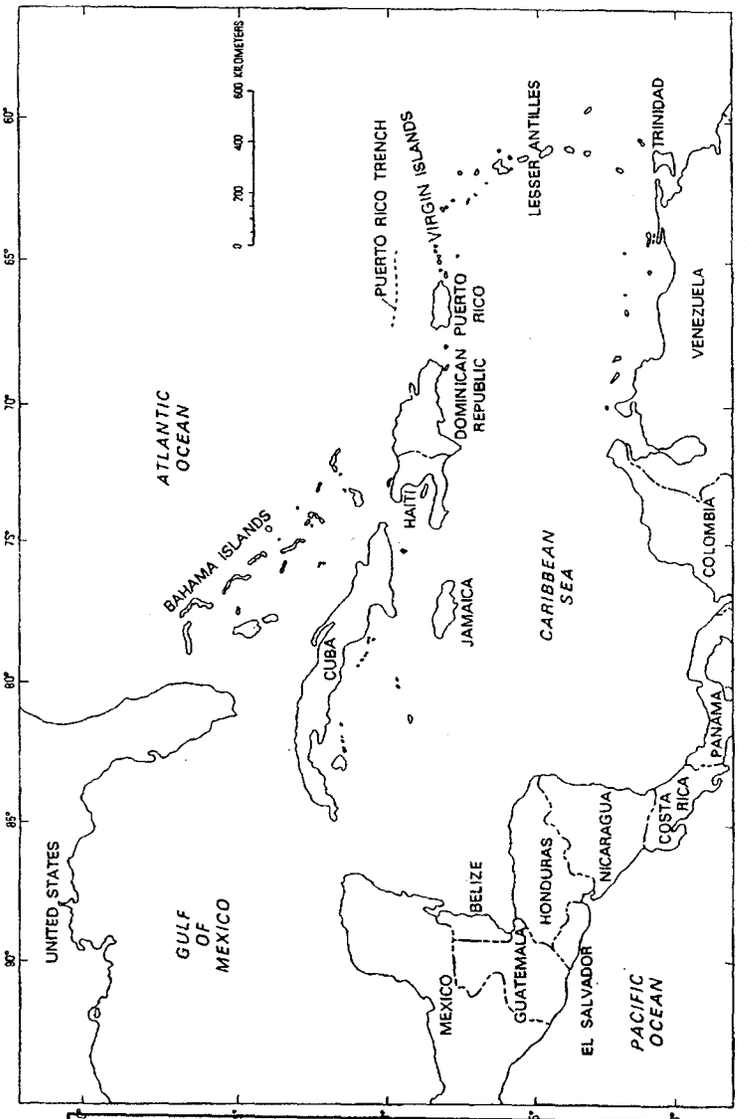

Figure 3.1. Map showing location of Puerto Rico in the Caribbean region.

Reproduced with permission of the copyright owner. Further reproduction prohibited without permission.

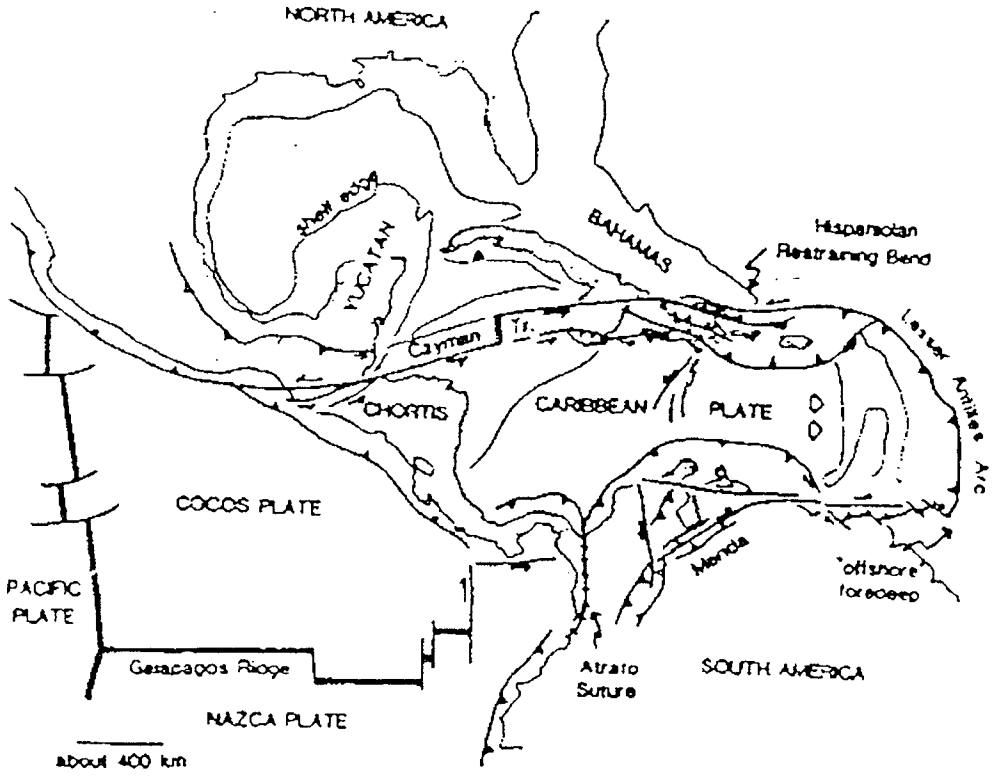

Figure 3.2a. Tectonic setting of Puerto Rico (Lewis and Draper, 1990).

along the Puerto Rico Trench (Masson and Scanlon, 1991). Along the Southern tectonic boundary, underthrusting is occurring in the western portion of the block and extension is occurring to the east (Masson and Scanlon, 1991). Rates of tectonic uplift during the Late Pleistocene along the western portion of Puerto Rico, determined from dating of marine terraces, were 0.03 to 0.05 mm/year (Taggart and Joyce, 1991). Geology of the four study basins is shown in figure 3.3.

Reproduced with permission of the copyright owner. Further reproduction prohibited without permission.

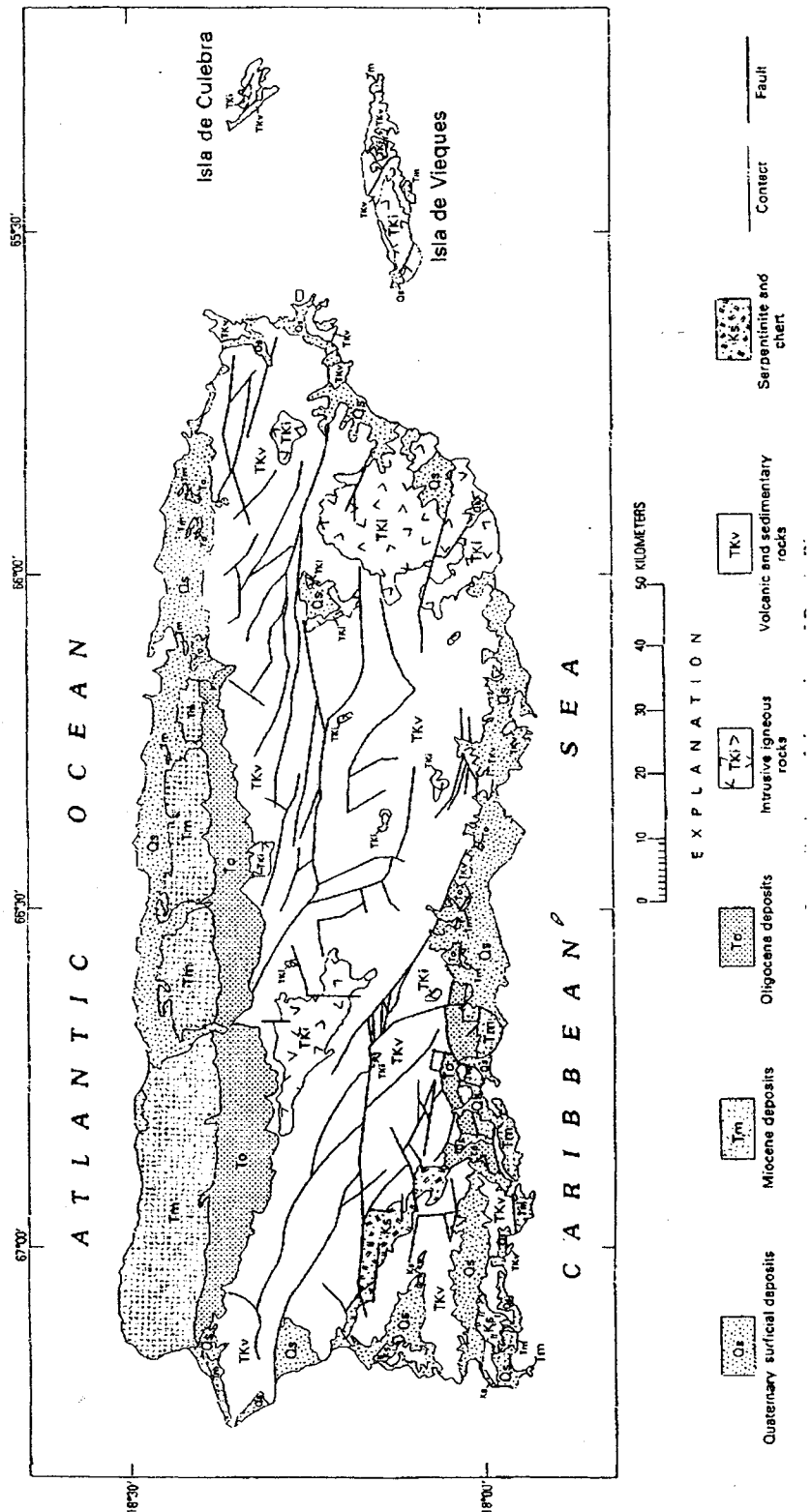

Figure 3.2b. Generalized map of the geology of Puerto Rico (Monroe, 1980b).

Reproduced with permission of the copyright owner. Further reproduction prohibited without permission.

Reproduced with permission of the copyright owner. Further reproduction prohibited without permission.

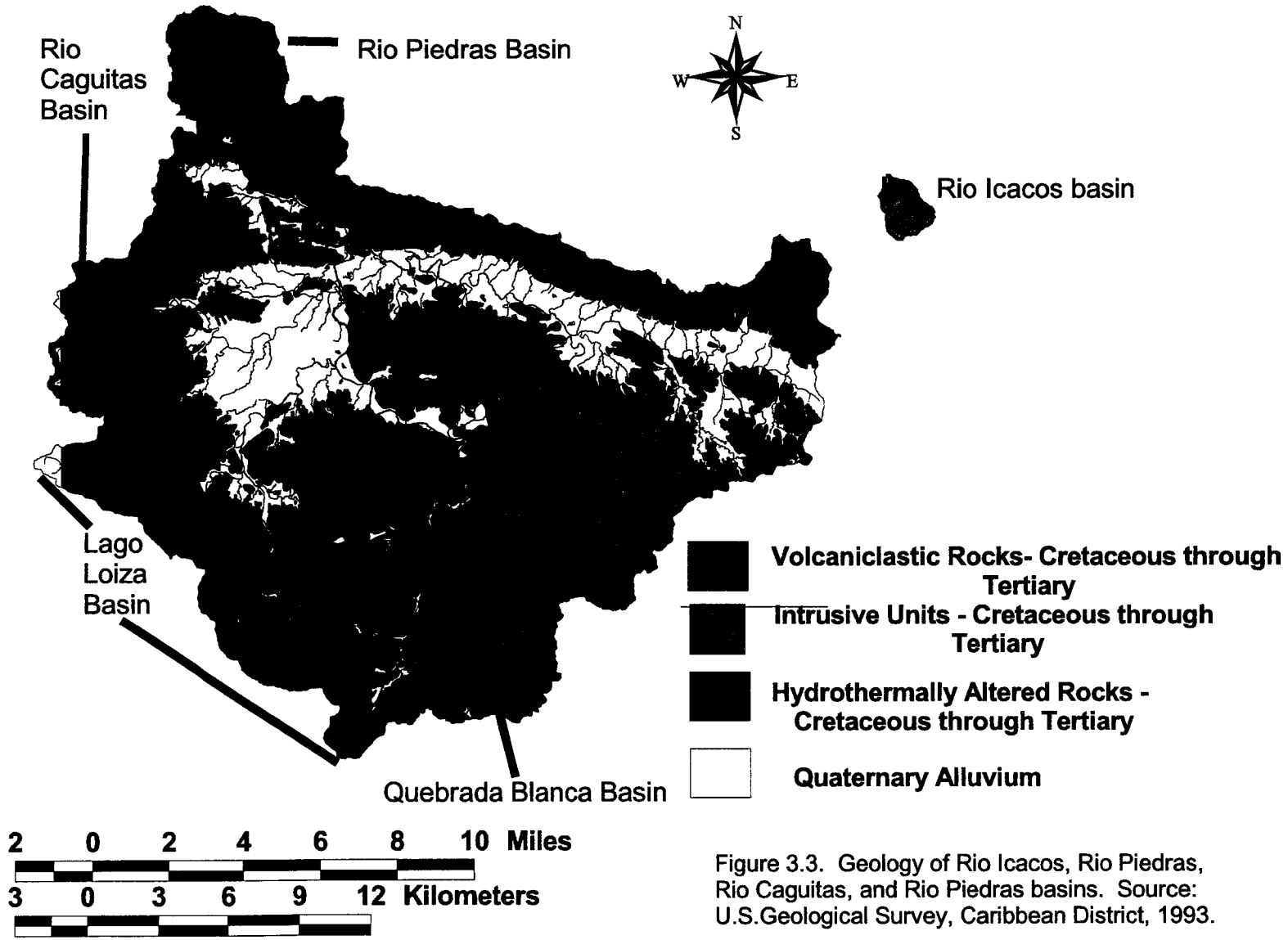

Figure 3.3. Geology of Rio Icacos, Rio Piedras, Rio Caguitas, and Rio Piedras basins. Source: U.S.Geological Survey, Caribbean District, 1993.

Monroe (1980b) describes a complex history of stream capture in the Rio Grande de Loiza basin that occurred during the Cenozoic. The river has lost several headwater tributaries on the southeastern and eastern portions of the basin. Quaternary terrace deposits in these valleys mark the site of capture. Extensive Quaternary deposits and alluvium cover more than 38 mi^2 (100 km^2) of the basin. The Quaternary terraces may be a result of either climatic, sea level, or tectonic influences. Little work has been performed on the Quaternary geology of Puerto Rico.

Puerto Rico has considerable pedologic diversity; 9 of the 10 orders of soil are represented (Barnett and others, 1972). Only Aridisols are missing. Inceptisols, soils in the early stages of development, which reflect active geomorphic surface processes that prohibit development of more mature soils are the most prevalent. The texture of soils in the Quebrada Blanca, Rio Piedras, Rio Icacos, and Rio Caguitas basins are strongly related to the underlying geology (fig. 3.4). The granodiorite and quartz diorite weather to sandy loams and loams such as Pandura sandy loams (Boccheciamp, 1978). The volcaniclastic rocks weather to clays and silty clay loams such as Mucara clay, Naranjito silty clay loam, and Caguabo clay loam. The alluvium weathers to clay such as Mabi clay and Rio Arriba clays. Characteristics of the major soils in the Quebrada Blanca, Rio Piedras, Rio Icacos, and Rio Caguitas basins are shown in Table 3.1. Variations in soil properties can be observed in the different soils. Pandura soils in the granodiorite have higher permeability but thinner soil profiles than the soils in the volcaniclastic rocks (Table 3.1).

Reproduced with permission of the copyright owner. Further reproduction prohibited without permission.

Reproduced with permission of the copyright owner. Further reproduction prohibited without permission.

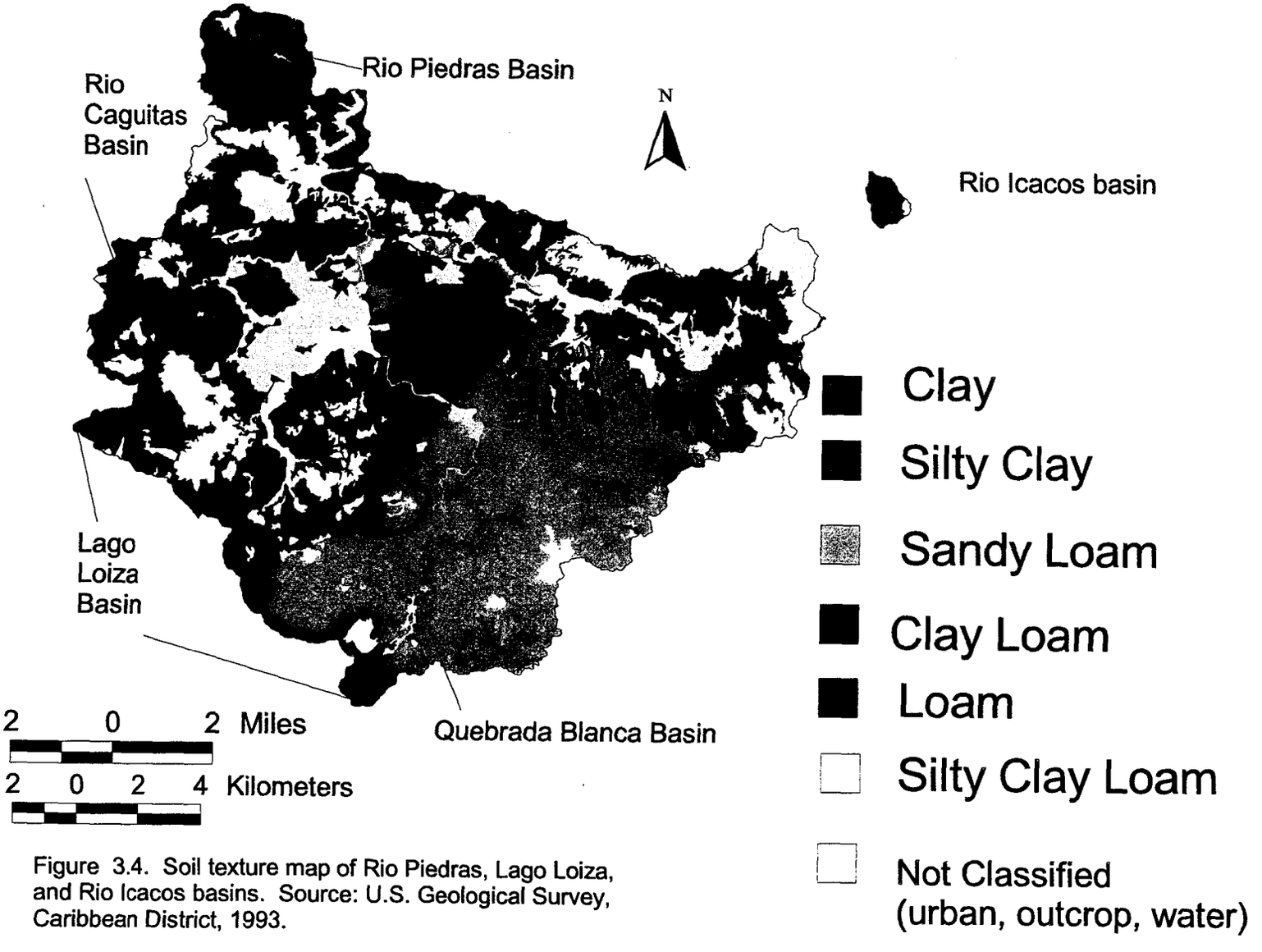

Figure 3.4. Soil texture map of Rio Piedras, Lago Loiza, and Rio Icacos basins. Source: U.S. Geological Survey, Caribbean District, 1993.

Table 3.1. Major soils in Quebrada Blanca basin (QB), Rio Icacos basin (I), Rio Caguitas basin (RC), and Rio Piedras basin (RP) (Boccheciamp, 1977, 1978).

Soil	Soil order	Typical setting	Soil textures	Dominant slopes %	Permeability (top 22-35 inches), inches per hour	Depth to bedrock, in	Water-shed where mapped
Mucara	Inceptisols	Steep volcanic uplands	Clay loam, clay	40-60	0.6 to 2.0	20-36	QB, RC, RP
Humatas	Ultisols	Steep volcanic uplands	Silty clay loam, clay	40-60	0.6 to 2.0	>60	RC, RP
Pandura	Inceptisols	Plutonic rocks	sandy loam	40-60	2.0 to 6.0	12-19	QB, I

Rio Icacos Basin

Two plutons, Upper Cretaceous granodiorite and Tertiary age quartz diorite, outcrop in the Rio Icacos basin and underly approximately 99 percent of the basin (fig. 3.3) (Briggs and Akers, 1965). Rio Icacos drains the Sierra de Luquillo mountains with elevations reaching 3,500 ft (1,074m) above mean sea level. The Luquillo mountains are asymmetrical, fault-block mountains and have been tectonically stable since the Tertiary (Scatena, 1995). Soils in the Rio Icacos basin are Pandura Sandy loams.

The 1.26 mi^2 (3.26 km^2) portion of the Rio Icacos basin being investigated (fig. 1.1) drains the eastern slope of the Sierra de Luquillo mountains and is in the Luquillo Experimental Forest (LEF), a 27,900 acre (11,300 ha) forested preserve (Waide and Lugo, 1992). Research in the LEF includes studies on mass wasting (Simon and others, 1990; Larsen and Simon, 1990; Larsen and Torres-Sanchez, 1990, 1992; Larsen and Simon, 1993), hydrology (Larsen and others, 1999), and ecology. Elevations vary from 2,021 to 2,467 feet (616 to 752 m). Mean slope of

Reproduced with permission of the copyright owner. Further reproduction prohibited without permission.

the watershed is 35.5%, while mean channel slope of the Rio Icacos is 15.1% (Larsen, 1997). Annual precipitation is 98 inches (2,500 mm) at the lower elevations to 195 inches (5,000 mm) at the higher elevations.

The Rio Icacos has a steep, sandy channel (fig. 3.5a). The channel gradient of Rio Icacos at the streamflow gaging station is 0.0014 (Larsen, 1997) and the median particle size of bed sediment at that location is 0.6 mm (fig. 3.5b). Channel geometry at the USGS gage is shown in figure 3.5c. Bankfull width and depth are approximately 8m and 2.25m , respectively (fig. 3.5c).

Because of the high annual rainfall amounts, steep slopes, and Spanish policies, human land-use has been limited (Larsen, 1997; Larsen and Torres-Sanchez, 1998). Minor tree cutting for charcoal and small subsistence farming may have been the only human impact. In 1883, the Rio Blanco watershed, of which the Rio Icacos is a subbasin, was set aside as a forest preserve. Because of the limited impact of humans and its designation as a protected watershed, the Rio Icacos was chosen in this study as a "natural" watershed to investigate sediment. The most recent land use map for the Rio Icacos basin was in 1977. Ninety-eight percent of the area was classified as forest (Larsen, 1997). Because of its status as a preserve, the land use has not changed since 1977.

Quebrada Blanca Basin

Quebrada Blanca at El Jagual drains 3.24 mi^2 (8.39 km^2) and is underlain by volcaniclastic rocks, intrusive rocks, and alluvium (Briggs and Akers, 1965) in dominantly granodiorite (fig. 3.3). Average slope for the basin is 33.4% (Gellis and others, 1999). Soils in the basin are related to the geology, with sandy soils on the granodiorite (Pandura Sandy loams) and clayey soils (Mucura Clay) on the volcaniclastics (fig. 3.4).

Reproduced with permission of the copyright owner. Further reproduction prohibited without permission.

Figure 3.5a. View of Rio Icacos looking upstream near USGS streamflow gaging station, 10/05/1989.

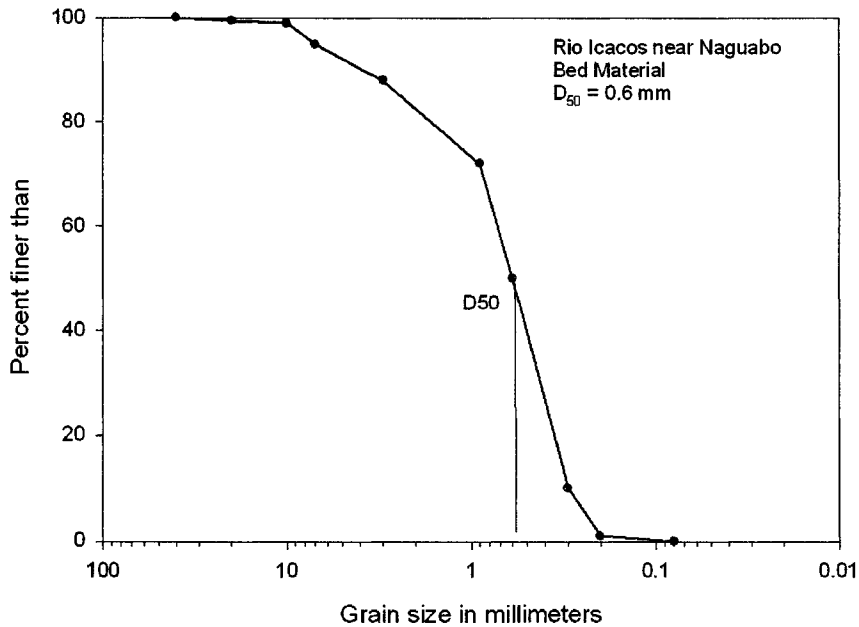

Figure 3.5b. Size analysis of bed material at Rio Icacos (after Larsen, 1997).

Reproduced with permission of the copyright owner. Further reproduction prohibited without permission.

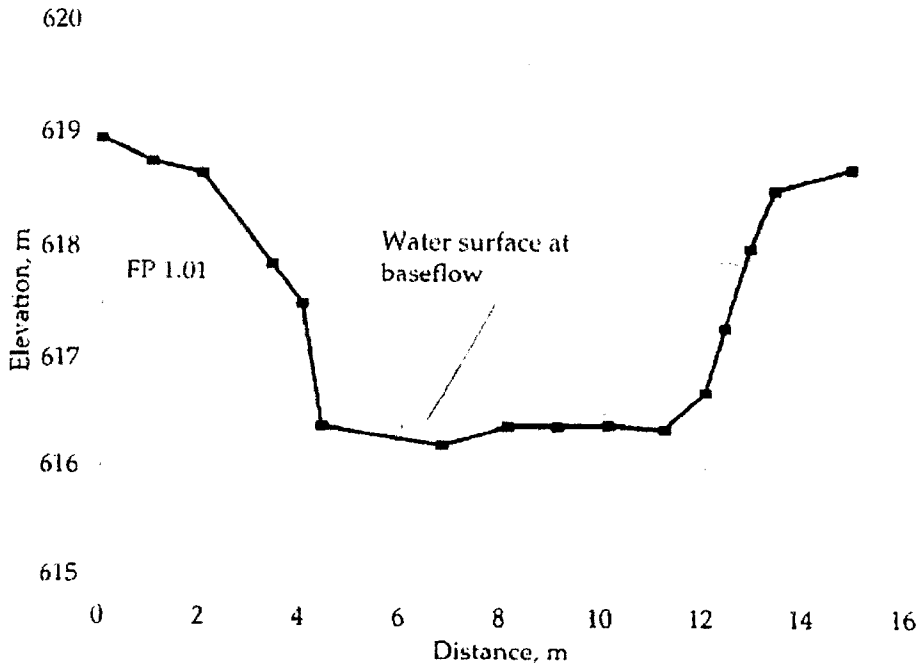

Reproduced with permission of the copyright owner. Further reproduction prohibited without permission.

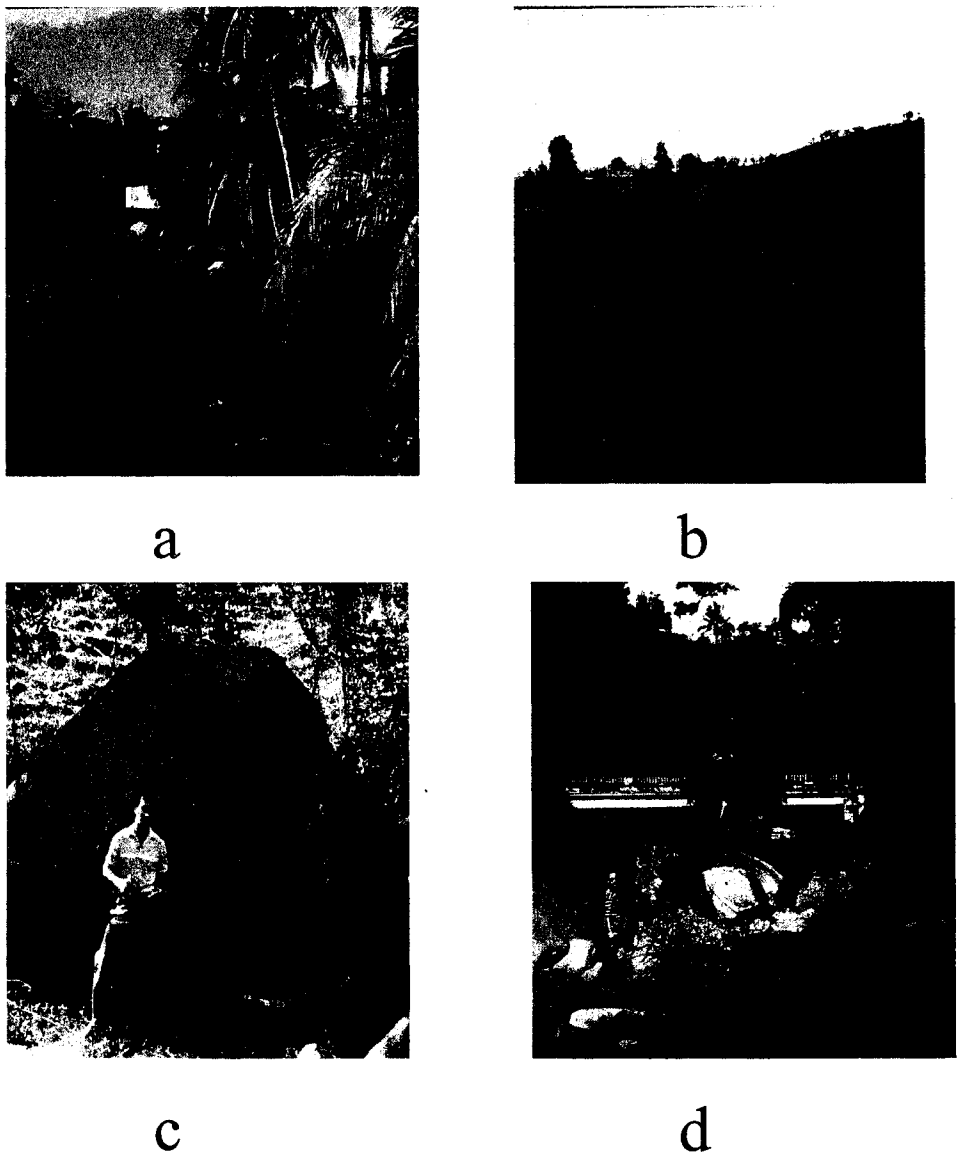

Figure 3.6. a) View looking upstream of Quebrada Blanca near gage, 11/071999. b) View of upper reaches of Quebrada Blanca watershed showing cropland, forested areas, and bare ground, 3/24/1990. c) Corestone on hillslope. Quebrada Blanca, 1/16/1990. d) Accumulation of boulders, possibly corestones, downstream of gage, 11/07/1999.

Reproduced with permission of the copyright owner. Further reproduction prohibited without permission.

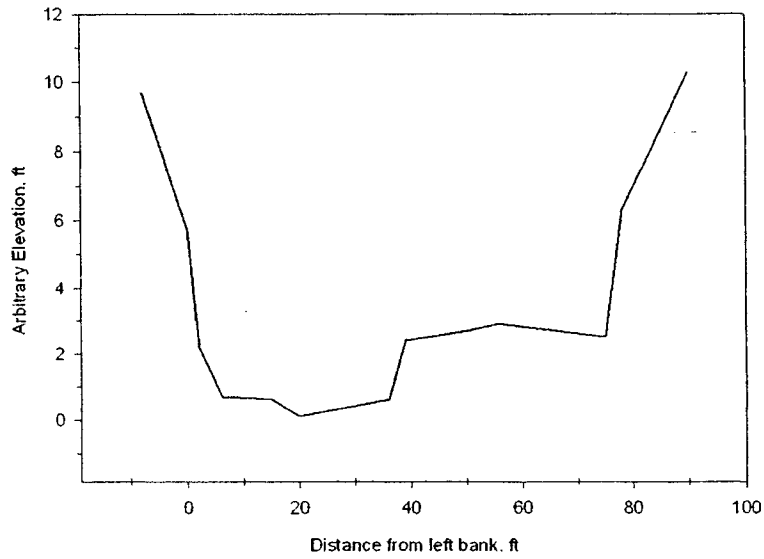

Figure 3.6e. View upstream of channel geometry near USGS streamflow station at Quebrada Blanca at El Jagual, August, 1986.

Many granodiorite corestones are in the watershed (fig. 3.6c). Bedrock is weathered below the ground surface by groundwater action along preferred orientations, such as joints, and exhumed by surface erosion to form corestones (Ruxton and Berry, 1957). In Quebrada Blanca, corestones form portions of the pool-riffle sequence and are important factors influencing channel morphology (fig. 3.6d).

Reproduced with permission of the copyright owner. Further reproduction prohibited without permission.

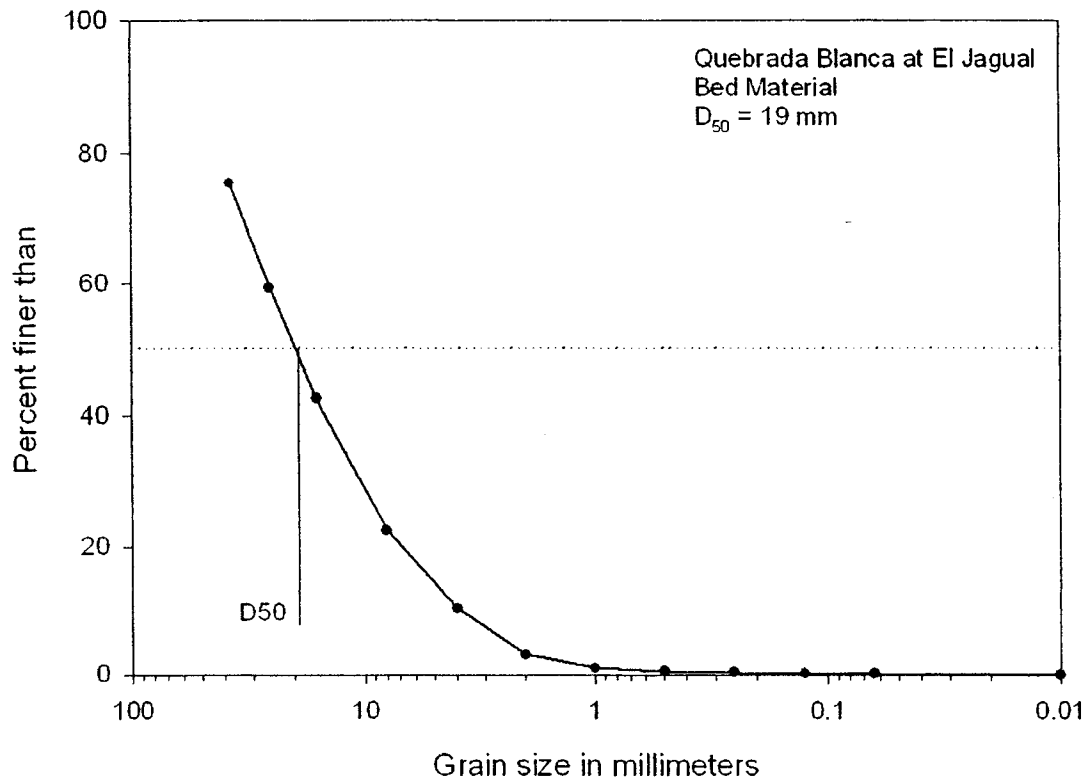

Figure 3.7. Size analysis of bed material at Quebrada Blanca near El Jagual, November 1999.

Land use in the Quebrada Blanca basin is dominantly pasture (54%), forest (21%), rural (15%), and cropland (8%) (fig. 3.8). Two percent of the basin was identified as bare ground (Gellis and others, 1999) (fig. 3.8). Sediment sources are minimal in the basin and include some cropland, small slips and landslides on the steep pasture and forested slopes.

Rio Caguitas Basin

The Rio Caguitas basin (8.5 mi^2; 13.6 km^2) drains the western part of the Rio Grande de Loiza basin (fig. 1.1). Rio Caguitas drains dominantly volcaniclastic rocks and the soils are Mucura

Reproduced with permission of the copyright owner. Further reproduction prohibited without permission.

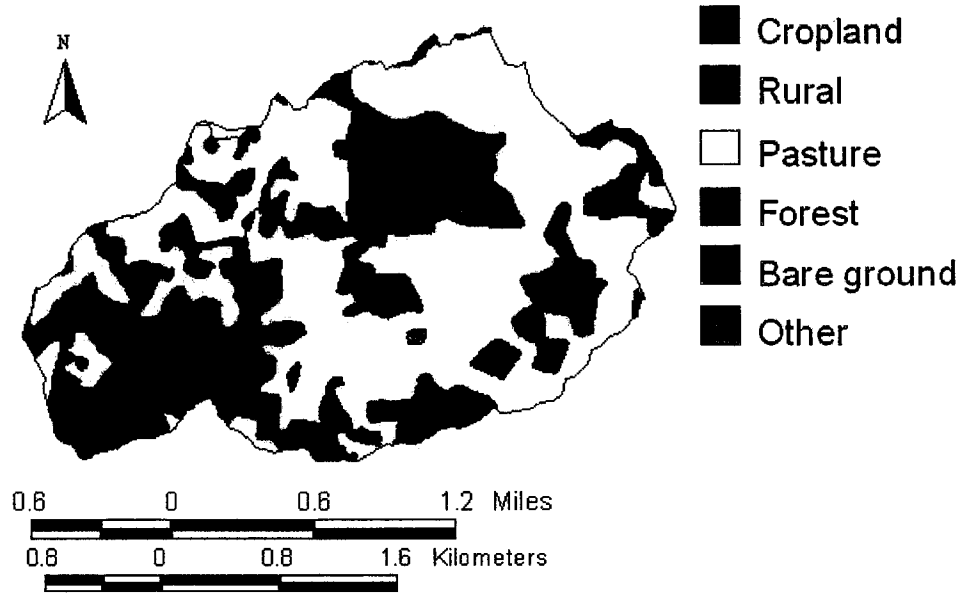

Figure 3.8. 1987 Land use of the Quebrada Blanca basin. Source: U.S. Geological Survey, Caribbean District, 1993.

Clay. Average slope for the basin is 33.2% (Gellis and others, 1999). Rio Caguitas is a steep, sand, cobble, and boulder channel, with bedrock outcropping in the river (fig. 3.9a). The median bed-material size at Rio Caguitas at the USGS gage is 8.0 mm (fig. 3.10). The slope of the channel bed at the USGS gage is 0.071. Bankfull width and depth are approximately 50 feet (15.2 m) and 8.0 feet (2.4 m), respectively (fig. 3.9b). Land use in the basin is forest (36%), pasture (27%), cropland (23%), and rural (11%) (fig. 3.11). Three percent of the basin was identified as bare ground (Gellis and others, 1999) with cropland the major source of sediment (fig. 3.11; 3.12).

Reproduced with permission of the copyright owner. Further reproduction prohibited without permission.

Figure 3.9a. View of Rio Caguitas near Aguas Buenas looking upstream near USGS streamflow gaging station.

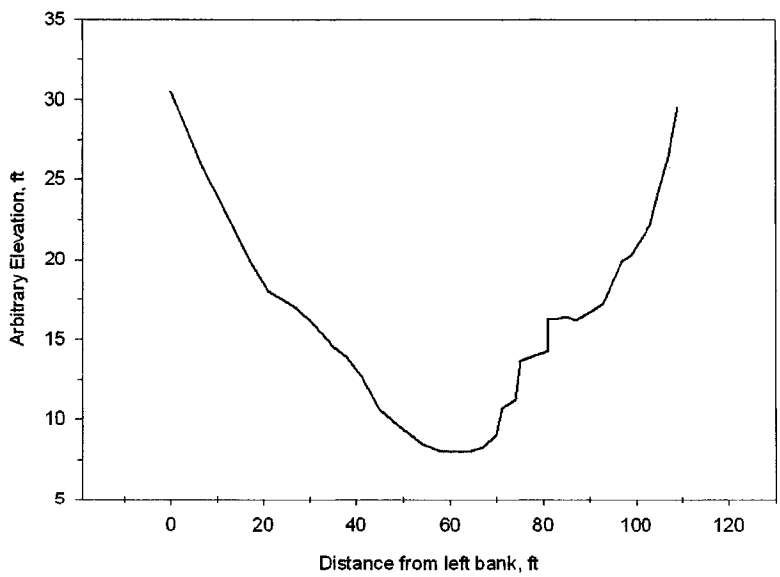

Figure 3.9b. View upstream of channel geometry of Rio Caguitas near Aguas Buenas near the USGS streamflow gaging station, August, 1990.

Reproduced with permission of the copyright owner. Further reproduction prohibited without permission.

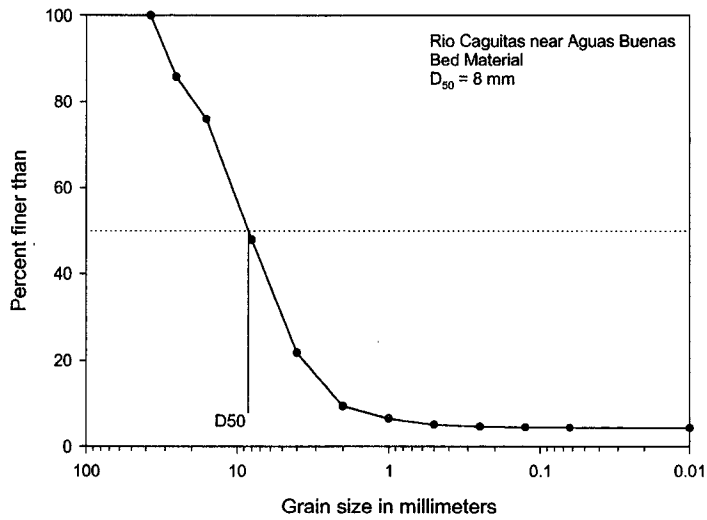

Figure 3.10. Size analysis of bed material at Rio Caguitas near Aguas Buenas, November 1999.

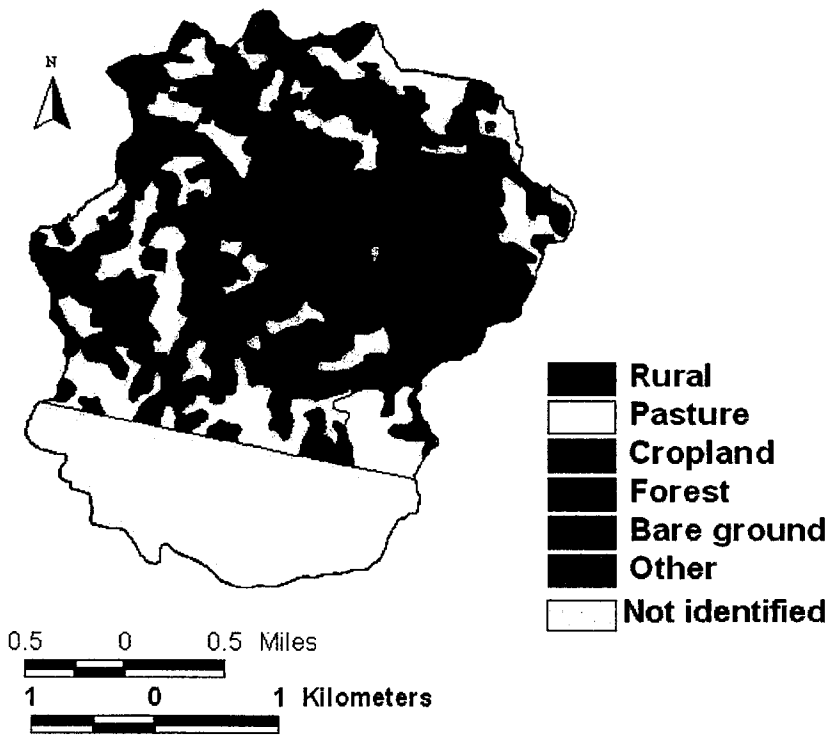

Figure 3.11. 1987 Land use of the Rio Caguitas basin. Source U.S. Geological Survey, Caribbean District, 1993.

Reproduced with permission of the copyright owner. Further reproduction prohibited without permission.

Figure 3.12. Cropland as bare ground during planting in the Rio Caguitas basin.

Rio Piedras Basin

The Rio Piedras basin is 8 miles (13 km) from metropolitan San Juan (fig. 1.1). Drainage area of the Rio Piedras at El Senorial at the USGS streamflow-gaging station is 7.49 mi^2 (19.4 km^2). Geology of the basin is dominantly volcaniclastics (thin bedded volcanic wackes and tuffaceous siltstone), and quartz diorite (Pease, 1968) (fig. 3.3). Soils in the basin are Macura clay. Elevations in the basin range from 151 to 984 feet (46 to 300 m).

The Rio Piedras is a fine-grained meandering channel (fig. 3.13a). The median grain size of the channel bed material is 2 mm (fig .3.14). Channel geometry at the USGS gage is shown in figure 3.13b. Bankful width and depth are approximately 57 feet (17.4 m) and 3.7 feet (1.1 m), respectively (fig. 3.13b).

Reproduced with permission of the copyright owner. Further reproduction prohibited without permission.

Figure 3.13a. View looking upstream from gage on the Rio Piedras at El Senorial, 11/07/1999.

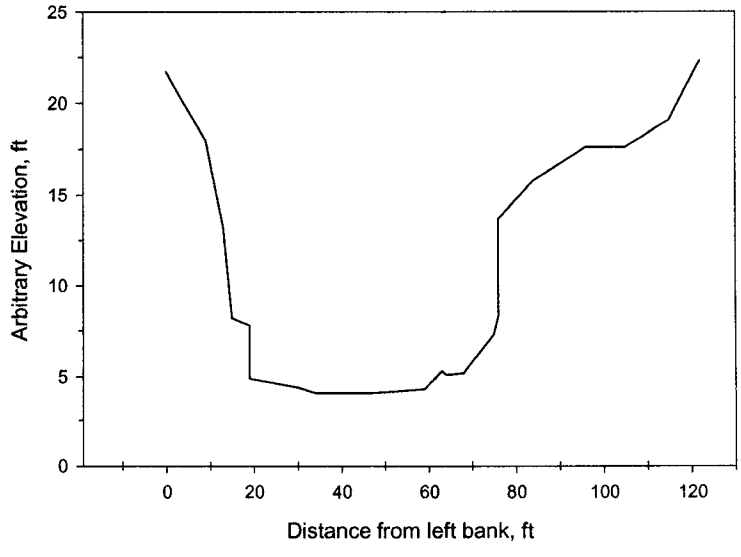

Figure 3.13b. View looking upstream of channel cross section at Rio Piedras at El Senorial near USGS streamflow gaging stations, May, 1989.

Reproduced with permission of the copyright owner. Further reproduction prohibited without permission.

The Rio Piedras basin contains the Barrios of Caimito and Cupey, which are within the municipality of San Juan. Population increased in the San Juan area in the 1950's to 1960's (fig. 3.15). The most recent land use map for the Rio Piedras basin was in 1977 and shows urban (77%) and forested (23%) areas (Webb and Gomez-Gomez, 1998) (fig 3.16). Since 1977 there has been considerable housing construction in the Rio Piedras basin (fig.3.17). Population in the barrios of Caimito and Cupey more than tripled between 1960 to 1990 (Table 3.2). Sediment sources in the Rio Piedras are widespread and are related to construction activity.

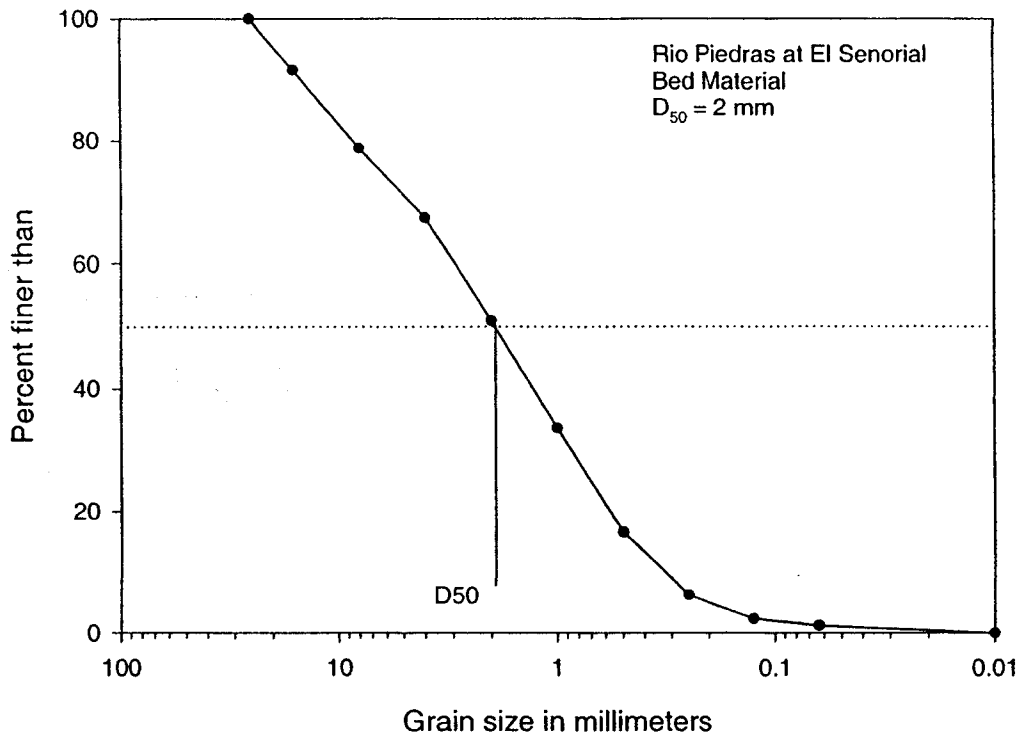

Figure 3.14. Size analysis of bed material at Rio Piedras at El Senorial, November 1999.

Reproduced with permission of the copyright owner. Further reproduction prohibited without permission.

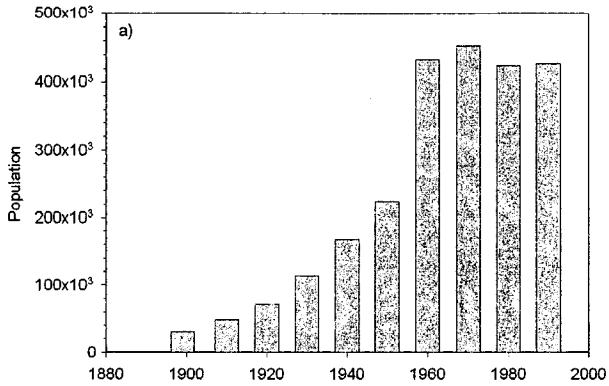

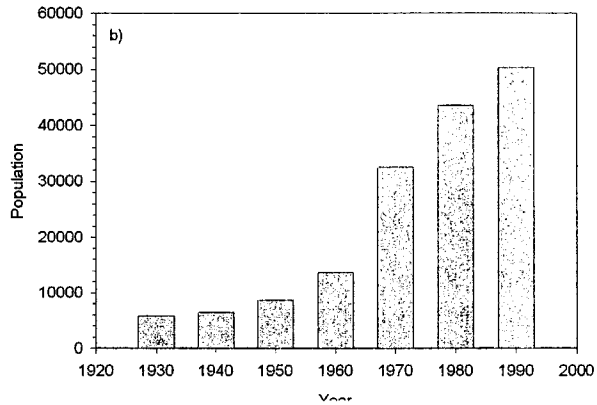

Figure 3.15 (a) Population of San Juan urban zone and (b) barrios in the Rio Piedras basin (Caimito and Cupey)(U.S. Dept. of Commerce Census reports (1935, 1949, 1959, 1969, 1973, 1978, 1982, 1987).

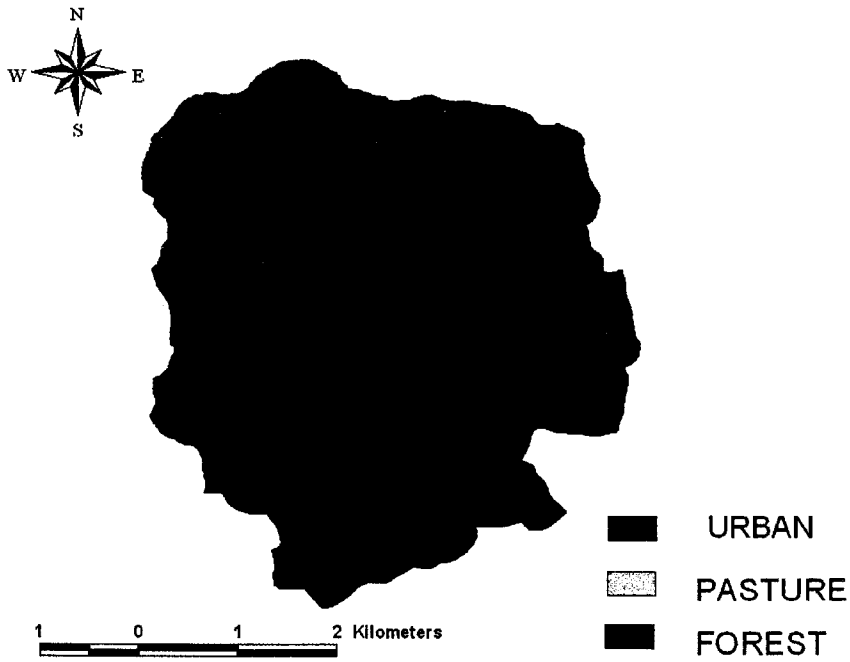

Figure 3.16. Land use map (1977) for the Rio Piedras basin. Source: U.S. Geological Surcey, Caribbean District.1991.

Reproduced with permission of the copyright owner. Further reproduction prohibited without permission.

Figure 3.17. View to a housing construction project in the Rio Piedras basin.

Table 3.2. Population changes in the vicinity of the Rio Piedras basin (U.S. Dept. of Commerce Census reports (1935, 1949, 1959, 1969, 1973, 1978, 1982, 1987).

	Barrio of Caimito and Cupey		San Juan Urban Zone
Year	Population	Year	Population
1930	5812	1899	32048
1940	6528	1910	48716
1950	8713	1920	71443
1960	13688	1930	114715
1970	32569	1940	169247
1980	43678	1950	224767
1990	50485	1960	432377
		1970	452749
		1980	424600
		1990	426832

Reproduced with permission of the copyright owner. Further reproduction prohibited without permission.

Climate and Hydrology of Puerto Rico and Study Area

Climate

The modern climate of Puerto Rico is humid tropical with annual average temperatures ranging from 10^0C to 30^0C. Climate is controlled by seasonal movements of the Intertropical Convergence Zone (ITCZ). In northern winter, the southward shift of the ITCZ imposes drier conditions on the Caribbean (Hastenrath, 1976). With the northward shift of the ITCZ into the northern hemisphere a rainy season develops in the Caribbean. Average annual rainfall varies from 40 inches (1,000 mm) in the drier southern coast to 155 inches (4,000 mm) in the eastern Sierra Luquillo mountains. The relative humidity in San Juan averages 80 percent throughout much of the year (Monroe, 1980b). Rates of annual evaporation recorded at sea level in San Juan are 82 inches (2,072 mm) and at Adjuntas, elevation 1500 feet (457 m), are 51 inches (1,294 mm) (Monroe, 1980b).

Puerto Rico is situated between the subtropical high pressure cells of the Atlantic and the low pressures of the equatorial region. Rainfall in Puerto Rico is produced by easterly waves and cold fronts. Over 70% of annual rainfall is produced by tropical waves, depressions, storms, and hurricanes (Larsen, 1997). Hurricanes and tropical disturbances are extremely important climatological features that are effective geomorphic agents (Gupta, 1988, Gellis, 1993; Coch, 1994; Larsen and Torres-Sanchez, 1995). For a storm to be classified as a hurricane it must be have wind speeds in excess of 65 knots (120 km/hrs). A hurricane hits Puerto Rico about once every 21 years (Larsen and Torres-Sanchez, 1998), and average rainfall associated with these storms can range from 5.3 to 28.5 inches (135 to 725 mm) (Scatena, 1995). Large floods associated with hurricanes may control the channel geometry of tropical rivers (Gupta, 1988).

Reproduced with permission of the copyright owner. Further reproduction prohibited without permission.

Hurricanes with heavy rains and wind can cause extensive flooding and erosion, especially in hilly regions where mass movements can occur (Larson and Torres-Sanchez, 1995).

Climate of the study basins

Precipitation records obtained from the National Weather Service raingages Rio Piedras, Caguas, Gurabo, Juncos, San Lorenzo, Lower Rio Blanco, and Upper Rio Blanco (fig. 3.18) show average annual rainfall between 63.8 to 158.9 inches (1,620 to 4,035) (fig. 3.19; Table 3.3). Rainfall is strongly influenced by orographic effects. The higher rainfall at the Lower Rio Blanco raingage is a result of its location in the Sierra de Luquillo Mountains at an elevation of 1,440 ft (439 m). There are two marked rainfall seasons in Puerto Rico (fig. 3.19). A drier season, from January through April, and a wetter season, from May through December which includes the hurricane season and has an average monthly rainfall close to twice that from January through April.

Human and Land-Use History

At the time of Columbus' exploration of the Caribbean, three groups of people inhabited the region: Guanahatabeys in western Cuba, Tainos in the Bahamas and Greater Antilles, and Caribs in the Lesser Antilles (Rouse, 1989). The Guanahatabeys were the first inhabitants of the Caribbean, migrating there from Belize to Cuba in 5,000 B.C. The Tainos, also called Arawaks, considered to be expert canoeists, migrated from Venezuela, around the mouth of the Orinoco River, to Hispaniola, Puerto Rico, and the Lesser Antilles between 600-1,000A.D. (Brenner and

Reproduced with permission of the copyright owner. Further reproduction prohibited without permission.

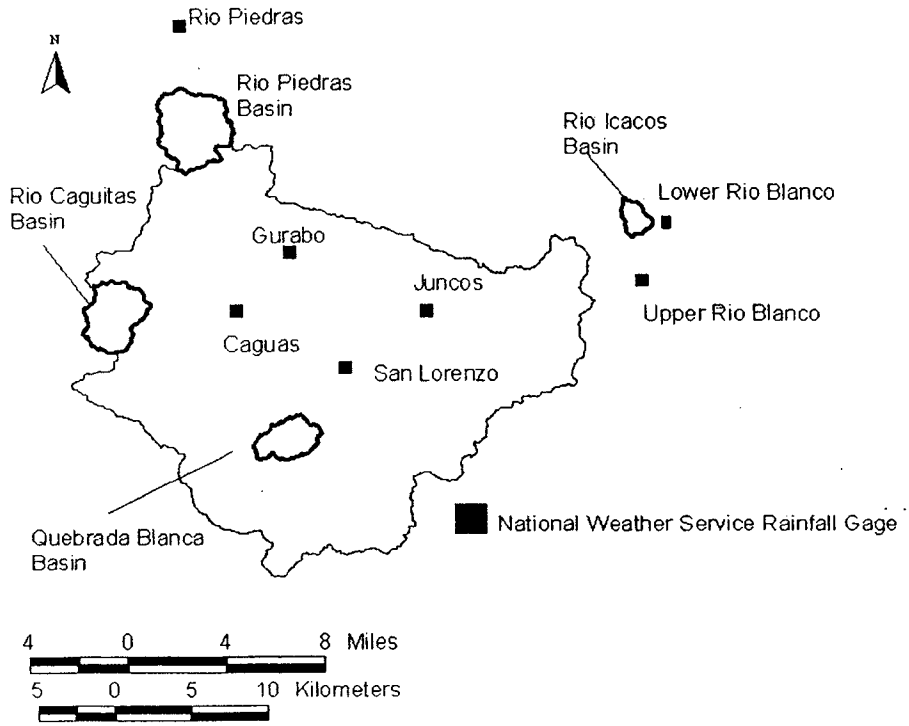

Figure 3.18. Location of National Weather Service raingages.

Table 3.3. Historic rainfall averages for National Weather Service raingages in study area.

National Weather Service raingage name	Years	Average annual rainfall, in
Rio Piedras Experimental Station	1911 to 1996	76.8
Gurabo Substation	1956 to 1996	63.8
Caguas	1931 to 1995	64.9
Juncos 1SE	1911 to 1996	64.7
San Lorenzo Farm	1954 to 1988	71.7
Rio Blanco Lower	1931 to 1996	109.4
Rio Blanca Upper	1931 to 1974	158.9

Reproduced with permission of the copyright owner. Further reproduction prohibited without permission.

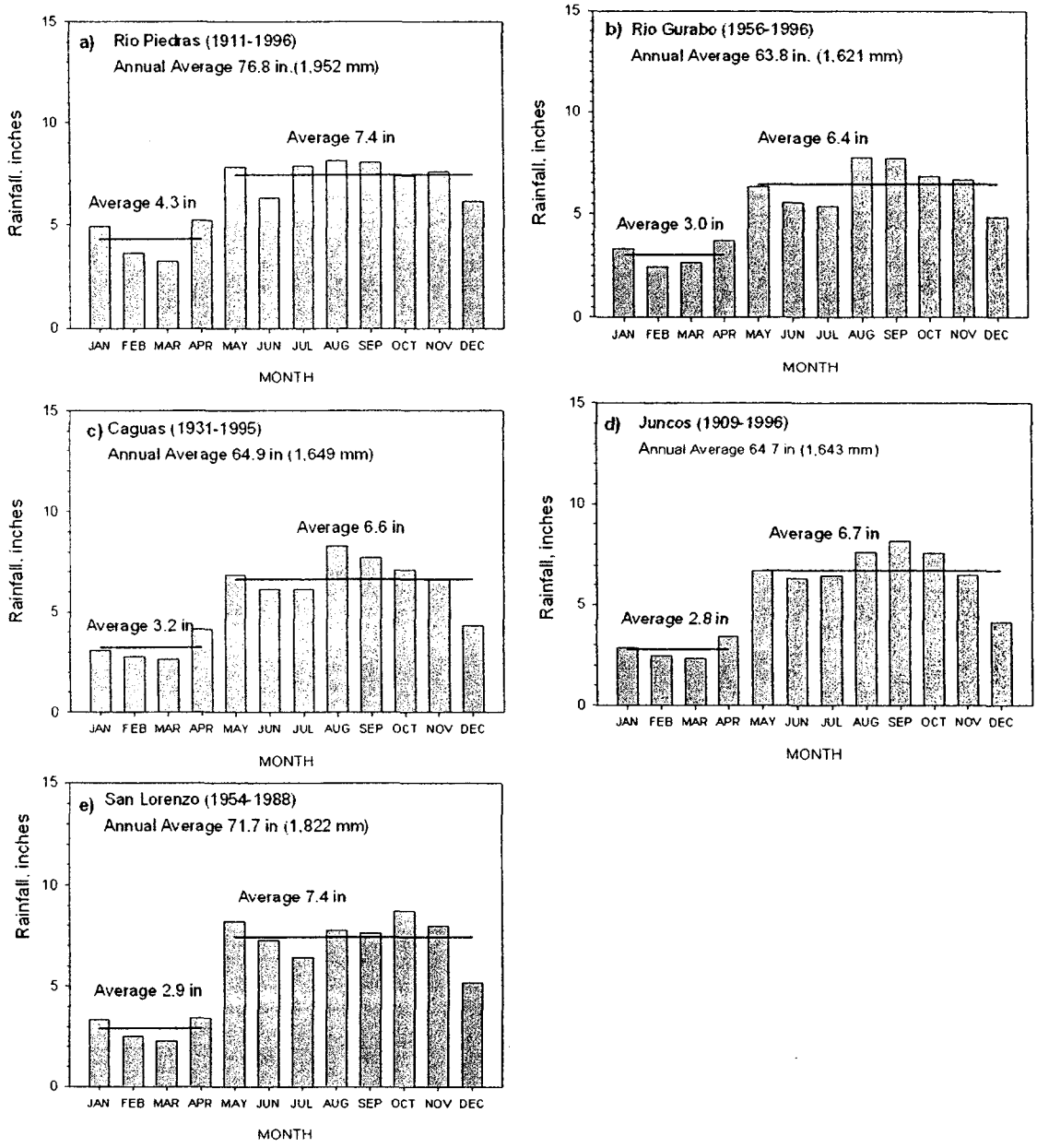

Figure 3.19. Historical monthly average rainfall and average seasonal rainfall (Jan-Apr; May-Dec) for National Weather Service rain gages: (a) Rio Piedras, (b) Rio Gurabo, (c) Caguas, (d) Juncos, (e) San Lorenzo, (f) Lower Rio Blanco, and (g) Upper Rio Blanca.

Reproduced with permission of the copyright owner. Further reproduction prohibited without permission.

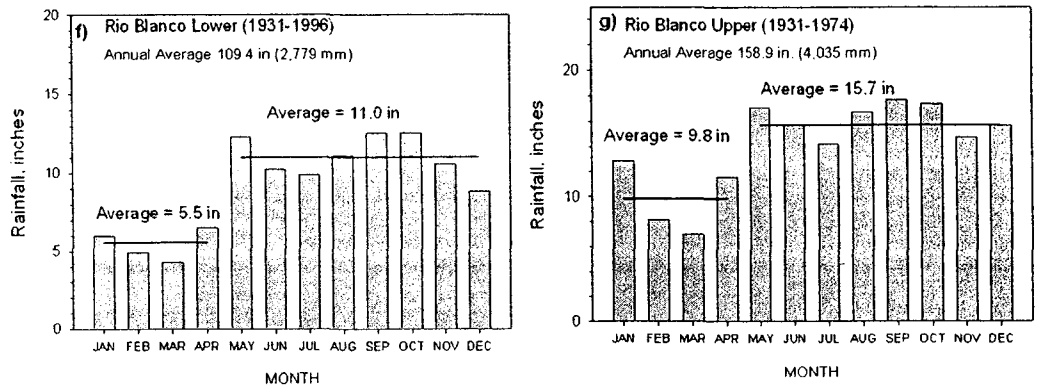

Figure 3.19. Continued.

Binford, 1988; Rouse, 1989; Kjellmark, 1996). The Taino migration north and west culminated between 800 and 1,200 A.D. and was blocked by encounters with the Guanahatabeys (Rouse, 1989). The fierce, warlike Caribs who migrated from the Guianas, South America, around 1,000 A.D., raided and pillaged most of the Taino villages and also adapted their culture. The word hurricane comes from the Carib language.

Christopher Columbus discovered Puerto Rico on his second voyage in 1493 when the Island was close to 100% forest cover. Early in the history of Spanish occupation Puerto Rico was used mainly as a military installation. Agricultural development was minimal and largely confined to the coast. Later in the Spanish occupation, agriculture (coffee and sugarcane) became more important (U.S. War Department, 1900). Land use for Puerto Rico in agriculture, pasture, and forest cover from 1828 to 1987 is shown in figure 3.20. In 1828, only 3% of the Island was in cropland, 24% pasture, and the remainder in forest (Murphy, 1916). At the time of U.S. occupation in 1898, 76% of the area of Puerto Rico was included within farms and of this area

Reproduced with permission of the copyright owner. Further reproduction prohibited without permission.

21% was in cropland (US War Department, 1900). Of this cropland, 41% was planted in coffee, 15% in sugarcane, and 1% in tobacco. After 1899, coffee, sugarcane, and tobacco became increasingly important. In 1935, 86.2% of the Island was included within farms and 43% of this area was cropland, more than twice the amount in 1899. Of the cropland in 1935, 21% was in coffee, 40% in sugarcane, and 13% in tobacco. Cropland reached its highest percentage of 47.5% of Puerto Rico in 1939 (fig. 3.20). Cropland was achieved at the expense of forest cover, which reached its lowest value of 6.5% in 1948. Pasture, used chiefly for livestock, reached its highest percentage of 55.8% in 1900. The dominant grass in pasture is Guinea Grass (*Panicum maximum*) (Alberts and Garcia-Molinari, 1943).

By the early 1940's, Puerto Rico's economy, which had centered around the cash crops of sugar cane, tobacco, and coffee was severely depressed (Lewis, 1963; Golding 1973). Beginning in 1942, a government program of economic aid and incentives was established to invigorate the Puerto Rican economy through industrial development. The development program is historically referred to as "Operation Bootstrap" (Lewis, 1963) and by 1957 industry had economically supplanted agriculture as the major source of income. The resulting shift from an agricultural to a manufacturing economy resulted in the large scale abandonment of farmland and a continual increase in forest cover since 1948. During the transition period, population shifted from the interior of Puerto Rico to manufacturing centers in and near San Juan and along the north coast. Exemption from certain taxes has also proven to be an incentive in attracting U.S. businesses to Puerto Rico. The tax exemption known as Section 936 of the U.S. tax code provided certain tax incentives for businesses through 1996, when the section was eliminated by

Reproduced with permission of the copyright owner. Further reproduction prohibited without permission.

the U.S. Congress. Thus, Puerto Rico has remained an industrial society and is one of the world leaders in the production of pharmaceutical products.

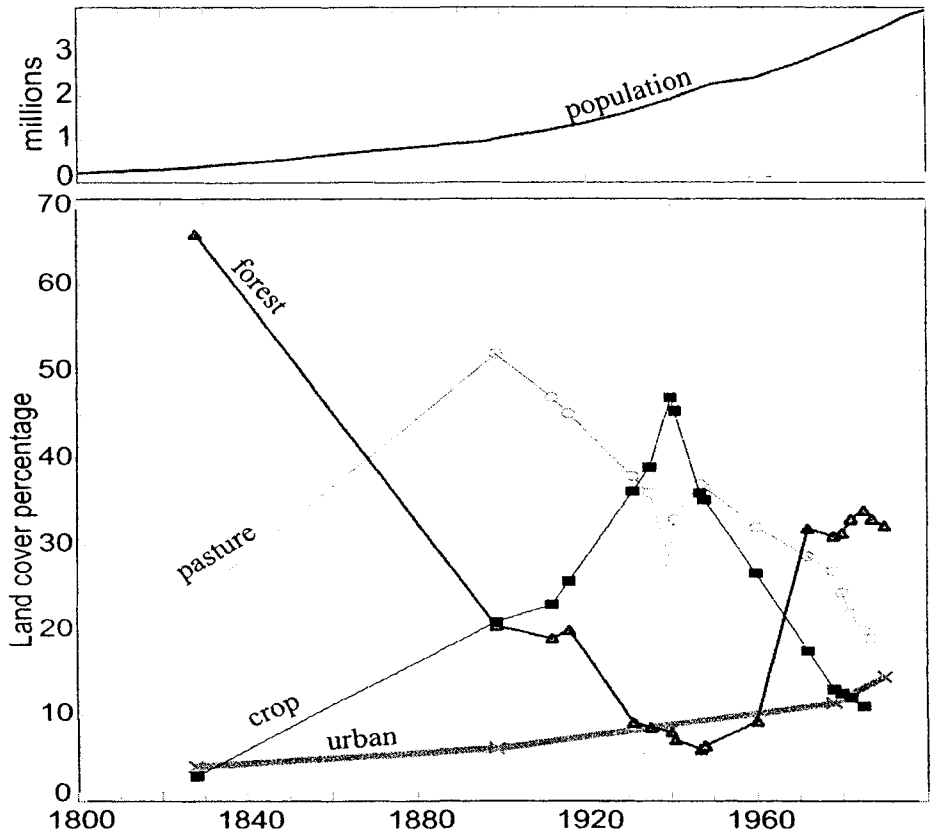

Figure 3.20. Land use changes over time for Puerto Rico (Gellis and others, 1999).

Land-use changes for the Lago Loiza basin in north-central Puerto Rico, 1950 through 1987, were documented by Gellis and others (1999). In 1950, the majority of the basin was in cropland (58%). Similar to the entire Island, cropland decreased through 1977 and was supplanted by forest and pasture. Cropland and forest both increased from 1977 to 1987. Pasture is the only land use that decreased since 1977, from 65.4% in 1977, to only 48.5% in 1987. Land previously in pasture was replaced by forest, cropland, and rural land. Rural land use is low density, residential development along roads away from major centers and may include small

Reproduced with permission of the copyright owner. Further reproduction prohibited without permission.

mixed-crop plots. It should be noted that as pasture was converted to cropland and rural land it went through a period of vegetation removal and bare ground. The amount of land in forest cover increased from 7.6 % in 1950 to 16 % in 1977, and then to 20.6 % in 1987. Using a GIS, Gellis and others (1999) determined how the same section of land in the Lago Loiza basin changed over time. Land classified as rural, pasture, cropland, and urban in 1987 was greater than 50% cropland in 1950. Only 32% of forest in 1987 was cropland in 1950, while the majority of forest was classified as pasture in 1950 (47%) (Gellis and others, 1999).

The Lago Loiza basin is 35 miles (22 km) from San Juan and urban and rural land use have increased in the Lago Loiza basin since 1950. The population in the Rio Grande de Loiza basin increased 77% from 1950 to 1990 and housing units increased 194% during the same period (Gellis and others, 1999). In 1990, 34% of the Lago Loiza basin population resided in the Caguas urban area. The population of Caguas almost tripled between 1950 and 1990, a period which spans the operation of the reservoir. The increasing population in Caguas can be attributed to a shift in population from metropolitan San Juan and the increase in industrial jobs (pharmaceutical and electronics) in the municipalities. The increase in urban area in the Lago Loiza basin caused more land to be disturbed for construction.

Based on analysis of 1987 and 1989 aerial photographs, disturbed ground locations in the Lago Loiza basin ranged from 0.002 to 102.3 acres (0.0008 to 41.4 hectares) and totaled 2,086 acres (844 hectares) (Gellis and others, 1999). Disturbed ground was classified as construction sites (63%), cropland (21%), mining (15% sand and gravel quarries), or landslides (1%). The mean area of bare ground was highest in construction sites (7.9 acres; 3.2 hectares), followed by

Reproduced with permission of the copyright owner. Further reproduction prohibited without permission.

mining (7.2 acres; 2.9 hectares), cropland (2.1 acres; 0.86 hectares), and landslides (0.42 acres; 0.17 hectares).

Reproduced with permission of the copyright owner. Further reproduction prohibited without permission.

CHAPTER IV

METHODS

A variety of field, laboratory, GIS, and statistical techniques were used to determine streamflow, fluvial suspended-sediment transport, rainfall, and hillslope erosion in Puerto Rico. A description of the methods used for both data collection and analysis will be summarized with a brief discussion of the errors involved. Numerous independent variables were assembled to determine their significance to suspended-sediment characteristics. Definitions and statistical analysis used on the independent variables are presented.

GIS

Several GIS coverages obtained from the USGS district office in San Juan, Puerto Rico were used in this analysis: geology, land use, soils, slope, and hydrography. The geology and soils coverages are digitizations of original publications (Briggs and Akers, 1965; Pease, 1968; Boccheciamp, 1977,1978). Land use for Quebrada Blanca and Rio Caguitas in 1950, 1977, and 1987 was obtained from aerial photographs and reports (Brockman, 1952; Puerto Rico Department of Natural and Environmental Resources, 1977; Gellis and others, 1999). Land-use information for the Rio Icacos basin was obtained from Larsen (1997). Land-use information for the Rio Piedras basin was obtained from CSA Architects and Engineers (1999).

Reproduced with permission of the copyright owner. Further reproduction prohibited without permission.

Rainfall

Collection

Rainfall in this analysis was recorded at the streamflow-gaging station in each study basin, neighboring streamflow-gaging stations, and in some cases stand-alone raingages that were constructed in select places in and around the study basins (fig.4.1). Rainfall recorders were tipping-bucket type raingages. They were programmed to accumulate rainfall totals every 15-minutes and at more frequent intervals during intense rainfall events based on a given threshold. The rainfall data were stored in Data Collection Platforms (DCP) and downloaded monthly. The rainfall collectors are calibrated by the manufacturers but were not calibrated in the field. Therefore, errors associated with the rainfall collection could include poor calibration by the manufacturer. During the monthly inspection and cleaning, dust was often noticed in the tipping buckets. This could present a small source of error. Rainfall data by the National Weather Service were also used in rainfall analysis (fig. 3.18).

Rainfall event definition

Typically the beginning of the rainfall event does not coincide with the beginning of the runoff event but begins some time period before the initial rise in discharge. The start of the runoff event is easy to discern for most events as an abrupt rise in discharge, while the determination of the beginning of the rainfall event is more subjective. In most observed cases, the beginning of a rainfall event is recognized as a burst of rain over a period of minutes to tens of minutes before the initial rise in the hydrograph. Sometimes lower intensity values of rainfall are observed before the

Reproduced with permission of the copyright owner. Further reproduction prohibited without permission.

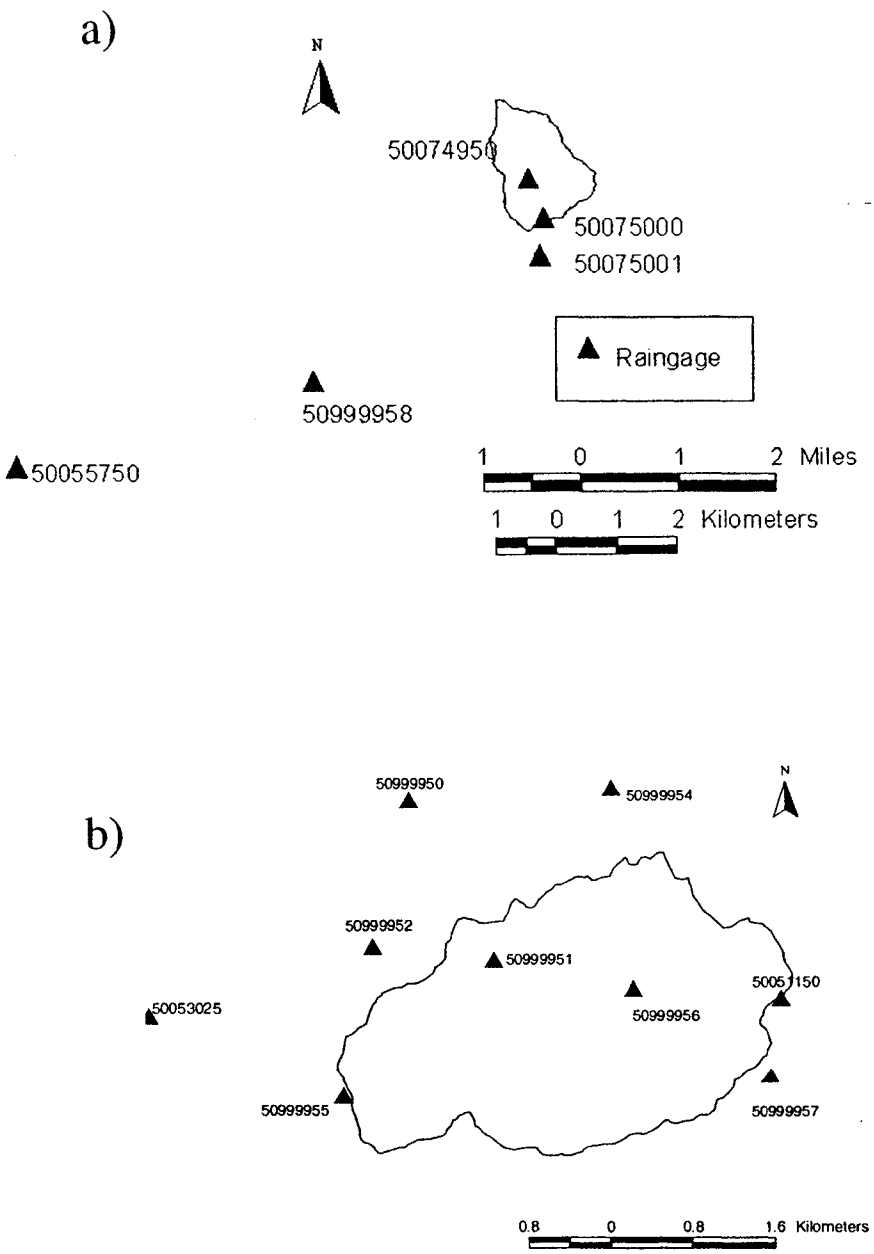

Figure 4.1. Location of raingages used in study in a) Rio Icacos and b) Quebrada Blanca.

Reproduced with permission of the copyright owner. Further reproduction prohibited without permission.

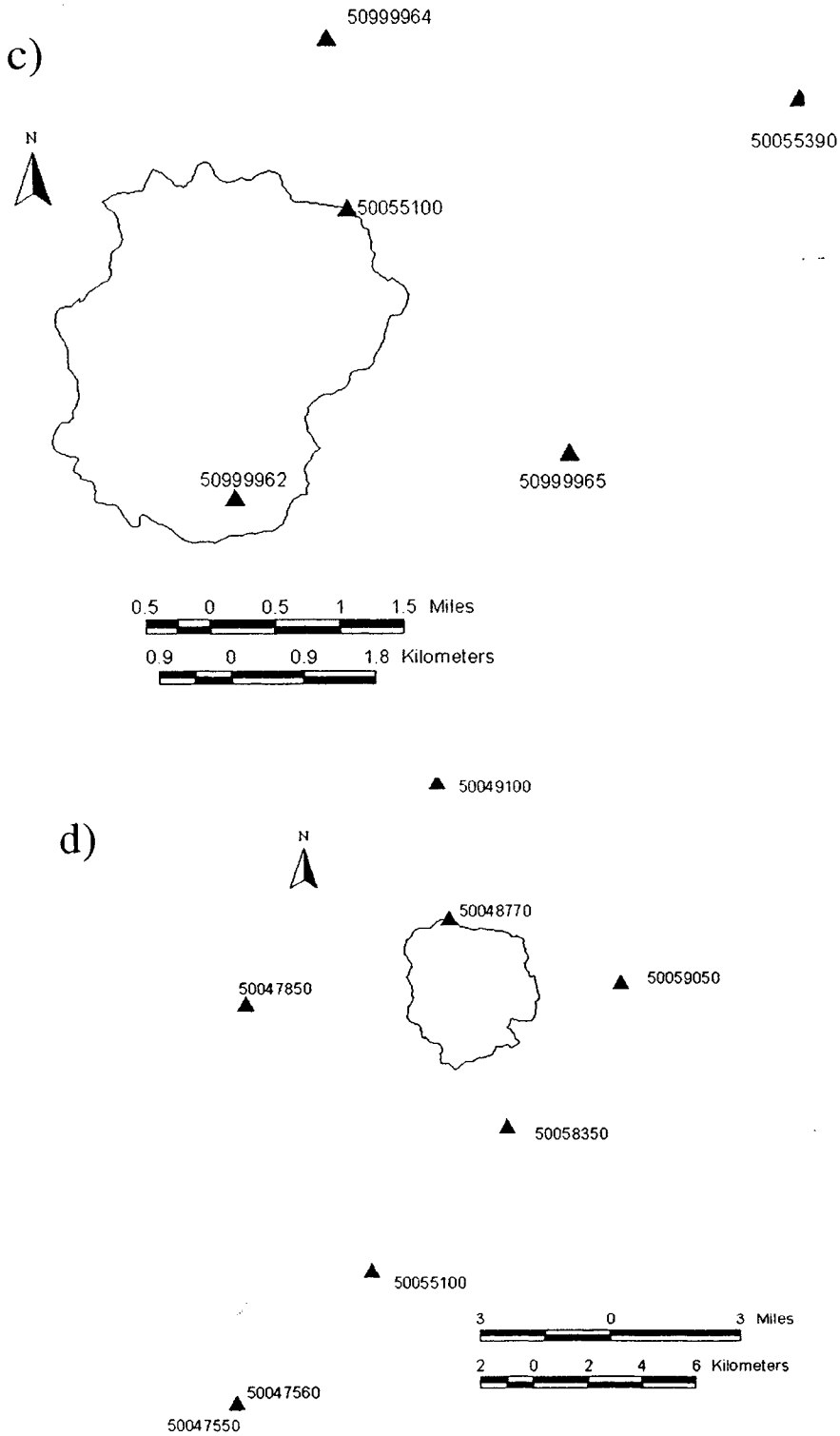

Figure 4.1. Location of raingages used in study in c) Rio Caguitas and d) Rio Piedras.

Reproduced with permission of the copyright owner. Further reproduction prohibited without permission.

the start of the runoff event, a break in rainfall amounts or intensity was used to determine the beginning of the rainfall event.

Rainfall intensity

Rainfall intensity for the runoff events was defined two ways. In one definition the maximum 15-minute intensity for the rainfall event was used. Because the two highest 15-minute rainfall intensity amounts for a given storm may be fairly close, rainfall intensity over a greater period of time was also examined. For example, the maximum 15-minute rainfall intensity may be 0.52 in/15-min (13.2 mm/15-min). The next highest 15-minute rainfall intensity may be 0.49 in/15-min (12.4 mm/15-min). To determine rainfall intensity for the event over a greater period of time, 75% of the rainfall was calculated and divided by the amount of time 75% of the rain fell. This factor is termed the '75-% Rainfall Intensity' and will be used in the statistical analysis presented later in this chapter.

Areal distribution

Rainfall producing the runoff event and rainfall intensity (maximum 15-minute and 75-% intensity) were quantified for each station for each storm event using raingages in the basin and surrounding basins (fig. 4.1). Estimates of precipitation over the entire basin were made using the Thiessen polygon Method (Brooks and others, 1991) in which polygons are determined around each gage from the perpendicular bisectors of nearby gages. Each polygon is weighted to the drainage area. A GIS was used to calculate the Thiessen Polygons. If one of the rainfall gages was not operational during the storm, the missing polygon represented by that gage was omitted and the estimated rainfall was based on the remaining gages and remaining area. If several gages were

Reproduced with permission of the copyright owner. Further reproduction prohibited without permission.

not operating or a missing rainfall gage covered more than 50% of the area, an average of rainfall for the storm event was calculated using the remaining gage(s). The Thiessen Method assumes a linear interpolation between gages and does not take orographic effects into account.

Streamflow

Collection

Streamflow from the four USGS gaging stations were analyzed in this study (fig. 1.1). Determination of streamflow follows USGS standards. At each station many direct and some indirect measurements of streamflow and water surface (stage) were made over a range of conditions to define the relationship between stage elevation and water discharge (Carter and Davidian, 1968). Streamflow measurements were made monthly on a routine basis and at select times during high flows. A rating curve was developed from discharge measurements and the stage of the river and was used to estimate water discharge when only stage was known (Kennedy, 1984).

The stage of the stream was recorded at each station using a mercury manometer. A pipe was fitted to a point near the bottom of the stream and connected to the mercury manometer, so that adjustments in the stage of the river were reflected in the pressure inside the pipe. The stage values were recorded with automatic digital recorders (ADR) and a DCP installed at each site using a 15-minute recording interval. The DCP also transmitted stage more frequently during high flows. These data were then used to compute mean daily streamflow.

The errors involved in making streamflow measurements include wind, boundary conditions, equipment, and measurement error (Sauer and Meyer, 1992). Most errors in

Reproduced with permission of the copyright owner. Further reproduction prohibited without permission.

streamflow measurements range from 3 to 6 % (Sauer and Meyer, 1992). During a runoff event the streambed may scour or fill and cause changes in the rating curve. These shifts in the streambed cannot be accurately quantified and are estimated by the persons working the streamflow record. During the course of operation of the gaging station, the record may be incomplete as a result of power disruptions, adverse weather conditions, and vandalism. In this study, missing periods of record were omitted from analyses.

Storm-generated event definition

What defines a "runoff event"? Rain falls on a basin and streamflow rises, but the discharge used as a threshold in the definition of an event is subjective. In this study, a runoff event was defined by a minimum peak discharge. Several methods were used in conjunction to determine the minimum peak discharge necessary to define an event.

One method examines the statistical percentiles of hourly discharge for the period of study. Hourly discharges were entered into a computer spreadsheet package which produces a table that contains the ordinal and percentage rank of each value in the data set. The percentile of each number is determined by its rank which is

$$m = \frac{P}{100}(n+1)$$

where m = the ranked value, P=desired percentile, n=total number of values. Linear interpolation is used when m is not a whole number.

The discharge value at the 95th percentile was used to define the minimum peak discharge for a runoff event.

Reproduced with permission of the copyright owner. Further reproduction prohibited without permission.

The other method used in conjunction with the 95th percentile method was based on examination of the relationship of instantaneous discharge to suspended-sediment concentration for a given gage, known as the sediment-transport curve. The value of peak flow selected from the 95th percentile analysis was examined on the transport curve to determine if this was the discharge where a noticeable increase in suspended-sediment concentration occurs relative to an increase in discharge. If the increase occurred before that discharge then the definition of an event was given a lower peak flow value. If an increase in suspended-sediment concentration occurs after the 95th percentile value then the definition of an event was given a higher value. If the transport curve is generally linear over a range of discharges, then the 95th percentile value was used.

The number of peaks in an event and their magnitudes are variables thought to influence suspended-sediment characteristics (Walling, 1974). Some runoff events only have one peak and the peak flow characteristics were defined for the one peak. Other events are multi-peaked, defined by troughs and peaks (fig. 4.2). Just as the definition of a runoff event is subjective, determining what are secondary peaks in an event is subjective. The runoff event in figure 4.2 has 3 peaks, but is there enough rise on some of the peaks to identify them as separate peaks? For this research, in multi-peaked events, a peak is defined by a minimum difference in discharge from the immediately preceding trough to the peak (fig. 4.2) The minimum difference in discharge used to define each peak varies over a range of discharges. At each station discharge was broken into classes to determine this minimum difference. Classes of discharge are log or semi-log cycles. If a peak does not meet these definitions, the higher peak, whether it was earlier or later in time, is determined as the peak (peak no. 2, in fig. 4.2).

Reproduced with permission of the copyright owner. Further reproduction prohibited without permission.

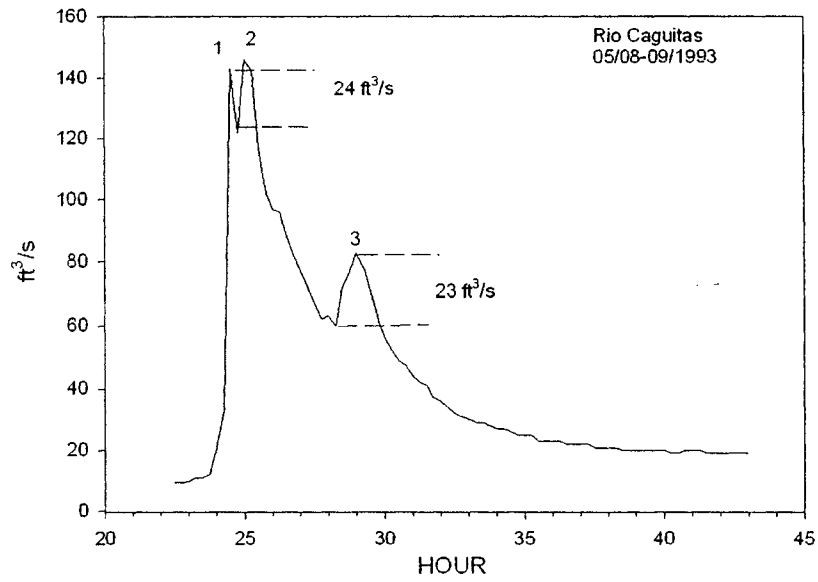

Figure 4.2. Example of a multi-peaked event at Rio Caguitas. The storm had 3 peaks. But as can be seen in the example the first peak reached 143 ft^3/s, dropped 24 ft^3/s, and rose to a higher peak (146 ft^3/s). In this example the first peak was not counted.

The minimum peak discharge used to define a stormflow runoff event for each streamflow station is shown in Table 4.1A. The minimum difference in discharge of the peak minus the previous trough was used to define each peak in a multi-peaked event. The minimum difference of the peak minus the previous trough was defined over a range of discharges for each station (Table 4.1B). For example, at Quebrada Blanca at El Jagual, a peak of 250 ft^3/s (7.1 m^3/s) would be a peak if the preceding trough discharge was 200 ft^3/s (5.4 m^3/s) or less (Table 4.1b).

Hydrograph Separation

Hydrograph separation techniques were used to separate base flow from stormwater runoff for select events at the four stations. During or following a precipitation event, water flows over

Reproduced with permission of the copyright owner. Further reproduction prohibited without permission.

Table 4.1. (A) Minimum peak discharge at each station used to define an event. (B) Difference in the peak flow minus the preceding trough used to define a peak in a multipeaked event.

A)

Station	Minimum discharge (ft^3/s)
Rio Icacos	30
Q. Blanca	15
Rio Caguitas	12
Rio Piedras	48

B)

Discharge (ft^3/s) of trough preceding peak flow in multi-peaked event	Difference in discharge (peak flow minus trough) (ft^3/s)			
	Rio Icacos	Q. Blanca	R. Caguitas	R. Piedras
>0-100	10	10	10	20
>100-500	45	50	40	50
>500-1000			150	100

and through the land surface and discharges into the nearby stream. The flood or runoff hydrograph records the start and end of stormwater runoff. A typical hydrograph illustrating the flow components is show in figure 4.3. The beginning of stormwater runoff is usually marked by a steep rise in the hydrograph shown as the "rising limb" in figure 4.3. The hydrograph gradually tapers off into a recession limb (fig. 4.3). The point of maximum curvature of the recession curve or inflection point is described as the point where overland flow and throughflow cease and base flow begins (Serrano, 1997). The shape of the hydrograph recession may be affected by the

Reproduced with permission of the copyright owner. Further reproduction prohibited without permission.

permeability of alluvial deposits lining the stream, soil moisture, and evapotranspiration (Pettyjohn and Henning, 1979).

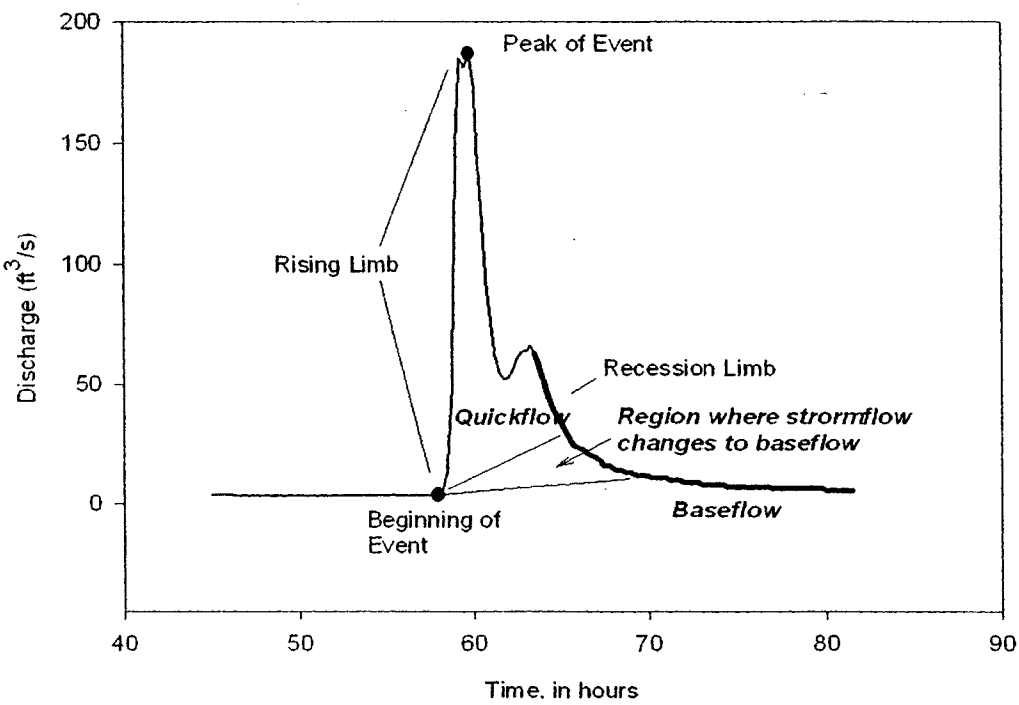

Figure 4.3. Typical hydrograph for Puerto Rican streams illustrating the components of the hydrograph.

Barnes (1939) separated hydrographs of the Upper Mississippi Valley into three components: surface-flow, storm-seepage, and base-flow. Surface flow is the direct route of precipitation over land to the stream channel without infiltration. This is often referred to as "Hortonian overland flow" and occurs when precipitation intensity exceeds infiltration capacity. If sediment sources are common on hillslopes, this type of flow may contribute a large amount of sediment to the stream. Saturation overland flow occurs when the soil profile becomes saturated via throughflow, the water table rises to the surface, and overland flow occurs. Storm-seepage, also referred to as interflow and throughflow, is movement of water through the upper soil layers

Reproduced with permission of the copyright owner. Further reproduction prohibited without permission.

that discharges into the river during and shortly after the rainfall event. Large increases in runoff may be a result of throughflow (Scanlon and others, 2001). Base flow is the contribution from storage in groundwater at a deeper level.

Scanlon and others (2001) refer to three conduits of flow that make up the hydrograph: (1) saturated overland flow (Hortonian), (2) shallow soil flow (throughflow), and (3) deeper groundwater flow. Hortonian flow is active only during the initial rise in the hydrograph and makes a small contribution to the overall volume of water (Scanlon and others, 2001). The two pathways that contribute most of the stream discharge are throughflow and groundwater. Throughflow is important when precipitation amounts are sufficient, antecedent conditions are wet, and the shallow water table may be perched. Preferential pathways can be through the A and B horizons (Hammermeister and others, 1982). Under these conditions throughflow can cause a rapid rise in the hydrograph and provide large volumes of water to stream discharge.

Hewlett and Hibbert (1967) described conventional methods of hydrograph separation as "...one of the most desperate analysis techniques in use in hydrology." Among other problems in defining the water budget for a hydrologic event involves the qualitative selection of where storm runoff begins and ends. Hewlett and Hibbert (1967) state that using graphical techniques, interflow is impossible to distinguish from base flow. Kulandaiswamy and Seetharaman (1969) cited the lack of adequate explanations in Barnes' (1939) detail of interflow delineations, which makes the "Barnes" method for the separation of the hydrograph into three components unsuitable. More recent work in separating hydrographs into surface flow, interflow, and base flow has been directed towards a quantitative approach using chemically-based hydrograph separation (Takeuchi and Sakamoto, 1986; Ogunkoya and Jenkins, 1993). In chemically-based hydrograph separation,

Reproduced with permission of the copyright owner. Further reproduction prohibited without permission.

ground water or 'old water' has a distinct chemical signature from 'new water' or incident precipitation, overland flow, and rapid subsurface flow (Ogunkoya and Jenkins (1993).

Hydrograph separation assumes that surface runoff causes the increases in streamflow from precipitation. The assumption that all floods may not be a result of surface runoff was argued by Hewlett and Hibbert (1967). In small forested watersheds of the American east (<20 mi^2; 52 km^2), Hewlett and Hibbert (1967) postulated that streamflow is a result of a shrinking and expanding source area; the variable source area concept. The portion of a watershed that contributes to streamflow expands and contracts depending on rainfall amounts and antecedent conditions. Adequate vegetation in the forests increases infiltration, and during precipitation events subsurface flows predominate. Work in forested watersheds using chemical tracers to separate groundwater from surface water support Hewlett and Hibbert's (1967) idea that groundwater may be more important in generating streamflow events. Ground water accounted for 74-90% of storm runoff in forested Appalachian watersheds (Swistock and others, 1989), and in forested areas of Scotland, groundwater accounted for 53-66% of runoff (Ogunkoya and Jenkins, 1993).

Runoff events at the four streamflow stations analyzed in this study were delineated using hydrograph separation techniques. The term 'quickflow' used by Hewlett and Hibbert (1967) for direct runoff which included overland flow and throughflow, is used in this manuscript. For the purposes of this research, the hydrograph was separated into quickflow (overland flow, saturated overland flow, and throughflow) and base flow. The beginning of a storm runoff event is defined by a steep rise in the hydrograph or as the departure from base flow. Most of the hydrographs at the streamflow stations showed abrupt rises and the beginning of the event was apparent. Defining

Reproduced with permission of the copyright owner. Further reproduction prohibited without permission.

the end of an event where quickflow ends and base flow begins is often a more difficult task (Pettyjohn and Henning, 1979).

Four graphical techniques were examined as part of this PhD dissertation to define the end of a runoff event and develop a consistent methodology. To determine the best graphical technique and therefore, lessen the ambiguity in selecting the end of stormflow runoff, hydrographs at three streamflow stations (50051150, 51151180, and 50075000; fig. 1.1) were used to develop a methodology

Method 1.

The areal extent equation (Linsley and others, 1982), defines the end of the event using the equation:

$$N = A^{0.2}$$

where; N = the number of days after a peak when surface runoff ceases, and A is the basin area in square miles.

Method 2.

The "eyeball " method (Pettyjohn and Henning, 1979) extends a straight line from the beginning of the event to the end of the event. The end of the event is described as the inflection point on the hydrograph recession curve.

Method 3.

The inflection point on the recession curve was obtained by drawing a 45-degree line tangent to the hydrograph recession curve. The equation for the recession curve was obtained by

Reproduced with permission of the copyright owner. Further reproduction prohibited without permission.

fitting a 3rd order regression line to this portion of the hydrograph. The equations for the 45-degree line and for the 3rd order regression were set equal to each other to find the point common to both curves.

Method 4.

The fourth method was developed as part of this research. It is based on graphical features of the hydrograph where the break in maximum curvature of the recession curve or inflection point is described as the point where surface flow ceases and base flow begins. The inflection point on the hydrograph recession curve was obtained by taking the second derivative of a 3rd order best-fit regression line to the recession portion of the hydrograph. The second derivative of a 3rd-order equation is the inflection point of the curve or where concavity changes (Hughes-Hallett, 1994).

In methods 2, 3, and 4, the recession limb of the hydrograph had to fall below a threshold discharge and reach a threshold slope for it to be considered the end of the event. A discharge was chosen at each station as a threshold based on analysis of base-flow recession curves. A base-flow recession curve slope was calculated as discharge over time during a period when a runoff event had not occurred for several days. Recession curves were developed for each station using methods outlined by Nathan and McMahon (1990) and Rutledge (1997). Examination of these curves determined the discharge at which base flow was dominant. This was the discharge selected at each station as the threshold discharge. The threshold slope was determined by analysis of the base flow recession curves. Recession slopes were developed for periods of known base flow and averaged to obtain one recession slope value. This slope was used as the threshold slope to determine when a runoff event was in base flow.

Reproduced with permission of the copyright owner. Further reproduction prohibited without permission.

Results of hydrograph separation methodologies

All four of the methods listed to determine the end of an event were examined for 3 stations (Quebrada Blanca at El Jagual 50051150; Quebrada Salvatierra near San Lorenzo 50051180; Rio Icacos near Naguabo 5007500; fig. 1.1) and the volume of quickflow compared (Table 4.2; fig. 4.4). The volume of quickflow was computed by drawing a straight line from the beginning to the end of the event, defined by each methodology, and calculating the area under the hydrograph.

Method 1 always predicted the end of the event the same number of days from the peak. For example, at Quebrada Blanca at El Jagual, the end point is always 1.27 days from the peak of the event. This method does not take into account the variance in magnitude of peak flows nor the number of peaks in an event. Many hydrographs in Puerto Rican streams peak at the same time from the beginning of the event but have different magnitudes of peak flows. Method 1 appears more suitable for large river basins where the end of the event may be recorded in days and therefore, this method to determine the end of the runoff event was not used.

Method 2, the selection of the end of the event by choosing an inflection by eye is subjective. The method appears suitable for single and multi-peaked events that have a sufficient time gap until the next event. It was found that in closely spaced events, this selection process was prone to errors associated with repeatability. This method was not used.

Method 3, drawing a 45-degree line tangent to the recession curve, proved to be somewhat subjective when the recession curve did not have a well-defined concavity and plotted early on the recession curve. This method was not used.

Reproduced with permission of the copyright owner. Further reproduction prohibited without permission.

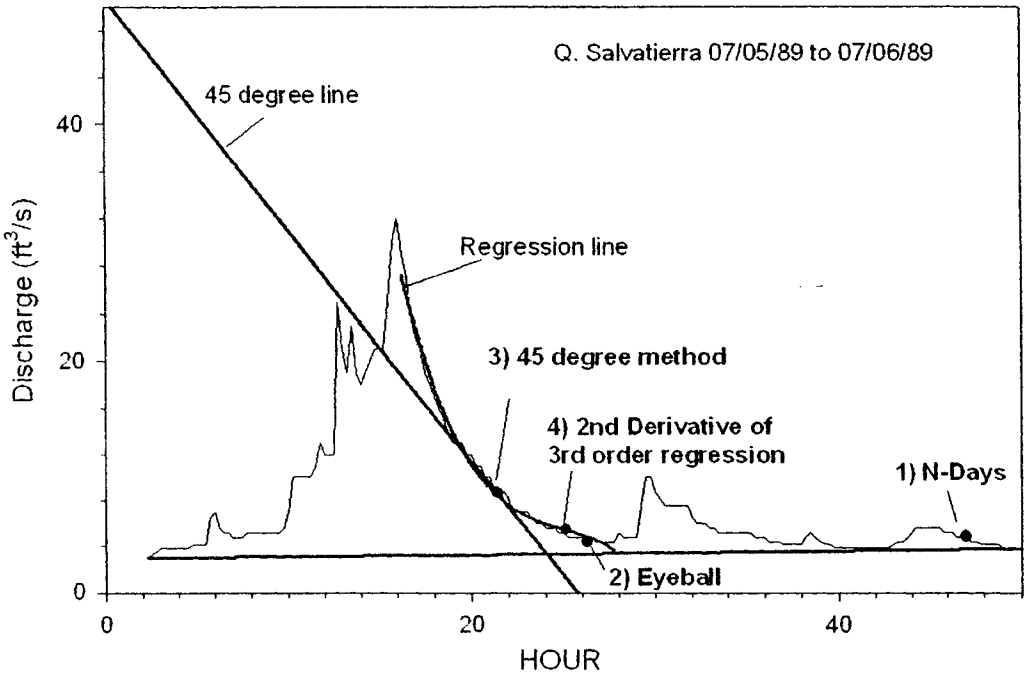

Figure 4.4. Comparison of methodologies to determine the end of the runoff event: 1) N-Days, 2) eyeball, 3) 45-degree method, and 4) 2nd derivative of a 3rd order best-fit regression.

Table 4.2. Results of methodologies to determine the end of the runoff event.
A) Quebrada Blanca at El Jagual

Method tested	Start date of event	Start time (hour: minute)	End date	End time (hour: minute)	Quickflow (ft^3)
Method 1- N-Days	6/20/1992	17:45	6/22/1992	11:15	2,218,140
Method 2 - Eye	6/20/1992	17:45	6/23/1992	12:00	2,973,690
Method 3 - 45-Degree	6/20/1992	17:45	6/23/1992	13:45	2,985,340
Method 4- 2^{nd} derivative	6/20/1992	17:45	6/22/1992	15:30	2,482,740

Reproduced with permission of the copyright owner. Further reproduction prohibited without permission.

Table 4.2 B) Quebrada Salvatierra near San Lorenzo.

Method tested	Start date of event	Start time	End date	End time	Quickflow (ft^3)
Method 1	7/05/1989	02:15	7/06/1989	23:00	The end point does not plot on the hydrograph recession but plots in the next event
Method 2	7/05/1989	02:15	7/06/1989	02:15	607,050
Method 3	7/05/1989	02:15	7/06/1989	01:00	569,340
Method 4	7/05/1989	02:15	7/05/1989	21:30	416,700

Table 4.2 C) Rio Icacos near Naguabo

Method tested	Start date of event	Start time	End date	End time	Quickflow (ft^3)
Method 1	11/06/1994	10:00	11/07/1994	12:30	The end point does not plot on the hydrograph recession but plots in the next event
Method 2	11/06/1994	10:00	11/07/1994	02:30	1,968,530
Method 3	11/06/1994	10:00	11/07/1994	03:00	2,190,960
Method 4	11/06/1994	10:00	11/06/1994	17:45	1,683,750

Method 4, using the 2nd derivative of a 3rd order best-fit regression to the recession curve, provided a consistent methodology and consistent results. Method 4 was used in this research to determine the end of a runoff event. For Method 4, a regression line is fitted to the recession curve

Reproduced with permission of the copyright owner. Further reproduction prohibited without permission.

of the hydrograph. The selection of the beginning and the end of the recession curve of an event can be difficult to determine. To be consistent, a methodology was developed to select the beginning and the end of the recession curve. The end of the recession curve of the hydrograph was selected where base flow should be dominant and the slope of the recession curve should flatten. The point where base flow should be dominant was based on recession slope analysis for each station (Table 4.3). For an event to be defined as a separate event, recession flow at a station would have to reach this threshold recession slope over a specified period of time and fall at or below a threshold base flow. The threshold base flow was based on observations of recession curves. The calculated inflection point used to mark the end of the event did not have to fall below this threshold base flow.

Once a threshold base flow is selected there still exists subjectiveness in selecting the beginning and the end of the recession portion of the hydrograph. To determine the variance in stormflow runoff by selection of the beginning of the recession curve, several beginning and end curves were selected, and a comparison of the volume of runoff calculated for each selection was made (Table 4.4).

The lowest and highest values of quickflow differed by 13% for Quebrada Blanca, 7% for Quebrada Salvatierra, and 8% for Rio Icacos. Selection of the beginning of the hydrograph recession curve immediately below the peak provided the most consistent results.

Complex Events

Events that are closely spaced in time are termed "complex events" (fig. 4.5). In complex events the recession portions of the storm hydrographs approach but never reach base flow as

Reproduced with permission of the copyright owner. Further reproduction prohibited without permission.

Table 4.3. Values for base flow and recession limb slope used in Method 4.

Station	Threshold recession limb slope over listed hours	Threshold base flow (ft^3/s)
R. Icacos	0.018 ft^3/s over 2.0 hours	10
Q. Blanca	0.005 ft^3/s over 2.5 hours	12
R. Caguitas	0.010 ft^3/s over 2.5 hours	12
R. Piedras	0.006 ft^3/s over 2.0 hours	10

Table 4.4. Analysis on the selection of the end of the runoff event using the 2nd-derivative for various start and end times on the hydrograph recession curve. A "*" denotes that this end time was selected as the best time to define the end of the event.

A) Quebrada Blanca at El Jagual - Start of event on 6/20/92 at 17:45

Hydrograph recession beginning date and time	Beginning discharge (ft^3/s)	Hydrograph recession end date and time	End discharge (ft^3/s)	End date and time of inflection point	End discharge (ft^3/s)	Quickflow (ft^3)
6/21/1992 @ 05:45	60	6/24/1992 @ 08:45	5.7	6/23/1992 @ 05:45	8.0	2,756,160
6/21/1992 @ 23:45	16	6/24/1992 @ 05:45	5.7	6/23/1992 @ 15:00	6.0	3,079,530
6/22/1992 @ 01:30	16	6/24/1992 @ 03:00	5.7	6/23/1992 @ 10:30	8.4	2,757,870
6/22/1992 @ 01:30	16	6/24/1992 @ 05:45	5.7	* 6/23/1992 @ 13:45	6.7	2,985,340
6/22/1992 @ 01:30	16	6/24/1992 @ 10:00	5.7	6/23/1992 @ 18:30	6.0	3,098,430
6/22/1992 @ 02:30	15	6/24/1992 @ 05:45	5.7	6/23/1992 @ 13:45	6.7	2,985,340
6/22/1992 @ 04:00	15	6/24/1992 @ 03:00	5.7	6/23/1992 @ 10:30	8.4	2,757,870
6/22/1992 @ 04:00	15	6/24/1992 @ 16:45	4.6	6/23/1992 @ 20:30	6.0	3,109,230

Reproduced with permission of the copyright owner. Further reproduction prohibited without permission.

Table 4.4 Continued

B) Quebrada Salvatierra near San Lorenzo - Start of event on 7/05/1989 at 02:15

Hydrograph recession beginning date and time	Beginning discharge (ft^3/s)	Hydrograph recession end date and time	End discharge (ft^3/s)	End date and time of inflection point	End discharge (ft^3/s)	Quickflow (ft^3)
7/05/89 @ 16:15	29	7/06/89 @ 03:45	4.4	* 7/06/89 @ 01:00	5.3	569,340
7/05/89 @ 17:00	22	7/06/89 @ 03:45	4.4	7/06/89 @ 03:00	4.4	609,300
7/05/89 @ 17:00	22	7/06/89 @ 02:00	4.8	7/06/89 @ 01:00	5.2	569,340
7/05/89 @ 17:45	18	7/06/89 @ 03:45	4.4	7/06/89 @ 05:45	10	The end point does not plot on the hydrograph recession but plots in the next event
7/05/89 @ 17:30	19	7/06/89 @ 03:45	4.4	7/06/89 @ 05:30	10	The end point does not plot on the hydrograph recession but plots in the next event
7/05/89 @ 18:15	16	7/06/89 @ 03:45	4.4	7/06/89 @ 20:30	5.6	The end point does not plot on the hydrograph recession but plots in the next event

Reproduced with permission of the copyright owner. Further reproduction prohibited without permission.

Table 4.4 Continued

C) Rio Icacos near Naguabo - Start of event on 11/06/1994 at 10:00am

Hydrograph recession beginning date and time	Beginning discharge (ft^3/s)	Hydrograph recession end date and time	End discharge (ft^3/s)	End date and time of inflection point	End discharge (ft^3/s)	Quickflow (ft^3)
11/06/1994 @ 15:30	63	11/07/1994 @ 09:30	5.7	* 11/07/1994 @ 3:00	7.2	2,160,960
11/06/1994 @ 15:30	63	11/07/1994 @ 08:00	5.7	11/07/1994 @ 2:15	8.0	2,130,330
11/06/1994 @ 16:00	51	11/07/1994 @ 02:30	7.2	11/06/1994 @ 23:15	10.0	2,051,360
11/06/1994 @ 16:00	51	11/07/1994 @ 05:00	6.4	11/07/1994 @00:45	9.0	2,092,200
11/06/1994 @ 16:30	41	11/07/1994 @ 09:30	5.7	11/07/1994 @ 03:45	7.2	2,165,860
11/06/1994 @ 16:30	41	11/07/1994 @ 08:00	5.7	11/07/1994 @ 03:00	7.2	2,160,960
11/06/1994 @ 17:30	27	11/07/1994 @ 08:00	5.7	11/07/1994 @ 03:45	7.2	2,165,860
11/06/1994 @18:00	24	11/07/1994 @ 02:30	7.2	11/07/1994 @ 00:15	9.0	2,087,280
11/06/1994 @ 18:00	24	11/07/1994 @ 08:00	5.7	11/07/1994 @ 04:00	7.2	2,167,500
11/06/1994 @ 19:30	16	11/07/1994 @ 08:00	5.7	11/07/1994 @ 06:00	6.4	2,205,470

defined for regular events. However, the individual runoff portions that make up the complex event may be considered isolated because discrete rainfalls are responsible for each rise in runoff. In addition, not all the major rises and falls in discharge in a complex event may be sampled for suspended sediment and removing a portion of the complex event eliminates the need to estimate sediment concentrations in unsampled portions of the hydrograph.

Reproduced with permission of the copyright owner. Further reproduction prohibited without permission.

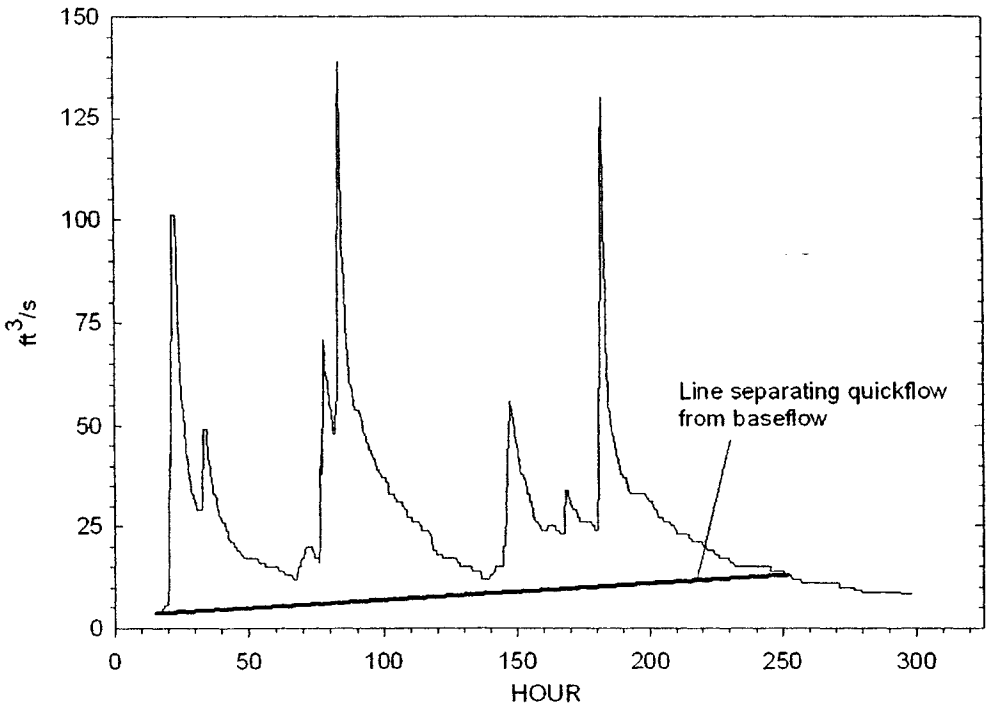

Figure 4.5. Example of a complex runoff event with several peak flows and concave portions on the recession limb, Quebrada Blanca 11/21/1991 to 12/01/1991.

Just as with the determination of a single runoff event, complex event hydrographs were delineated into separate runoff events if the hydrograph recession fell below a threshold discharge and reached a threshold slope. This threshold discharge could still be in quickflow but is close to base flow. The threshold discharge was based on examination of recession curves and was always higher than the value used to determine the end of a single event. If the hydrograph recession met the threshold discharge and threshold slope criteria, the end of the event was selected just before the next hydrograph rise. The final recession limb of the complex event had to meet the criteria established for a single event. In addition to the threshold definitions above, a plot of rainfall with the hydrograph helped to determine when complex events should be separated into individual events. The values used to define complex events are shown in table 4.5.

Reproduced with permission of the copyright owner. Further reproduction prohibited without permission.

Table 4.5. Values for base flow and recession limb slope used to define complex events.

Station	Threshold recession limb slope (cfs/hour) over listed hours	Threshold discharge (ft^3/s)
R. Icacos	0.5 over 2 hours	17
Q. Blanca	0.5 over 2 hours	15
R. Caguitas	0.5 over 2 hours	16
R. Piedras	0.5 over 2 hours	20

Quickflow Calculation

There are at least 3 methods to quantify quickflow from base flow once the beginning and end of the hydrograph have been defined (Dunne and Leopold, 1978; Pettyjohn and Henning, 1979) (fig. 4.6). The first method continues the pre-storm base flow under the peak. A line is then drawn from the point under the peak to the end of the event (fig. 4.6a). The second method projects the base flow recession increasing under the peak of the event. A line is then drawn from the beginning of the event to this point under the peak (fig. 4.6b). These conditions of groundwater rise during the event are thought to occur in small catchments (Hall, 1971). A third method simply draws a straight line from the beginning to the end of the event (fig. 4.6c).

Reproduced with permission of the copyright owner. Further reproduction prohibited without permission.

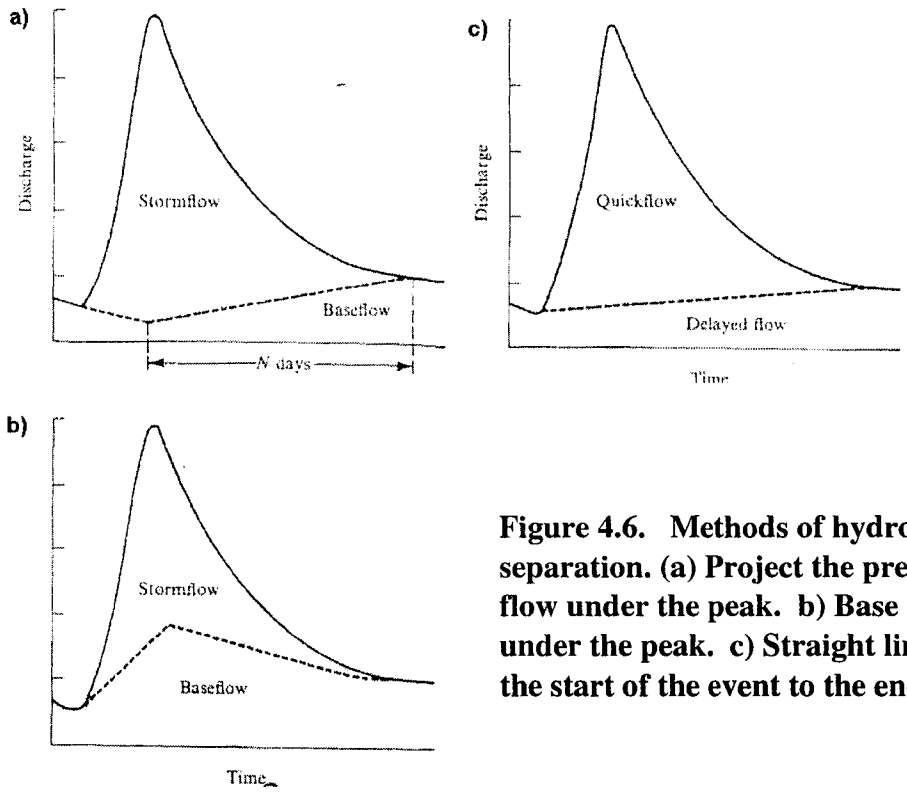

Figure 4.6. Methods of hydrograph separation. (a) Project the pre-storm base flow under the peak. b) Base increase under the peak. c) Straight line drawn from the start of the event to the end.

Differences in the separation of the hydrograph into quickflow using the straight line method in figure 4.6 versus the other methods were analyzed for two stations (50051150, 500511800 (fig. 4.7; Table 4.6). Several rates of either base flow increase or decrease under the peak flow were selected. For Quebrada Blanca, the straight line method (Method 3) had a maximum difference of 27% with respect to a base flow rise under the peak flow (Method 1) and a maximum difference of 5% for a base flow decrease under the peak flow (Method 2). For Quebrada Salvatierra, Method 3 had a maximum difference of 13% with respect to both Methods 1 and 2.

Reproduced with permission of the copyright owner. Further reproduction prohibited without permission.

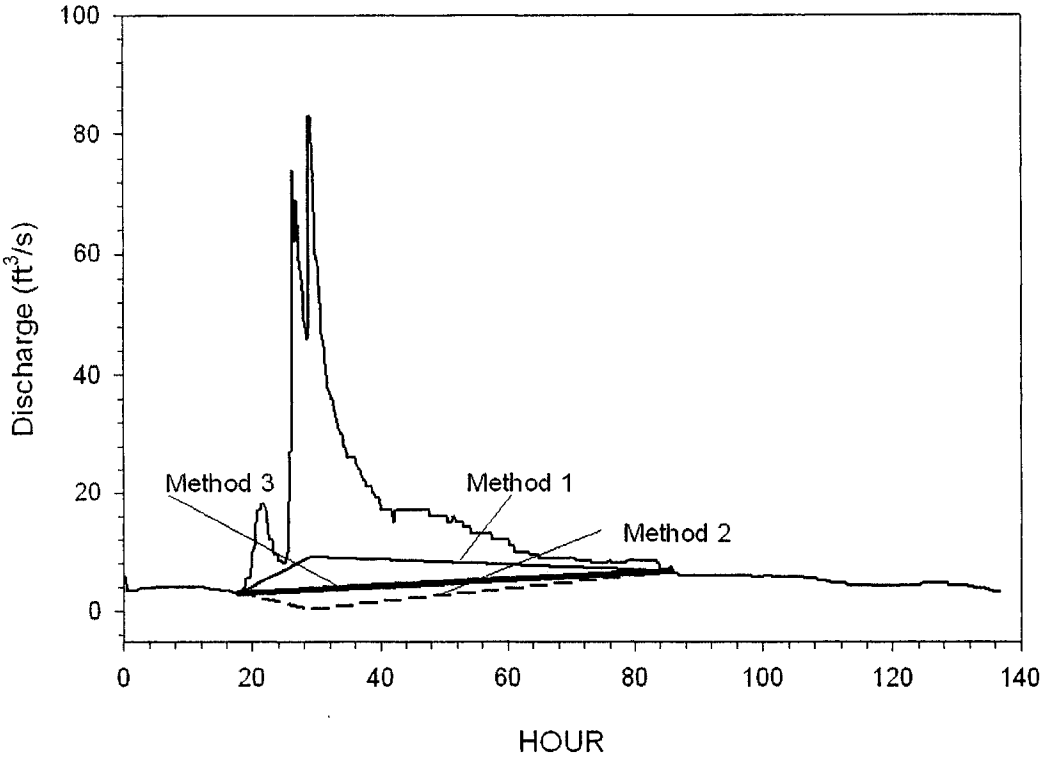

Figure 4.7. Differences in quickflow determinations using an event at Quebrada Blanca near El Jagual (6/20-23/1992) for the three methods outlined in figure 4.6.

Determining whether base flow recession increases or decreases under peak flow requires knowledge of the physical and biologic components controlling groundwater; particularly the geology of the basin and streamside deposits. Information on groundwater characteristics for the Puerto Rican streams analyzed in this study was not available, and therefore, the hydrograph was separated by drawing a straight line from the beginning of the event to the end of the event. In complex events a line was drawn from the beginning of the first runoff event to the end of the entire event. In complex events the discharge at the end of each event would not be base flow. Base flow would plot below the end discharge and the difference in discharge between the two values was recorded (fig. 4.8).

Reproduced with permission of the copyright owner. Further reproduction prohibited without permission.

Table. 4.6. Results of analysis of methodology to determine the volume of quickflow in a runoff event. *(Method 1 - base flow rise under peak flow; Method 2 - base flow decrease under peak flow; Method 3 - straight line from beginning to the end of the event.*

A) Quebrada Blanca at El Jagual - Event from 6/20/92 @ 17:45 to 6/23/92 @ 13:45

Base flow recession (ft^3/s per hour)	**Quickflow (ft^3)**	**Method tested**
0.061	2,180,140	Method 1
0.050	2,256,880	Method 1
0.042	2,312,700	Method 1
0.061	3,140,740	Method 2
0.050	3,125,920	Method 2
0.042	3,115,150	Method 2
	2,985,340	Method 3

B) Quebrada Salvatierra near San Lorenzo - Event from 7/05/89 @ 02:15 to 7/06/89 @ 10:45

Base flow recession (ft^3/s per hour)	**Quickflow (ft^3)**	**Method tested**
0.10	496,840	Method 1
0.08	504,220	Method 1
0.0042	532,160	Method 1
0.04	646,30	Method 2
0.017	633,170	Method 2
0.0042	626,160	Method 2
	569,340	Method 3

Reproduced with permission of the copyright owner. Further reproduction prohibited without permission.

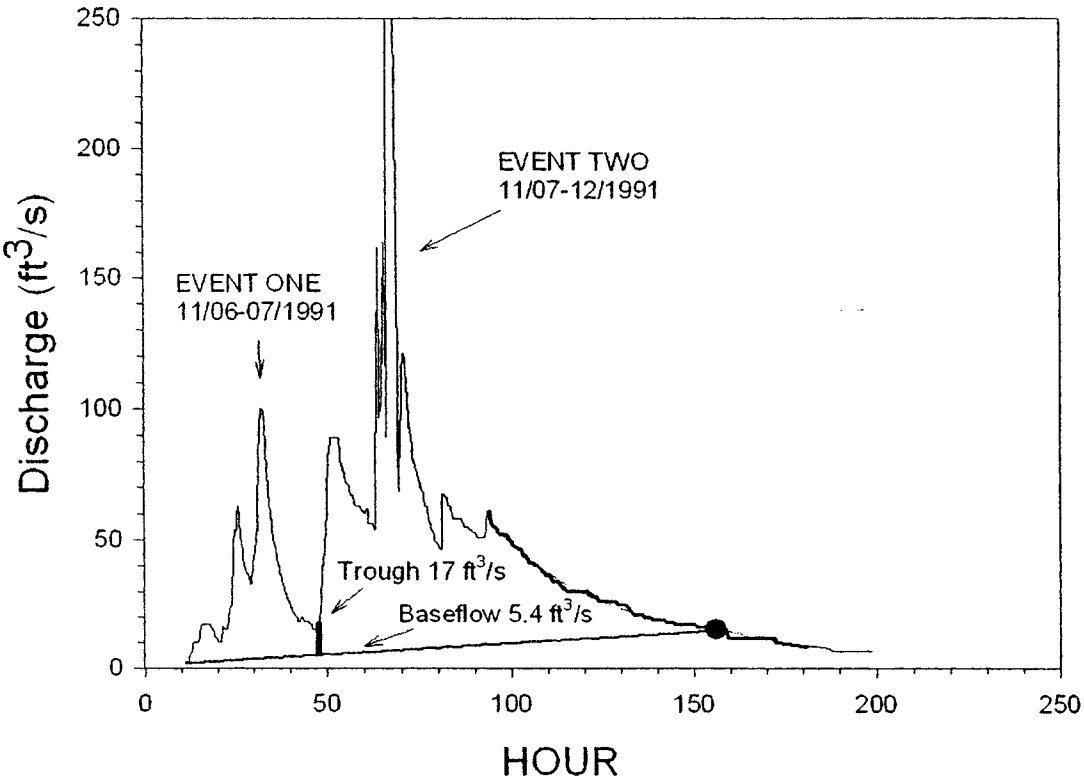

Figure 4.8. Example of a complex event for Quebrada Blanca near El Jagual illustrating the difference from the end of an event to base flow. In this example, the difference was 17 ft^3/s - 5 ft^3/s = 12 ft3/s.

Sediment Transport and Erosion

Hillslope erosion

Sheetwash and rainsplash are responsible for most hillslope erosion. Sheetwash is the erosion and transport of soil from a hillslope by tiny streams that move back and forth across the hillslope during a rainstorm (Dunne and Leopold, 1978). To determine sheetwash erosion on hillslopes of different land cover in Puerto Rico, Gellis and others (1999) and Larsen (1997) instrumented hillslopes with sediment traps. Data used in their reports are analyzed and summarized in this study. A description of their collection methods follows.

Reproduced with permission of the copyright owner. Further reproduction prohibited without permission.

Twelve slopes representing principal land-use categories in the Lago Loiza basin (forest, pasture, agriculture, and constructions sites) were selected for measurement of sheetwash erosion (fig. 4.9). The period of data collection from Gellis and others (1999) extended from February 7, 1991 through December 12, 1992 and Larsen (1997) from November 27, 1991 through February 22, 1995. Hillslope runoff and sediment were collected in a sediment trap or Gerlach trough in unbounded plots (Gerlach, 1967). The Gerlach trough was a collection trough 52 cm wide and 8.5 cm deep. To prevent raindrops from entering the trap, a lid made of sheet metal was fitted with a hinge to the back of the trap. Two 1.27 cm (½ inch) diameter holes were drilled into the side of the trap, one at the bottom and one in the center and fitted with a 1.9 cm (3/4 inch) hose barb. Both holes were connected to 18.9 liter (5 gallon) collection buckets. The center hole was designed to operate if the bottom hole became clogged with organic debris. Traps were visited at selected time intervals. If water was present in the bucket, the bucket was weighed in the field with a hand scale, water was poured out, and sediment from the collection bucket and trough was transferred to another bucket and brought to the laboratory. At select times a sample of the poured water was taken back to the laboratory to determine the amount of sediment. The water-sediment mixture was dried at 105^0 C for 24 hours and weighed. Selected samples with a high organic content were dried at 550^0 C for 1-hour.

Gerlach troughs were installed at each hillslope in unbounded plots. To determine contributing areas, Gellis and others (1999) used a total station to survey the hillslope. The coordinates of each surveyed point were entered into a computer software package and a topographic map was generated for each site. The contributing area for each trap was then delineated and digitized to compute contributing area and slope. Larsen (1997) estimated the

Reproduced with permission of the copyright owner. Further reproduction prohibited without permission.

Reproduced with permission of the copyright owner. Further reproduction prohibited without permission.

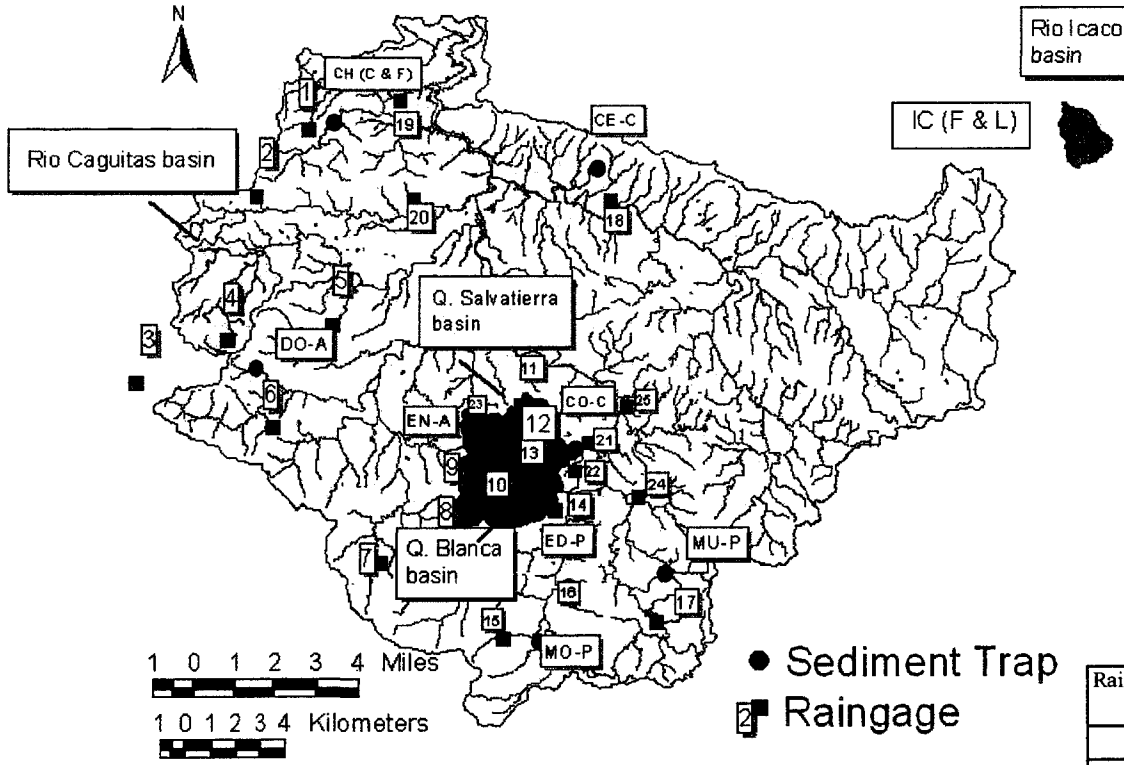

Site ID	Land Cover	Soils	Vegetation
CE-C	*Construction* site	*Naranjito silty* clay loam	*bare*
CH-C	Construction site	Humatas clay	bare w/ some shrubs
CO-C	Construction site	Cayaguas sandy loam	bare to minimal vegetation
EN-A	Cropland	Naranjito silty clay loam	mixed fruits (plaintains, tanniers, ams, pigeon peas, and bananas)
DO-A	Cropland	Humatas clay	mixed fruits (plaintains, grapefruits, and oranges)
ED-P	Pasture	Pandura sandy loam	grass
MO-P	Pasture	Pandura sandy loam	grass
MU-P	Pasture	Pandura sandy loam	grass
CH-F	Forest	Naranjito silty clay loam	secondary growth forest
IC-F	Forest	Humatas clay	Colorado forest
IC-L	Landslide scar	Humatas clay	bare

Rain ID	USGS Station ID	Rain ID	USGS Station ID
1	50999963	14	50999957
2	50999964	15	50999902
3	50075500	16	50050900
4	50999962	17	50999960
5	50999965	18	50057000
6	50999966	19	50058350
7	50999961	20	50055390
8	50999955	21	50051180
9	50999952	22	50051150
10	50999951	23	50999950
11	50999953	24	50051310
12	50999954	25	50051800
13	50999956		

Figure 4.9. Location of sediment traps and rangages used in this research.

contributing area with a metric trap and noted that the drainage area estimated in this way may be off by as much as a factor of two. Bounding the contributing area to the Gerlach Troughs with an impervious material may be a more satisfactory method (Loughran; 1989; Gellis and others, 2001).

Erosion rates for each trap were determined as the volume-weighted sediment concentration and sediment yield. The volume-weighted sediment concentration, reported as ppm, is the sum of the total sediment mass retained divided by the runoff (sediment and water) for the period of record. Not all traps were operating during the same period of time. The volume-weighted sediment concentration normalizes the data for differences in collection period by dividing sediment by runoff. Sediment yield is defined as cumulative sediment, in grams, divided by drainage area, in square feet, and by the number of days the trap was in operation (grams/ft^2/day).

Fluvial sediment

This study emphasizes suspended-sediment transport at a station. Bedload was not measured as part of this study. Larsen (1997) quantified bedload transport in the Rio Icacos using bed material transport equations and Gellis and others (1999) quantified bedload transport in the Rio Gurabo, a tributary to Lago Loiza, using resurveys of a sediment pool. Results from these studies are cited in this report.

Data Collection

Suspended-sediment samples were collected during low and high flows at each station. Low flow suspended-sediment samples were collected by USGS personnel or local observers

Reproduced with permission of the copyright owner. Further reproduction prohibited without permission.

using conventional USGS depth-integrating samplers: either a DH-48 hand-held sampler or a D-74 bridge sampler (Edwards and Glysson, 1988). Suspended-sediment samples were collected with the DH-48 hand-held sampler and the D-74 bridge sampler at a single vertical in the channel cross section. At select times the DH-48 hand-held sampler collected samples at various points in the cross section using the equal width increment (EWI) method (Edwards and Glysson, 1988). During high flows suspended-sediment samples were collected with the EWI method using a sediment sampler attached to a crane or at a single vertical in the channel using a D-74 bridge sampler.

All of the streamflow stations were instrumented with an automatic pump sampler that was activated during high flows. The automatic pump sampler is a device capable of collecting 24 separate, sequential water-sediment samples. The pump sampler had an intake pipe with a sensor that was installed close to or just below the bankfull discharge elevation. The sensor detected water and activated the pump sampler. The pump sampler then collected samples at pre-programmed intervals. At some streamflow stations the pump sampler was activated by the Data Collection Platform (DCP). The DCP had an encoder that is calibrated to read the gage height of the water, in feet. A gage height was entered into the DCP program which was set to emit an electrical charge when the water reached the programmed gage height to activate the automatic sampler (Richards, 1991). After activation, the automatic pump sampler collects samples at programmed time intervals. The time intervals were based on investigation of hydrographs for that stream. The automatic samplers utilized a peristaltic pump system to transport the sample from the stream to the sample bottle. The suction line was cleared by the sampler before and after each sample was collected.

Reproduced with permission of the copyright owner. Further reproduction prohibited without permission.

For this study a record of suspended-sediment samples collected at the four basins were obtained from the USGS Caribbean District. Many of the automatic pump samplers were activated by stage. Many of the times recorded on the record sheets provided by the USGS were rounded off to the nearest 15-minute value. Some of the values were also incorrect. The gage height at which the automatic sampler was activated is known. To obtain the most accurate time for each sample, the time at which the automatic sampler was activated was interpolated between15-minute gage-height values.

The most accurate method for obtaining a representative suspended-sediment concentration for a channel cross sections is using the EWI method (Edwards and Glysson, 1988). All other suspended-sediment sampling methods (single vertical and automatic pump samplers) should be calibrated to an EWI. When single vertical or automatic pump samplers are collected in conjunction with an EWI, a calibration coefficient is calculated. The calibration coefficient is the suspended-sediment concentration of the EWI divided by the suspended-sediment concentration from the sampling method. The calibration coefficient is applied to the single vertical and automatic pump suspended-sediment samples at that time of collection. Investigation of the data determined whether the calibration coefficient was applied to samples collected at other times. This decision was based on the number of times samples are calibrated and their distribution of collection times relative to discharge. Because suspended-sediment concentrations vary with water discharge, all values should be considered as instantaneous and representative only of the discharge at the given location and time. At each station every attempt was made to calibrate the bridge samplers and the automatic pump samplers to an EWI. Because of the 'flashiness' of most runoff events and the hours in the day they would occur, the automatic pump samplers were seldom calibrated.

Reproduced with permission of the copyright owner. Further reproduction prohibited without permission.

Suspended-sediment samples were brought to the USGS laboratory for analysis of concentration and selected samples were analyzed for particle sizes. Determination of suspended-sediment concentration was made by the evaporation or filtration method (Guy, 1969). In the evaporation method, sediment was allowed to settle in the bottom of the sample bottle and the supernatant liquid was decanted. The sediment was washed into an evaporating dish, dried in an oven, and later weighed. Similar steps were followed in the filtration method except that instead of washing the sediment into an evaporating dish, the sediment was filtered through a glass-fiber filter (mesh size of 0.4 micrometers) into a crucible, and was then oven dried.

The concentration of suspended-sediment is equal to the ratio of the dry weight of sediment to the volume of the water-sediment mixture. This concentration was computed as a weight to weight ratio and is expressed in parts per million (ppm). A conversion factor was used to convert ppm to milligrams per liter (mg/L) using the assumption that water density is equal to 1,000 mg/mL plus or minus 0.005, temperature is from 0^0 to 29^0C, specific gravity of suspended sediment is 2.65 g/mL, and the dissolved solids concentration is less than 10,000 ppm (Guy, 1969). For concentrations less than 15,900 ppm the conversion factor is equal to unity. Particle-size analysis of suspended sediment included percent sand (>0.062 mm) and percent silt and clay (<0.062 mm). Size analysis was performed by sieving the sample through a 0.064 mm screen.

Sediment-Transport Curves

The relationship of instantaneous water discharge to suspended-sediment concentration is referred to as a sediment-transport curve (Glysson, 1987). Sediment-transport curves are often used to estimate suspended-sediment concentrations when data are not available. Frequently this

Reproduced with permission of the copyright owner. Further reproduction prohibited without permission.

is performed during the calculation of suspended-sediment loads. Sediment-transport curves can also be used to determine differences in the transport of sediment as a result of seasons (Curtis and others, 1978; Lopes and Ffolliott, 1993), land use (Gellis, 1991), geology (Larsen, 1997), and storm events (Gellis, 1993).

Sediment-transport curves were generated for each station for the period being analyzed. Several types of curves were generated. A sediment-transport curve was generated for all data and a least-squares linear regression line was fitted through the data using a standard software graphing package. Visual inspection of the data was used to determine if the best-fit line should be separated into two or more portions. Sediment-transport curves were further separated into samples collected on the rising and falling limbs of the hydrograph to the highest peak discharge as well as relative to the flow of an individual peak. Sediment transport curves were also developed for different seasons.

The hypothesis that previous events and previous peaks in the current event affect suspended-sediment concentrations was tested. To determine whether previous events affect the current event suspended-sediment concentration, samples taken on the rising limb to the highest peak discharge were separated into groups defined by the previous-event runoff divided by the time since the end of the previous event and plotted against suspended-sediment concentration. The hypothesis tested is that samples collected very close to a large runoff event would have lower suspended-sediment concentrations than those samples collected after a large time interval since the last runoff event. To determine if previous peaks in a multipeaked event were affecting suspended-sediment concentrations, suspended samples of the current event were separated into

Reproduced with permission of the copyright owner. Further reproduction prohibited without permission.

groups categorized by the magnitude of the previous peak flow. It is expected that samples collected after a large peak discharge would show lower suspended-sediment concentrations.

Walling (1996) reported that in most rivers the amount of sand in suspension is controlled by hydraulic variables and increases with increased discharge. To test the relationship of discharge to suspended sand, sediment-transport curves of discharge versus percent sand were generated. Sediment-transport curves of percent sand were then separated into rising and falling samples relative to the highest peak discharge. Sediment-transport curves of suspended-sediment concentration versus percent sand were also generated to determine whether at higher suspended-sediment concentrations the percent of sand in transport changes.

In this analysis of sediment-transport curves, Walling's (1974) four variables: 1) discharge minus base flow, 2) time relation of sample to major peak, 3) base flow at start of the event, and 4) index of flood intensity, were analyzed to determine whether this improved the relation of suspended-sediment concentrations to discharge. Discharge with and without base flow was examined. Base flow was determined by a linear equation from the beginning to the end of each event and subtracted from the discharge of each suspended-sediment sample. The dependent variable, suspended-sediment concentration, was also separated into rising and falling samples. The time relation of the sample, in minutes, is negative before the peak and positive afterwards. Flood intensity was defined the same way as Walling (1974), as follows:

$$\textit{Flood intensity} = \frac{\textit{hydrograph peak - flow level preceding storm hydrograph } (ft^3/s/hour)}{\textit{Time of rise}}$$

Flood intensity is similar to the peakedness index used by Guy (1964). Forward stepwise regression was applied to the four variables to determine their significance. The probability for F-

Reproduced with permission of the copyright owner. Further reproduction prohibited without permission.

to-enter and F-to-remove was set at an alpha value of 0.05. Details on the forward stepwise regression procedure are reported later in this chapter under the heading, "Multiple Linear Regression Analysis".

Calculation of Suspended-Sediment Loads

Suspended-sediment loads were quantified for those storms that were adequately sampled for suspended sediment. A runoff event was determined to be sampled adequately if at least one suspended-sediment sample was collected on the rising limb to the highest peak discharge and at least 50% of the total suspended-sediment load had to be calculated between the first and last sample for it to be used in the statistical analysis.

The suspended-sediment load transported during an event was computed following procedures outlined by Porterfield (1972). The first step in the computation of suspended-sediment load was to create a continuous temporal concentration curve. Samples of suspended-sediment concentration collected during runoff events were plotted with instantaneous water discharge over the time of the event (fig. 4.10). In a continuous temporal concentration curve there needs to be a suspended-sediment concentration for each calculated value of instantaneous water discharge. Water discharge typically was calculated at 15-minute intervals. Linear interpolation was used to calculate water discharge for suspended-sediment samples collected between 15-minute intervals.

Reproduced with permission of the copyright owner. Further reproduction prohibited without permission.

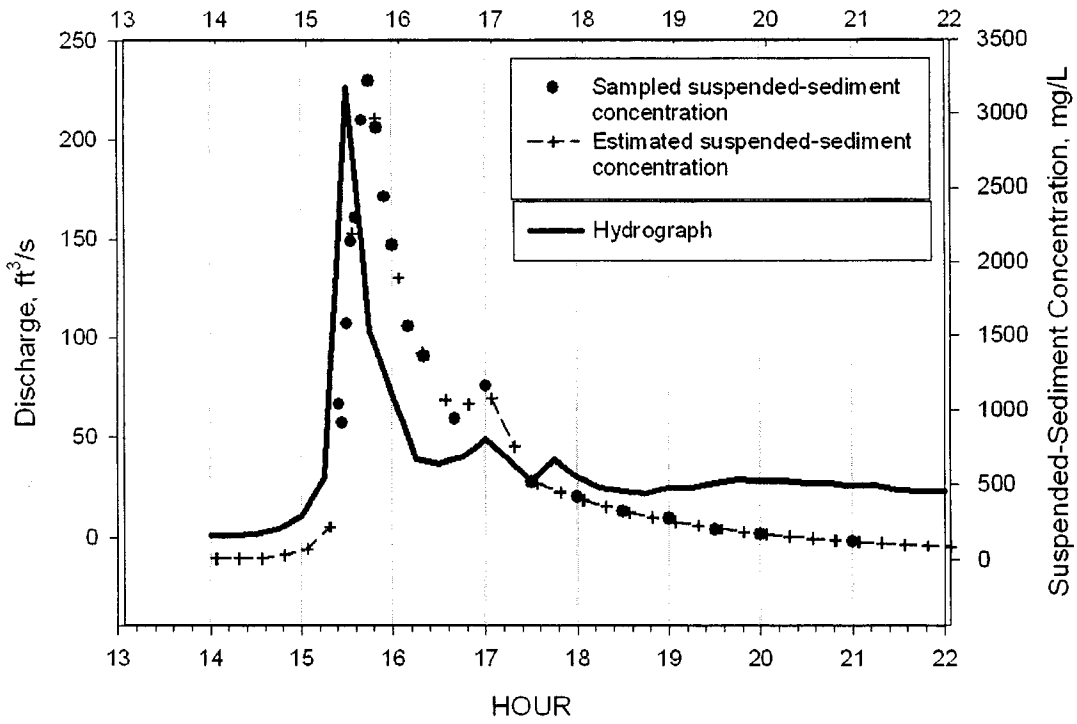

Figure 4.10. Example of a continuous temporal suspended-sediment concentration trace for Quebrada Blanca, 6/14/1990 to 6/15/1990.

Two methods were used to estimate suspended-sediment concentration for times when no sample was collected. If the time of the estimated suspended-sediment concentration was between two collected samples and reasonably close in time to these samples, linear interpolation was used to estimate the suspended-sediment concentration. Sediment-transport curves were also used to estimate suspended-sediment concentrations. If enough samples were collected during the event, rising and falling sediment-transport curves were developed for this specific event and the equations generated from linear regression was used to estimate suspended-sediment concentrations. If not enough samples were collected in the single storm event to define sediment-transport curves, then transport curves developed from all storm samples relative to rising and falling hydrograph

Reproduced with permission of the copyright owner. Further reproduction prohibited without permission.

conditions were used. The estimated concentrations were plotted with the sampled concentrations on the hydrograph to determine visually the validity of the concentration trace (fig. 4.10). If the concentration curve did not appear adequate, selected estimated values were modified. Porterfield (1972) states that the visual procedure method to construct continuous temporal concentration curves is the most common and accurate method when supplemented with transport curves.

When the continuous temporal concentration curves is complete the next step in the computation of suspended-sediment discharge is to subdivide the suspended-sediment concentration curve. A maximum time increment of 15-minutes was used in subdividing the event. Finer increments of time were used if samples were collected between 15-minute values. Each increment is the mid-interval or a time interval that extends halfway to the preceding and succeeding value times. For each increment the suspended-sediment discharge (Q_s) is computed as:

$$\mathbf{Q_s = Q_w \times C_s \times k}$$

where; Q_s = *suspended-sediment load, in tons*
Q_w = *instantaneous discharge, in* ft^3/s
C_s = *instantaneous suspended-sediment concentration, in mg/L*
k = *a coefficient for conversion of water discharge and sediment concentration to a mass, in tons, and assumes a density of water of 62.4 pounds per cubic foot.*

$$k = \frac{(60 \text{ minutes} \times 60 \text{ seconds} \times \text{hours of event}) \times 62.4 \text{ pounds/ft}^3}{2{,}000 \text{ pounds/ton} \times 1{,}000{,}000}$$

Each subdivision increment is a percentage of the time of the runoff event and weighted for the time of the event. The sum of the suspended-sediment discharge for all increments is the suspended-sediment load for the event. The suspended-sediment load for several storms was

Reproduced with permission of the copyright owner. Further reproduction prohibited without permission.

calculated without base flow to see whether this changed the total load. In most cases the total load did not change by more than 10 % and therefore, in the calculation of suspended-sediment, the base flow component was not removed.

Geomorphic Measurements

Channel cross-sectional surveys are performed by the USGS when a streamflow station is established or when a major shift in the discharge-rating curve occurs. These cross-sectional surveys were used to describe the cross-sectional geometry and slope of the study channels at the USGS gage.

Statistical Analysis of Discharge and Sediment data

This section describes the statistical analyses of instantaneous suspended-sediment and storm generated suspended-sediment loads. Methods used in the statistical descriptions of instantaneous sediment and discharge are presented. The dependent and independent variables used, and the various types of storm hydrographs used in the statistical analysis, are listed.

Descriptive statistics

Streamflow and sediment analyzed in this report represent samples of a population. By statistically analyzing the data one hopes to make conclusions about the population. The first consideration in the analysis of data is to determine the characteristics of the data. Discharge, precipitation, and suspended sediment were described at each station analyzed in this report for the period of investigation, 1989 through 1996, and for the period of record at each station. Annual mean daily discharges were calculated for each station from data provided by the USGS

Reproduced with permission of the copyright owner. Further reproduction prohibited without permission.

databases. Annual and monthly mean daily discharge flow duration curves were described for each station. Peak flows for the period of period of investigation and the period of record were obtained from USGS databases.

Quantile plots and box plots were used to display the distribution of the data visually. Quantile plots display the distribution of data by plotting the data along the x-axis against the quantile. There are several methods to quantify quantile. Helsel and Hirsch (1992) list the advantages of each and recommend the Cunnane method. In the Cunnane method the quantile is found by:

$$p_i = (i-0.4/(n+0.2)$$

where p_i is the ordinate value of the quantile, i is the rank from 1 to n; n being the total number of values

Quantile plots in this research used the Cunnane method. Box plots are a convenient method to illustrate the distribution of the data and major percentiles. Box plots created for this research use the median 10, 25, 75, and 90 percentiles. Because suspended sediment concentrations vary over several orders of magnitude, quantile plots and box plots of suspended sediment are shown on log scale.

Probability plots display the suspended-sediment data on the x-axis against the standardized theoretical distribution of the data or expected value in a normal distribution. This is a convenient method to determine whether the data are normally distributed. If the data are normally distributed the plotted values fall on approximately a straight line. If the original data are not normally distributed often a transformation, such as a log transformation is necessary to normalize the data (Helsel and Hirsch, 1992).

Reproduced with permission of the copyright owner. Further reproduction prohibited without permission.

Statistical analysis of storm sediment loads

The steps used to analyze storm-generated suspended sediment are shown in figure 4.11. Independent variables were assembled for the quickflow portion and runoff of the entire storm hydrograph. Skoklevski and Velickov (1995) observed that the best correlations for rivers in the Republic of Macedonia were observed for rising runoff. To test whether the rising limb of the hydrograph is statistically more significant in explaining sediment characteristics than the entire storm hydrograph, only the portion of the storm hydrograph rising to highest peak discharge was used. Normality of the independent variables was tested and, if necessary data were transformed to improve normality. At this point, two distinct approaches to reducing the number of variables were used to assess potential analytical and interpretive advantages. The first approach was an inspection of the Pearson's product-moment correlation matrix to remove highly correlated ($R \geq 0.80$) variables. The second approach was a more involved principal component analysis of the correlation matrix. Principal components analysis is a statistical tool used to reduce the dimensionality of the data scatter onto a new set of axes (Davis, 1973) and to compute new composite variables that are uncorrelated. The first axis explains most of the variance in the data, and subsequent axes explain the remaining variance. In factor analysis, a smaller number of principal components are selected to determine a simplified structure to the data. The smaller number of principal components was based on examination of the scree plot which is a plot of eigenvalues against their principal component axis. The uncorrelated variables resulting from the two approaches were then subjected to forward-stepwise multiple regression, with the F-to-enter and F-to-remove level of significance set at 0.05.

Reproduced with permission of the copyright owner. Further reproduction prohibited without permission.

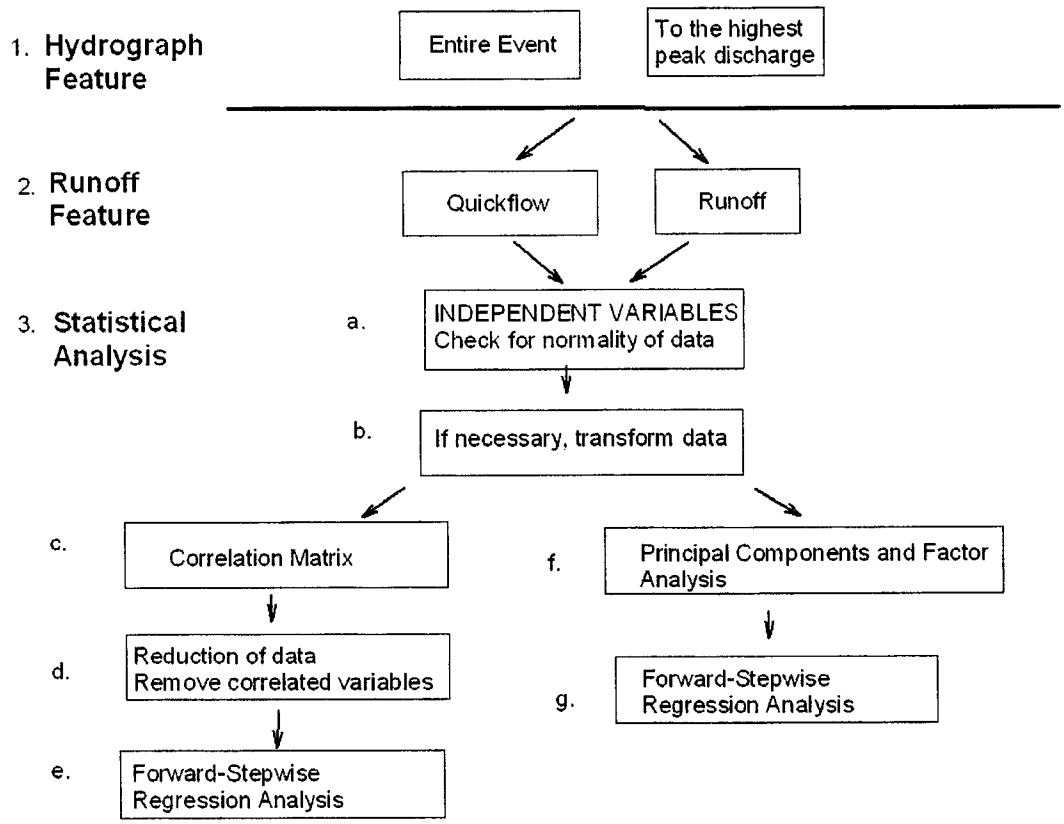

Figure 4.11. Steps used in statistical analysis.

Dependent variables

A major objective of this PhD dissertation was to determine the factors controlling suspended sediment characteristics at the four gaging stations. These factors include hydrologic and meteorologic variables. Suspended sediment as a dependent variable was defined for two portions of the storm hydrograph: 1) the entire runoff hydrograph and 2) the portion of the hydrograph rising to the highest peak. For the two portions of the hydrograph, sediment as a dependent variable was defined two ways: 1) suspended-sediment load and 2) discharge-weighted sediment concentration. Computation of suspended-sediment load was outlined earlier.

Reproduced with permission of the copyright owner. Further reproduction prohibited without permission.

Discharge-weighted sediment concentration is the suspended-sediment load for the event divided by the runoff or quickflow of the event.

$$C = 3.203 \times 10^{7} \frac{Qs}{Qw}$$

where; C is the discharge-weighted sediment concentration, in mg/L (sediment weight per unit volume of the water-sediment mixture), Qs is the suspended-sediment load for the storm event, in tons, and Qw is the runoff or quickflow computed for the storm event, in cubic feet

Guy (1964) used a similar dependent variable which he termed the "water-discharge-weighted storm event concentration" in his analysis of factors affecting storm-period sediment transport for seven streams in the Atlantic coast area of the United States. Because of the intercorrelation of water discharge and sediment load, Guy (1964) regarded the water-discharge-weighted storm event concentration as a better dependent variable than sediment discharge. The physical meaning of the discharge-weighted sediment concentration is the mass of sediment passing the monitoring site during the storm divided by the volume of runoff passing the same site for the same storm. As such it is not an instantaneous measurement of suspended sediment but an estimate of the mean suspended-sediment concentration of the storm event. It is analogous to collecting the entire storm runoff in a giant bottle and taking it to the laboratory for drying and concentration.

Both dependent variables were tested to determine whether they were normally distributed, and if necessary, a transformation was used to improve the normal distribution. A list of abbreviations of dependent and independent variables that will be used in the text are shown in Table 4.7. To avoid problems with spurious relations among the dependent and independent

Reproduced with permission of the copyright owner. Further reproduction prohibited without permission.

Table 4.7. Abbreviations of dependent and independent variables used in quickflow and runoff analysis for events defined for: the entire runoff event and to the highest peak flow.

Dependent Variables

Abbreviation	*Characteristic*
SEDCONC	Discharge-weighted suspended sediment concentration, mg/L (using quickflow or runoff in the calculation)
SED	Suspended-sediment load, tons

Independent Variables

Abbreviation	*Characteristic*	*Used in analysis for: Quickflow (Q), Runoff (R)*	*Used in analysis for: 1- entire runoff event 2- to the highest peak flow*
1-QUICK	Quickflow,ft^3/s	Q	12
2-RUN	Runoff, ft^3/s	R	12
3-BASE	Base flow at start of event, ft^3/s	QR	12
4-PKBS	Peak flow minus base flow, ft^3/s	Q	12
5-PK	Peak flow, ft^3/s	R	12
6-MXTMJPK	Maximum rate of hydrograph rise from start of event to the highest peak flow, ft^3/min	QR	12
7-MXTRP	Maximum rate of rise for any peak from preceding trough to peak flow, ft^3/min	QR	1
8-SMPKBS	Sum of current peak flows minus base flow, ft^3/s	Q	1
9-SMPK	Sum of current peak flows, ft^3/s	R	1
10-RAIN	Rainfall for the current event, in	QR	1
11-INT15	Maximum 15-minute rainfall intensity of current event, in/min	QR	12
12-SFIVE	Seventy-five % rainfall intensity of current event, in/min	QR	1
13-RRISE	Rainfall on the rising limb of the hydrograph to the highest peak flow, in	QR	12
14-RAINFOL	Rainfall amount after the highest peak flow, in	QR	1
17-RNBTWTI	Runoff since the end of the previous event divided by the time since the previous event, $ft^{3/}$ hour	QR	12
18-PPTBTW	The amount of precipitation since the end of the previous event divided by the time since the previous event, in/hour	QR	12

Reproduced with permission of the copyright owner. Further reproduction prohibited without permission.

Table 4.7. Continued.

19-INTBET	Maximum 15-minute rainfall intensity since the end of the previous event divided by the time since the previous event, in/min	QR	12
20-LSPKBTI	The previous-event peak flow minus base flow divided by the time since the previous-event peak flow, $ft^3/s/hour$	Q	12
21-LSPKTI	The previous-event peak flow divided by the time since the previous-event peak flow, $ft^3/s/hour$	R	12
22-SMLSPKBS	Sum of peak flows in previous event minus base flow divided by time since the previous event, $ft^3/s/hour$	Q	12
23-SMLSPK	Sum of peak flows in previous event divided by time since the previous event, $ft^3/s/hour$	R	12
24-QULST	Previous-event quickflow divided by time since the previous event, $ft^3/hour$	Q	12
25-RULST	Previous-event runoff divided by time since the previous event, $ft^3/hour$	R	12
26-PPTLSTI	Rainfall of the previous event divided by the time since the previous event, in/hour	QR	12
27-INTLST	The maximum 15-minute rainfall intensity of the previous event divided by the time since the previous event, in/min/hour	QR	12
28-LS75OTI	Seventy-five % rainfall intensity of the previous event divided by the time since the previous event, in/min/hour	QR	12
29-SUM3PPTI	Sum of the 3 previous rainfall events divided by the time over the 3 previous events, in/hour	QR	12
30-QU3EVT	Combined quickflow of previous 3 events divided by the time over the previous 3 events, ft^3 /hour	Q	12
31-RU3EVT	Combined runoff of previous 3 events divided by the time over the previous 3 events, ft^3 /hour	R	12

variables, the quickflow (runoff minus base flow) and runoff of the current event were removed as independent variables when examining discharge-weighted sediment concentration as a dependent variable in forward-stepwise regression analyses.

Reproduced with permission of the copyright owner. Further reproduction prohibited without permission.

Another objective of this study was to determine whether quickflow or runoff for each type of event were each better statistical factors to characterize storm-generated suspended-sediment loads. Hydrograph separation into quickflow eliminates the base flow contribution to storm runoff. The technique of hydrograph separation was defined earlier (fig. 4.3). Separate statistical analyses were performed for each of the 3 portions of the runoff event using quickflow and runoff variables (fig. 4.3).

Walling (1974) Sediment-Transport Curve Approach

A rigorous study of sediment characteristics during storm events was provided by Walling (1974). A stepwise-regression model of the dependent variable, instantaneous sediment concentration, and four independent variables: (1) discharge, (2) rising or falling stage, (3) flow level at beginning of event, and (4) the shape of the hydrograph (index of flood intensity), were used to determine statistical relationships. These variables were also considered in this study.

Independent variables

Independent variables thought to influence sediment characteristics at-a-station included meteorologic, hydrologic, and sedimentologic variables (Table 4.8). Meteorologic and hydrologic factors thought to influence suspended-sediment concentrations at-a-station were divided into three time categories: 1) previous-event factors, 2) factors between events, and 3) current-event factors (Table 4.8).

For this analysis, flow characteristics in the sampled event that control suspended-sediment concentrations included: 1) base flow or discharge immediately prior to the hydrograph rise,

Reproduced with permission of the copyright owner. Further reproduction prohibited without permission.

Table 4.8. Independent variables thought to influence suspended-sediment concentrations, separated into three time categories.

(Used in analysis for: 1-used in the analysis for the entire runoff event, 2-used in the analysis to the highest peak flow

CHARACTERISTICS OF THE PREVIOUS EVENT	CHARACTERISTICS BETWEEN EVENTS	CHARACTERISTICS OF THE CURRENT EVENT
Peak flow of the previous event (using quickflow or runoff) divided by hours since the peak flow *12*	Rainfall Between Events Divided by Hours Since the Previous Event *12*	Quickflow *12*
Sum of peak flows of the previous event (using quickflow and runoff) divided by hours since the previous event *12*	Maximum 15-minute Rainfall Intensity Between Events Divided by Hours Since the Previous Event *12*	Runoff *12*
Quickflow of the Previous Event Divided by Hours Since the Previous Event *12*	Runoff Between Events Divided by Hours Since the Previous Event *12*	Rainfall *1*
Runoff of the Previous Event Divided by Hours Since the Previous Event *12*		Maximum 15-minute Rainfall Intensity *12*
Combined Quickflow of last Events Divided by Time Over the Last Events *12*		75-Percent Rainfall Intensity *1*
Rainfall of the Previous Event Divided by Hours Since the Previous Event *12*		Base flow at Start of Event *12*
Maximum !5-minute Intensity of The Previous Event Divided by Hours Since the Previous Event *12*		Maximum Peak flow (using either quickflow and runoff) *12*
75 Percent Intensity of The Previous Event Divided by Hours Since the Previous Event *12*		Sum of Peak flows In Event (using either quickflow and runoff) *1*
Sum of Last 3 Events Rainfall Divided by Time Over the Last 3 Events *12*		Hysteresis Characteristic *1*
Combined Runoff of last 3 events Divided by Time Over the Last 3 Events *12*		Rainfall on Rising Limb to Highest Peak flow *12*
		Rainfall on Falling Limb After Highest Peak flow *1*

Reproduced with permission of the copyright owner. Further reproduction prohibited without permission.

Table 4.8 Continued.

CHARACTERISTICS OF THE PREVIOUS EVENT	CHARACTERISTICS BETWEEN EVENTS	CHARACTERISTICS OF THE CURRENT EVENT
		Maximum Rate of Hydrograph Rise For Any Peak, From Preceding Trough to Peak *1*
		Maximum Rate of Hydrograph Rise From Start of Event to the Highest Peak flow *12*

2) highest peak flow, 3) sum of all peak flows, 3) quickflow, 4) runoff, and 5) the rate of rise for the highest peak, and 6) the rate of rise for peaks other than the highest peak. Walling and Webb (1982) showed that the base flow component is essentially a dilution factor. When base flow was removed, there was no slope in the positive relationship between discharge and suspended-sediment concentration (Walling and Webb, 1982). The rate of hydrograph rise was found to control suspended-sediment concentrations in Oregon Coast Range drainages (Beschta, 1987).

Current-event meteorologic factors of precipitation magnitude, intensity, and duration can affect runoff response (Brooks and others, 1991). Rainfall amounts and rainfall intensities can be important factors influencing suspended-sediment characteristics (Guy, 1964; Walling, 1974). Walling (1974) concluded that the most important variables controlling storm generated suspended sediment concentrations were rainfall, maximum 15-minute rainfall intensity, and the kinetic energy of the storm. Meteorologic variables in this statistical analysis included rainfall and rainfall intensity.

To test whether rainfall at the beginning of the runoff event was more important in influencing sediment characteristics than later in the runoff event, rainfall was divided into two components (1) from the beginning of the runoff event to the highest peak flow and (2) after the

Reproduced with permission of the copyright owner. Further reproduction prohibited without permission.

highest peak flow to the end of the event. Rainfall intensity included maximum 15-minute rainfall intensity and the 75% rainfall intensity.

Meteorologic and hydrologic characteristics since the previous runoff event may also influence suspended-sediment characteristics of the current event (Wood, 1977; Moore, 1984, Beschta, 1987). Physical and biologic processes that occur between runoff events may increase the sediment available for transport (Walling and Webb, 1982). Light rains occurring between runoff events may move sediment from the hillslopes to low-order channels or the main channel and floodplain where it remains in storage until high flows of the next runoff event mobilize it. Characteristics between events that were examined included rainfall and runoff. The values were normalized by the elapsed time since the previous event.

The characteristics of the last few storm events may also influence the suspended-sediment concentrations of the current event (Walling and Webb, 1982; Beschta, 1987). If the previous runoff event was high, sediment may have been flushed from hillslopes and the channel and the suspended-sediment characteristics of the current event may be low. The effects of previous storms may diminish as time since previous events increases, a period of time Walling and Webb (1982) referred to as the "recovery period". A 1,000 cfs (28.3 cms) peak in a previous event may influence the characteristics of suspended sediment in a later event but its effect may be greater if the peak occurred 10 hours prior to the runoff event as opposed to 10 days. Therefore, the hydrologic and meteorologic characteristics of the previous event were divided by the number of hours since the last event. To determine how many previous events should be examined, forward stepwise regression was run on the dependent variable (suspended-sediment load) and independent variables (current quickflow, previous-event quickflow divided by the time since the

Reproduced with permission of the copyright owner. Further reproduction prohibited without permission.

previous-event runoff). Events back to the 6th previous event were used to in this analysis. The alpha value was set to 0.15. Three previous events were used as a minimum. If more than 3 previous events were shown to be significant, this number of previous events was used.

Runoff, quickflow, and rainfall for the previous events were calculated as follows:

$$\text{Sum } (n \text{ last events}) =$$

$$\text{LOG } \frac{\text{(Previous event \{rainfall or runoff\}}}{\text{(hours since previous event)}} +$$

$$\frac{\text{LOG (2nd previous event \{rainfall or runoff\}}}{\text{(hours since 2nd previous event)}} + \ldots. +$$

$$\frac{\text{LOG (nth previous event \{rainfall or runoff\}}}{\text{(hours since nth previous event)}}$$

Hysteresis

For most streams, higher suspended-sediment concentrations are found on the rising limb of the hydrograph and lower concentrations on the falling limb (Wood, 1977). This relationship, when plotted, is known as hysteresis (fig. 4.12). In the statistical analysis, a value of "1" was given to the event if the plot of discharge versus suspended-sediment concentration over time (hysteresis loop) was clockwise, with higher concentrations on the rising limb. A value of "0" was given to the event if the hysteresis was other than a clockwise loop. Visual inspection of hysteresis plots was used to determine the assigned value of the event. The characteristic hysteresis curve, of peak suspended-sediment concentrations preceding peak flow, is thought to be related to exhaustion of in-channel sediment sources (Walling and Webb, 1982) or to an increase in base flow on the recession limb (Wood, 1977). Exhaustion of sediment sources may include decreased detachment of soil particles at the cessation of rainfall, dilution effects from groundwater increases, and progressive wetting and armoring of soil (Walling and Webb, 1982).

Reproduced with permission of the copyright owner. Further reproduction prohibited without permission.

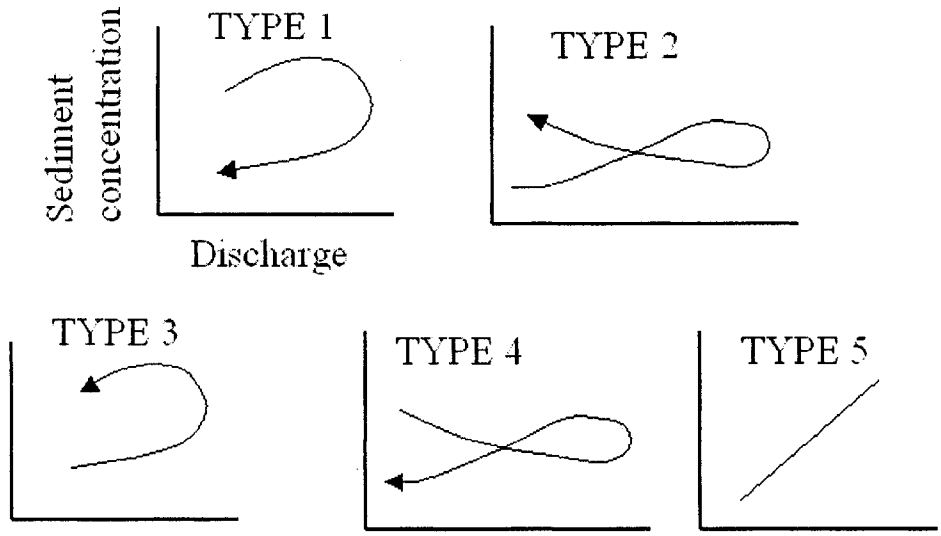

Figure 4.12. Description of hysteresis types used in this report. Arrows indicate direction through time. Type 1 - clockwise, Type - 2 clockwise early in storm reversing to counterclockwise, Type 3 - counterclockwise, Type 4 - counterclockwise early in storm reversing to clockwise, Type 5 - no exhaustion.

The sampled runoff events were analyzed for the timing of peak suspended-sediment concentration relative to the highest peak discharge and to the type of hysteresis. If the runoff event contained multiple peaks, the timing of the peak suspended-sediment concentration was determined relative to the timing of individual flow peaks. Hysteresis characteristics were classified into five types (fig. 4.12). Type 1 is a clockwise hysteresis over time with exhaustion of sediment. Type 2 is a "figure 8" hysteresis shape with clockwise rotation from sediment exhaustion that is reversed later in the event to counterclockwise rotation and increased supply of sediment. Type 3 is a counterclockwise hysteresis over time in which suspended-sediment concentrations increases as flow decreases. Type 4 is a "figure 8" hysteresis shape with counterclockwise rotation from increased sediment supply that is reversed later in the event to clockwise rotation and sediment

Reproduced with permission of the copyright owner. Further reproduction prohibited without permission.

exhaustion. Type 5 has no observed exhaustion or increase in suspended-sediment concentration. This classification of hysteresis types is similar to those used by Kurashige (1994) and Williams (1989).

To gain insight into the controls of sediment exhaustion and sediment increases during a storm, hysteresis loops around the highest peak discharge were examined for the amount of sediment exhaustion (Type 1) and sediment increases (Type 3). The width of the hysteresis loop or the amount of sediment exhaustion and sediment increase around the highest peak discharge was quantified by taking the difference in suspended-sediment concentration values on the rising limb and the falling limb at the same discharge. The widest portion of the hysteresis curve was chosen. Williams (1989) used a similar method to determine the increase or decrease in suspended sediment in a hysteresis loop by taking the ratio of suspended sediment to discharge (C/Q) at the same discharge. Hydrologic variables related to the storm hydrograph that might be influencing the amount of sediment exhaustion and sediment increases were selected and used in the statistical analysis of the hysteresis loop (Table 4.9). The dependent variable used in this statistical analysis is the width of the hysteresis loop or the amount of sediment exhaustion and increase. Forward stepwise regression was used in the statistical analysis of hysteresis loops. Hysteresis loops were generalized into Type-1 and Type-3 loops. Type-4 loops were categorized as Type-3 and Type-2 loops were categorized as Type-1 loops.

Storm hydrograph variables of rainfall and runoff thought to be influencing the hysteresis loops were selected and were the same as those used in the statistical analysis for storm-generated sediment (Table 4.2; Table 4.9). Runoff variables, not quickflow, were used in these statistical analyses. An additional variable included in this analysis of hysteresis loops was the slope of the

Reproduced with permission of the copyright owner. Further reproduction prohibited without permission.

Table 4.9. Independent variables used in the analysis of hysteresis loops and tested against the width of the hysteresis loops for clockwise (Type 1) and counterclockwise (Type 3) storms..

Abbreviation	*Characteristic*
2-RUN	Current runoff, ft^3/s
6-MXTMJPK	Maximum rate of hydrograph rise from start of event to the highest peak flow. ft^3/min
9-SMPK	Sum of current peaks, ft^3/s
12-SFIVE	Seventy five percent rainfall intensity of current event, in/min
13-RRISE	Rainfall on the rising limb of the hydrograph to the highest peak flow
14-RAINFOL	Rainfall amount after the peak flow, inches
17-RNBTWTI	Total runoff since the end of the previous event divided by the time since the previous event, $ft^{3/}$ hour
25-RULST	Previous event runoff divided by time since the previous event, ft^3/s/hour
31-RU3EVT	Combined runoff of previous 3 events divided by the time over the previous 3 events, ft^3 /hour
32-RATE_RISE	Slope of sediment transport curve on rising limb
33-RATE_FALL	Slope of sediment transport curve on falling limb
34-TIME_PKCON	Time of peak sediment concentration relative to peak flow

sediment transport curve for each storm event (32-RATE_RISE, 33-RATE_FALL; Table 4.9). The slope of the sediment transport curve was calculated for the rising and falling-limb sediment samples relative to the highest peak discharge. Steep slopes for sediment transport curves on the Rhine River were indicative of large quantities of sediment available for transport (Asselman, 1999). Changes in the slope of sediment transport curves were used by Beschta (1987) to show exhaustion of sediment and changing sediment sources after the annual peak discharge for rivers draining the Oregon Coast Range. The amount of sediment exhaustion or increase in each flood may be related therefore to the sediment available for transport exemplified by the slope of the sediment transport curve for that storm.

Reproduced with permission of the copyright owner. Further reproduction prohibited without permission.

Normality

The first step in statistical analysis was to determine whether the dependent and independent variables were normally distributed. After a quickflow or runoff data set was created, the variables were tested for normality by three methods: (1) visual inspection of histograms of data, (2) visual inspection of residuals generated by linear regression of the independent variables against the dependent variable sediment load (Helsel and Hirsch, 1992; Swan and Sandilands, 1995), and (3) using a standard computer software package. The computer software package tests the normality using the Kolmogorov-Smirnov test (Swan and Sandilands, 1995). The Kolmogorov-Smirnov test for normality is based on the maximum difference between the sample cumulative distribution and the hypothesized cumulative distribution. Given N ordered data points $Y_1, Y_2, ..., Y_N$, the hypothesized cumulative distribution is defined as:

$$E_N = n(i)/N$$

where $n(i)$ is the number of points less than Y_i and the Y_i are ordered from the smallest to the largest value. This is a step function that increases by $1/N$ at the value of each ordered data point. The test for normality is based on the maximum distance between these two curves. Variables found to have a non-normal distribution were transformed using methods outlined by Helsel and Hirsch (1992), using log transform, square root, and square of the value. Values were then tested for normality after the transform.

The principles of regression analysis are violated if the independent variables contain values of zero. This can be corrected by adding a constant. Selection of a constant value was determined by using the constant value that provided a better normal distribution to the data or transformed

Reproduced with permission of the copyright owner. Further reproduction prohibited without permission.

data. Visual inspection of histograms were used to determine which constant provided a better normal distribution. Typically, the constant used was the lowest value of the data set.

Multiple linear regression analysis

Suspended-sediment characteristics are likely to be related to many independent variables. Multiple regression statistical techniques, an extension of simple linear regression, can be used to determine relationships when many independent variables are involved. In simple linear regression a line is found to minimize the sum of squared deviations from the data points to the line. In multiple linear regression, depending on the number of independent variables, a best-fitting plane or hyperplane is generated.

The multiple linear regression model as denoted by Helsel and Hirsch (1992) is:

$$y = \beta o + \beta_1 x_1 + \beta_2 x_2 + ... + \beta_k x_k + \varepsilon$$

where y is the dependent variable
βo is the intercept
β_1 is the slope coefficient for the first independent variable
β_2 is the slope coefficient for the second independent variable
β_k is the slope coefficient for the kth independent variable
and ε is the error

Forward stepwise regression is a multiple linear regression statistical technique used to define the most important independent variables explaining the dependent variable. It is a useful technique for large data sets (Swan and Sandilands, 1995). In forward stepwise regression, independent variables are added one at a time beginning with the best predictor to find which independent variables best explain the dependent variable (Younger, 1979). The forward selection begins by selecting the independent variable which provides the best R^2 value. Additional variables

Reproduced with permission of the copyright owner. Further reproduction prohibited without permission.

are selected in a stepwise procedure and variables are selected if they add to the model's prediction of the dependent variable. The addition of a variable is based on the probability of F-to-enter limit and probability of F-to-remove limit. Forward stepwise regression for all analyses in this study used a probability for F-to-enter and F-to-remove at an alpha value of 0.05. At this value the F-to-enter would have to improve significantly the relation by 0.05. At the first step, a value is selected if it falls above the F-to-enter. Once a variable is added, all the variables are examined. If a variable in the model has a new F value that falls below the F-to-remove limit it is removed.

The F value, also called a partial F value, is defined as:

$$F = \frac{\text{Residual sum of squares}}{\text{Residual Mean Square}}$$

The residual sum of squares = Total sum of squares - regression sum of squares
The regression sum of squares is bSxy
where b = the slope of the regression line
and Sxy is the covariance defined as:

$$Sxy = \Sigma(X_i - \bar{X})(Y_i - \bar{Y})$$

where $\bar{X} = \Sigma x_i/n$

and $\bar{Y} = \Sigma Y_i/n$

The total sum of squares is Syy

where $Syy = \Sigma(Y_i - \bar{Y})^2$

The residual mean square is the residual sum of squares divided by the degrees of freedom (d.f.) of the residuals. The d.f. of the residuals is the difference of the d.f. (equal to n-1), minus the regression d.f. (equal to the number of independent variables).

Reproduced with permission of the copyright owner. Further reproduction prohibited without permission.

Correlation matrix

A high correlation between two independent variables is known as multi-collinearity and can be a problem in multiple regression analysis (Helsel and Hirsch, 1992). Slope coefficients may be unrealistic and unstable and stepwise multiple regression procedures may produce an inaccurate model (Helsel and Hirsch, 1992). A solution to the problem of multi-collinearity is to remove one or more of the variables that have a high correlation. Correlation coefficients measure the strength of association between two variables. The Pearson's product-moment correlation coefficient (r) is a dimensionless measure of correlation (Swan and Sandilands, 1995). It is calculated by:

$$r = \frac{\sum(X_i - \bar{X})(Y_i - \bar{Y})}{(n-1)S_x S_y}$$

Where x_i and y_i are individual data points from i=1 to i=n
n is the total number of data points
and S_x and S_y are the standard deviations of the x and y variables

Correlation matrices of the dependent and independent variables using the Pearson's product-moment correlation coefficient were generated using a statistical computer package. Independent variables with r values of 0.8 and higher may have a high correlation and were examined to determine whether one or more should be removed (Wulder, 2000). The decision to remove an independent variable is based on the knowledge of the variables and the assumption that one is a surrogate for another.

Principal component and factor analysis

Principal component analysis is a statistical tool to reduce the dimensionality of the data scatter onto a new set of axes (Davis, 1973). Most of the variance in the data is explained along

Reproduced with permission of the copyright owner. Further reproduction prohibited without permission.

the first axis and subsequent axes explain the remaining variability. Factor analysis seeks to explain the variance of the data based on fewer variables. It is a technique that looks for structure or patterns to the data. It is emphasized that principal components analysis is primarily an exploratory tool rather than a predictive tool.

The process of principal components is to rotate the data into a new set of axes to allow maximum variance of the data along the new rotated axes. The first principal component explains most of the variance. Successive components explain the remaining variance and are mutually orthogonal. If the variables in the analysis have different scales, a correlation matrix is calculated from the original data matrix (Swan and Sandilands, 1995). A correlation matrix effectively standardizes the data. The principal components are found by calculating the eigenvectors and eigenvalues of the correlation matrix. The eigenvectors define the axes of the components whereas the eigenvalues are the length or variance of each component axis. The number of components is equal to the number of correlated variables.

The original values are projected onto a principal axis by multiplying the original value by the eigenvector of each principal axis. The eigenvector values are called weights (Swan and Sandilands, 1995). The transformed data points are linear combinations of their original data values. The loadings are calculated as the correlation coefficients between the original variables and the new variables (principal components). The similarity and the magnitude of the loadings (positive or negative) suggests how closely related and significant the variables are. The value a loading must have to be considered significant is subjective. Values of loadings on a principal component should be viewed relative to one another. For example, if loadings on a principal component are around 0.9, a loading of 0.6 may be ignored. For this analysis, interpretations of

Reproduced with permission of the copyright owner. Further reproduction prohibited without permission.

the significance of factor loadings were examined relative to each other and in general, unless factor loadings were less than +/- 0.6, a +/- 0.6 loading threshold was used.

Rotation of the principal components axis can be used to interpret the factors more clearly (Daultrey, 1976; Davis, 1986). In this statistical analysis, rotations of the principal components axis were performed using the varimax rotation. Varimax rotation maximizes the variances to obtain loadings close to 0 or 1. The factor scores were saved after varimax rotation and forward stepwise regression was performed on the factor scores against all three dependent variables.

In factor analysis a smaller number of principal components are selected to determine a simplified structure to the data. Selection of the number of principal components can be based on an eigenvalue greater than 1.0, the "Rule of 1" (Davis, 1986). Another method examines the scree plot of the principal components and looks at a break in slope (SYSTAT, 1997). A scree plot is eigenvalues plotted against their principal axis. Both methods, the 'rule of 1' and the scree plot, were used to select factors. The factor model is:

$$X_j = \sum^{p}_{r=1} a_{jr} f_r + \varepsilon_j$$

where f_r is the rth common factor, p is the specified number of factors, the coefficient a_{jr} is the loading on the j_{th} factor, and ε_j is the random variation unique to the original variable X_j (Davis, 1986).

Because only the partial variance of the data is included in factor analysis, an error term is introduced. Factor analysis can be separated into R-mode analysis and Q-mode analysis. R-mode analysis examines variances among variables and Q-mode examines similarities among observations to determine patterns or groups.

Reproduced with permission of the copyright owner. Further reproduction prohibited without permission.

In this statistical analysis, principal components provided a means of reducing the data into categories. Principal component analysis was first performed on the data set using the "Rule of 1.0" and the scree plot; fewer principal component axes were selected for factor analysis. Using factor analysis (R-mode), loadings on each principal component were used to categorize or label the axes. Multiple-regression analysis of forward stepwise regression was performed on the new scores or principal components against the three dependent variables described earlier.

Reproduced with permission of the copyright owner. Further reproduction prohibited without permission.

CHAPTER V

SUSPENDED-SEDIMENT TRANSPORT AT RIO ICACOS

Statistical results are discussed first for Rio Icacos, a forested basin. The period of investigation at Rio Icacos (50075000) (fig. 3.5), was chosen from May 5, 1992 through September 20, 1994, based on the best record of storm samples for suspended sediment. Rainfall, discharge, and suspended-sediment characteristics are described for this period.

Rainfall and Discharge for the Study Period

Average annual rainfall for water years (WY) 1901 to 1994, recorded at the National Weather Service raingage in Canonvanas, was 76 in (1,930 mm). Average water-year rainfall at Canonvanas raingage was missing for WY1994 and a comparison of average long-term conditions to the study period could not be made. Rainfall amounts for the study period used in the statistical analyses were obtained from three USGS stations, 50075001, 50075000, and 50074950 (fig. 4.1). When these stations were not operating, data were augmented with USGS stations 50999958, 50065549, 50065500, and 50055750 (fig. 4.1a). Using these raingages the mean daily rainfall for the period May 5, 1992 through September 20, 1994 was 0.26 in (6.6 mm).

For the period being investigated the mean daily flow at Rio Icacos near Naguabo was 10.2 ft^3/s (0.29 m^3/s). For the period of record, July 1, 1945 through September 30, 1995, the mean daily flow was 13.6 ft^3 (0.38 m^3/s). Mean flow during the study period was 25% lower than the longer-term average. Flow durations for the period of investigation and the period of record

Reproduced with permission of the copyright owner. Further reproduction prohibited without permission.

are shown in figure 5.1. Peak flow for the period of record was 2,860 ft^3/s (81.0 m^3/s) on April 21, 1983. Peak flows during the period of investigation are listed in Table 5.1.

Table 5.1. Peak flows greater than 1.01-year recurrence (494 ft^3/s; 14 m^3/s) at Rio Icacos near Naguabo during the period of investigation (May, 1992 to September 1994).

Date	Peak flow (ft^3/s)
05/06/1992	1,260
12/29/1992	567
02/19/1994	872

Suspended-Sediment Load and Yield

Daily and annual suspended-sediment loads for the study period at Rio Icacos were not published and annual suspended-sediment loads for the period October 1, 1995 to September 30, 2000 were obtained directly from unpublished data in the USGS-Caribbean District (Matthew Larsen, personnel communication, 2002). The average annual suspended-sediment load for the period was 8,610 tons (7,810) metric tons), the average annual sediment yield was 6,830 tons/mi^2 (2,390 metric tons/ km^2), and the average annual discharge-weighted sediment concentration was 510 mg/L. On average, for water years 1995 through 2000, 75% of the annual suspended-sediment load was transported in 11 days, 90% of the load was transported in 28 days, and 30% of the load was transported in one day. On August 23, 2000, 61% of the suspended-sediment load for that year (6,590 tons; 5,980 metric tons) was transported.

Reproduced with permission of the copyright owner. Further reproduction prohibited without permission.

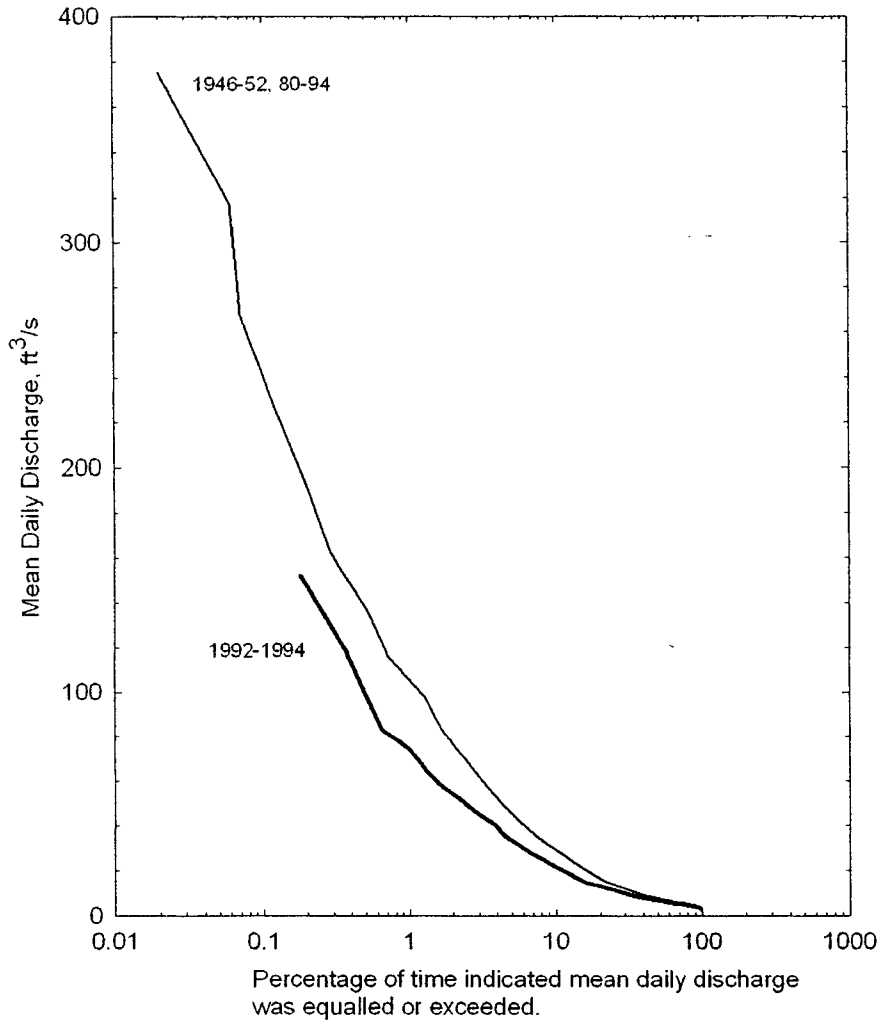

Figure 5.1 Flow durations for period of investigation(water year 1992-1994) and period of record (1946-52, 1980-94) for Rio Icacos near Naguabo (50075000).

Suspended-Sediment Analysis

During the period May 5, 1992 through September 30, 1994, 632 water samples were collected for suspended-sediment concentration at the station Rio Icacos near Naguabo. Of the samples, 74 were collected during base flow, 240 on the rising limb of the hydrograph to the

Reproduced with permission of the copyright owner. Further reproduction prohibited without permission.

highest peak, and 318 on the falling limb of the hydrograph following the highest peak. Forty samples were collected using the Equal-Width Increment (EWI) method, 525 samples were collected with an automatic sampler, and 67 samples were taken at single vertical (SV) in the channel. During the period of analysis, there was no calibration of either the SV or automatic samples to EWI samples. Because the samples were not calibrated, it is recognized that some error may be incurred in this analysis of suspended sediment.

The lowest and highest suspended-sediment concentrations were 0.3 mg/L and 3,545 mg/L, The mean concentration for this data set was 382 mg/L, the median suspended-sediment value is 241 mg/L, and the sample standard deviation was 484 mg/L (fig. 5.2). Samples were taken over a range of discharges from 2.7 to 634 ft^3/s (0.08 to 18.0 m^3/s). The distribution of sampled discharge shows 42% of sediment was sampled at moderate flows between 10 to 200 ft^3/s (0.28 to 5.66 m^3/s) (fig. 5.3).

Quantile plots of the suspended-sediment data (fig. 5.4.a,b) show that most of the samples collected were of low concentrations. Seventy-seven percent of the suspended-sediment concentration were less than 466 mg/L. Box plots of the data show the 10^{th}, 25^{th}, 50^{th}, 75^{th}, and 90^{th} percentiles of suspended sediment are 19, 108, 241, 466, and 849 mg/L, respectively (fig. 5.2). Probability plots show that the suspended-sediment data are not normally distributed (fig. 5.4a,c); therefore, applying a log transform to the data was found to be appropriate (fig. 5.4d).

Sediment-transport curves

Sediment-transport curves were created: 1) for all samples, 2) samples rising to the highest peak flow, 3) samples falling from the highest peak flow, 4) samples rising to any peak flow, 5)

Reproduced with permission of the copyright owner. Further reproduction prohibited without permission.

samples falling from any peak, and 6) samples collected at base flow (fig. 5.5). Two clusters are observed in the sediment transport curve (fig. 5.5a) and are a result of sampling frequency. Low-discharge samples are frequently collected by observers and USGS technicians. High-discharge samples are collected by an automatic sampler. The transport curve breaks in slope around 30 ft^3/s and best-fit regression lines were determined for discharges less than and greater than 27 ft^3/s (fig. 5.5a). The correlation coefficient for the low flow samples is 0.56 and is 0.62 for the high flows (fig. 5.5a). Correlation coefficients did not improve if the suspended-sediment samples were divided into rising and falling flows from the highest peak flow or rising and falling from any peak flow (fig. 5.5b,c).

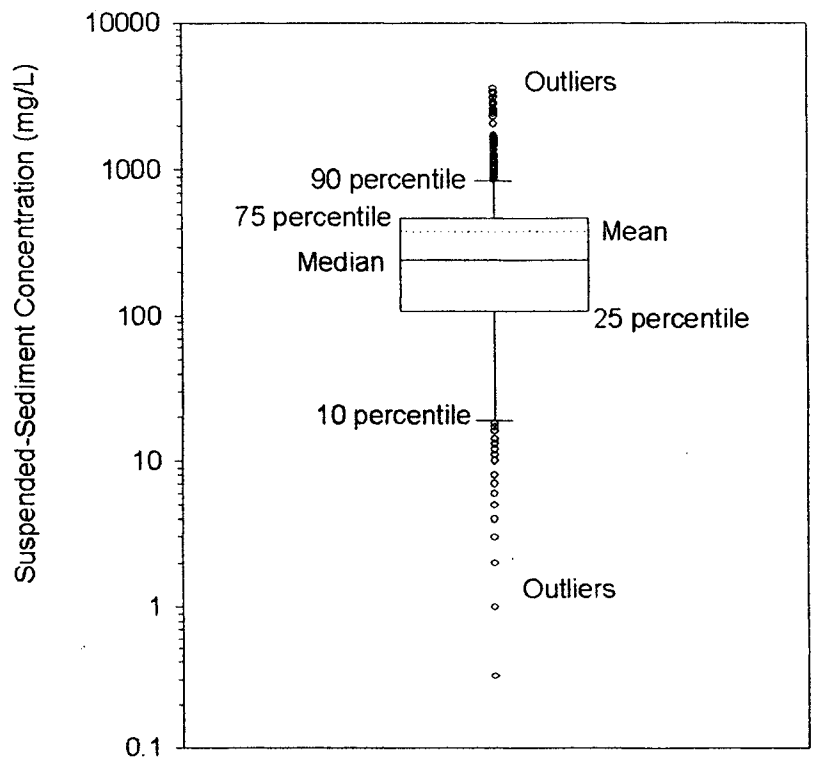

Figure 5.2. Box plot of suspended-sediment concentrations (n=632) for Rio Icacos near Naguabo.

Reproduced with permission of the copyright owner. Further reproduction prohibited without permission.

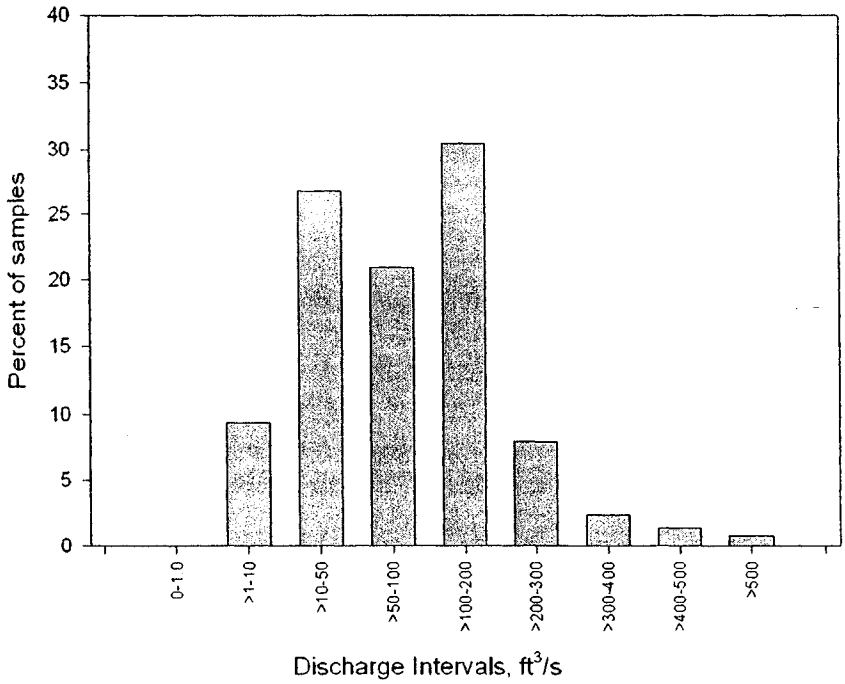

Figure 5.3. Frequency of discharges for suspended-sediment samples, Rio Icacos near Naguabo.

To test the hypothesis that previous storm-generated runoff events flush sediment, suspended-sediment samples were analyzed relative to the last event and to peak flows of the current event (fig.5.6). If previous events flushed sediment from the system, then suspended-sediment samples may have low concentrations after a large recent runoff event. Suspended-sediment samples were separated into four classes categorized by the runoff of the previous event divided by time since the previous event (fig. 5.6a). Only sediment on the rising limb may be affected by previous events and therefore, only samples rising to the highest peak flow were in the previous runoff analysis. Figure 5.6a shows that as the magnitude and closeness in time of previous runoff events increases, the best-fit regression lines for suspended-sediment concentration at a

Reproduced with permission of the copyright owner. Further reproduction prohibited without permission.

given discharge show a decrease in slope. This may indicate that large recent flows lower the current-event suspended-sediment concentrations.

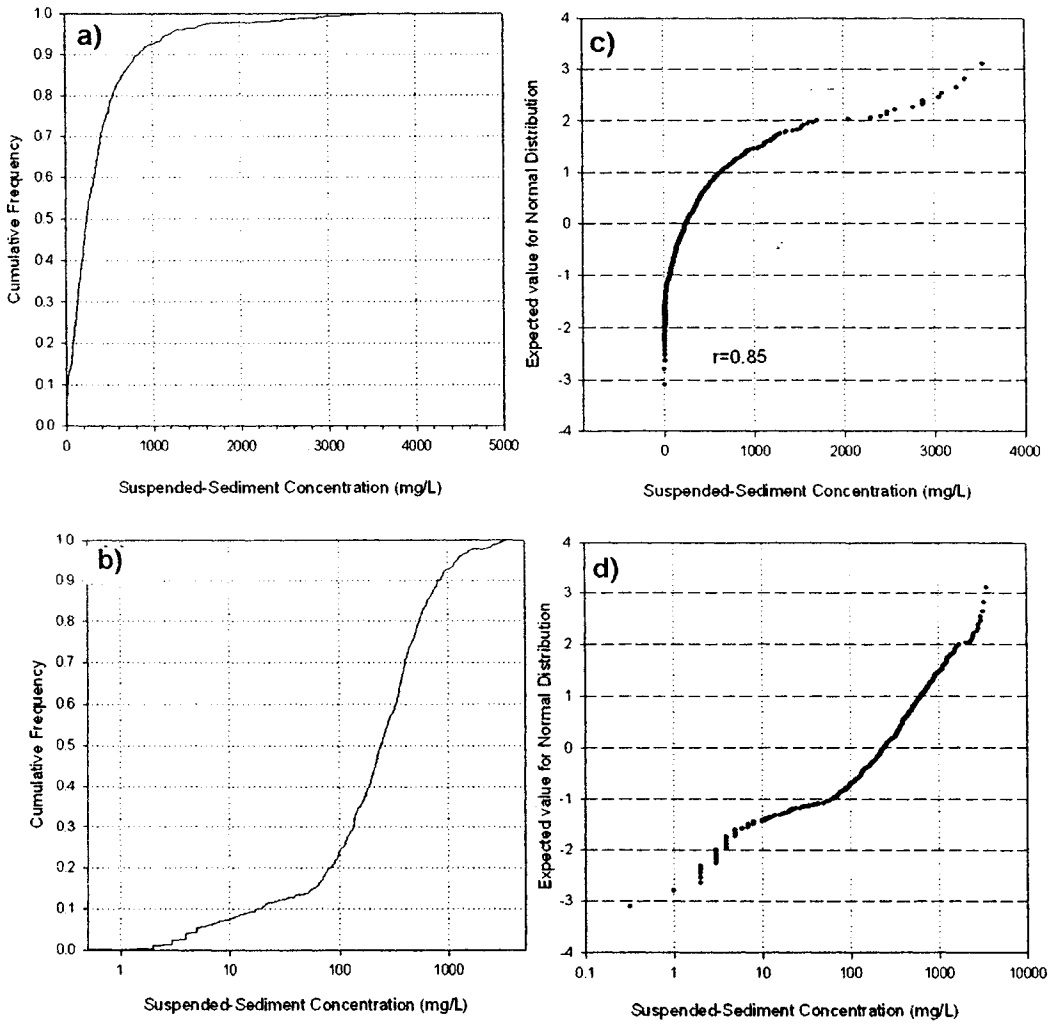

Figure 5.4. Quantile plots for Rio Icacos near Naguabo showing (a) suspended sediment and (b) log transformed suspended sediment. Probability plots of Rio Icacos near Naguabo showing (c) suspended sediment and (d) log transformed suspended sediment.

Suspended-sediment samples were separated by the previous peak flow in the current event (fig. 5.6b). The data bins were defined by the number of samples. Figure 5.6b does not show a consistent pattern. At low discharges, samples collected after intermediate peak flows

Reproduced with permission of the copyright owner. Further reproduction prohibited without permission.

(100-199 ft^3/s) have the highest suspended-sediment concentrations. At high flows samples collected after intermediate peak flows have the lowest suspended-sediment concentrations. Thus, it does not appear that peak flows in the current event are influencing suspended-sediment concentrations.

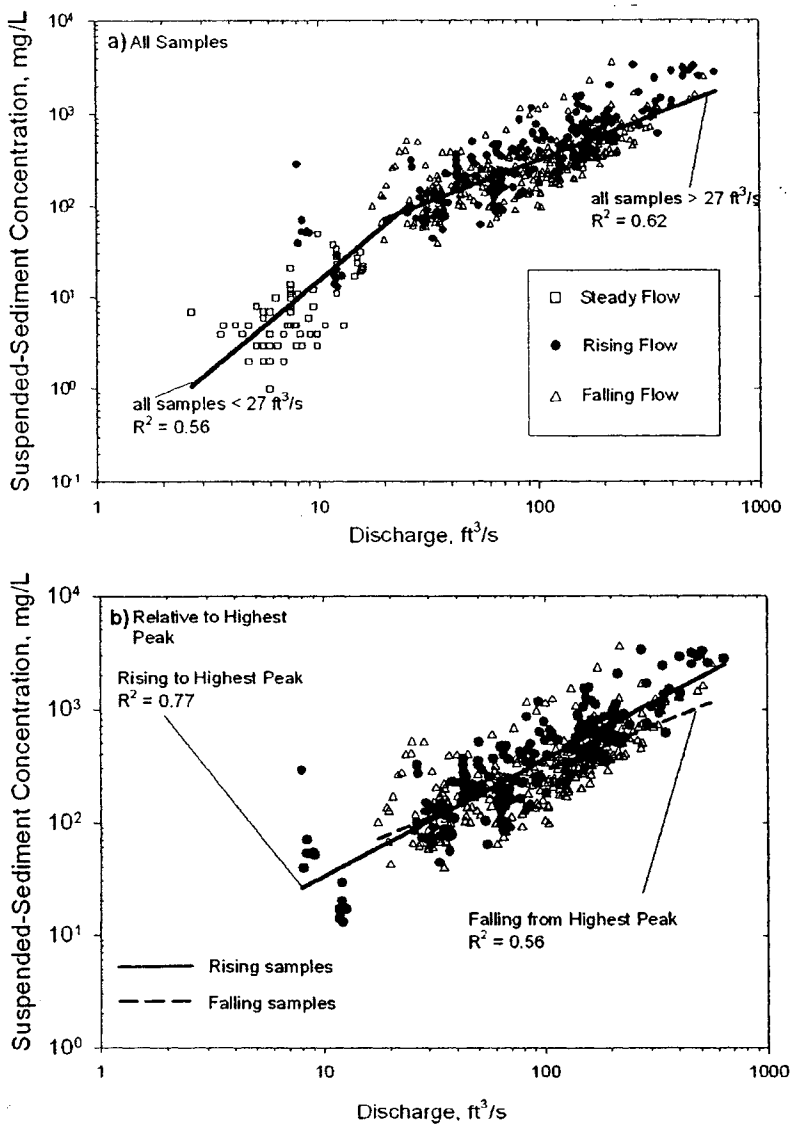

Figure 5.5. Suspended-sediment transport curves for Rio Icacos near Naguabo. a) All samples, and b) rising and falling hydrograph samples relative to the highest peak.

Reproduced with permission of the copyright owner. Further reproduction prohibited without permission.

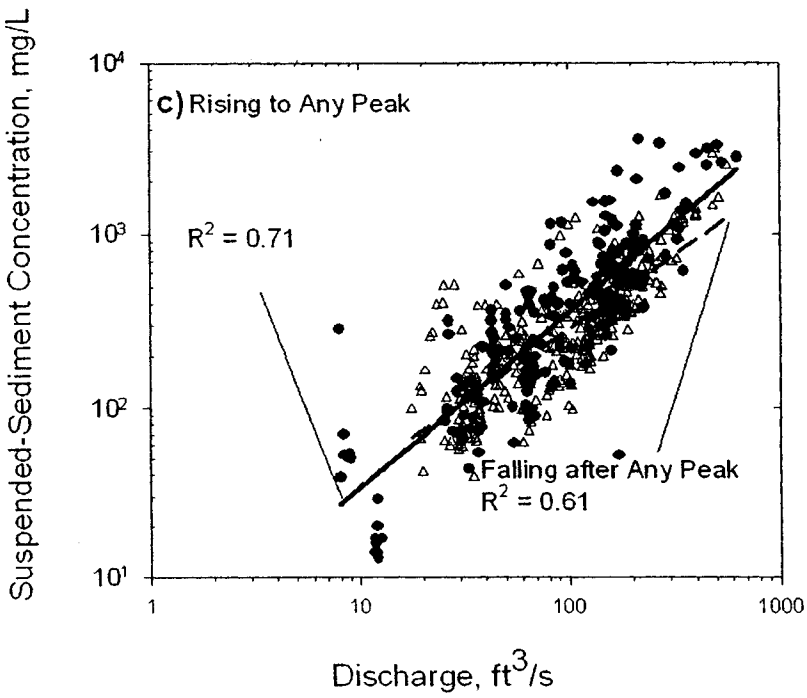

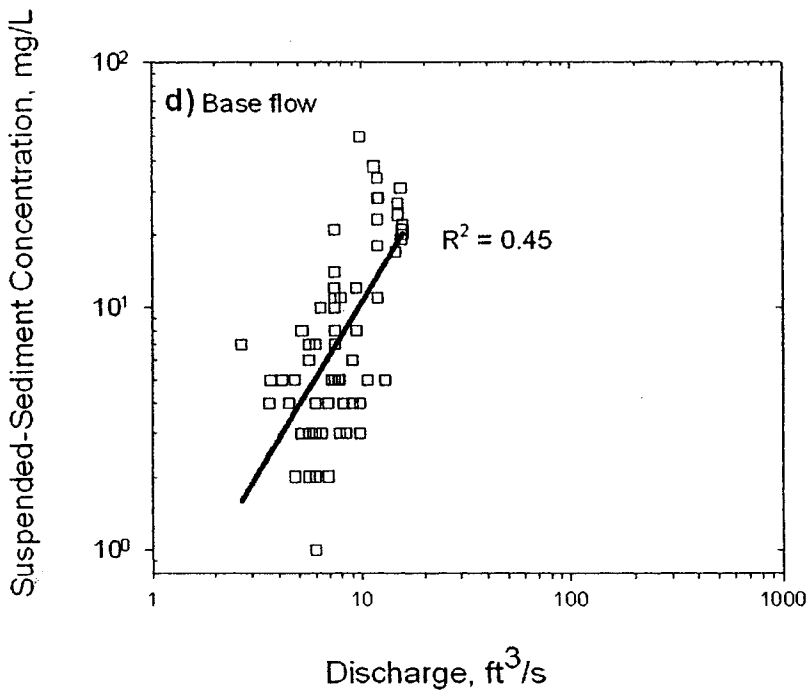

Figure 5.5. Continued, c) rising and falling hydrograph samples relative to any peak, and d) base flow samples.

Reproduced with permission of the copyright owner. Further reproduction prohibited without permission.

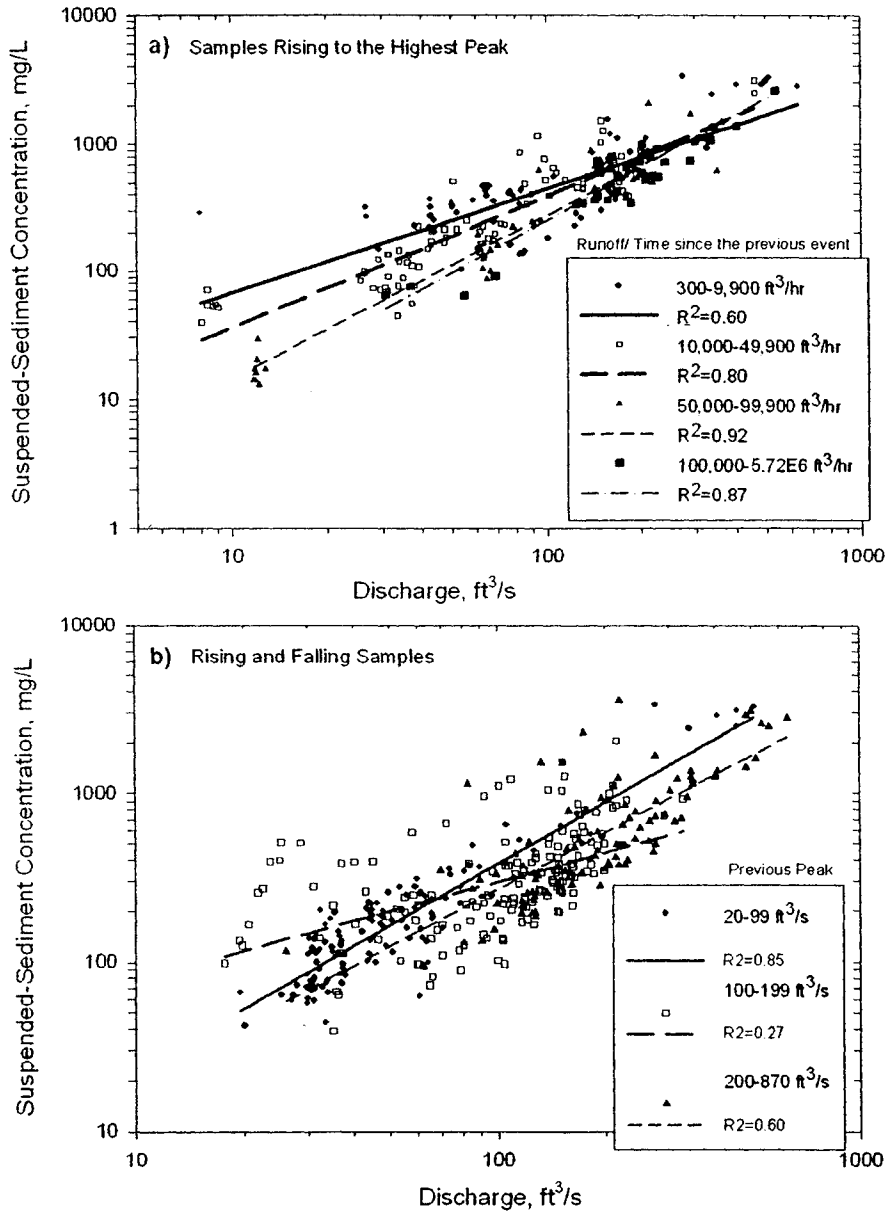

Figure 5.6. Suspended-sediment transport curves for Rio Icacos near Naguabo. a) Samples collected on the rising limb to the highest peak flow separated by runoff of the previous event divided by the time since the previous event and b) rising and falling hydrograph samples separated by the previous peak flow in the current event.

Rainfall has a strong seasonal component in Puerto Rico (fig. 3.18). Seasonal suspended-sediment transport groups separated into May through December and January through April are

Reproduced with permission of the copyright owner. Further reproduction prohibited without permission.

shown in figure 5.7 The R^2 values for each season are generally high. A plot of all samples shows that the best-fit regression line is lower for January through April compared to May through December (fig. 5.7a). Separation of seasonal suspended-sediment samples into rising and falling relative to the highest peak flow show generally the same results as for all samples; R^2 values are relatively high and suspended-sediment concentrations are low for January through April (fig. 5.7b,c). May through December is hurricane season and more sediment relative to other times of year may be generated.

Larsen (1997) examined the transport of silt and clay (<0.062 mm) for six samples in the Rio Icacos (fig. 5.8). The percent of sand (>0.062 mm) in suspension increased with discharge. For all samples the average amount of sand in suspension was 52.4% +/- 24.0 %, and ranged from 19 to 82%. Larsen (1997) acknowledged the small sample size of the data set but attributed increases in sand at high discharges to the abundant supply of sand in the channel. The intrusive bedrock of the basin weathers to medium-quartz sand. At high flows with increased stream power, sand on the bed of the channel is resuspended.

Walling (1974) Sediment-Transport Curve Approach

Results using Walling's (1974) four independent variables of discharge, time relation of sample, base flow, and flood intensity (described in Chapter 4) are listed in Table 5.2. The dependent variables were separated into all samples, samples on the rising hydrograph to the highest peak flow, and samples on the falling hydrograph from the highest peak flow. Analysis included discharge with and without base flow.

Reproduced with permission of the copyright owner. Further reproduction prohibited without permission.

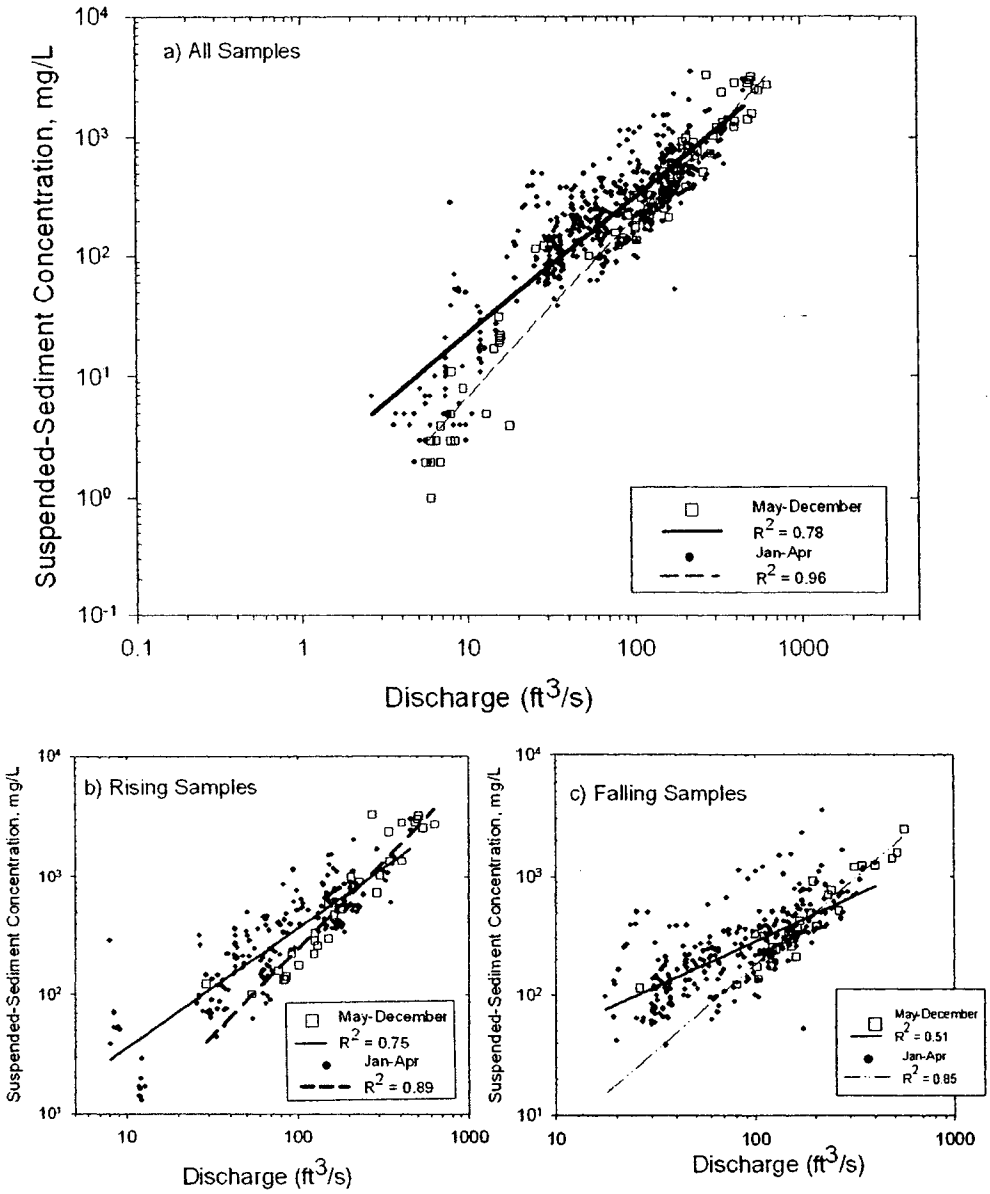

Figure 5.7. Seasonal suspended-sediment transport curves (May-Dec; Jan-Apr) for Rio Icacos near Naguabo. a) All samples, b) Rising hydrograph samples relative to the highest peak flow, and c) Falling hydrograph samples relative to the highest peak flow.

Reproduced with permission of the copyright owner. Further reproduction prohibited without permission.

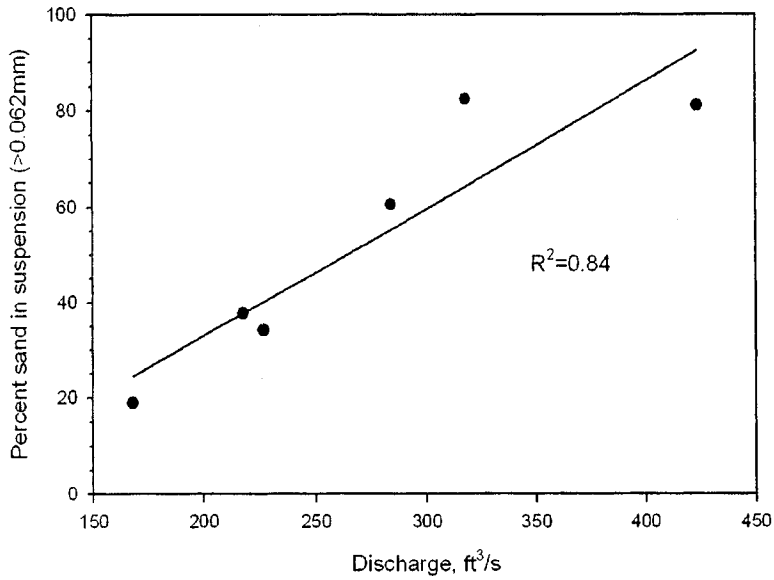

Fig. 5.8. Percent sand in suspension versus discharge, Rio Icacos (After Larsen, 1997).

The regression coefficient improved by separating samples on the rising hydrograph. For samples with baseflow discharge was the most important variable explaining suspended-sediment concentrations and had a positive slope of the best-fit regression line, indicating that discharge was correlated directly to suspended-sediment concentration. For rising samples without base flow, the base flow at the start of the event was significant and the slope of the best-fit regression line was negative, indicating that high base flows at the start of the event are diluting concentrations. For samples on the falling hydrograph without base flow, flood intensity was significant in the second step and the slope of the best-fit regression line was positive, indicating a direct correlation to the rate of hydrograph rise.

For samples with base flow removed, the most important factor explaining sediment concentrations was discharge, which had a positive slope (Table 5.2). For all samples and samples on the falling hydrograph (without base flow), flood intensity was important in the second

Reproduced with permission of the copyright owner. Further reproduction prohibited without permission.

Reproduced with permission of the copyright owner. Further reproduction prohibited without permission.

Table 5.2. Results of forward stepwise regression using Walling's (1974) four variables to explain suspended-sediment concentration. A) Discharge including base flow, B) Discharge subtracting base flow.

A)

Step	Independent variable using all samples (rising and falling)	R^2	Coefficient	Independent variable using rising samples	R^2	Coefficient	Independent variable using falling samples	R^2	Coefficient
Step one	Discharge	0.66	0.94	Discharge	0.77	1.04	Discharge	0.54	0.82
Step two	Flood Intensity	0.68	0.18	Base flow	0.78	-0.24	Flood Intensity	0.59	0.24
	Discharge		0.85	Discharge		1.05	Discharge		0.70

B)

Step	Independent variable using all samples (rising and falling)	R^2	Coefficient	Independent variable using rising samples	R^2	Coefficient	Independent variable using falling samples	R^2	Coefficient
Step one	Discharge	0.66	0.92	Discharge	0.77	1.03	Discharge	0.55	0.79
Step two	Flood Intensity	0.68	0.18	Base flow	0.79	-0.25	Flood Intensity	0.60	0.24
	Discharge		0.84	Discharge		1.04	Discharge		0.69

step of forward stepwise regression and had a positive slope, indicating that storms with rapidly rising hydrographs had high suspended-sediment concentrations. For samples on the rising hydrograph, base flow at the start of the event was the most important variable and had a negative slope, indicating that sediment may be diluted during high base flow.

Statistical Results at Rio Icacos

The statistical results performed on storm-generated suspended-sediment loads and concentrations for Rio Icacos are summarized below. Discussion on statistical results follows the flow chart of figure 4.11. Abbreviations for the statistical analysis are summarized in Table 4.7.

Entire event analysis

This section describes the results of statistical analysis at-a-station for Rio Icacos at Naguabo using characteristics of the entire runoff event. At Rio Icacos, the most accurate period of storm event suspended-sediment collection was from 05/05/1992 through 09/20/1994, during which 194 runoff events defined by a peak flow over 30 ft^3/s (0.85 m^3/s) occurred. Of these runoff events, 48 were sampled adequately to define suspended-sediment loads for the entire event (Table 5.3) and 13 were defined as complex events (Table 5.3).

The average suspended-sediment load for the 48 events was 41.4 tons (37.5 metric tons) (fig. 5.9). The maximum sediment load during the study period was 404 tons (366 metric tons) on 2/19/1994 (Table 5.3). Runoff associated with this event was 6.67×10^6 ft^3 (1.89×10^5 m^3) when 3.34 inches (85 mm) of rain fell. The largest runoff event of 1.05×10^7 ft^3 (2.96×10^5 m^3)

Reproduced with permission of the copyright owner. Further reproduction prohibited without permission.

occurred 02/19-20/1994 when 6.11 in (155 mm) of rain fell on the basin and 368 tons (334 metric tons) of sediment was transported.

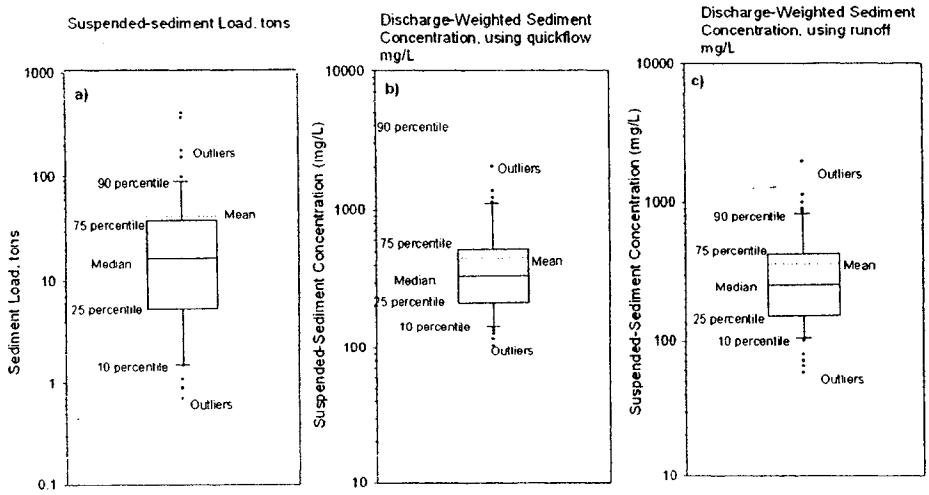

Figure 5.9. Box plots of dependent variables, a) suspended-sediment load, b) discharge-weighted sediment concentration using quickflow and c) discharge-weighted sediment concentrations using runoff, for Rio Icacos near Naguabo.

A plot of the discharge-weighted sediment concentration, using runoff, for each event over the period of study is shown in figure 5.10. There is considerable variation in the discharge-weighted sediment concentration: 58 to 1,940 mg/L (fig. 5.9b,c; 5.10). The average discharge-weighted sediment concentration of all events using runoff was 360 mg/L (fig. 5.9c). The average discharge-weighted sediment concentration of all events using quickflow was 452 mg/L (fig. 5.9b). The maximum discharge-weighted sediment concentration, for both quickflow and runoff, 2,040 mg/L and 1,940 mg/L, respectively, occurred 2/19/1994.

Peak flows of the 48 events ranged from 30 to 872 ft^3/s (0.85 to 24.7 m^3/s). Quickflow for the 48 events ranged from 1.91×10^5 to 9.86×10^6 ft^3 (5.42×10^3 to 2.74×10^5 m^3) and runoff ranged from 3.60×10^5 to 1.05×10^7 ft^3 (1.02×10^4 to 2.96×10^5 m^3). Rainfall contributing to runoff for the 48 events ranged from 0.13 to 6.11 in (3.3 to 155 mm).

Reproduced with permission of the copyright owner. Further reproduction prohibited without permission.

Reproduced with permission of the copyright owner. Further reproduction prohibited without permission.

Table 5.3. Summary of runoff events sampled adequately to determine suspended-sediment loads at Rio Icacos near Naguabo.

(Mna = Complex event, n=number of complex event, a,b,c, = sequence of each event in the entire multiple event; a=1st event, b=2nd, etc.)*

Start Date	Start Time (hour)	Start Discharge (ft3/s	End Date	End Time (hour)	Ending Discharge (ft3/s	Event Duration (hour)	Number of Peaks in Event	Peak Flow (ft3/s	Quickflow (ft3)	Runoff (ft3)	Suspended Sediment Load (tons)	M=Part of Complex Event
5/23/1992	0.25	9.0	5/23/1992	15.25	26.0	15.00	1	107	1282186	1904130	45.0	M1a
6/1/1992	11.00	15.0	6/2/1992	3.00	15.0	16.00	2	505	2320200	3184200	99.0	
7/8/1992	4.00	9.8	7/8/1992	9.25	12.0	5.25	1	76	369900	575910	3.9	
7/16/1992	22.75	9.4	7/17/1992	3.50	30.0	4.75	1	90	631777	812430	5.8	M2a
7/24/1992	2.75	9.0	7/24/1992	7.00	12.0	4.25	1	48	198900	359550	1.6	
7/26/1992	21.25	7.4	7/27/1992	3.00	9.8	5.75	1	41	191340	369360	0.9	
8/5/1992	1.25	12.0	8/5/1992	9.75	18.0	8.50	1	252	1539000	1998000	53.9	
8/14/1992	10.50	12.0	8/14/1992	22.50	12.0	12.00	2	66	614700	1133100	4.0	
8/30/1992	23.50	9.4	8/31/1992	8.75	11.0	9.25	1	82	718920	1058580	5.0	
9/4/1992	14.25	8.4	9/4/1992	20.00	8.4	5.75	1	31	213300	387180	0.7	
9/16/1992	2.00	6.0	9/16/1992	9.50	14.0	7.50	1	65	460800	730800	4.8	
9/18/1992	21.25	6.9	9/19/1992	4.25	10.0	7.00	1	37	272475	485415	1.1	
9/23/1992	18.25	7.9	9/24/1992	2.00	9.8	7.75	1	44	308250	555165	1.1	
9/30/1992	13.00	5.6	9/30/1992	17.75	9.8	4.75	1	44	232200	363870	1.5	
10/22/1992	16.50	2.9	10/22/1992	23.50	6.0	7.00	1	106	655335	767475	7.7	
11/2/1992	21.25	4.8	11/3/1992	7.00	7.4	9.75	1	83	725400	939510	6.1	
11/3/1992	14.50	4.8	11/4/1992	12.50	21.0	22.00	5	171	4026249	4502070	31.3	M3a
11/12/1992	15.00	3.6	11/12/1992	20.50	9.4	5.50	1	72	405360	534060	1.9	
11/16/1992	8.50	5.6	11/16/1992	22.00	9.4	13.50	1	175	1628460	1992960	19.2	
11/18/1992	2.00	9.8	11/18/1992	10.50	21.0	8.50	1	64	953691	1259460	4.0	M4a
11/20/1992	13.50	7.9	11/20/1992	22.75	10.0	9.25	1	162	1030320	1328355	18.0	
11/22/1992	6.76	20.0	11/23/1992	7.25	10.0	24.49	1	181	3691476	4573236	16.3	M5c
12/6/1992	4.25	9.8	12/6/1992	14.00	14.0	9.75	1	145	1205820	1623510	17.1	
12/25/1992	19.25	10.0	12/26/1992	9.75	20.0	14.50	2	177	2150594	2746800	22.0	M6a
12/26/1992	9.76	20.0	12/26/1992	20.75	15.0	10.99	1	343	2996772	3547732	67.7	M6b
12/29/1992	12.50	8.4	12/30/1992	16.00	21.0	27.50	3	410	7810560	9265860	169.8	
1/22/1993	4.00	11.0	1/23/1993	4.50	15.0	24.50	2	191	3505500	4652100	24.0	
2/20/1993	12.50	9.0	2/21/1993	17.50	16.0	29.00	3	162	4639950	5944950	31.9	
4/30/1993	9.76	27.0	4/30/1993	18.75	25.0	8.99	2	292	2796813	3471625	45.4	M7b
5/1/1993	11.75	16.0	5/2/1993	5.25	30.0	17.50	3	239	4328772	5352300	149.5	M8a
5/2/1993	12.51	24.0	5/2/1993	23.25	17.0	10.74	1	207	1606286	2257922	18.9	M8c
5/8/1993	17.00	5.6	5/9/1993	7.75	12.0	14.75	1	138	1137510	1604790	8.3	
5/9/1993	12.75	9.4	5/9/1993	19.75	16.0	7.00	1	192	1336590	1656630	14.2	
7/7/1993	12.00	7.4	7/7/1993	20.50	12.0	8.50	1	236	1625670	1922490	27.6	
7/22/1993	16.01	9.4	7/22/1993	23.00	11.0	6.99	1	198	1189743	1436294	15.4	M9b
9/15/1993	19.00	3.9	9/16/1993	10.75	11.0	15.75	3	328	3641498	4007745	47.6	M10a
9/16/1993	11.00	11.0	9/16/1993	23.00	13.0	12.00	1	337	2698740	3174345	44.7	M0b
10/7/1993	1.50	6.4	10/7/1993	12.25	11.5	10.75	1	231	1439712	1787373	19.5	
10/22/1993	16.50	6.0	10/22/1993	22.75	13.5	6.25	1	171	1013838	1233491	13.7	
12/19/1993	20.25	10.6	12/20/1993	1.00	21.2	4.75	1	151	870882	1050087	11.5	M11a
2/19/1994	5.50	5.2	2/19/1994	20.00	14.1	14.50	3	872	6341562	6671443	404.3	M12a
2/19/1994	20.01	14.1	2/20/1994	19.75	11.1	23.74	3	562	9677284	10468754	368.1	M12b
6/17/1994	9.00	6.4	6/18/1994	2.50	13.1	17.50	1	169	2066111	2681496	13.0	
7/17/1994	23.00	5.1	7/18/1994	19.00	15.0	20.00	1	169	2544940	3266932	15.3	
8/18/1994	19.75	10.0	8/19/1994	7.25	13.1	11.50	1	340	2612138	3091234	45.8	
8/23/1994	17.00	3.1	8/24/1994	2.00	10.0	9.00	1	190	1298856	1511671	8.3	
9/7/1994	18.50	3.5	9/8/1994	5.75	15.0	11.25	1	228	1754910	2130227	17.0	
9/20/1994	5.26	10.7	9/20/1994	22.75	10.0	17.49	1	240	3567650	4117597	28.3	M13b

A simple accounting of rainfall to quickflow can be made by assuming that the contributing area to the streamflow-gaging station, 1.26 mi^2 (3.26 km^2), is impervious and calculating the volume of quickflow resulting from each rainfall event. The results of this comparison are listed in Appendix 5.1. One event on 9/16/1993, had a ratio of computed quickflow to theoretical quickflow of 129 % (Appendix 5.1). This event was the second of a complex event. The ratio of computed quickflow to theoretical quickflow for the entire complex event, 9/15-16/1993, is 76 %. For the second complex event on 9/16/1993 to have over 100 % ratio may indicate that rainfall totals were poorly recorded for that event or that the volume of quickflow was overestimated. Nearby raingages to the Rio Icacos at Naguabo raingage showed similar amounts of rainfall and therefore, the rainfall measurements for this event may be appropriate. The event prior to the 9/16/1993 event was relatively large (8^{th} on record) and therefore, the base flow contribution to this event may have been larger than calculated with the hydrograph separation methodology used here. Excluding the 9/16/1993 event, rainfall to quickflow ranged from 7 to 66 % and averaged 42 % (Appendix 5.1).

The dependent variables used to describe sediment for the entire storm event are:

1) suspended-sediment load, in tons;

2) discharge-weighted sediment concentration, in mg/L

Plots of runoff versus the two dependent variables are shown in figure 5.11. Suspended-sediment load has the better relation to runoff (R^2=0.83) (fig. 5.11a). This is in part a spurious relation because discharge is used in the calculation of suspended-sediment load. There is considerable scatter in runoff versus discharge-weighted sediment concentration (fig. 5.11b), implying that some factor(s) other than runoff are controlling sediment concentration.

Reproduced with permission of the copyright owner. Further reproduction prohibited without permission.

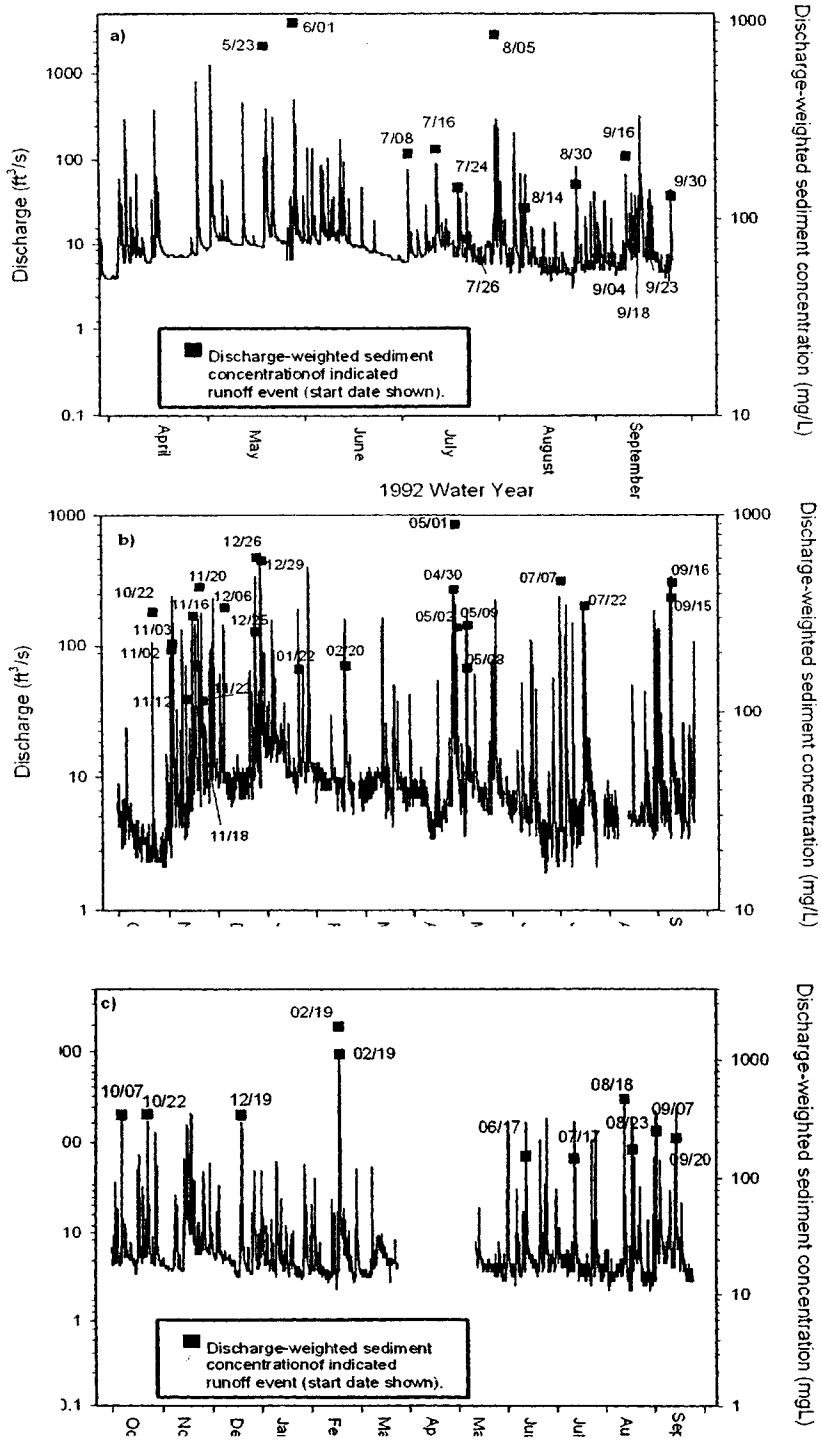

Figure 5.10. Instantaneous discharge and discharge-weighted sediment concentration for Rio Icacos near Naguabo, for period of investigation, a) May 1992 through September 1992, b) water year 1993, and c) water year 1994.

Reproduced with permission of the copyright owner. Further reproduction prohibited without permission.

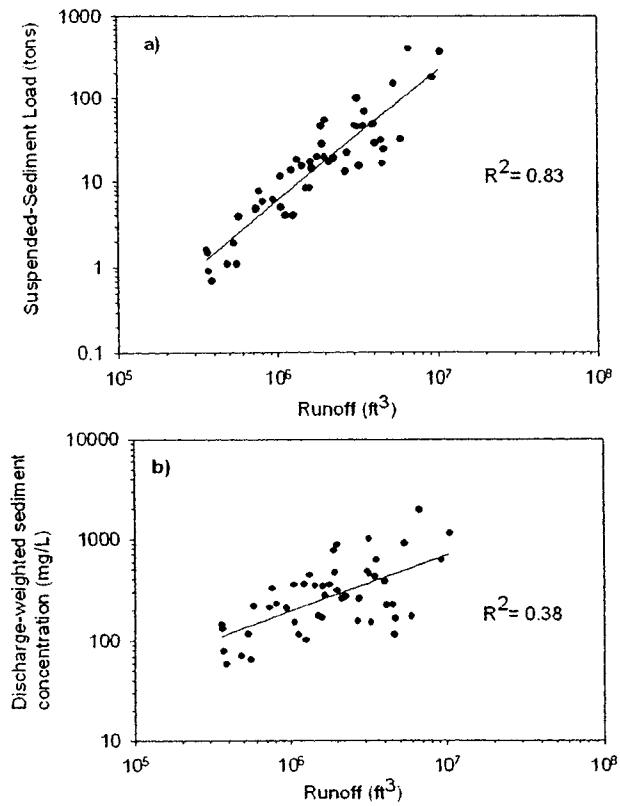

Figure 5.11. Plots of storm-generated runoff versus a) suspended-sediment load, and b) discharge-weighted sediment concentration for Rio Icacos near Naguabo.

The two dependent variables were tested against the independent variables shown in Table 4.8. Statistical analysis was performed against two portions of the runoff hydrograph:

1) the entire runoff event, and

2) to the highest peak of the event

Forward stepwise regression for suspended-sediment load against previous runoff events back to the 6th event indicated that only the current runoff event was significant (alpha = 0.15; R^2=0.68). A minimum of three previous events was used. Hydrographs were separated into quickflow and runoff. For the 48 storms that were adequately sampled, the base flow contribution was 5 to 48% of runoff.

Reproduced with permission of the copyright owner. Further reproduction prohibited without permission.

Quickflow Results (entire event)

The independent variables assembled to analyze the relation of suspended-sediment characteristics to quickflow characteristics are listed in Appendix 5.2. Tests for normality using the residuals indicated that 17 of the 23 independent variables needed a log transformation and three were transformed using the square root (Appendix 5.2).

Analysis of the correlation matrix showed a high correlation ($r>0.80$) among select variables (Appendix 5.3). Many of the characteristics of the previous event (20-LSPKBTI, 22-SMLSPKBS, 24-QULST, 26-PPTLSTI, 27-INTLST, 28-LS75OTI) and three previous events (29-SUM3PPTI, 30-QU3EVT) were correlated. Two of these variables (20-LSPKBTI, 27-INTLST) were removed. 1-QUICK and 10-RAIN had a high correlation (0.87) and 10-RAIN was removed. Current-event characteristics of 8-SMPKBS and 4-PKBS were intercorrelated; 4-PKBS was removed. Rate of hydrograph rise to the highest peak flow (6-MXTMJPK) and for any peak flow (7-MXTRP) were intercorrelated (0.99) and 6-MXTMJPK was removed. The high correlation of the highest peak flow (6-MXTMJPK) and for any peak flow (7-MXTRP) was because many of the events on Rio Icacos were single peak events.

Suspended-sediment load was highly correlated to peak flow (4-PKBS) and quickflow (1-QUICK) (fig. 5.12a,b). Correlation coefficients were lower using the discharge-weighted sediment concentration as a dependent variable and showed the peak flow (4-PKBS) and the sum of peak flows (9-SMPKBS) with the two highest R^2 values (fig. 5.12c,d) (Appendix 5.1).

Reproduced with permission of the copyright owner. Further reproduction prohibited without permission.

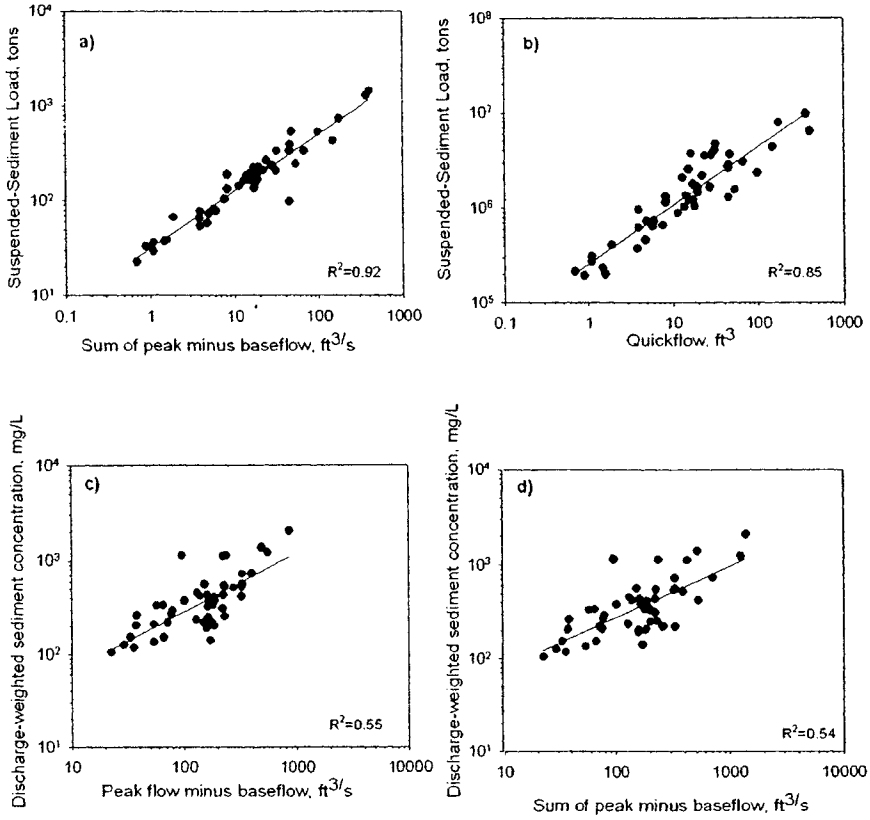

Figure 5.12. Graphical relations at Rio Icacos near Naguabo of independent variables with highest R^2 values using quickflow characteristics of the entire event against dependent variables. (a,b) suspended-sediment load and (c,d) discharge-weighted sediment concentration.

Forward stepwise regression (entire event, quickflow)

Forward stepwise regression was run on the 18 independent variables against the two dependent variables (Table 5.4). Both dependent variables (suspended-sediment load and discharge-weighted sediment concentration) showed the sum of peak flows (8-SMPKBS) was significant in the first step of forward stepwise regression (Table 5.4). The coefficient of the regression line was positive. Quickflow was not significant using suspended-sediment load as a dependent variable.

Reproduced with permission of the copyright owner. Further reproduction prohibited without permission.

Discharge-weighted sediment concentration as a dependent variable showed the maximum rate of hydrograph rise for any peak (7-MXTRP) was significant in the second step, and base flow preceding the start of the event (3-BASE) was significant in the third step (Table 5.4). The coefficient for the best-fit regression line was positive for both independent variables, indicating a direct correlation to the discharge-weighted sediment concentration.

Table 5.4. Results of forward stepwise regression for entire event using quickflow characteristics.

Dependent Variable	Step	Variables in the Model	R^2	F Statistic	Coefficient	Constant
suspended- sediment load, tons	One	8-SMPKBS	0.92	542	1.54	-2.20
discharge-	One	8-SMPKBS	0.54	53.3	0.54	1.36
weighted sediment	Two	7-MXTRP	0.60	7.34	0.31	1.83
concentration, mg/L		8-SMPKBS		8.12	0.31	
	Three	3-BASE	0.64	4.55	0.02	1.71
		7-MXTRP		7.21	0.29	
		8-SMPKBS		8.12	0.30	

Factor analysis - (entire event, quickflow)

Principal component analysis was performed on two sets of independent variables associated with quickflow characteristics of the event. One set contained 23 independent variables, including quickflow, the other set did not include quickflow (Appendices 5.4, 5.5). The scree plot showed a break in slope for six components which were selected for factor analysis.

Factor analysis for the data set with and without quickflow showed similar results. Over 73% of the variance was explained by the first three axes (Appendices 5.4, 5.5). Forward

Reproduced with permission of the copyright owner. Further reproduction prohibited without permission.

stepwise regression was performed on the factor scores from principal components analysis against both dependent variables (sediment loads and discharge-weighted sediment concentration) (Table 5.5). Both dependent variables had the same results and indicated PC2 as the most significant principal component in the first step of forward stepwise regression and PC1 in the second step (Table 5.5). PC2 has strong positive loadings (>0.6) on characteristics of the current event (1-QUICK, 4-PKBS, 8-SMPKBS, 10-RAIN, 13-RRISE). PC1 has strong positive loadings (>0.8) on characteristics of the previous event (>0.8) (24-QULST, 30-QU3EVT, 22-SMLSPKBS, 26-PPTLSTI, 29-SUM3PPTI, 27-INTLST, 28-LS75OTI). High negative loadings on PC1 (<-0.6) include characteristics between events (17-RNBTWTI, 18-PPTBTW, 19-INTBET). The slope of the best-fit regression line for PC2 and PC1 was positive, indicating a direct correlation to characteristics of the current event (PC1) and to characteristics of the previous event (PC2). The negative loadings on PC2 associated with characteristics between events indicated an inverse relation to suspended-sediment load and to the discharge-weighted sediment concentration.

Interpretations from factor analysis for the entire event using quickflow indicated that current-event characteristics and previous-event characteristics were directly correlated to sediment load and discharge- weighted sediment concentration. Hydrologic characteristics between events were inversely correlated to the dependent variables. In this interpretation, large previous events increase sediment supply and between-event characteristics flush sediment.

Varimax rotation (entire event, quickflow)

Rotations of the principal components axis was performed using the varimax rotation. The factor scores were saved after varimax rotation and forward stepwise regression was performed

Reproduced with permission of the copyright owner. Further reproduction prohibited without permission.

Table 5.5. Results of forward stepwise regression on the principal components for the entire event using quickflow characteristics.

Dependent Variable	Step	Variables in the Model	R^2	F Statistic	Coefficient	Constant
suspended-sediment load, tons	One	PC2	0.44	36.0	0.43	1.16
	Two	PC1	0.88	158	0.43	1.16
		PC2		159	0.43	
discharge-weighted sediment concentration, mg/L	One	PC2	0.36	25.6	0.18	2.54
	Two	PC1	0.52	15.5	0.12	2.54
		PC2		33.7	0.18	

on the factor scores against the dependent variables (Table 5.6) (Appendices 5.6; 5.7). Using suspended-sediment load as a dependent variable indicated PC2 was important in the first step of forward stepwise regression and PC5 important in the second step (Table 5.6) PC2 showed high positive loadings (>0.7) on characteristics of the current event (1-QUICK, 10-RAIN, 13-RRISE, 14-RAINFOL), and PC5 had strong positive loadings (>0.8) on characteristics related to the rate of hydrograph rise (6-MXTMJPK, 7-MXTRP) (Appendix 5.6).

Using the discharge-weighted sediment concentration as a dependent variable showed that PC5 and PC2 was significant in the first and second steps of forward stepwise regression, respectively (Table 5.6). PC5 had high positive loadings (>0.6) on characteristics related to peak flow and the rate of hydrograph rise (4-PKBS, 6-MXTMJPK, 7-MXTRP,). The coefficient for PC5 was positive and the loadings were positive, indicating a direct relation between the rate of hydrograph rise and discharge-weighted sediment concentration. PC2 was significant in the second step of forward stepwise regression (Table 5.6) and had high loadings on characteristics of the current event (1-QUICK, 10-RAIN, 13-RRISE, 14-RAINFOL) and the slope of the best-fit

Reproduced with permission of the copyright owner. Further reproduction prohibited without permission.

regression line was positive (Appendix 5.6, 5.7). Before varimax rotation current-event, previous-event, and between-event characteristics were significant, and after varimax rotation only current-event characteristics were significant.

Table 5.6. Results of forward stepwise regression on the principal components after varimax rotation for the entire event using quickflow characteristics.

Dependent Variable	Step	Variables in the Model	R^2	F Statistic	Coefficient	Constant
suspended-sediment load, tons	One	PC2	0.61	72.2	0.51	1.16
	Two	PC5	0.88	96.8	0.33	1.16
		PC2		222	0.51	
discharge-weighted sediment concentration, mg/L	One	PC5	0.47	40.8	0.21	2.54
	Two	PC2	0.64	20.9	0.12	2.54
		PC5		58.5	0.21	

Runoff Results (entire event)

The independent variables assembled to analyze the relation of suspended-sediment characteristics to runoff characteristics are listed in Appendix 5.8. Tests for normality using the residuals indicated that 21 of the 23 independent variables required a log transformation (Appendix 5.8).

Analysis of the correlation matrix showed a high correlation ($r>0.80$) among select variables (Appendix 5.9). Many of the characteristics of the previous event (21-LSPKTI, 23-SMLSPK, 25-RULST, 26-PPTLSTI, 27-INTLST, 28-LS75OTI) and three previous events (29-SUM3PPTI, 31-RU3EVT) were correlated. Two of these variables (21-LSPKTI, 27-INTLST) were removed. The remaining variables were retained because they were perceived to be important. 2-RUN and 10-RAIN showed a high correlation (0.87) and 10-RAIN was removed.

Reproduced with permission of the copyright owner. Further reproduction prohibited without permission.

Current-event characteristics of peak flow (9-SMPK and 5-PK) were intercorrelated; 5-PK was removed. Rates of hydrograph rise (6-MXTMJPK and 7-MXTRP) were intercorrelated (0.99) and 6-MXTMJPK was removed.

Peak flow and the sum of peak flows were the two variables showing the highest correlation coefficients with suspended-sediment load and discharge-weighted sediment concentration (fig. 5.13) (Appendix 5.9). Compared to the dependent variable suspended-sediment load, correlation coefficients were lower using discharge-weighted sediment concentration.

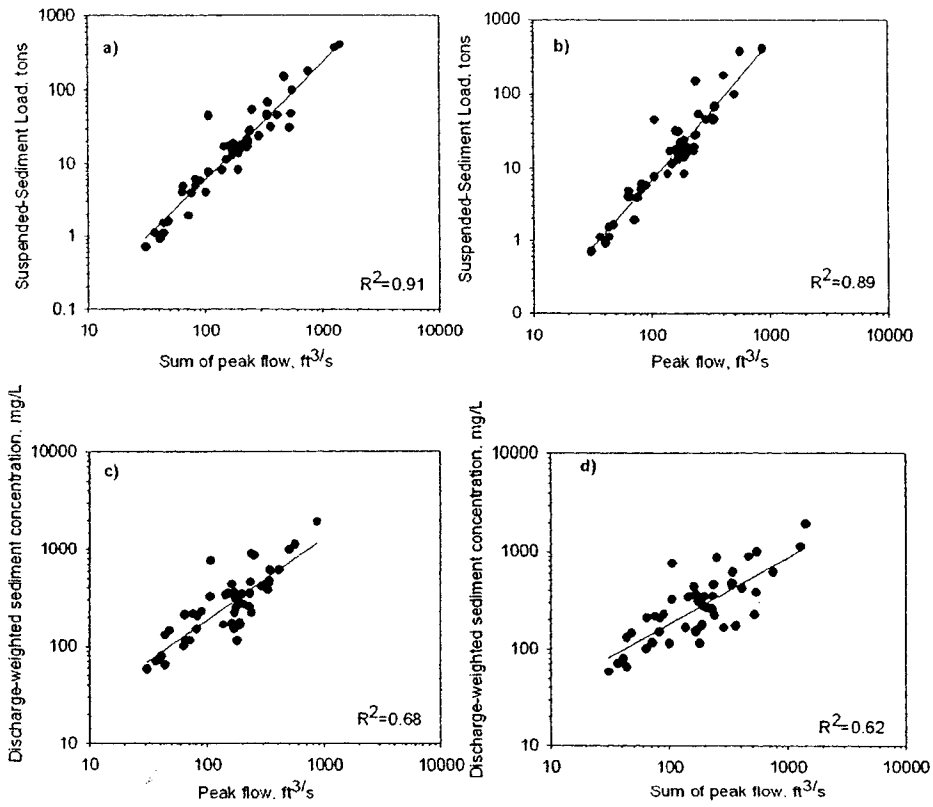

Figure 5.13. Graphical relations at Rio Icacos of independent variables with highest R^2 values using runoff characteristics of the entire event against dependent variables: (a,b) suspended-sediment load and (c,d) discharge-weighted sediment concentration.

Reproduced with permission of the copyright owner. Further reproduction prohibited without permission.

Forward stepwise regression (entire event, runoff)

Results of forward stepwise regression on the remaining 18 independent variables against the two dependent variables are listed in Table 5.7. Suspended-sediment load and discharge-weighted sediment concentration showed the sum of peak flows (8-SMPKBS) was significant in the first step of forward stepwise regression (Table 5.7). The coefficient of the regression line was positive. Using suspended-sediment load as a dependent variable showed base flow preceding the event (3-BASE) was significant in the second step of forward stepwise regression (Table 5.7). The coefficient of the regression was positive, indicating that as flow immediately preceding the event increases, the suspended-sediment load increases. Using the discharge-weighted sediment concentration as a dependent variable indicated the maximum rate of hydrograph rise for any peak (7-MXTRP) was significant in the second step of forward stepwise regression (Table 5.7). The coefficient of the regression was positive, indicating a direct correlation of the maximum rate of hydrograph rise for any peak to the discharge-weighted sediment concentration.

Table 5.7. Results of forward stepwise regression for entire event using runoff characteristics.

Dependent Variable	Step	Variables in the Model	R^2	F Statistic	Coefficient	Constant
suspended - sediment load, tons	One	9-SMPK	0.91	474	1.59	-2.40
	Two	3-BASE	0.92	5.29	0.02	-2.51
		9-SMPK		489	1.57	
discharge-weighted sediment concentration, mg/L	One	9-SMPK	0.62	74.1	0.68	0.89
	Two	7-MXTRP	0.68	9.51	0.34	1.46
		9-SMPK		13.8	0.42	
	Two	3-BASE	0.57	46.1	0.02	1.89
		7-MXTRP		7.00	0.46	

Reproduced with permission of the copyright owner. Further reproduction prohibited without permission.

.Factor analysis - (entire event, runoff)

Principal component analysis was performed on two sets of independent variables associated with quickflow characteristics of the event. One set contained 23 independent variables, including quickflow, the other set did not include quickflow (Appendices 5.10, 5.11). Six components were selected for factor analysis.

Factor analysis for the data set with and without quickflow gave similar results. Over 73% of the total variance was explained by the first three axes. Forward stepwise regression was performed on the factor scores from principal components analysis against both dependent variables (suspended-sediment load and the discharge-weighted sediment concentration (Table 5.8). Both dependent variables had the same result and indicated PC2 was the most significant principal component in the first step of forward stepwise regression and PC1 in the second step (Table 5.8). PC2 has strong positive loadings (>0.6) on characteristics of the current event (5-PK, 9-SMPK, 10-RAIN, 13-RRISE). PC1 has strong positive loadings (>0.8) on characteristics of the previous event (>0.8) (25-RULST, 31-RU3EVT, 23-SMLSPKTI, 26-PPTLSTI, 29-LST3PPTI, 27-INTLST, 28-LST75OTI). High negative loadings on PC1 (<-0.6) included characteristics between events (17-RNBTWTI, 18-PPTBTW, 19-INTBET). The slope of the best-fit regression line for PC2 and PC1 was positive, indicating a direct correlation to characteristics of the current event (PC1) and characteristics of the previous event (PC2). Negative loadings on PC2 indicated an inverse correlation of suspended-sediment load and the discharge-weighted concentration to characteristics between events. This was similar to the results using quickflow and indicated that large previous events contribute sediment to the system and between-event characteristics flush sediment.

Reproduced with permission of the copyright owner. Further reproduction prohibited without permission.

Interpretations from factor analysis for the entire event using runoff were similar to quickflow and indicated that current-event characteristics and previous-event characteristics were directly correlated to sediment load and discharge-weighted sediment concentration. Hydrologic characteristics between events were inversely correlated to the dependent variables.

Table 5.8. Results of forward stepwise regression on the principal components for the entire event using runoff characteristics.

Dependent Variable	Step	Variables in the Model	R^2	F Statistic	Coefficient	Constant
suspended - sediment load, tons	One	PC2	0.44	36.9	0.43	1.16
	Two	PC1	0.88	154	0.42	1.16
		PC2		160	0.43	
discharge-weighted sediment concentration, mg/L	One	PC2	0.42	33.8	0.22	-2.42
	Two	PC1	0.62	24.1	0.15	2.42
		PC2		50.8	0.22	

Varimax rotation (entire event, runoff)

Rotations of the principal components axes were performed using the varimax rotation. The factor scores were saved after varimax rotation and forward stepwise regression was run on the factor scores against the dependent variables (Table 5.9) (Appendices 5.12; 5.13).

Using suspended-sediment load as a dependent variable indicated PC2 was important in the first step of forward stepwise regression and PC5 was important in the second step (Table 5.9). PC2 showed high positive loadings (>0.7) on characteristics of the current event (1-QUICK, 9-SMPK, 10-RAIN, 13-RRISE, 14-RAINFOL) and PC5 showed high positive loadings (>0.8) on characteristics related to the rate of hydrograph rise (6-MXTMJPK, 7-MXTRP) (Appendix 5.12).

Reproduced with permission of the copyright owner. Further reproduction prohibited without permission.

The dependent variable discharge-weighted sediment concentration showed PC5 and PC2 were significant in the first and second steps of forward stepwise regression, respectively (Table 5.9). PC5 showed high positive loadings (>0.8) on characteristics related to the rate of hydrograph rise (6-MXTMJPK, 7-MXTRP). The coefficient for PC5 was positive and the loadings were positive, indicating a direct relation between the rate of hydrograph rise and suspended-sediment load. In the second step of forward stepwise regression PC2 was significant. PC2 had high loadings on characteristics of the current event and the slope of the best-fit regression line was positive (Appendices 5.12; 5.13). Results after varimax rotation using runoff were similar to results using quickflow and indicated that only current-event characteristics were significant after rotation.

Table 5.9. Results of forward stepwise regression on the principal components after varimax rotation for the entire event using runoff characteristics.

Dependent Variable	Step	Variables in the Model	R^2	F Statistic	Coefficient	Constant
suspended-sediment load, tons	One	PC2	0.62	75.1	0.51	1.16
	Two	PC5	0.88	92.5	0.33	1.16
		PC2		225	0.51	
discharge-weighted sediment concentration, mg/L	One	PC5	0.48	42.0	0.23	2.42
	Two	PC2	0.71	36.2	0.16	2.42
		PC5		74.2	0.23	

Discussion

For the entire event, separating storm runoff into quickflow did not improve the statistical significance or interpretations of the controlling variables. Multiple regression analysis of the independent variables, using quickflow and runoff, showed current-event characteristics of peak

Reproduced with permission of the copyright owner. Further reproduction prohibited without permission.

flow as important and directly correlated to the two dependent variables. Base flow was directly correlated to the two dependent variables, indicating that in storms with high base flows prior to the beginning of the event, more sediment was transported.

The results of forward stepwise regression analysis on the principal components before varimax rotation were similar for quickflow and runoff (Tables 5.5, 5.8). Factor analysis for the entire event, using quickflow or runoff, showed that current-event characteristics and previous-event characteristics were positively correlated to suspended-sediment load and the discharge-weighted concentration. Characteristics between events were negatively correlated.

Highest peak flow analysis

This section describes the results of statistical analysis for Rio Icacos near Naguabo using characteristics measured to the highest peak flow of the event. The 48 storms sampled adequately to the highest peak flow are summarized in Table 5.10. Two dependent variables were used to describe sediment to the highest peak flow: 1) suspended-sediment load, in tons, and 2) discharge-weighted sediment concentration, in mg/L.

The average suspended-sediment load for the 48 events was 18 tons (16 metric tons) (fig. 5.14a). The average discharge-weighted sediment concentration, using quickflow was 568 mg/L (fig. 5.14b). The average discharge-weighted sediment concentration, using runoff was 486 mg/L (fig. 5.14c). The maximum discharge-weighted sediment concentration using quickflow (2,700 mg/L) and runoff (2,960 mg/L) occurred for the storm event on 2/19/1994.

Reproduced with permission of the copyright owner. Further reproduction prohibited without permission.

Reproduced with permission of the copyright owner. Further reproduction prohibited without permission.

Table 5.10. Summary of runoff events sampled adequately to the highest peak of the event at Rio Icacos near Naguabo.

Start Date	Start Time (hours)	Start discharge (ft3/s)	End Date	End Time	Peak flow (ft3/s)	Quickflow (ft3)	Runoff (ft3)	Suspended-sediment load (tons)	Discharge-weighted sediment concentration (Quickflow) mg/L	Discharge-weighted sediment concentration (Runoff) mg/L
5/23/1992	0.25	9.0	5/23/1992	3.75	107	2.51E+005	3.72E+005	3.65	465	314
6/1/1992	11.00	15.0	6/1/1992	19.25	505	8.84E+005	1.33E+006	37.0	1342	893
7/8/1992	4.00	9.8	7/8/1992	6.25	76	1.73E+005	2.56E+005	1.57	291	196
7/16/1992	22.75	9.4	7/17/1992	0.25	90	1.62E+005	2.15E+005	1.47	291	220
7/24/1992	2.75	9.0	7/24/1992	3.75	48	6.13E+004	9.50E+004	0.62	324	209
7/26/1992	21.25	7.4	7/26/1992	22.00	41	3.47E+004	5.51E+004	0.28	260	164
8/5/1992	1.25	12.0	8/5/1992	2.00	252	2.58E+005	2.92E+005	13.3	1647	1460
8/14/1992	10.50	12.0	8/14/1992	17.00	66	3.50E+005	6.31E+005	2.04	186	103
8/30/1992	23.50	9.4	8/31/1992	1.75	82	2.12E+005	2.90E+005	1.21	183	134
9/4/1992	14.25	8.4	9/4/1992	15.25	31	4.33E+004	7.35E+004	0.23	169	100
9/16/1992	2.00	6.0	9/16/1992	3.25	65	1.07E+005	1.37E+005	1.57	470	367
9/18/1992	21.25	6.9	9/18/1992	23	37	8.72E+004	1.33E+005	0.35	129	84.6
9/23/1992	18.25	7.9	9/23/1992	19.25	44	6.66E+004	9.63E+004	0.43	209	144
9/30/1992	13.00	5.6	9/30/1992	14.00	44	7.57E+004	9.68E+004	0.84	355	278
10/22/1992	16.50	2.9	10/22/1992	18.00	106	2.19E+005	2.36E+005	3.36	493	456
11/2/1992	21.25	4.8	11/2/1992	23.00	83	1.77E+005	2.09E+005	2.81	507	430
11/3/1992	14.50	4.8	11/4/1992	3.00	171	1.69E+006	1.94E+006	12.4	234	204
11/12/1992	15.00	3.6	11/12/1992	16.50	72	1.51E+005	1.75E+005	0.82	174	151
11/16/1992	8.50	5.6	11/16/1992	13.25	175	5.39E+005	6.46E+005	3.79	225	188
11/18/1992	2.00	9.8	11/18/1992	6.00	64	6.10E+005	7.52E+005	3.17	167	135
11/20/1992	13.50	7.9	11/20/1992	15.25	162	2.96E+005	3.47E+005	8.43	912	778
11/22/1992	6.76	20.0	11/22/1992	9.75	181	8.17E+005	9.25E+005	5.76	226	200
12/6/1992	4.25	9.8	12/6/1992	8.25	145	5.75E+005	7.28E+005	12.9	719	568
12/25/1992	19.25	10.0	12/26/1992	1.00	177	9.63E+005	1.18E+006	13.9	462	377
12/26/1992	9.76	20.0	12/26/1992	11.75	343	6.17E+005	7.11E+005	18.5	958	832
12/29/1992	12.50	8.4	12/29/1992	17.25	410	1.34E+006	1.51E+006	50.0	1191	1063
1/22/1993	4.00	11.0	1/22/1993	14.75	191	1.16E+006	1.62E+006	7.10	196	141
2/20/1993	12.50	9.0	2/20/1993	20.75	162	2.06E+006	2.36E+006	15.2	236	206
4/30/1993	9.76	27.0	4/30/1993	14.50	292	1.71E+006	1.94E+006	32.0	598	529
5/1/1993	11.75	16.0	5/1/1993	14.25	239	9.18E+005	1.06E+006	29.1	1016	878
5/2/1993	12.51	24.0	5/2/1993	13.75	207	3.93E+005	4.68E+005	7.07	576	484
5/8/1993	17.00	5.6	5/8/1993	22.00	138	2.52E+005	3.73E+005	3.30	419	284
5/9/1993	12.75	9.4	5/9/1993	13.75	192	3.39E+005	3.75E+005	6.18	583	528
7/7/1993	12.00	7.4	7/7/1993	15.50	236	6.21E+005	7.26E+005	10.2	526	450
7/22/1993	16.01	9.4	7/22/1993	17.25	198	4.64E+005	5.03E+005	10.3	709	653
9/15/1993	19.00	3.9	9/15/1993	21.50	328	9.16E+005	9.54E+005	20.5	718	689
9/16/1993	11.00	11.0	9/16/1993	12.50	337	8.44E+005	8.94E+005	16.6	629	594
10/7/1993	1.50	6.4	10/7/1993	4.25	231.32	4.86E+005	5.56E+005	11.3	744	650
10/22/1993	16.50	6.0	10/22/1993	18.25	171.23	3.80E+005	4.25E+005	5.72	481	431
12/19/1993	20.25	10.6	12/19/1993	21.25	151.34	2.24E+005	2.62E+005	2.52	360	308
2/19/1994	5.50	5.2	2/19/1994	13.75	871.86	3.18E+006	3.35E+006	268	2697	2558
2/19/1994	20.01	14.1	2/20/1994	0.25	547.9	3.99E+006	4.11E+006	173	1390	1350
6/17/1994	9.00	6.4	6/17/1994	11.00	168.5	3.92E+005	4.40E+005	4.51	369	328
7/17/1994	23.00	5.1	7/18/1994	5.50	168.5	8.62E+005	1.02E+006	5.93	220	187
8/18/1994	19.75	10.0	8/18/1994	21.75	339.51	8.65E+005	9.39E+005	25.4	943	868
8/23/1994	17.00	3.1	8/23/1994	19.00	189.54	4.08E+005	4.36E+005	5.32	418	391
9/7/1994	18.50	3.5	9/7/1994	20.25	227.51	5.29E+005	5.57E+005	8.52	516	490
9/20/1994	5.26	10.7	9/20/1994	8.50	240.31	9.41E+005	1.03E+006	9.72	331	302

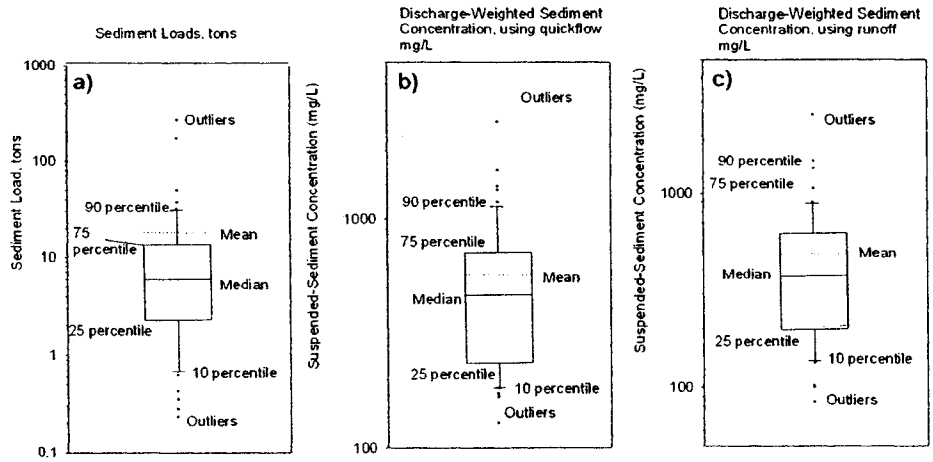

Figure 5.14. Box plots of dependent variables to the highest peak flow, a) sediment load, b) discharge-weighted sediment concentrations using quickflow, and c) discharge-weighted sediment concentration using runoff.

Quickflow Results (highest peak)

The independent variables assembled to analyze the relation of suspended-sediment characteristics to quickflow characteristics for the portion of the hydrograph rising to the highest peak flow are listed in Appendix 5.14. Tests for normality using the residuals and inspection of histograms indicated that 10 of the 17 independent variables required a log transformation and 3 were transformed using the square root (Appendix 5.14). Analysis of the correlation matrix showed a high correlation ($r>0.80$) among select variables (Appendix 5.15). Variables that showed a high correlation were related to the previous event or the three previous events (24-QULST, 22-SMLSPKBS, 26-PPTLSTI, 27-INTLST, 20-LSPKBTI, 29-SUM3PPTI, and 30-QU3EVT (Appendix 5.15). Two of these variables (20-LSPKBTI, 27-INTLST) were removed.

Reproduced with permission of the copyright owner. Further reproduction prohibited without permission.

Forward stepwise regression (highest peak, quickflow)

Results of forward stepwise regression on the remaining independent variables with both dependent variables are listed in Table 5.11. The peak flow of the current event minus base flow (4-PKBS) was significant in either the first or second step of forward stepwise regression for both dependent variables (Table 5.11). For both dependent variables, the coefficient of the regression equation was positive, indicating a direct correlation of peak flow to suspended-sediment load and concentration. The rate of hydrograph rise to the highest peak flow (6-MXTMJPK) was significant in the first step of forward stepwise regression using the discharge-weighted sediment concentration as a dependent variable and was significant in the second step using suspended-sediment load as the dependent variable. The coefficient of the best-fit regression line was positive.

Table 5.11. Results of forward stepwise regression measured to the highest peak flow of the event using quickflow characteristics.

Dependent Variable	Step	Variables in the Model	R^2	F Statistic	Coefficient	Constant
suspended-sediment load, tons	One	4-PKBS	0.88	328	0.12	-0.82
	Two	1-QUICK	0.94	56.0	0.64	-3.77
		4-PKBS		8.12	0.31	
	Three	6-MXTMJPK	0.95	5.67	0.27	-4.04
		1-QUICK		65.4	0.73	
		4-PKBS		17.5	0.05	
discharge-weighted sediment concentration, mg/L	One	6-MXTMJPK	0.67	91.8	0.63	2.59
	Two	4-PKBS	0.72	7.95	0.02	2.33
		6-MXTMJPK		14.8	0.40	

Reproduced with permission of the copyright owner. Further reproduction prohibited without permission.

Quickflow was significant in the second step using suspended-sediment load as a dependent variable. Results were similar to the entire event in showing that peak flows and rate of hydrograph rise were significant. Quickflow was significant for statistical relations to the highest peak flow but was not significant when considering the entire event.

Factor analysis - (highest peak, quickflow)

Principal component analysis was performed on two sets of independent variables associated with quickflow characteristics of the event. One set was used in forward stepwise regression against the dependent variables, suspended-sediment load (Appendices 5.16; 5.17). Six components were selected for factor analysis.

Both sets of factor analysis had similar results. Over 80% of the total variance was explained by the first three axes. Both dependent variables showed PC2 to be important in the first step of forward stepwise regression (Table 5.12). For all dependent variables PC2 had high loadings on characteristics of the current event (1-QUICK, 4-PKBS, 6-MXTMJPK, 11-INT15, 13-RRISE,) (Appendix 5.16). The coefficient of regression for each dependent variable was correlated directly with PC2.

Suspended-sediment load and discharge-weighted sediment concentration showed PC1 to be important in the second step of forward stepwise regression (Table 5.12). PC1 had strong positive loadings (>0.8) on the previous event and previous three event characteristics (21-LSPKBTI, 22-SMLSPKBS, 24-QULST, 26-PPTLSTI,27-INTLST, 28- LS75OTI, 29-SUM3PPTI, 30-QU3EVT). Strong negative loadings (<-0.7) for PC1 were on characteristics between events (17-RNBTWTI, 18-PPTBTW, 19-INTBTW). The coefficient of regression was

Reproduced with permission of the copyright owner. Further reproduction prohibited without permission.

positive, indicating that previous-event characteristics were directly correlated to suspended-sediment load of the current event and inversely correlated to characteristics between events.

Interpretations from factor analysis to the highest peak flow using quickflow were similar for the entire event and show that current-event characteristics and previous-event characteristics were directly correlated to sediment load and discharge weighted sediment concentration. Hydrologic characteristics between events were inversely correlated to the dependent variables.

Table 5.12. Results of forward stepwise regression on the principal components measured to the highest peak of the event using quickflow characteristics.

Dependent Variable	Step	Variables in the Model	R^2	F Statistic	Coefficient	Constant
suspended-sediment load, tons	One	PC2	0.62	74.1	0.52	0.75
	Two	PC1	0.89	109	0.34	0.75
		PC2		248	0.52	
discharge-weighted sediment concentration, mg/L	One	PC2	0.49	43.5	-0.21	2.66
	Two	PC1	0.59	11.4	0.10	2.66
		PC2		53.4	-0.21	

Varimax rotation (highest peak, quickflow)

Rotations of the principal components axes were performed using the varimax rotation. Over 70% of the variability was explained by the first three principal component axes. The factor scores were saved after varimax rotation and forward stepwise regression was performed on the factor scores against the dependent variables (Table 5.13) (Appendices 5.18; 5.19).

Both dependent variables showed either PC2 or PC5 was significant in the first or second step of forward stepwise regression (Table 5.13). PC2 for both dependent variables had high

Reproduced with permission of the copyright owner. Further reproduction prohibited without permission.

positive loadings (>0.6) on characteristics of the current event (1-QUICK, 4-PKBS, 6-MXTMJPK,11-INT15, 13-RRISE) (Appendix 5.18; 5.19). The coefficient of regression was positive, indicating that suspended-sediment load was directly correlated with PC2.

PC5 had a strong positive loadings (>0.5 peak flow (4-PKBS) and on the rate of hydrograph rise to the highest peak (6-MXTMJPK) (Appendices 5.18; 5.19). The regression coefficient was positive, indicating that peak flow characteristics were directly correlated with suspended-sediment load. Results after varimax rotation using quickflow to the highest peak flow were similar to results for the entire event and indicated that only current-event characteristics were significant after rotation.

Table 5.13. Results of forward stepwise regression on the principal components after varimax rotation to the highest peak flow using quickflow characteristics.

Dependent Variable	Step	Variables in the Model	R^2	F Statistic	Coefficient	Constant
suspended-sediment load, tons	One	PC2	0.68	96.5	0.55	0.75
	Two	PC5	0.86	56.9	0.28	0.75
		PC2		214	0.55	
discharge-weighted sediment concentration, mg/L	One	PC5	0.58	64.5	0.3	2.64
	Two	PC2	0.71	20.4	0.11	2.64
		PC5		91.7	0.23	

Runoff Results (highest peak)

The independent variables assembled to analyze the relation of suspended-sediment characteristics to quickflow characteristics for the portion of the hydrograph rising to the highest peak flow are listed in Appendix 5.20. Analysis of the correlation matrix showed the same results as for the entire event (Appendix 5.21). Variables that showed a high correlation (r>0.80) were

Reproduced with permission of the copyright owner. Further reproduction prohibited without permission.

removed and included the previous event peak flow (20-LSPKTI) and the previous event 15-minute rainfall intensity (27-INTLST).

Forward stepwise regression (highest peak, runoff)

Results of forward stepwise regression for both dependent variables indicated that current-event characteristics were significant in all steps. Peak flow (5-PK) was significant in the first step of forward stepwise regression using suspended-sediment load and significant in the second step using discharge-weighted sediment concentration (Table 5.14). The coefficient of regression was positive. The rate of hydrograph to the highest peak (6-MXTMJPK) was significant in the first step of forward stepwise regression using discharge-weighted sediment concentration and the coefficient was positive (Table 5.14). Using suspended-sediment load as a dependent variable showed runoff (2-RUN) was significant in the second step of forward stepwise regression and the coefficient was positive (Table 5.14). Runoff was significant forstatistical relations to the highest peak flow but was not significant when looking at the entire event.

Factor analysis - (highest peak, runoff)

Principal component analysis was performed on two sets of independent variables associated with runoff characteristics to the highest peak flow (Appendix 5.22; 5.23). Six components were selected for factor analysis. Both sets of factor analysis have similar results. Over 80% of the total variance was explained by the first three axes.

Results of forward stepwise regression on the principal components were identical to using quickflow variables to the highest peak (Table 5.12; 5.15). Both dependent variables showed PC2 to be important in the first step of forward stepwise regression (Table 5.15).

Reproduced with permission of the copyright owner. Further reproduction prohibited without permission.

Table 5.14. Results of forward stepwise regression measured to the highest peak flow of the event using runoff characteristics.

Dependent Variable	Step	Variables in the Model	R^2	F Statistic	Coefficient	Constant
suspended-sediment load, tons	One	5-PK	0.88	325	0.13	-0.91
	Two	2-RUN	0.94	45.7	0.62	-3.89
		5-PK		100	0.08	
discharge-weighted sediment concentration, mg/L	One	6-MXTMJPK	0.67	91.8	0.62	2.59
	Two	5-PK	0.72	8.14	0.02	2.31
		6-MXTMJPK		14.7	0.40	

PC2 had high loadings on characteristics of the current event (2-RUN, 5-PK, 6-MXTMJPK, 11-INT15, 13-RRISE,) (Appendices 5.22; 5.23). The coefficient of the best-fit regression line for each dependent variable was directly correlated with PC2.

Dependent variables, suspended-sediment load and discharge-weighted sediment concentration, showed PC1 to be important in the second step of forward stepwise regression (Table 5.15). PC1 has strong positive loadings (>0.8) on previous event and previous three event characteristics (21-LSPKBTI, 22-SMLSPKBS, 24-QULST, 26-PPTLSTI,27-INTLST, 28-LS75OTI, 29-SUM3PPTI, 30-QU3EVT). Strong negative loadings (<-0.7) are for between-events characteristics (17-RNBTWTI, 18-PPTBTW, 19-INTBTW). The coefficient of regression was positive, indicating that suspended-sediment load and the discharge-weighted sediment concentration were directly correlated to the previous-event characteristics and inversely correlated to characteristics between events.

Interpretations from factor analysis for the entire event using runoff to the highest peak flow were similar for the quickflow to the highest peak flow and show that current-event characteristics

Reproduced with permission of the copyright owner. Further reproduction prohibited without permission.

and previous-event characteristics were directly correlated to sediment load and discharge weighted sediment concentration. Hydrologic characteristics between events were inversely correlated to the dependent variables.

Table 5.15. Results of forward stepwise regression on the principal components measured to the highest peak of the event using runoff characteristics.

Dependent Variable	Step	Variables in the Model	R^2	F Statistic	Coefficient	Constant
suspended-sediment load, tons	One	PC2	0.62	76.6	0.52	0.75
	Two	PC1	0.89	106	0.34	0.75
		PC2		251	0.52	
discharge-weighted sediment concentration, mg/L	One	PC2	0.53	52.7	-0.24	2.56
	Two	PC1	0.66	16.0	0.12	2.56
		PC2		70.0	-0.24	

Varimax rotation (highest peak, runoff)

Rotations of the principal components axes were performed using the varimax rotation. Over 70% of the variability was explained by the first three principal component axes. The factor scores were saved after varimax rotation and forward stepwise regression was performed on the factor scores against the dependent variables (Table 5.16) (Appendices 5.24; 5.25).

Results were similar to using quickflow variables to the highest peak flow. Both dependent variables showed either PC2 or PC5 was significant in the first or second step of forward stepwise regression (Table 5.16). PC2 had high positive loadings (>0.7) on characteristics of the current event (2-RUN, 5-PK, 11-INT15, 13-RRISE) (Appendices 5.24; 5.25). The coefficient of regression was positive, indicating that suspended-sediment load was correlated directly with PC2.

Reproduced with permission of the copyright owner. Further reproduction prohibited without permission.

Table 5.16. Results of forward stepwise regression on the principal components after varimax rotation to the highest peak using runoff characteristics.

Dependent Variable	Step	Variables in the Model	R^2	F Statistic	Coefficient	Constant
suspended-sediment load, tons	One	PC2	0.65	85.5	0.54	0.75
	Two	PC5	0.86	63.2	0.30	0.75
		PC2		201	0.54	
discharge-weighted sediment concentration, mg/L	One	PC5	0.61	73.0	0.26	2.56
	Two	PC2	0.76	26.7	0.13	2.56
		PC5		114	0.26	

PC5 has strong positive loadings (>0.5) on characteristics of the current peak flow (5-PK, 6-MXTMJPK) (Appendices 5.24; 5.25). The regression coefficient was positive, indicating that as peak flow characteristics increased the sediment load of the current event increased. Results after varimax rotation using runoff to the highest peak flow were similar to results for the entire event and indicated that only current-event characteristics were significant after rotation.

Discussion

Statistical results to the highest peak flow, using quickflow or runoff, for forward stepwise regression on the independent variables in each case indicated characteristics of the current event related to peak flow (peak flow, rate of hydrograph rise) were significant and directly correlated to suspended-sediment load and the discharge-weighted concentration. Runoff and quickflow were significantly correlated to suspended-sediment load. Factor analysis to the highest peak flow, using quickflow or runoff, showed that current-event characteristics and previous-event

Reproduced with permission of the copyright owner. Further reproduction prohibited without permission.

characteristics were positively correlated to suspended-sediment load and the discharge-weighted concentration. Characteristics between events were negatively correlated.

Hysteresis

Hysteresis loops of the 48 sampled events were analyzed for the timing of the peak suspended-sediment concentration relative to peak flow, the type of hysteresis, and the width of the hysteresis loop (Table 5.17). For the entire event, 35 of the 48 events had the peak suspended-sediment concentration sampled between 1 to 183 minutes before the highest peak flow. Six events had the peak suspended-sediment concentration collected 2 to 38 minutes after peak flow, and seven events had the suspended-sediment concentration coincide with peak flow.

For the entire event, hysteresis Type 1 (clockwise) is most common (fig.), occurring in 36 of the 48 events (75%). One event was characterized as Type 2 (spiral loop), two events were Type 3 (counterclockwise), two events were Type 4 (spiral) and two events were Type 5 (straight line) (fig. 5.15). Five events did not have enough samples to define adequately the hysteresis loop. Eleven of the events were multipeaked but only 4 were sampled adequately to define a hysteresis type for the secondary peaks. Therefore, the hysteresis types for multipeaked events are not shown.

Hysteresis loops around the highest peak flow were examined to determine the maximum width of the hysteresis loop, which quantifies how much exhaustion or replenishment of sediment occurred during the runoff event. Analysis into the causes for exhaustion and replenishment of sediment were examined. Hysteresis loops were categorized into Type-1 and Type-3 occurrences (Appendix 5.26).

Reproduced with permission of the copyright owner. Further reproduction prohibited without permission.

Reproduced with permission of the copyright owner. Further reproduction prohibited without permission.

Table 5.17. Summary of hysteresis characteristics for Rio Icacos near Naguabo.
In events with more than one peak, the highest peak is in bold.
See figure 4.12 for a description of the hysteresis type.

Start Date	Start Hour	End Date	End Hour	Number of Peaks	Peak discharge, ft3/s	Peak sediment concentration mg/L	Time of peak suspended-sediment concentration relative to peak discharge, min (-) indicates prior to peak	Hysteresis type for the entire event	Hysteresis type for the highest peak
5/23/1992	0.25	5/23/1992	15.25	1	113	394	-10	1	1
6/1/1992	11.00	6/2/1992	3	2	505	2780	-3	5	5
7/8/1992	4.00	7/8/1992	9.25	1	77	419	0	1	1
7/16/1992	22.75	7/17/1992	3.5	1	90	411	-10	1	1
7/24/1992	2.75	7/24/1992	7	1	50	271	-10	2	2
7/26/1992	21.25	7/27/1992	3	1	48	199	0	ot enough samples	
8/5/1992	1.25	8/5/1992	9.75	1	275	1660	-0	1	1
8/14/1992	10.50	8/14/1992	22.5	2	66	237	15	1	1
8/30/1992	23.50	8/31/1992	8.75	1	82	343	15	4	4
9/4/1992	14.25	9/4/1992	20	1	32	100	0	1	1
9/16/1992	2.00	9/16/1992	9.5	1	65	462	-16	1	1
9/18/1992	21.25	9/19/1992	4.25	1	37	120	-30	1	1
9/23/1992	18.25	9/24/1992	2	1	44	172	-20	ot enough samples	
9/30/1992	13.00	9/30/1992	17.75	1	45	367	-19	1	1
10/22/1992	16.50	10/22/1992	23.5	1	106	556	-11	1	1
11/2/1992	21.25	11/3/1992	7	1	83	467	-40	1	1
11/3/1992	14.50	11/4/1992	12.5	5	171	756	-15	1	1
11/12/1992	15.00	11/12/1992	20.5	1	72	236	0	3	3
11/16/1992	8.50	11/16/1992	22	1	175	638	38	4	4
11/18/1992	2.00	11/18/1992	10.5	1	64	193	-183	1	1
11/20/1992	13.50	11/20/1992	22.75	1	167	868	0	1	1
11/22/1992	6.76	11/23/1992	7.25	1	181	364	-23	1	1
12/6/1992	4.25	12/6/1992	14	1	146	1160	-75	1	1
12/25/1992	19.25	12/26/1992	9.75	2	177	652	-60	1	1
12/26/1992	9.76	12/26/1992	20.75	1	349	1193	0	1	1
12/29/1992	12.50	12/30/1992	16	3	410	1700	-50	1	1
1/22/1993	4.00	1/23/1993	4.5	2	191	540	-8	1	1
2/20/1993	12.50	2/21/1993	17.5	3	162	367	2	1	1
4/30/1993	9.76	4/30/1993	18.75	2	292	996	-37	1	1
5/1/1993	11.75	5/2/1993	5.25	3	239	3540	14	3	3
5/2/1993	12.51	5/2/1993	23.25	1	207	724	-1	1	1
5/8/1993	17.00	5/9/1993	7.75	1	138	563	-5	ot enough samples	
5/9/1993	12.75	5/9/1993	19.75	1	192	645	-6	ot enough samples	
7/7/1993	12.00	7/7/1993	20.5	1	236	1190	-6	1	1
7/22/1993	16.01	7/22/1993	23	1	198	683	-15	1	1
9/15/1993	19.00	9/16/1993	10.75	1	328	1110	-21	1	1
9/16/1993	11.00	9/16/1993	23	1	337	947	9	1	1
10/7/1993	1:50	10/7/1993	12.25	1	249	886	-20	1	1
10/22/1993	16.50	10/22/1993	22.75	1	171	638	-5	5	5
12/19/1993	20.25	12/20/1993	1	1	164	698	-20	1	1
2/19/1994	5.50	2/19/1994	20	3	872	3340	-90	1	1
2/19/1994	20.01	2/20/1994	19.75	3	562	2570	-20	1	1
6/17/1994	9.00	6/18/1994	2.5	1	169	460	-15	1	1
7/17/1994	23.00	7/18/1994	19	1	169	400	-15	ot enough samples	
8/18/1994	19.75	8/19/1994	7.25	1	340	1110	-21	1	1
8/23/1994	17.00	8/24/1994	2	1	198	423	-25	1	1
9/7/1994	18.50	9/8/1994	5.75	1	228	575	-25	1	1
9/20/1994	5.26	9/20/1994	22.75	1	240	563	-10	1	1

Reproduced with permission of the copyright owner. Further reproduction prohibited without permission.

Table 5.17. Continued.

Start Date	Start Hour	End Date	End Hour	First peak peak ft3/s	First peak suspended sediment concentration, mg/L	Time of 1st peak suspended-sediment concentration relative to peak discharge, min	Hysteresis type of first peak	Second peak ft3/s	Second peak suspended sediment concentration, mg/L	Time of 2nd peak suspended-sediment concentration relative to peak discharge, min	Hystersis Type
5/23/1992	0.25	5/23/1992	15.25								
6/1/1992	11.00	6/2/1992	3.00	48	183	0	3				
7/8/1992	4.00	7/8/1992	9.25								
7/16/1992	22.75	7/17/1992	3.50								
7/24/1992	2.75	7/24/1992	7.00								
7/26/1992	21.25	7/27/1992	3.00								
8/5/1992	1.25	8/5/1992	9.75								
8/14/1992	10.50	8/14/1992	22.50	not enough samples							
8/30/1992	23.50	8/31/1992	8.75								
9/4/1992	14.25	9/4/1992	20.00								
9/16/1992	2.00	9/16/1992	9.50								
9/18/1992	21.25	9/19/1992	4.25								
9/23/1992	18.25	9/24/1992	2.00								
9/30/1992	13.00	9/30/1992	17.75								
10/22/1992	16.50	10/22/1992	23.50								
11/2/1992	21.25	11/3/1992	7.00								
11/3/1992	14.50	11/4/1992	12.50	97	248	11	3	118	221	-45	1
11/12/1992	15.00	11/12/1992	20.50								
11/16/1992	8.50	11/16/1992	22.00								
11/18/1992	2.00	11/18/1992	10.50								
11/20/1992	13.50	11/20/1992	22.75								
11/22/1992	6.76	11/23/1992	7.25								
12/6/1992	4.25	12/6/1992	14.00								
12/25/1992	19.25	12/26/1992	9.75	50	not sampled						
12/26/1992	9.76	12/26/1992	20.75								
12/29/1992	12.50	12/30/1992	16.00	228	1140	145	2	118	ot enough samples		
1/22/1993	4.00	1/23/1993	4.50	97							
2/20/1993	12.50	2/21/1993	17.50	128	not sampled			74	ot enough samples		
4/30/1993	9.76	4/30/1993	18.75	121							
5/1/1993	11.75	5/2/1993	5.25	157	735	-16	1				
5/2/1993	12.51	5/2/1993	23.25								
5/8/1993	17.00	5/9/1993	7.75								
5/9/1993	12.75	5/9/1993	19.75								
7/7/1993	12.00	7/7/1993	20.50								
7/22/1993	16.01	7/22/1993	23.00								
9/15/1993	19.00	9/16/1993	10.75								
9/16/1993	11.00	9/16/1993	23.00								
10/7/1993	1.50	10/7/1993	12.25								
10/22/1993	16.50	10/22/1993	22.75								
12/19/1993	20.25	12/20/1993	1.00								
2/19/1994	5.50	2/19/1994	20.00	20	ot enough samples			531	3340	-30	nough sam
2/19/1994	20.01	2/20/1994	19.75	423	ot enough samples			303	777	25	nough sam
6/17/1994	9.00	6/18/1994	2.50								
7/17/1994	23.00	7/18/1994	19.00								
8/18/1994	19.75	8/19/1994	7.25								
8/23/1994	17.00	8/24/1994	2.00								
9/7/1994	18.50	9/8/1994	5.75								
9/20/1994	5.26	9/20/1994	22.75								

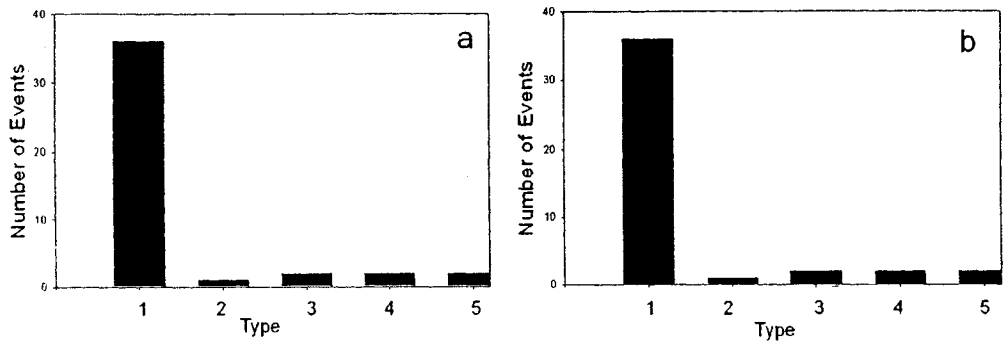

Figure 5.15. Hysteresis loops described at Rio Icacos near Naguabo for a) the entire event and (b) near the highest peak flow.

Analysis of the correlation table showed two variables with high intercorrelation (25-RULST and 31-RU3EVT) and 25-RULST was removed. Because only four storms were classified as counterclockwise loops (Type-3), results of forward stepwise regression on the storm characteristics related to hysteresis are only shown for clockwise hysteresis loops (Table 5.18) (Appendix 5.26).

In the first step of forward stepwise regression runoff (2-RUN) was significant in explaining the clockwise hysteresis width and the slope of the best-fit line was positive (Table 5.18) (Appendix 5.26). In the second step of forward stepwise regression, the time of the peak sediment concentration relative to peak flow (34-TIME_PKCON) was significant (fig. 5.16b; Table 5.18) and the slope of the best-fit regression line was negative, indicating that the earlier the sediment concentration reaches its peak before the highest peak flow, the more sediment exhaustion occurs. These results suggest that the channel was a sediment source during the event. Results of forward stepwise regression on hysteresis widths for Type-1 events indicated that large runoff events had sediment concentrations peak before the highest peak flow and exhaust sediment.

Reproduced with permission of the copyright owner. Further reproduction prohibited without permission.

Table 5.18. Results of forward stepwise regression for (clockwise (Type 1) hysteresis.

Step	Independent variable using all samples (rising and falling)	R^2	F Statistic	Coefficient	Constant
one	2-RUN	0.68	73.5	1.09	-0.35
two	34-TIME_PKCON	0.72	5.02	-0.01	-0.41
	2-RUN		81.7	1.09	

Summary of Results for Rio Icacos

During the study period, May 5, 1992 through September 30, 1994, 632 suspended-sediment samples were collected for concentration at the station Rio Icacos near Naguabo. Most of the samples were collected at moderate flows between 10 to 200 ft^3/s (0.28 to 5.66 m^3/s) (fig. 5.3). Fifty percent of the samples collected were of low suspended-sediment concentrations (<241 mg/L). Runoff and rainfall conditions during the collection period were 25% drier than the long-term average.

Examination of transport curves showed that the best correlation coefficient of sediment-transport curves was for all samples (0.87); although two data clusters at either end of the best-fit regression line may be affecting this relation (fig. 5.5a). Sediment-transport curves at Rio Icacos did not show an improvement in the relation of discharge to suspended-sediment concentration by separating samples into rising and falling limb either relative to the highest peak flow or relative to any peak flow in the event (figs. 5.6 a,b).

Generation of sediment-transport curves to show the effect of previous events at Rio Icacos showed that large previous events which are close in time to the current event, lower the current-event suspended-sediment concentrations in low to moderate flows and may indicate a

Reproduced with permission of the copyright owner. Further reproduction prohibited without permission.

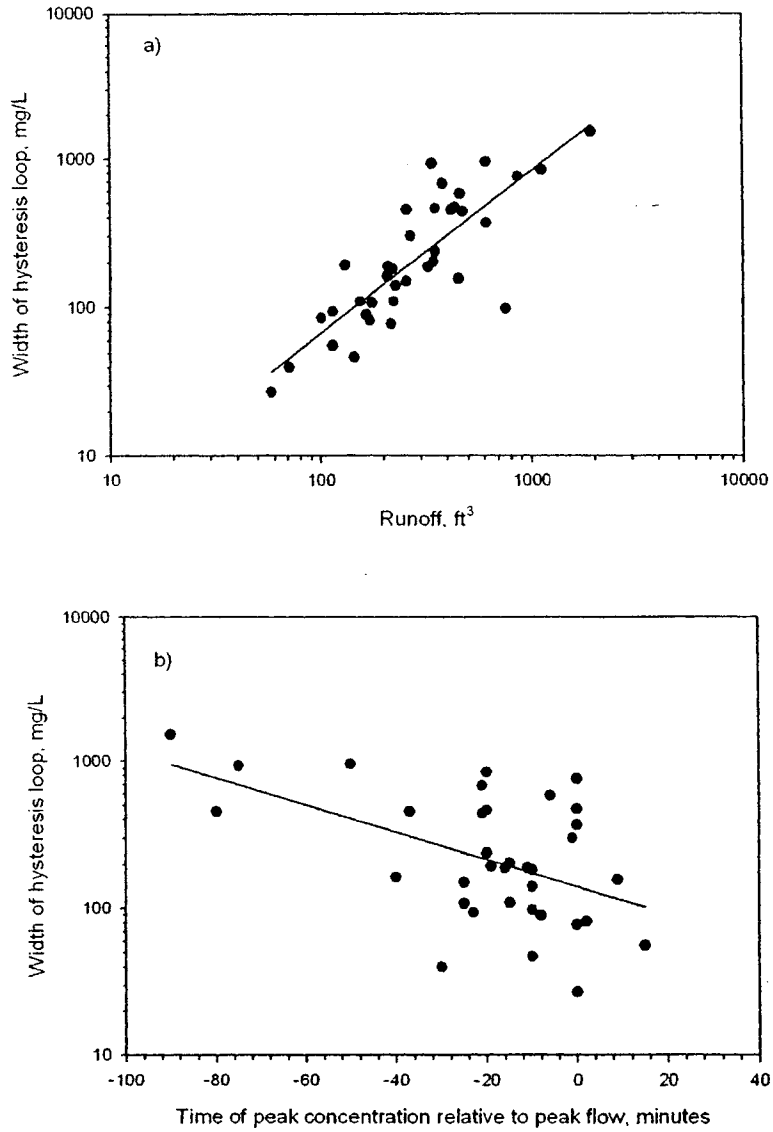

Figure 5.16. Graphs showing relations of hysteresis loops. (a) Runoff plotted against clockwise hysteresis width. (b) The time of the peak sediment concentration relative to the peak flow plotted against clockwise hysteresis width. The event on 11/18/1992 had the peak sediment concentration occur 183 minutes before peak flow and was an outlier. This datum was removed from the plot but not from the multiple regression analysis.

Reproduced with permission of the copyright owner. Further reproduction prohibited without permission.

flushing mechanism (fig 5.6a). The R^2 values for the regression lines are relatively high (fig. 5.6a). It does not appear that peak flows in the current event influence suspended-sediment concentrations (fig. 5.6b).

Separation of samples by season indicated that samples collected May through December, which is the wet season, had higher suspended-sediment concentration than samples collected January through April (fig. 5.7a). The percent sand in suspension in Rio Icacos samples increased with discharge (fig. 5.8). This increase is likely related to the rock types in the basin which weathers to sand and produces significant amounts of sand-size bed material.

Results, using Walling's (1974) four independent variables (discharge, time relation of sample, base flow, and flood intensity), showed that for samples with and without base flow, discharge was the most important factor explaining sediment concentrations and had a positive slope (Table 5.2). Flood intensity was significant in the second step, with and without base flow, for all samples and falling hydrograph samples, and had a positive slope, indicating that fast rising flows had high suspended-sediment concentrations. For rising hydrograph samples, with and without base flow, base flow at the start of the event was the most important variable but had a negative slope, indicating that suspended-sediment concentrations may be diluted during high base flow. The opposite result, that base flow was directly correlated to suspended-sediment concentration was shown for the entire event using all samples without base flow. This difference in the interpretation of base flow may be explained that on the falling limb increases in base flow during the storm lead to resuspension and high sediment concentrations. This effect would not be seen on the rising limb, for which there was a negative correlation. Introduction of sediment on the rising limb may be immediately diluted by the high base flow.

Reproduced with permission of the copyright owner. Further reproduction prohibited without permission.

A summary of forward stepwise regression for all statistical analyses (independent variables, principal components with and without varimax rotation) for the entire event or to the highest peak flow using quickflow or runoff, at Rio Icacos is listed in Table 5.19. For each statistical analysis, the dependent variable, suspended-sediment load, generally showed the highest correlation coefficient with the independent variables. Correlation coefficients did not seem to improve by subtracting out the base flow portion of the hydrograph. Results did not seem to improve by analyzing only the rising portion of the hydrograph to the highest peak.

For the entire event and to the highest peak flow, using quickflow or runoff, forward stepwise regression on the independent variables always indicated characteristics of the current event related to aspects of peak flow (peak flow, sum of peak flows, rate of hydrograph rise) were significant and were directly correlated to suspended-sediment load and the discharge-weighted concentration. Base flow was significant for the entire event, using runoff, and was directly correlated to suspended-sediment load. This result was similar to those using Walling's (1974) four variables. However, in Walling's (1974) study, base flow at the start of the event was inversely correlated to suspended-sediment concentrations. In Rio Icacos, high base flows may be transporting sand as bed load. The independent variables, quickflow and runoff, were not significant when considering the entire event but were significant when looking to the highest peak flow.

Principal components analysis showed strikingly similar results for the entire event and to the highest peak flow (using quickflow and runoff). Current-event and previous-event characteristics were directly correlated to the dependent variables, and characteristics between events were inversely correlated (Table 5.19). Large previous events in this forested basin are

Reproduced with permission of the copyright owner. Further reproduction prohibited without permission.

Table 5.19. A) Summary of the first two steps of forward stepwise regression analyses for Rio Icacos near Naguabo for the entire event. The value in the parenthesis is the correlation coefficient (R^2). The '+' or '-' sign indicate the slope for the line of best fit.

	Quickflow suspended-sediment load	**Runoff** suspended-sediment load	**Quickflow** discharge-weighted sediment concentration	**Runoff** discharge-weighted sediment concentration
Forward stepwise regression on variables	+ sum of peak flows (0.92)	+ sum of peak flows (0.91) + base flow (0.92)	+ sum of peak flows (0.54) + maximum rate of hydrograph rise (0.60)	+ sum of peak flows (0.62) + maximum rate of hydrograph rise (0.68)
Forward stepwise regression on principal components	**+ PC2 (0.44)** + current rain, quickflow, peak flows **+ PC1 (0.88)** + previous-event characteristics of peak flow, quickflow, rainfall + previous 3 event rainfall, quickflow - rainfall, runoff, and rainfall intensity since the previous event	**+ PC2 (0.44)** + current rain, peak flow **+ PC1 (0.88)** + previous-event characteristics of peak flow, quickflow, rainfall + previous 3 event rainfall, quickflow - rainfall, runoff, and rainfall intensity since the previous event	**+ PC2 (0.36)** + current rain, peak flows **+ PC1 (0.52)** + previous-event characteristics of peak flow, quickflow, rainfall + previous 3 event rainfall, quickflow - rainfall, runoff, and rainfall intensity since the previous event	**+ PC2 (0.42)** + current rain, peak flow **+ PC1 (0.62)** + previous-event characteristics of peak flow, runoff, rainfall + previous 3 event rainfall, runoff - rainfall, runoff, and rainfall intensity since the previous event
Forward stepwise regression on rotated principal components	**+ PC2** (0.61) + current rain, quickflow, peak flow **+ PC5** (0.88) current rate of hydrograph rise, peak flow	**+ PC2** (0.62) + current rain, runoff, peak flow **+ PC5** (0.88) current rate of hydrograph rise, peak flow	**+ PC5** (0.47) current rate of hydrograph rise, peak flow **+ PC2** (0.64) + current rain, , peak flow	**+ PC5** (0.48) + current rate of hydrograph rise, peak flow **+ PC2** (0.71) + current rain, peak flow

Reproduced with permission of the copyright owner. Further reproduction prohibited without permission.

Table 5.19 B) Summary of the first two steps of forward stepwise regression analyses for Rio Icacos near Naguabo to the highest peak flow. The value in the parenthesis is the correlation coefficient (R^2). The '+' or '-' sign indicate the slope for the line of best fit.

	Quickflow suspended-sediment load	**Runoff** suspended-sediment load	**Quickflow** discharge-weighted sediment concentration	**Runoff** discharge-weighted sediment concentration
Forward stepwise regression on variables	+ peak flow (0.88) + quickflow (0.94)	+ peak flow (0.88) + runoff (0.94)	+ rate of hydrograph rise - (0.67) + peak flow (0.72)	+ rate of hydrograph rise (0.67) + peak flow (0.72)
Forward stepwise regression on principal components	**+ PC2 (0.62)** + Current rain, rain intensity quickflow, peak flow **+ PC1 (0.89)** + previous-event characteristics of peak flow, quickflow, rainfall + previous 3 event rainfall, quickflow - rainfall, runoff, and rainfall intensity between the previous event	**+ PC2 (0.62)** + Current rain, rain intensity runoff, peak flow, maximum rate of hydrograph rise **+ PC1 (0.89)** + previous-event characteristics of peak flow, runoff, rainfall + previous 3 event rainfall, runoff - rainfall, runoff, and rainfall intensity since the previous event	**- PC2 (0.49)** - Current rain, rain intensity, peak flow **+ PC1 (0.59)** + previous-event characteristics of peak flow, quickflow, rainfall + previous 3 event rainfall, quickflow - rainfall, runoff, and rainfall intensity since the previous event	**- PC2 (0.53)** - Current rain, rain intensity runoff, peak flow, maximum rate of hydrograph rise **+ PC1 (0.66)** + previous-event characteristics of peak flow, runoff, rainfall + previous 3 event rainfall, runoff - rainfall, runoff, and rainfall intensity since the previous event
Forward stepwise regression on rotated principal components	**+ PC2 (0.68)** + Current rain, quickflow, peak flow **+ PC5 (0.86)** + maximum rate of hydrograph rise	**+ PC2 (0.65)** + Current rain, quickflow, peak flow, rainfall intensity **+ PC5 (0.86)** + maximum rate of hydrograph rise, peak flow	**+ PC5 (0.58)** + maximum rate of hydrograph rise, peak flow **+ PC2 (0.71)** + Current rain, rainfall intensity	**+ PC5 (0.61)** + maximum rate of hydrograph rise, peak flow **+ PC2 (0.76)** + Current rain, peak flow, rainfall intensity

Reproduced with permission of the copyright owner. Further reproduction prohibited without permission.

supplying sediment to the channel that increases sediment loads and concentrations in the current event. Larger amounts of runoff occurring since the previous event to the start of the current event flush sediment. After varimax rotation, for the entire event and to the highest peak flow (using quickflow and runoff) only characteristics of the current event were significant (Table 5.19).

Analysis of hysteresis indicates that clockwise loops occurred in 75% of the events. Runoff (2-RUN) and the time of the peak sediment concentration relative to peak flow (34-TIME_PKCON) were significant in explaining the amount of sediment exhaustion. Runoff was positively correlated to the amount of sediment exhaustion, indicating that large events cause the most sediment removal. The time of the peak sediment concentration relative to peak flow was inversely correlated to the amount of sediment exhaustion, indicating that the earlier the sediment concentration peaks relative to the highest peak flow the more sediment removal occurs.

Rio Icacos drains dominantly forest. Sources of sediment in this basin are landslides and sediment stored in 1st and 2nd order channels. Brown and others (1995) determined that 55% of channel sand is from landslides and 45% from sheetwash. Results from the sediment-transport curves and statistical operations provide information on how the sediment conveyor belt in this forested humid-tropical basin operates. Sediment is supplied to the channel from sources of landslides and 1st and 2nd order channels. The source material is dominantly sand and by the time it reaches the main channel, flow is receding and the sediment is deposited. This channel source of sediment becomes the major source of sediment for the next event as indicated by clockwise hysteresis loops. Increases in runoff events between events flush sediment.

Reproduced with permission of the copyright owner. Further reproduction prohibited without permission.

CHAPTER VI

SUSPENDED-SEDIMENT TRANSPORT AT QUEBRADA BLANCA

Suspended-sediment transport is discussed for Quebrada Blanca, which drains primarily pasture (54%) in sandy and clayey soils. The period of investigation at Quebrada Blanca at El Jagual (fig. 1,1; 3.6), was chosen for March 8, 1989 through September 30, 1995, based on the best record of storm samples for suspended sediment. Rainfall, discharge, and suspended-sediment characteristics are described for the 1989 WY to the 1995 WY.

Rainfall and Discharge for the Study Period

Average annual long-term rainfall for WYs 1931 through 1995, recorded at the National Weather Service raingage in San Lorenzo, located approximately 3.5 miles (5.6 km) from the streamflow station at Quebrada Blanca, was 98 in (2490 mm). Average annual rainfall at the San Lorenzo raingage during WY's 1989 to 1995 was 82 in (2080 mm) and therefore, conditions during the study period at Quebrada Blanca may be 16% drier than indicated by the long-term record.

The mean daily flow at Quebrada Blanca at El Jagual for WYs 1989 to 1995 was 5.2 ft^3/s (0.15 m^3/s), which is 25% lower than the annual mean discharge of 6.9 ft^3/s (0.20 m^3/s) for a longer period, 1984 to 1997. Flow durations for the period of investigation are shown in figure 6.1. Peak flow for the period of record was 7,400 ft^3/s (210 m^3/s) on May 17, 1985. The highest

Reproduced with permission of the copyright owner. Further reproduction prohibited without permission.

peak flow during the period of investigation was 7,180 ft^3/s (203 m^3/s), recorded during the Three King's Day storm, January 5, 1992 (Table 6.1).

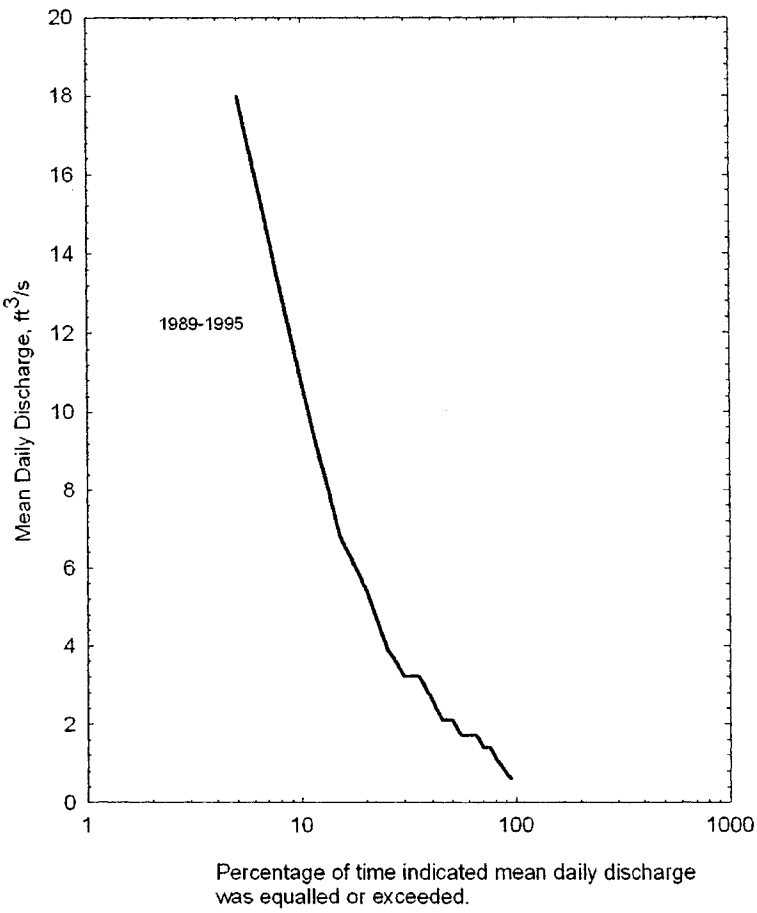

Figure 6.1 Flow durations for period of investigation (water year 1989-1995) for Quebrada Blanca near El Jagual (50051150).

Suspended-Sediment Load and Yield

Suspended-sediment loads at Quebrada Blanca WY 1989 through 1995 were obtained from the USGS-Caribbean District's annual surface-water data reports. The average annual suspended-sediment load was 2,820 tons (2,560 metric tons), the average annual sediment

Reproduced with permission of the copyright owner. Further reproduction prohibited without permission.

Table 6.1. Peak flows greater than 1.05 year recurrence (832 ft^3/s; 23.6 m^3/s) at Quebrada Blanca at El Jagual during the period of investigation, October, 1988 through September 1995

Date	Peak flow (ft^3/s)
11/17/1988	2,430
8/10/1990	889
10/20/1990	1,360
1/5/1992	7,180
7/11/1993	3,730

yield was 870 tons/mi^2 (305 metric tons/ km^2), and the average annual discharge-weighted sediment concentration was 500 mg/L. During the period, 1989 through 1995, 90% of the annual suspended-sediment load was transported in 12 days, 75% in 5 days, and 50% in one day. In just one day, on September 20, 1994, 84% of the average annual suspended-sediment load (2,260 tons; 2,050 metric tons) was transported.

Suspended-Sediment Analysis

During the period March 8, 1989 through September 30, 1995, 923 suspended-sediment samples were collected at the station Quebrada Blanca near El Jagual (50051150). Of the 923 samples, 374 were collected during base flow, 212 were collected on the rising limb of the hydrograph to the highest peak, and 337 were collected on the falling limb of the hydrograph after the highest peak. Sixty-four samples were collected using the EWI method, 462 were collected with the automatic suspended-sediment sampler, and 397 were taken at a single vertical (SV) in the channel. Because SV and automatic samples are not representative of the channel cross section, a calibration should be made to EWI samples.

Reproduced with permission of the copyright owner. Further reproduction prohibited without permission.

Thirty-one SV samples were collected in conjunction with EWI samples. Calibration of EWI samples to SV samples (EWI/SV) shows a wide scatter around 1.0 for discharges less than 20 ft^3/s (0.57 m^3/s). Discharges greater than 20 ft^3/s (0.57 m^3/s) show a calibration of 1.0 (fig. 6.2). An examination of the suspended-sediment samples by season did not show a relation to time of year. Because there was not a consistent relation of EWI to SV, a calibration coefficient was not applied to SV samples at Quebrada Blanca at El Jagual.

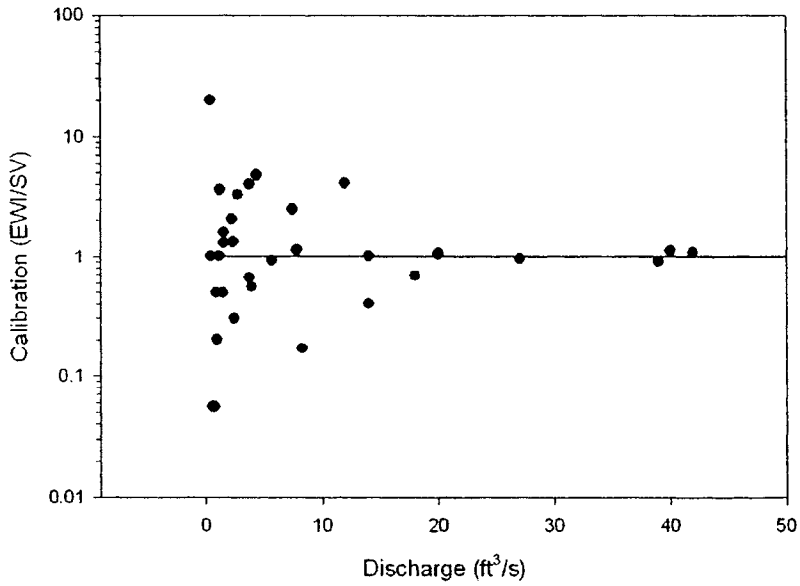

Figure 6.2. Graph showing calibration of suspended-sediment concentrations taken with equal width increments (EWI) and single vertical (SV) samples at Quebrada Blanca near El Jagual (50051150).

The streamflow gaging station, Quebrada Blanca at El Jagual, is not at a bridge and therefore it was not possible to calibrate the automatic sampler for high flow events. Automatic suspended-sediment samples were calibrated to four EWI samples for an event on August 10, 1990. Suspended-sediment samples were taken over a range of discharges (40 to 44 ft^3/s; 1.1

Reproduced with permission of the copyright owner. Further reproduction prohibited without permission.

to 1.2 m^3/s) and the calibration coefficient averaged 0.84, which means the automatic sampler was sampling higher sediment concentrations than the EWI samples.

Because of the low number of suspended-sediment samples that were available to calibrate the suspended-sediment samples collected by the automatic sampler, these samples were only adjusted for the flow event on August 10, 1990 for a range of discharges from 40 to 44 ft^3/s (1.1 to 1.2 m^3/s). A calibration coefficient was not applied to other suspended-sediment samples collected by the automatic sampler. Therefore, it is recognized that an inadequate number of sediment samples were calibrated and some error may be incurred in this analysis.

The lowest and highest suspended-sediment concentrations sampled were 0.1 mg/L and 5,070 mg/L. The mean suspended-sediment concentration for all samples was 500 mg/L, the median suspended-sediment concentration was 153 mg/L, and the sample standard deviation was 740 mg/L (fig. 6.3). Suspended sediment was sampled at discharges ranging from 0.46 to 547 ft^3/s (0.013 to 12.4 m^3/s). This distribution of sampled discharge shows that most suspended-

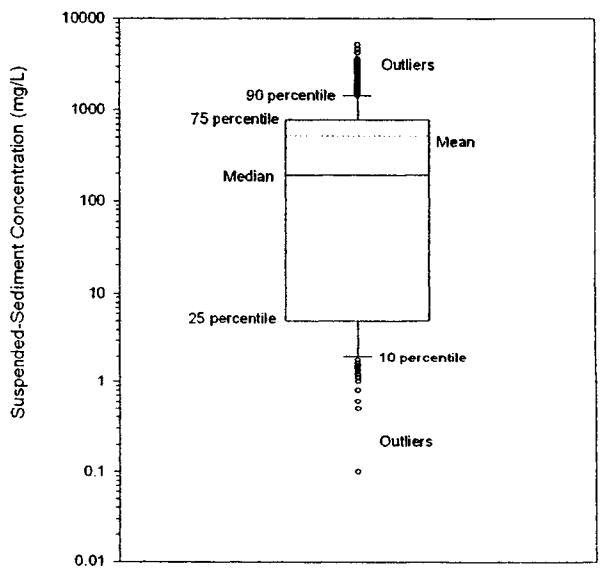

Figure 6.3. Box plot of suspended-sediment concentrations (n=926) for Quebrada Blanca near El Jagual.

Reproduced with permission of the copyright owner. Further reproduction prohibited without permission.

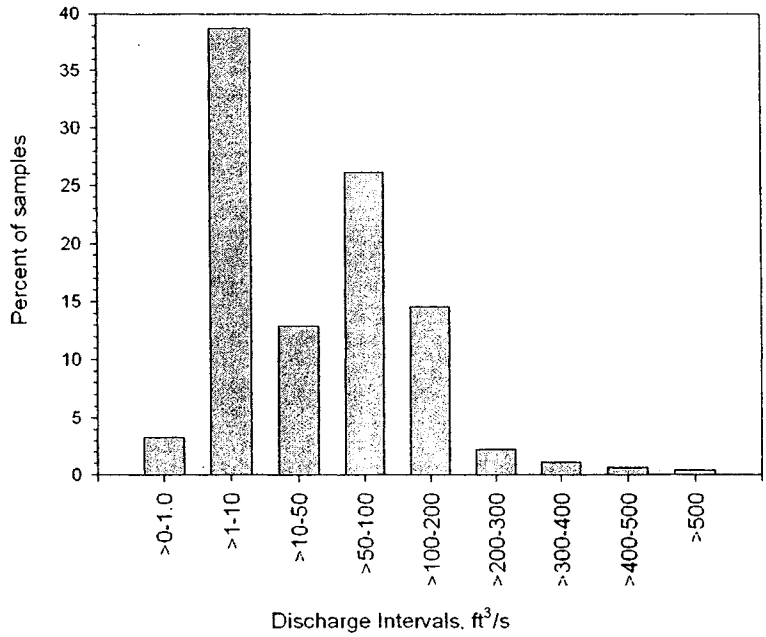

Figure 6.4. Bar graph showing frequency of discharges for suspended-sediment samples, Quebrada Blanca near El Jagual.

sediment samples were taken at low to moderate flows, from 1.0 to 100 ft^3/s (0.028 to 2.83 m^3/s) (fig. 6.4).

Quantile plots of the suspended-sediment data (fig. 6.5a,b) show that most of the samples had low concentrations. Thirty-seven percent of the suspended-sediment concentrations were below 10 mg/L. Box plots of the data show the 10^{th}, 25^{th}, 75^{th}, and 90^{th} percentiles of suspended-sediment concentration are 2.0, 5.0, 760, and 1,420 mg/L, respectively (fig. 6.3). Probability plots of the suspended-sediment data show that the data are not normally distributed (fig. 6.5c) and therefore, applying a log transform to the data was found to be appropriate (fig. 6.5d).

Reproduced with permission of the copyright owner. Further reproduction prohibited without permission.

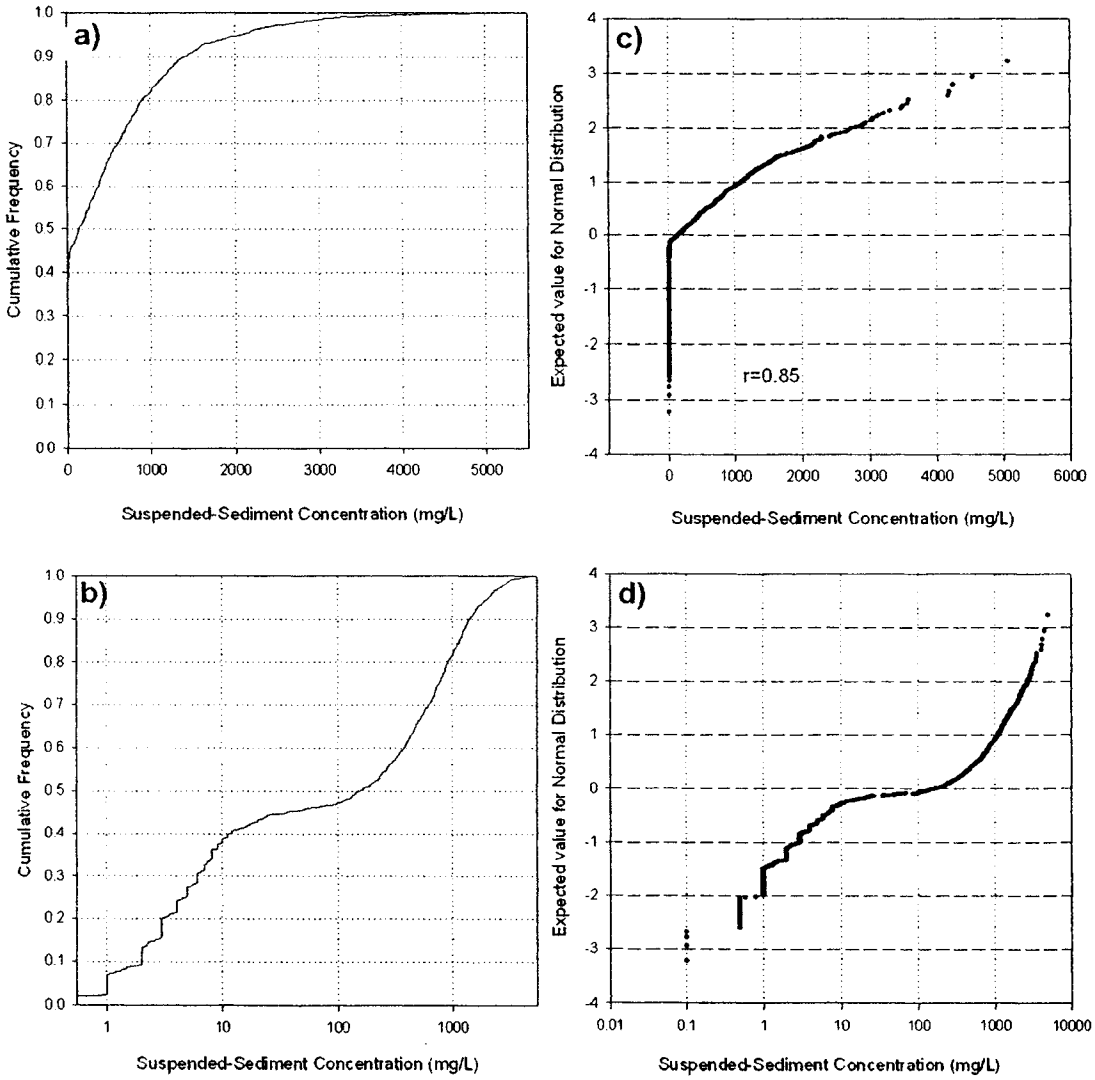

Figure 6.5. Quantile plots for Quebrada Blanca near El Jagual showing a) suspended sediment and b) log transformed suspended sediment. Probability plots of Quebrada Blanca near El Jagual showing c) suspended sediment and d) log transformed suspended sediment.

Sediment-transport curves

Sediment-transport curves were created: 1) for all samples, 2) samples rising to the highest peak flow, 3) samples falling from the highest peak flow, 4) samples rising to any peak flow, 5)

Reproduced with permission of the copyright owner. Further reproduction prohibited without permission.

samples falling from any peak flow, and 6) samples collected at base flow (fig. 6.6). Two clusters in the sediment-transport curves are related to sampling frequency. Low discharge samples are frequently collected by observers and USGS technicians, whereas high discharge samples are collected by the automatic sampler. The low number of suspended-sediment samples taken at intermediate discharges, 20 to 60 ft^3/s (0.6 to 1.7 m^3/s), illustrated the difficulty in either a technician or an observer reaching the site when the event is beginning or ending. The correlation coefficient for all samples in the sediment transport curve is 0.87 (fig. 6.6a). Because outliers influence linear regression, the high correlation coefficient for all samples reflects the effect of the two clusters on the regression line (fig. 6.6a). A change in slope in the relation of discharge to suspended-sediment concentration is observed at 100 ft^3/s (2.83 m^3/s). Osterkamp (2002) used three best-fit lines for different segments of the transport curve at Quebrada Blanca (0.5 to 12 ft^3/s, 12 to 46 ft^3/s, and 46 to 547 ft^3/s) (fig. 6.6). Segmentation of the transport curve into three segments represents different flow regimes as they relate to channel geometry. The lowest flows are base flow, intermediate flows are falling and rising stormflow runoff, and the highest flows are overbank onto the floodplain (Osterkamp, 2002). Segmentation of the transport curve produced a low correlation coefficient for each line compared to the best-fit line for all the data (fig. 6.6). Correlation coefficients did not improve when the suspended-sediment samples were divided into rising and falling from the highest peak flow or rising and falling from any peak flow (fig. 6.6b,c). Base flow suspended-sediment samples show a wide scatter in concentrations and a poor relation of discharge to sediment concentration (fig. 6.6d).

Reproduced with permission of the copyright owner. Further reproduction prohibited without permission.

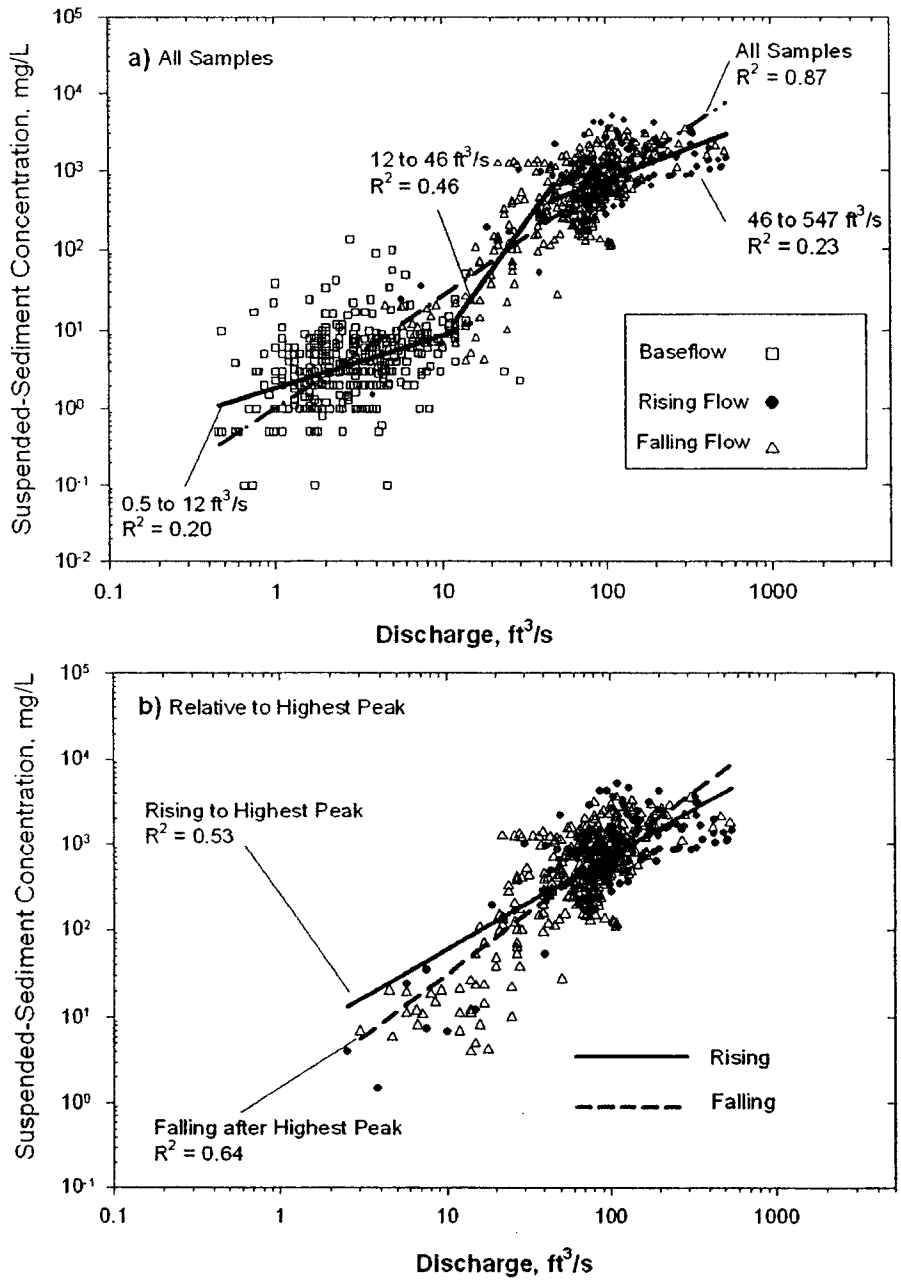

Figure 6.6. Graphs showing suspended-sediment transport curves for Quebrada Blanca near El Jagual. a) All samples, and b) rising and falling samples relative to the highest peak flow.

Reproduced with permission of the copyright owner. Further reproduction prohibited without permission.

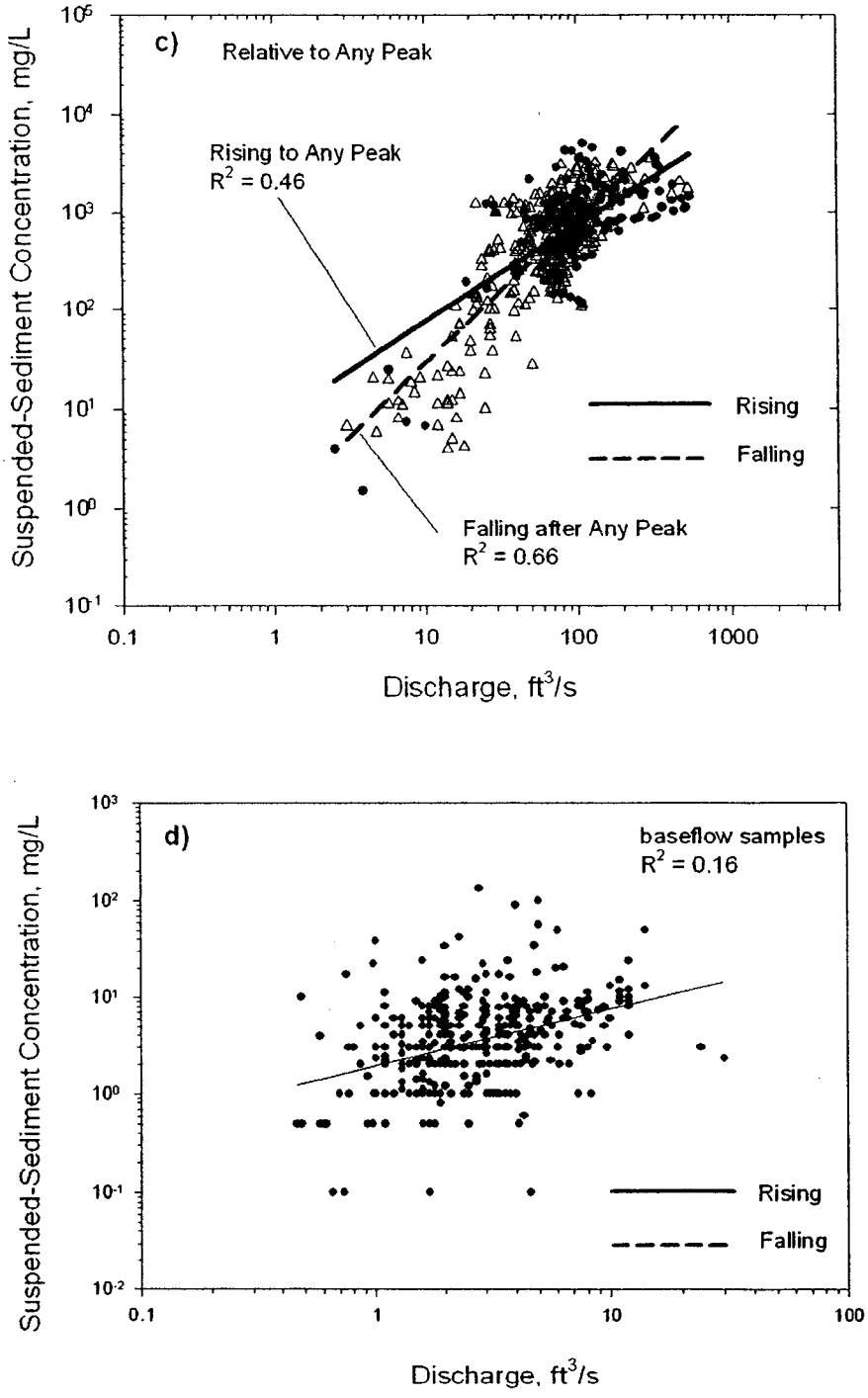

Figure 6.6. Continued, c) rising and falling samples relative to any peak flow, and d) base flow samples.

Reproduced with permission of the copyright owner. Further reproduction prohibited without permission.

To test the hypothesis that previous storm events flush sediment, suspended-sediment samples were analyzed relative to the last flow event and to peak flows of the current event. If previous events flush sediment from the system, suspended-sediment samples may show low concentrations after a large recent runoff event. Suspended-sediment samples were separated into three classes categorized by runoff of the previous event divided by time since the previous event. Only sediment on the rising limb may be affected by previous events and therefore, only samples rising to the highest peak flow are in the previous runoff analysis. Plots of runoff of the previous event divided by the time since the previous event initially showed outliers at the low discharges that may influence the best-fit regression lines. Swan and Sandilands (1995) recommended removing the outliers and repeating the regression. The outliers were removed and regression analysis was run for discharges greater than 55 ft^3/s (1.6 m^3/s) (fig. 6.7a). Suspended-sediment samples, separated by the runoff of the previous event divided by the time since the last event, at high discharges show the lowest suspended-sediment concentrations for the largest runoff category, 1 x 10^6 to 29.5 x 10^6 ft^3/hr (28,300 to 835,400 m^3/hr) (fig. 6.7a). Sediment flushing may occur at high discharges. Because of data scatter and the low correlation coefficient, this interpretation remains inconclusive.

The times at which sediment samples were taken after individual peaks in the current event may influence suspended-sediment concentrations (Walling and Webb, 1982). Sediment samples separated into classes defined by the previous peak flow of the current event did not show clear results and outliers at the low discharges may influence the best-fit regression lines. Regression analysis was run for discharges greater than 30 ft^3/s (0.85 m^3/s) (fig. 6.7b). Suspended-sediment samples separated by the previous peak flow in the current event show for most discharges that

Reproduced with permission of the copyright owner. Further reproduction prohibited without permission.

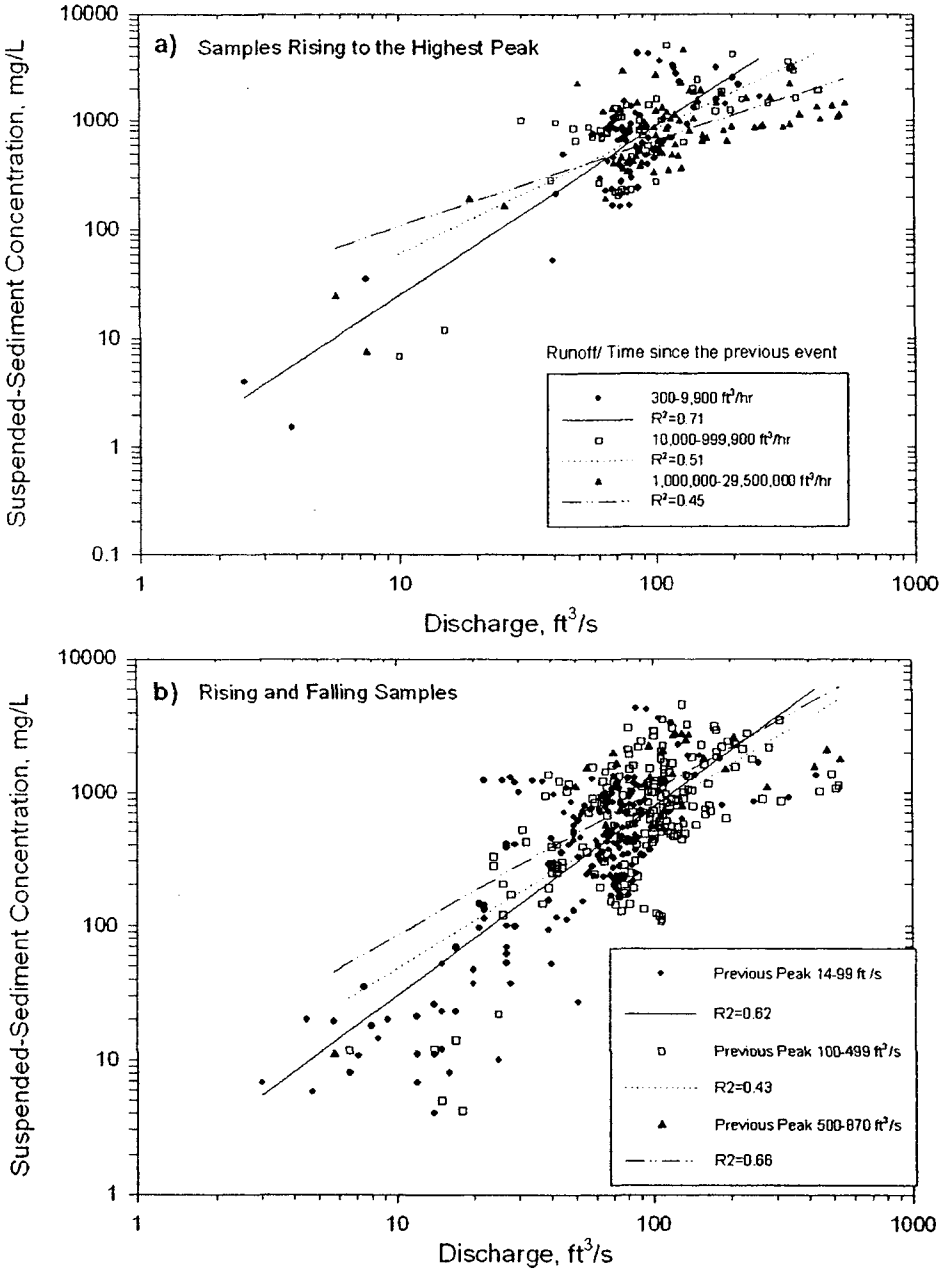

Figure 6.7. Suspended-sediment transport curves for Quebrada Blanca near El Jagual. a) Samples collected on the rising limb (>55 ft³/s) to the highest peak flow separated by runoff of the previous event divided by the time since the previous event and b) rising and falling samples (>30 ft³/s) separated by the previous peak flow in the current event.

Reproduced with permission of the copyright owner. Further reproduction prohibited without permission.

samples taken after high peak flows have low concentrations. This implies that sediment flushing by large previous peak flows may occur in Quebrada Blanca.

Rainfall is strongly seasonal in Puerto Rico (fig. 3.18). Sediment-transport data separated into seasonal groups, May through December (wet season) and January through April (drier season), are shown in figure 6.8. A plot of all samples shows that the regression line for January through April is slightly below the regression line for May to December (fig. 6.8a). Separation of seasonal suspended-sediment samples into rising and falling limbs relative to the highest peak flow (fig. 6.8b,c) improved the regression coefficient for January through April falling limb samples (R^2=0.94) (fig. 6.8c). Analysis of figure 6.9 does not lead to the conclusion that separation of suspended-sediment samples by season for Quebrada Blanca improves the least-squares regression coefficients.

The percent sand (>0.062 mm) in suspension versus discharge and suspended-sediment concentration were examined (fig. 6.9). Sixty-one samples of suspended sediment, collected August 1989 through August 1993, were analyzed for the percent sand and the percent silt and clay (<0.062 mm). For all samples, the average amount of sand in suspension was 7.6 %, (+/- 5.9 %), and varied from zero to 31%. Plots for all samples do not show any relation of percent sand to increasing discharge or suspended-sediment concentration (fig. 6.9a,b). Regression coefficients improved slightly with separation of samples rising relative to the highest peak flow but still showed much scatter (fig. 6.9c,d). Samples collected on the falling limb showed no relation of discharge to percent sand in suspension (fig. 6.9e,f). Based on these transport curves the amount of sand in suspension did not show a significant correlation with flow or suspended-sediment concentration.

Reproduced with permission of the copyright owner. Further reproduction prohibited without permission.

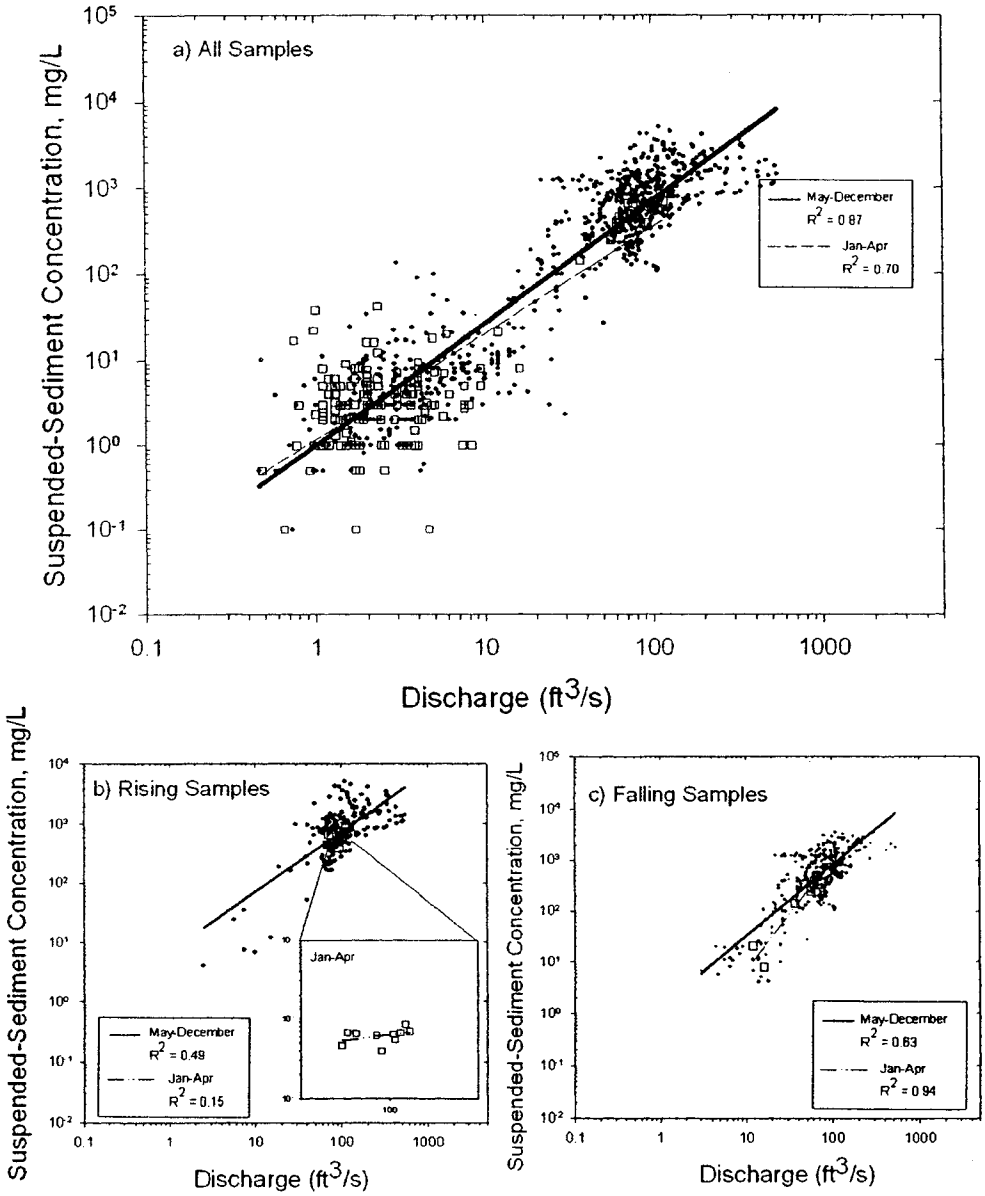

Figure 6.8. Seasonal suspended-sediment-transport curves (May-Dec; Jan-Apr) for Quebrada Blanca near El Jagual. a) All samples, b) Rising samples relative to the highest peak flow, and c) Falling samples relative to the highest peak flow.

Reproduced with permission of the copyright owner. Further reproduction prohibited without permission.

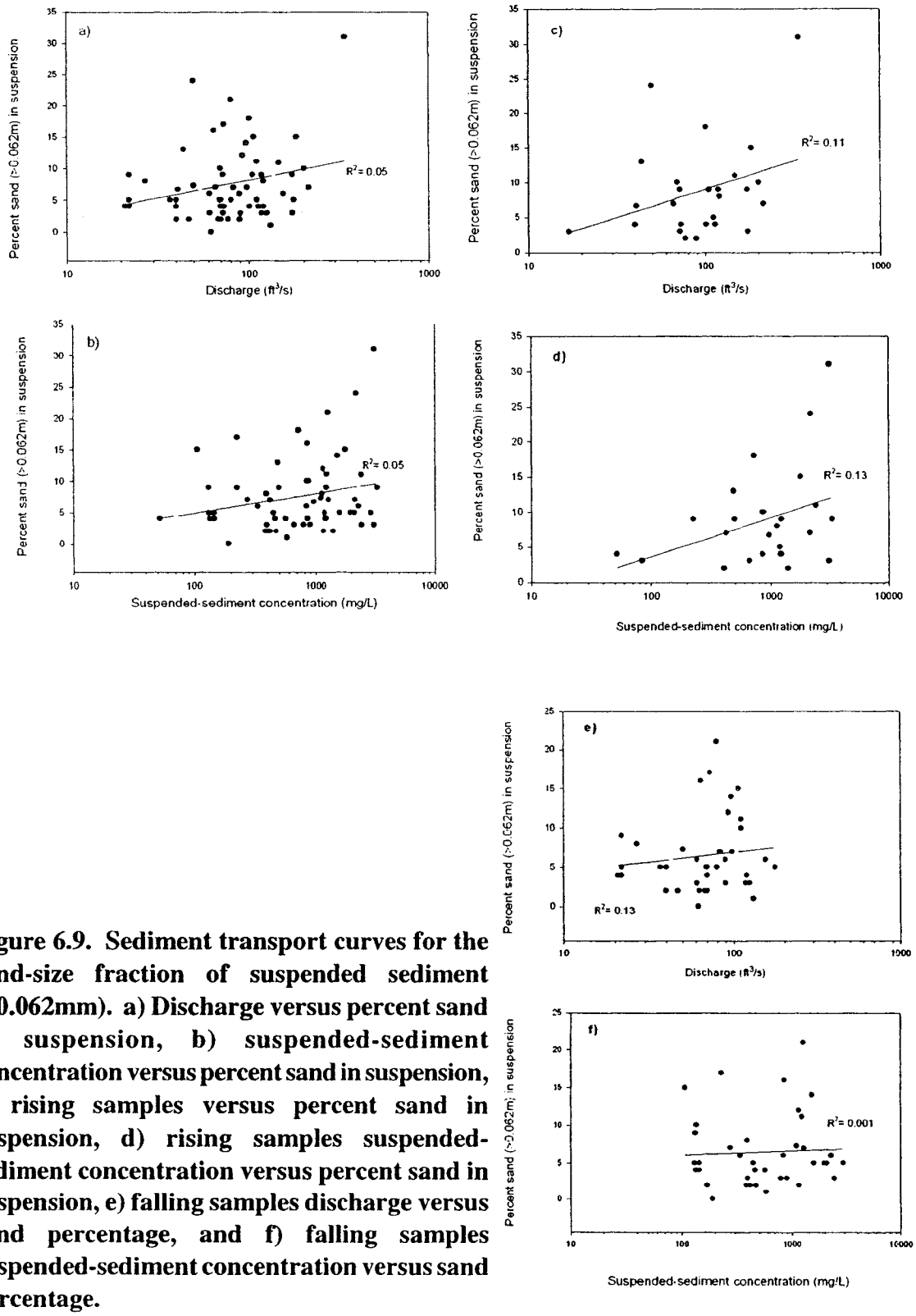

Figure 6.9. Sediment transport curves for the sand-size fraction of suspended sediment (>0.062mm). a) Discharge versus percent sand in suspension, b) suspended-sediment concentration versus percent sand in suspension, c) rising samples versus percent sand in suspension, d) rising samples suspended-sediment concentration versus percent sand in suspension, e) falling samples discharge versus sand percentage, and f) falling samples suspended-sediment concentration versus sand percentage.

Reproduced with permission of the copyright owner. Further reproduction prohibited without permission.

Walling (1974) Sediment-Transport Curve Approach

Results using Walling's (1974) four independent variables of discharge, time relation of sample, base flow, and flood intensity, described in Chapter 4, are listed in Table 6.2. The dependent variables were separated into all samples, samples rising to the highest peak flow, and samples falling from the highest peak flow. Analysis included discharge with and without base flow. Results were similar for samples with and without base flow. The regression coefficient did not improve by separating samples into rising and falling discharge. In each analysis, the most important factor explaining sediment concentration is discharge, followed in the second step by the time relation of sediment (Table 6.2). The slope of the regression line was positive for discharge and negative for the time relation of sediment. This implies that samples collected later in the event have low concentrations, although the slope of the line is very low.

Statistical Results at Quebrada Blanca

The statistical results performed on suspended-sediment loads and concentrations for Quebrada Blanca are summarized below. Discussion on statistical results will follow the flow chart of figure 4.11. Abbreviations used for the statistical analysis are summarized in Table 4.7.

Entire Event Analysis

This section describes the results of statistical analysis at-a-station for Quebrada Blanca at El Jagual using characteristics of the entire runoff event. At Quebrada Blanca the most accurate period of storm-event suspended-sediment collection occurred between March 1989 through September, 1993. During this period, 153 runoff events defined by a peak flow over 15 ft^3/s (0.42 m^3/s) occurred. Of these runoff events, 23 were sampled adequately to define suspended-

Reproduced with permission of the copyright owner. Further reproduction prohibited without permission.

Reproduced with permission of the copyright owner. Further reproduction prohibited without permission.

Table 6.2. Results of forward stepwise regression using Walling's (1974) four independent variables to explain suspended-sediment concentration.

A) Discharge including base flow

Step	Independent variable using all samples (rising and falling)	R^2	Coefficient	Independent variable for rising samples	R^2	Coefficient	Independent variable for falling samples	R^2	Coefficient
one	Discharge	0.61	1.31	Discharge	0.54	1.08	Discharge	0.63	1.44
two	Discharge	0.64	1.18	Discharge	0.62	0.94	Discharge	0.73	1.07
	Time relation of sample		-0.001	Time relation of sample		0.001	Time relation of sample		-0.001
three	Discharge	0.65	1.09	Discharge	0.62	0.96	Discharge	0.74	0.95
	Time relation of sample		-0.001	Time relation of sample		0.001	Time relation of sample		-0.001
	Flood intensity		0.11	Base flow		-0.12	Flood intensity		0.16
four	Discharge	0.66	1.11						
	Time relation of sample		-0.001						
	Flood intensity		0.10						
	Base flow		-0.09						

Reproduced with permission of the copyright owner. Further reproduction prohibited without permission.

B) Table 6.2. Continued. Discharge minus base flow.

Step	Independent variable using all samples (rising and falling)	R^2	Coefficient	Independent variable for rising samples	R^2	Coefficient	Independent variable for falling samples	R^2	Coefficient
one	Discharge	0.64	1.06	Discharge	0.56	0.94	Discharge	0.65	1.12
two	Discharge	0.65	0.98	Discharge	0.63	0.82	Discharge	0.71	0.84
	Time relation of sample		-0.001	Time relation of sample		0.001	Time relation of sample		-0.001
three	Discharge	0.66	0.90				Discharge	0.73	0.74
	Time relation of sample		-0.001				Time relation of sample		-0.001
	Flood intensity		0.11				Flood intensity		0.17

Reproduced with permission of the copyright owner. Further reproduction prohibited without permission.

Table 6.3. Summary of runoff events sampled adequately to determine suspended-sediment loads at Quebrada Blanca near El Jagual. (* Mna = Complex event, n=number of complex event, a,b,c, = sequence of each event in the entire complex event; a=1st event, b=2nd, etc.).

Start Date	Start Time hour	Start Discharge (ft^3/s)	End Date	End Time hour)	Ending Discharge (ft^3/s)	Event Duration (hour)	Number of Peaks in Event	Peak Flow (ft^3/s))	Quickflow (ft3)	Runoff (ft3)	Suspended Sediment Load (tons)	M=Part of Complex Event
08/11/1989	16	0.98	08/12/1989	5.75	3.7	13.75	1	86	742990	858820	6.5	
08/18/1989	22	3.1	08/19/1989	23.25	8.1	25.25	1	231	2079900	2588940	62.7	
09/13/1989	21.5	3.1	09/14/1989	20	8.1	22.5	2	115	1027890	1481490	12.3	
09/18/1989	2.75	7.3	09/20/1989	7.75	7.5	53	3	537	11147630	12330270	376	M1b
09/22/1989	9	4.4	09/22/1989	21.5	12	12.5	2	335	1537030	1752210	52.1	M2b
10/01/1989	13.75	7	10/02/1989	1.25	9.3	11.5	1	55	403070	740480	5.2	
05/09/1990	19.25	0.73	05/10/1990	20	3	24.75	1	507	1452430	1537050	34.1	M3a
06/14/1990	14	1.4	06/15/1990	11.5	13	21.5	1	226	1257480	1814760	35.8	
08/07/1990	17	3.3	08/09/1990	13.5	11	44.5	1	62	1788130	2436800	7.9	M4a
08/09/1990	14	12	08/12/1990	21.75	7.5	79.75	3	838	6219530	7984940	98.9	M5b
10/16/1990	12	2.1	10/17/1990	14.75	6.2	26.75	1	109	1727660	1996250	19.3	M6a
10/24/1990	18.75	7	10/25/1990	15.25	23	20.5	2	118	2314490	2841050	15.5	M7a
11/04/1990	12.25	4.1	11/05/1990	14.5	17	26.25	2	110	2815080	3290810	48.1	M8a
12/30/1990	19.25	2	01/02/1991	6.75	9.3	59.5	2	91	4610390	5820620	34.1	
07/15/1991	13.25	0.65	07/16/1991	2.75	26	13.5	1	97	1564080	1619200	16	M9a
08/27/1991	10	0.75	08/28/1991	15.25	10	29.25	2	255	3048940	3614930	49.3	
09/17/1991	2.42	0.98	09/18/1991	10.75	6.4	32.33	3	340	3940770	4370280	75.1	
09/22/1991	8.5	3.2	09/23/1991	17.75	10	33.25	3	132	3372600	4162620	49	
11/28/1991	12.25	24	12/01/1991	11.75	13	71.5	1	130	3861880	6840670	22.5	M10e
05/16/1992	4	2	05/17/1992	8.75	8	28.75	2	128	1449420	1966920	55.1	
06/04/1992	8.5	4.3	06/05/1992	13.5	8	29	1	347	2377040	3019100	115	
07/22/1993	16	5.9	07/23/1993	2.75	15	10.75	1	501	2694810	2946110	97.0	
08/15/1993	21.5	5.3	08/17/1993	17	12	43.5	6	234	6476630	7831220	152	

sediment loads for the entire event (Table 6.3). Of the 23 events, 10 were defined as complex events. Six of the complex events had suspended-sediment sampled in the first storm-generated hydrograph, 3 were sampled in the second storm-generated hydrograph, and one was sampled on the fifth storm-generated hydrograph (Table 6.3).

The average suspended-sediment load for the 23 events was 62.6 tons (56.8 metric tons) (fig.6.10a). The maximum sediment load during the study period was 376 tons (341 metric tons) on 9/18/1989 during Hurricane Hugo. The runoff associated with this event, 1.23 x 10^6 ft^3 (3.48 x 10^5 m^3), was the most during the period of study, when 7.2 inches (180 mm) of rain, recorded at seven rain gages, fell in the basin.

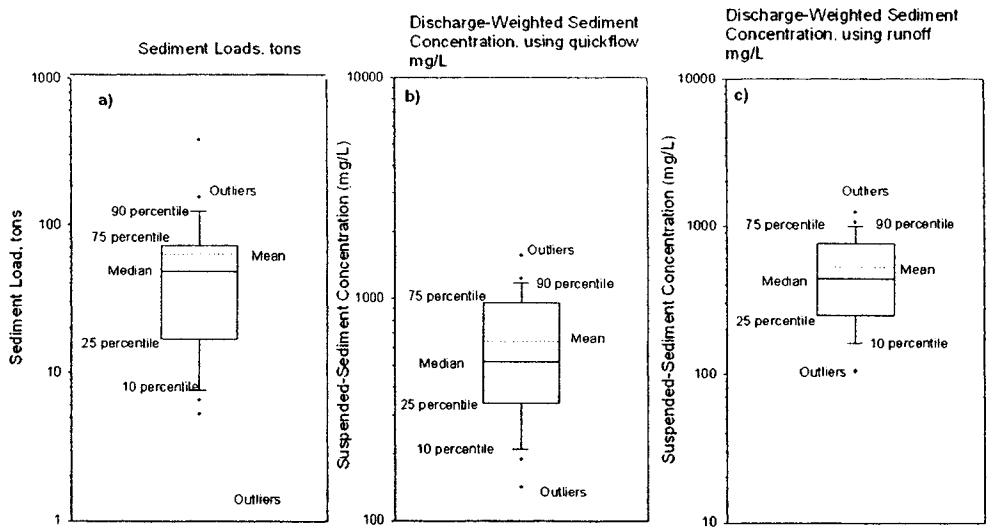

Figure 6.10. Box plot of dependent variables, a) sediment load, b) discharge-weighted sediment concentrations using quickflow, and c) discharge-weighted sediment concentrations using runoff for Quebrada Blanca near El Jagual.

A plot of the discharge-weighted sediment concentration, using runoff, for each event during the period of study is shown in figure 6.11. There is considerable variation in the discharge-weighted sediment concentration, 103 to 1,220 mg/L (fig. 6.10; 6.11). The average discharge-

Reproduced with permission of the copyright owner. Further reproduction prohibited without permission.

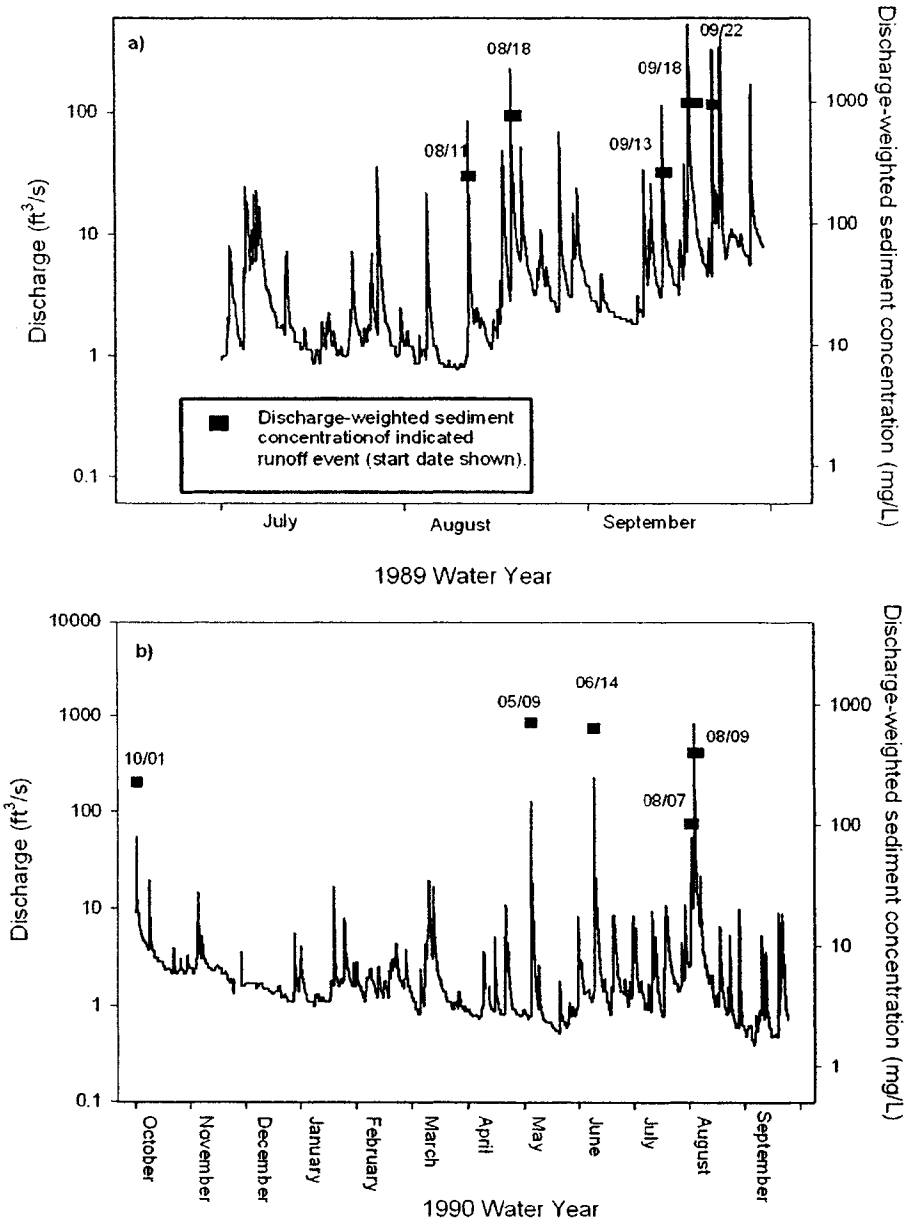

Figure 6.11. Instantaneous discharge and discharge-weighted sediment concentration for Quebrada Blanca at El Jagual, for period of investigation: a) July-September,1989 and b) water year 1990.

Reproduced with permission of the copyright owner. Further reproduction prohibited without permission.

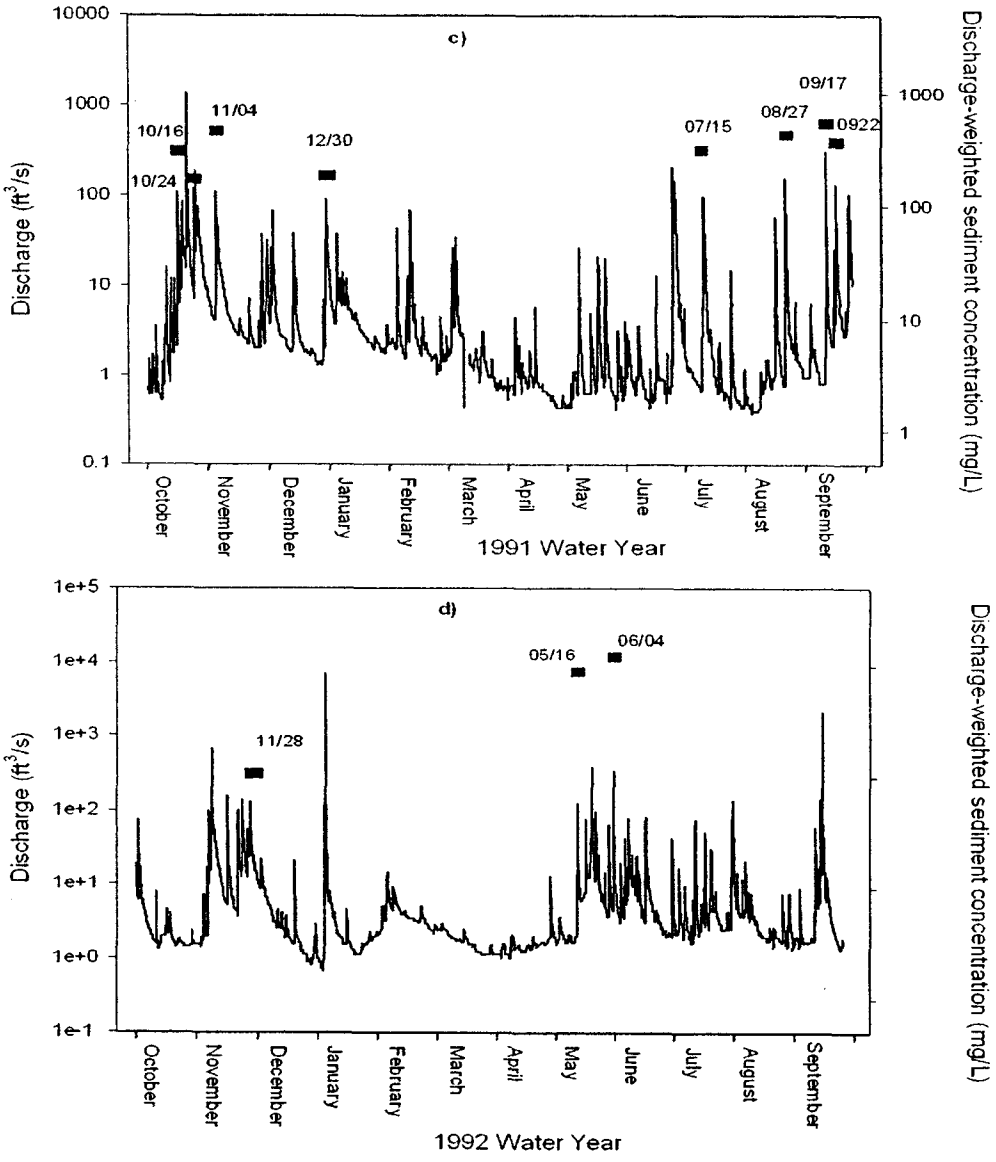

Figure 6.11. Continued. c) water year 1991 and d) water year 1992.

Reproduced with permission of the copyright owner. Further reproduction prohibited without permission.

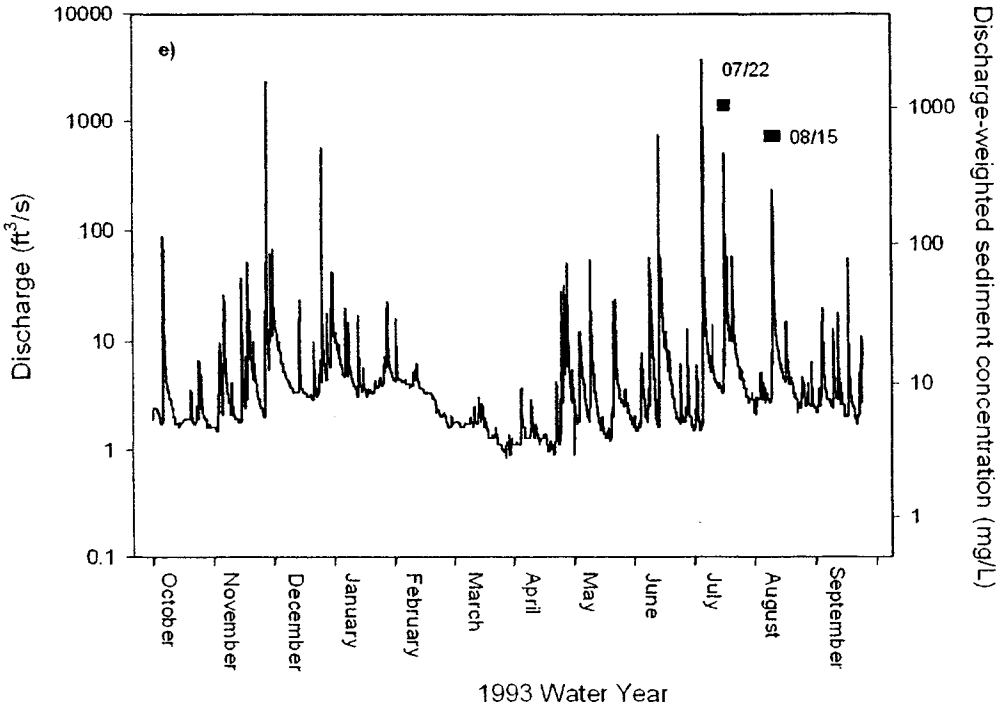

Figure 6.11. Continued. e) water year 1993.

weighted sediment concentration of all events using runoff was 522 mg/L (fig. 6.10c). The average discharge-weighted sediment concentration of all events using quickflow was 638 mg/L (fig. 6.10b) and the maximum discharge-weighted sediment concentration, for both quickflow and runoff, 1,550 mg/L and 1,220 mg/L, respectively, occurred on 6/4/1992 through 6/5/1992.

The peak flows of the 23 sampled events ranged from 55 to 838 ft^3/s (1.6 to 23.7 m^3/s). Quickflow ranged from 4.03 x 10^5 to 112 x 10^5 ft^3 (0.11 x 10^5 to 3.16 x 10^5 m^3) and runoff ranged from 7.40 x 10^5 to 123 x 10^5 ft^3 (0.210 x 10^5 to3.49 x 10^5 m^3). Hydrographs for the 23 events were separated into quickflow and runoff. For the 23 storms that were adequately sampled, the base flow contribution was between 3 to 45% of the runoff.

Reproduced with permission of the copyright owner. Further reproduction prohibited without permission.

Rainfall contributing to runoff for the 23 events ranged from 0.52 to 7.22 in (13 to 183 mm). A simple accounting of rainfall to quickflow can be made by assuming that the contributing area to the streamflow-gaging station (3.25 mi^2; 5.23 km^2) is impervious and calculating the volume of quickflow resulting from each rainfall event. The results of this comparison are listed in Appendix 6.1. Based on these computations, 4 to 98% of rainfall was quickflow and averaged 22 % (Appendix 6.1). The 98% value (for a runoff event from 11/28/1991 to 12/01/1991) occurred when only three rainfall stations were operating and thus, reflects the localized nature of rainfall which may be missed when only a few stations are operating.

The dependent variables used to describe sediment for the entire storm event are:

1) suspended-sediment load, in tons;

2) discharge-weighted sediment concentration, in mg/L

The dependent variables were tested against the independent variables shown in Table 4.8. Statistical analysis was performed against two portions of the runoff hydrograph, 1) the entire runoff event and 2) to the highest peak flow of the event. Forward stepwise regression for suspended-sediment load against previous quickflow events divided by the time since the previous quickflows back to the 6^{th} event indicated that the current quickflow, the previous quickflow, and the 2^{nd} previous quickflow were significant (alpha = 0.15; R^2=0.82). A minimum of three previous events were used in this statistical analysis to calculate previous runoff and previous-event rainfall characteristics.

Histograms of the dependent variables showed that suspended-sediment load and the discharge-weighted sediment concentration have normal distributions following a log transformation. Suspended-sediment load has the better relation to runoff (R^2=0.54) (fig. 6.12a),

Reproduced with permission of the copyright owner. Further reproduction prohibited without permission.

in part a spurious relation because discharge is used in the calculation of suspended-sediment load. There is considerable scatter in runoff versus discharge-weighted sediment concentration (fig. 6.12), implying that factor(s) other than runoff control sediment concentration.

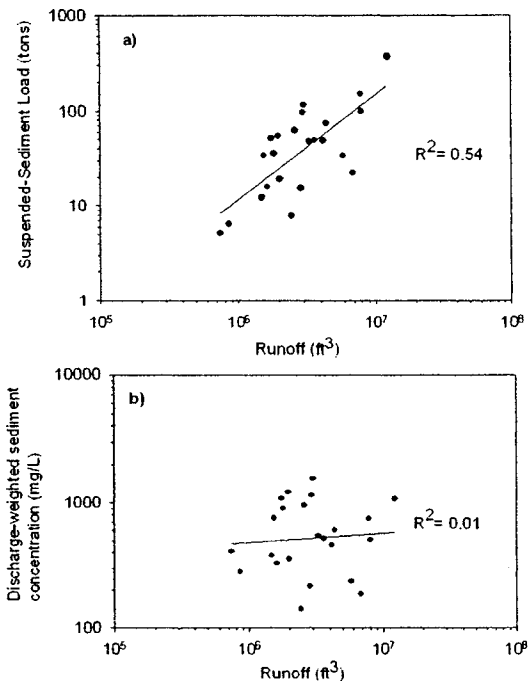

Figure 6.12. Plots of storm generated runoff versus a) suspended-sediment load and b) discharge-weighted sediment concentration for Quebrada Blanca at El Jagual.

Quickflow Results (entire event)

The independent variables assembled to analyze the relation of suspended-sediment characteristics to quickflow characteristics are listed in Appendix 6.2. Tests for normality using the residuals indicated that 17 of the 23 independent variables needed a log transformation (Appendix 6.2). Analysis of the correlation matrix showed a high correlation ($r>0.80$) among the following variables of the previous event(s): 20-LSPKBTI, 22-SMLSPKBS, 24-QULST, 26-

Reproduced with permission of the copyright owner. Further reproduction prohibited without permission.

PPTLSTI, 27-INTLST, 29-SUM3PPTI, and 30-QU3EVT (Appendix 6.3) so 20-LSPKBTI and 27-INTLST were removed. Variables of the current event that showed a high correlation included 4-PKBS, 8-SMPKBS, 6-MXTMJPK, 7-MXTRP, 10-RAIN, and 13-RRISE (Appendix 6.3) so 4-PKBS, 6-MXTMJPK, and 10-RAIN were removed. Three variables showed a high correlation among each other, 24-QULST, 22-SMLSPKBS, and 26-PPTLSTI, but were left in because they were perceived to be important.

High correlations of the dependent variables to the independent variables that were observed in the correlation matrix included suspended-sediment load to the sum of peak flows minus base flow (24-SMPKBS) and quickflow (28-QUICK). Discharge-weighted sediment concentration was correlated to the maximum rate of hydrograph rise for any peak in the event (16-MXTRP) (fig. 6.13).

Forward stepwise regression (entire event, quickflow)

Forward stepwise regression was run on the remaining 18 independent variables against the two dependent variables (Table 6.4). In general, the three most important independent variables are related to the characteristics of the current runoff event (Table 6.4).

The first step of forward stepwise regression using suspended-sediment load as a dependent variable indicated that the sum of peak flows minus base flow (8-SMPKBS) was significant. The correlation coefficient (R^2) for the line of best fit is high (0.72) and the slope of the best-fit line or coefficient was positive, indicating a direct correlation (fig. 6.13a). In the second

Reproduced with permission of the copyright owner. Further reproduction prohibited without permission.

step of forward stepwise regression analysis, using sediment load as a dependent variable, quickflow (1-QUICK) was significant and the coefficient was positive (fig. 6.13b, Table 6.4).

Table 6.4. Results of forward stepwise regression for entire event using quickflow characteristics.

Dependent Variable	Step	Variables in the Model	R^2	F Statistic	Coefficient	Constant
suspended-sediment, tons	One	8-SMPKBS	0.73	56.3	1.03	-0.87
	Two	1-QUICK	0.80	7.01	0.52	-3.47
		8-SMPKBS		18.4	0.72	
discharge-weighted sediment concentration, mg/L	One	7-MXTRP	0.50	20.9	0.46	2.63
	Two	13-RRISE	0.62	6.04	0.45	2.58
		7-MXTRP		21.3	0.43	

Using the discharge-weighted sediment concentration as a dependent variable indicated that the maximum rate of hydrograph rise for any peak (7-MXTRP) was significant in the first step of forward stepwise regression and the coefficient was positive (fig. 6.13c,d; Table 6.4). Rainfall on the rising limb of the hydrograph (13-RRISE) was important in the second step of forward stepwise regression using the discharge-weighted sediment concentration as the dependent variable and the coefficient was positive (Table 6.4).

Reproduced with permission of the copyright owner. Further reproduction prohibited without permission.

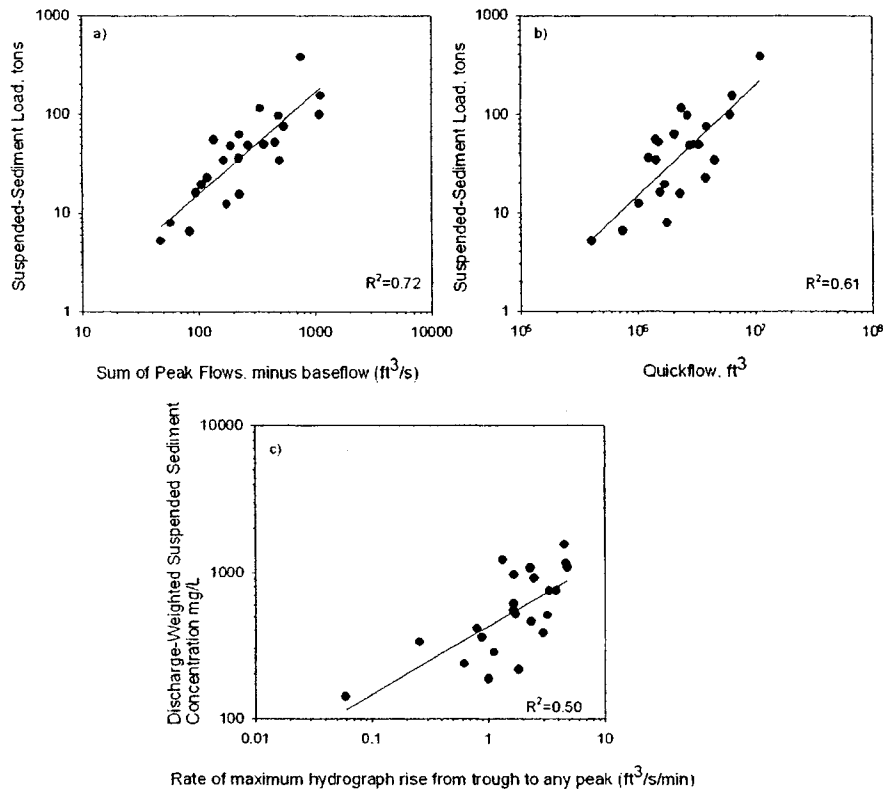

Figure 6.13. Graphical relations at Quebrada Blanca near El Jagual of independent variables with highest R^2 values using quickflow characteristics of the entire event against dependent variables: (a,b) suspended-sediment load and (c) discharge-weighted sediment concentration.

Factor analysis (entire event, quickflow)

Principal component analysis was performed on two sets of independent variables associated with quickflow characteristics of the event. One set contained 23 independent variables, including quickflow, the other set did not include quickflow (Appendices 6.4, 6.5). Six components were selected for factor analysis, determined from the scree plot. Forward stepwise regression was performed on both data sets using the dependent variables suspended-sediment load and discharge-weighted sediment concentration.

Reproduced with permission of the copyright owner. Further reproduction prohibited without permission.

Factor analysis for the data set with and without the variable quickflow gave similar results. Over 69% of the variance was explained by the first three axes. Forward stepwise regression was performed on the factor scores from principal component analysis against the two dependent variables (Table 6.5). Using the suspended-sediment load as a dependent variable indicated PC2 as the most significant principal component in the first step of forward stepwise regression and PC1 was significant in the second step (Table 6.5). PC2 represented characteristics of the current event and had high negative loadings (<-0.70) on rainfall (10-RAIN, 13-RRISE) and peak flow characteristics (4-PKBS, 8-SMPKBS) (Appendix 6.4). The coefficient of the best-fit line for PC2 was negative (-0.32), indicating that suspended-sediment load is directly correlated to characteristics with negative loadings (rainfall and peak flow characteristics of the current event).

Table 6.5. Results of forward stepwise regression on the principal components for the entire event using quickflow characteristics.

Dependent Variable	Step	Variables in the Model	R^2	F Statistic	Coefficient	Constant
suspended sediment, tons	One	PC2	0.50	21.4	-0.32	1.57
	Two	PC1	0.72	15.8	0.21	1.57
		PC2		36.5	-0.32	
discharge-weighted sediment concentration, mg/L	One	PC2	0.41	14.5	0.18	2.72
	Two	PC3	0.54	5.42	0.10	2.72
		PC2		17.6	0.18	

PC1 is important in the second step of forward stepwise regression explaining suspended-sediment load and had high positive loadings (>0.70) on characteristics of the previous event (20-LSPKBTI, 22-SMLSPKBS, 24-QULST, 26-PPTLSTI, 27-INTLST, 28-LS75OTI), three

Reproduced with permission of the copyright owner. Further reproduction prohibited without permission.

previous events (30-QU3EVT, 29-SUM3PPTI), and base flow (Appendix 6.4). The coefficient of the regression line was positive, indicating suspended-sediment load correlates with PC1 (Table 6.5). The direct correlation indicates that as magnitudes of variables of the previous events and three previous events increase, sediment in the current event increases. This supports the hypothesis that previous events supply sediment which is transported in the current event.

Observations of sediment load for the entire event based on factor analysis indicated that sediment load is directly proportional to previous-event characteristics (peak flow, quickflow, rainfall and rainfall intensity), the sum of the last three previous events (quickflow and rainfall), and current-event characteristics (rain, peak flow). Suspended-sediment load is a function of runoff and suspended-sediment concentration and thus, increases in either of these variables increase sediment load. Increases in previous-event rainfall and runoff will increase soil moisture. High antecedent soil moisture conditions generate runoff in the current event and thereby increase sediment loads. Rainfall in the current event increases sediment load by increasing the detachment of sediment from hillslopes and its delivery to the fluvial system. High rainfall amounts on the rising limb of the hydrograph and wet antecedent soil conditions may lead to an increase in the rate of hydrograph rise and the energy available to mobilize and transport sediment.

Using discharge-weighted sediment concentration as a dependent variable showed PC2 was significant in the first step of forward stepwise regression (Table 6.5). PC2 had high positive loadings (>0.70) from rainfall (10-RAIN, 13-RRISE) and flow characteristics of the current event (4-PKBS, 9-SMPKBS) (Appendix 6.5). The coefficient of forward stepwise regression was positive, indicating that as current-event characteristics of rainfall and flow increase, the discharge-weighted sediment concentration increases.

Reproduced with permission of the copyright owner. Further reproduction prohibited without permission.

PC3 was important in the second step of forward stepwise regression using discharge-weighted sediment concentration as a dependent variable (Table 6.7). PC3 had high positive loadings (>0.5) on rate of current-event hydrograph rise (6-MXTMJPK, 7-MXTRP), variables between events (17-RNBTWTI, 18-PPTBTW, 19-INTBET), and current rainfall intensity (12-SFIVE) (Appendix 6.5). The coefficient was positive, indicating that as the magnitude of these variables increase the discharge-weighted sediment concentration increases.

Interpretations of discharge-weighted sediment concentration characteristics based on factor analysis indicated that the sediment concentration of the current event is directly correlated to current-event variables and between-event variables. Rainfall and runoff between events may be supplying sediment which is transported in the sampled event.

Varimax rotation (entire event, quickflow)

Varimax rotation was performed on the principal components. The factor scores were saved after varimax rotation and forward stepwise regression was performed on the factor scores against the two dependent variables (Table 6.6). Using suspended-sediment load as a dependent variable showed that PC2 was important in the first step of forward stepwise regression and PC6 was important in the second step. PC2 had high positive loadings after rotation (>0.7) on current-event rainfall characteristics (10-RAIN, 13-RRISE, 14-RAINFOL) (Appendix 6.6). The coefficient of the regression line was positive, indicating that suspended-sediment load is correlated directly with current-event rainfall characteristics (Table 6.6). PC6 had high positive loadings on the maximum rate of hydrograph rise (7-MXTRP) and peak flow characteristics (4-PKBS, 8-SMPKBS) (Appendix 6.6). Interpretations of sediment load characteristics, based on factor

Reproduced with permission of the copyright owner. Further reproduction prohibited without permission.

analysis after varimax rotation, indicated that current rainfall and hydrograph characteristics increased sediment loads.

Table 6.6. Results of forward stepwise regression on the principal components after varimax rotation for the entire event using quickflow characteristics.

Dependent Variable	Step	Variables in the Model	R^2	F Statistic	Coefficient	Constant
suspended - sediment, tons	One	PC2	0.47	18.6	0.31	1.57
	Two	PC2	0.74	21.6	0.24	1.57
		PC6		31.7	0.31	
discharge-weighted sediment Concentration, mg/L	One	PC3	0.44	16.4	0.19	2.72
	Two	PC2	0.59	7.12	0.11	2.72
		PC3		21.2	0.19	

Using the discharge-weighted sediment concentration as a dependent variable showed PC3 was significant in the first step of forward stepwise regression (Table 6.6). PC3 had high positive loadings (> 0.6) on the maximum rate of hydrograph rise (7-MXTRP) and peak flow characteristics (4-PKBS, 8-SMPKBS) (Appendix 6.7). PC2 was important in the second step of forward stepwise regression (Table 6.6) and had high positive loadings (>0.90) on rainfall characteristics (11-RAIN, 13- RRISE). The coefficient of the regression was positive, indicating that as rainfall increased sediment concentration increased. Interpretations using the discharge-weighted sediment concentration as a dependent variable, based on factor analysis after varimax rotation, indicated that only current rainfall and hydrograph characteristics affected sediment concentrations, whereas previous-event and between-event characteristics did not have an effect.

Reproduced with permission of the copyright owner. Further reproduction prohibited without permission.

Runoff Results (entire event)

The independent variables assembled to analyze the relation of suspended-sediment characteristics to runoff characteristics are listed in Appendix 6.8. Seventeen of the 23 independent variables required a log transformation (Appendix 6.8).

. Analysis of the correlation matrix showed a high correlation (r>0.80) among select variables (Appendix 6.9). Five variables that showed high correlations were the same as in the quickflow analysis and were removed. Variables that were removed included 20-LSPKTI, 27-INTLST, 10-RAIN, 6-MXTMJPK, and 5-PK. Three variables that showed a high correlation among each other, 25-RULST, 23-SMLSPK, and 26PPTLSTI, were left in because they were perceived to be important.

Important relations of the dependent variables to the independent variables observed in the correlation matrix are suspended-sediment load to sum of peak flows (9-SMPK) and runoff (2-RUN). Discharge-weighted sediment concentration is correlated to rate of hydrograph rise for any peak (7-MXTRP) and the sum of peak flows (9-SMPK) (fig.6.14).

Forward stepwise regression (entire event, runoff)

Forward stepwise regression was run on the 18 independent variables against the two dependent variables (Table 6.7). The three most important variables explaining both dependent variables were similar to the quickflow analysis and were related to the characteristics of the current runoff event. Variables related to the current peak flow (9-SMPK, 7-MXTRP) were significant in the first step of stepwise regression against the dependent variables (Table 6.7). The slopes of

Reproduced with permission of the copyright owner. Further reproduction prohibited without permission.

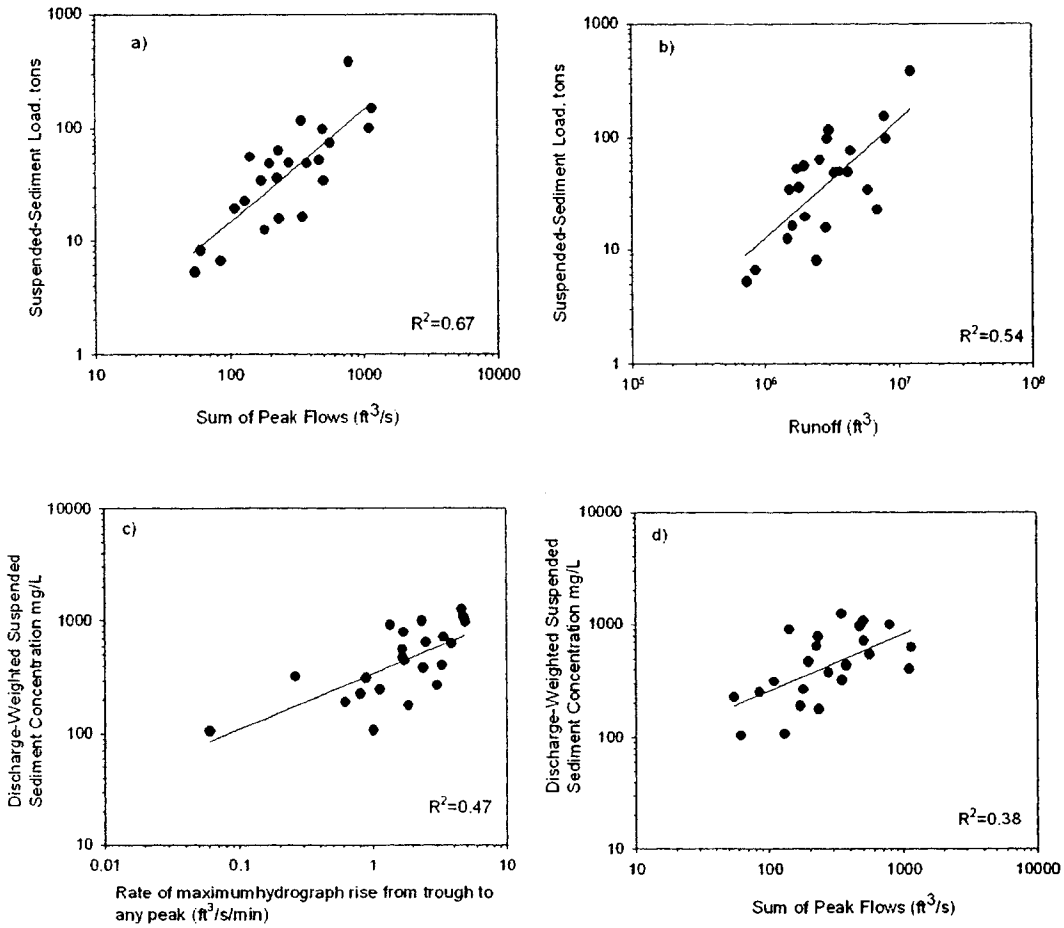

Figure 6.14. Graphical relations at Quebrada Blanca near El Jagual of independent variables with highest R^2 values using runoff characteristics of the entire event against dependent variables: (a,b) suspended-sediment load and (c,d) discharge-weighted sediment concentration.

the line of best-fit for the dependent variables were positive, indicating a direct correlation of the dependent variables with the independent variables.

Using suspended-sediment load as a dependent variable showed runoff (2-RUN) was significant in the second step of forward stepwise regression. Unlike the quickflow results, the maximum rate of hydrograph rise for any peak (7-MXTRP) was significant in the third step (Table

Reproduced with permission of the copyright owner. Further reproduction prohibited without permission.

Table 6.7. Results of forward stepwise regression for entire event using runoff characteristics.

Dependent Variable	Step	Variables in the Model	R^2	F Statistic	Coefficient	Constant
Suspended sediment, tons	One	9-SMPK	0.67	42.9	1.03	-0.92
	Two	2-RUN	0.76	7.86	0.57	-3.88
		9-SMPK		19.1	0.75	
Discharge-weighted sediment concentration, mg/L	One	7-MXTRP	0.47	18.8	0.49	2.53
	Two	13-RRISE	0.65	10.3	0.60	2.46
		7-MXTRP		212	0.44	

6.7). The slope of the regression coefficient was positive, indicating that as the highest rate of hydrograph rise for any peak increased, sediment load increased.

Using the discharge-weighted sediment concentration as a dependent variable showed that rainfall on the rising limb of the hydrograph (13-RRISE) was significant in the second step (Table 6.7). The slope of the regression coefficient was positive, indicating that as rainfall on the rising limb increased sediment load increased.

Factor analysis - (entire event, runoff)

Principal component analysis was performed on two sets of independent variables associated with runoff characteristics of the event. One set contained 23 independent variables, including runoff, the other set did not include runoff (Appendices 6.10, 6.11). Six components were selected for factor analysis. Seventy percent of the total variance was explained by the first three axes. Forward stepwise regression was performed on the two data sets using the dependent variables, suspended-sediment load and discharge-weighted sediment concentration.

Reproduced with permission of the copyright owner. Further reproduction prohibited without permission.

Results of factor analysis using runoff for the entire event were similar to the results using quickflow (Table 6.8). PC2 is significant in the first step of forward stepwise analysis explaining suspended-sediment load (Table 6.8) and had high negative loadings on current-event characteristics (5-PK, 9-SMPK, 10-RAIN, 13-RRISE,) (Appendix 6.10). A high positive loading (0.55) was on the runoff between events (17-RNBTWTI) (Appendix 6.10). The slope of the best-fit line was negative and the loadings were negative, indicating a direct correlation of sediment load to current-event characteristics and an indirect correlation with the runoff between events.

Using suspended-sediment load as an independent variable showed PC1 to be important in the second step of forward stepwise regression (Table 6.8). PC1 had high positive loadings (>0.7) on features of the previous event (21-LSPKTI, 23-SMLSPK, 25-RULST, 26-PPTLSTI, 27-INTLST, 28-LS75OTI), three previous events (31-RU3EVT, 29-SUM3PPTI), and base flow (3-BASE) (Appendix 6.10). The slope of the line of best fit was positive, indicating that as the magnitude of characteristics of the previous event(s) increased, sediment load increased.

Table 6.8. Results of forward stepwise regression on the principal components for the entire event using runoff characteristics.

Dependent Variable	Step	Variables in the Model	R^2	F Statistic	Coefficient	Constant
suspended sediment, tons	One	PC2	0.48	19.7	-0.32	1.57
	Two	PC1	0.71	15.8	0.22	1.57
		PC2		33.7	-0.32	
discharge-weighted sediment concentration, mg/L	One	PC2	0.47	18.3	0.21	2.62
	Two	PC3	0.61	7.43	0.12	2.62
		PC2		23.9	0.21	

Reproduced with permission of the copyright owner. Further reproduction prohibited without permission.

Interpretations of suspended-sediment load characteristics based on factor analysis were similar to results using quickflow. Previous-event characteristics were supplying sediment to the system and increases in rainfall and peak flow of the current event were increasing suspended-sediment load.

The results of forward-stepwise regression on the principal components using the discharge-weighted sediment concentration as a dependent variable were similar to the results using quickflow and showed PC2 was significant in the first step (Table 6.8). PC2 had high positive loadings (> 0.60) from rainfall (13-RAIN, 20-RRISE, 21-RAINFOL) and peak flow characteristics (17-PK, 18-SMPK) of the current event (Appendix 6.11). The coefficient of forward stepwise regression was positive, indicating that as current-event characteristics of rainfall and peak flow increase, the discharge-weighted sediment concentration increases.

Using the discharge-weighted sediment concentration as a dependent variable showed that PC3 was important in the second step of forward stepwise regression (Table 6.8). PC3 had high positive loadings (>0.5) on variables between events (17-RNBTWTI, 18-PPTBTW, 19-INTBET), rate of current-event peak rise (6-MXTMJPK, 7-MXTRP), and current rainfall intensity (12-SFIVE) (Appendix 6.11). The coefficient was positive, indicating that as these variables increased the discharge-weighted sediment concentration increased. Interpretations of discharge-weighted sediment concentration characteristics based on factor analysis did not indicate that previous-event characteristics are significant. Sediment concentration of the current event increased as a function of current rainfall and hydrograph peak flow characteristics. Rainfall and runoff between events introduced sediment to the channel.

Reproduced with permission of the copyright owner. Further reproduction prohibited without permission.

Varimax rotation (entire event, runoff)

Rotation of the principal components axis were performed using the varimax rotation. Varimax rotation using sediment load as a dependent variable showed similar results to before rotation and indicated that PC2 was significant in the first step of forward stepwise regression (Table 6.9). PC2 had high positive loadings (>0.70) from rainfall (13-RAIN, 20-RRISE, 21-RAINFOL) (Appendix 6.12) and the slope of the line of best fit was positive, indicating that as current-event characteristics of rainfall increased, sediment load increased. PC6 was significant in the second step of forward stepwise regression (Table 6.9). This is different from the results before rotation, which showed that PC1 was significant in the second step of forward stepwise regression. PC6 had high loadings (>0.80) on characteristics of the hydrograph rise (6-LMXTMJPK, 7-MXTRPK) (Appendix 6.12) and the slope was positive, indicating that as the rate of hydrograph rise increased the sediment load increased.

Table 6.9. Results of forward stepwise regression on the principal components after varimax rotation for the entire event using quickflow characteristics.

Dependent Variable	Step	Variables in the Model	R^2	F Statistic	Coefficient	Constant
suspended sediment, tons	One	PC2	0.45	17.0	0.31	1.57
	Two	PC6	0.73	21.5	0.24	1.57
		PC2		33.6	0.31	
discharge-weighted sediment concentration	One	PC3	0.44	16.2	0.19	2.72
	Two	PC2	0.60	8.00	0.12	2.72
		PC3		21.5	0.19	

Reproduced with permission of the copyright owner. Further reproduction prohibited without permission.

Using the discharge-weighted sediment concentration as a dependent variable indicated that PC3 was significant in the first step of forward stepwise regression and PC2 was significant in the second step (Table 6.9). These are the same principal components that were significant before rotation but the order of significance was reversed after rotation. PC3 had high loadings (>0.80) on characteristics of the hydrograph rise (6-MXTMJPK, 7-MXTRPK) (Appendix 6.13) and the slope was positive, indicating that as the rate of hydrograph rise increased the sediment load increased. PC2 had high positive loadings (> 0.70) from rainfall (13-RAIN, 20-RRISE, 21-RAINFOL) (Appendix 6.13) and as these variables increased, sediment load increased. The interpretation after varimax rotation is that suspended-sediment load transported is directly correlated to characteristics of the current event.

Discussion

Results of forward stepwise regression analysis for the entire event using independent variables related to runoff (Table 6.10) closely match the results using variables related to quickflow (Table 6.6). In both the quickflow and runoff analyses, the sum of peak flows in the current event is important in explaining suspended-sediment load, and the maximum rate of hydrograph rise for any peak is important in explaining the discharge-weighted sediment concentration. Forward stepwise regression using the discharge-weighted sediment concentration as a dependent variable also indicated that rainfall on the rising limb of the hydrograph was significant.

The results of forward stepwise regression analysis on the principal components before varimax rotation are generally similar for both quickflow and runoff (Tables 6.5, 6.8). For both

Reproduced with permission of the copyright owner. Further reproduction prohibited without permission.

Reproduced with permission of the copyright owner. Further reproduction prohibited without permission.

Table 6.10. Summary of runoff events sampled adequately to the highest peak of the event at Quebrada Blanca near El Jagual.

(* Mna = Complex event, n=number of complex event, a,b,c, = sequence of each event in the entire multiple event; a=1st event, b=2nd, etc)

Start Date	Start Time	Start discharge ft3/s	End Date	End Time	End discharge ft3/s	Event Duration (hour)	Peak Flow (cfs)	Total quickflow (ft3)	Runoff (ft3)	Suspended-sediment load (tons)
8/11/1989	16.00	0.98	8/11/1989	17.25	86	1.25	86	57750	62720	1.3
8/18/1989	22.00	3.1	8/19/1989	0.25	231	2.25	231	174640	201560	9.3
9/13/1989	21.50	3.1	9/14/1989	0.75	115	3.25	115	229640	270140	4.7
9/18/1989	2.75	7.3	9/18/1989	9.00	537	6.25	537	4849670	9141620	154
9/22/1989	9.00	4.4	9/22/1989	10.25	335	1.25	335	379980	828810	20.2
5/9/1990	19.25	0.73	5/9/1990	21.75	507	2.50	507	270540	52920	6.5
6/14/1990	14.00	1.4	6/14/1990	15.50	226	1.50	226	136860	277320	5.3
8/9/1990	13.75	12	8/10/1990	7.50	838	17.75	838	1694040	146610	30.7
10/16/1990	12.00	2.1	10/16/1990	14.00	109	2.00	109	188670	3012300	2.5
10/24/1990	18.75	7.0	10/24/1990	20.25	118	1.50	118	131580	1076400	3.0
12/30/1990	19.25	2.0	12/31/1990	4.75	91	9.50	91	758210	544240	14.3
9/17/1991	2.42	0.98	9/17/1991	9.33	340	6.92	340	1113560	1116410	21.9
9/22/1991	8.5	3.2	9/23/1991	17.75	10	33.25	132	908150	846540	25.9
11/16/1991	13.25	5.1	11/16/1991	14.50	154	1.25	154	217200	557030	9.3
11/21/1991	15.50	3.6	11/21/1991	22.00	101	6.50	101	367370	1912290	3.0
11/28/1991	12.25	24	11/28/1991	14.00	130	1.75	130	362500	1142220	9.3
5/16/1992	4.00	2.0	5/16/1992	13.25	128	9.25	128	495980	240800	30.6
6/4/1992	8.50	4.3	6/4/1992	9.75	347	1.25	347	500240	454680	47.0
7/22/1993	16.00	5.9	7/22/1993	17.75	501	1.75	501	982320	594720	47.7
8/15/1993	21.50	5.3	8/16/1993	9	234	11.50	234	2391130	519950	101

dependent variables, current rainfall and peak flow characteristics were significant. After varimax rotation, current-event rainfall and rate of hydrograph rise were significant and directly correlated to both dependent variables. Interpretations of sediment characteristics based on factor analysis indicated that sediment is entrained from hillslopes by rainfall during the current event and that steep, rapid rises in the storm hydrograph provide energy for sediment transport.

Highest peak flow analysis

This section describes the results of statistical analysis at-a-station for Quebrada Blanca at El Jagual using characteristics measured to the highest peak flow of the event. Twenty of the 23 storms were sampled adequately to the highest peak flow of the event (Table 6.10)

Two dependent variables were used to describe sediment to the highest peak flow: 1) suspended-sediment load, in tons and 2) discharge-weighted sediment concentration, in mg/L. Histograms of the dependent variables showed that suspended-sediment load and the discharge-weighted sediment concentration required a log transformation.

The average suspended-sediment load for the 20 events was 27.3 tons (fig. 6.15a) and the average discharge-weighted sediment concentration using quickflow, was 1,100 mg/L (fig. 6.15b). The maximum discharge-weighted sediment concentration, for both quickflow and runoff, 3,000 mg/L and 2,890 mg/L, occurred on 6/4/1992.

Quickflow Results (highest peak)

The independent variables assembled to analyze the relation of suspended-sediment characteristics to quickflow characteristics for the portion of the hydrograph rising to the highest

Reproduced with permission of the copyright owner. Further reproduction prohibited without permission.

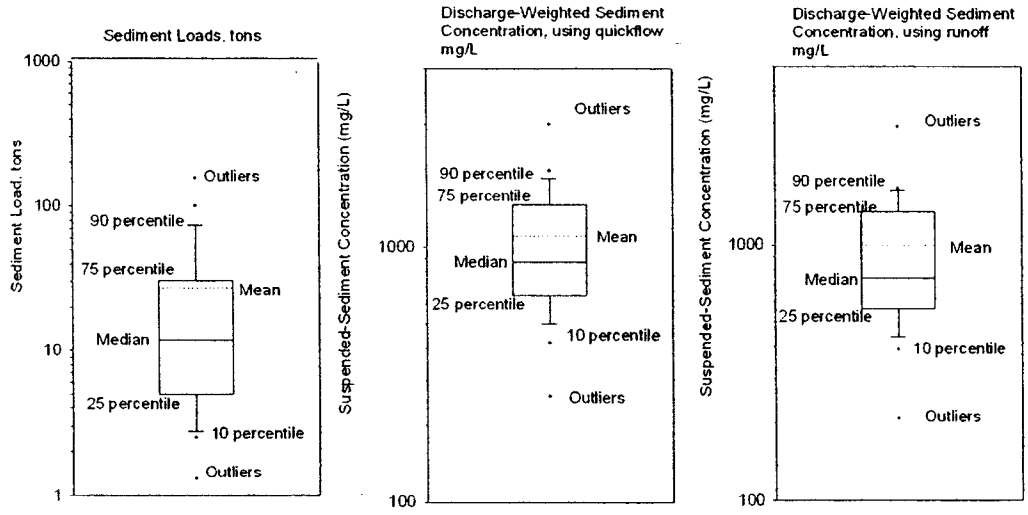

Figure 6.15. Box plot of dependent variables to the highest peak flow, a) sediment load, b) discharge-weighted sediment concentrations using quickflow, and c) discharge-weighted sediment concentration using runoff.

peak flow are listed in Appendix 6.14. Tests for normality using the residuals and histograms indicated that 13 of the 17 independent variables needed a log transformation (Appendix 6.14). Analysis of the correlation matrix showed the same results as for the entire event (Appendix 6.15). Variables that showed a high correlation ($r>0.80$) and were removed included: 20-LSPKBTI, 27-INTLST, and 19-INTBET.

Relations of the dependent variables to the independent variables that appear important in the correlation matrix are the suspended-sediment load to quickflow (1-QUICK) and to peak flow minus base flow (4-PKBS) (fig. 6.16a,b; Appendix 6.15). The discharge-weighted sediment concentration showed the best relation to the rate of hydrograph rise to the highest peak (6-MXTMJPK) (fig. 6.16c).

Reproduced with permission of the copyright owner. Further reproduction prohibited without permission.

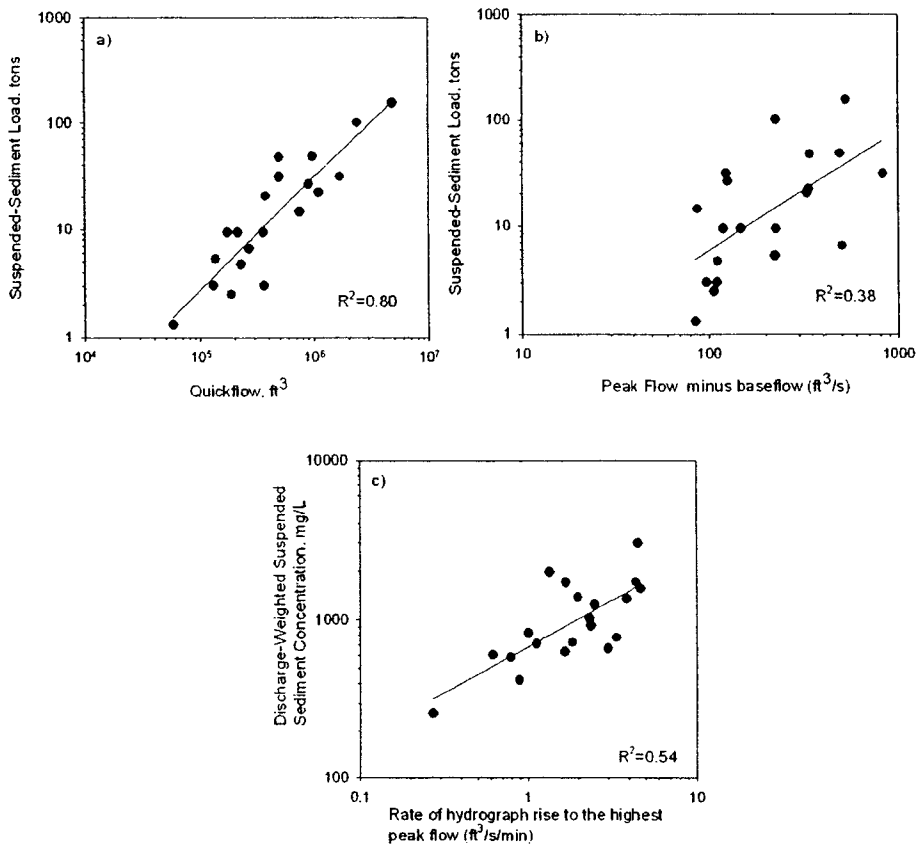

Figure 6.16. Graphical relations at Quebrada Blanca near El Jagual of independent variables with highest R^2 values using quickflow characteristics to the highest peak flow against dependent variables: (a,b) suspended-sediment load and (c) discharge-weighted sediment concentration.

Forward stepwise regression (highest peak, quickflow)

Forward stepwise regression was performed on the 14 independent variables against both dependent variables describing sediment (suspended-sediment load and discharge-weighted sediment concentration) for the portion of the hydrograph to the highest peak flow.

Results of forward stepwise regression on the remaining independent variables against the two dependent variables are listed in Table 6.11. In general, the three most important variables

Reproduced with permission of the copyright owner. Further reproduction prohibited without permission.

explaining the dependent variables were related to the characteristics of the current runoff. The maximum rate of rise to the highest peak flow (6-MXTMJPK) is significant against both dependent variables (Table 6.11).

The quickflow (1-QUICK) of the current event was significant in the first step of the forward stepwise regression against suspended-sediment load. In the second step of forward stepwise regression, the maximum rate of rise to the highest peak flow (6-MXTMJPK) was significant (Table 6.11). In both steps the slope of the best fit line was positive.

Table 6.11. Results of forward stepwise regression measured to the highest peak flow of the event using quickflow characteristics.

Dependent Variable	Step	Variables in the Model	R^2	F Statistic	Coefficient	Constant
suspended-sediment load, tons	One	1-QUICK	0.79	69.5	1.00	-4.80
	Two	6-MXTMJPK	0.90	19.4	0.57	-4.66
		1-QUICK		125	1.00	
discharge-weighted sediment concentration, mg/L	One	6-MXTMJPK	0.54	20.9	0.57	2.83

Factor analysis - (highest peak, quickflow)

Principal component analysis was performed on two sets of independent variables associated with quickflow characteristics to the highest peak flow. One set contained 17 independent variables, including quickflow, the other set did not include quickflow (Appendices 6.16; 6.17). Six components were selected for factor analysis. Over 59% of the variance was explained by the first three axes in both the principal component data sets with or without quickflow (Appendices 6.16, 6.17).

Reproduced with permission of the copyright owner. Further reproduction prohibited without permission.

Using suspended-sediment load as a dependent variable indicated that PC4 was significant in the first step of forward stepwise regression and PC2 was significant in the second step (Table 6.12). PC4 had a high positive loading (> 0.5) on quickflow (1-QUICK) and a high negative loading (<0.5) on the rainfall intensity of the previous event (28-LS75OTI) and current event (11-INT15) (Appendix 6.16). The slope of the line of best-fit was positive, indicating that suspended-sediment load was correlated directly with quickflow and inversely correlated with the rainfall intensity of the previous event and rainfall intensity of the current event.

Using suspended-sediment load as a dependent variable indicated that PC2 was significant in the second step of forward stepwise regression (Table 6.12) and had high positive loadings (> 0.6) on characteristics between events (17-RNBTWTI, 18-PPTBTW, 19-INTBET) and high negative loadings (< -0.5) on characteristics of the current event (1-QUICK, 4-PKBS, 13-RRISE) (Appendix 6.16). The coefficient of PC2 was negative, indicating that suspended-sediment load of the current event was inversely correlated to characteristics between events and directly correlated with characteristics of the current event.

Results of factor analysis for sediment load characteristics, calculated to the highest peak flow, indicated that rainfall intensity of the previous event and current event decreased sediment loads on the rising portion of the current hydrograph. Runoff and precipitation since the previous event flushed sediment from the current event. Quickflow, peak flow, and rainfall increased sediment loads in the current event.

Using the discharge-weighted sediment concentration as a dependent variable indicated that PC3 was significant in the first step of forward stepwise regression and PC4 was significant in the second step (Table 6.12). PC3 had high positive loadings (> 0.6) on characteristics of the

Reproduced with permission of the copyright owner. Further reproduction prohibited without permission.

current-event, peak flow minus base flow (4-PKBS) and the maximum rate of hydrograph rise to the highest peak flow (6-MXTMJPK) (Appendix 6.17). The slope of the line of best fit was positive, indicating that the discharge-weighted sediment concentration of the current event was directly correlated to characteristics of the current event (Table 6.12).

Using the discharge-weighted sediment concentration as a dependent variable indicated that PC4 was significant in the second step of forward stepwise regression. PC 4 had high positive loadings (> 0.5) on rainfall intensity of the previous event (28-LS75OTI) (Appendix 6.17). The

Table 6.12. Results of forward stepwise regression on the principal components measured to the highest peak of the event using quickflow characteristics.

Dependent Variable	Step	Variables in the Model	R^2	F Statistic	Coefficient	Constant
suspended-sediment load, tons	One	PC4	0.39	11.7	0.35	1.12
	Two	PC2	0.65	12.8	-0.28	1.12
		PC4		19.4	0.35	
discharge-weighted sediment concentration, mg/L	One	PC3	0.29	7.34	0.14	2.97
	Two	PC4	0.55	10.0	-0.13	2.97
		PC3		11.0	0.14	

slope of the line of best fit was positive, indicating that the discharge-weighted sediment concentration of the current event was directly correlated to characteristics of the current event (Table 6.12).

Using the discharge-weighted sediment concentration as a dependent variable indicated that PC4 was significant in the second step of forward stepwise regression. PC 4 had high positive loadings (> 0.5) on rainfall intensity of the previous event (28-LS75OTI) (Appendix 6.17). The

Reproduced with permission of the copyright owner. Further reproduction prohibited without permission.

slope of the line of best fit was negative, indicating that suspended-sediment load was inversely correlated with rainfall intensity of the previous event.

Interpretations of discharge-weighted sediment concentration characteristics based on factor analysis indicated that between-event rainfall characteristics (such as rainfall intensity between events)decreased sediment for transport on the rising portion of the current hydrograph. Peak flow, and rainfall characteristics of the current event increased sediment loads. Rainfall intensity of the current event was directly correlated with the discharge-weighted sediment concentration but inversely correlated with sediment load. The reason for this difference is unclear.

Varimax rotation (highest peak, quickflow)

Principal components axes were rotated using the varimax rotation. Varimax rotation using suspended-sediment load as a dependent variable showed results similar to those before rotation and indicated that PC4 was significant in the first step of forward stepwise regression (Table 6.13). Correlation coefficient (R^2) values were lower than before rotation. High positive loadings on PC4 (0.73) were on quickflow (1-QUICK) and high negative loadings (-0.87) were on rainfall intensity (11-INT15) (Appendix 6.18). The correlation coefficient was positive, indicating that sediment load was directly correlated to quickflow and inversely correlated to rainfall intensity.

Using suspended-sediment load as a dependent variable indicated that PC5 was significant in the second step of forward stepwise regression (Table 6.13). PC5 had a high positive loading (0.91) on the rate of hydrograph rise to the highest peak (16-MXTMJPK) (Appendix 6.18). The coefficient was positive, indicating that as the rate of hydrograph rise to the highest peak flow increased, sediment load increased.

Reproduced with permission of the copyright owner. Further reproduction prohibited without permission.

Interpretations of sediment load characteristics, based on varimax rotation of the principal components and factor analysis, indicated that increases in quickflow and the rate of hydrograph rise to the highest peak flow increased sediment loads. The rainfall intensity of the current event decreased sediment loads.

Using the discharge-weighted sediment concentration as a dependent variable indicated that PC6 was significant in the first step of forward stepwise regression and the correlation coefficients were higher than before rotation (Table 6.13). PC6 had a high positive loading on the rate of hydrograph rise to the highest peak flow (16-MXTMJPK) (Appendix 6.19) and the coefficient of the regression was positive. Interpretations of discharge-weighted sediment concentration characteristics based on factor analysis indicated that steep, fast rising hydrographs increased sediment concentrations. The rate of hydrograph rise (16-MXTMJPK) was also significant before varimax rotation. However, before rotation five variables were considered significant in explaining the discharge-weighted sediment concentration and only one variable was important after varimax rotation.

Table 6.13. Results of forward stepwise regression on the principal components after varimax rotation measured to the highest peak of the event using quickflow characteristics.

Dependent Variable	Step	Variables in the Model	R^2	F Statistic	Coefficient	Constant
suspended-sediment load, tons	One	PC4	0.29	7.26	0.30	1.12
	Two	PC5	0.54	9.05	0.28	1.12
		PC4		10.5	0.30	
discharge-weighted sediment concentration, mg/L	One	PC6	0.38	11.0	0.16	2.97

Reproduced with permission of the copyright owner. Further reproduction prohibited without permission.

Runoff Results (highest peak)

The independent variables assembled to analyze the relation of suspended-sediment characteristics to runoff characteristics for the portion of the hydrograph rising to the highest peak flow are listed in Appendix 6.20. Tests for normality using the residuals indicated that 13 of the 17 independent variables needed a log transformation (Appendix 6.20).

Analysis of the correlation matrix showed a high correlation ($r>0.80$) among select variables (Appendix 6.21). These variables were the same as in the quickflow analysis and were removed (21-LSPKTI, 27-INTLST, and 19-INTBET). Three variables showed a high correlation among each other, 25-RULST, 23-SMLSPK, and 26-PPTLSTI, but were left in because they were perceived to be important (Appendix 6.21).

Relations of the dependent variables to the independent variables that appear important in the correlation matrix were suspended-sediment load to runoff (2-RUN) and to peak flow (5-PK). Discharge-weighted sediment concentration was correlated to the maximum rate of hydrograph rise to the highest peak flow (6-MXTMJPK) (fig. 6.17).

Forward stepwise regression (highest peak, runoff)

Forward stepwise regression was performed on the 14 independent variables against both dependent variables describing sediment (suspended-sediment load and discharge-weighted sediment concentration) for the portion of the hydrograph rising to the highest peak flow. The results of forward stepwise regression shown in Table 6.14 were similar to the quickflow analysis for the first step of forward stepwise regression to the highest peak (Table 6.12). In general, the three most important variables explaining both dependent variables were related to the

Reproduced with permission of the copyright owner. Further reproduction prohibited without permission.

characteristics of the current runoff. The maximum rate of rise to the highest peak flow (6-MXTMJPK) was significant against both dependent variables and the slope of the line of best fit was positive, indicating a direct relation of sediment characteristics to the rate of hydrograph rise (Table 6.14).

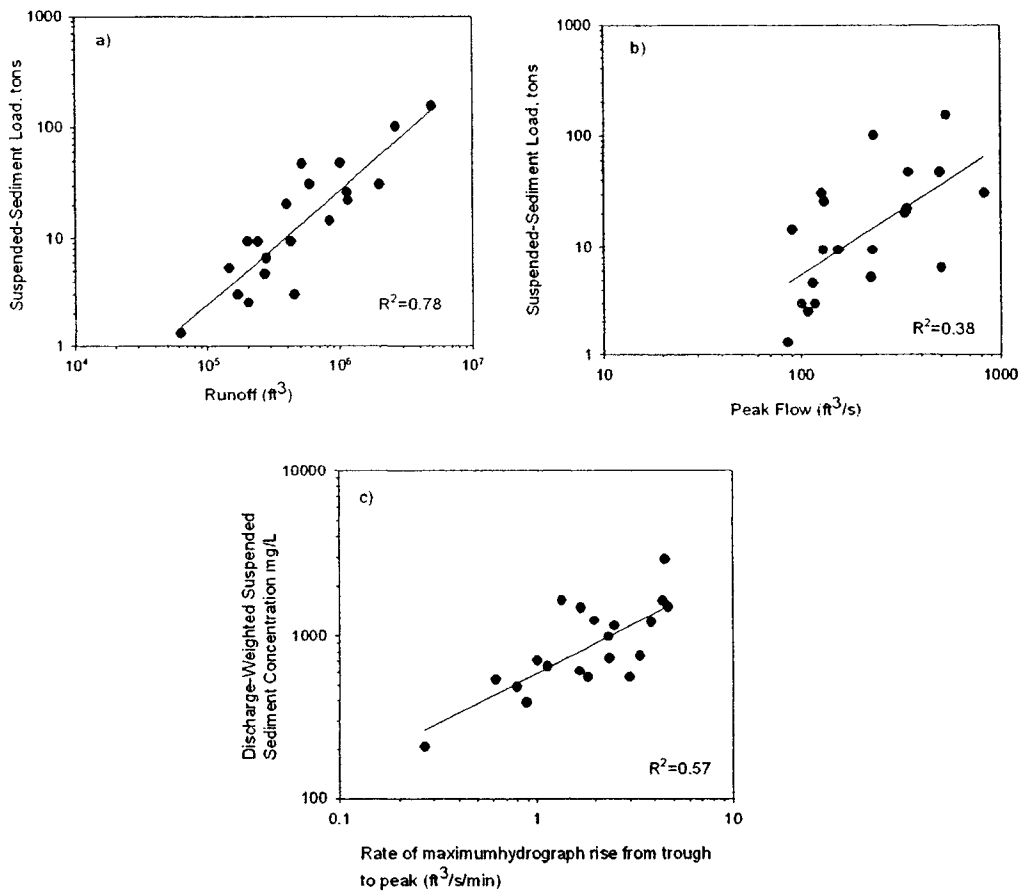

Figure 6.17. Graphical relations at Quebrada Blanca near El Jagual of independent variables with highest R^2 values using runoff characteristics to the highest peak against dependent variables: a), b) suspended-sediment load, and c) discharge-weighted sediment concentration.

Using suspended-sediment load as a dependent variable showed runoff (2-RUNOFF) was significant in the first step of forward stepwise regression (Table 6.14). The slope of the line of best fit was positive, indicating a direct correlation of sediment load to runoff.

Reproduced with permission of the copyright owner. Further reproduction prohibited without permission.

Table 6.14. Results of forward stepwise regression measured to the highest peak flow of the event using runoff characteristics.

Dependent Variable	Step	Variables in the Model	R^2	F Statistic	Coefficient	Constant
suspended-sediment load, tons	One	2-RUN	0.77	61.8	1.0	-4.84
	Two	6-MXTMJPK	0.90	22.4	0.62	-4.75
		2-RUN		123	1.0	
discharge-weighted sediment concentration, mg/L	One	6-MXTMJPK	0.57	24.1	0.62	2.77

Factor analysis - (highest peak, runoff)

Principal component analysis was performed on two sets of independent variables associated with runoff characteristics to the highest peak (Appendix 6.22, Appendix 6.23). Six components were selected for factor analysis.

Factor analyses on both data sets have results similar to the quickflow analysis. Using suspended-sediment load as a dependent variable indicated that PC4 was significant in the first step of forward stepwise regression and PC2 was significant in the second step (Table 6.15). PC4 had a high positive loadings (0.57) on runoff (2-RUN), and a high negative loading (-0.51) on the rainfall intensity of the previous event (28-LS75OTI) and rainfall intensity of the current event (11-INT15) (-0.48) (Appendix 6.22). The coefficient of regression was positive, indicating that suspended-sediment load was correlated directly with runoff and inversely correlated with the rainfall intensities of the previous and current event.

Using suspended-sediment load as a dependent variable indicated that PC2 was significant in the second step of forward stepwise regression (Table 6.15) and had high negative loadings (<

Reproduced with permission of the copyright owner. Further reproduction prohibited without permission.

-0.5) on characteristics of the current event (2-RUN, 5-PK, 13-RRISE) (Appendix 6.22). High positive loadings (> 0.6) were on characteristics between events (17-RNBTWTI, 18-PPTBTW, 19-INTBET). The coefficient of PC2 was negative, indicating that suspended-sediment load was directly correlated with characteristics of the current event and inversely correlated to characteristics between events.

Table 6.15. Results of forward stepwise regression on the principal components measured to the highest peak flow of the event using runoff characteristics.

Dependent Variable	Step	Variables in the Model	R^2	F Statistic	Coefficient	Constant
suspended-sediment load, tons	One	PC4	0.43	13.7	0.37	1.12
	Two	PC2	0.68	13.3	-0.28	1.12
		PC4		23.0	0.37	
discharge-weighted sediment concentration, mg/L	One	PC3	0.32	8.32	0.15	2.92
	Two	PC4	0.58	10.7	-0.14	2.92
		PC3		12.8	0.15	

Interpretations of sediment load characteristics to the highest peak flow using runoff characteristics based on factor analysis indicated that previous-event rainfall intensity removed sediment for transport that would be available on the rising portion of the current hydrograph. Runoff and precipitation since the previous event flushed sediment from the current event. Quickflow, peak flow, and rainfall of the current event increased sediment loads.

Using the discharge-weighted sediment concentration as a dependent variable indicated that PC3 was significant in the first step of forward stepwise regression and PC4 was significant in the second step (Table 6.15). PC3 had high positive loadings (>0.5) on characteristics of the

Reproduced with permission of the copyright owner. Further reproduction prohibited without permission.

current event (5-PK, 6-MXTMJPK, 11-INT15) (Appendix 6.23). The slope of the line of best fit was positive, indicating that discharge-weighted sediment concentration was directly correlated to characteristics of the current event (Appendix 6.23). PC4 was significant in the second step of forward stepwise regression and had high positive loadings (>0.5) on rainfall intensity of the previous event (28-LS75OTI) (Appendix 6.23). The slope of the line of best fit was negative, indicating that discharge-weighted sediment concentration was correlated directly with current rate of hydrograph rise to the highest peak and inversely correlated with rainfall intensity of the previous event.

Interpretations of discharge-weighted sediment concentration characteristics based on factor analysis indicated that previous-event rainfall intensity removed sediment available for transport to the rising portion of the current hydrograph. Peak flow and rainfall characteristics of the current event increased sediment concentration.

Varimax rotation (highest peak, runoff)

Principal components axes were rotated using the varimax rotation. Varimax rotation using sediment load as a dependent variable showed results similar to those before rotation and indicated that PC4 was significant in the first step of forward stepwise regression. R^2 values were lower than before rotation (Table 6.16). High positive loadings (>0.7) on PC4 were on runoff (2-RUN) and high negative loadings (<-0.8) were on rainfall intensity of the current event (11-INT15) (Appendix 6.24). The slope of the line of best fit was positive, indicating that as runoff increased, sediment load to the highest peak increased and as the rainfall intensity on the rising limb of the hydrograph increased, sediment load decreased (Table 6.16).

Reproduced with permission of the copyright owner. Further reproduction prohibited without permission.

In the second step of forward stepwise regression, PC5 was significant (Table 6.21). PC5 had a high positive loading (0.92) on the rate of hydrograph rise to the highest peak (6-MXTMJPK) (Appendix 6.24). The slope of the line of best fit was positive, indicating that as the rate of hydrograph rise to the highest peak flow increased the sediment load increased.

Table 6.16. Results of forward stepwise regression on the principal components using varimax rotation measured to the highest peak flow of the event using runoff characteristics.

Dependent Variable	Step	Variables in the Model	R^2	F Statistic	Coefficient	Constant
suspended - sediment load, tons	One	PC4	0.30	7.60	0.30	1.12
	Two	PC5	0.55	9.82	0.28	1.12
		PC4		11.3	0.30	
discharge-weighted sediment concentration, mg/L	One	PC6	0.41	12.6	0.17	2.92

Interpretations of the sediment load characteristics to the highest peak flow based on factor analysis after varimax rotation indicated that increases in runoff and the rate of hydrograph rise to the highest peak, increased sediment loads. As was observed in previous analyses, the current-event rainfall intensity (11-INT15) was inversely correlated to sediment load.

Using the discharge-weighted sediment concentration as a dependent variable indicated that PC6 was significant and the correlation coefficients (R^2) were higher than before rotation (Table 6.16). PC6 had a high positive loading (>0.8) on the rate of hydrograph rise to the highest peak flow (6-MXTMJPK) (Appendix 6.25) and the slope of the line of best fit was positive (Table 6.16). Interpretations of the discharge-weighted sediment concentration characteristics to the highest peak flow based on factor analysis after varimax rotation indicated that one characteristic

Reproduced with permission of the copyright owner. Further reproduction prohibited without permission.

of the current event, the rate of hydrograph rise to the highest peak, was significant and had a direct correlation to sediment concentration.

Discussion

Statistical results using runoff characteristics to the highest peak flow (Table 6.15) were similar to the results using quickflow (Table 6.12). Forward stepwise regression indicated that either runoff or quickflow is important in explaining suspended-sediment load, and the maximum rate of hydrograph rise to the highest peak flow was significant in explaining the discharge-weighted sediment concentration.

The results of forward stepwise regression analysis on the principal components generated for the portion of the hydrograph to the highest peak flow were similar using both quickflow and runoff characteristics (Appendices 6.16, 6.17, 6.22, 6.23). PC4 is the most important principal component explaining both dependent variables. Variables on PC4 that were directly correlated with the dependent variables are characteristics of the current event (quickflow, maximum rate of hydrograph rise for any peak). Variables on PC4 that are inversely correlated to both dependent variables are characteristics of previous events (the previous event 75% rainfall intensity).

After varimax rotation, only current-event characteristics of runoff and the rate of hydrograph rise to the highest peak flow were significantly correlated to sediment characteristics. Characteristics of the previous events and characteristics since the previous events were not significant. Current-event rainfall intensity was negatively correlated to sediment loads. Sediment loosened by increased rainfall intensity may not travel to the gage before the highest peak flow.

Reproduced with permission of the copyright owner. Further reproduction prohibited without permission.

Results of factor analysis for sediment load characteristics, calculated to the highest peak flow, indicated that rainfall intensity of the previous event and current event decreased sediment loads on the rising portion of the current hydrograph. Runoff and precipitation since the previous event flushed sediment from the current event. Quickflow, peak flow, and rainfall increased sediment loads in the current event. Rainfall intensity increased erosion and basin sediment yields (Guy, 1964; Dunne and Leopold, 1978). Previous-event rainfall intensity may remove sediment from hillslopes that could be available for transport in the current event. The inverse relation of current-event rainfall intensity to storm loads is difficult to explain. Because only sediment characteristics to the highest peak flow were examined, the sediment moved from high rainfall intensity may appear after the peak flow and would not be included in this analyses.

Hysteresis

Hysteresis loops of the 23 sampled events were analyzed for the timing of the peak suspended-sediment concentration relative to peak flow, the type of hysteresis, and the width of the hysteresis loop (Table 6.17). Close to half of the events (12 events) had the peak sediment concentration sampled between 1 to 456 minutes before the highest peak flow. Ten events had the peak suspended-sediment concentration collected 1 to 365 minutes after peak flow (Table 6.17). One sample was collected at the time of the peak flow.

Observation of the hysteresis loops for the entire event showed that clockwise hysteresis (Type 1; fig. 4.7) was the most common type observed in 11 of the 23 events (fig. 6.18a). Six of the 23 events showed a counter clockwise hysteresis (Type-3) loop (Fig. 6.18a), three of the events showed a figure eight (Type 4), and three events were indeterminate relative to hysteresis

Reproduced with permission of the copyright owner. Further reproduction prohibited without permission.

Reproduced with permission of the copyright owner. Further reproduction prohibited without permission.

Table 6.17. Summary of hysteresis characteristics for Quebrada Blanca near El Jagual. In events with more than one peak, the highest peak is in bold.

See figure 4.12 for a description of the hysteresis type.

Start Date	Start Hour	End Date	End Hour	Number of Peaks	Peak Discharge ft3/s	Peak sediment Concentration, mg/L	Time of peak suspended-sediment concentration relative to peak discharge, min (-) indicates prior to peak	Hysteresis type For the entire event	Hysteresis type For the highest peak
8/11/1989	16.00	8/12/1989	5.75	1	86	1350	-1	1	1
8/18/1989	22.00	8/19/1989	23.25	1	231	5070	-10	4	3
9/13/1989	21.50	9/14/1989	20.00	2	115	1000	-32	1	1
9/18/1989	2.75	9/20/1989	7.75	3	537	2080	24	3	3
9/22/1989	9.00	9/22/1989	21.50	2	335	2200	-22	4	3
10/1/1989	13.75	10/2/1989	1.25	1	55	869	0	Not enough samples	Not enough samples
5/9/1990	19.25	5/10/1990	20.00	1	507	1640	50	3	3
6/14/1990	14.00	6/15/1990	11.50	1	226	3220	11	3	3
8/7/1990	17.00	8/9/1990	13.50	1	62	443	24	Not enough samples	Not enough samples
8/9/1990	13.75	8/12/1990	21.75	3	838	1770	7	3	3
10/16/1990	12.00	10/17/1990	14.75	1	109	1250	17	3	3
10/24/1990	18.75	10/25/1990	15.25	2	118	867	-10	1	1
11/4/1990	12.25	11/5/1990	14.50	2	110	1700	1	1	1
12/30/1990	19.25	1/2/1991	6.75	2	91	982	-27	1	1
7/15/1991	13.25	7/16/1991	2.75	1	97	1400	365	1	1
8/27/1991	10.00	8/28/1991	15.25	2	255	3510	18	Not enough samples	Not enough samples
9/17/1991	2.42	9/18/1991	10.75	3	340	1770	13	3	3
9/22/1991	8.50	9/23/1991	17.75	3	132	1330	-61	1	1
11/28/1991	12.25	12/1/1991	11.75	1	130	1190	-20	1	1
5/16/1992	4.00	5/17/1992	8.75	2	128	4250	-32	1	1
6/4/1992	8.50	6/5/1992	13.50	1	347	4180	-20	1	1
7/22/1993	16.00	7/23/1993	2.75	1	501	1930	-9	1	1
8/15/1993	21.50	8/17/1993	17	6	234	3120	-456	4	1

Reproduced with permission of the copyright owner. Further reproduction prohibited without permission.

Table 6.17. Continued.

Start Date	Start Hour	End Date	End Hour	First peak ft3/s	First peak suspended-sediment concentration, mg/L	Time of 1st peak suspended-sediment concentration relative to peak discharge, min	Hysteresis type of first peak	Second peak ft3/s	Second peak suspended-sediment concentration, mg/L	Time of 2nd peak suspended-sediment concentration relative to peak discharge, min	Hysteresis tyoe
8/11/1989	16.00	8/12/1989	5.75								
8/18/1989	22.00	8/19/1989	23.25								
9/13/1989	21.50	9/14/1989	20.00	65	766	0	3	**115**	**1000**	**-27**	**1**
9/18/1989	2.75	9/20/1989	7.75	132	725	19	3	**537**	**2080**	**24**	**3**
9/22/1989	9.00	9/22/1989	21.50	**335**	**2200**	**-22**	**3**	**136**	896	0	1
10/1/1989	13.75	10/2/1989	1.25								
5/9/1990	19.25	5/10/1990	20.00								
6/14/1990	14.00	6/15/1990	11.50								
8/7/1990	17.00	8/9/1990	13.50								
8/9/1990	13.75	8/12/1990	21.75	**838**	**1770**	7	**3**	150	720	-18	1
10/16/1990	12.00	10/17/1990	14.75								
10/24/1990	18.75	10/25/1990	15.25	**118**	**867**	**-10**	**1**	115	711	-45	1
11/4/1990	12.25	11/5/1990	14.50	**110**	**1700**	1	**1**	87	718	30	enough sam
12/30/1990	19.25	1/2/1991	6.75	80	854	3	3	**91**	**982**	**-27**	**1**
7/15/1991	13.25	7/18/1991	7.50								
8/27/1991	10.00	8/28/1991	15.25	**255**	**3510**	**18**	t enough samp	121	2187	-22	1
9/17/1991	2.42	9/18/1991	10.75	90	391	-2	1	**340**	**1770**	**13**	**3**
9/22/1991	8.50	9/23/1991	17.75	65	Not enough samples			80	1330	-16	1
11/28/1991	12.25	12/1/1991	11.75								
5/16/1992	4.00	5/17/1992	8.75	14	Not enough samples			**128**	**4250**	**-32**	**1**
6/4/1992	8.50	6/5/1992	13.50								
7/22/1993	16.00	7/23/1993	2.75								
8/15/1993	21.50	8/17/1993	17	203	3120	9	3	216	682	14	3

Reproduced with permission of the copyright owner. Further reproduction prohibited without permission.

Table 6.17. Continued.

Start Date	Start Hour	End Date	End Hour	Third peak ft3/s	Third peak suspended-concentration concentration, mg/L	Time of 3rd peak suspended-sediment concentration relative to peak discharge, min	Hysteresis type	Fourth peak ft3/s
8/11/1989	16.00	8/12/1989	5.75					
8/18/1989	22.00	8/19/1989	23.25					
9/13/1989	21.50	9/14/1989	20.00					
9/18/1989	2.75	9/20/1989	7.75	122	Not enough samples			
9/22/1989	9.00	9/22/1989	21.50					
10/1/1989	13.75	10/2/1989	1.25					
5/9/1990	19.25	5/10/1990	20.00					
6/14/1990	14.00	6/15/1990	11.50					
8/7/1990	17.00	8/9/1990	13.50					
8/9/1990	13.75	8/12/1990	21.75					
10/16/1990	12.00	10/17/1990	14.75					
10/24/1990	18.75	10/25/1990	15.25					
11/4/1990	12.25	11/5/1990	14.50					
12/30/1990	19.25	1/2/1991	6.75					
7/15/1991	13.25	7/18/1991	7.50					
8/27/1991	10.00	8/28/1991	15.25					
9/17/1991	2.42	9/18/1991	10.75					
9/22/1991	8.50	9/23/1991	17.75	**132**	**732**	**-61.00**	**1**	
11/28/1991	12.25	12/1/1991	11.75					
5/16/1992	4.00	5/17/1992	8.75					
6/4/1992	8.50	6/5/1992	13.50					
7/22/1993	16.00	7/23/1993	2.75					
8/15/1993	21.50	8/17/1993	17	**234**	**1030**	**-16**	**4**	Not enough samples

(fig. 6.18; Table 6.22). Examination of the hydrographs for just the highest peak flow indicated that 12 events showed Type 1 and eight events showed Type 3 (fig. 6.18b). Thirteen of the events were multipeaked (Table 6.22). Examination for just the first peak, which is not the highest peak, showed more Type-3 occurrences (n= 6) than Type 1 (n=2) (fig. 6.18c). Sediment concentration did not correlate to the first peak flow and may suggest a hillslope source of sediment. For the second peak that was not the highest peak flow, exhaustion of sediment was common (fig. 6.18d).

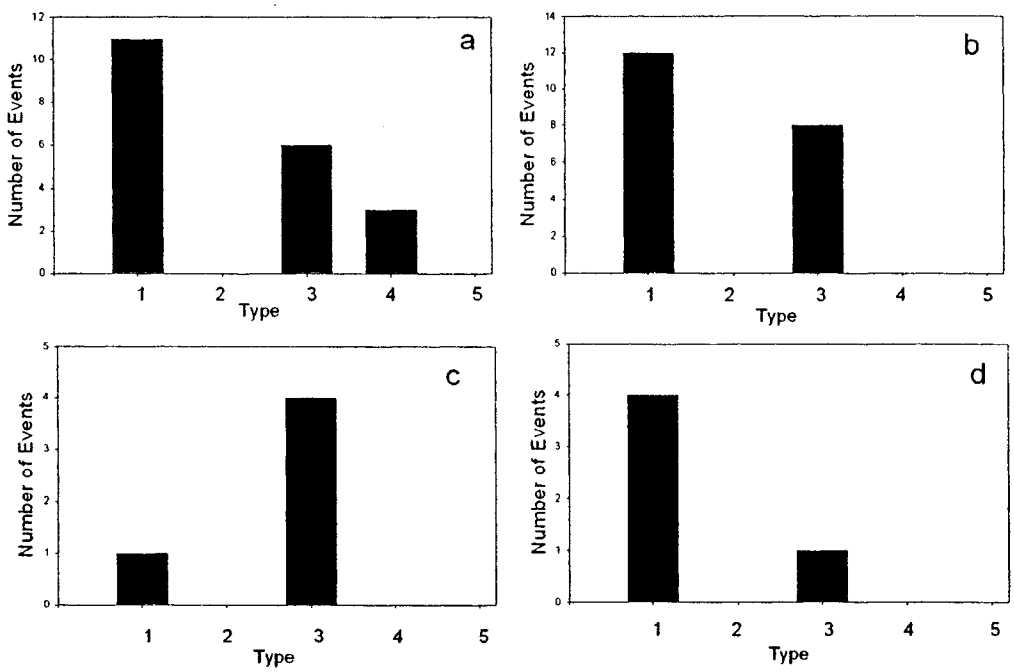

Figure 6.18. Hysteresis loops described at Quebrada Blanca near El Jagual for (a) the entire event, (b) near the highest peak flow, (c) first peak (not the highest peak), and (d) second peak (not the highest peak).

Average maximum width for Type-1 and Type-3 storms were similar, 693 and 791 mg/L, respectively (Appendix 6.26). Averages for the characteristics used to describe hysteresis indicated differences in Type-1 versus Type-3 storms. Sediment load, discharge weighted-

Reproduced with permission of the copyright owner. Further reproduction prohibited without permission.

sediment concentration, rainfall, and runoff averages were higher for Type-3 hysteresis events than Type-1 hysteresis events (Appendix 6.26), implying that large storms, with more rainfall and runoff, increase erosion and sediment delivery, resulting in high suspended-sediment concentrations after the highest peak flow. Previous-event runoff was higher for Type-3 hysteresis but the sum of runoff for the three previous events was higher for Type-1 hysteresis and the runoff between events was higher for Type-1 hysteresis. A previous event by itself might not introduce sediment to the channel to cause Type-1 hysteresis but large magnitude, closely spaced events may introduce large amounts of sediment to lead to Type-1 events.

The number of Type-1 storms with positive or negative slopes on the rising-limb sediment-transport curve were similar (Appendix 6.26). About half of the Type-1 storms showed a rapid decrease of suspended sediment with increasing discharge. On the falling limb of the hydrograph, positive slopes of the sediment-transport curves for Type-1 storms were steeper than for Type-3 storms, reflecting rapid exhaustion of sediment.

Variables thought to influence the maximum width of the hysteresis loops were statistically examined through forward stepwise regression (Table 4.4). Results were separated into Type-1 and Type-3 events (Table 6.18). Analysis of the correlation table showed two variables with high intercorrelation (25-RULST and 31-RU3EVT); 25-RULST was removed. Results of forward stepwise regression on the variable for Type-1 storms indicated that the sum of the three previous runoff events (31-RU3EVT) was significant in the first step (Table 6.24). The slope of the regression line was negative, indicating that as the sum of runoff the three previous events increased, the width of the hysteresis loop or the amount of sediment exhaustion decreased (fig. 6.19a). Wide clockwise hysteresis loops are associated with samples having high suspended-sediment

Reproduced with permission of the copyright owner. Further reproduction prohibited without permission.

concentrations on the rising limb of the hydrograph (fig. 6.19b; Appendix 6.26). Large, closely spaced runoff events in time decreased the width of the hysteresis loops by limiting the amount of sediment available for transport.

Table 6.18. Results of forward stepwise regression for (A) clockwise (Type 1) hysteresis and (B) counterclockwise (Type 3) hysteresis.

A)

Step	Independent variable using all samples (rising and falling)	R^2	F Statistic	Coefficient	Constant
Step one	31-RU3EVT	0.45	8.06	-0.10	3.96

B)

Step	Independent variable using all samples (rising and falling)	R^2	F Statistic	Coefficient	Constant
Step one*	12-SFIVE	0.44	4.66	-1.66	0.05
Step two*	14-RAINFOL	0.77	7.42	-0.10	0.05
	12-SFIVE		14.9	-2.20	

* *The probability for F-to-enter and F-to-remove was increased to 0.10*

Statistical analysis of Type-3 hysteresis did not show significant intercorrelation and therefore, no variables were removed. Results of forward stepwise regression indicated that the rainfall intensity (12-SFIVE) was significant in the first step and the slope of the regression was negative (fig. 6.19c). Rainfall on the falling limb (14-RAINFOL) was significant in the second step (Table 6.18) and the slope of the regression limb was negative. The width of the counterclockwise hysteresis loop was normalized by taking the inverse of the square root and, therefore, the width of counterclockwise hysteresis loops was positively correlated to both variables. Increases in rainfall intensity and high rainfall amounts on the falling limb of the hydrograph increased the amount of sediment replenished after the peak flow.

Reproduced with permission of the copyright owner. Further reproduction prohibited without permission.

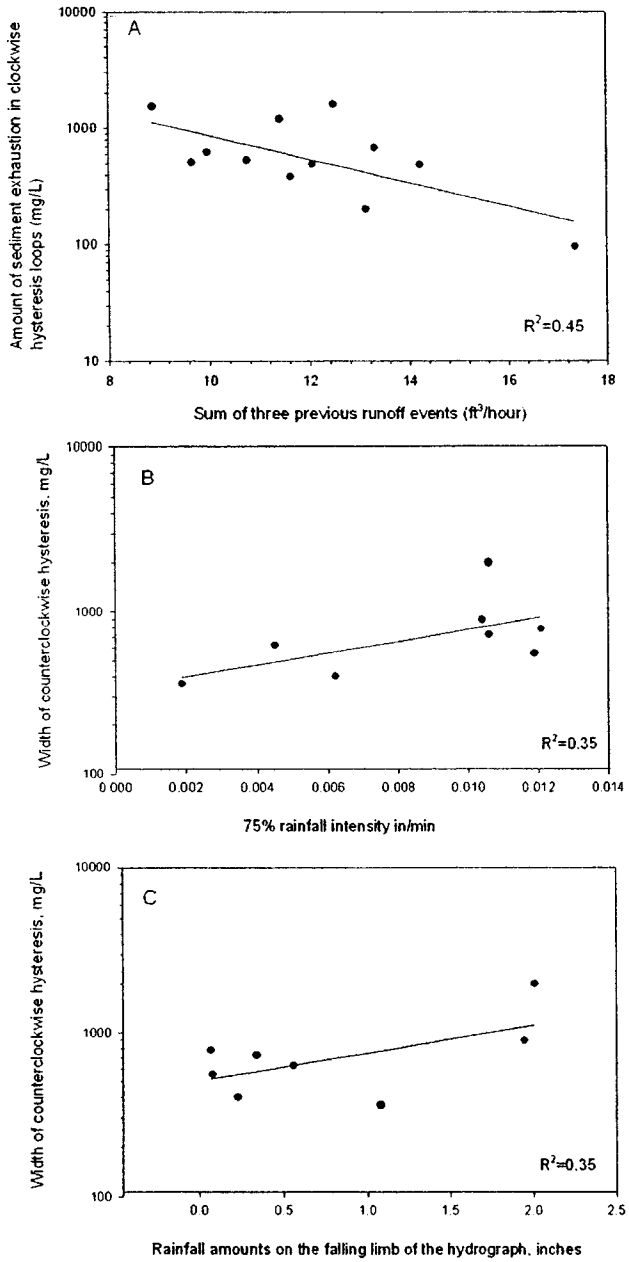

Figure 6.19. Graphs showing relations of hysteresis loops. a) Sum of three previous runoff events plotted against clockwise hysteresis width. b) 75% rainfall intensity plotted against counterclockwise hysteresis width, and c) rainfall on the falling limb of the hydrograph plotted against counterclockwise hysteresis width.

Reproduced with permission of the copyright owner. Further reproduction prohibited without permission.

Summary of Results for Quebrada Blanca

During the period, March 8, 1989 through September 30, 1995, 949 suspended-sediment samples were collected for concentrations at the station Quebrada Blanca near El Jagual. Most suspended-sediment samples were collected at low to moderate flows (1.0 to 100 ft^3/s; 0.028 to 2.83 m^3/s) (fig. 6.4) and 37% of the suspended-sediment samples had concentrations below 10 mg/L (fig. 6.5ab). Runoff and rainfall conditions during the collection period were 16% drier than the long-term average.

Examination of transport curves showed the best correlation coefficient of sediment-transport curves was for all samples (0.87), although two data clusters at either end of the best-fit regression line may be affecting this relation (fig. 6.6a). Sediment-transport curves at Quebrada Blanca do not show an improvement in the relation of discharge to suspended-sediment concentration by separating samples into rising and falling, either relative to the highest peak flow or relative to any peak in the event (figs. 6.6b.c). Quebrada Blanca has greater than 90% silt and clay in suspension for most flows. The percent of sand in suspension did not increase with increasing discharge. This is surprising considering that close to one-half of the basin is underlain by granodiorite which weathers to sand. Based on analysis of the sediment-transport curves it does not appear that previous runoff events significantly affect suspended-sediment concentrations at Quebrada Blanca. At high discharges, a weak relation of low suspended-sediment concentrations following closely spaced previous runoff events was observed (fig. 6.7a). Suspended-sediment concentrations did not decrease following peak flows in the current event but were generally high. It appears that peak flows remobilize sediment.

Reproduced with permission of the copyright owner. Further reproduction prohibited without permission.

A summary of forward stepwise regression for all statistical analyses is shown in Table 6.24. The dependent variable, suspended-sediment load, generally showed the highest correlation with the independent variables. Correlation coefficients did not improve by subtracting the base flow portion of the hydrograph into quickflow. Results did not seem to improve by analyzing only the rising portion of the hydrograph to the highest peak. Correlation coefficients did not improve by removing complex events.

Significant independent variables in the first step of forward stepwise regression for both the entire event and to the highest peak flow were related to the characteristics of the current event (Table 6.24). Except for suspended-sediment load for the entire event, the rate of hydrograph rise appears significant in the first step of forward stepwise regression for both dependent variables. Beschta (1987) observed that the slope of the rising limb hydrograph on Oregon Coast drainages is directly related to suspended-sediment concentrations. During high rates of hydrograph rise sediment sources are evacuated at a high rate.

Results did not improve by analyzing only the rising portion of the hydrograph to the highest peak flow. In forward stepwise regression analysis using principal components, characteristics of the current event were significant for both the entire event and to the highest peak flow for both dependent variables and in all cases were directly correlated to the dependent variables (Table 6.24). For the entire event, using sediment load as a dependent variable, characteristics of the previous event and three previous events were significant and were directly correlated to sediment load. Runoff since the previous event was inversely correlated to sediment load but directly correlated to the discharge-weighted sediment concentration.

Reproduced with permission of the copyright owner. Further reproduction prohibited without permission.

Table 6.24. A) Summary of the first two steps of forward stepwise regression analyses for Quebrada Blanca near El Jagual for the entire event. The value in the parenthesis is the correlation coefficient (R^2). The '+' or '-' sign indicate the slope for the line of best fit.

	Quickflow sediment load	**Runoff** sediment load	**Quickflow** discharge-weighted sediment concentration	**Runoff** discharge-weighted sediment concentration
Forward stepwise regression on variables	+ peak flow (0.73) + quickflow (0.80)	+ sum of current peak flows (0.67) + runoff (0.76)	+ highest rate of hydrograph rise for any peak (0.50) + rainfall on rising limb (0.62)	+ highest rate of hydrograph rise for any peak (0.47) + rainfall on rising limb (0.65)
Forward stepwise regression on principal components	- **PC2** (0.50) - Current rain, peak flow **+PC1** (0.72) + previous-event characteristics of peak flow, quickflow, rainfall, and rainfall intensity + three previous-events rainfall and quickflow + base flow at the start of event	- **PC2** (0.48) - current rain, peak flow **+PC1** (0.71) + previous-event characteristics of peak flow, runoff, rainfall, and rainfall intensity + three previous-events rainfall and runoff + base flow at the start of event	+ **PC2** (0.41) + current rain and peak flow + **PC3** (0.54) + runoff and rainfall since previous event + rate of hydrograph rise, current rainfall intensity	+ **PC2** (0.47) + current rain and peak flow + **PC3** (0.61) + runoff and rainfall since previous event + runoff, rate of hydrograph rise, current rainfall intensity
Forward stepwise regression on rotated principal components	+ **PC2** (0.47) + current rain + **PC6** (0.74) + rate of hydrograph rise, peak flow	+ **PC2** (0.45) + current rain + **PC6** (0.73) + rate of hydrograph rise	+ **PC3** (0.44) + rate of hydrograph rise, peak flow + **PC2** (0.59) + current rain	+ **PC3** (0.44) + rate of hydrograph rise + **PC2** (0.60) + current rain

Reproduced with permission of the copyright owner. Further reproduction prohibited without permission.

Table 6.24. B) Summary of the first two steps of forward stepwise regression analyses for Quebrada Blanca near El Jagual to the highest peak flow. The value in the parenthesis is the correlation coefficient (R^2). The '+' or '-' sign indicate the slope for the line of best fit.

	Quickflow sediment load	**Runoff** sediment load	**Quickflow** discharge-weighted sediment concentration	**Runoff** discharge-weighted sediment concentration
Forward stepwise regression on variables	+ quickflow (0.79) + rate of hydrograph rise to highest peak (0.90)	+ runoff (0.77) + rate of hydrograph rise to highest peak (0.90)	+ rate of hydrograph rise to highest peak (0.54)	+ rate of hydrograph rise to highest peak (0.57)
Forward stepwise regression on principal components	**+ PC4** (0.39) + quickflow - current rainfall intensity - rainfall intensity of the previous event **- PC2** (0.65) -current quickflow, peak flow, rainfall + rainfall, rainfall intensity, and quickflow between events	**+ PC4** (0.43) + runoff - current rainfall intensity - rainfall intensity of the previous event **- PC2** (0.68) - runoff, peak flow, rainfall + rainfall, rainfall intensity, and runoff between previous event	**+ PC3** (0.29) + peak flow, rate of hydrograph rise to highest peak, rainfall intensity **- PC4** (0.55) + rainfall intensity of the previous event	**+ PC3** (0.32) + peak flow, rate of hydrograph rise to highest peak, rainfall intensity **- PC4** (0.58) + rainfall intensity of the previous event
Forward stepwise regression on rotated principal components	**+ PC4** (0.29) + quickflow - current rainfall intensity **+ PC5** (0.54) + rate of hydrograph rise to highest peak	**+ PC4** (0.30) + runoff - current rainfall intensity **+ PC5** (0.55) + rate of hydrograph rise to highest peak	**+ PC6** (0.38) + rate of hydrograph rise to highest peak	**+ PC6** (0.41) + rate of hydrograph rise to highest peak

Characteristics of the current event, such as magnitude of peak flow and rate of hydrograph rise, increased suspended-sediment loads and concentrations by increasing the ability of flows to entrain sediment. Characteristics between the current and previous events, such as runoff can

Reproduced with permission of the copyright owner. Further reproduction prohibited without permission.

either increase or decrease suspended-sediment loads and concentrations by entraining and adding sediment as well as flushing sediment from the system. Previous-event characteristics of runoff and precipitation may increase sediment loads of the current event by increased erosion on hillslopes.

Forward stepwise analysis of the principal components to the highest peak showed an inverse relation between sediment load and rainfall and runoff since the previous event. The discharge-weighted sediment concentration was inversely correlated to previous-event rainfall intensity and current-event rainfall intensity.

After varimax rotation, current rainfall, quickflow, runoff, and rate of hydrograph rise were significant for both dependent variables for the entire event and to the highest peak (Table 6.24). Previous-event characteristics were significant and inversely correlated to the discharge-weighted sediment concentration for the entire event and to the highest peak flow.

Clockwise hysteresis loops were the most common for the sampled storm events and indicated that exhaustion of sediment occurred in most events. Storm events with high rainfall and runoff had counterclockwise hysteresis loops, implying that large storms increase erosion and sediment delivery, resulting in high suspended-sediment concentrations after the highest peak flow. Large storms may increase the contributing area of runoff and erosion, a concept referred to as the 'variable contributing area' concept (Dunne and others, 1975; Hornberger and others, 1998). Previous-event runoff and runoff between events were larger for Type-1 storms than Type-3 storms. Sediment delivered to the channel from these large previous events may lead to sediment deposition and cause Type-1 hysteresis loops.

Results of forward stepwise regression on the Type-1 hysteresis loops indicated that large, closely spaced previous runoff events may decrease the width of clockwise loops by limiting the

Reproduced with permission of the copyright owner. Further reproduction prohibited without permission.

amount of sediment available for transport. Results of forward stepwise regression on the Type-3 hysteresis loops indicated that wide counterclockwise loops are associated with samples having high suspended-sediment concentrations on the falling limb of the hydrograph (Table 6.23). Intense rainfall and rainfall on the falling limb increase the amount of sediment available for transport and lead to counterclockwise hysteresis.

Conclusions drawn from the sediment-transport curves and statistical operations are that previous events and rainfall and runoff between events supply sediment to the system at Quebrada Blanca but that sediment does not reach the monitoring station before the highest peak flow. This observation suggests that during a storm event the channel network does not deliver sediment as quickly in Quebrada Blanca as in Rio Icacos. Based on the hysteresis loops, in-channel sediment and upland sediment sources were equally important.

Reproduced with permission of the copyright owner. Further reproduction prohibited without permission.

CHAPTER VII

SUSPENDED-SEDIMENT TRANSPORT AT RIO CAGUITAS

Suspended-sediment transport is discussed for Rio Caguitas which drains a mixed land-use basin of forest (36%), cropland (23%), and pasture (27%), all in clayey soils. The period of investigation at Rio Caguitas near Aguas Buenas (500551000) (fig. 3.5), is November 24, 1991 through May 23, 1996, based on the best record of storm samples for suspended sediment. Rainfall, discharge, and suspended-sediment characteristics are described for this period.

Rainfall and Discharge for the Study Period

Average annual rainfall for water years 1932 through 1994, recorded at the National Weather Service (NWS) raingage in Caguas, located approximately 3.8 miles (6.1 km) from the streamflow station at Rio Caguitas, was 64 in (1630 mm). Average rainfall at the NWS Caguas raingage was missing for WY1991 and a comparison of average long-term conditions to the study period could not be made. Rainfall amounts for the study period used in the statistical analyses were obtained from three USGS stations, 50055100, 50999962, and 50999965 (fig. 4.1c). Using these raingages the average annual rainfall for WY 1992 through 1996 was 50.9 in (1290 mm) and, therefore, rainfall conditions for the study period may have been drier than the long-term average recorded at the NWS Caguas station.

For the period being investigated, November 24, 1991 through May 23, 1996, the mean daily flow at Rio Caguitas near Aguas Buenas was 6.25 ft^3/s (0.18 m^3/s). Flow duration for the

Reproduced with permission of the copyright owner. Further reproduction prohibited without permission.

period of investigation is shown in figure 7.1 and peak flows are listed in Table 7.1. Peak flow for the period of record is 4,490 ft^3/s (127 m^3/s) on September 10, 1996.

Table 7.1. Peak flows greater than 1.03 year recurrence (199 ft^3/s; 5.64 m^3/s) at Rio Caguitas during the period of investigation, November, 1991 through May, 1996.

Date	Peak flow (ft^3/s)
1/05/1992	1,760
9/18/1993	2,990
11/16/1993	392
9/6/1995	1,480

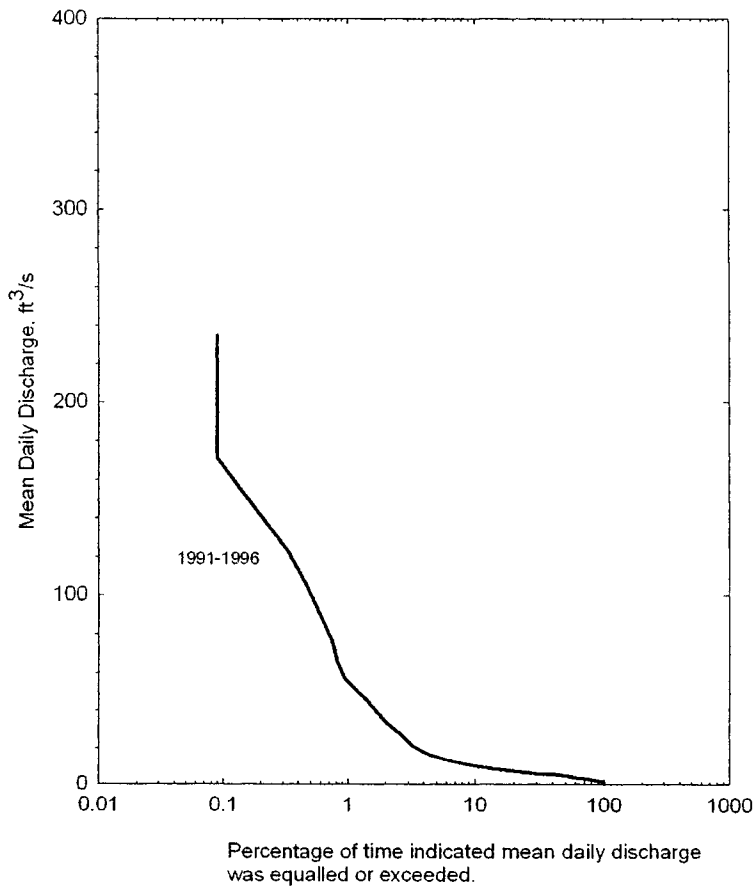

Figure 7.1 Flow durations for period of investigation (water years 1991-1996) for Rio Caguitas near Aguas Buenas (50055100).

Reproduced with permission of the copyright owner. Further reproduction prohibited without permission.

Suspended-Sediment Load and Yield

Suspended-sediment loads at Rio Caguitas from WY 1991 through 1996 were obtained from the USGS-Caribbean District's annual surface-water data reports. The average annual suspended-sediment load, from WY1991 through 1996, was 9,140 tons (8,290 metric tons), the average annual sediment yield was 1,720 tons/mi^2 (602 metric tons/km^2), and the average annual discharge-weighted sediment concentration was 1,360 mg/L. On average, from 1991 to 1996, 90% of the annual suspended-sediment load was transported in 12 days, 75% in 5 days, and 47% in one day. On September 10, 1996, 82% of the average annual suspended-sediment load (24,460 tons; 22,180 metric tons) was transported.

Suspended-Sediment Analysis

During the period November 24, 1991 through May 23, 1996, 1,011 water samples were collected for suspended sediment at the station Rio Caguitas near Aguas Buenas. Of the samples, 525 were collected during base flow, 127 on the rising limb of the hydrograph to the highest peak flow, and 359 on the falling limb of the hydrograph following the highest peak flow. Eighteen samples were collected using the EWI method, 469 were collected with the automatic sampler, and 524 were taken at a single vertical (SV) in the channel. During the period of analysis, there was no calibration of the automatic samples to the EWI samples. Because the samples were not calibrated, it is recognized that some error may be incurred in this analysis of suspended sediment. On 10 occasions the SV samples were calibrated to an EWI sample, but discharges were low during the calibration (2.8 to 11 cfs). Calibration of the samples is expressed as the ratio of EWI:SV which ranged from 0.38 to 4.5. There was no relation of the calibration coefficient to

Reproduced with permission of the copyright owner. Further reproduction prohibited without permission.

discharge. Because there was no relation of the calibration coefficient to discharge and because of the limited number of samples, no calibration was applied to the SV samples. When an EWI sample and a SV sample were taken together, only the EWI sample was used in analysis.

The lowest and highest suspended-sediment concentrations were 0.4 mg/L and 35,970 mg/L. The mean concentration for this data set was 1,230 mg/L, the median suspended-sediment value was 231 mg/L, and the sample standard deviation is 484 mg/L (fig. 7.2). Samples were collected over a range of discharges from 1.2 to 1,712 ft^3/s (0.03 to 48.5 m^3/s). The distribution of sampled discharge shows that 74% of the suspended-sediment samples were sampled at low flows between 1 and 50 ft^3/s (0.03 to 1.42 m^3/s) (fig. 7.3).

Quantile plots of the suspended-sediment data (fig. 7.4.a,b) show that the sediment samples were adequately distributed (fig. 7.4b). Box plots of the data show the 10^{th}, 25^{th}, 50, 75^{th}, and 90^{th} percentiles of suspended sediment are 7, 16, 231, 1460, and 3350 mg/L, respectively (fig. 7.2). Probability plots indicated that the suspended-sediment data were not normally distributed (fig. 7.4c), therefore, applying a log transform to the data was found to be appropriate (fig 7.4d).

Sediment-transport curves

Sediment-transport curves were created: 1) for all samples, 2) samples rising to the highest peak, 3) samples falling from the highest peak flow, 4) samples rising to any peak flow, 5) samples falling from any peak flow, and 6) samples collected at base flow (fig. 7.5). Significant scatter of the sediment data occurs at all flows (fig. 7.5). The correlation coefficient for all samples is 0.71 (fig. 7.5a). Correlation coefficients did not improve when the suspended-sediment samples were

Reproduced with permission of the copyright owner. Further reproduction prohibited without permission.

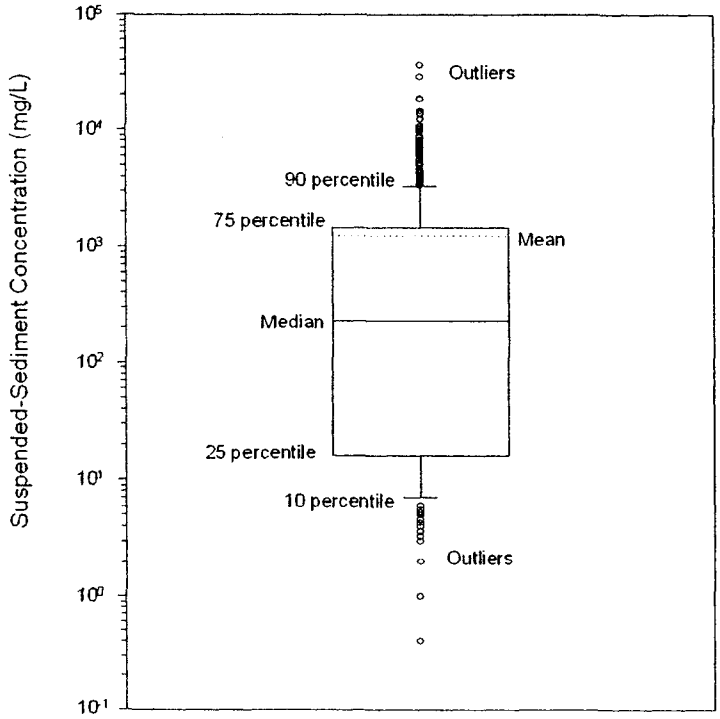

Figure 7.2. Box plot of suspended-sediment concentrations (n=1011 for Rio Caguitas near Aguas Buenas.

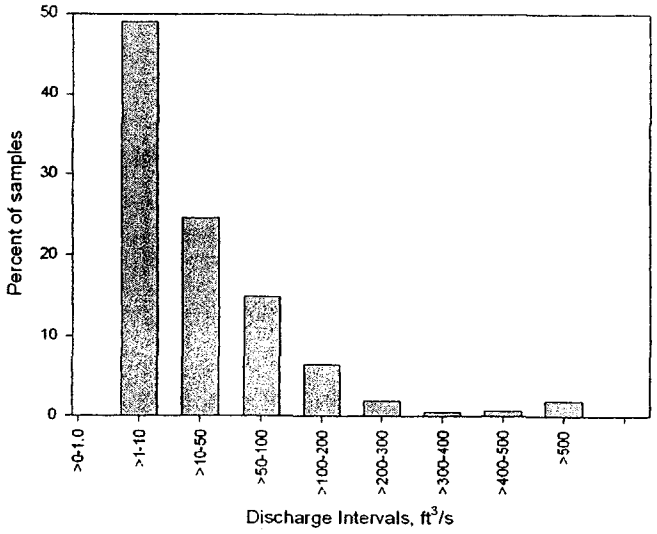

Figure 7.3. Frequency of discharges for suspended-sediment samples, Rio Caguitas near Aguas Buenas.

Reproduced with permission of the copyright owner. Further reproduction prohibited without permission.

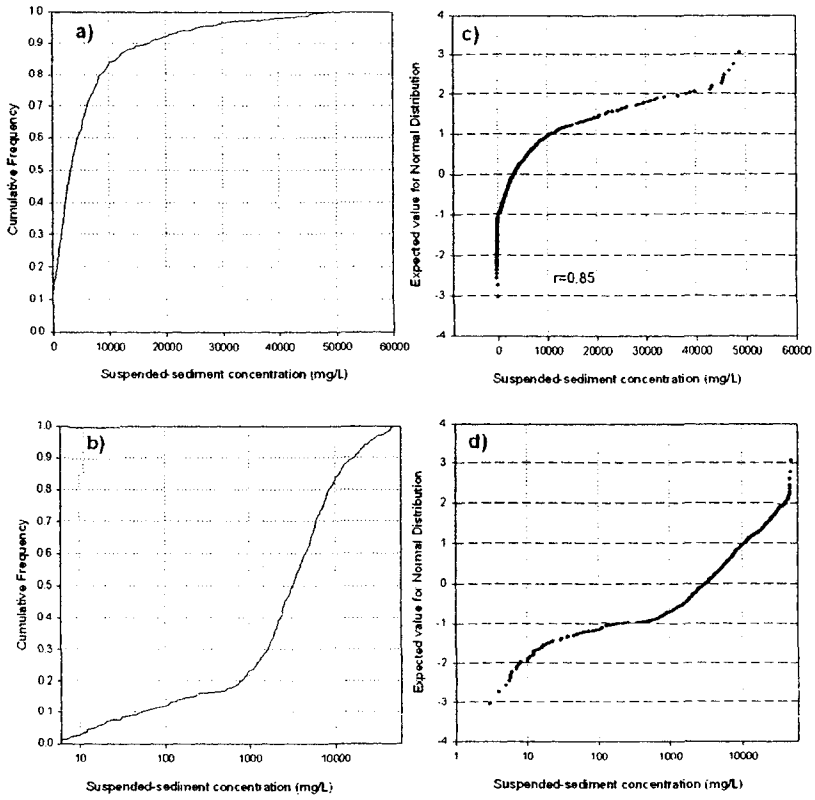

Figure 7.4. Quantile plots for Rio Caguitas near Aguas Buenas showing a) suspended sediment and b) log transformed suspended sediment. Probability plots of Rio Caguitas showing c) suspended sediment and d) log transformed suspended sediment.

divided into rising and falling from the highest peak flow or into rising and falling from any peak flow (fig. 7.5b,c).

To test the hypothesis that recent events flush sediment, suspended-sediment samples were analyzed relative to the last event and to peak flows of the current event (fig. 7.6a). Suspended-sediment samples were separated into 4 classes defined by the runoff of the previous event divided by the time since the previous event (fig. 7.6a). Only samples rising to the highest peak flow were

Reproduced with permission of the copyright owner. Further reproduction prohibited without permission.

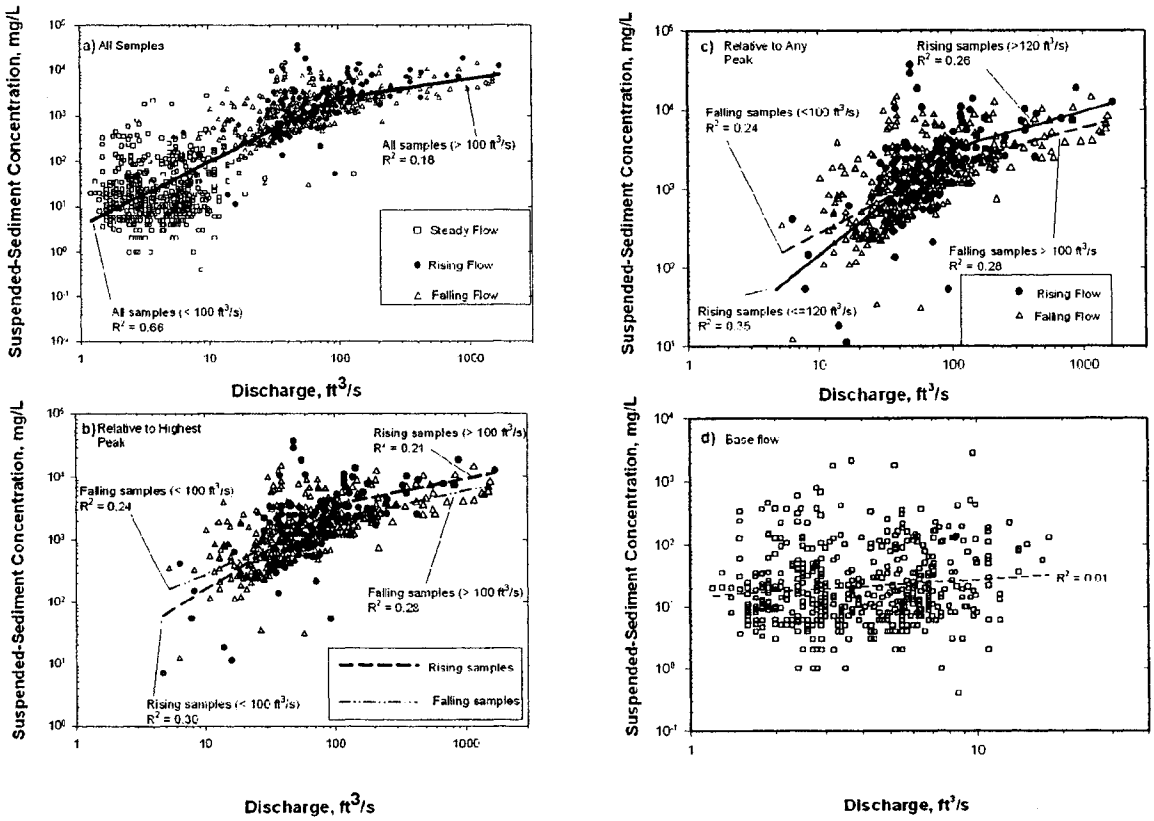

Figure 7.5. Suspended-sediment transport curves for Rio Caguitas near Aguas Buenas: a) All samples, b) rising and falling samples relative to the highest peak flow, c) rising and falling samples relative to any peak flow, and d) base flow samples.

used in this analysis. Samples collected at discharges less than 100 ft^3/s showed low suspended-sediment concentrations after large, recent runoff events, although the R^2 values were low (fig. 7.6a). This may indicate that large, previous runoff events reduced suspended-sediment concentrations at low discharges on the rising limb. Suspended-sediment samples separated by the previous peak flow in the current event did not show any significant differences (fig. 7.6b).

Reproduced with permission of the copyright owner. Further reproduction prohibited without permission.

Seasonal sediment-transport curves separated into May through December and January through April are shown in figures 7.7. The R^2 values for each season show a good correlation (fig. 7.7). A plot for all samples did not show any significant difference between the drier season (January through April) and the wet season (May through December) (fig. 7.7a). The relation of discharge to suspended-sediment concentration did not improve when the samples were separated by flow (fig. 7.7b,c).

The percent sand (>0.062 mm) in suspension versus discharge and sediment concentration were examined (fig. 7.8). Thirty-four samples of suspended sediment, collected between November 1991 through May 1996 were analyzed for percent sand. For all samples the average amount of sand in suspension was 6.4%, +/- 7.6 %, and ranged from 1 to 36%. The low percentage of sand reflects the geology of the basin, volcaniclastics which weather to clay and silt-size material. Plots for all samples showed an increase of sand with increasing discharge (fig. 7.8a). For high flows an exponential increase in sand percent is observed (fig. 7.8a). A significant relation between suspended-sediment concentration and percent sand was not observed (fig.7.8b). Analysis of samples rising to the highest peak flow or falling from the highest peak flow showed that as discharge increased more sand was suspended (fig. 7.8c,d). This may indicate that under the right hydraulic conditions the channel is a source of sand.

Reproduced with permission of the copyright owner. Further reproduction prohibited without permission.

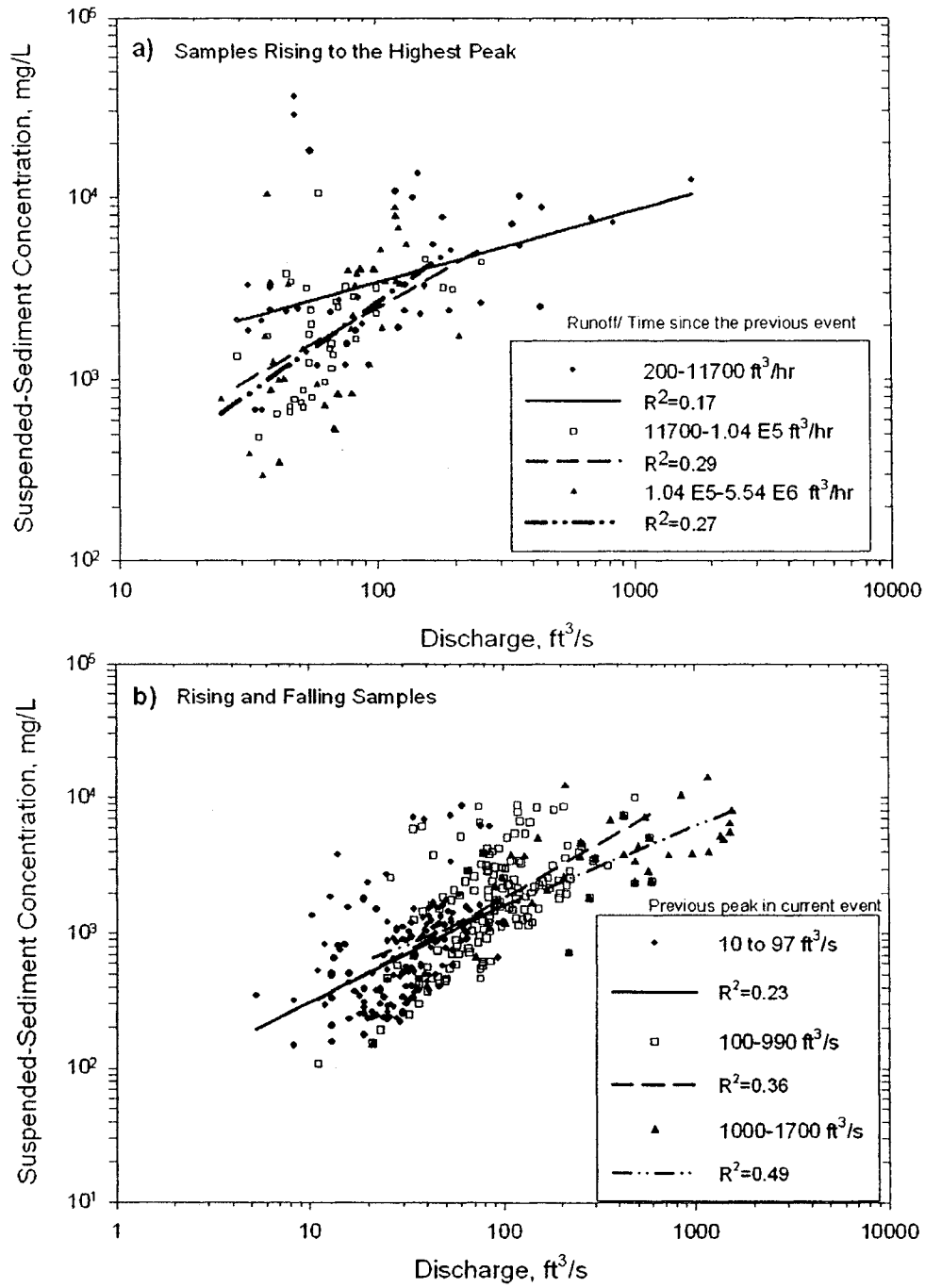

Figure 7.6. Suspended-sediment transport curves for Rio Caguitas near Aguas Buenas: a) Samples collected on the rising limb to the highest peak flow separated by runoff of the previous event divided by the time since the previous event and b) rising and falling samples separated by the previous peak flow in the current event.

Reproduced with permission of the copyright owner. Further reproduction prohibited without permission.

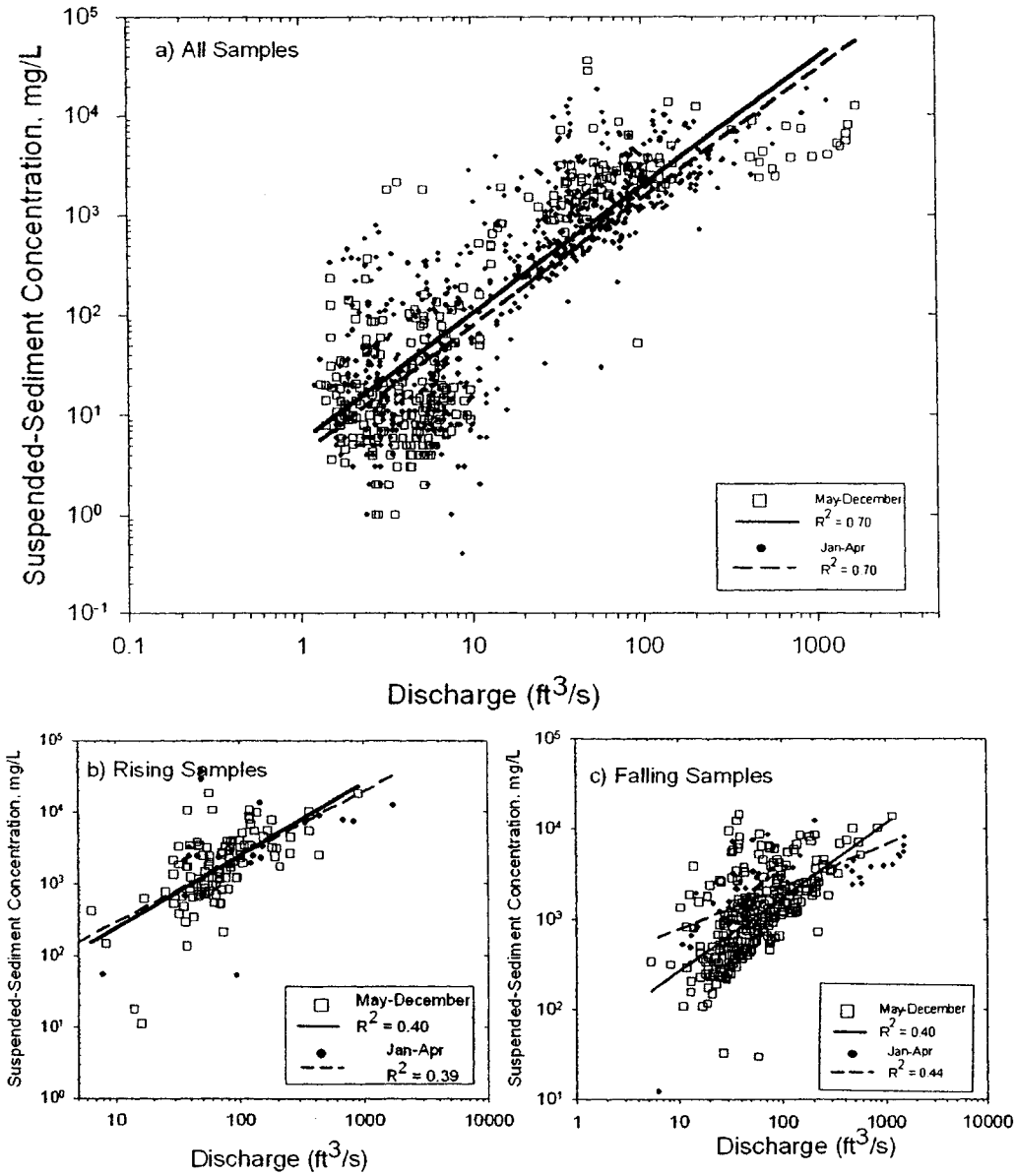

Figure 7.7. Seasonal suspended-sediment transport curves (May-Dec; Jan-Apr) for Rio Caguitas near Aguas Buenas: a) All samples, b) Rising limb samples relative to the highest peak flow, and c) Falling limb samples relative to the highest peak flow.

Reproduced with permission of the copyright owner. Further reproduction prohibited without permission.

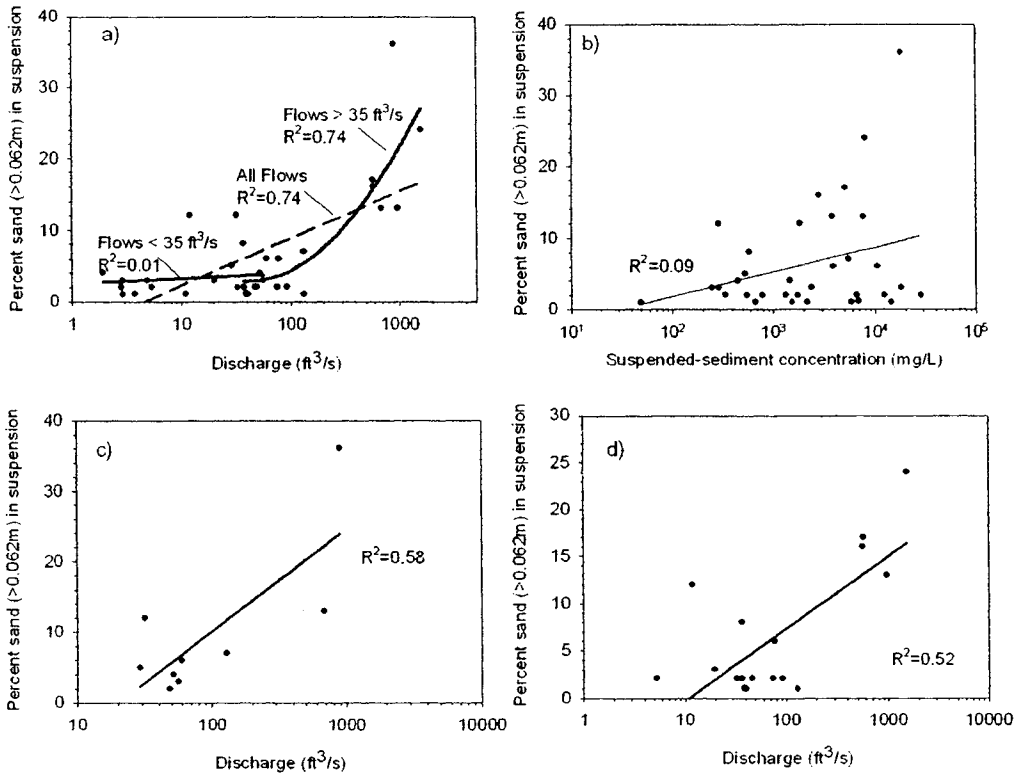

Figure 7.8. Sediment transport curves for the sand-size fraction of suspended sediment (>0.062mm). a) discharge versus percent sand in suspension , b) suspended-sediment concentration versus percent sand in suspension, c) rising limb discharge versus percent sand in suspension, and d) falling limb discharge versus percent sand in suspension.

Walling (1974) Sediment-Transport Curve Approach

Results using Walling's (1974) four independent variables of discharge, time relation of sample, base flow, and flood intensity, described in Chapter 4, are listed in Table 7.2. The dependent variables were separated into all samples, samples rising to the highest peak flow, and samples falling from the highest peak flow. Results were similar for samples with and without base flow. The regression coefficient did not improve by separating samples into rising samples. For

Reproduced with permission of the copyright owner. Further reproduction prohibited without permission.

Reproduced with permission of the copyright owner. Further reproduction prohibited without permission.

Table 7.2. Results of forward stepwise regression using Walling's (1974) four variables to explain suspended-sediment concentration. A) Discharge including base flow and B) discharge subtracting out base flow.

A)

Step	Independent variable using all samples (rising and falling)	R^2	Coefficient	Independent variable using rising samples	R^2	Coefficient	Independent variable using falling samples	R^2	Coefficient
Step one	Discharge	0.48	0.79	Discharge	0.44	0.97	Discharge	0.43	0.70
Step two	Base flow	0.53	-0.47	Flood Intensity	0.52	0.41	Base flow	0.58	-0.71
	Discharge		0.80	Discharge		0.67	Discharge		0.72

B)

Step	Independent variable using all samples (rising and falling)	R^2	Coefficient	Independent variable using rising samples	R^2	Coefficient	Independent variable using falling samples	R^2	Coefficient
Step one	Discharge	0.48	0.77	Discharge	0.44	0.96	Discharge	0.43	0.68
Step two	Base flow	0.53	-0.46	Flood Intensity	0.55	0.41	Base flow	0.58	-0.60
	Discharge		0.78	Discharge		0.67	Flood Discharge		0.70

each analysis, the most important factor explaining sediment concentrations was discharge and the slope of the best-fit regression line was positive (Table 7.2). For all samples and falling limb samples, base flow at the start of the event was the most significant variable and the slope of the best-fit regression line was negative, indicating that sediment may be diluted as a result of high base flows at the start of the event. For rising limb samples, flood intensity was important in the second step of forward stepwise regression and the slope of the best-fit regression line was positive (Table 7.2).

Statistical Results at Rio Caguitas

Entire Event Analysis

This section describes the results of statistical analysis for Rio Caguitas near Aguas Buenas using characteristics of the entire runoff event. At Rio Caguitas near Aguas Buenas the most accurate period of storm-event suspended-sediment collection occurred 11/24/1991 through 5/23/1996 when 127 runoff events defined by a peak flow over 12 ft^3/s (0.34 m^3/s) occurred. Of these runoff events, 23 were sampled adequately to define suspended-sediment loads for the entire event (Table 7.3). Of these 23 events, 7 were defined as complex events (Table 7.3).

The average suspended-sediment load for the 27 events was 464 tons (421 metric tons) (fig.7.9a). The maximum sediment load during the study period was 3,800 tons (3,450 metric tons) on 1/05/1992 (Table 7.3). The runoff associated with this event was the largest sampled, 6.67×10^6 ft^3 (1.89×10^5 m^3) when 5.76 inches (150 mm) of rain fell.

Reproduced with permission of the copyright owner. Further reproduction prohibited without permission.

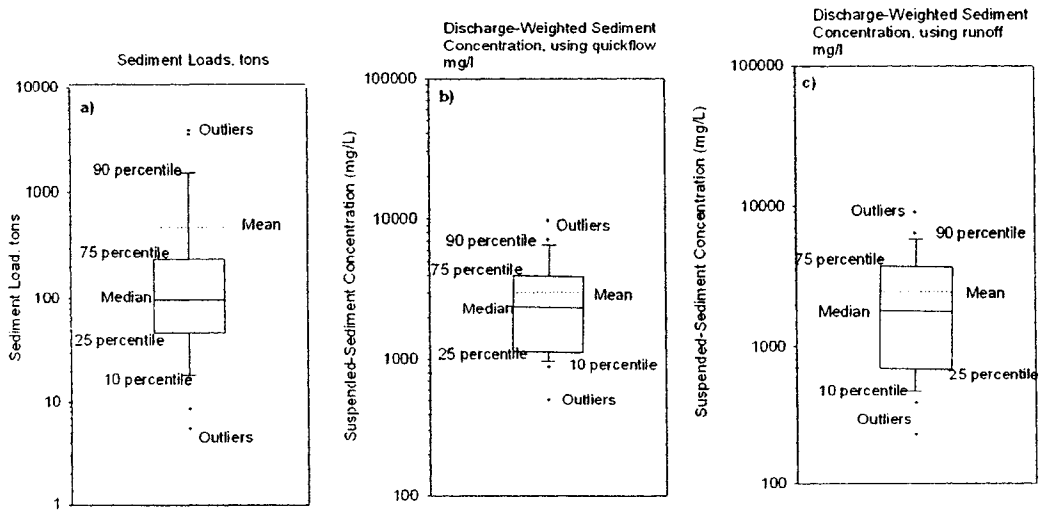

Figure 7.9. Box plot of dependent variables, a) sediment load, b) discharge-weighted sediment concentrations using quickflow, and c) runoff, for Rio Caguitas near Aguas Buenas.

A plot of the discharge-weighted sediment concentration using runoff, for each event over the period of study is shown in figure 7.10. There is considerable variation in the discharge-weighted sediment concentration using runoff; 227 to 8,840 mg/L (fig. 7.9b,c; 7.10). The average discharge-weighted sediment concentration of all events using runoff was 2,480 mg/L (fig. 7.9c) and using quickflow was 2,990 mg/L (fig. 7.9b). The maximum discharge-weighted sediment concentration, for both quickflow and runoff, 9,560 mg/L and 8,840 mg/L, respectively, occurred in a runoff event from 9/6-7/1995.

The peak flow of the 23 events ranged from 34 to 1,730 ft^3/s (0.96 to 49.0 m^3/s). Quickflow for the 23 events (including those not sampled for sediment) ranged from 3.11×10^5 to 2.88×10^7 ft^3 (8.81×10^3 to 8.14×10^5 m^3) and runoff ranged from 7.04×10^5 to 3.04×10^7 ft^3 (1.99×10^4 to 8.60×10^5 m^3). Rainfall contributing to runoff for the 50 events ranged from 0.13

Reproduced with permission of the copyright owner. Further reproduction prohibited without permission.

Reproduced with permission of the copyright owner. Further reproduction prohibited without permission.

Table 7.3. Summary of runoff events sampled adequately to determine suspended-sediment loads at Rio Caguitas near Aguas Buenas.

(* Mna = Complex event, n=number of complex event, a,b,c, = sequence of each event in the entire multiple event; a=1st event, b=2nd, etc)

Start Date	Start Time (hour)	Start Discharge (ft3/s)	End Date	End Time (hour)	Ending Discharge (ft3/s)	Event Duration (hour)	Number of Peaks in Event	Peak Flow (cfs)	Quickflow (ft3)	Runoff (ft3)	Rainfall (inches)	Suspended-Sediment Load (tons)	M=Part of Complex Event
1/5/1992	15.75	6.4	1/7/1992	6	17.0	38.25	3	1730	2.88E+007	3.04E+007	5.76	3803	
9/22/1992	13.75	6.4	9/23/1992	9.75	10.0	20.00	1	66	1.18E+006	1.77E+006	0.52	38.2	
12/1/1992	12.5	11.0	12/1/1992	22	12.0	9.50	2	41	3.11E+005	7.04E+005	0.30	8.47	
12/29/1992	12.25	13.0	12/30/1992	4	15.0	15.75	2	78	5.99E+005	1.35E+006	0.78	21.0	M1b
1/7/1993	13.25	8.6	1/8/1993	5.75	15.0	16.50	1	162	1.72E+006	2.42E+006	0.65	139	
5/1/1993	14.75	9.3	5/2/1993	16	18.0	25.25	2	102	2.26E+006	3.28E+006	0.95	71.6	M2a
5/6/1993	14.25	8.9	5/7/1993	1.25	16.0	11.00	1	100	9.81E+005	1.47E+006	0.29	73.5	
5/26/1993	13.5	8.2	5/26/1993	23.5	18.0	10.00	1	237	1.49E+006	1.96E+006	0.64	109	
7/3/1993	10.75	7.3	7/4/1993	0.75	9.3	14.00	1	34	3.49E+005	7.67E+005	0.50	5.43	
7/13/1993	16.75	11.0	7/14/1993	4.25	18.0	11.50	1	145	1.35E+006	1.95E+006	0.27	51.9	
7/22/1993	13.75	8.9	7/23/1993	2	19.0	12.25	1	359	2.33E+006	2.77E+006	0.84	191.4	M3a
8/15/1993	23.75	13.0	8/16/1993	7.75	24.0	8.00	1	94	5.92E+005	1.01E+006	1.37	20.7	M4a
8/18/1995	11.25	6.2	8/19/1995	9	27.7	21.75	1	615	4.95E+006	5.59E+006	2.61	351	M5a
9/6/1995	2.25	8.9	9/7/1995	3.75	12.8	25.50	1	1483	1.17E+007	1.27E+007	3.16	3500	M6b
9/7/1995	11.5	9.9	9/8/1995	6.5	12.8	19.00	1	97	1.63E+006	2.40E+006	0.63	49.8	
9/15/1995	21.75	8.3	9/17/1995	8.42	19.8	34.67	5	597	1.08E+007	1.16E+007	2.87	1030	M7b
9/27/1995	14.25	2.7	9/27/1995	21.5	9.5	7.25	1	85	5.75E+005	7.34E+005	0.25	96.5	
10/27/1995	14.75	2.6	10/28/1995	2	8.6	11.25	1	485	2.04E+006	2.27E+006	0.89	452	
11/4/1995	13.75	2.6	11/5/1995	6	9.2	16.25	1	237	2.29E+006	2.63E+006	1.34	147	
12/25/1995	16.25	1.7	12/25/1995	23.5	10.9	7.25	1	210	1.25E+006	1.41E+006	0.66	250	
3/15/1996	13.5	1.9	3/16/1996	1.25	3.9	11.75	1	66.5	8.47E+005	9.70E+005	1.49	46.1	
4/3/1996	14.5	1.4	4/3/1996	22	8.9	7.5	2	145	8.54E+005	9.93E+005	0.46	165.9	
5/23/1996	1.75	1.8	5/23/1996	13.25	6.5	11.5	2	98.2	7.16E+005	8.87E+005	1.76	64.2	

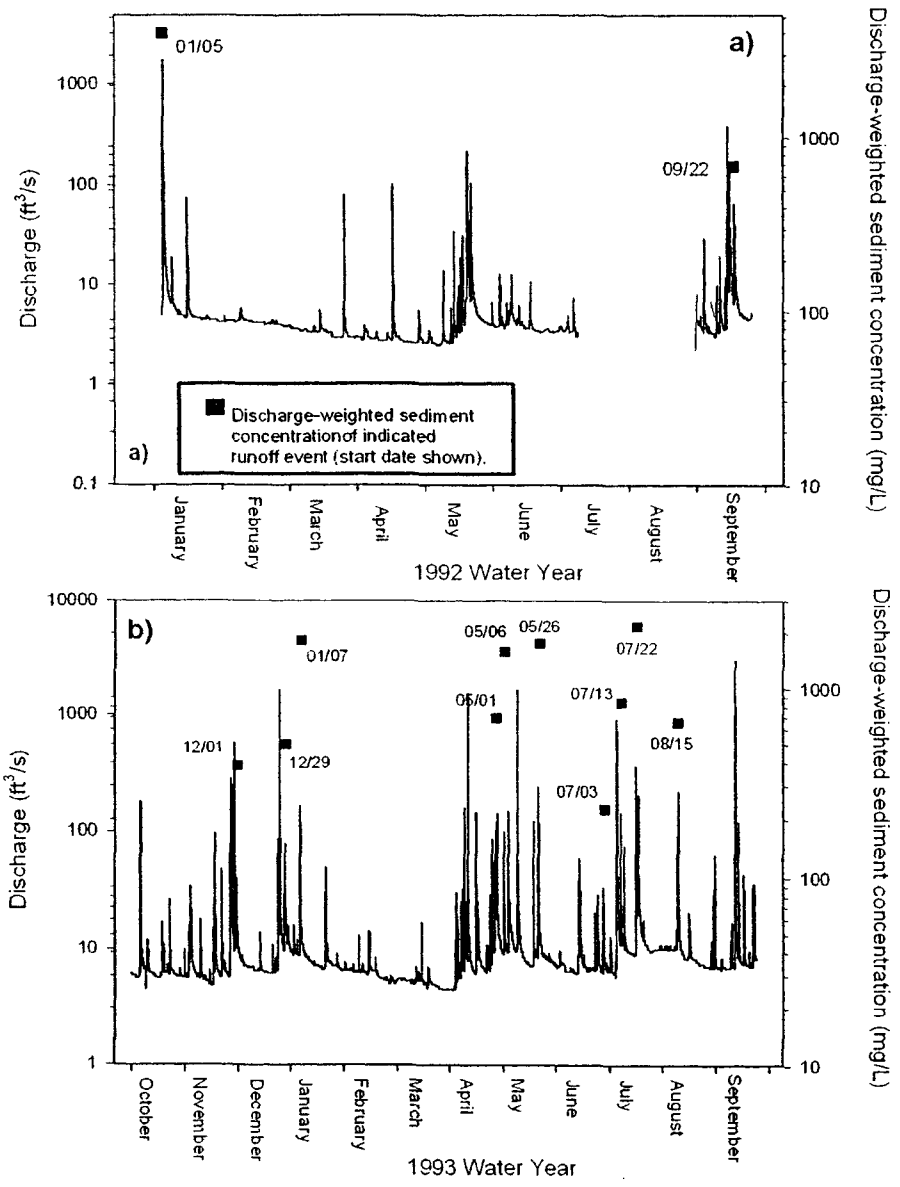

Figure 7.10. Instantaneous discharge and discharge-weighted sediment concentration for Rio Caguitas near Aguas Buenas for period of investigation, a) November 1991 through September 1992 and b) water year 1993.

Reproduced with permission of the copyright owner. Further reproduction prohibited without permission.

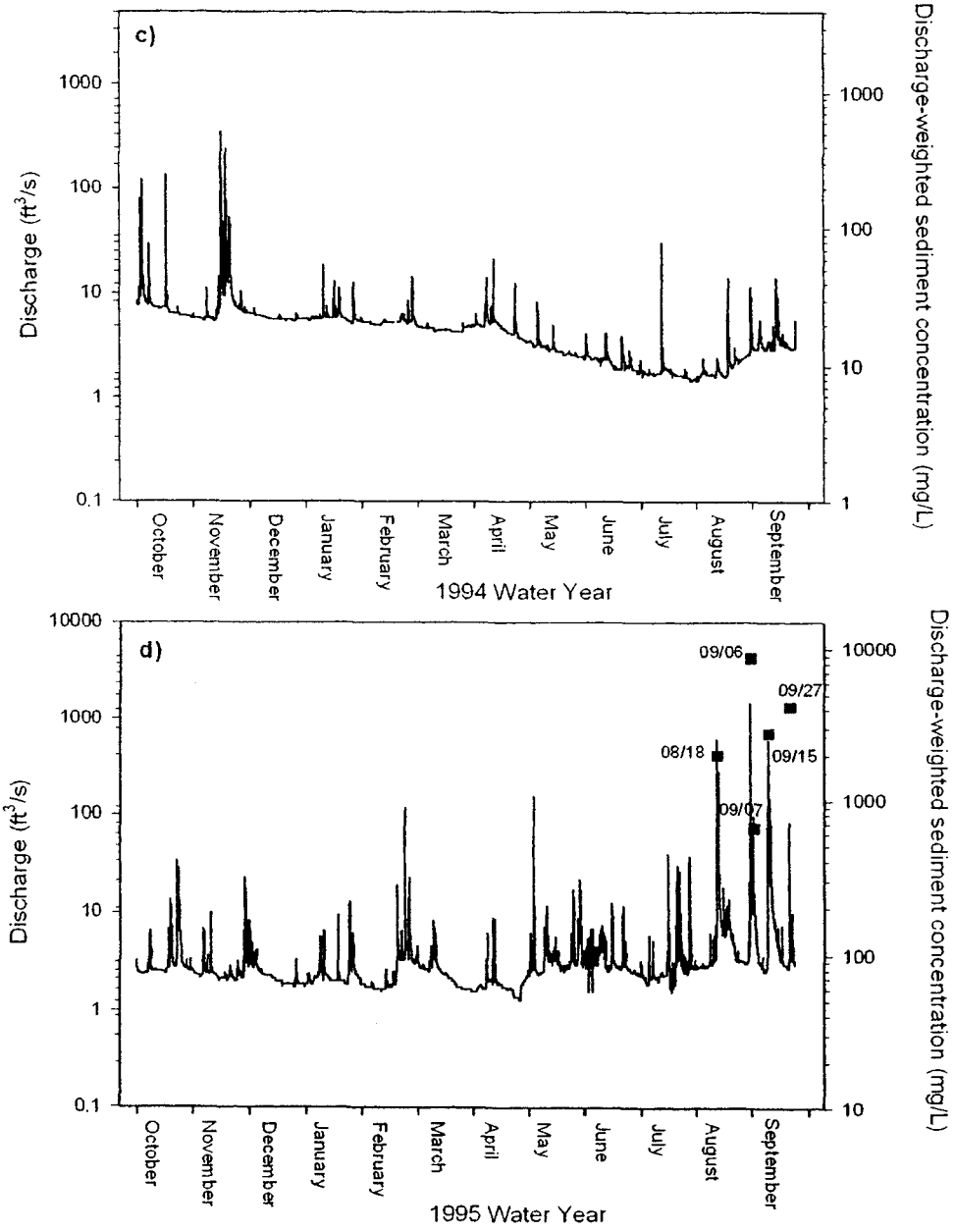

Figure 7.10. Instantaneous discharge and discharge-weighted sediment concentration for Rio Caguitas near Aguas Buenas for c)water year 1994 and d) water year 1995.

Reproduced with permission of the copyright owner. Further reproduction prohibited without permission.

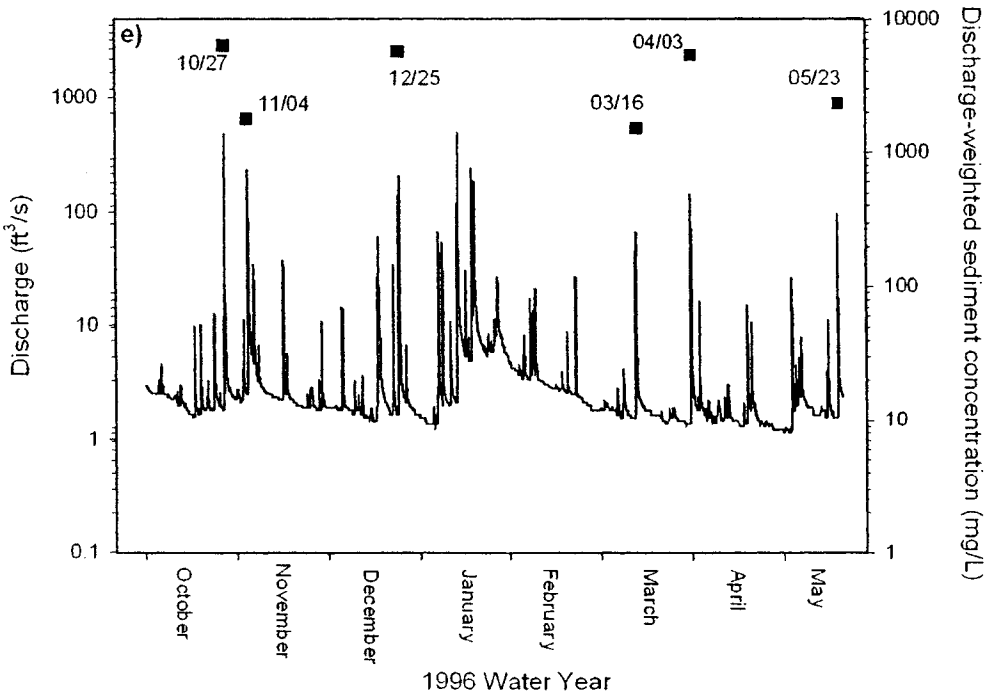

Figure 7.10. Instantaneous discharge and discharge-weighted sediment concentration for Rio Caguitas near Aguas Buenas for e)water year 1996.

to 6.11 in (3.3 to 155 mm). A simple accounting of rainfall to quickflow can be made by assuming that the contributing area to the streamflow-gaging station (5.30 mi^2) is impervious and calculating the volume of quickflow resulting from each rainfall event (Appendix 7.1). Based on these computations, 3 to 41% of rainfall was quickflow with an average of 18% (Appendix 7.1).

Two dependent variables were used to described sediment for the entire storm event:

1) suspended-sediment load, in tons;

2) discharge-weighted sediment concentration, in mg/L

Histograms of the two dependent variables indicate a better normal distribution with a log transformation. Plots of runoff versus the two dependent variables are shown in figure 7.11.

Reproduced with permission of the copyright owner. Further reproduction prohibited without permission.

Suspended-sediment load has the best relation to runoff (R^2=0.83) (fig. 7.11a). There is generally a good relation for runoff versus discharge-weighted sediment concentration(fig. 7.11b), but the R^2 values are low.

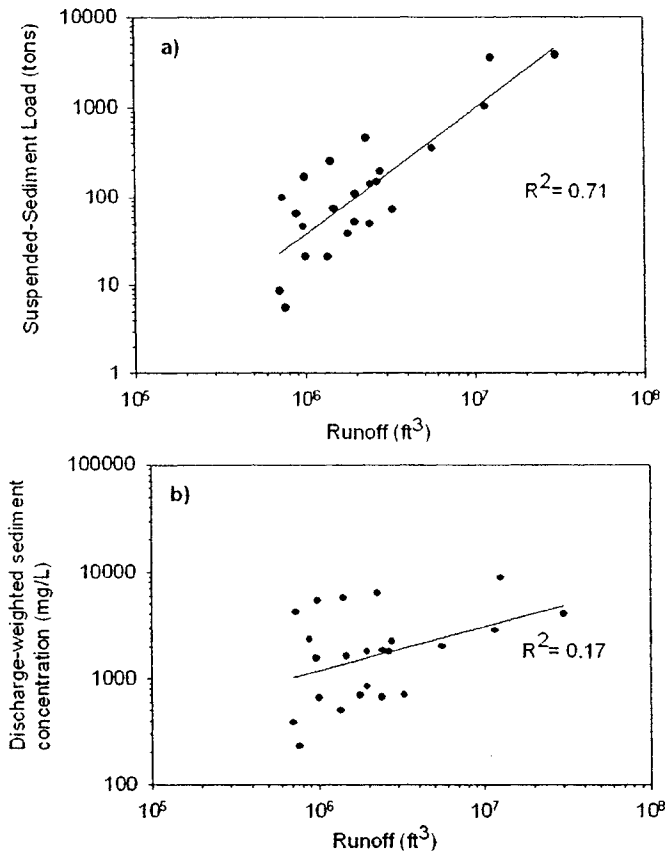

Figure 7.11. Plots of storm generated runoff versus a) suspended-sediment load and b) discharge-weighted sediment concentration for Rio Caguitas near Aguas Buenas.

The two dependent variables were tested against the independent variables shown in Table 4.2. Statistical analysis was performed against two portions of the runoff hydrograph:

1) the entire runoff event and

2) to the highest peak flow

Reproduced with permission of the copyright owner. Further reproduction prohibited without permission.

Forward stepwise regression for suspended-sediment load against previous runoff events back to the 6th event, indicated that only the current runoff event was significant (alpha = 0.15; R^2=0.73). A minimum of three previous events was used. Hydrographs were further separated into quickflow and runoff. For the 50 storms that were adequately sampled, the base flow contribution ranged from 5 to 48 % of the runoff.

Quickflow Results (entire event)

The independent variables assembled to analyze the relation of suspended-sediment characteristics to quickflow characteristics are listed in Appendix 7.2. Tests for normality indicated that 18 of the 23 independent variables needed a log transformation (Appendix 7.2). Analysis of the correlation matrix showed a high correlation (r>0.80) among select variables (Appendix 7.3). Many of the characteristics of the previous event (20-LSPKBTI, 22-SMLSPKBS, 24-QULST, 26-PPTLSTI, 27-INTLSTI) and three previous events (29-SUM3PPTI, 30-QU3EVT) were correlated. Two of these variables (20-LSPKBTI, 27-INTLST) were removed. Current-event characteristics of 1-QUICK, 8-SMPKBS and 4-PKBS were intercorrelated; 4-PKBS was removed. Rate of hydrograph rise 6-MXTMJPK and 7-MXTRP were intercorrelated (r=0.97) and 6-MXTMJPK was removed. The high correlation of the rate of hydrograph rise was because many of the events on Rio Caguitas were single peaked events.

Important relations of the dependent variables to the independent variables observed in the correlation matrix are suspended-sediment load to 1-QUICK, 4-PKBS, 6-MXTMJPK, and 8-SMPKBS (fig. 7.12).

Reproduced with permission of the copyright owner. Further reproduction prohibited without permission.

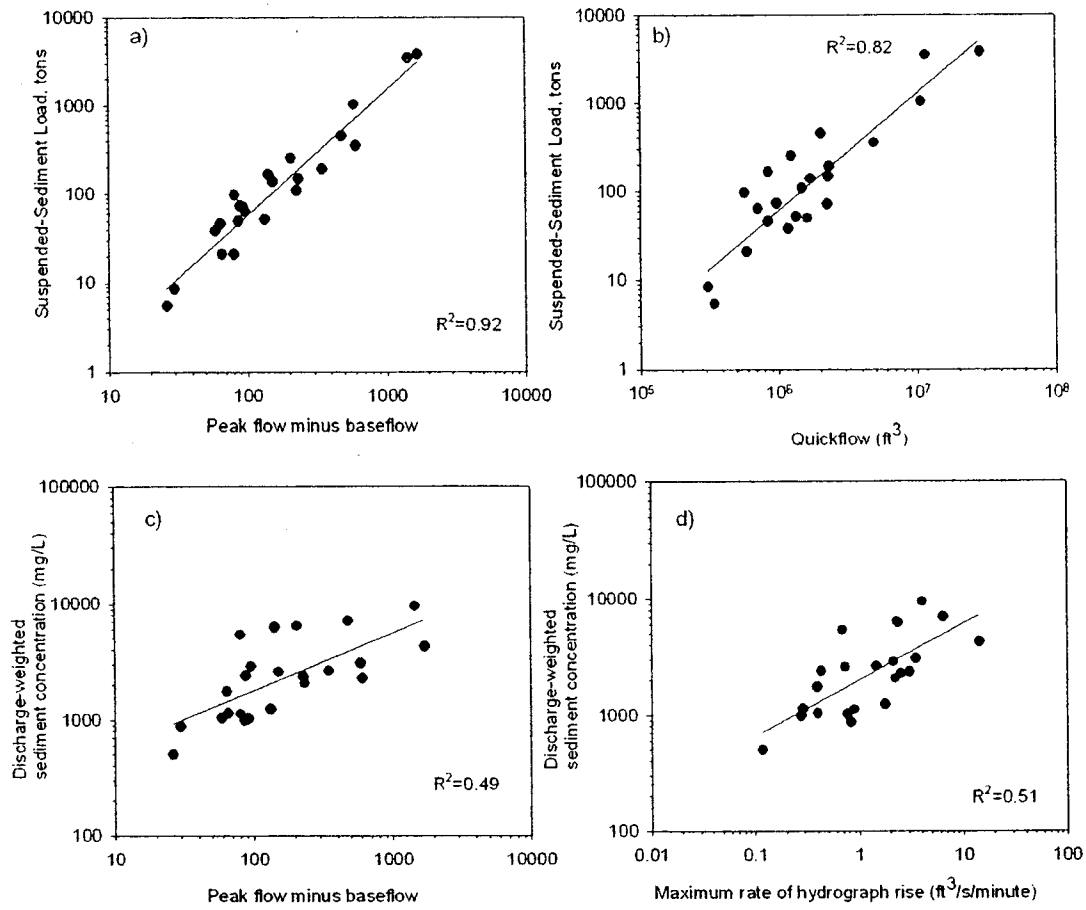

Figure 7.12. Graphical relations at Rio Caguitas near Aguas Buenas of independent variables with highest R^2 values using quickflow characteristics of the entire event against dependent variables. (a,b) suspended sediment load and (c,d) discharge weighted sediment concentration.

Forward stepwise regression (entire event, quickflow)

Forward stepwise regression was run on the 19 independent variables against the two dependent variables. Using suspended-sediment load as a dependent variable indicated that the sum of peak flows of the current event (8-SMPKBS) was significant in the first step of forward stepwise regression and the coefficient of the regression line was positive. Base flow at the start of the event (3-BASE) was important in the second step (Table 7.4) and the slope was negative,

Reproduced with permission of the copyright owner. Further reproduction prohibited without permission.

indicating that as base flow increased sediment load decreased. A similar negative correlation of base flow to suspended sediment concentration was found in the Walling (1974) analysis (Table 7.2).

Table 7.4. Results of forward stepwise regression for entire event using quickflow characteristics.

Dependent Variable	Step	Variables in the Model	R^2	F Statistic	Coefficient	Constant
suspended-sediment load, tons	One	8-SMPKBS	0.89	170	1.31	-0.94
	Two	3-BASE	0.92	5.88	-0.02	-0.83
		8-SMPKBS		208	1.39	
discharge-weighted sediment concentration, mg/L	One	7-MXTRP	0.46	18.0	0.48	3.29
	Two	17-RNBTWTI	0.56	4.72	0.00	3.46
		7-MXTRP		8.12	0.31	

Using the discharge-weighted sediment concentration as a dependent variable indicated the maximum rate of hydrograph rise for any peak (7-MXTRP) was important (Table 7.4). The slope of the best-fit regression line was positive, indicating a direct correlation of the rate of hydrograph rise to the discharge-weighted sediment concentration. The runoff between events was significant in the second step using the discharge-weighted sediment concentration as a dependent variable but there was no slope to the best-fit regression line (Table 7.4).

Factor analysis (entire event, quickflow)

Principal component analysis was performed on two sets of independent variables associated with quickflow characteristics of the event. One set contained 23 independent

Reproduced with permission of the copyright owner. Further reproduction prohibited without permission.

variables, including quickflow, the other set did not include quickflow (Appendices 7.4, 7.5). Six components were selected for factor analysis. Factor analyses for the principal components with and without quickflow had similar results. Over 76% of the total variance was explained by the first three axes (Appendices 8.2, 8.3). Forward stepwise regression was performed on the factor scores from principal components analysis against the two dependent variables (Table 7.5). The two dependent variables had differing results. Using suspended-sediment load as a dependent variable indicated PC2 was the most significant principal component in the first step of forward stepwise regression and PC1 in the second step (Table 7.5). PC2 had high positive loadings (> 0.6) on characteristics of the current event (1-QUICK, 4-PKBS, 6-MXTMJPK, 7-MXTRP, 8-SMPKBS, 10-RAIN, 13-RRISE) and characteristics of the previous event (26-PPTLSTI, 27-INTLST, 28-LS75OTI) (Appendix 7.4). The coefficient of the best-fit regression line was positive, indicating a direct correlation of suspended-sediment load to previous-event rainfall and previous-event rainfall intensity.

Table 7.5. Results of forward stepwise regression on the principal components for the entire event using quickflow characteristics.

Dependent Variable	Step	Variables in the Model	R^2	F Statistic	Coefficient	Constant
suspended-Sediment load, tons	One	PC2	0.56	26.9	0.53	2.05
	Two	PC1	0.75	15.6	0.31	2.05
		PC2		45.6	0.53	
discharge-weighted sediment concentration, mg/L	One	PC2	0.26	7.26	0.17	3.35
	Two	PC4	0.50	9.94	-0.17	3.35
		PC2		10.4	0.17	

Reproduced with permission of the copyright owner. Further reproduction prohibited without permission.

In the second step of forward stepwise regression, using suspended-sediment load as a dependent variable indicated that PC1 was significant (Table 7.5). PC1 had high positive loadings (>0.6) on rainfall (10-RAIN), hysteresis (16-HYSTER), and rainfall between events (18-PPTBTW, 19-INTBET) (Appendix 7.4). High negative loadings (<-0.8) on PC1 were on previous-event characteristics (20-LSPKBTI, 24-QULST) and previous three event quickflow and rainfall events (30-QU3EVT, 29-SUM3PPTI). The coefficient of the best-fit regression line was positive, indicating a direct correlation of suspended-sediment load to current-event characteristics (rainfall and hysteresis) and between-event characteristics (rainfall and rainfall intensity). The direct correlation to hysteresis indicated that clockwise hysteresis storms (Type-1) transported high suspended-sediment loads. Suspended-sediment load was inversely correlated to the previous-event peak flow and quickflow and three previous-event characteristics (rainfall and quickflow).

Using suspended-sediment load as a dependent variable indicated that previous-event characteristics were significant and directly correlated to PC2 but inversely correlated to PC1. Interpretations on the influence of characteristics of the previous event on the discharge-weighted sediment concentration were different on each principal component. PC2 showed previous-event rainfall and rainfall intensity as being directly correlated to suspended-sediment load. PC1 showed previous-event quickflow and peak flow and the three previous-events quickflow and rainfall as inversely correlated to suspended-sediment load. High amounts of previous-event rainfall and rainfall intensity may be supplying sediment from hillslopes and high previous-event quickflow and peak flows flush sediment. Rainfall and rainfall intensity between events were correlated directly with suspended-sediment load and were supplying sediment to the system.

Reproduced with permission of the copyright owner. Further reproduction prohibited without permission.

Using discharge-weighted sediment concentration as a dependent variable indicated that PC2 was significant in the first step of forward stepwise regression and PC4 was significant in the second step (Table 7.5). PC2 had high positive loadings (> 0.6) on characteristics of the current event (4-PKBS, 6-MXTMJPK, 7-MXTRP, 8-SMPKBS, 10-RAIN, 11-INT15, 13-RRISE) (Appendix 7.5). The coefficient of the best-fit regression line was positive, indicating that characteristics of the current event were directly correlated to sediment concentration.

PC4 was significant in the second step of forward stepwise regression using sediment concentration as a dependent variable (Table 7.5). PC4 had a high positive loading (0.57) on rainfall intensity of the current event (11-INT15) (Appendix 7.5). The coefficient of the regression was negative, indicating that increases in rainfall intensity of the current event were decreasing sediment concentrations. Rainfall intensity (11-INT15) was correlated with the discharge-weighted sediment concentration on PC2 and inversely correlated on PC4. The loadings are high for PC2, thus more weight is given to rainfall intensity as being directly correlated to sediment concentration. However, under some circumstances increases in rainfall intensity may be reducing sediment concentrations. This may occur when rainfall intensity increases runoff but not sediment.

Interpretations from factor analysis for the entire event using quickflow indicated that current-event characteristics were directly correlated to sediment load and discharge weighted sediment concentration. Previous-event rainfall intensity increased sediment loads and previous-event(s) quickflow flushed sediment.

Reproduced with permission of the copyright owner. Further reproduction prohibited without permission.

Varimax rotation (entire event, quickflow)

Principal components axes were rotated using the varimax rotation. The factor scores were saved after varimax rotation and forward stepwise regression was performed on the factor scores against the dependent variables (Table 7.6). After varimax rotation both dependent variables showed that PC2 was significant in the first step of forward stepwise regression. For both sets of factor scores (with and without the variable quickflow), PC2 had high positive loadings (>0.8) on characteristics of the current-event peak flow (1-QUICK, 4-PKBS, 6-MXTMJPK, 7-MXTRP, 8-SMPKBS) (Appendices 7.6, 7.7). The coefficient of the best-fit regression line was positive, indicating a direct correlation of current-event characteristics to suspended-sediment load.

Using suspended-sediment load as a dependent variable indicated PC4 was important in the second step (Table 7.6). PC4 had high positive loadings (>0.8) on current-event rainfall characteristics (10-RAIN, 11-INT15) (Appendix 7.6). The coefficient of the regression was positive, indicating a direct correlation of rainfall characteristics to suspended-sediment load.

Using the discharge-weighted sediment concentration as a dependent variable indicated PC3 was important in the second step of forward stepwise regression (Table 7.6). PC3 had a high positive loading (0.89) on base flow at the start of the event (3-BASE) (Appendix 7.7). The coefficient of the best-fit regression line was negative, indicating that as base flow increased sediment concentration of the current event decreased. Before varimax rotation, current-event and previous-event characteristics were significant and after varimax rotation only current-event characteristics were significant.

Reproduced with permission of the copyright owner. Further reproduction prohibited without permission.

Table 7.6. Results of forward stepwise regression on the principal components after varimax rotation for the entire event using quickflow characteristics.

Dependent Variable	Step	Variables in the Model	R^2	F Statistic	Coefficient	Constant
suspended-sediment load, tons	One	PC2	0.82	94.2	0.64	2.05
	Two	PC4	0.87	7.55	0.16	2.05
		PC2		124	0.64	
discharge-weighted sediment concentration, mg/L	One	PC2	0.52	22.9	0.24	3.35
	Two	PC3	0.61	4.82	-0.10	3.35
		PC2		27.0	0.24	

Runoff Results (entire event)

The independent variables assembled to analyze the relation of suspended-sediment characteristics to runoff characteristics are listed in Appendix 7.8. Tests for normality using the residuals and histogram plots indicated that 18 of the 23 independent variables needed a log transformation (Appendix 7.8). Analysis of the correlation matrix was similar to quickflow interpretations and showed a high correlation ($r>0.80$) among select variables (Appendix 7.9). Many of the characteristics of the previous event (21-LSPKTI, 23-SMLSPK, 25-RULST, 26-PPTLSTI, 27-INTLSTI) and three previous events (29-SUM3PPTI, 31-RU3EVT) were correlated. Two of these variables (21-LSPKTI, 27-INTLST) were removed. Current-event characteristics of 2-RUN, 9-SMPK and 5-PK were intercorrelated and 5-PK was removed. Rate of hydrograph rise (6-MXTMJPK and 7-MXTRP) were intercorrelated ($r=0.97$) and the maximum rate of hydrograph rise to the highest peak flow (6-MXTMJPK) was removed.

Important relations of the dependent variables to the independent variables that were observed in the correlation matrix are suspended-sediment load to peak flow (5-PK) and to runoff

Reproduced with permission of the copyright owner. Further reproduction prohibited without permission.

(2-RUN). The discharge-weighted sediment concentration showed a correlation to peak flow (5-PK) and to the maximum rate of hydrograph rise for any peak (7-MXTRP) (fig. 7.13). The high correlation of the rate of hydrograph rise was because many of the events on Rio Caguitas were single-peaked events.

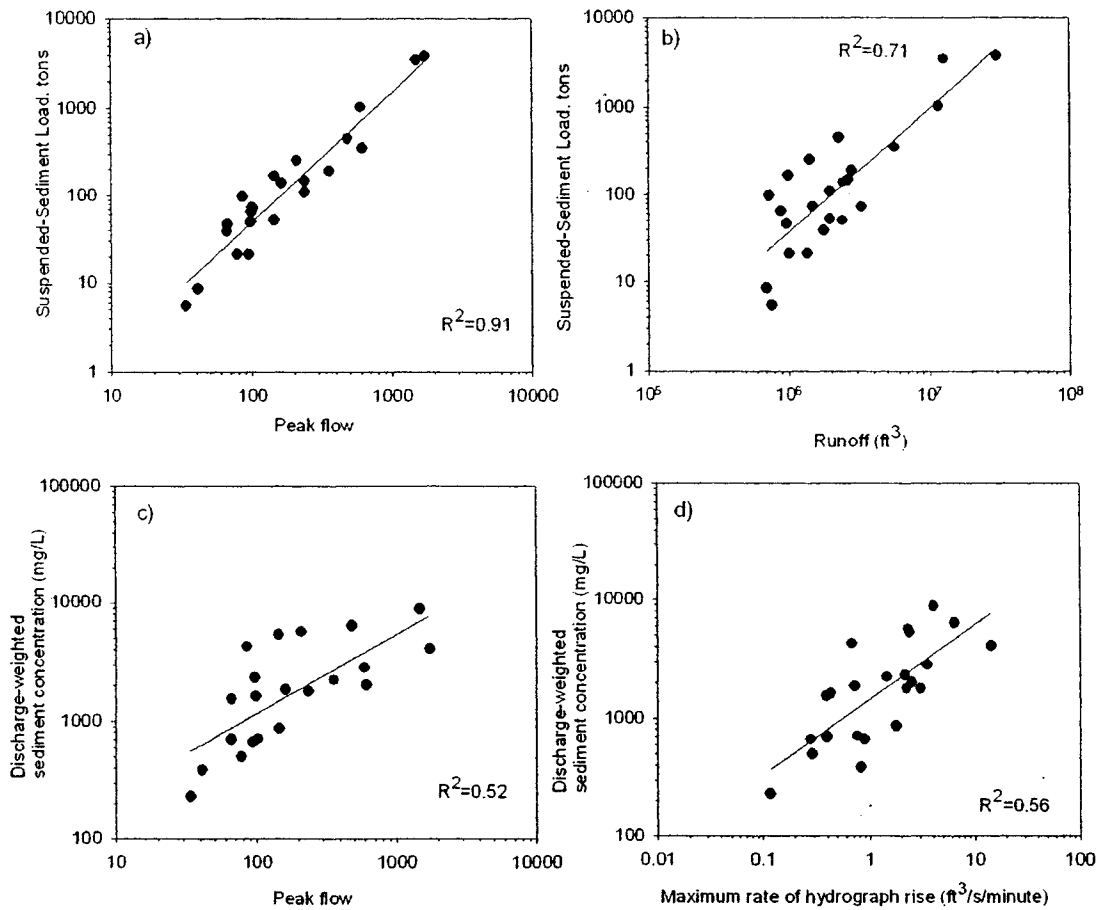

Figure 7.13. Graphical relations at Rio Caguitas near Aguas Buenas of independent variables with highest R^2 values using runoff characteristics of the entire event against dependent variables: (a,b) suspended-sediment load and (c,d) discharge-weighted sediment concentration.

Reproduced with permission of the copyright owner. Further reproduction prohibited without permission.

Forward stepwise regression (entire event, runoff)

Forward stepwise regression was run on the 19 independent variables against the two dependent variables. Results were similar to statistics run with quickflow variables. Using suspended-sediment load as the dependent variable indicated that the sum of peak flows of the current event (9-SMPK) was significant in the first step of forward stepwise regression and the coefficient of the regression line was positive. Base flow at the start of the event (3-BASE) was important in the second step (Table 7.7) and the slope was negative, indicating that as base flow increased sediment load decreased.

Table 7.7. Results of forward stepwise regression for entire event using runoff characteristics.

Dependent Variable	Step	Variables in the Model	R^2	F Statistic	Coefficient	Constant
suspended-sediment load, tons	One	9-SMPK	0.88	148	1.36	-1.08
	Two	3-BASE	0.90	6.03	-0.02	-0.99
		9-SMPK		182	1.45	
discharge-weighted sediment concentration, mg/L	One	7-MXTRP	0.49	19.9	0.62	3.14
	Two	17-RNBTWTI	0.58	4.54	0.00	3.35
		7-MXTRP		12.5	0.50	

Using the discharge-weighted sediment concentration as a dependent variable indicated the maximum rate of hydrograph rise for any peak (7-MXTRP) was important (Table 7.7). The coefficient of the regression was positive. The runoff between events was significant in the second step using the discharge-weighted sediment concentration as a dependent variable but there was no slope to the best-fit regression line (Table 7.7).

Reproduced with permission of the copyright owner. Further reproduction prohibited without permission.

Factor analysis (entire event, runoff)

Principal component analysis was performed on two sets of independent variables associated with runoff characteristics of the event. One set contained 22 independent variables, including runoff, the other set did not include quickflow (Appendices 7.10, 7.11). Six components were selected for factor analysis.

Factor analysis for the data set with and without the variable runoff had similar results. Over 77% of the total variance was explained by the first 3 axes. Forward stepwise regression was performed on the factor scores from principal components analysis against the two dependent variables (Table 7.8). Using suspended-sediment load as a dependent variable indicated PC2 was the most significant principal component in the first step of forward stepwise regression and PC1 was significant in the second step (Table 7.8). PC2 had high positive loadings (> 0.7) on characteristics of the current event (2-RUN, 5-PK, 9-SMPK) and characteristics of the previous-event rainfall (26-PPTLSTI, 27-INTLST, 28-LS75OTI) (Appendix 7.10). The coefficient of the best-fit regression line was positive, indicating that suspended-sediment load was directly correlated to current-event characteristics and previous-event rainfall and rainfall intensity.

In the second step of forward stepwise regression, PC1 was significant (Table 7.8). PC1 had high positive loadings (>0.6) on current-event characteristics (6-MXTMJPK, 7-MXTRP, 10-RAIN, 13-RRISE, 14RFOL, 16-HYSTER) and rainfall between events (18-PPTBTW) (Appendix 7.10). High negative loadings (<-0.7) on PC1 were on previous-event characteristics (21-LSPKTI, 25-RULST) and previous three events (29-SUM3PPTI 31-RU3EVT). The coefficient of the best-fit regression line was positive, indicating that current-event characteristics and rainfall between events were directly correlated with suspended-

Reproduced with permission of the copyright owner. Further reproduction prohibited without permission.

sediment load and the previous-event and three previous-event characteristics were inversely correlated.

Table 7.8. Results of forward stepwise regression on the principal components for the entire event using runoff characteristics.

Dependent Variable	Step	Variables in the Model	R^2	F Statistic	Coefficient	Constant
suspended-Sediment load, tons	One	PC2	0.46	17.6	0.48	2.05
	Two	PC1	0.74	21.8	0.38	2.05
		PC2		35.0	0.48	
discharge-weighted sediment concentration, mg/L	One	PC1	0.25	6.91	0.21	3.22
	Two	PC4	0.48	9.19	-0.21	3.22
		PC1		9.60	0.21	

Similar to the results using suspended-sediment load as a dependent variable in quickflow analysis, in this runoff analysis previous-event characteristics were significant and directly correlated to PC2 but inversely correlated to PC1. PC2 showed previous-event rainfall and rainfall intensity as being directly correlated to suspended-sediment load. PC1 showed previous-event quickflow and peak flow and the three previous-events quickflow and rainfall as inversely correlated to suspended-sediment load. High amounts of previous-event rainfall and rainfall intensity supplied sediment from hillslopes and high previous-event quickflow and peak flows flushed sediment. Rainfall and rainfall intensity between events were correlated directly with suspended-sediment load and supplied sediment to the system.

Using the discharge-weighted sediment concentration as the dependent variable indicated that PC1 was significant in the first step of forward stepwise regression and PC4 was significant

Reproduced with permission of the copyright owner. Further reproduction prohibited without permission.

in the second step (Table 7.8). PC1 had high loadings (>0.6) on hysteresis (16-HYSTER), rainfall (10-RAIN), and rainfall characteristics between the previous event (18-PPTBTW, 19-INTBET) (Appendix 7.11). High negative loadings (<-0.7) on PC1 were on previous-event characteristics (21-LSPKTI, 25-RULST) and previous three events (29-SUM3PPTI 31-RU3EVT). The coefficient of the regression line was positive, indicating that rainfall between events supplied sediment, and peak flow and runoff of the previous event and three previous events decreased sediment. The results using the dependent variable discharge-weighted sediment concentration with runoff characteristics was different than using quickflow. Using quickflow did not show previous-event or between-event characteristics as significant.

PC4 was significant in the second step using sediment concentration as a dependent variable (Table 7.8). PC4 had a high loading (>0.5) on rainfall intensity (11-INT15) of the current event. (Appendix 7.11). The coefficient of the regression was negative, indicating that increases in rainfall intensity of the current event decreased sediment concentration. Quickflow analysis showed a similar interpretation, that rainfall intensity (11-INT15) was correlated with the discharge-weighted sediment concentration on PC2 and inversely correlated on PC4.

Varimax rotation (entire event, runoff)

Principal components axes were rotated using the varimax rotation. The factor scores were saved after varimax rotation and forward stepwise regression was performed on the factor scores against the dependent variables (Table 7.9). Results were similar to the results using quickflow and showed for both dependent variables that PC2 was significant in the first step of forward stepwise regression. For both sets of factor scores (with and without quickflow), PC2

Reproduced with permission of the copyright owner. Further reproduction prohibited without permission.

had high positive loadings (>0.8) on characteristics of the current-event peak flow (5-PK, 6-MXTMJPK, 7-MXTRP, 9-SMPK) (Appendices 7.12, 7.13). The coefficient of the best-fit regression line was positive, indicating that as characteristics of the peak flow increased, sediment load and sediment concentration increased. Before varimax rotation, previous-event and between-event characteristics were significant. After varimax rotation, only current-event characteristics were significant.

Table 7.9. Results of forward stepwise regression on the principal components after varimax rotation for the entire event using runoff characteristics.

Dependent Variable	Step	Variables in the Model	R^2	F Statistic	Coefficient	Constant
suspended- sediment load, tons	Step One	PC2	0.80	81.9	0.64	2.05
discharge-weighted sediment concentration, mg/L	Step One	PC2	0.56	26.4	0.32	3.22

Discussion

For the entire event, separating storm events into quickflow did not improve statistical significance. Interpretations of quickflow versus runoff were for the most part similar. In forward stepwise regression of the independent variables, using quickflow and runoff, the sum of peak flows in the current event was important in explaining suspended-sediment load and the discharge-weighted sediment concentration. Base flow at the start of the event was significant and was inversely correlated to suspended-sediment load and the discharge-weighted sediment concentration, implying that base flow was diluting sediment concentrations. The maximum rate

Reproduced with permission of the copyright owner. Further reproduction prohibited without permission.

of hydrograph rise for any peak was important in the second step in explaining suspended-sediment load and the discharge-weighted sediment concentration.

The results of forward stepwise regression analysis on the principal components before varimax rotation were similar for both quickflow and runoff (Tables 7.5; 7.8). Factor analysis for the entire event, using quickflow or runoff, showed that current-event characteristics and previous-event characteristics of rainfall were positively correlated to suspended-sediment load and the discharge-weighted concentration. Previous-event runoff and peak flow and the sum of the three previous-events runoff and precipitation were negatively correlated to the dependent variables. Rainfall and rainfall intensity between the previous event and the beginning of the current event were negatively correlated to the dependent variables. In the mixed land use basin of Rio Caguitas, high previous-event rainfall and rainfall intensity supplied sediment from hillslopes and high previous-event quickflow and peak flows flushed sediment. Rainfall and rainfall intensity between events supply sediment to the system.

Highest peak flow analysis

This section describes the results of statistical analysis Rio Caguitas near Aguas Buenas using characteristics measured to the highest peak flow of the event. Twenty-one storms were used in this analysis (Table 7.10). Two dependent variables were used:

1) suspended-sediment load, in tons and

2) discharge-weighted sediment concentration, in mg/L

Histograms of the dependent variables showed that they have a better normal distribution with a log transformation.

Reproduced with permission of the copyright owner. Further reproduction prohibited without permission.

Reproduced with permission of the copyright owner. Further reproduction prohibited without permission.

Table 7.10. Summary of runoff events sampled adequately to the highest peak of the event at Rio Caguitas near Aguas Buenas.

Start Date	Start Time	Start discharge ft3/s	End Date	End Time	Peak Flow ft3/s	Event Duration (hour)	Total quickflow (ft3)	Runoff (ft3)	Suspended-sediment load (tons)	Discharge-weighted sediment concentration Quickflow mg/L	Discharge-weighted sediment concentration Runoff mg/L
1/5/1992	15.75	6.4	1/5/1992	17.75	1730	2	4.55E+006	4.60E+006	1390	9785	9683
9/22/1992	13.75	6.4	9/22/1992	16.25	66	2.5	1.41E+005	2.01E+005	3.39	768	540
12/1/1992	12.50	11.0	12/1/1992	15.5	41	3	1.19E+005	2.39E+005	1.95	524	260
12/29/1992	12.25	13.0	12/29/1992	16	78	3.75	1.03E+005	2.64E+005	3.30	1024	400
1/7/1993	13.25	8.6	1/7/1993	16.75	162	3.5	4.51E+005	5.68E+005	37.6	2673	2123
5/1/1993	14.75	9.3	5/1/1993	16.75	102	2	1.84E+005	2.53E+005	20.2	3517	2561
5/6/1993	14.25	8.9	5/6/1993	17.75	100	3.5	3.52E+005	4.78E+005	15.3	1389	1022
7/3/1993	10.75	7.3	7/3/1993	14.5	34	3.75	8.72E+004	1.89E+005	1.83	671	309
7/13/1993	16.75	11.0	7/13/1993	18	145	1.25	2.20E+005	2.71E+005	8.24	1202	975
7/22/1993	13.75	8.9	7/22/1993	17.75	359	4	4.54E+005	6.12E+005	38.3	2705	2004
8/15/1993	23.75	13.0	8/16/1993	1.25	94	1.5	1.37E+005	1.99E+005	7.07	1648	1137
8/18/1995	11.25	6.2	8/18/1995	19.25	615	8	1.67E+006	1.87E+006	243	4656	4158
9/6/1995	2.25	8.9	9/6/1995	8.25	1483	6	3.56E+006	3.75E+006	1560	14061	13374
9/7/1995	11.5	9.9	9/7/1995	16.75	97	5.25	5.91E+005	7.85E+005	24.0	1301	980
9/15/1995	21.75	8.3	9/16/1995	4.25	597	6.5	2.88E+006	3.03E+006	415	4626	4395
9/27/1995	14.25	2.7	9/27/1995	16.25	85	2	2.08E+005	2.34E+005	36.3	5600	4972
10/27/1995	14.75	2.6	10/27/1995	16	485	1.25	5.69E+005	5.82E+005	175	9837	9613
11/4/1995	13.75	2.6	11/4/1995	15.5	237	1.75	6.63E+005	6.82E+005	70.7	3415	3322
12/25/1995	16.25	1.7	12/25/1995	17.75	210	1.5	3.78E+005	3.92E+005	101	8564	8256
3/15/1996	13.5	1.9	3/15/1996	16.25	67	2.75	1.52E+005	1.73E+005	11.0	2324	2043
4/3/1996	14.5	1.4	4/3/1996	15.5	145	1	1.07E+005	1.14E+005	71.9	21454	20189

The average suspended-sediment load for the 21 events was 202 tons (183 metric tons) (fig.7.14a). The average discharge-weighted sediment concentration using quickflow was 4,840 mg/L (fig 7.14b) and using runoff was 4,400 mg/L (fig. 7.14c). The maximum discharge weighted sediment concentration for quickflow (21,400 mg/L) and runoff (20,200 mg/L) both occurred for the runoff event on 4/03/1996.

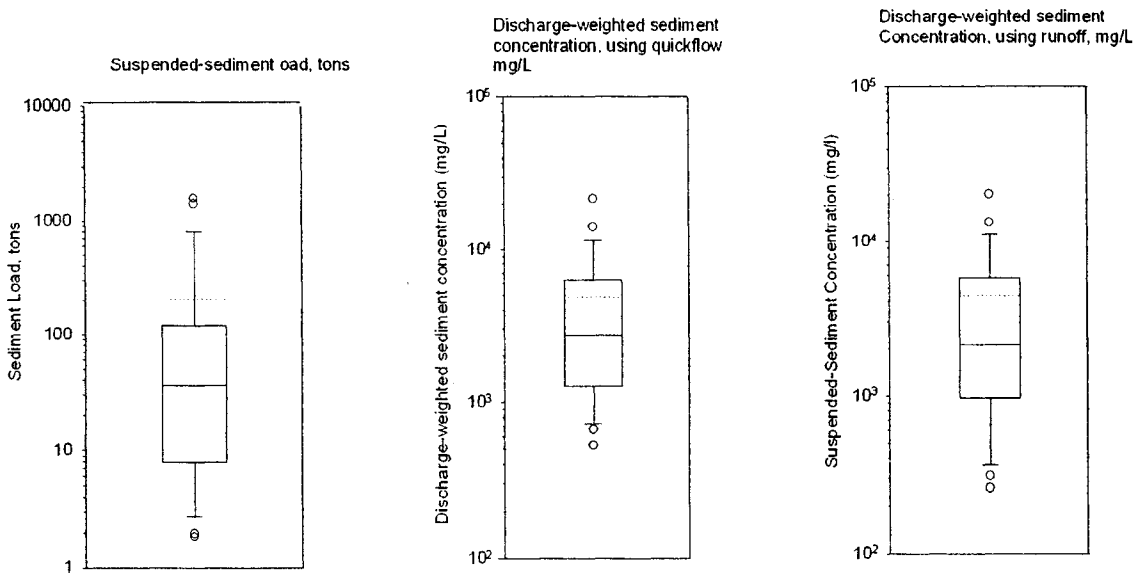

Figure 7.14. Box plot of dependent variables to the highest peak flow, a) sediment load, b) discharge-weighted sediment concentrations using quickflow, and c) discharge-weighted sediment concentration using runoff.

Quickflow Results (highest peak)

The independent variables assembled to analyze the relation of suspended-sediment characteristics to quickflow characteristics for the portion of the hydrograph rising to the highest peak flow are listed in Appendix 7.14. Tests for normality using the residuals indicated that 13 of the 17 independent variables needed a log transformation (Appendix 7.14). Analysis of the

Reproduced with permission of the copyright owner. Further reproduction prohibited without permission.

correlation matrix showed the same results as for the entire event (Appendix 7.15). Variables that showed a high correlation (r>0.80) were removed (20-LSPKBTI, 27-INTLST).

Forward stepwise regression (highest peak, quickflow)

Forward stepwise regression was performed on 15 independent variables against two dependent variables describing sediment (suspended-sediment load and discharge-weighted sediment concentration) for the portion of the hydrograph to the highest peak flow. Results were similar to the results for the entire event using quickflow characteristics (Table 7.11), although R^2 values were significant to the highest peak flow.

Using suspended-sediment load as the dependent variable indicated that peak flow of the current event (4-PKBS) was significant in the first step of forward stepwise regression and the coefficient of the regression line was positive. Using the discharge-weighted sediment concentration as a dependent variable indicated the rate of hydrograph rise to the highest peak (6-MXTMJPK) was significant (Table 7.11). The coefficient of the regression was positive. The runoff between events was significant in the second step using the discharge-weighted sediment concentration as a dependent variable but there was no slope to the best-fit regression line (Table 7.11).

Factor analysis (highest peak, quickflow)

Principal component analysis was performed on two sets of independent variables associated with quickflow characteristics of the event. One set contained 17 independent

Reproduced with permission of the copyright owner. Further reproduction prohibited without permission.

Table 7.11. Results of forward stepwise regression measured to the highest peak flow of the event using quickflow characteristics.

Dependent Variable	Step	Variables in the Model	R^2	F Statistic	Coefficient	Constant
suspended- sediment load, tons	One	4-PKBS	0.90	170	1.61	-2.02
discharge-	One	6-MXTMJPK	0.57	254.	0.67	3.42
weighted sediment	Two	17-RNBTWTI	0.70	7.37	0.00	3.66
concentration, mg/L		6-MXTMJPK		19.5	0.55	

variables, including quickflow; the other set did not include quickflow (Appendices 7.16, 7.17). Six components were selected for factor analysis.

Factor analyses for the data set with and without quickflow had similar results. Over 80% of the variance was explained by the first three axes. Forward stepwise regression was performed on the factor scores from principal components analysis against the two dependent variables (Table 7.12). The dependent variables all had similar results and showed PC2 as the most significant principal component in the first step of forward stepwise regression. PC2 for both sets with and without quickflow showed high positive loadings (>0.7) for current-event characteristics (1-QUICK, 4-PKBS, 6-MXTMJPK, 11-INT15, 13-RRISE) and a high negative loading (<-0.7) on the runoff between events (17-RNBTWTI) (Appendices 7.16, 7.17). The coefficient of the best-fit regression line was positive, indicating that current-event characteristics were directly correlated with suspended-sediment load and the runoff between events was inversely correlated.

The second step of forward stepwise regression using suspended-sediment load as a dependent variable showed that PC4 was significant (Table 7.12). PC4 had a high positive loading

Reproduced with permission of the copyright owner. Further reproduction prohibited without permission.

on rainfall intensity (11-INT15) (Appendix 7.16). The coefficient of the best-fit regression line was positive, indicating that rainfall of the current event increased sediment load.

Using the discharge-weighted sediment concentration as a dependent variable indicated that PC4 was significant in the second step of forward stepwise regression (Table 7.12). PC4 had a high negative loading (-0.52) on the rate of hydrograph rise to the highest peak (6-MXTMJPK) (Appendix 7.17). The coefficient of the best-fit regression line was negative, indicating that sediment load and the rate of hydrograph rise to the highest peak flow were directly correlated.

Interpretations from factor analysis to the highest peak flow using quick flow showed current-event characteristics were significant and directly correlated to suspended-sediment load and the discharge-weighted sediment concentration. Runoff between events was inversely correlated to suspended-sediment load, implying that large flows between events flushed sediment. Factor analysis did not show that previous events or that the sum of the three previous events was significant.

Table 7.12. Results of forward stepwise regression on the principal components measured to the highest peak flow of the event using quickflow characteristics.

Dependent Variable	Step	Variables in the Model	R^2	F Statistic	Coefficient	Constant
suspended-sediment load, tons	One	PC2	0.75	56.3	0.74	1.54
	Two	PC4	0.85	12.3	-0.27	1.54
		PC2		89.8	0.74	
discharge-weighted sediment concentration, mg/L	One	PC2	0.54	22.4	0.33	3.47
	Two	PC4	0.64	5.00	-0.14	3.47
		PC2		27.1	0.33	

Reproduced with permission of the copyright owner. Further reproduction prohibited without permission.

Varimax rotation (to the highest peak, quickflow)

Principal components axes were rotated using the varimax rotation. Over 70% of the variance was explained by the first three axes (Appendices 7.18, 7.19). The factor scores were saved after varimax rotation and forward stepwise regression was performed on the factor scores against the dependent variables (Table 7.13). Results were similar to those before rotation and both dependent variables showed PC2 as significant in the first step of forward stepwise regression. PC2, for both sets with and without quickflow, showed high loadings on current-event characteristics (1-QUICK, 4-PKBS, 6-MXTMJPK) (Appendices 7.18, 7.19) and was directly correlated to the dependent variables.

The second step of forward stepwise regression using suspended-sediment load as a dependent variable showed PC6 was significant (Table 7.13). PC6 had high positive loadings (> 0.5) on rainfall between events(18-PPTBTW, 19-INTBET) (Appendix 7.18). The coefficient of the best-fit regression line was positive, indicating that rainfall between events was inversely correlated to suspended-sediment load. This implies that large rainfall between events transported sediment from hillslopes and supplied sediment to the current event.

Runoff Results (highest peak)

The independent variables assembled to analyze the relation of suspended-sediment characteristics to runoff characteristics for the portion of the hydrograph rising to the highest peak flow are listed in Appendix 7.20. Tests for normality indicated that 13 of the 17 independent variables needed a log transformation (Appendix 7.20). Analysis of the correlation matrix showed

Reproduced with permission of the copyright owner. Further reproduction prohibited without permission.

the same results as for the entire event (Appendix 7.21). Variables that showed a high correlation (r>0.80) and were removed included (20-LSPKTI and 27-INTLST).

Table 7.13. Results of forward stepwise regression on the principal components after varimax rotation for the entire event using quickflow characteristics.

Dependent Variable	Step	Variables in the Model	R^2	F Statistic	Coefficient	Constant
suspended-sediment load, tons	One	PC2	0.87	122	0.80	1.54
	Two	PC6	0.90	5.50	0.15	1.54
		PC2		150	0.80	
discharge-weighted sediment concentration, mg/L	One	PC2	0.54	22.7	-0.33	3.47

Forward stepwise regression (highest peak, runoff)

Forward stepwise regression was performed on the 15 independent variables against the two dependent variables describing sediment (suspended-sediment load and discharge-weighted sediment concentration) for the portion of the hydrograph to the highest peak flow (Table 7.14). Results were similar to quickflow analysis to the highest peak flow.

Using suspended-sediment load as the dependent variable indicated that peak flow of the current event (4-PKBS) was significant in the first step of forward stepwise regression and the coefficient of the regression line was positive. Using the discharge-weighted sediment concentration as a dependent variable indicated the rate of hydrograph rise to the highest peak (6-MXTMJPK) was significant (Table 7.14) and the coefficient of the regression was positive. The runoff between events was significant in the second step using the discharge-weighted sediment

Reproduced with permission of the copyright owner. Further reproduction prohibited without permission.

concentration as a dependent variable and there was no slope to the best-fit regression line (Table 7.14).

Table 7.14. Results of forward stepwise regression measured to the highest peak flow of the event using runoff characteristics.

Dependent Variable	Step	Variables in the Model	R^2	F Statistic	Coefficient	Constant
suspended- sediment load, tons	One	5-PK	0.89	148	1.70	-2.27
discharge-	One	6-MXTMJPK	0.61	29.6	0.76	3.30
weighted sediment	Two	17-RNBTWTI	0.70	5.53	0.00	3.55
concentration, mg/L		6-MXTMJPK		22.0	0.70	

.

Factor analysis (highest peak, runoff)

Principal component analysis was performed on two sets of independent variables associated with runoff characteristics to the highest peak flow. One set contained 17 independent variables, including runoff, the other set did not include runoff (Appendices 7.22, 7.23). Six components were selected for factor analysis.

Factor analysis for the data set with and without runoff had similar results. Over 80% of the variance was explained by the first three axes (Appendices 7.22, 7.23). Forward stepwise regression was performed on the factor scores from principal components analysis against the two dependent variables (Table 7.15). The two dependent variables all had similar results and showed PC2 as the most significant principal component in the first step of forward stepwise regression. PC2 for both sets with and without runoff showed high positive loadings (>0.7) for current-event characteristics (4-PKBS, 11-INT15, 6-MXTMJPK, 13-RRISE) and a high negative loading (<-

Reproduced with permission of the copyright owner. Further reproduction prohibited without permission.

0.67) on the runoff between events (17-RNBTWTI) (Appendices 7.22, 7.23). The coefficient of the best-fit regression line was positive, indicating that current-event characteristics were directly correlated with suspended-sediment load and the runoff between events was inversely correlated.

The second step of forward stepwise regression using suspended-sediment load as a dependent variable showed PC4 was significant (Table 7.15). PC4 had a high positive loading on rainfall intensity (11-INT15) (Appendix 7.22). The coefficient of the best-fit regression line was negative, indicating a direct correlation of suspended-sediment load to rainfall intensity.

Using the discharge-weighted sediment concentration as a dependent variable indicated that PC4 was significant in the second step of forward stepwise regression (Table 7.15). PC4 had a high negative loading (-0.54) on the maximum rate of hydrograph rise to the highest peak (6-MXTMJPK) (Appendix 7.23). The coefficient of the best-fit regression line was negative, indicating a direct correlation of discharge-weighted sediment concentration to the maximum rate of hydrograph rise.

Table 7.15. Results of forward stepwise regression on the principal components measured to the highest peak flow of the event using runoff characteristics.

Dependent Variable	Step	Variables in the Model	R^2	F Statistic	Coefficient	Constant
suspended-sediment load, tons	One	PC2	0.76	60.3	0.75	1.54
	Two	PC4	0.87	14.9	-0.28	1.54
		PC2		104	0.75	
discharge-weighted sediment concentration, mg/L	One	PC2	0.49	18.6	0.38	3.35
	Two	PC4	0.62	5.82	-0.19	3.35
		PC2		23.3	0.38	

Reproduced with permission of the copyright owner. Further reproduction prohibited without permission.

Varimax rotation (entire event, runoff)

Principal components axes were rotated using the varimax rotation. Over 70% of the variance was explained by the first three axes (Appendices 7.24, 7.25). The factor scores were saved after varimax rotation and forward stepwise regression was performed on the factor scores against the dependent variables (Table 7.16). PC2 was significant in the first step of forward stepwise regression and for both data sets, with and without runoff, PC2 showed high positive loadings (>0.8) for current-event characteristics (2-RUN,4-PKBS, 6-MXTMJPK) (Appendices 7.24, 7.25). The coefficient of the best-fit regression line was positive, indicating that current-event characteristics were directly correlated to suspended-sediment load.

Table 7.16. Results of forward stepwise regression on the principal components after varimax rotation for the entire event using runoff characteristics.

Dependent Variable	Step	Variables in the Model	R^2	F Statistic	Coefficient	Constant
suspended-sediment load, tons	One	PC2	0.84	100	0.79	1.54
	Two	PC4	0.88	5.73	0.17	1.54
		PC2		126	0.79	
discharge-weighted sediment concentration, mg/L	One	PC2	0.57	25.5	0.41	3.35

The second step of forward stepwise regression, using suspended-sediment load as a dependent variable showed PC4 was significant (Table 7.16). PC4 had high positive loadings (> 0.7) on current-event rainfall characteristics (11-INT15, 14-RRISE) (Appendix 7.24). The coefficient of the best-fit regression line was positive, indicating that current-event characteristics were directly correlated to suspended-sediment load. Before varimax rotation current event and

Reproduced with permission of the copyright owner. Further reproduction prohibited without permission.

between-event characteristics were significant and after varimax only the current-event characteristics were significant.

Discussion

Statistical results to the highest peak flow slightly improved the R^2 values compared to using data for the entire event. Separating storm events into quickflow did not improve the statistical significance and interpretations of quickflow versus runoff were for the most part similar. In forward stepwise regression of the independent variables, using quickflow and runoff, peak flow and the maximum rate of hydrograph rise were important in explaining suspended-sediment load and the discharge-weighted sediment concentration. The slope of the best-fit line was positive, indicating that the current-event characteristics were directly correlated to the dependent variables.

The results of forward stepwise regression analysis on the principal components before varimax rotation were similar for both quickflow and runoff (Tables 7.16, 7.20). Factor analysis, to the highest peak flow, using quickflow or runoff, showed that characteristics between events were inversely correlated to suspended-sediment load and to the discharge-weighted concentration. After varimax rotation, rainfall and rainfall intensity were significant and were directly correlated to suspended-sediment load. By examining the rising portion of the hydrograph, sediment supply was directly correlated to current-event characteristics and to the rainfall between events. Sediment on the rising portion of the hydrograph was flushed by runoff between events.

Hysteresis

Hysteresis loops of the 23 sampled events were analyzed for the timing of the peak suspended-sediment concentration relative to peak flow, the type of hysteresis, and the width of

Reproduced with permission of the copyright owner. Further reproduction prohibited without permission.

the hysteresis loop (Table 7.17). For the entire event, the majority of events (14 of the 23 events) had the peak suspended-sediment concentration sampled before the peak flow, ranging from 3 to 258 minutes before the highest peak flow. Seven events had peak suspended-sediment concentration 8 to 225 minutes after peak flow. Two suspended-sediment concentration samples were collected at the peak.

The 17 events sampled adequately to define hysteresis loops at Rio Caguitas were divided between Type-1 and Type-3. For the entire event, Type 1 occurred in 9 of the 17 events (53%), 7 events were Type 3 (41%), and 1 event was Type 4 (fig. 7.15). Six events did not have enough samples to adequately define the hysteresis loop. Seven of the events were multipeaked but only 4 events had secondary peaks sampled (fig. 7.15c).

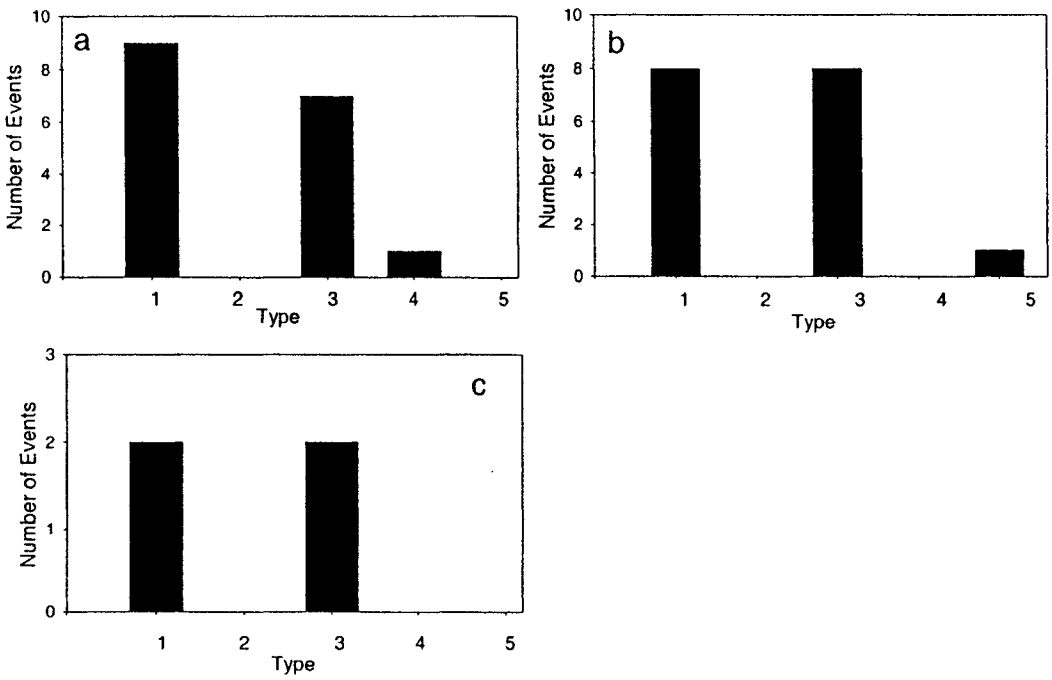

Figure 7.15. Hysteresis loops described at Rio Caguitas near Aguas Buenas for a) the entire event, b) near the highest peak flow, and c) for the first peak that is not the highest peak flow.

Reproduced with permission of the copyright owner. Further reproduction prohibited without permission.

Reproduced with permission of the copyright owner. Further reproduction prohibited without permission.

Table 7.17. Summary of hysteresis characteristics for Rio Cagultas near Aguas Buenas for the entire event In events with more than one peak, the highest peak is in bold.

See figure 4.12 for a description of the hysteresis type.

Start Date	Start Hour	End Date	End Hour	Number of Peaks	Entire event peak Discharge, ft3/s	Entire event Peak Concentration, mg/L	Time of peak suspended-sediment concentration relative to peak discharge, min	Entire event Hysteresis Type	Hysteresis type For the highest peak	First peak ft3/s	First peak suspended-sediment concentration, mg/L	Time of 1st peak suspended-sediment concentration relative to peak discharge, min
1/5/1992	15.75	1/7/1992	6	3	1730	12400	-3	1	1	**1730**	**12400**	**-3**
9/22/1992	13.75	9/23/1992	9.75	1	66	1620	176	3	3			
12/1/1992	12.5	12/1/1992	22	2	41	816	152	3	3	Not enough samples		
12/29/1992	12.25	12/30/1992	4	2	83	3260	-0	Not enough samples	Not enough samples	**83**	**3260**	**0**
1/7/1993	13.25	1/8/1993	5.75	1	162	3290	-43	1	1			
5/1/1993	14.75	5/2/1993	16	2	102	3800	-15	1	1	**102**	**3800**	**-15**
5/6/1993	14.25	5/7/1993	1.25	1	100	2930	75	3	3			
5/26/1993	13.5	5/26/1993	23.5	1	237	4480	8	Not enough samples	Not enough samples			
7/3/1993	10.75	7/4/1993	0.75	1	34	676	0	Not enough samples	Not enough samples			
7/13/1993	16.75	7/14/1993	4.25	1	145	1590	92	3	3			
7/22/1993	13.75	7/23/1993	2	1	359	4000	22	3	3			
8/15/1993	23.75	8/16/1993	7.75	1	94	2010	-13	Not enough samples	Not enough samples			
8/18/1995	11.25	8/19/1995	9	2	615	18100	-83	1	3	**615**	**18100**	**-83**
9/6/1995	2.25	9/7/1995	3.75	1	1483	18300	-24	1	1			
9/7/1995	11.5	9/8/1995	6.5	1	99	10400	-220	3	3			
9/15/1995	21.75	9/17/1995	8.42	5	597	8760	-258	4	5	123	4000	-3
9/27/1995	14.25	9/27/1995	21.5	1	85	10600	-8	2	2			
10/27/1995	14.75	10/28/1995	2	1	485	10100	-10	Not enough samples	Not enough samples			
11/4/1995	13.75	11/5/1995	6	1	237	4582	-43	Not enough samples	1			
12/25/1995	16.25	12/25/1995	23.5	1	210	9920	-28	1	1			
3/15/1996	13.5	3/16/1996	1.25	1	67	3190	-44	1	1			
4/3/1996	14.5	4/3/1996	22	2	145	35972	-14	1	1	**145**	**35972**	**-14**
5/23/1996	1.75	5/23/1996	13.25	1	98	5505	225	Not enough samples	Not enough samples	36	5505	-15

Hysteresis loops near the highest peak flow were examined to determine the maximum width of the loop or how much exhaustion or replenishment of sediment occurred during the runoff event. Possible causes for the exhaustion and replenishment of sediment were examined. Results were separated into Type-1 and Type-3 loops (Appendix 7.26). Type-4 hysteresis were grouped into Type-3 hysteresis because before and after the peak flow, the hysteresis loop is counterclockwise (fig. 4.7). Type-5 loops were not included in this analysis.

The average values for some of the storm characteristics showed differences between Type-1 and Typ-3 loops (Table 7.23). The average maximum width for Type-1 loops (4,940 mg/L) was three times that of Type-3 loops (1,670 mg/L) (Appendix 7.26). The average sediment load for Type-1 loops (1,020 tons) was an order-of-magnitude higher than for Type-3 loops (108 tons). Rainfall, rate of hydrograph rise, sum of peak flows and storm runoff were all higher for Type-1 compared to Type-3 (Appendix 7.26). Type 1 loops may occur during larger events that transported more sediment than Type-3 loops. The finding that Type-1 storms transported more sediment was also a statistical result of the principal components analysis for the entire event using quickflow (Appendix 7.26), which showed a direct correlation between suspended-sediment load and hysteresis. The discharge-weighted sediment concentration of Type-1 storms (3,720 mg/L) was more than twice the discharge-weighted sediment concentration of Type-3 storms (1,580). The sum of runoff of the three previous events and runoff between events were both higher for Type-3 storms (Appendix 7.26). This may indicate that channel sediment is flushed by these events which would reduce the likelihood of a Type-1 event.

Variables thought to influence the maximum width of the hysteresis loops around the peak flow were statistically examined using forward stepwise regression (Table 4.4). Results were

Reproduced with permission of the copyright owner. Further reproduction prohibited without permission.

separated into Type-1 and Type-3 events (Appendix 7.26). Analysis of the correlation table showed the sum of peak flows (9-SMPK) and previous-event runoff (25-RULST) were highly correlated with other variables and both were removed. Results of forward stepwise regression for Type 1 storms indicated that the time of peak suspended-sediment concentration relative to peak flow (34-TIME_PKCON) was significant in the first step (Table 7.18). The slope of the regression line was positive, indicating that as the time of the sediment peak concentration approaches the time of peak flow, the amount of exhaustion increased (fig. 7.16a).

The correlation matrix for Type-3 loops showed the sum of peak flows (9-SMPK) and previous-event runoff (25-RULST) to be highly correlated with other variables and both were removed. Results of forward stepwise regression on variables used to describe Type-3 loops indicated that the runoff between events (17RNBTWTI) was significant in the first step (Table 7.18; fig. 7.16b). The slope of the best-fit regression line was negative, indicating that as runoff between events increased, the width of the hysteresis loop decreased. Runoff between events was inversely correlated to suspended-sediment load to the highest peak flow. Runoff between events flushed sediment from the system, and therefore there is a limited amount of sediment available for Type-3 hysteresis loops.

Summary of Results for Rio Caguitas

During the study period, November 24, 1991 through May 23, 1996, 1,011 suspended-sediment samples were collected for concentrations at the station Rio Caguitas near Aguas Buenas. Most of the samples (74%) were collected at low flows between 1 and 50 ft^3/s

Reproduced with permission of the copyright owner. Further reproduction prohibited without permission.

Table 7.18. Results of forward stepwise regression for (A) clockwise (Type 1) hysteresis and (B) counterclockwise (Type 3) hysteresis.

A)

Step	Independent variable using all samples (rising and falling)	R^2	F Statistic	Coefficient	Constant
Step one	34-TIME-PKCON	0.54	7.05	0.02	4.07

B)

Step	Independent variable using all samples (rising and falling)	R^2	F Statistic	Coefficient	Constant
Step one	17-RNBTWTI	0.55	7.27	-0.001	9.04

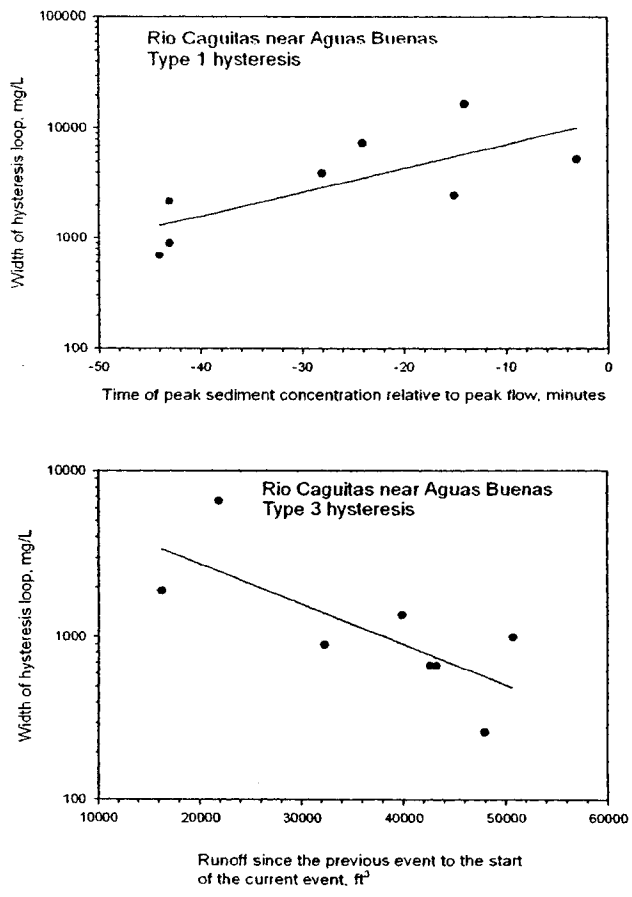

Figure 7.16. Relationships of hysteresis loops. a) The time of peak sediment concentration relative to peak flow plotted against clockwise hysteresis width. b) The runoff between events plotted against counterclockwise hysteresis loops.

Reproduced with permission of the copyright owner. Further reproduction prohibited without permission.

(0.03 to 1.42 m^3/s) (fig. 7.3). Fifty percent of the samples were of low suspended-sediment concentrations (< 231 mg/L). Rainfall conditions during the collection period were drier than the long-term average.

Sediment-transport curves generated to show the effect of previous events at Rio Caguitas indicated that large, previous runoff events reduced suspended-sediment concentrations on the rising limb for samples collected at low discharges (<100 ft^3/s) (fig. 7.6a). Suspended-sediment samples separated by the previous peak flow in the current event did not show a significant difference (fig. 7.6b).

Examination of sediment-transport curves showed that the best correlation coefficient was for all samples (0.71) (fig. 7.5a). Correlation coefficients did not improve when suspended-sediment samples were divided into rising and falling from the highest peak flow or rising and falling from any peak flow (fig. 7.5b,c). No significant difference in the relation of discharge to suspended-sediment concentration was observed when the samples were separated into the drier season (January to April) and the wet season (May to December) (fig. 7.7a).

For all samples the average amount of sand in suspension was 6.4 %, +/- 7.6%, and ranged from 1 to 36%. The low percentage of sand reflects the geology of the basin, volcaniclastics, which weathers to clay and silt size material. Plots for all samples showed an increase of sand with increasing discharge (fig. 7.8a). For high flows an exponential increase in sand percent seem to apply (fig. 7.8a).

Results using Walling's (1974) four independent variables (discharge, time relation of sample, base flow, and flood intensity), showed that the most important factor explaining sediment concentrations was discharge and the slope of the best-fit regression line was positive (Table 7.2).

Reproduced with permission of the copyright owner. Further reproduction prohibited without permission.

For all samples and falling samples, base flow at the start of the event was the most significant variable and the slope of the best-fit regression line was negative, indicating that sediment was diluted as a result of high base flows at the start of the event. For rising samples, flood intensity was important in the second step of forward stepwise regression and the slope of the best-fit regression line was positive. Results were similar for samples with and without base flow.

A summary of forward stepwise regression for all statistical analyses (independent variables, principal components with and without varimax rotation) for the entire event or to the highest peak flow using quickflow or runoff, at Rio Caguitas is shown in Table 7.19. For each statistical analysis, the dependent variable suspended-sediment load generally showed the highest correlation coefficients to the independent variables. Correlation coefficients did not improve by removing the base flow portion of the hydrograph. Results improved slightly by analyzing only the rising portion of the hydrograph to the highest peak flow.

For the entire event and to the highest peak flow, using quickflow or runoff, forward stepwise regression on the independent variables always indicated characteristics of the current event related to peak flow (peak flow, sum of peak flows, rate of hydrograph rise) were significant and were directly correlated to suspended-sediment load and to the discharge-weighted concentration. Base flow was significant for the entire event, using runoff, and was inversely correlated to suspended-sediment load. This was similar to the results using Walling's (1974) four variables. The independent variables quickflow and runoff were not significant when looking at the entire event or to the highest peak flow (Table 7.19).

Principal components analysis showed similar results for the entire event and to the highest peak flow (using quickflow and runoff). Current-event and between-event characteristics of rainfall

Reproduced with permission of the copyright owner. Further reproduction prohibited without permission.

Table 7.19. A) Summary of the first two steps of forward stepwise regression analyses for Rio Caguitas near Aguas Buenas for the entire event. The value in the parenthesis is the correlation coefficient (R^2). The '+' or '-' sign indicate the slope for the line of best fit. A '0' indicates no slope.

	Quickflow sediment load	**Runoff** sediment load	**Quickflow** discharge-weighted sediment concentration	**Runoff** discharge-weighted sediment concentration
Forward stepwise regression on variables	+ sum of peak flows (0.89) - base flow (0.92)	+ sum of peak flows (0.88) - base flow (0.90)	+ maximum rate of hydrograph rise (0.46) 0 runoff between events (0.56)	+ maximum rate of hydrograph rise (0.49) 0 runoff between events (0.58)
Forward stepwise regression on principal components	**+ PC2 (0.56)** + current rain, quickflow, peak flow, maximum rate of hydrograph rise + previous rainfall and rainfall intensity **+ PC1 (0.75)** + current rainfall, hysteresis + rainfall between the previous event - previous peak flow, quickflow - sum three previous rainfall	**+ PC2 (0.46)** + current rain, runoff, peak flow, maximum rate of hydrograph rise + previous rainfall and rainfall intensity **+ PC1 (0.74)** + current rainfall, hysteresis + rainfall between the previous event - previous peak flow, runoff - sum three previous rainfall and runoff events	**+ PC2 (0.26)** + current rain, peak flow, maximum rate of hydrograph rise **- PC4 (0.50)** + current rainfall intensity	**+ PC1 (0.25)** + current rain, hysteresis + rainfall and rainfall intensity between events **- PC4 (0.48)** + current rainfall intensity
Forward stepwise regression on rotated principal components	**+ PC2 (0.82)** + current quickflow, peak flow, maximum rate of hydrograph rise **+ PC4 (0.87)** + current rainfall and rainfall intensity	**+ PC2 (0.80)** + current peak flow, maximum rate of hydrograph rise	**+ PC2 (0.52)** + current peak flow, maximum rate of hydrograph rise **- PC3 (0.61)** + base flow	**+ PC2 (0.56)** + current peak flow, maximum rate of hydrograph rise

Reproduced with permission of the copyright owner. Further reproduction prohibited without permission.

Table 7.19 B) Summary of the first two steps of forward stepwise regression analyses for Rio Caguitas to the highest peak flow. The value in the parenthesis is the correlation coefficient (R^2). The '+' or '-' sign indicate the slope for the line of best fit.

	Quickflow sediment load	**Runoff** sediment load	**Quickflow** discharge-weighted sediment concentration	**Runoff** discharge-weighted sediment concentration
Forward stepwise regression on variables	+ peak flow (0.90)	+ peak flow (0.89)	+ rate of hydrograph rise (0.57) 0 runoff since previous event (0.70)	+ rate of hydrograph rise (0.61) 0 runoff since previous event (0.70)
Forward stepwise regression on principal components	**+ PC2 (0.75)** + current rain, quickflow, rainfall intensity, peak flow, maximum rate of hydrograph rise - runoff between events **+ PC4 (0.85)** + current rainfall intensity	**+ PC2 (0.76)** + current rain, runoff, rainfall intensity, peak flow, maximum rate of hydrograph rise - runoff between events **+ PC4 (0.87)** + current rainfall intensity	**+ PC2 (0.54)** + current rain, rainfall intensity, peak flow, maximum rate of hydrograph rise - runoff between events **+ PC4 (0.64)** - maximum rate of hydrograph rise	**+ PC2 (0.49)** + current rain, rainfall intensity, peak flow, maximum rate of hydrograph rise - runoff between events **+ PC4 (0.62)** - maximum rate of hydrograph rise
Forward stepwise regression on rotated principal components	**+ PC2 (0.87)** + quickflow, peak flow, maximum rate of hydrograph rise **+ PC6 (0.90)** + rainfall and rainfall intensity between the previous event	**+ PC2 (0.75)** +runoff, peak flow, maximum rate of hydrograph rise **+ PC4 (0.88)** + current rainfall and rainfall intensity	**+ PC2 (0.54)** + peak flow, maximum rate of hydrograph rise	**+ PC2 (0.58)** + peak flow, maximum rate of hydrograph rise

were directly correlated to the dependent variables and runoff characteristics between events were inversely correlated (Table 7.19). For the entire event, previous-event rainfall supplied sediment and previous-event runoff and peak flow, and the sum of the three previous-events runoff and

Reproduced with permission of the copyright owner. Further reproduction prohibited without permission.

rainfall flushed sediment. Previous-event characteristics were not observed to be significant to the highest peak flow. After varimax rotation, for the entire event and to the highest peak flow (using either quickflow and runoff), characteristics of the current event were significant and previous-event and between-event characteristics were not significant (Table 7.19). An exception was analysis to the highest peak flow which showed rainfall and rainfall intensity as significant after varimax rotation and directly correlated to suspended-sediment load.

Analysis of hysteresis loops indicated that clockwise and counterclockwise hysteresis loops are both common. Clockwise loops transported more sediment, had high sediment concentrations, and had wider loops than Type-3 loops. Type-1 loops were associated with large runoff and rainfall events. The time of peak suspended-sediment concentration relative to peak flow (34-TIME_PKCON) was significant in explaining the amount of sediment exhaustion in Type-1 events (Table 7.18). The slope of the regression line was positive, indicating that as the time of the sediment peak concentration approached the time of peak flow, the amount of exhaustion increased (fig. 7.16a). For Type-3 events, runoff between events was inversely correlated to the width of Type-3 hysteresis loops (fig. 7.16a). Runoff between events flushed sediment from the system, and therefore there was a limited amount of sediment available in Type-3 events.

Rio Caguitas drains mixed land-use of cropland (23%), pasture (27%), and forest (36%). Sources of sediment are cropland and the channel corridor (bed and banks). Analysis of sediment characteristics for Rio Caguitas suggests that both sources are important. Current-event characteristics of peak flow and the rate of hydrograph rise were significant in transporting suspended-sediment. Rio Caguitas drains volcaniclastics and the suspended sediment is typically fine grained. Increases in base flow at the start of the event led to low sediment loads. An increase

Reproduced with permission of the copyright owner. Further reproduction prohibited without permission.

of sand in suspension, up to 36%, was observed at high flows and indicated the channel as a source of sediment. Sediment was supplied to the system from hillslopes during large previous-event rainfall and between-event rainfall events. Sediment was flushed by previous-event runoff, the sum of the three previous-events runoff and rainfall, and from runoff between events. Type-1 hysteresis was more common in large events where sediment in the channel is suspended. The sum of runoff of the three previous events and runoff between events were both high for Type-3 storms (Appendix 7.26). This may indicate that channel sediment is flushed by these events, which would reduce the likelihood of a Type-1 event.

Reproduced with permission of the copyright owner. Further reproduction prohibited without permission.

CHAPTER VIII

SUSPENDED-SEDIMENT TRANSPORT AT RIO PIEDRAS

Suspended-sediment transport is described for Rio Piedras, which drains urban (77%) and forested (23%) areas in clayey soils. At the time of this PhD study, substantial areas of the basin were undergoing clearance for housing construction (fig. 3.15; 3.17). The period of investigation at Rio Piedras at El Senorial (50048770) (fig. 3.5) was chosen as October, 1991 through September, 1995 based on the best record of storm samples for suspended sediment. Rainfall, discharge, and suspended-sediment characteristics are described for this period.

Rainfall and Discharge for the Study Period

Average annual rainfall for water years 1912 through 1995, recorded at the National Weather Service raingage in Rio Piedras was 76 in (1930 mm). For the period of study, WY 1991-95, the average rainfall was 62 inches (1,580), which is 13% drier than the long-term average.

Rainfall amounts for the study period used in the statistical analyses were obtained from three USGS stations, 50048770, 50058350, and 50059050 (fig. 4.1d). When these stations were not operating, data was augmented with USGS stations (50047850, 50055100, 50059000, 50059100, 50999963, and 50999964) (fig. 4.1d), and National Weather Service raingages (Rio Piedras Experimental Station and the San Juan airport). The mean daily rainfall for the period October 1, 1991 through September 30, 1995 was 0.16 inches (4.0 mm).

Reproduced with permission of the copyright owner. Further reproduction prohibited without permission.

For the period being investigated the mean daily flow at Rio Piedras at El Senorial was 16.4 ft^3/s (0.46 m^3/s). Flow duration for the period of investigation is shown in figure 8.1. Peak flow for the period of record was 4,680 ft^3/s (133 m^3/s) on August 24, 1988. Peak flows during the period of investigation are listed in Table 8.1.

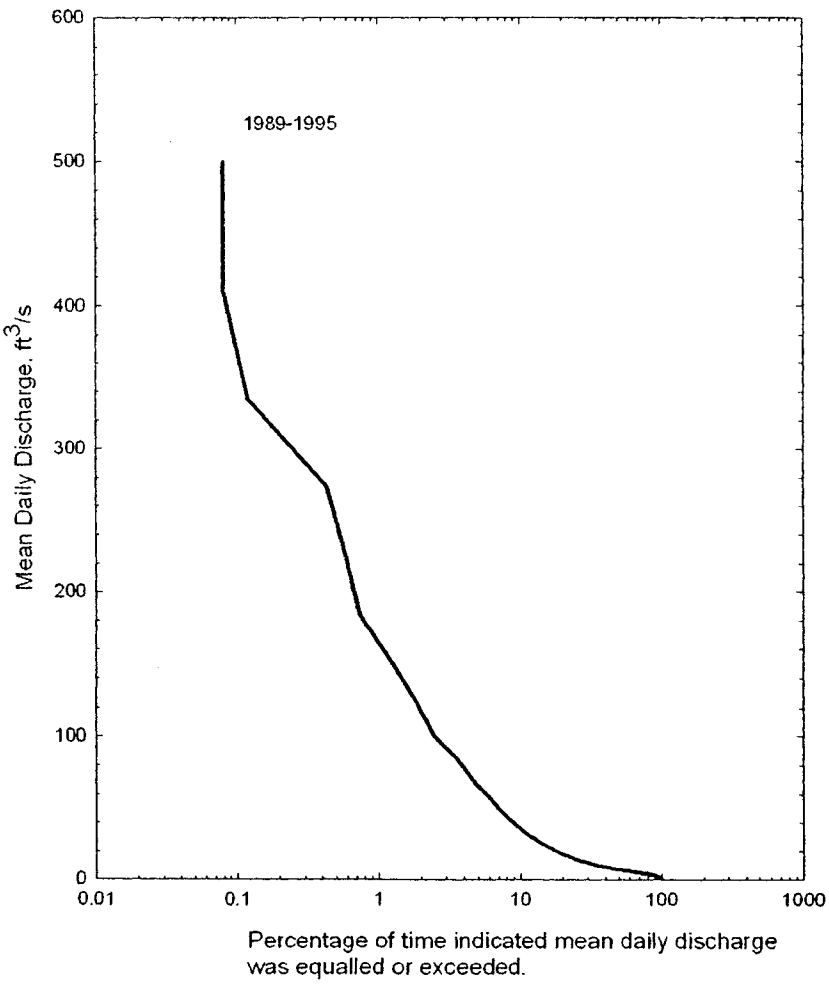

Figure 8.1 Flow durations for period of investigation (water year 1991-1995) for Rio Piedras at El Senorial (50048770).

Reproduced with permission of the copyright owner. Further reproduction prohibited without permission.

Table 8.1. Peak flows greater than 1.01 year recurrence (1,500 ft^3/s; 42.5 m^3/s) at Rio Piedras at El Senorial during the period of investigation, October, 1991 through September 1995.

Date	Peak flow (ft^3/s)
8/21/1992	4,250
11/18/1992	3,540
08/28/1994	2,130
09/06/1995	2,960

Suspended-Sediment Load and Yield

Suspended-sediment loads at Rio Piedras from WY 1989 through 1995 were obtained from the USGS-Caribbean District's annual surface-water data reports. The average annual suspended-sediment load was 127,400 tons (115,500 metric tons), the average annual sediment yield was 17,000 tons/mi^2 (5,950 metric tons/km^2), and the average annual discharge-weighted sediment concentration was 7,620 mg/L. On average, for water years 1989 through 1995, 90% of the annual suspended-sediment load was transported in 24 days, 75% in 11 days, and 25% in one day. On August 21, 1992, 44% of the suspended-sediment load for that year (114,000 tons; 103,400 metric tons) was transported.

Suspended-sediment Analysis

Between the period December 5, 1991 through September 30, 1995, 527 suspended-sediment samples were collected at the station Rio Piedras at El Senorial. Of the samples, 85 were collected during base flow, 168 were collected on the rising limb of the hydrograph to the highest peak flow, and 274 were collected on the falling limb of the hydrograph following the highest peak

Reproduced with permission of the copyright owner. Further reproduction prohibited without permission.

flow. Only one of the samples was collected using the EWI method, 429 were collected with the automatic suspended-sediment sampler, and 97 were taken at a single vertical (SV) in the channel. During the period of analysis, there was no calibration of the either the SV or automatic samples to EWI samples. Because the samples were not calibrated, it is recognized that some error may be incurred in this analysis of suspended sediment.

The lowest and highest suspended-sediment concentrations were 3 mg/L and 48,770 mg/L. The mean concentration for this data set is 6,290 mg/L, the median suspended-sediment value was 3,260 mg/L, and the sample standard deviation was 8,820 mg/L (fig. 8.2). Samples were taken over a range of discharges from 1.4 to 2,965 ft^3/s (0.04 to 84.0 m^3/s). The distribution of sampled discharge shows that 57% of the suspended-sediment samples were taken at high flows between 100 and 500 ft^3/s (2.83 to 14.2 m^3/s) (fig. 8.3).

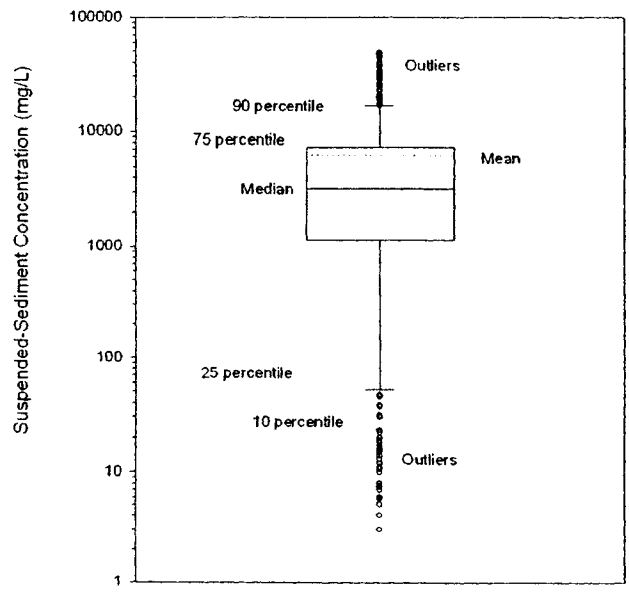

Figure 8.2. Box plot of suspended-sediment concentrations (n=527) for Rio Piedras at El Senorial.

Reproduced with permission of the copyright owner. Further reproduction prohibited without permission.

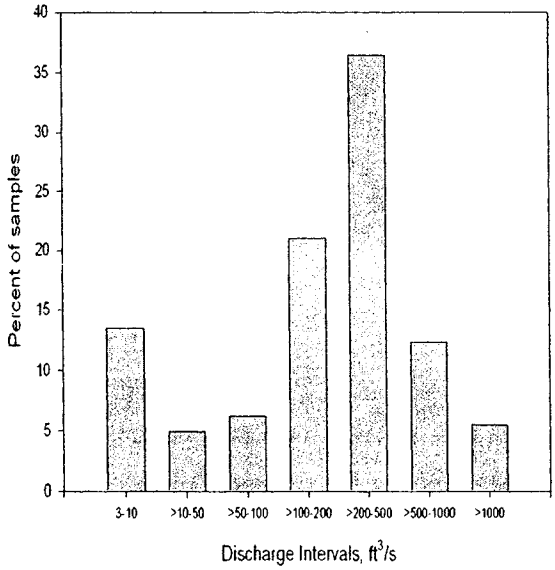

Figure 8.3. Frequency of discharges for suspended-sediment samples, Rio Piedras at El Senorial.

Quantile plots of the suspended-sediment data (fig. 8.4.a, b) show that most of the samples collected were of high concentrations. Seventy-seven percent of the suspended-sediment samples were above 1,000 mg/L. Box plots of the data show the 10^{th}, 25^{th}, 75^{th}, and 90^{th} percentiles of suspended sediment are 52, 1,150, 7,340, and 16,650 mg/L, respectively (fig. 8.2). Probability plots show that the suspended-sediment data are not normally distributed (fig. 8.4c), therefore, applying a log transform to the data was found to be appropriate (fig 8.4d).

Sediment-Transport Curves

Sediment-transport curves were created: 1) for all samples, 2) samples rising to the highest peak flow, 3) samples falling from the highest peak flow, 4) samples rising to any peak low, 5) samples falling from any peak flow, and 6) samples collected at base flow (fig. 8.5). Two clusters in the sediment-transport curves are related to sampling frequency. Low-discharge samples are

Reproduced with permission of the copyright owner. Further reproduction prohibited without permission.

frequently collected by observers and USGS technicians. High-discharge samples are collected by the automatic sampler. The low number of suspended-sediment samples collected at intermediate discharges, 20 to 100 ft^3/s (0.57 to 2.83 m^3/s), illustrates the difficulty in either a technician or an observer reaching the site when the event is beginning or ending.

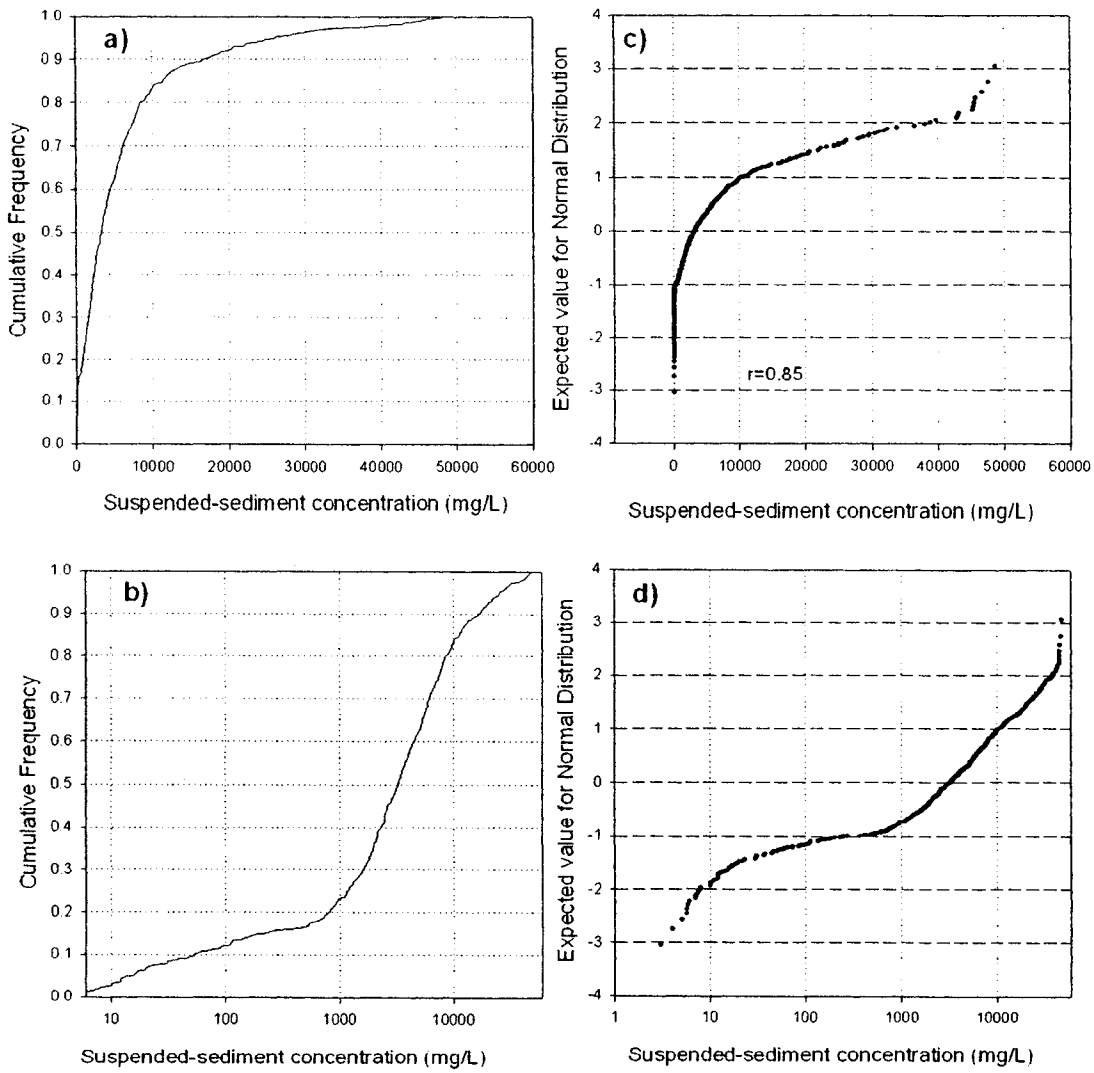

Figure 8.4. Quantile plots for Rio Piedras at El Senorial showing (a) suspended sediment and (b) log transformed suspended sediment. Probability plots of Rio Senorial showing (c) suspended sediment and (d) log transformed suspended sediment.

Reproduced with permission of the copyright owner. Further reproduction prohibited without permission.

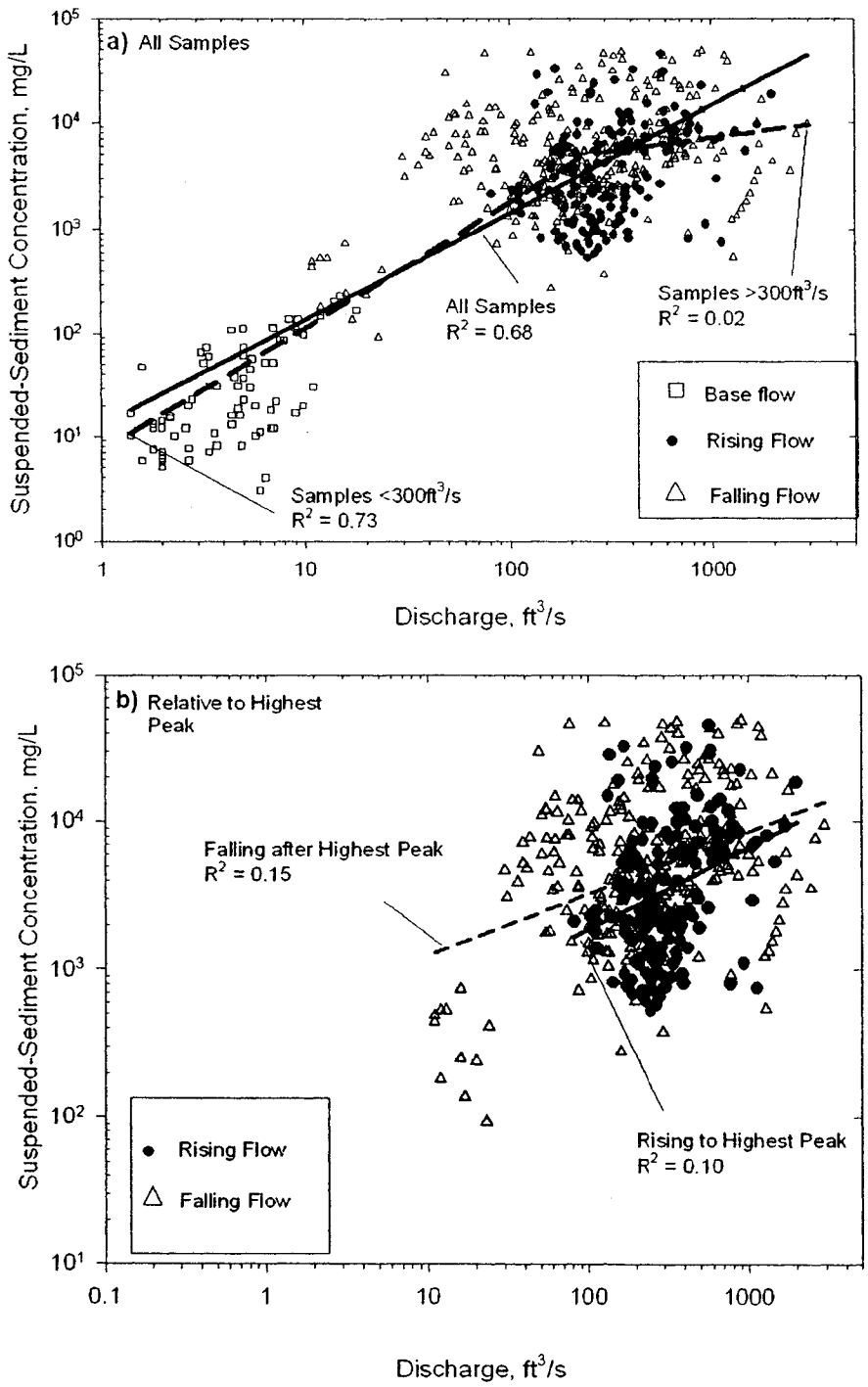

Figure 8.5. Suspended-sediment transport curves for Rio Piedras at El Senorial : a) All samples and b) rising and falling samples relative to the highest peak.

Reproduced with permission of the copyright owner. Further reproduction prohibited without permission.

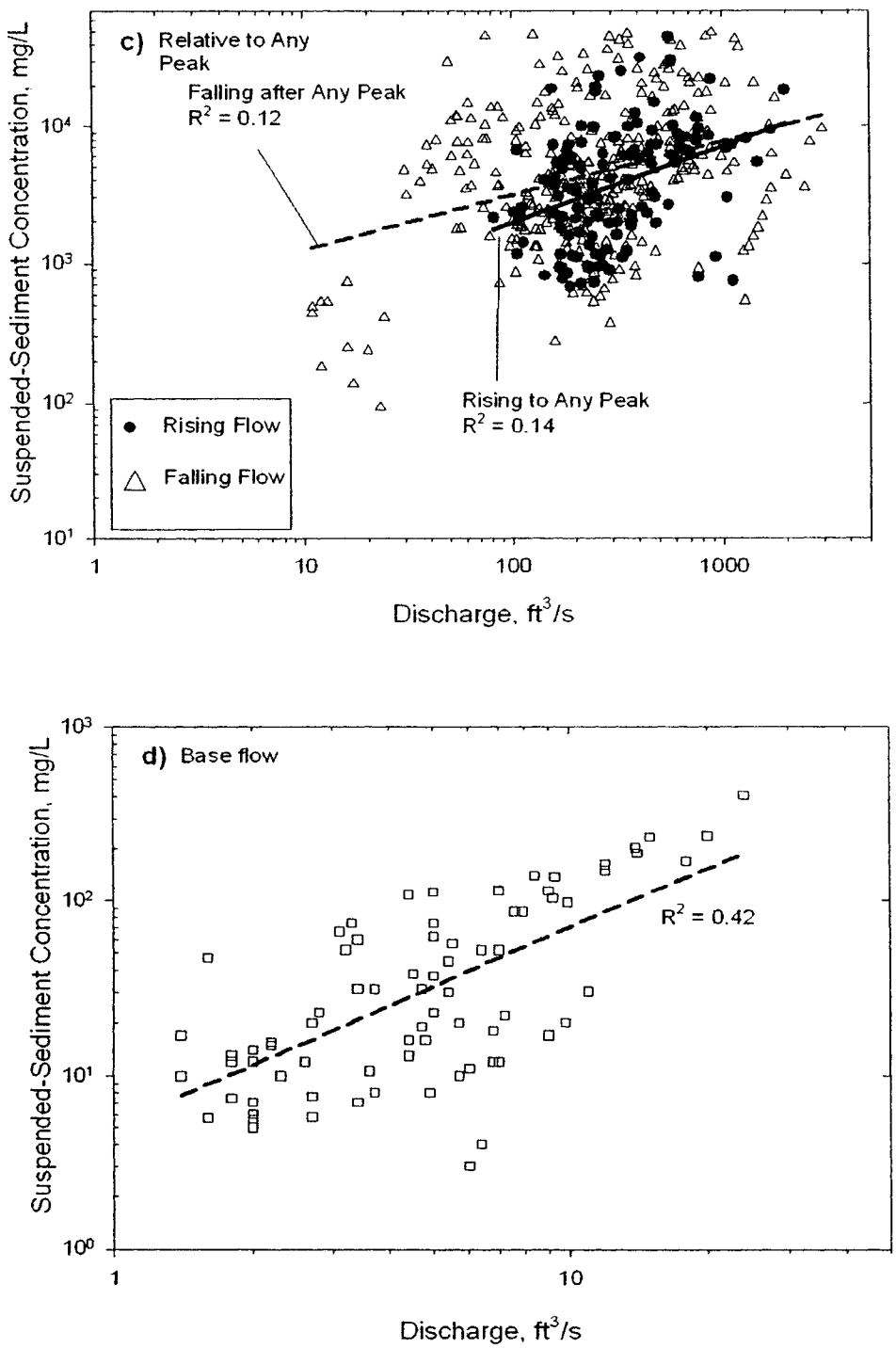

Figure 8.5. Continued. c) Rising and falling samples relative to any peak flow and d) base flow samples.

Reproduced with permission of the copyright owner. Further reproduction prohibited without permission.

The correlation coefficient for all samples is 0.68 (fig.8.5a). Correlation coefficients did not improve when the suspended-sediment samples were divided into rising and falling from the highest peak flow or rising and falling from any peak (fig. 8.5b,c). Samples separated into rising and falling showed high suspended-sediment concentrations for falling flow. Base flow samples showed concentrations up to 233 mg/L (fig. 8.5d).

To test the hypothesis that previous runoff events flush sediment, suspended-sediment samples were analyzed relative to the last event and to peak flows of the current event (fig. 8.6a). If previous events flushed sediment from the system, then suspended-sediment samples may have low concentrations after a large recent runoff event. Suspended-sediment samples were separated into 4 classes defined by the runoff of the previous event divided by the difference in time of the sample to the end of the previous event (fig. 8.6a). Only samples rising to the highest peak flow were in this analysis. The line of best fit for samples in the largest class (500,000 to 2,800,000 ft^3/hr) or samples collected shortly after a previous event showed the lowest suspended-sediment concentrations for a given discharge (fig. 8.6a). However, the smallest class (700-9,900 ft^3/hr) of samples, which were collected following a long time period did not show the highest suspended-sediment concentrations (fig. 8.6a).

Suspended-sediment samples separated by the previous peak flow in the current event showed for all discharges that samples taken after the highest peak flow have lower concentrations (fig. 8.6b). Flushing of sediment after previous peaks in the current event may be occurring, but the R^2 value was low (0.26) (fig. 8.6b).

Reproduced with permission of the copyright owner. Further reproduction prohibited without permission.

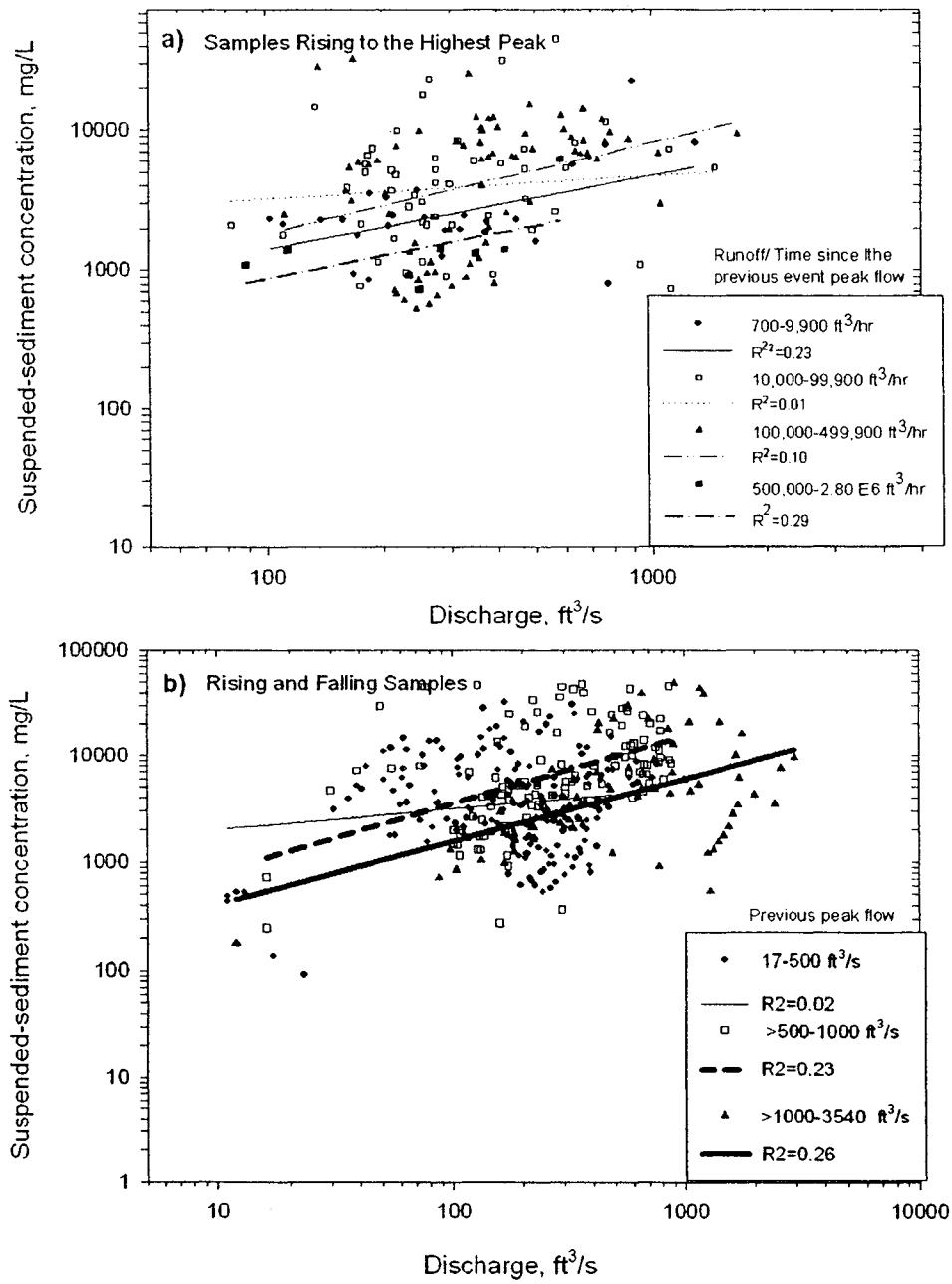

Figure 8.6. Suspended-sediment transport curves for Rio Piedras at El Senorial: a) Samples collected on the rising limb to the highest peak flow separated by runoff of the previous event divided by the time since the previous-event and b) rising and falling samples separated by the previous peak flow in the current event.

Reproduced with permission of the copyright owner. Further reproduction prohibited without permission.

Seasonal sediment transport groups separated into May through December and January through April are shown in figure 8.7. The R^2 values for each season are generally high. A plot of all samples shows very little difference in the line of best fit for January to April compared to

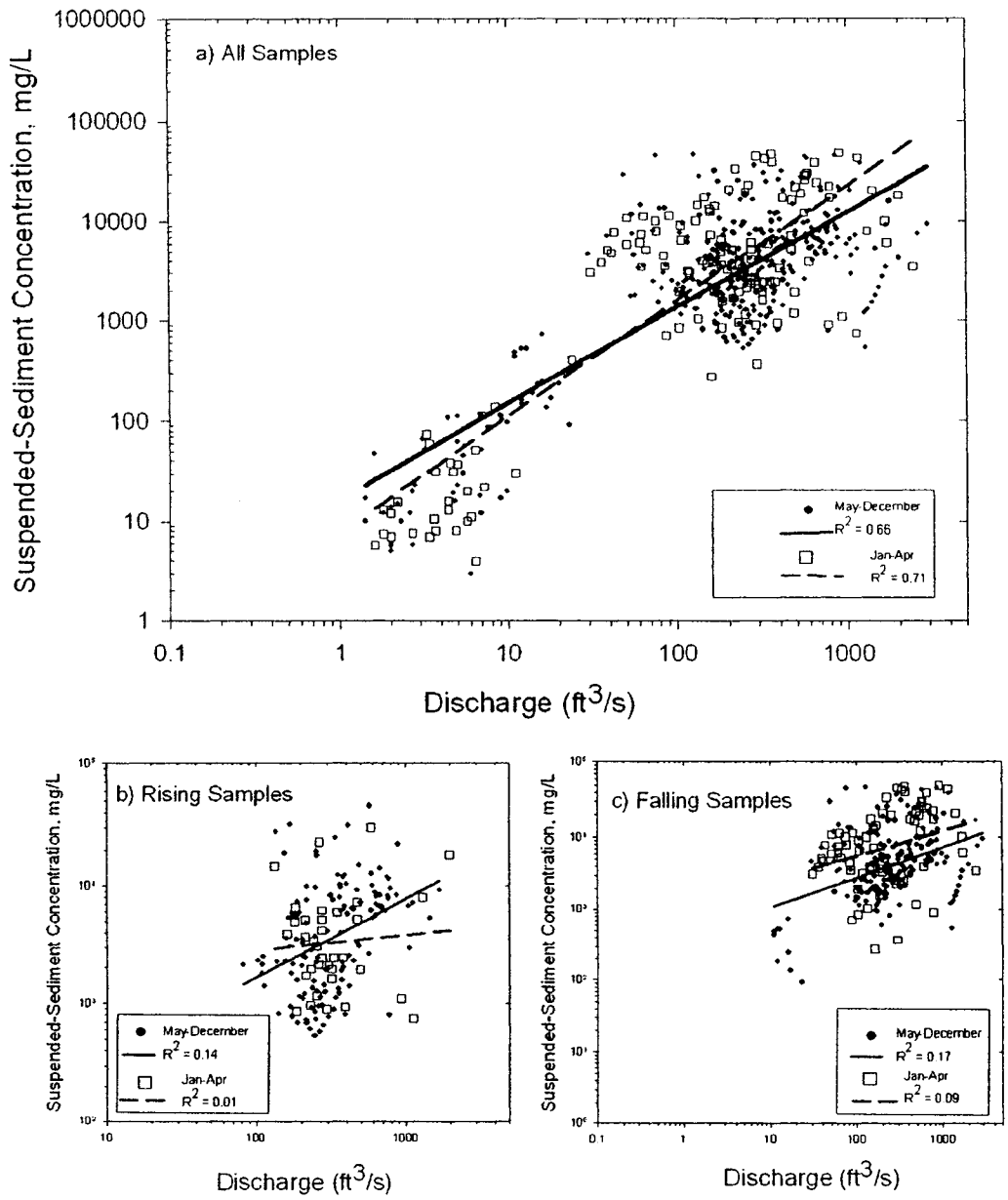

Figure 8.7. Seasonal suspended-sediment transport curves (May-Dec; Jan-Apr) for Rio Piedras at El Senorial: a) all samples, b) rising samples relative to the highest peak flow, and c) falling samples relative to the highest peak flow.

Reproduced with permission of the copyright owner. Further reproduction prohibited without permission.

May through December (fig. 8.7). Separation of seasonal suspended-sediment samples into rising and falling relative to the highest peak flow showed generally poor correlations (fig. 8.7b,c). Analysis of figure 8.7 does not lead to the conclusion that separation of suspended-sediment samples by season improved the least-squares regression coefficients or showed any significance in suspended-sediment transport.

Sediment transport of the percent sand (>0.062 mm) in suspension versus discharge and sediment concentration were examined (fig. 8.8). Forty-nine samples of suspended- sediment samples, collected November 1991 through September 1995, were analyzed for percent sand. For all samples the average amount of sand in suspension was 13.5% +/- 12.6%, and varied from 1 to 52%. The percent of sand in suspension for all samples showed increasing sand percentage with increasing discharge and suspended-sediment concentrations, although the R^2 values were low (fig. 8.8a,b). Analysis for samples rising to the highest peak flow showed increasing sand percentage with increasing discharge, a high R^2 value, and a slightly higher slope (fig. 8.8c). A plot for samples falling from the highest peak flow showed increasing sand percentage with discharge and a high R^2 (0.62) (fig. 8.8d). The high percentage of silt and clay in suspension at Rio Piedras at El Senorial reflects both the soil textures in the basin, which are generally fine-grained, and human disturbance in the watershed leading to accelerated upland erosion.

Walling (1974) Sediment-Transport Curve Approach

Results using Walling's (1974) four independent variables of discharge, time relation of sample, base flow, and flood intensity, described in Chapter 4, are listed in Table 8.2. The dependent variables were separated into all samples, samples on the rising hydrograph to the

Reproduced with permission of the copyright owner. Further reproduction prohibited without permission.

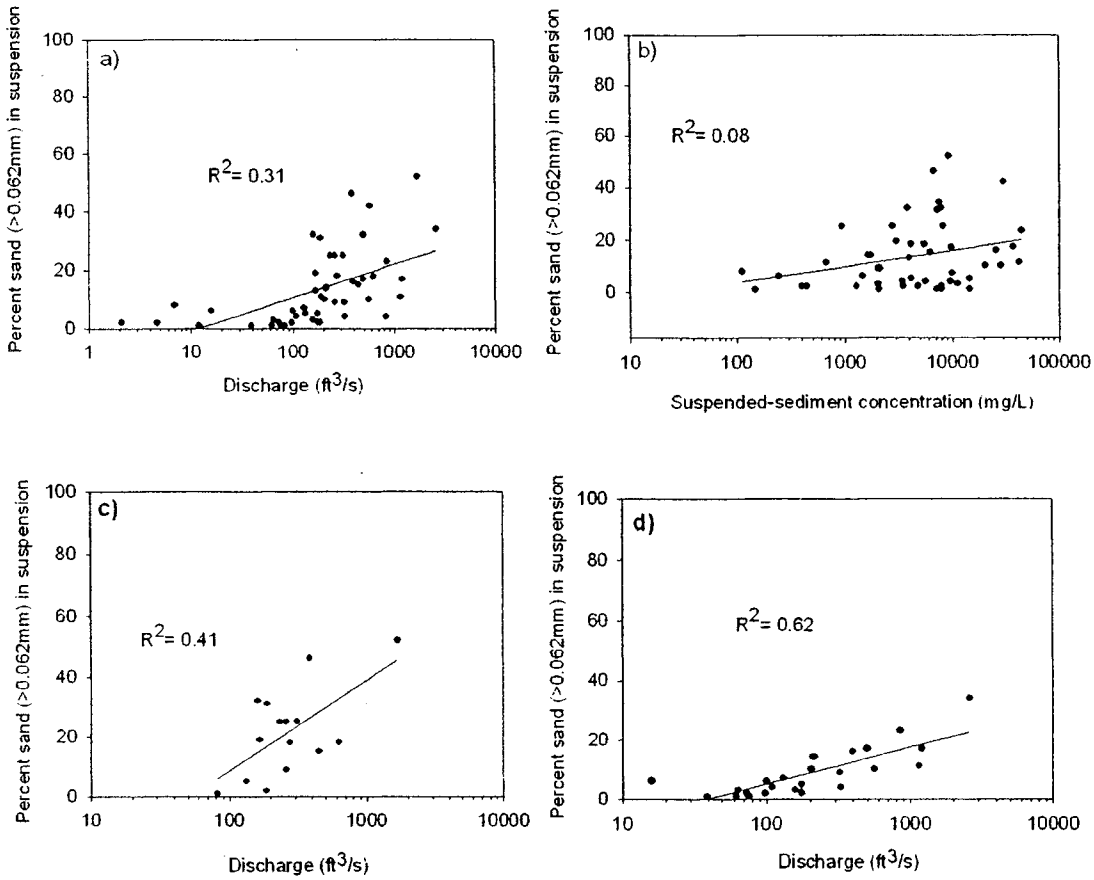

Figure 8.8. Sediment transport curves for the sand-size fraction of suspended sediment (>0.062mm). a) Discharge versus percent sand in suspension, b) suspended-sediment concentration versus percent sand in suspension, c) rising discharge versus percent sand in suspension, and d) rising samples suspended-sediment concentration versus percent sand in suspension.

highest peak flow, and samples on the falling hydrograph from the highest peak flow. Analysis included discharge with and without base flow. Results were similar for samples with and without base flow, and regression coefficients did not improve by separating samples into rising limb and falling limb discharge. For each analysis, the most important factor explaining suspended-sediment concentrations varied. For all sediment samples, discharge was the most important variable and had a positive slope (Table 8.2). For rising limb samples, base flow at the start of the event was

Reproduced with permission of the copyright owner. Further reproduction prohibited without permission.

Reproduced with permission of the copyright owner. Further reproduction prohibited without permission.

Table 8.2. Results of forward stepwise regression using Walling's (1974) four independent variables to explain dependent variable suspended-sediment concentration. Results with A) discharge including base flow and B) discharge minus base flow.

A)

Step	Independent variable using all samples (rising and falling)	R^2	Coefficient	Independent variable using rising samples	R^2	Coefficient	Independent variable using falling samples	R^2	Coefficient
Step one	Discharge	0.10	0.38	Base flow	0.12	0.50	Time relation of sample	0.19	-0.08
Step two	Base flow	0.13	0.39	Discharge	0.21	0.54	Discharge	0.21	0.19
	Discharge		0.29	Base flow		0.49	Time relation of sample		-0.06

B)

Step	Independent variable using all samples (rising and falling)	R^2	Coefficient	Independent variable using rising samples	R^2	Coefficient	Independent variable using falling samples	R^2	Coefficient
Step one	Base flow	0.11	0.36	Base flow	0.12	0.50	Time relation of sample	0.19	-0.08
Step two	Discharge	0.14	0.38	Discharge	0.21	0.50	Discharge	0.21	0.19
	Base flow		0.30	Base flow		0.53	Time relation of sample		-0.05

the most important variable and had a positive slope, indicating that base flow increased sediment transport. For falling samples, the time of the sample was most important and had a negative slope (Table 8.2) This implies that samples collected later in the event had low concentrations. In each analysis the R^2 values were generally low.

Statistical Results at Rio Piedras

Entire Event Analysis

This section describes the results of statistical analysis at-a-station for Rio Piedras at El Senorial using characteristics of the entire runoff event. From 10/01/1991 through 9/15/1995, 280 runoff events defined by a peak flow over 48 ft^3/s (1.36 m^3/s) occurred. Of these runoff events, 26 were sampled adequately to define suspended-sediment loads for the entire event (Table 8.3). Of these 26 events, 1 was defined as a complex event (Table 8.3).

The average suspended-sediment load for the 26 events was 1,430 tons (1,300 metric tons) (fig.8.9a). The maximum sediment load transported during the study period was 4,680 tons (4,240 metric tons) transported 5/1-5/3/1992 (Table 8.3). The runoff associated with this event, 2.48×10^7 ft^3 (7.02×10^5 m^3), was the second largest runoff event during the period of study associated with 2.3 inches (58 mm) of rainfall. The largest runoff event (2.48×10^7 ft^3, 7.76×10^5 m^3) during the study period (9/6 to 9/7/1995) transported 3,720 tons (3,380 metric tons) of sediment when 2.91 in (74 mm) of rain fell on the basin.

A plot of the discharge-weighted sediment concentration using runoff for each event over the period of study is shown in figure 8.10. There is considerable variation in the discharge-weighted sediment

Reproduced with permission of the copyright owner. Further reproduction prohibited without permission.

Reproduced with permission of the copyright owner. Further reproduction prohibited without permission.

Table 8.3. Summary of runoff events sampled adequately to determine suspended-sediment loads at Rio Piedras at El Senorial

(* Mnb = Complex event, n=number of complex event, a,b,c,etc = sequence of each event in the entire multiple event; a=1st event, b=2nd, c

Start Date	Start Time (hour)	Start Discharge (ft3/s)	End Date	End Time (hour)	Ending Discharge (ft3/s)	Event Duration (hour)	Number of Peaks in Event	Peak Flow (ft3/s)	Quickflow (ft3)	Runoff (ft3)	Suspended-Sediment Load	M=Part of Complex Event
3/28/1992	15.25	3.5	3/29/1992	4.00	8.6	12.8	1	1800	7286203	7564038	4302	
4/19/1992	12.00	4.1	4/20/1992	6.00	8.1	18.0	2	596	3870608	4264268	2051	
4/29/1992	17.25	2.1	4/30/1992	16.75	8.0	23.5	2	844	12340215	12767445	3696	
5/1/1992	16.75	2.6	5/3/1992	14.50	9.8	45.8	3	874	24788070	25809210	4679	
5/16/1992	11.00	2.8	5/17/1992	9.00	13.0	22.0	1	919	8409330	9035010	2960	
7/20/1992	10.75	6.4	7/21/1992	6.00	18.0	19.3	4	434	3499830	4345290	457	
8/5/1992	2.00	8.0	8/6/1992	10.50	23.6	32.5	1	1300	13428000	15278063	3306	
9/6/1992	13.25	6.8	9/6/1992	21.50	15.8	8.3	2	593	2924535	3260640	398	
9/23/1992	10.50	6.4	9/23/1992	21.00	16.0	10.5	2	718	2762820	3186180	349	
6/9/1993	11.25	7.6	6/9/1993	23.00	14.0	11.8	2	420	2871330	3328170	1348	
6/29/1993	17.00	8.4	6/30/1993	2.50	11.3	9.5	1	202	1424283	1760896	283	
9/6/1993	17.00	8.9	9/7/1993	6.00	11.0	13.0	1	1060	6763784	7229444	888	
1/11/1994	0.50	4.3	1/11/1994	19.25	9.6	18.8	3	214	3680422	4146560	526	
1/23/1994	14.25	6.0	1/24/1994	3.00	8.9	12.8	2	269	2663274	3003606	1187	
4/10/1994	7.50	3.2	4/10/1994	19.50	9.2	12.0	1	1292	6304760	6573773	244	
7/2/1994	8.83	3.7	7/2/1994	23.25	5.0	14.4	3	547	2661619	2889210	354	
11/19/1994	16.17	6.2	11/20/1994	2.50	8.9	10.3	1	1082	5661957	5942418	489	
12/1/1994	14.75	9.9	12/2/1994	3.75	18.1	13.0	1	249	2061697	2717894	80	
12/2/1994	11.25	13.3	12/3/1994	15.25	20.8	28.0	3	742	7339530	9055045	769	
2/25/1995	15.00	2.8	2/26/1995	23.75	18.1	32.8	1	2500	17727461	18507524	3358	M2a
5/15/1995	18.00	2.8	5/16/1995	2.75	3.9	8.8	1	767	2438436	2544198	453	
6/10/1995	11.50	1.5	6/10/1995	22.50	5.5	11.0	1	471	3249718	3387599	198	
6/15/1995	11.50	1.4	6/15/1995	21.25	4.4	9.8	2	388	1926114	2028512	186	
6/16/1995	12.50	2.0	6/16/1995	23.75	3.7	11.3	1	1134	4170431	4286447	483	
7/21/1995	17.50	1.5	7/22/1995	4.25	8.9	10.8	2	1039	5183263	5383249	497	
9/6/1995	3.75	3.9	9/7/1995	2.50	13.8	22.7	2	2965	27415546	28138203	3721	

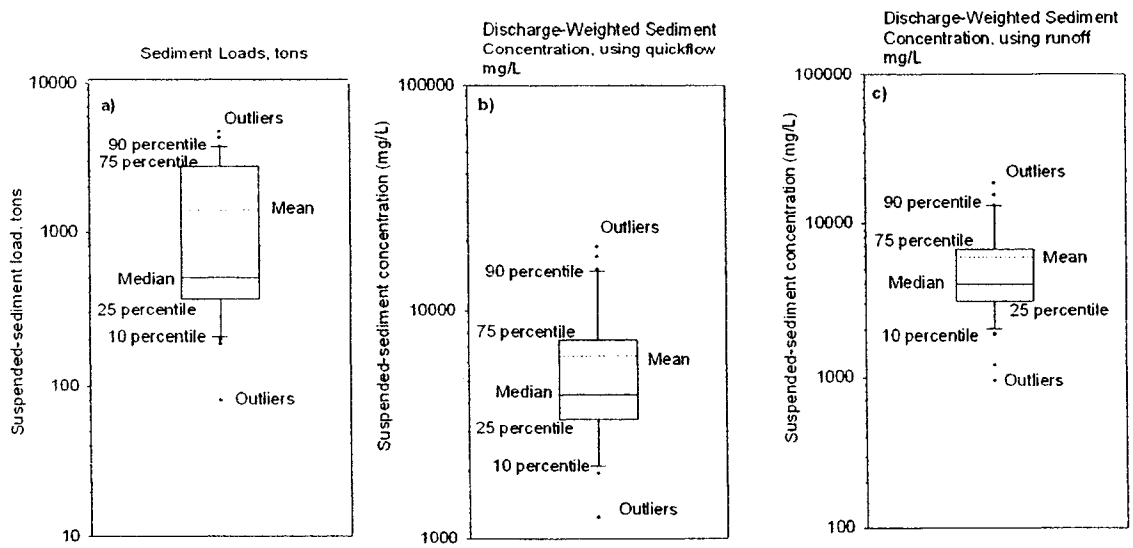

Figure 8.9. Box plot of dependent variables, a) sediment load, b) discharge-weighted sediment concentrations using quickflow and c) runoff, for Rio Piedras at El Senorial.

concentration, 944 to 18,220 mg/L (fig. 8.9; 8.10). The average discharge- weighted sediment concentration of all events using runoff was 5,380 mg/L (fig. 8.9c). The average discharge-weighted sediment concentration of all events using quickflow was 6,490 mg/L (fig. 8.9b). The maximum discharge-weighted sediment concentration, for both quickflow and runoff, 18,920 mg/L and 18,220 mg/L, respectively, occurred 3/28/99 to 3/29/1992.

The peak flow of the sampled events ranged from 202 to 2,965 ft^3/s (5.72 to 84.0 m^3/s). Quickflow for the 26 events ranged from $1.42x\ 10^6$ to $2.74\ x\ 10^7\ ft^3$ (4.03×10^4 to $7.76 \times 10^5\ m^3$) and runoff ranged from 1.76×10^6 to $2.81 \times 10^7\ ft^3$ (4.99×10^4 to $7.97 \times 10^5\ m^3$). Rainfall of the events ranged from 0.32 to 3.90 in (8.0 to 99.0 mm). A simple accounting of rainfall to quickflow can be made by assuming that the contributing area to the streamflow-gaging station (7.49 mi^2, 19.4 km^2) was impervious and calculating the volume of quickflow resulting from each rainfall event. The results of this comparison are listed in Appendix 8.1. Based on this comparison,

Reproduced with permission of the copyright owner. Further reproduction prohibited without permission.

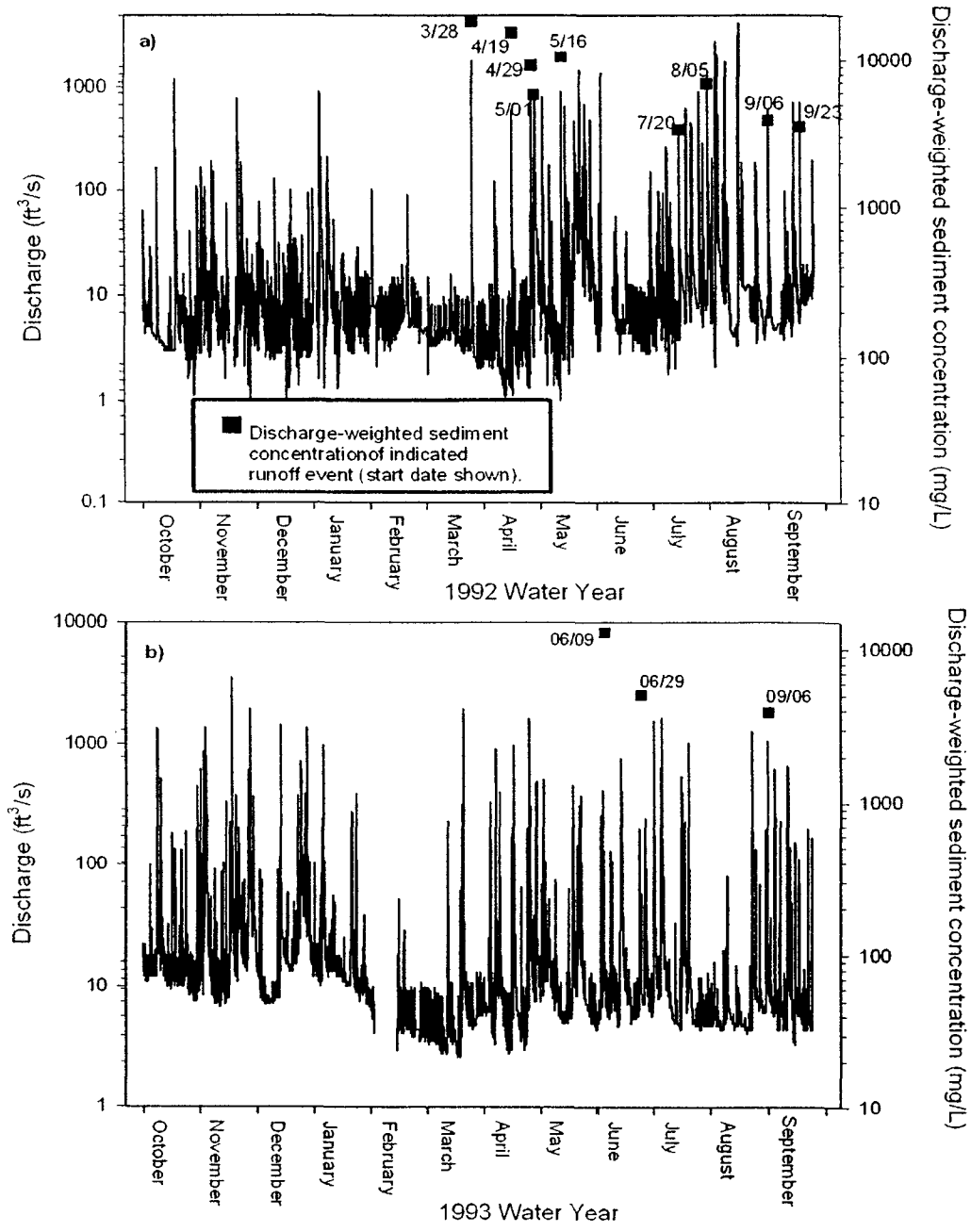

Figure 8.10. Instantaneous discharge and discharge-weighted sediment concentration for Rio Piedras at El Senorial for a) water year 1992 and b) water year 1993.

Reproduced with permission of the copyright owner. Further reproduction prohibited without permission.

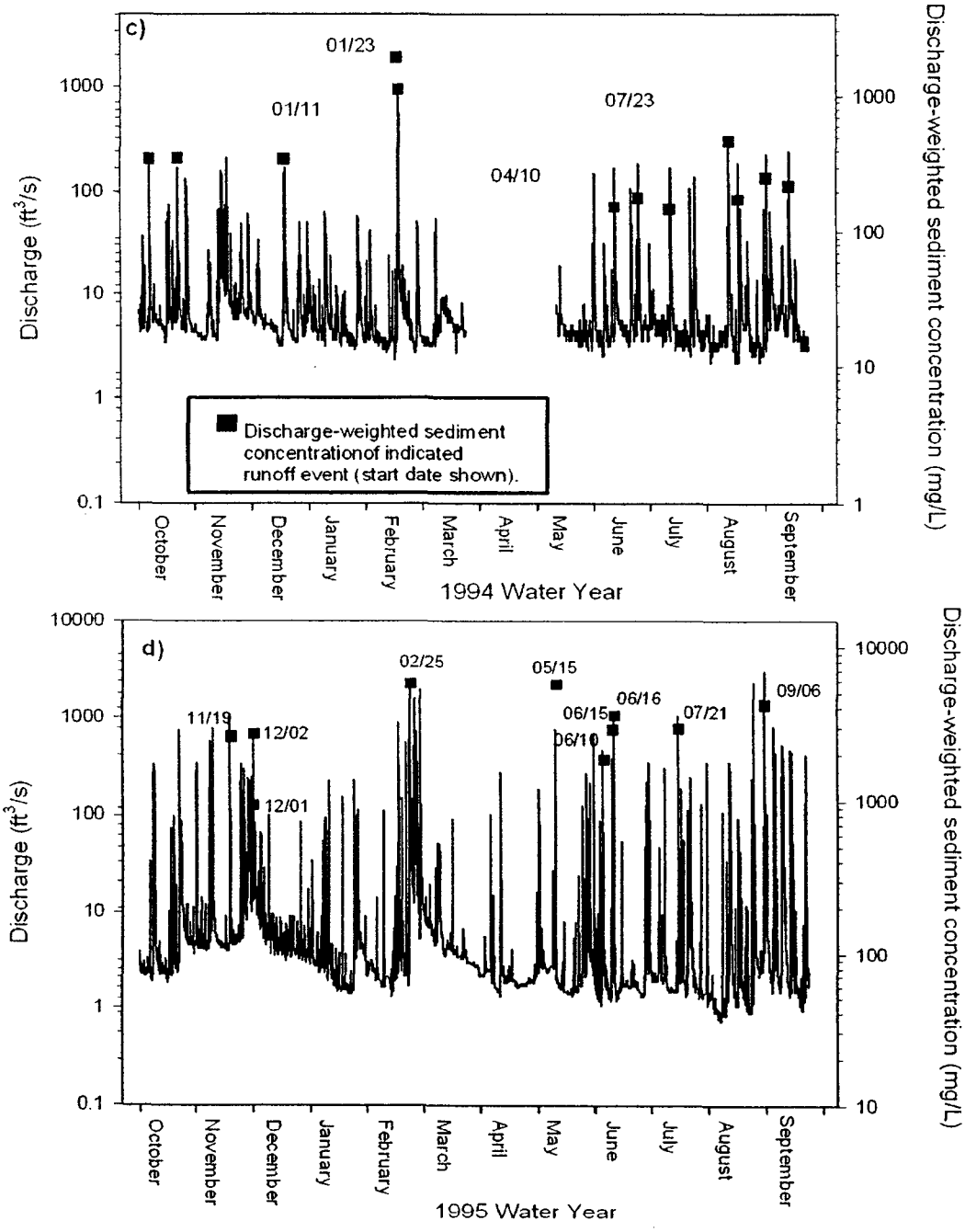

Figure 8.10. Instantaneous discharge and discharge-weighted sediment concentration for Rio Piedras at El Senorial for c)water year 1994 and d) water year 1995.

Reproduced with permission of the copyright owner. Further reproduction prohibited without permission.

9 to 71% of rainfall was quickflow with an average of 35% (Appendix 8.1). This range is related to a number of causes, including poor rainfall data and errors involved in the quickflow separation procedure used here.

Two dependent variables were used to described sediment for the entire storm event:

1) suspended-sediment load, in tons and

2) discharge-weighted sediment concentration (with and without quickflow), in mg/L

Histograms of the dependent variables indicated that a log transformation was necessary to obtain a normal distribution. Plots of runoff versus the two dependent variables are shown in figure 8.11. Suspended-sediment load had the best relation to runoff (R^2=0.61) (fig. 8.11a). This is in part a spurious relation because discharge is used in the calculation of suspended-sediment load. There is considerable scatter in runoff versus discharge-weighted sediment concentration (fig. 8.11a), implying that some factor(s) other than runoff were controlling sediment concentration.

The two dependent variables were tested against the independent variables shown in Table 4.8. Statistical analysis was performed against two portions of the runoff hydrograph:

1) the entire runoff event and

2) to the highest peak flow of the event.

Hydrographs were separated into quickflow and runoff. For the 26 storms that were adequately sampled, the base flow contribution was 3 to 24% of runoff.

Reproduced with permission of the copyright owner. Further reproduction prohibited without permission.

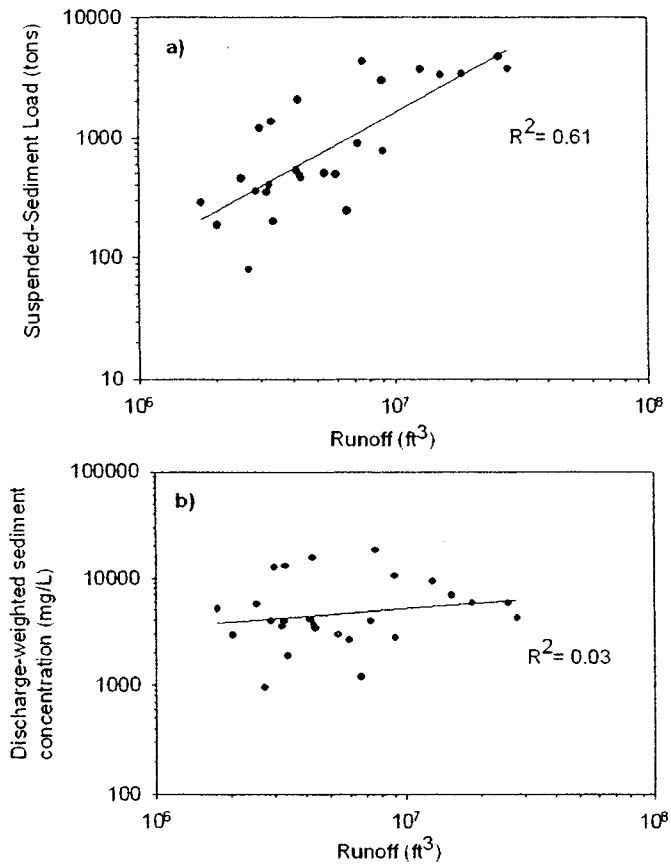

Figure 8.11. Plots of storm generated runoff versus a) suspended-sediment load and b) discharge-weighted sediment concentration for Rio Piedras at El Senorial.

Quickflow results (entire event)

The independent variables assembled to analyze the relation of suspended-sediment characteristics to quickflow characteristics are listed in Appendix 8.2. Tests for normality indicated that 18 of the 23 independent variables needed a log transformation (Appendix 8.2). Analysis of the correlation matrix showed a high correlation ($r>0.80$) among select variables (Appendix 8.3). Many of the characteristics of the previous event (20-LSPKBTI, 22-SMLSPKBS, 24-QULST, 26-PPTLSTI, 27-INTLST, 28-LS75OTI) and three previous events (29-SUM3PPTI, 30-

Reproduced with permission of the copyright owner. Further reproduction prohibited without permission.

QU3EVT) were correlated. Two of these variables (20-LSPKBTI, 27-INTLST) were removed. Current-event characteristics of 1-QUICK, 8-SMPKBS and 4-PKBS were intercorrelated; 4-PKBS was removed. Base flow (3-BASE) and runoff between events (17-RNBTWTI) were correlated but were left in because they were both perceived to be important.

Important relations of the dependent variables to the independent variables that were observed in the correlation matrix are: suspended-sediment load to quickflow (1-QUICK) and to the sum of peak flows minus base flow (8-SMPKBS) (fig. 8.12). There were no significant relations observed using the discharge-weighted sediment concentration.

Forward stepwise regression (entire event, quickflow)

Results of forward stepwise regression on the 20 remaining independent variables against the two dependent variables are listed in Table 8.4. In forward stepwise regression using suspended-sediment, only one variable, quickflow (1-QUICK), was significant. In the analysis using the discharge-weighted sediment concentration, no variables were significant. The probability for F-to-enter and F-to-remove was increased to 0.10 for these two analyses and more variables were found to be significant (Table 8.4). Quickflow (1-QUICK) was significant in the first step and the sum of the previous-event peak flows (22-SMLSPKBS) was important in the second step in explaining the suspended-sediment load. The best-fit regression line indicated a direct relation with quickflow and an inverse relation with the sum of the previous-event peak flows, indicating that previous-event peak flows flushed sediment.

In forward stepwise regression analysis using the independent variable discharge-weighted sediment concentration, the precipitation between events (18-PPTBTW) was important in the first

Reproduced with permission of the copyright owner. Further reproduction prohibited without permission.

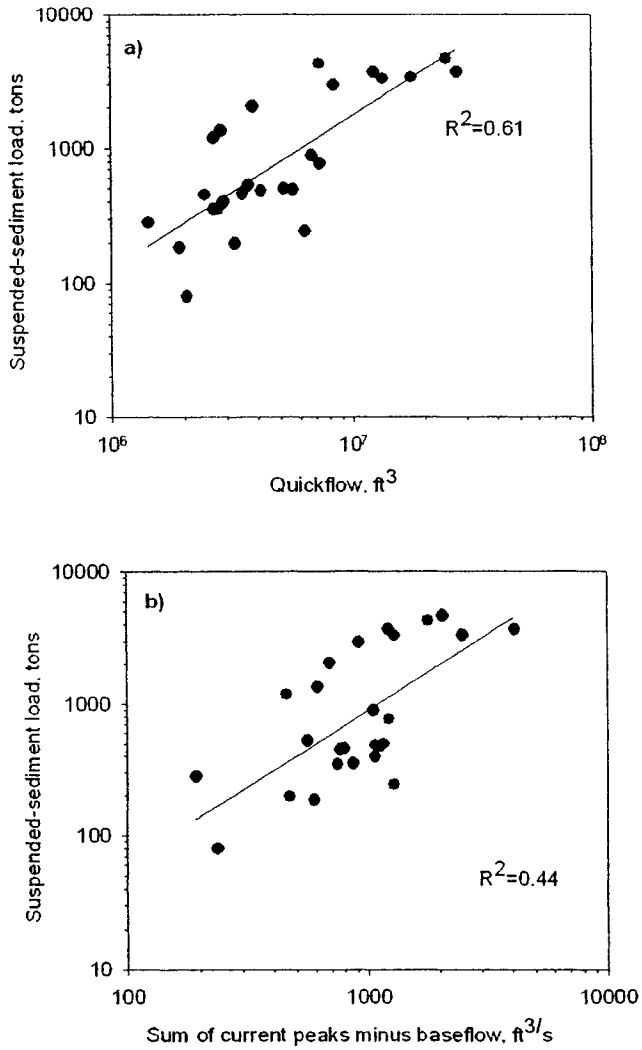

Figure 8.12. Graphical relations at Rio Piedras at El Senorial of independent variables with highest R^2 values using quickflow characteristics of the entire event against dependent variables. a) quickflow versus suspended-sediment load and b) the sum of current peak flow minus base flow versus suspended-sediment load There were no significant relations observed using the discharge-weighted sediment concentration.

step of forward stepwise regression and the previous-event sum of peak flows (22-SMLSPKBS) was significant in the second step (Table 8.4). The slope of the best-fit regression line for the precipitation between events (18-PPTBTW) and the previous-event sum of peak flows (22-SMLSPKBS) was negative, indicating an inverse relation to the discharge-weighted sediment concentration. In the third step of forward stepwise regression, using the discharge-weighted

Reproduced with permission of the copyright owner. Further reproduction prohibited without permission.

sediment concentration as the dependent variable, the rainfall intensity between events (19-INTBET) was significant and the slope of the best-fit regression line was positive, indicating a direct correlation to the discharge-weighted sediment concentration. Interpretations from multiple regression analysis on the independent variables indicated that the previous-event peak flows and the rainfall between events flushed sediment. Rainfall intensity between events supplied sediment

Table 8.4. Results of forward stepwise regression for entire event using quickflow characteristics

Dependent Variable	Step	Variables in the Model	R^2	F Statistic	Coefficient	Constant
suspended-sediment load, tons *	One	1-QUICK	0.61	38.2	1.14	-4.7
	Two	22-SMLSPKBS	0.67	3.75	-0.16	-5.1
		1-QUICK		46.0	1.21	
	Three	18-PPTBTW	0.74	6.54	-0.20	-5.1
		22-SMLSPKBS		7.36	-0.20	
		1-QUICK		47.1	1.12	
discharge-weighted sediment concentration, mg/L *	One	18-PPTBTW	0.13	3.64	-0.15	3.2
	Two	22-SMLSPKBS	0.34	7.09	-0.20	3.2
		18-PPTBTW		7.82	-0.20	
	Three	19-INTBET	0.44	4.30	0.08	3.5
		22-SMLSPKBS		11.1	-0.24	
		18-PPTBTW		9.86	-0.22	

.* *The probability for F-to-enter and F-to-remove was increased to 0.10*

Factor analysis - Quickflow

Principal component analysis was performed on two sets of independent variables associated with quickflow characteristics of the event. One set contained 23 independent variables, including quickflow; the other set did not include quickflow (Appendices 8.4, 8.5). Six

Reproduced with permission of the copyright owner. Further reproduction prohibited without permission.

components were selected for factor analysis. Factor analysis for the data set with and without the variable quickflow showed similar results. Over 65% of the variance is explained by the first three axes. Forward stepwise regression was performed on the factor scores from principal components analysis against the two dependent variables (Table 8.5). Using suspended-sediment load as a dependent variable indicated PC2 as the most significant principal component in the first step of forward stepwise regression and PC1 in the second step (Table 8.5). PC2 had strong loadings (> 0.7) on characteristics of the current event (1-QUICK, 4-PKBS, 8-SMPKBS, 13-RRISE) (Appendix 8.4). The coefficient of regression was positive, indicating a direct relation of characteristics of the current event to suspended-sediment load.

Table 8.5. Results of forward stepwise regression on the principal components for the entire event using quickflow characteristics.

Dependent Variable	Step	Variables in the Model	R^2	F Statistic	Coefficient	Constant
suspended-sediment load, tons	One	PC2	0.46	20.1	0.34	2.90
	Two	PC4	0.56	5.36	-0.16	2.90
		PC2		23.7	0.34	
discharge weighted sediment concentration, mg/L	One	None				

PC4 was significant in the second step of forward stepwise regression (Table 8.5) and had a high positive loading (0.62) on current-event rainfall intensity (12-SFIVE) (Appendix 8.4). The slope of the best fit line was negative, indicating an inverse relation between rainfall intensity and suspended-sediment load. This statistical result is difficult to interpret. Increases in rainfall intensity are usually associated with increased erosion. Using the discharge-weighted sediment concentration as a dependent variable with a significance level of 0.05 or 0.10 did not show any

Reproduced with permission of the copyright owner. Further reproduction prohibited without permission.

significant variables. Interpretations from principal components analysis only showed current-event characteristics (quickflow, peak flow, and rainfall) as being significant in Rio Piedras. Rainfall intensity was significant and was inversely correlated to suspended-sediment load.

Varimax rotation (entire event, quickflow)

The principal components axes were rotated using the varimax rotation. The factor scores were saved after varimax rotation and forward stepwise regression was performed on the factor scores against the dependent variables (Table 8.6). The dependent variable, suspended-sediment load, showed the same results as without varimax rotation; namely that PC2 was the most important principal component explaining the dependent variable. PC2 had strong positive loadings (>0.79) on characteristics of the current event (1-QUICK, 4-PKBS, 8-SMPKBS,10-RAIN, 11-INT15) (Appendix 8.6).

Table 8.6. Results of forward stepwise regression on the principal components after varimax rotation for the entire event using quickflow characteristics.

Dependent Variable	Step	Variables in the Model	R^2	F Statistic	Coefficient	Constant
suspended sediment load, tons	One	PC2	0.46	20.7	0.34	2.90
	Two	PC5	0.56	5.38	0.16	2.90
		PC2		24.5	0.34	
discharge-weighted sediment concentration, mg/L *	Step One	PC1	0.14	3.86	-0.12	3.70

* *The probability for F-to-enter and F-to-remove was increased to 0.10*

Using suspended-sediment load as a dependent variable showed PC5 as important in the second step (Table 8.6). PC5 had a high positive loading (0.79) on hysteresis (Appendix 8.6) and

Reproduced with permission of the copyright owner. Further reproduction prohibited without permission.

the slope of the best-fit regression line was positive, indicating that clockwise hysteresis loops were directly correlated with suspended-sediment loads. This implied that clockwise hysteresis loops had high suspended-sediment loads. PC5 had a high negative loading (-0.79) on the precipitation between events and was inversely correlated to the suspended-sediment load indicating that rainfall between events flushed sediment.

Using the discharge-weighted sediment concentration as a dependent variable did not show any significant variables at a probability to enter of 0.05. The probability to enter was increased to 0.10 and PC1 was shown to be significant (Table 8.6). PC1 had high positive loadings (>0.8) on characteristics of the previous event ((20-LSPKBTI, 22-SMLSPKBS, 24-QULST, 26-PPTLSTI, 27-INTLST, 28-LS75OTI) (Appendix 8.7). The coefficient of the best-fit regression line was negative, indicating that previous events were inversely correlated to the discharge-weighted sediment concentration, although the R^2 value was very low (0.14). Afer varimax rotation, the significant variables still remained as current-event characteristics (quickflow, peak flow, and rainfall) and rainfall intensity was not found to be significant. Using the discharge-weighted sediment concentration showed that previous events flushed sediment, although the correlation coefficient was low.

Runoff Results (entire event)

The independent variables assembled to analyze the relation of suspended-sediment characteristics to runoff characteristics are listed in Appendix 8.8. Tests for normality using the residuals indicated that 18 of the 23 independent variables required a log transformation (Appendix 8.8). Analysis of the correlation matrix showed a high correlation (r>0.80) among select variables

Reproduced with permission of the copyright owner. Further reproduction prohibited without permission.

(Appendix 8.9). Many of the characteristics of the previous event (21-LSPKTI, 23-SMLSPK, 25-RULST, 26-PPLSTI, 27-INTLST) were correlated. Two of these variables (20-LSPKBTI, 27-INTLST) were removed. Current-event characteristics of 2-RUN, 9-SMPK and 5-PK, were intercorrelated; 5-PK was removed. Base flow (3-BASE) and runoff between events (17-RNBTWTI) were correlated but were left in because they were both perceived to be important. Important relations of the dependent variables to the independent variables that were observed in the correlation matrix are: suspended-sediment load to runoff (2-RUN) (fig. 8.11a).

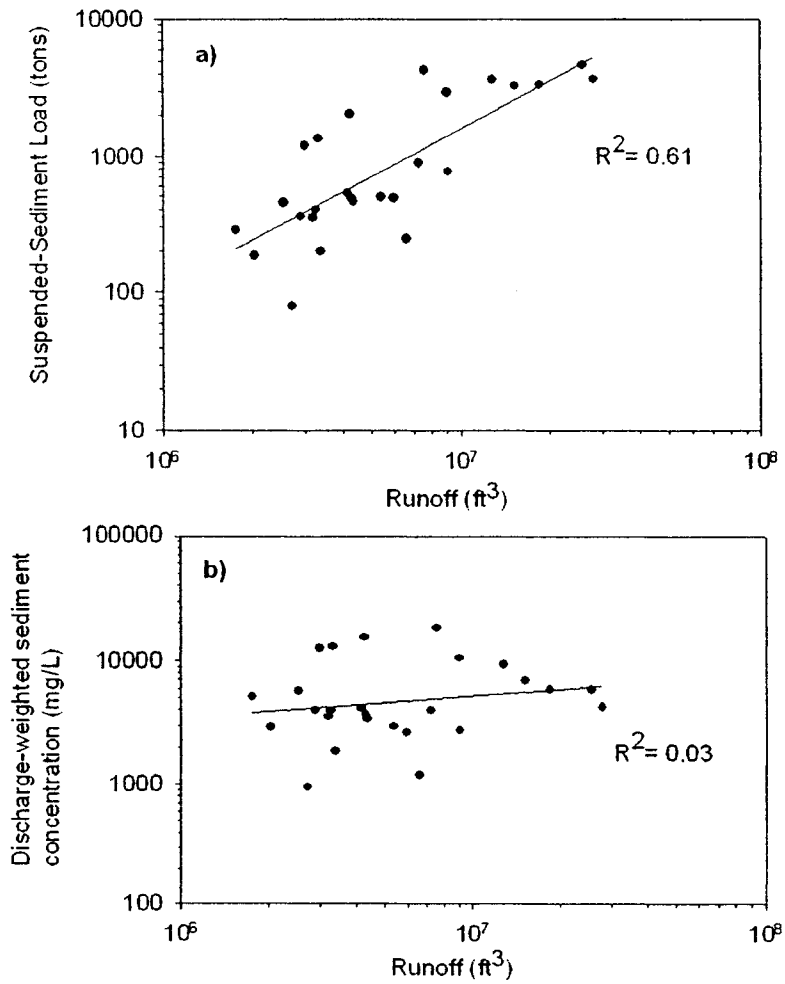

Figure 8.11. Plots of storm generated runoff versus a) suspended-sediment load and b) discharge-weighted sediment concentration for Rio Piedras near El Senorial.

Reproduced with permission of the copyright owner. Further reproduction prohibited without permission.

Forward stepwise regression (entire event, runoff)

Results of forward stepwise regression on the remaining 20 independent variables against the two dependent variables are listed in Table 8.7. In forward stepwise regression using suspended-sediment load, runoff (2-RUN) was significant in the first step of forward stepwise regression and the slope of the regression was positive. In the second step, the rainfall of the previous event (26-PPTLSTI) was significant and the slope of the regression line was negative, indicating an inverse relation between rainfall of the previous event and suspended-sediment load (Table 8.7).

Table 8.7. Results of forward stepwise regression for entire event using runoff characteristics.

Dependent Variable	Step	Variables in the Model	R^2	F Statistic	Coefficient	Constant
suspended-sediment load, tons	One	2-RUN	0.61	37.1	1.18	-5.0
	Two	26-PPTLSTI	0.67	4.54	-0.19	-5.7
		2-RUN		44.7	1.21	
discharge-* weighted sediment concentration, mg/L	One	18-PPTBTW	0.15	4.11	-0.16	3.15
	Two	23-SMLSPK	0.37	8.14	-0.21	3.10
		18-PPTBTW		9.07	-0.22	
	Three	19-INTBET	0.46	3.69	0.08	3.37
		23-SMLSPK		11.0	-0.23	
		18-PPTBTW		9.90	-0.22	

.* *The probability for F-to-enter and F-to-remove was increased to 0.10*

In forward stepwise regression analysis using discharge-weighted sediment concentration, no significant variables were found at a probability of 0.05. The probability was increased to 0.10 and the rainfall on the rising limb of the hydrograph (13-RRISE) became significant, although the

Reproduced with permission of the copyright owner. Further reproduction prohibited without permission.

R^2 value was low (0.13) (Table 8.7). The slope of the regression was positive, indicating a direct relation between the rainfall on the rising limb and suspended-sediment load. In the second step of forward stepwise regression, the precipitation between events (18-PPTBTW) was significant and the slope was negative, indicating an inverse relation of precipitation between events to suspended-sediment load.

Factor analysis - (entire event, runoff)

Principal component analysis was performed on two sets of independent variables associated with quickflow characteristics of the event. One set contained 23 independent variables, including quickflow, the other set did not include runoff (Appendices 8.10, 8.11). Six components were selected for factor analysis.

Factor analysis for the data set with and without the variable runoff had similar results. Over sixty-five percent of the variance was explained by the first three axes. Forward stepwise regression was performed on the factor scores from principal components analysis against the two dependent variables (Table 8.8). Using suspended-sediment load as a dependent variable showed similar results as in the quickflow analysis and indicated PC2 was significant in the first step of forward stepwise regression (Table 8.8). PC2 had high loadings (>0.7) on characteristics of the current event (2-RUN, 5-PK, 9-SMPK, 10-RAIN, 11-INT15) (Appendix 8.10). The coefficient of the regression was positive, indicating a direct relation of the characteristics of the current event to suspended-sediment load. Similar to the results using quickflow, PC5 was significant in the second step of forward-stepwise regression. PC5 had a high loading (0.61) on rainfall intensity (12-SFIVE) (Appendix 8.10). The coefficient was negative, indicating that as rainfall intensity

Reproduced with permission of the copyright owner. Further reproduction prohibited without permission.

increased the suspended-sediment load decreased. Using discharge-weighted sediment concentration did not show any significant variables at an alpha of 0.05 or 0.10.

Table 8.8. Results of forward stepwise regression on the principal components for the entire event using runoff characteristics.

Dependent Variable	Step	Variables in the Model	R^2	F Statistic	Coefficient	Constant
suspended-sediment load, tons	One	PC2	0.46	20.2	0.34	2.90
	Two	PC4	0.56	5.09	-0.16	2.90
		PC2		23.7	0.34	
discharge-weighted sediment concentration, mg/L	One	none				

Principal components analysis using both quickflow and runoff with the dependent variable suspended-sediment load showed that only current-event characteristics of runoff, peak flow, and rainfall were significant in Rio Piedras. Rainfall intensity was significant and was inversely correlated to suspended-sediment load.

Varimax rotation (entire event, runoff)

The principal components axes were rotated using the varimax rotation. The factor scores were saved after varimax rotation and forward stepwise regression was performed on the factor scores against the dependent variables (Table 8.9). The dependent variable suspended-sediment load showed the same results as without varimax rotation; that PC2 was the most important principal component explaining the dependent variable. PC2 had high loadings (>0.7) on characteristics of the current event (2-RUN, 5-PK, 9-SMPK, 10-RAIN, 13-RRISE) (Appendix

Reproduced with permission of the copyright owner. Further reproduction prohibited without permission.

8.12). The coefficient of the regression was positive, indicating a direct relation for characteristics of the current event to suspended-sediment load.

Table 8.9. Results of forward stepwise regression on the principal components after varimax rotation for the entire event using runoff characteristics.

Dependent Variable	Step	Variables in the Model	R^2	F Statistic	Coefficient	Constant
suspended-sediment load, tons	One	PC2	0.46	20.7	0.34	2.90
	Two	PC5	0.57	5.42	-0.16	2.90
		PC2		24.6	0.34	
discharge- * weighted sediment concentration, mg/L	One	PC1	0.14	3.98	-0.12	3.66

* *The probability for F-to-enter and F-to-remove was increased to 0.10*

Using the discharge-weighted sediment concentration as a dependent variable did not indicate any significant variables at a probability to enter of 0.05. The probability to enter was increased to 0.10 and PC1 was shown to be significant (Table 8.9). PC1 had high positive loadings (>0.8) on characteristics of the previous event ((21-LSPKTI, 22-SMLSPKBS, 25-RULST, 26-PPTLSTI, 27-INTLST, 28-LS75OTI) (Appendix 8.12). The coefficient of the best-fit regression line was negative, indicating that previous events are inversely correlated to the discharge-weighted sediment concentration, although the R^2 value is very low (0.14).

After varimax rotation the significant variables still remained as current-event characteristics (runoff, peak flow, and rainfall) and rainfall intensity was not found to be significant. Using the discharge-weighted sediment concentration showed that previous events flushed sediment, although the correlation coefficient was low.

Reproduced with permission of the copyright owner. Further reproduction prohibited without permission.

Discussion

For the entire event, separating storm events into quickflow did not improve the statistical significance or interpretations of the controlling variables. Suspended-sediment load showed more significance as a dependent variable than the discharge-weighted sediment concentration. This is in part related to discharge being used in the calculation of suspended-sediment loads and many of the independent variables are correlated to discharge. Multiple-regression analysis of the independent variables showed the current-event characteristic of runoff as important and directly correlated to the two dependent variables. Sum of previous peak flows and previous rainfall were inversely correlated to the dependent variables and flushed sediment. Rainfall intensity between events supplied sediment and rainfall between events flushed sediment.

In forward stepwise regression of the independent variables using quickflow and runoff, suspended-sediment load was the only dependent variable that showed significant results. Current-event characteristics of quickflow, peak flow, and rainfall were directly correlated to suspended-sediment load and rainfall intensity was inversely correlated to suspended-sediment load. After varimax rotation, results indicated clockwise hysteresis loops had high suspended-sediment loads. After varimax rotation, using the discharge-weighted sediment as a dependent variable showed previous-event characteristics (quickflow, runoff, peak flows, rainfall) were significant, although the R^2 values were low.

Highest peak flow analysis

This section describes the results of statistical analysis at-a-station for Rio Piedras at El Senorial using characteristics measured to the highest peak flow of the event. A summary of the 26 storms sampled adequately to the highest peak flow are listed in Table 8.10.

Reproduced with permission of the copyright owner. Further reproduction prohibited without permission.

Two dependent variables were used to described sediment to the highest peak flow:

1) suspended-sediment load, in tons and

2) discharge-weighted sediment concentration, in mg/L

Histograms of the dependent variables showed that suspended-sediment load and the discharge-weighted sediment concentration have a better normal distribution with a log transformation.

The average suspended-sediment load for the 26 events was 430 tons (390 metric tons) (fig.8.13a). The average discharge-weighted sediment concentration using quickflow was 6,870 mg/L (fig 8.13b). The average discharge-weighted sediment concentration using runoff was 6,400 mg/L (fig 813c). The maximum discharge-weighted sediment concentration for quickflow (29,650 mg/L) occurred for the runoff event on 2/25/1995 and the maximum discharge-weighted sediment concentration using runoff (19,970 mg/L) occurred on 6/9/1993.

Quickflow Results (highest peak)

The independent variables assembled to analyze the relation of suspended-sediment characteristics to quickflow characteristics for the portion of the hydrograph rising to the highest peak flow are listed in Appendix 8.14. Tests for normality indicated that 14 of the 17 independent variables needed a log transformation (Appendix 8.14). Analysis of the correlation matrix showed the same results as for the entire event (Appendix 8.15). Variables that were removed included (20-LSPKBTI, 27-INTLST).

Reproduced with permission of the copyright owner. Further reproduction prohibited without permission.

Reproduced with permission of the copyright owner. Further reproduction prohibited without permission.

Table 8.10. Summary of runoff events sampled adequately to the highest peak of the event at Rio Piedras at El Senorial

Start Date	Start Time	Start discharge (ft3/s)	End Date	End Time	End discharge (ft3/s)	Peak flow (ft3/s)	Total quickflow (ft3)	Runoff (ft3)	Suspended-sediment load (tons)	Discharge-weighted sediment concentration Quickflow mg/L	Discharge-weighted sediment concentration Runoff mg/L
3/28/1992	15.25	3.50	3/28/1992	16.25	1800	1800	1248015	1261350	244	6263	6197
4/19/1992	12.00	4.10	4/19/1992	12.75	596	596	404893	416745	84.2	6659	6470
4/29/1992	17.25	2.10	4/29/1992	21.00	844	844	3342140	3376845	419	4020	3979
5/1/1992	16.75	2.60	5/1/1992	23.50	874	874	10161053	10266300	2939	9266	9171
5/16/1992	11.00	2.80	5/16/1992	12.25	919	919	1591606	1605510	506	10191	10102
7/20/1992	10.75	6.40	7/20/1992	17.00	434	434	1231790	1418160	113	2936	2550
8/5/1992	2.00	8.00	8/6/1992	2.5	1300	1300	1162584	1177200	376	10355	10226
9/6/1992	13.24	6.97	9/6/1992	14.75	593	593	1629243	1671593	220	4317	4208
9/23/1992	10.50	6.40	9/23/1992	13.25	718	718	1046674	1122480	121	3702	3452
6/9/1993	11.25	7.60	6/9/1993	13.00	420	420	743487	794370	495	21337	19970
6/29/1993	17.00	8.40	6/29/1993	17.75	202	202	232793	255780	26.8	3686	3355
9/6/1993	17.00	8.90	9/6/1993	17.75	1060	1060	1272211	1296405	257	6470	6349
1/11/1994	0.50	4.25	1/11/1994	3.75	214	214	208858	263971	11.6	1783	1411
1/23/1994	14.25	5.97	1/23/1994	15.50	269	269	711734	739219	248	11173	10757
4/10/1994	7.50	3.25	4/10/1994	10.50	1292	1292	2908709	2951826	139	1535	1513
7/2/1994	8.83	3.72	7/2/1994	10.25	547	547	942919	962231	120	4066	3985
11/19/1994	16.17	6.22	11/19/1994	16.75	1082	1082	1133604	1146812	84.9	2399	2371
12/1/1994	14.75	9.93	12/1/1994	15.25	249	249	309357	327508	14.9	1541	1455
12/2/1994	11.25	13.28	12/2/1994	13.25	742	742	2116940	2214472	255	3855	3685
2/25/1995	15.00	2.82	2/25/1995	16.00	2500	2500	2754361	4946953	2549	29650	16508
5/15/1995	18.00	2.82	5/15/1995	19.25	767	767	373960	387010	167	14282	13801
6/10/1995	11.50	1.47	6/10/1995	13.00	471	471	1134875	1144302	70.4	1988	1971
6/15/1995	11.50	1.40	6/15/1995	12.00	388	388	412629	415280	49.9	3871	3847
6/16/1995	12.50	2.01	6/16/1995	13.50	1134	1134	1647268	1654771	169	3277	3262
7/21/1995	17.50	1.47	7/21/1995	20.50	1039	1039	1871793	1898827	198	3385	3337
9/6/1995	3.75	3.89	9/6/1995	7.00	2874	2965	6334457	6388229	1310	6623	6567

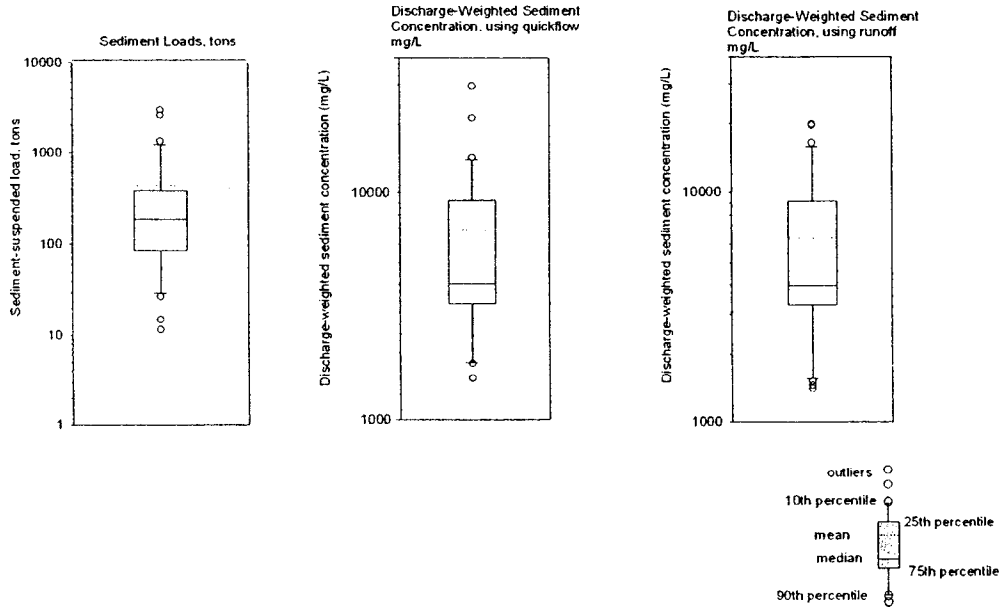

Figure 8.13. Box plot of dependent variables to the highest peak flow, a) sediment load, b) discharge-weighted sediment concentrations using quickflow, and c) discharge-weighted sediment concentration using runoff.

Important relations of the dependent variables to the independent variables that were observed in the correlation matrix are suspended-sediment load to quickflow (1-QUICK) and to peak flow (4-PKBS) (Appendix 8.15). The discharge-weighted sediment concentration did not show any significant relation to the independent variables (Appendix 8.15).

Forward stepwise regression (highest peak, quickflow)

Results of forward stepwise regression on the remaining 15 independent variables against the two dependent variables are listed in Table 8.11. The rainfall between events was significant in either the first or second step of forward stepwise regression for both dependent variables (Table 8.11). In all cases the coefficient of the regression equation was negative, indicating that the rainfall

Reproduced with permission of the copyright owner. Further reproduction prohibited without permission.

between events was inversely correlated to suspended-sediment load and discharge-weighted sediment concentration (Table 8.11). Using sediment load as a dependent variable indicated quickflow was significant in the first step of forward stepwise regression and the coefficient was positive (Table 8.11).

Table 8.11. Results of forward stepwise regression measured to the highest peak flow of the event using quickflow characteristics.

Dependent Variable	Step	Variables in the Model	R^2	F Statistic	Coefficient	Constant
suspended-sediment load, tons	One	QUICK	0.67	49.3	1.15	-4.72
	Two	PPTBTW	0.73	4.59	-0.19	-4.75
		QUICK		44.4	1.06	
discharge-weighted sediment concentration, mg/L	One	PPTBTW	0.19	5.64	-0.20	3.08

Factor analysis (highest peak, quickflow)

Principal component analysis was performed on two sets of independent variables associated with quickflow characteristics of the event. One set was used in forward stepwise regression against the dependent variable, suspended-sediment load (Appendix 8.16), and the other set was used in forward stepwise regression against discharge-weighted sediment concentration (Appendix 8.17). Four components were selected for factor analysis.

Both sets of factor analysis had similar results. Over 70% of the variance was explained by the first three axes. Using suspended-sediment load showed PC2 as significant in the first step of forward stepwise regression and PC5 in the second step (Table 8.12). PC2 had high positive loadings (> 0.7) on characteristics of the current event (1-QUICK, 11-INT15, 4-PKBS)

Reproduced with permission of the copyright owner. Further reproduction prohibited without permission.

(Appendix 8.16). The coefficient of regression was positive, indicating that suspended-sediment load was correlated directly with PC2. PC5 was significant in the second step of forward stepwise regression and had a high negative loading (<-0.9) on the rainfall between events (18-PPTBTW). The slope of the line of best fit was positive, indicating that suspended-sediment load was inversely correlated with the rainfall between events.

Using the discharge-weighted sediment concentration as a dependent variable indicated that PC2 was significant in the first step of forward stepwise regression although the R^2 value was low (0.16) (Table 8.12). PC2 had high positive loadings (> 0.7) on characteristics of the current event (6-MXTMJPK, 11-INT15, 4-PK) (Appendix 8.17). The coefficient of regression was positive, indicating that discharge-weighted sediment concentration was correlated directly with characteristics of the current event. Interpretations from factor analysis indicated that current-event characteristics of quickflow, peak flow, and rainfall intensity increases suspended-sediment loads and concentrations, and rainfall between events flushed sediment.

Table 8.12. Results of forward stepwise regression on the principal components measured to the highest peak flow of the event using quickflow characteristics.

Dependent Variable	Step	Variables in the Model	R^2	F Statistic	Coefficient	Constant
suspended-sediment load, tons	One	PC2	0.55	30.5	0.43	2.26
	Two	PC5	0.68	8.72	-0.20	2.26
		PC2		40.4	0.43	
discharge-weighted sediment concentration, mg/L	One	PC2	0.19	5.56	0.15	3.70

Reproduced with permission of the copyright owner. Further reproduction prohibited without permission.

Varimax rotation (peak flow, quickflow)

The principal components axis were rotated using the varimax rotation. The factor scores were saved after varimax rotation and forward stepwise regression was performed on the factor scores against the dependent variables (Table 8.13) (Appendices 8.18, 8.19). The dependent variable suspended-sediment load showed that PC2 was important in the first step of forward stepwise regression. PC2 had high loadings (>0.6) on characteristics of the current event (1-QUICK, 13-RRISE) (Appendix 8.18) and the coefficient of regression was positive, indicating a direct correlation with suspended-sediment load. PC5 was significant in the second step of forward stepwise regression and had a high positive loading (<-0.9) on the precipitation between events (18-PPTBTW) (Appendix 8.18). The coefficient of regression was positive, indicating that the precipitation between events was inversely correlated to suspended-sediment load.

Table 8.13. Results of forward stepwise regression on the principal components after varimax rotation to the highest peak flow using quickflow characteristics.

Dependent Variable	Step	Variables in the Model	R^2	F Statistic	Coefficient	Constant
suspended-sediment load, tons	One	PC2	0.54	28.8	0.43	2.26
	Two	PC5	0.71	13.0	0.23	2.26
		PC2		43.3	0.43	
discharge-weighted sediment concentration, mg/L	One	PC4	0.21	6.22	0.15	3.70

The dependent variable, discharge-weighted sediment concentration, showed that PC4 was significant in the first step of forward stepwise regression (Table 8.13). PC4 had a high negative loading (<-0.9) on the precipitation between events (18-PPTBTW) (Appendix 8.19) and

Reproduced with permission of the copyright owner. Further reproduction prohibited without permission.

the regression coefficient was positive, indicating an inverse relation of sediment concentration to the rainfall between events. Results after varimax rotation were similar to results before rotation and indicated that suspended-sediment load and discharge-weighted sediment concentration were directly correlated to current-event characteristics and inversely correlated to between-event rainfall.

Runoff Results (highest peak)

The independent variables assembled to analyze the relation of suspended-sediment characteristics to runoff characteristics for the portion of the hydrograph rising to the highest peak flow are listed in Appendix 8.20. Tests for normality using the residuals indicated that 12 of the 17 independent variables required a log transformation (Appendix 8.20).

Analysis of the correlation matrix showed a high correlation ($r>0.80$) among select variables (Appendix 8.21). Variables that showed a high correlation among each other were related to the previous event or the three previous events (25-RULST, 23-SMLSPK, 26-PPTLSTI, 27-INTLST, 28-LS75OTI, and 21-LSPKTI (Appendix 8.21). Two of these variables (20-LSPKTI, 27-INTLST) were removed. Significant relations of the dependent variables to the independent variables that were observed in the correlation matrix are the suspended-sediment load to runoff (2-RUN) and to the current peak flow (5-PK) (Appendix 8.21).

Forward stepwise regression (highest peak, runoff)

Results of forward stepwise regression on the remaining 15 independent variables against the two dependent variables are listed in Table 8.14. Results are identical to quickflow analysis to the highest peak flow (Table 8.11). Both dependent variables showed that rainfall between

Reproduced with permission of the copyright owner. Further reproduction prohibited without permission.

events (18-PPTBTW) was significant in either the first or second step of forward stepwise regression (Table 8.14). The coefficient was negative, indicating that both dependent variables are inversely correlated to the rainfall between events.

Table 8.14. Results of forward stepwise regression measured to the highest peak flow of the event using runoff characteristics.

Dependent Variable	Step	Variables in the Model	R^2	F Statistic	Coefficient	Constant
suspended-sediment load, tons *	One	2-RUN	0.70	56.5	1.2	-4.89
	Two	18-PPTBTW	0.74	3.63	-0.16	-4.85
		2-RUN		48.5	1.1	
discharge-weighted sediment concentration, mg/L	One	18-PPTBTW	0.17	4.86	-0.18	3.12

* *The probability for F-to-enter and F-to-remove was increased to 0.10*

In forward stepwise regression using suspended-sediment, only quickflow (1-QUICK) was significant (Table 8.14). The probability for F-to-enter and F-to-remove was increased to 0.10 and the rainfall between events (PPTBTW) was significant in the second step of forward stepwise regression (Table 8.14). The coefficient of the best-fit regression line was negative, indicating an inverse relation to suspended-sediment load.

Factor analysis (highest peak, runoff)

Principal component analysis was performed on two sets of independent variables associated with runoff characteristics of the event. One set was used in forward stepwise regression against the dependent variables, suspended-sediment load (Appendix 8.22) and the

Reproduced with permission of the copyright owner. Further reproduction prohibited without permission.

other set was used in the analysis of the discharge-weighted sediment concentration (Appendix 8.23). Six components were selected for factor analysis.

Factor analysis on both data sets have results similar to the quickflow analysis to the highest peak flow. Over 70% of the variance is explained by the first three axes. Using suspended-sediment load and the discharge-weighted sediment concentration as dependent variables showed similar results; PC2 was significant in the first step of forward stepwise regression and PC1 was significant in the second step (Table 8.15). PC2 had high positive loadings (>0.7) on characteristics of the current event (2-RUN, 5-PK, 11-INT15) (Appendices 8.22, 8.23). The coefficient of regression was positive, indicating that suspended-sediment load was correlated directly with PC2. PC1 was significant in the second step of forward stepwise regression and had a high loading (>0.8) on previous event and the sum of the three previous-event characteristics (23-SMLSPK, 25-RULST, 27-INTLST 21-LSPKTI). The coefficient of the best-fit regression line was positive, indicating that previous-event characteristics were directly correlated with suspended-sediment load. Interpretations from factor analysis to the highest peak flow using runoff characteristics indicated that current-event characteristics (runoff, peak flow, and rainfall intensity) and previous event(s) (runoff, peak flow, rainfall) increased suspended-sediment loads and concentrations.

Varimax rotation (highest peak, runoff)

The principal components axis were rotated using the varimax rotation. The factor scores were saved after varimax rotation and forward stepwise regression was performed on the factor

Reproduced with permission of the copyright owner. Further reproduction prohibited without permission.

scores against the dependent variables (Table 8.16). The dependent variable suspended-sediment load showed the same results as without varimax rotation; PC2

Table 8.15. Results of forward stepwise regression on the principal components measured to the highest peak flow of the event using runoff characteristics.

Dependent Variable	Step	Variables in the Model	R^2	F Statistic	Coefficient	Constant
suspended- sediment load, tons	One	PC2	0.57	31.6	0.44	2.26
	Two	PC1	0.68	8.31	0.20	2.26
		PC2		41.2	0.44	
discharge-weighted sediment concentration, mg/L	One	PC2	0.17	5.04	0.14	3.68

was the most important principal component in the first step of forward stepwise regression. PC2 had high positive loadings (>0.6) on characteristics of the current event (2-RUN, 13-RRISE) and the slope of the regression line was positive (Table 8.16; Appendix 8.24). PC5 was significant in the second step of forward stepwise regression (Table 8.16). PC5 had a high negative loading (<-0.9) on the rainfall intensity between events (19-INTBET) (Appendix 8.24). The slope of the regression line was positive, indicating an inverse relation. Increases in rainfall intensity between events cause sediment loads in the current event to decrease.

Using the discharge-weighted sediment concentration as a dependent variable showed PC4 was significant in the first step of forward stepwise regression (Table 8.16). PC4 had a high negative loading (< -0.9) on the rainfall between events (18-PPTBTW) (Appendix 8.25). The slope of the regression line was positive, indicating an inverse relation of rainfall between events to the discharge-weighted sediment concentration. Results after varimax rotation were similar to

Reproduced with permission of the copyright owner. Further reproduction prohibited without permission.

results before rotation and indicated that dependent variables were directly correlated to current-event characteristics. After varimax rotation between-event rainfall was significant and was inversely correlated to both dependent variables.

Table 8.16. Results of forward stepwise regression on the principal components after varimax rotation to the highest peak flow using runoff characteristics.

Dependent Variable	Step	Variables in the Model	R^2	F Statistic	Coefficient	Constant
suspended-sediment load, tons	One	PC2	0.53	27.1	0.42	2.26
	Two	PC5	0.69	12.2	0.23	2.26
		PC2		39.8	0.42	
discharge-weighted sediment concentration, mg/L*	One	PC4	0.15	4.14	0.13	3.68

.* *The probability for F-to-enter and F-to-remove was increased to 0.10*

Discussion

Statistical results were consistent for all of the tests to the highest peak flow and showed that current-event characteristics (quickflow, runoff, rainfall) were significant and directly correlated to the dependent variables. Rainfall between events was inversely correlated to the dependent variables and flushed sediment.

Hysteresis

Hysteresis characteristics of the 26 sampled events were analyzed for the timing of the peak suspended-sediment concentration relative to peak flow, the type of hysteresis, and the width of the hysteresis loop (Table 8.17). Sixty-five percent of the events (17 events) had the peak sediment concentration sampled 5 to 335 minutes after the highest peak flow. The remaining 9

Reproduced with permission of the copyright owner. Further reproduction prohibited without permission.

Reproduced with permission of the copyright owner. Further reproduction prohibited without permission.

Table 8.17. Summary of hysteresis characteristics for Rio Piedras at El Senorial
In events with more than one peak, the highest peak is in bold.
See figure 4.12 for a description of the hysteresis type.

Start Date	Start Hour	End Date	End Hour	Number of Peaks	Peak Discharge, ft3/s	Peak sediment Concentration, mg/L	Time of peak suspended-sediment concentration relative to peak discharge, min (-) indicates prior to peak	Hysteresis type For the entire event	Hysteresis type For the highest peak
3/28/1992	15.25	3/29/1992	4.00	1	1800	48770	35	3	3
4/19/1992	12.00	4/20/1992	6.00	2	596	47600	35	3	3
4/29/1992	17.25	4/30/1992	16.75	2	844	28700	45	3	3
5/1/1992	16.75	5/3/1992	14.50	3	874	14990	-210	1	3
5/16/1992	11.00	5/17/1992	9.00	1	919	45700	14	3	3
7/20/1992	10.75	7/21/1992	6.00	4	434	7830	75	Not enough sampl	Not enough samples
8/5/1992	2.00	8/6/1992	10.50	1	1300	38100	9	4	4
9/6/1992	13.25	9/6/1992	21.50	2	593	8300	14	3	3
9/23/1992	10.50	9/23/1992	21.00	1	718	6920	12	3	3
6/9/1993	11.25	6/9/1993	23.00	2	420	32340	-51	1	4
6/29/1993	17.00	6/30/1993	2.50	1	202	11970	42	3	3
9/6/1993	17.00	9/7/1993	6.00	1	1060	6440	-20	1	1
1/11/1994	0.50	1/11/1994	19.25	3	214	11310	335	3	Not enough samples
1/23/1994	14.25	1/24/1994	3.00	2	269	23300	-6	5	5
4/10/1994	7.50	4/10/1994	19.50	1	1292	3860	-67	1	1
7/2/1994	8.83	7/2/1994	23.25	3	547	9860	-61	3	3
11/19/1994	16.17	11/20/1994	2.50	1	1082	4100	31	3	3
12/1/1994	14.75	12/2/1994	3.75	1	249	4110	7	3	3
12/2/1994	11.25	12/3/1994	15.25	3	742	6130	-8	1	1
2/25/1995	15.00	2/26/1995	23.75	1	2500	30400	-39	1	1
5/15/1995	18.00	5/16/1995	2.75	1	767	8630	5	3	3
6/10/1995	11.50	6/10/1995	22.50	1	471	2990	11	3	3
6/15/1995	11.50	6/15/1995	21.25	2	388	5430	20	3	3
6/16/1995	12.50	6/16/1995	23.75	1	1134	6830	11	4	4
7/21/1995	17.50	7/22/1995	4.25	2	1039	5584	-5	1	1
9/6/1995	3.75	9/7/1995	2.50	2	2965	9500	7	1	1

Reproduced with permission of the copyright owner. Further reproduction prohibited without permission.

Table 8.17. Continued.

Start Date	Start Hour	End Date	End Hour	First peak ft3/s	First peak suspended-sediment concentration, mg/L	Time of 1st peak suspended-sediment concentration relative to peak discharge, min	Hysteresis type of first peak	Second peak ft3/s	Second peak suspended-sediment concentration, mg/L	Time of 2nd peak suspended-sediment concentration relative to peak discharge, min	Hysteresis type
3/28/1992	15.25	3/29/1992	4.00								
4/19/1992	12.00	4/20/1992	6.00	**596**	**47600**	**35**	**3**	Not enough samples			
4/29/1992	17.25	4/30/1992	16.75	379	5660	85	2	**844**	**28700**	**45**	**3**
5/1/1992	16.75	5/3/1992	14.50	449	12290	30	3	759	14990	-60	3
5/16/1992	11.00	5/17/1992	9.00								
7/20/1992	10.75	7/21/1992	6.00								
8/5/1992	2.00	8/6/1992	10.50								
9/6/1992	13.25	9/6/1992	21.50	490	7610	14	3	**593**	**8300**	**14**	**3**
9/23/1992	10.50	9/23/1992	21.00								
6/9/1993	11.25	6/9/1993	23.00	210	32340	14	Not enough samples	**410**	**31000**	**19**	**4**
6/29/1993	17.00	6/30/1993	2.50								
9/6/1993	17.00	9/7/1993	6.00								
1/11/1994	0.50	1/11/1994	19.25	**214**	**5280**	**0**	Not enough samples	177	11310	115	2
1/23/1994	14.25	1/24/1994	3.00	200	14730	19	Not enough samples	**269**	**23300**	**-6**	**5**
4/10/1994	7.50	4/10/1994	19.50								
7/2/1994	8.83	7/2/1994	23.25	263	9860	-1	Not enough samples	547	7980	79	3
11/19/1994	16.17	11/20/1994	2.50								
12/1/1994	14.75	12/2/1994	3.75								
12/2/1994	11.25	12/3/1994	15.25	392	5810	32	Not enough samples	742	6130	-8	3
2/25/1995	15.00	2/26/1995	23.75								
5/15/1995	18.00	5/16/1995	2.75								
6/10/1995	11.50	6/10/1995	22.50								
6/15/1995	11.50	6/15/1995	21.25	**388**	**5430**	**20**	**3**	210	1640	0	Not enough samples
6/16/1995	12.50	6/16/1995	23.75								
7/21/1995	17.50	7/22/1995	4.25	**1039**	**5584**	**-5**	**1**	Not enough samples			
9/6/1995	3.75	9/7/1995	2.50	**2965**	**9500**	**0**	**1**	Not enough samples			

Reproduced with permission of the copyright owner. Further reproduction prohibited without permission.

Table 8.17. Continued.

Start Date	Start Hour	End Date	End Hour	Third peak ft3/s	Third peak suspended-sediment concentration, mg/L	Time of 3rd peak suspended-sediment concentration relative to peak discharge, min	Hysteresis type
3/28/1992	15.25	3/29/1992	4.00				
4/19/1992	12.00	4/20/1992	6.00				
4/29/1992	17.25	4/30/1992	16.75				
5/1/1992	16.75	5/3/1992	14.50	**874**	**11290**	**30**	**3**
5/16/1992	11.00	5/17/1992	9.00				
7/20/1992	10.75	7/21/1992	6.00				
8/5/1992	2.00	8/6/1992	10.50				
9/6/1992	13.25	9/6/1992	21.50				
9/23/1992	10.50	9/23/1992	21.00				
6/9/1993	11.25	6/9/1993	23.00				
6/29/1993	17.00	6/30/1993	2.50				
9/6/1993	17.00	9/7/1993	6.00				
1/11/1994	0.50	1/11/1994	19.25	185	4010	-15	Not enough samples
1/23/1994	14.25	1/24/1994	3.00				
4/10/1994	7.50	4/10/1994	19.50				
7/2/1994	8.83	7/2/1994	23.25	Not enough samples			
11/19/1994	16.17	11/20/1994	2.50				
12/1/1994	14.75	12/2/1994	3.75				
12/2/1994	11.25	12/3/1994	15.25	Not enough samples			
2/25/1995	15.00	2/26/1995	23.75				
5/15/1995	18.00	5/16/1995	2.75				
6/10/1995	11.50	6/10/1995	22.50				
6/15/1995	11.50	6/15/1995	21.25				
6/16/1995	12.50	6/16/1995	23.75				
7/21/1995	17.50	7/22/1995	4.25				
9/6/1995	3.75	9/7/1995	2.50				

events had the peak suspended-sediment concentration collected 5 to 210 minutes before peak flow (Table 8.17).

Observation of the hysteresis loops for the entire event showed that counterclockwise hysteresis loops (Type 3) (fig. 8.14) were the most common type in 14 of the 26 events (54%) (fig. 8.14). Eight of the 24 (33%) events showed clockwise hysteresis loops (Type 1) (Fig. 8.14a), two of the events (8%) showed a figure eight (Type 4), one event showed no exhaustion (Type 5), and one event did not have enough samples to determine the hysteresis loop type (fig. 8.14a; Table 8.17). Examination of the hydrographs for just the highest peak flow showed 14 events with Type-3 loops, 5 events with Type-1 loops, 3 events with Type-4 loops, and 1 event with Type-5 loops (fig. 8.14b).

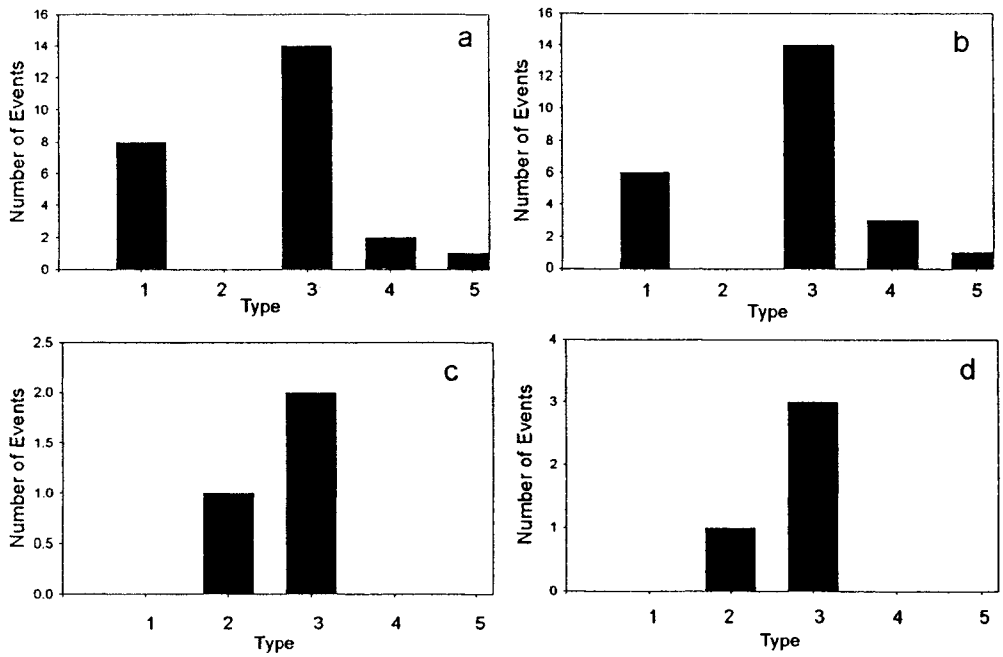

Figure 8.14. Hysteresis loops described at Rio Piedras at El Senorial for a) the entire event, b) near the highest peak flow, c) the first peak (not the highest peak), and d) the second peak (not the highest peak).

Reproduced with permission of the copyright owner. Further reproduction prohibited without permission.

Fourteen of the events were multipeaked (Table 8.3). Only three of these events had the first peak sampled for sediment and showed two events with Type-3 loops and one with a Type-2 loop (fig. 8.14c). For the second peak that was not the highest peak flow, four events were sampled and showed three with Type-3 loops and one with Type-2 loop (fig. 8.14d).

Hysteresis loops near the highest peak flow were examined to determine the maximum width of the hysteresis loop or how much exhaustion or replenishment of sediment occurred during the runoff event, as well as possible causes for the exhaustion and replenishment of sediment. Results were separated into Type-1 and Type-3 loops (Appendix 8.26). Type-4 loops were grouped into Type-3 loops because before and after the peak flow the hysteresis loop is counterclockwise (fig. 4.12).

The average values for the storm characteristics show differences between Type-1 and Type-3 storms (Appendix 8.26). The average maximum width for Type-3 storms (9,830 mg/L) was twice the width of Type-1 storms (4,820 mg/L) (Appendix 8.26). Sediment loads were similar for Type-1 (1,579 tons) and Type-3 storms (1,507 tons). Storm runoff was close to twice as high for Type-1 storms (1.25×10^7 ft^3) compared to Type-3 storms (6.47×10^6 ft^3). The similarity of sediment loads but differences in storm generated runoff between Type-1 and Type-3 events was reflected in the discharge-weighted sediment concentration which was almost twice as high in Type-3 storms (6,660 mg/L) compared to Type-1 storms (3,480 mg/L) (Appendix 8.26). The sum of peak flows and the rate of hydrograph rise were higher for Type-1 than Type-3 storms (Appendix 8.26). Analysis of sediment-transport curves for preceding peaks in the current event (fig. 8.6) showed low suspended-sediment concentrations for the highest class of peak flows (1000-3540 ft^3/s). Events with high peak flows showed Type-1 loops (Appendix 8.26). Rainfall

Reproduced with permission of the copyright owner. Further reproduction prohibited without permission.

was higher for Type-1 storms but rainfall intensity was higher for Type-3 storms. Previous-event runoff and between-event runoff were similar for Type-1 and Type-3 storms (Appendix 8.26). Interpretations of the differences between Type-1 and Type-3 hysteresis indicated that Type-3 loops occurred in smaller rainfall-runoff events.

In Type-3 storms, 15 of the 17 events had a positive slope on the rising limb sediment-transport curves and 11 of the 17 events had negative slopes on the falling limb sediment-transport curves (Appendix 8.26). The high number of events on the falling limb with negative slopes for the transport curve indicated that as discharge was falling, suspended-sediment concentration increased. The slopes of the sediment-transport curves, either positive or negative, were steeper for Type-3 than Type-1 storms indicating more available sediment for transport.

Variables thought to influence the maximum width of the hysteresis loops were statistically examined through forward stepwise regression (Table 4.4). Analysis of the correlation table showed 9-SUMPK, 6-MXTMJPK, 25-RULST to be intercorrelated with several other variables and these variables were all removed. Results of forward stepwise regression on the variable for Type-1 storms indicated that the rainfall on the falling limb (13-RRISE) was significant in the first step (Table 8.18A). The slope of the regression line was positive, indicating that as the rainfall on the rising limb of the hydrograph increased, the width of the hysteresis or the amount of sediment exhaustion increased (Table 8.18A). Greater rainfall on the rising limb was mobilizing sediment that increased sediment concentrations on the rising limb causing Type-1 loops with more sediment exhaustion (fig. 8.15a).

Statistical analysis of Type-3 loops did not show any significant intercorrelation and all variables were left in. Results of forward stepwise regression on variables used to describe Type-3

Reproduced with permission of the copyright owner. Further reproduction prohibited without permission.

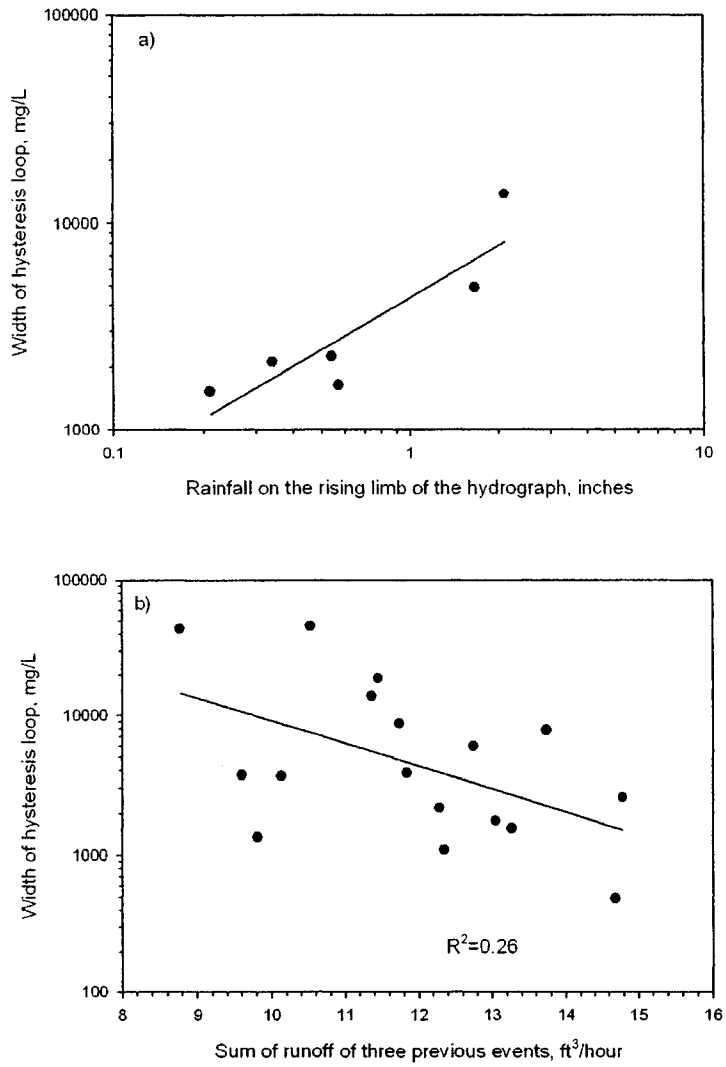

Figure 8.15. Relationships of hysteresis loops. (a) Rainfall totals on the rising limb plotted against clockwise hysteresis width. (b) The sum of the three previous runoff events plotted against counterclockwise hysteresis width.

storms indicated that the runoff of the three previous events (31-RU3EVT) was significant in the first step and the slope of the regression was negative (Table 8.18; fig. 8.15b). The slope of the best-fit regression line was negative, indicating that as runoff of the three previous events increased, the width of the hysteresis loop decreased. Previous runoff events flushed sediment from the

Reproduced with permission of the copyright owner. Further reproduction prohibited without permission.

system and therefore, there is a limited amount of sediment available for Type-3 hysteresis loops. Statistical analysis for the entire event using the discharge-weighted sediment concentration as a dependent variable also indicted that previous events flushed sediment Table 8.4).

Table 8.18. Results of forward stepwise regression for A) clockwise (Type-1) hysteresis and B) counterclockwise (Type-3) hysteresis.

A

Step	Independent variable using all samples (rising and falling)	R^2	F Statistic	Coefficient	Constant
Step one	13-RRISE	0.79	15.0	0.84	3.64

B

Step	Independent variable using all samples (rising and falling)	R^2	F Statistic	Coefficient	Constant
Step one	31-RU3EVT	0.26	5.38	-0.16	5.59

Summary of Results for Rio Piedras

During the study period, December 5, 1991 through September 30, 1995, 527 suspended-sediment samples were collected for concentrations at the station Rio Piedras at El Senorial. The distribution of sampled discharge showed that 57% of the suspended-sediment samples were sampled at high flows between 100 and 500 ft^3/s (2.83 to 14.2 m^3/s) (fig. 8.3). Runoff and rainfall conditions during the collection period were 13% drier than the long-term average.

Examination of sediment-transport curves showed the best correlation coefficient of sediment-transport curves was for all samples (0.68), although data clusters at either end of the best-fit regression line may be effecting this relation (fig.8.5a). Sediment-transport curves at Rio

Reproduced with permission of the copyright owner. Further reproduction prohibited without permission.

Piedras did not show an improvement in the relation of discharge to suspended-sediment concentration by separating samples into rising and falling limbs, either relative to the highest peak flow or relative to any peak flow in the event (figs. 8.5 b,c). Falling limb suspended-sediment samples had higher concentrations than rising limb samples.

Sediment-transport curves generated to show the effect of previous events at Rio Piedras indicated that samples collected shortly after a large storm event had the lowest suspended-sediment concentrations for a given discharge (fig. 8.6a). However, samples collected following a long time period since the previous event did not show the highest suspended-sediment concentrations (fig. 8.6a).

Separation of samples by wet season (May to December) to a drier season (January to April) did not show any difference (fig. 8.7a). There is a large amount of silt and clay in suspension at most flows in Rio Piedras (fig. 8.8). This is related to the geology of the basin which weathers to silt and clay. Also, human disturbances in the basin may be introducing large quantities of hillslope-derived fine sediment.

Results using Walling's (1974) four independent variables (discharge, time relation of sample, base flow, and flood intensity), showed that for all sediment samples discharge was the most important variable and had a positive slope (Table 8.2). For rising samples, base flow at the start of the event was the most important variable and had a positive slope, indicating that base flow is increasing sediment transport. For falling samples, the time of the sample was most important and had a negative slope (Table 8.2) This implies that samples collected later in the event have low concentrations. In each analysis the R^2 values were low.

Reproduced with permission of the copyright owner. Further reproduction prohibited without permission.

A summary of forward stepwise regression for all statistical analyses (independent variables, principal components with and without varimax rotation) for the entire event or to the highest peak flow using quickflow or runoff at Rio Piedras is shown in Table 8.19A,B. For each statistical analysis, the dependent variable suspended-sediment load showed the highest correlation coefficients. Correlation coefficient values did not seem to improve by subtracting the base flow portion of the hydrograph. Results improve sightly by analyzing only the rising portion of the hydrograph to the highest peak.

Table 8.19. A) Summary of the first two steps of forward stepwise regression analyses for Rio Piedras at El Senorial for the entire event. The value in the parenthesis is the correlation coefficient (R^2). The '+' or '-' sign indicate the slope for the line of best fit.

	Quickflow sediment load	**Runoff** sediment load	**Quickflow** discharge-weighted sediment concentration	**Runoff** discharge-weighted sediment concentration
Forward stepwise regression on variables	+ quickflow (0.61) - sum of last peak flows (0.67)	+ runoff (0.61) - sum of last peak flows (0.67)	- rainfall between the previous event (0.13) - sum of last peak flows (0.34)	- rainfall between the previous event (0.15) - sum of last peaks (0.37)
Forward stepwise regression on principal components	**+ PC2** (0.46) + current rain, quickflow, peak flow **- PC4** (0.56) + rainfall intensity	**+ PC2** (0.46) + current rain, runoff, peak flow, rainfall intensity **- PC4** (0.56) + rainfall intensity	none	none
Forward stepwise regression on rotated principal components	**+ PC2** (0.46) + current rain, quickflow, peak flow, rainfall, rainfall intensity **+ PC5** (0.56) + hyster	**+ PC2** (0.46) + current rain, quickflow, peak flow, rainfall **+ PC5** (0.57) + hyster	**- PC1** (0.14) + previous-event quickflow, peak flow, rainfall intensity	**- PC1** (0.14) + previous-event runoff, peak flow, rainfall intensity

Reproduced with permission of the copyright owner. Further reproduction prohibited without permission.

Table 8.19 B) Summary of the first two steps of forward stepwise regression analyses for Rio Piedras at El Senorial to the highest peak flow. The value in the parenthesis is the correlation coefficient (R^2). The '+' or '-' sign indicate the slope for the line of best fit.

	Quickflow sediment load	**Runoff** sediment load	**Quickflow** discharge-weighted sediment concentration	**Runoff** discharge-weighted sediment concentration
Forward stepwise regression on variables	+ quickflow (0.67) - rainfall since the last event (0.73)	+ runoff (0.70) - rainfall since the last event (0.74)	- rainfall since the last event (0.19)	- rainfall since the last event (0.17)
Forward stepwise regression on principal components	**+ PC2** (0.56) + Current, quickflow, peak flow, rainfall intensity **- PC5** (0.68) + rainfall between events	**+ PC2** (0.57) + current, quickflow, peak flow, rainfall intensity **+ PC1** (0.68) + Previous-event peak flow, runoff, rainfall intensity + sum of three previous-events rainfall and runoff	**+PC2** (0.17) + current peak flow, rate of hydrograph rise to highest peak, rainfall intensity	**+PC2** (0.17) +current peak flow, rate of hydrograph rise to highest peak, rainfall intensity
Forward stepwise regression on rotated principal components	**+PC2** (0.54) + current quickflow rainfall **+ PC5** (0.71) - rainfall between events	**+PC2** (0.53) + current quickflow rainfall **+ PC5** (0.69) - rainfall between events	**+ PC4** (0.21) - rainfall between events	**+ PC4** (0.15) - rainfall between events

For the entire event and to the highest peak flow, using quickflow or runoff, forward stepwise regression on the independent variables always showed runoff (or quickflow) was significant and directly correlated to suspended-sediment load and to the discharge-weighted concentration. The sum of the previous-event peaks flushed sediment. To the highest peak flow, forward stepwise regression on the independent variables showed runoff (or quickflow) was

Reproduced with permission of the copyright owner. Further reproduction prohibited without permission.

significant and directly correlated with the dependent variables. Rainfall intensity of the current event reduced suspended-sediment loads.

Principal components analysis for the entire event (using quickflow and runoff) only showed results for suspended-sediment load and indicated that current-event characteristics (rain, runoff, peak flows, rainfall intensity) were significant and directly correlated. After varimax rotation, hysteresis was significant and indicated that clockwise hysteresis loops (Type 1) were directly correlated to suspended-sediment load.

To the highest peak flow, suspended-sediment load (using quickflow) and discharge-weighted sediment concentration (using quickflow and runoff) showed that rainfall between events flush sediment. For runoff to the highest peak flow using suspended-sediment load, previous-event characteristics (peak flow, runoff, rainfall intensity) and the sum of the three previous-events characteristics (rainfall and runoff) were significant and were increasing sediment. After varimax rotation (using quickflow and runoff) suspended-sediment load showed current-event characteristics (quickflow, runoff, and rainfall) were directly correlated to suspended-sediment load. The rainfall between events was significant and inversely correlated to both dependent variables, indicating that increases in rainfall between events flush sediment

Analysis of hysteresis loops indicated that counterclockwise hysteresis loops were more common, occurring during 54% of the events (fig. 8.14). Sediment loads were similar for Type-1 (1,579 tons) and Type-3 storms(1,507 tons). Storm runoff was close to twice as high for Type-1 storms ($1.25 \times 10^7 ft^3$) compared to Type-3 storms ($6.47 \times 10^6 ft^3$). The sediment concentration was almost twice as high in Type-3 storms (6,660 mg/L) compared to Type-1 storms (3,480 mg/L) (Appendix 8.26).

Reproduced with permission of the copyright owner. Further reproduction prohibited without permission.

In Rio Piedras, Type-3 hysteresis may occur in smaller rainfall-runoff events. In Type-3 storms, there is a high number of events (11 of the 17 events) on the falling limb with negative transport curve slopes that indicate as discharge was falling, suspended-sediment concentration was increasing. The highest peak flows in the current event were associated with Type-1 hysteresis.

Results of forward stepwise regression to determine the controls of sediment exhaustion for Type-1 hysteresis indicated that the rainfall on the rising limb (13-RRISE) was significant and was directly correlated to the amount of sediment exhaustion (Table 8.18). Greater rainfall amounts on the rising limb were mobilizing sediment that increased sediment concentrations on the rising limb, causing Type-1 hysteresis with more sediment exhaustion. For Type-3 events, runoff of the three previous events (31-RU3EVT) was significant in the first step and inversely correlated to the width of the hysteresis loop. Large previous runoff events flushed sediment from the system, and therefore there is a limited amount of sediment available for Type-3 hysteresis loops. Sediment flushing was also observed in the statistical analysis for the entire event using the discharge-weighted sediment concentration as a dependent variable (Table 8.4).

The Rio Piedras watershed was being converted to urban areas during this study period. Many housing and commercial developments with large areas of bare ground were observed in the basin. Therefore, this basin is not considered supply limited. Analysis of storm-generated sediment characteristics for Rio Piedras illustrate a hillslope source of sediment. Hysteresis loops are dominantly counterclockwise implying that the sediment source has some travel time to the monitoring stations, as would be expected from a non-channel source. Bedrock geology in the basin weathers to silt and clay and this hillslope-derived sediment remains in suspension during

Reproduced with permission of the copyright owner. Further reproduction prohibited without permission.

storm events, leaving a small amount of sediment in the channel for the next event. High between-event rainfall intensities supplied sediment to the system and are being flushed by high runoff between events.

Reproduced with permission of the copyright owner. Further reproduction prohibited without permission.

CHAPTER IX

SHEETWASH EROSION

A total of 891 sheetwash samples were collected from 46 sediment traps on five different land- cover types (Appendix 9.1). Eleven traps were installed on construction sites, 10 on cropland, 15 on pasture, 8 in forest, and 2 on a landslide (fig. 4.9). A concern about sampling erosion at the scale of the sediment traps is the representativeness of the measurements. The sediment traps were installed on hillslopes characteristic of the major land-use types for the four study basins, as well as the Island of Puerto Rico. The sediment traps were installed on soil types that are common in the four basins (fig. 4.9). Slopes for the traps installed in the Lago Loiza basin closely parallel the slopes for each land-use type (fig. 9.1). Slopes for the forested site and the landslide site in the Rio Icacos basin were not analyzed.

Plots of runoff, rainfall, and sediment are shown for each land-cover site in figure 9.2. Rainfall showed a weak correlation to runoff, with R^2 values ranging from 0.22 to 0.55 (fig. 9.2). The relation of rainfall to runoff is complex and factors such as the extent of the forest canopy, antecedent soil moisture conditions, intensity of rainfall, and soil infiltration rates are important. Plots of runoff versus sediment showed a good correlation for the forest, cropland, and pasture sites, and a poor correlation for construction and landslide sites (fig. 9.2). The best relationship of runoff to total sediment was observed at the forested sites. The trap collection times varied for each land-cover site. To normalize the amount of rainfall that fell between collection periods, rainfall was divided by the number of days since the last collection to produce a rainfall intensity,

Reproduced with permission of the copyright owner. Further reproduction prohibited without permission.

in inches per day. Plotting this rainfall intensity versus total sediment did not produce a good correlation for any land-cover site (fig. 9.2). This may explain why rainfall intensity did not show up as a strong variable in the statistical analysis for each sediment station.

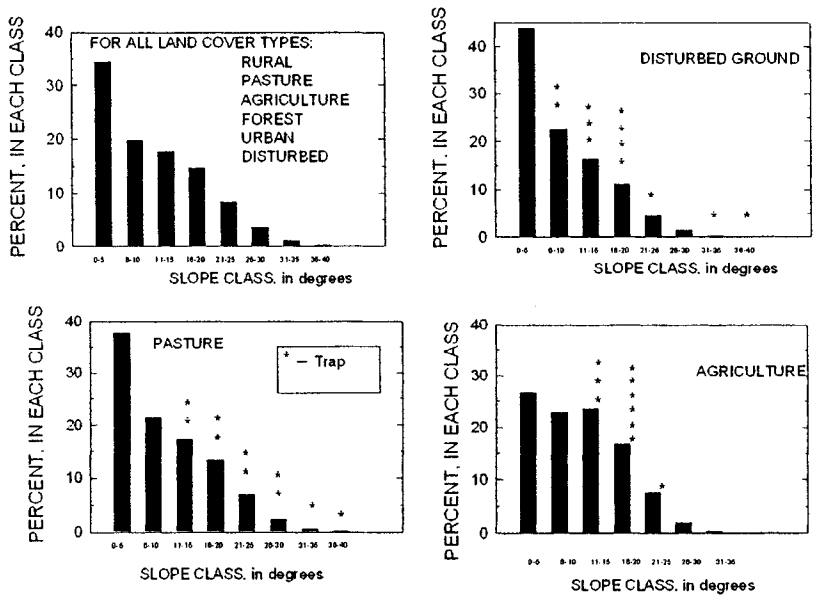

Figure 9.1. Distribution of slopes for three land-cover types instrumented with sediment traps in the Lago Loiza basin (after Gellis and others, 1999).

Sheetwash erosion is affected over time by vegetation changes, seasonal differences, and land-use change (Bryan, 1991). Sheetwash concentration for the land-cover sites changed through time for select sites (fig. 9.3). Disturbed sites showed the most change in sediment concentration where early in the study period sheetwash erosion was high and decreased over time (fig. 9.3 h,i,j,k). Larsen (1997) noted an increase in vegetation (mainly ferns) as the cause for the decrease in erosion over time at the landslide scar (IC-L; fig. 9.3). Towards the end of the study period, erosion rates on the landslide scar were lower than on the forest traps (Larsen, 1997).

Reproduced with permission of the copyright owner. Further reproduction prohibited without permission.

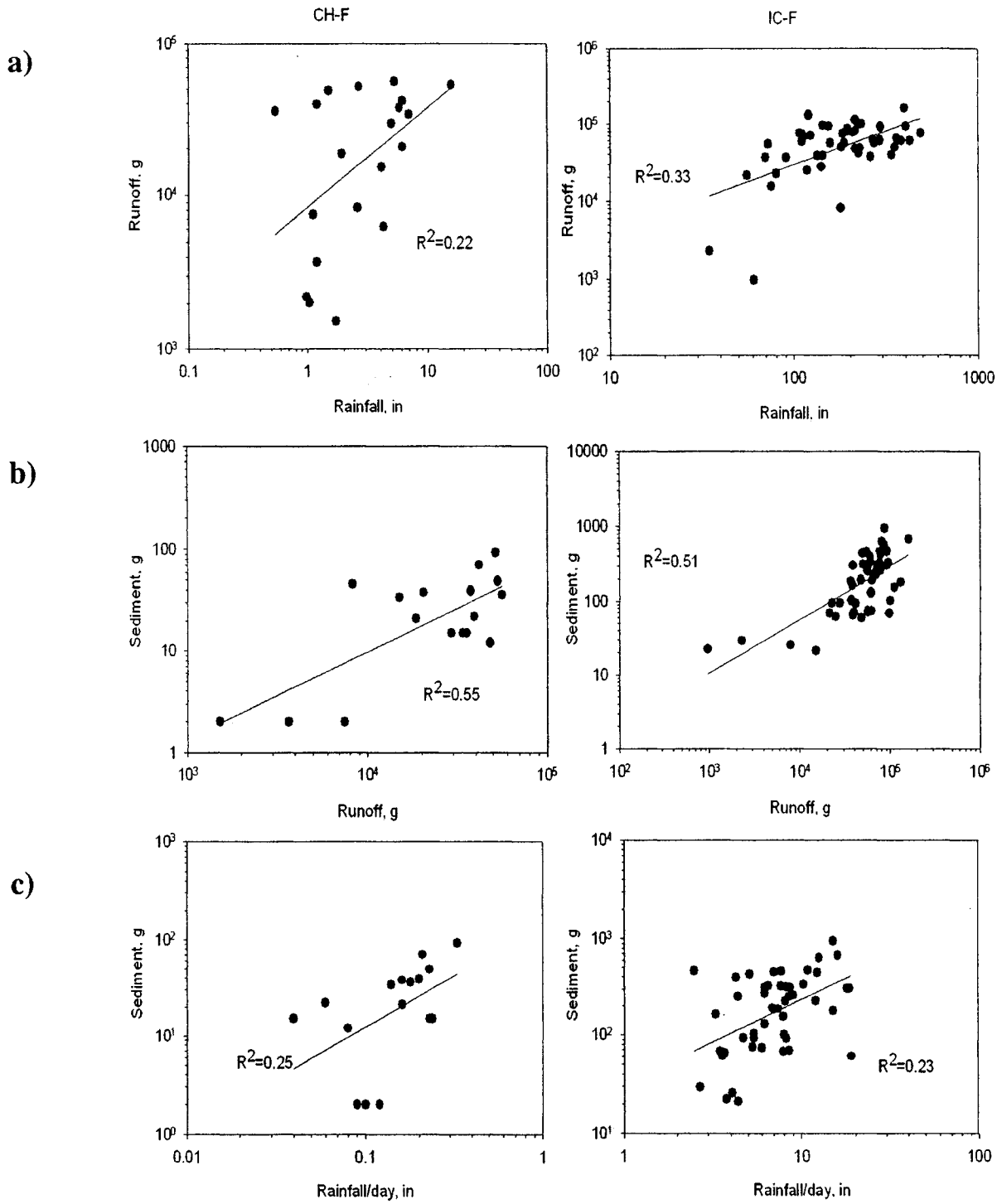

Figure 9.2. Sediment trap relations at forest sites CH-F and IC-F in a) relation of rainfall to runoff, b) runoff to sediment, and c) rainfall per day to total sediment.

Reproduced with permission of the copyright owner. Further reproduction prohibited without permission.

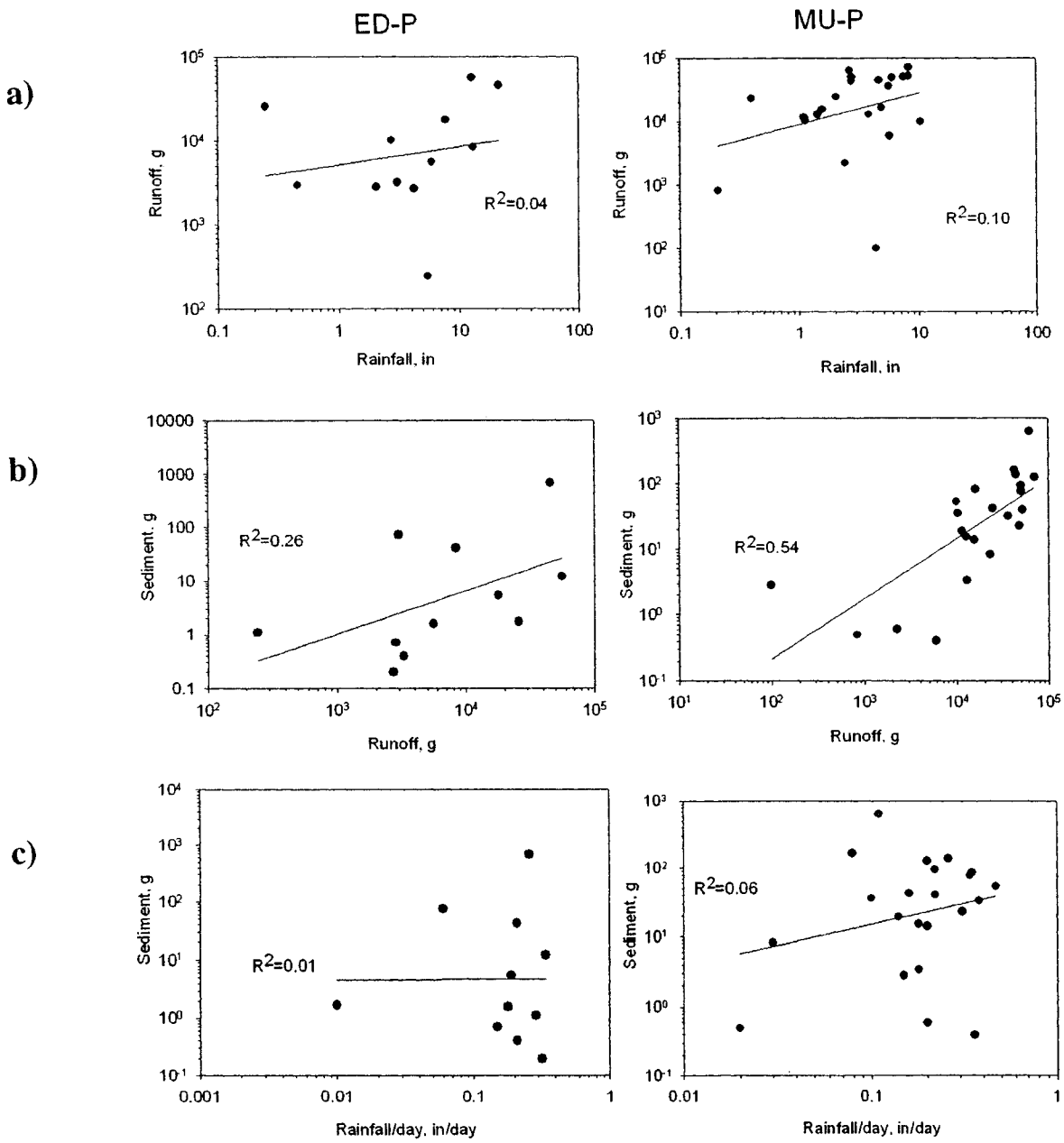

Figure 9.2. Continued. Sediment trap relations at pasture sites ED-P and MU-P a) relation of runoff to total sediment, b) runoff to sediment, and c) rainfall per day to total sediment.

Reproduced with permission of the copyright owner. Further reproduction prohibited without permission.

a)

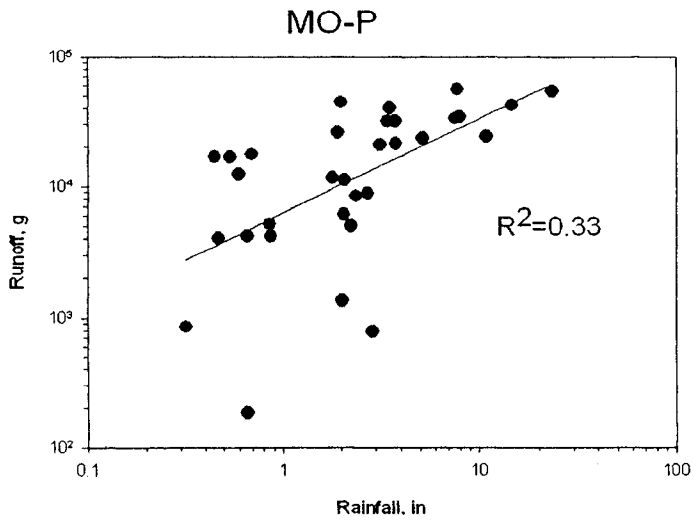

b)

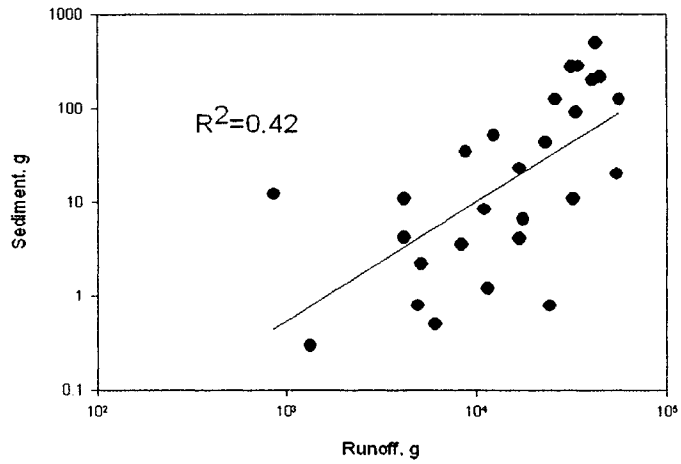

c)

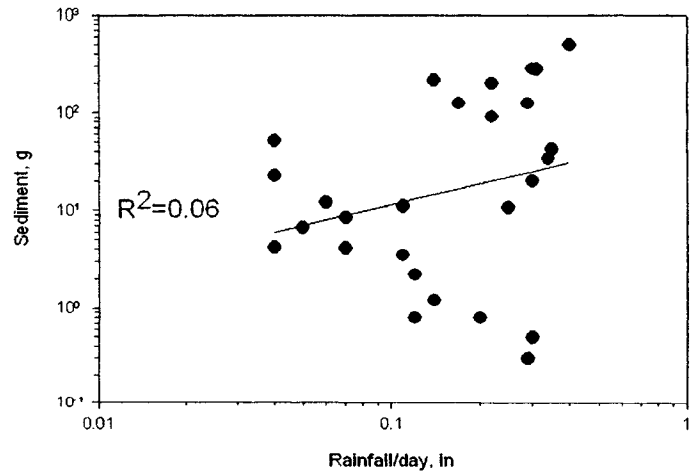

Figure 9.2. Continued. Sediment trap relations at pasture site MO-P, a) relation of runoff to total sediment, b) runoff to sediment, and c) rainfall per day to total sediment.

Reproduced with permission of the copyright owner. Further reproduction prohibited without permission.

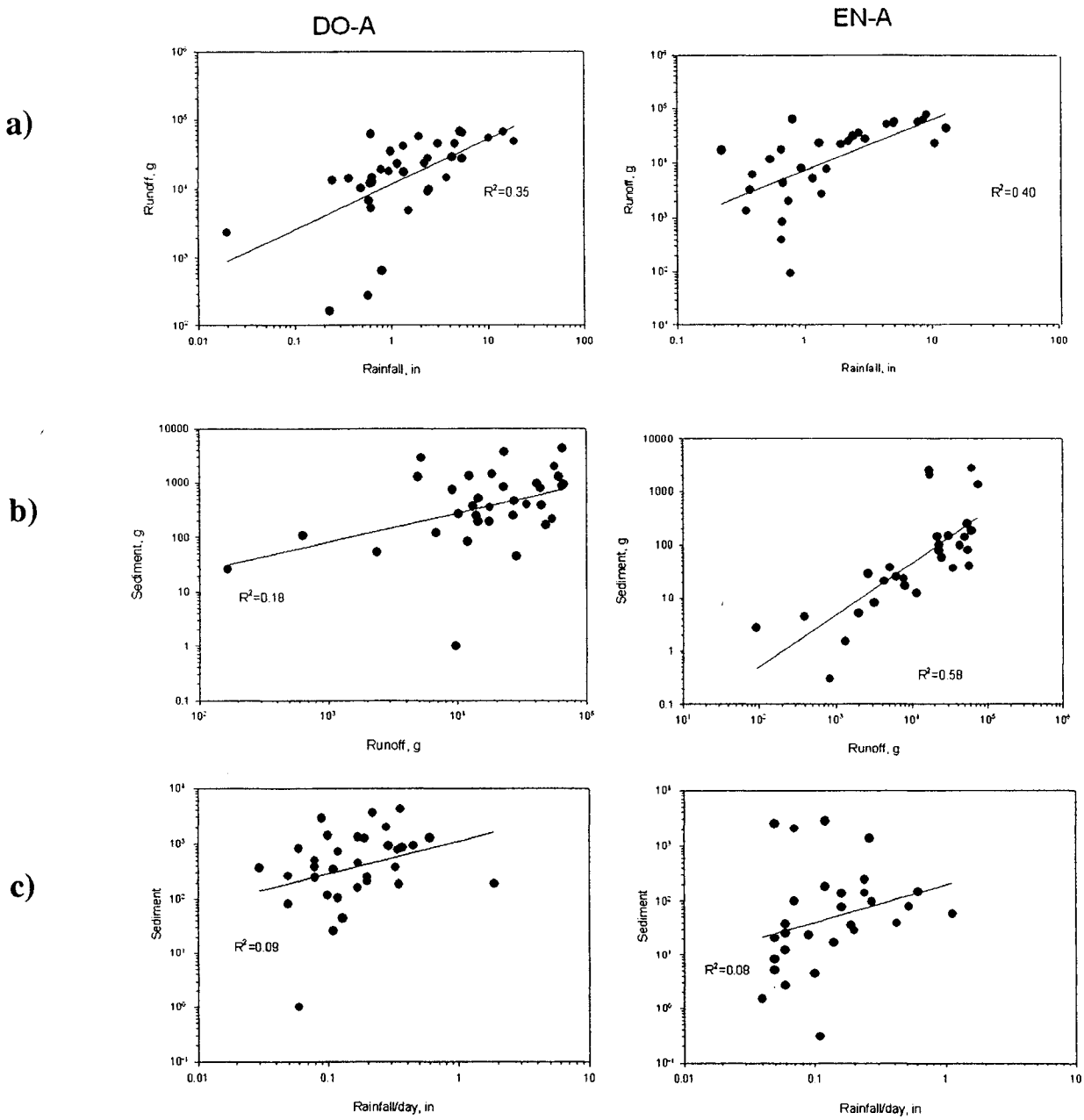

Figure 9.2. Continued. Sediment trap relations at cropland site DO-A and EN-A in a) relation of runoff to total sediment, b) runoff to sediment, and c) rainfall per day to total sediment.

Reproduced with permission of the copyright owner. Further reproduction prohibited without permission.

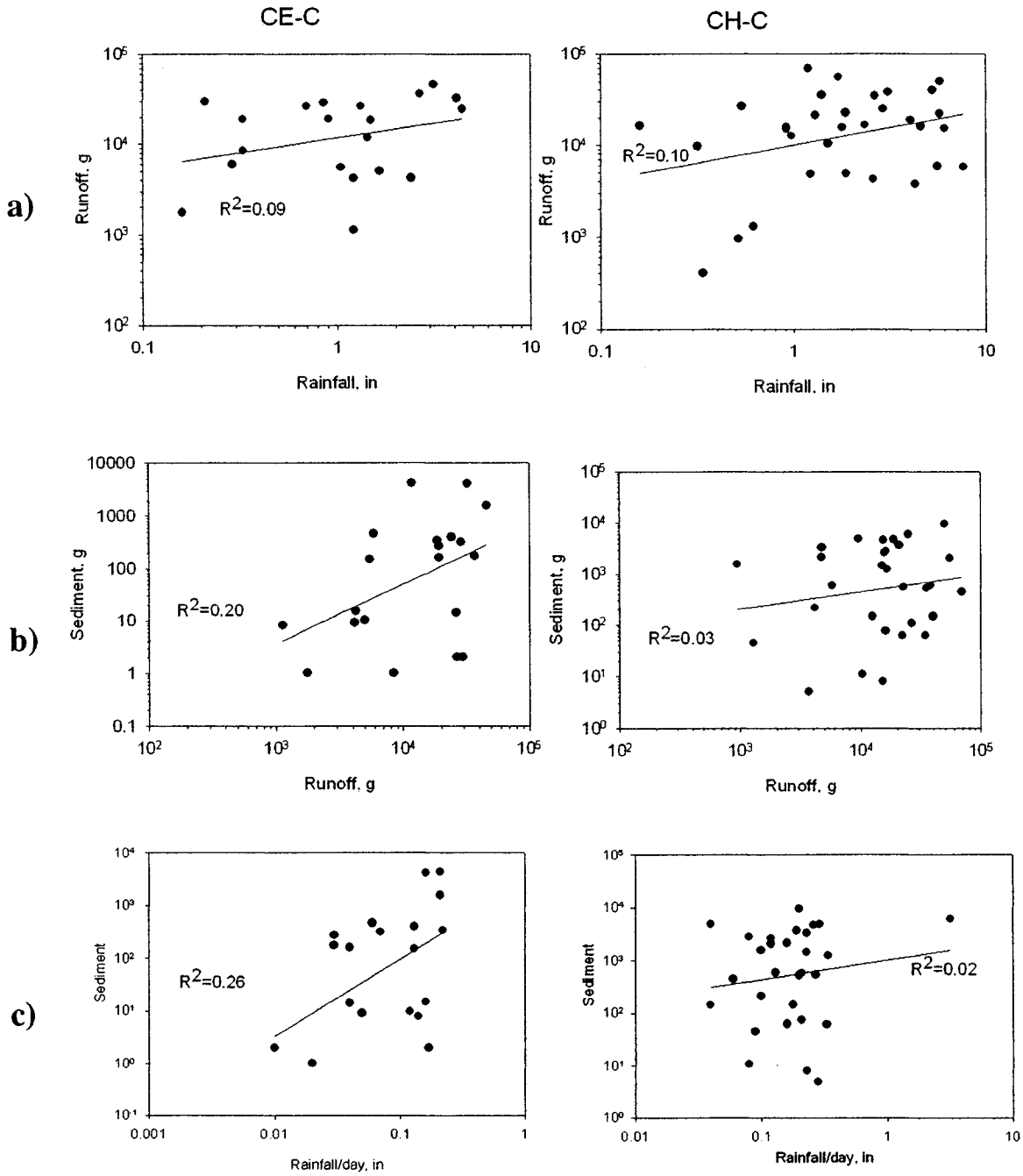

Figure 9.2. Continued. Sediment trap relations at construction sites CE-C and CH-C in a) relation of runoff to total sediment, b) runoff to sediment, and c) rainfall per day to total sediment.

Reproduced with permission of the copyright owner. Further reproduction prohibited without permission.

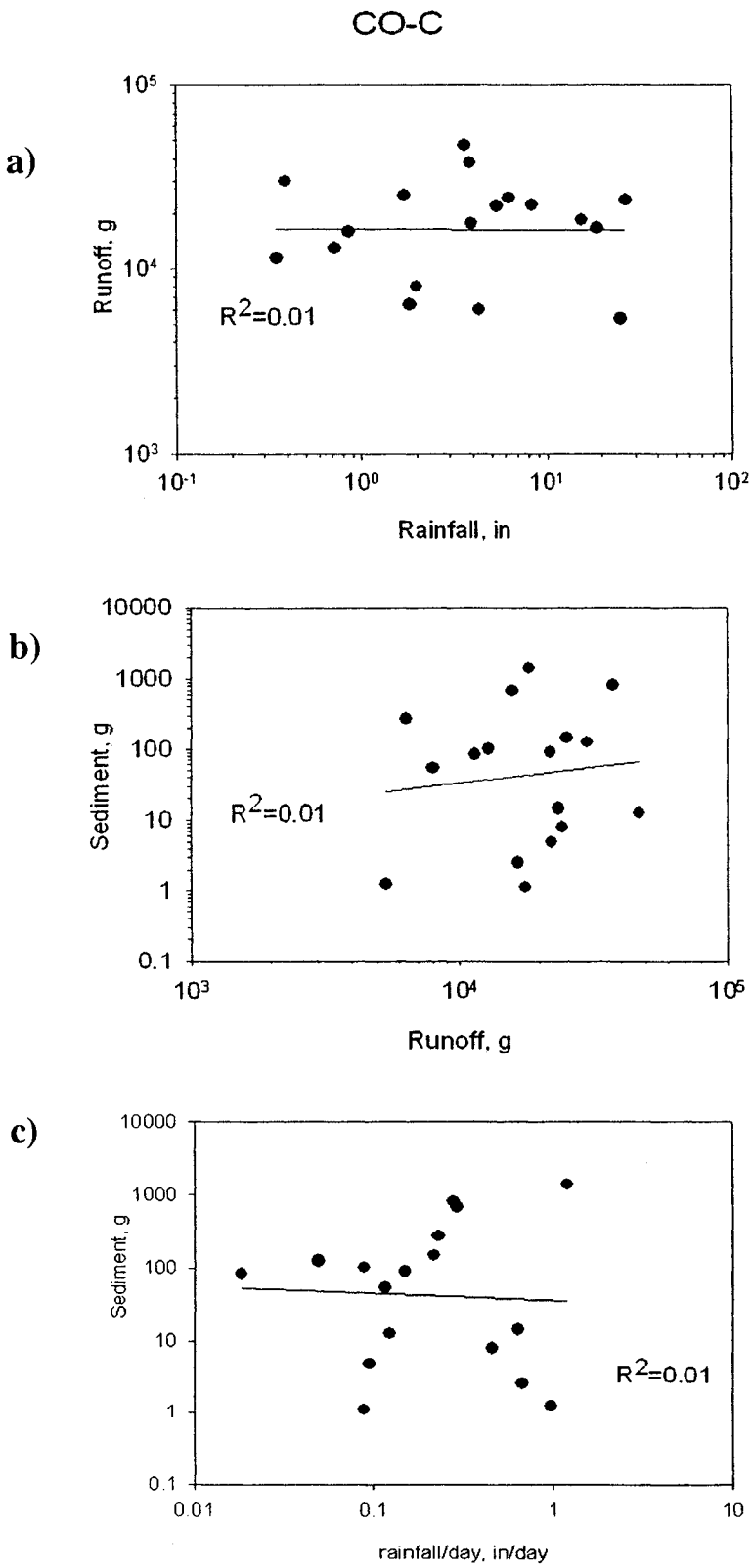

Figure 9.2. Continued. Sediment trap relations at construction site CO-C in a) relation of runoff to total sediment, b) runoff to sediment, and c) rainfall per day to total sediment.

Reproduced with permission of the copyright owner. Further reproduction prohibited without permission.

a)

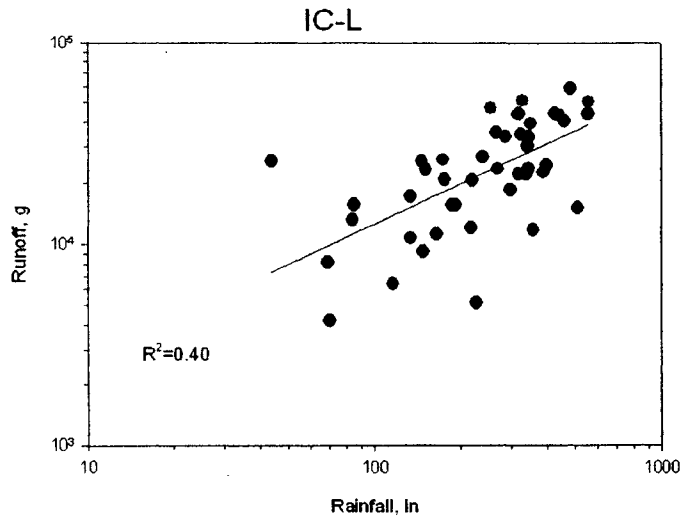

b)

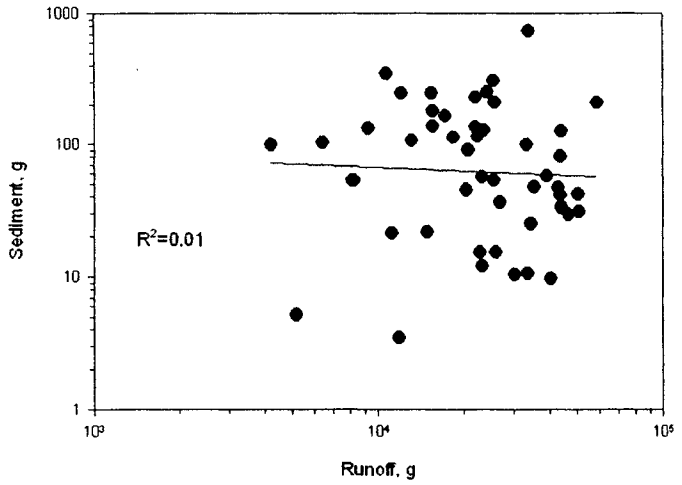

c)

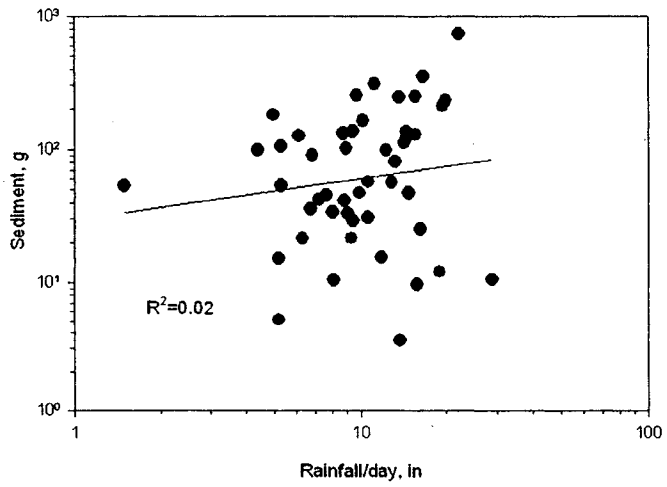

Figure 9.2. Concluded. Sediment trap relations at landslide site IC-L in a) relation of runoff to total sediment, b) runoff to sediment, and c) rainfall per day to total sediment.

Reproduced with permission of the copyright owner. Further reproduction prohibited without permission.

a)

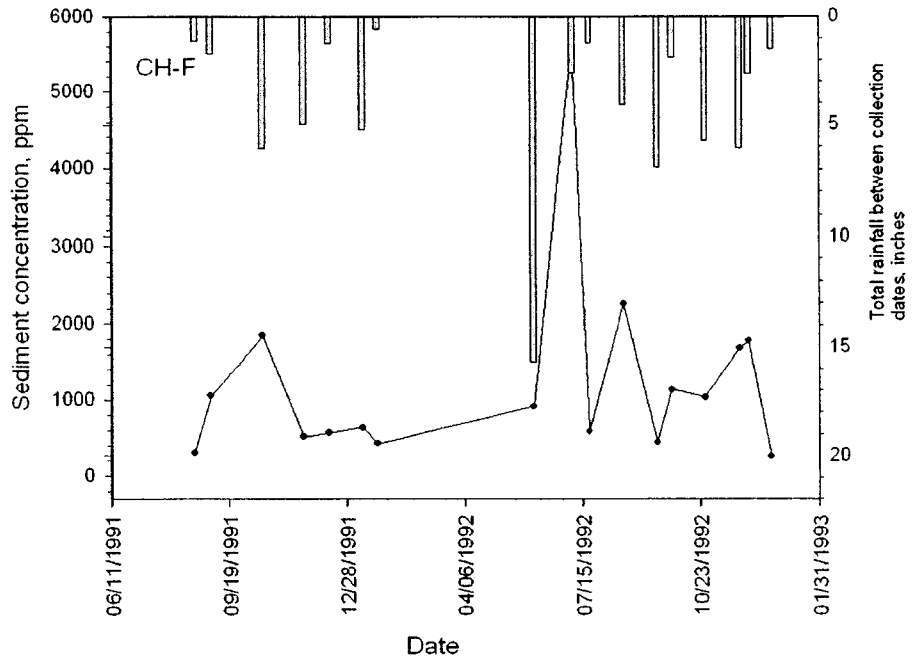

b)

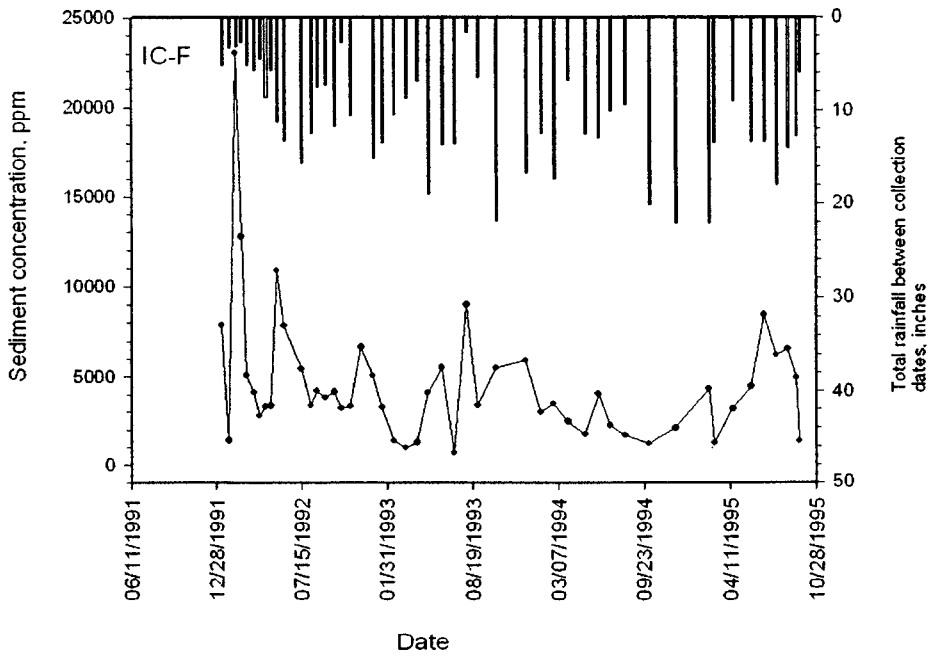

Figure 9.3. Relation of measured sediment concentration and rainfall over time at forest sites a) CH-F and b) IC-F.

Reproduced with permission of the copyright owner. Further reproduction prohibited without permission.

c)

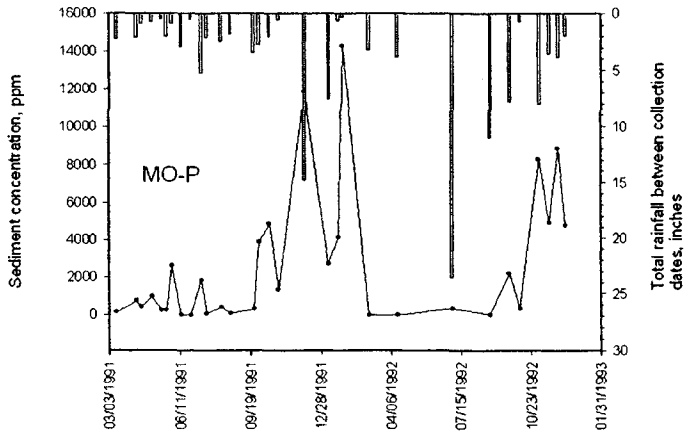

d)

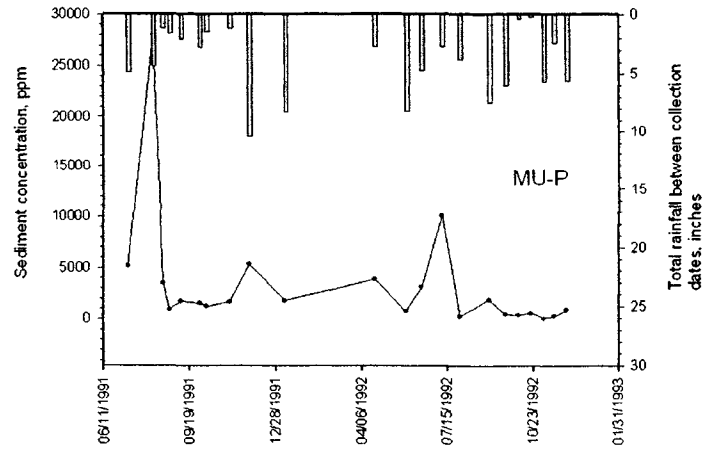

e)

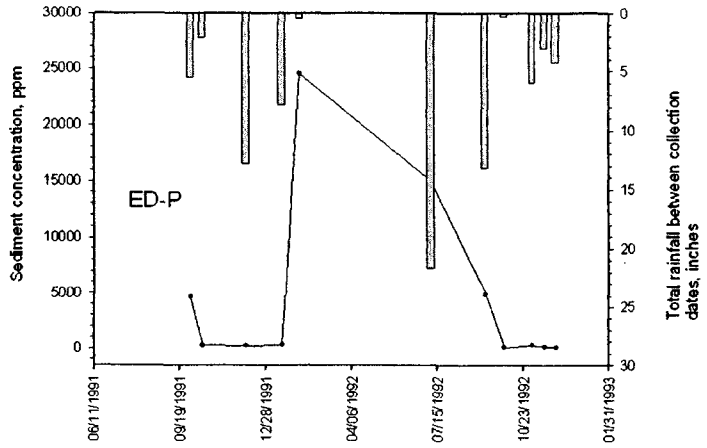

Figure 9.3. Continued. Relation of measured sediment concentration and rainfall over time at pasture sites c) MO-P, d) MU-P, and e) ED-P.

Reproduced with permission of the copyright owner. Further reproduction prohibited without permission.

f)

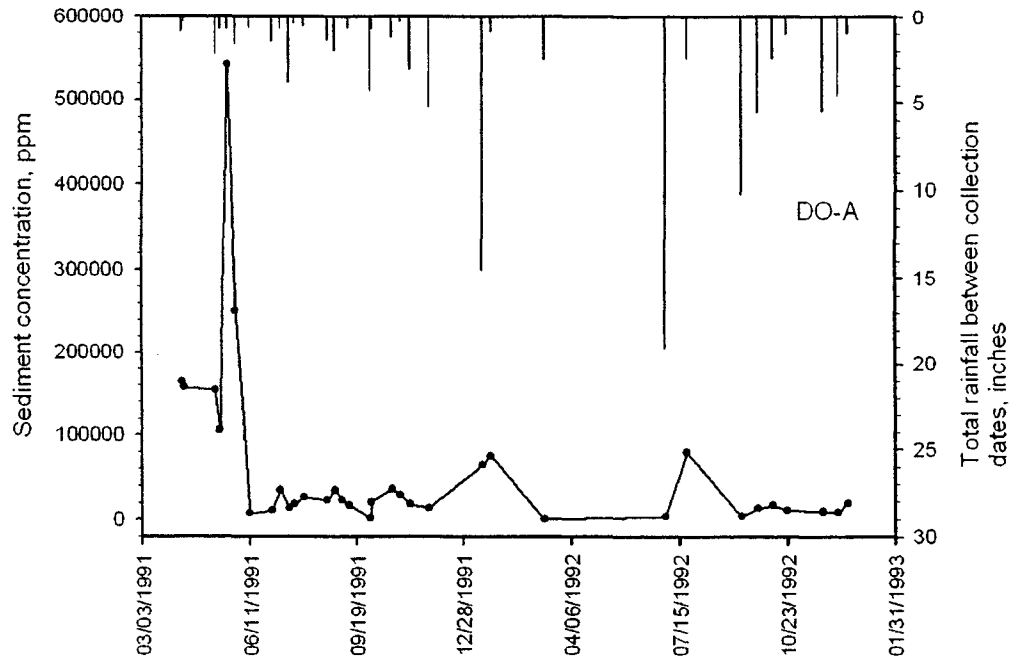

g)

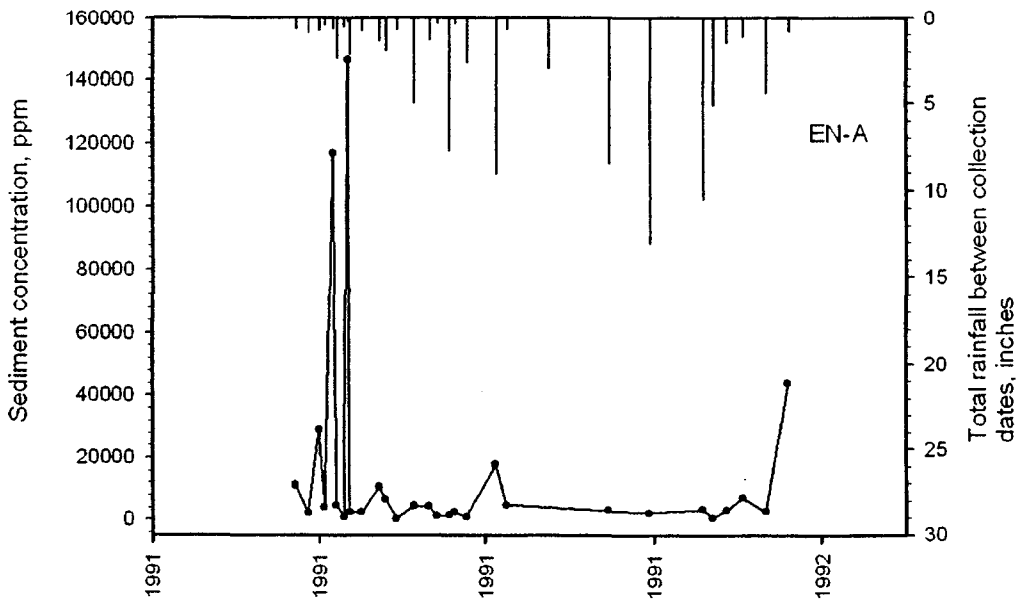

Figure 9.3. Continued. Relation of measured sediment concentration and rainfall over time at cropland sites f) DO-A, g) EN-A.

Reproduced with permission of the copyright owner. Further reproduction prohibited without permission.

h)

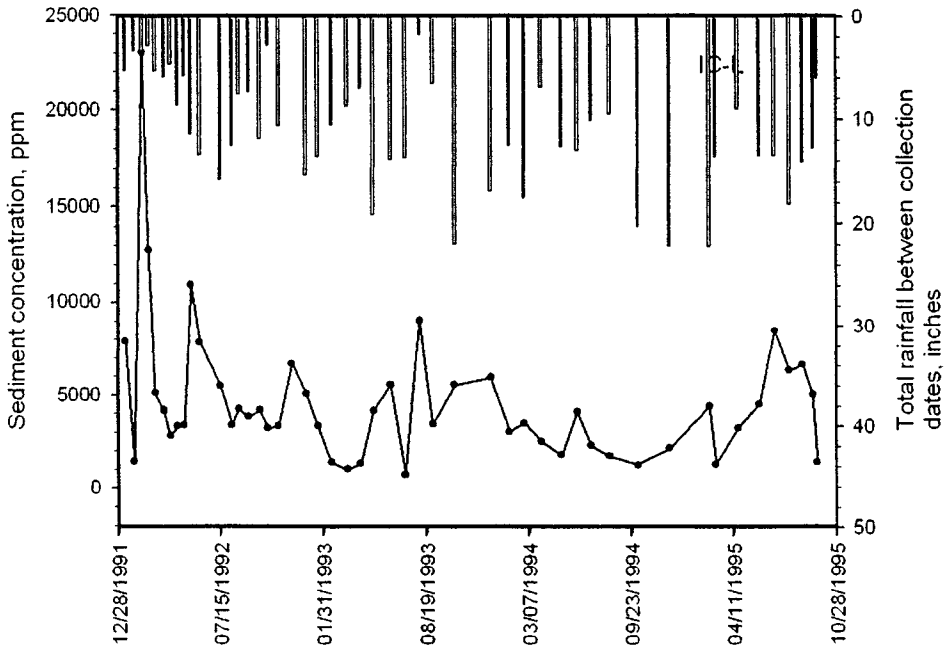

i)

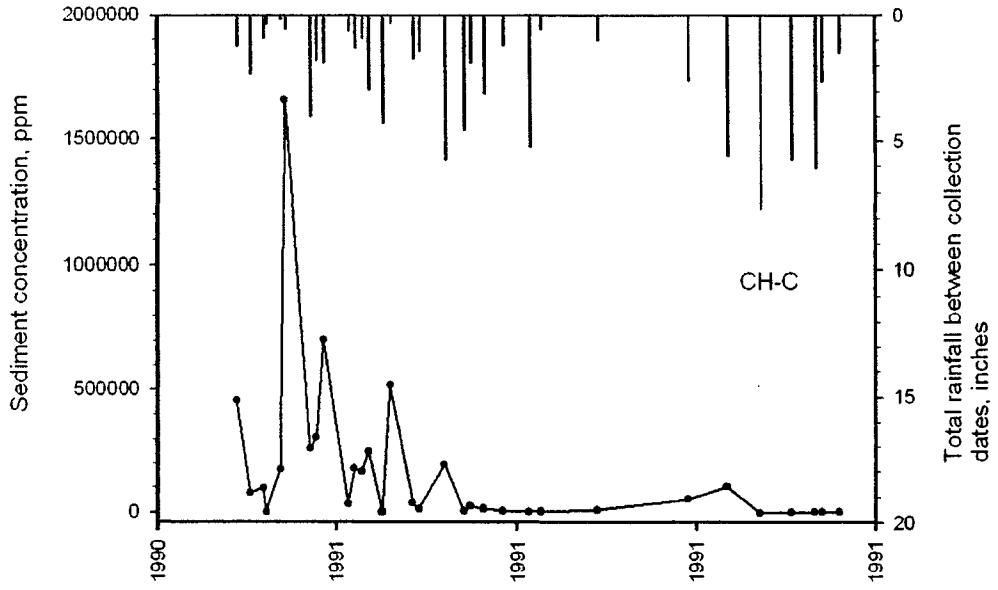

Figure 9.3. Continued. Relation of measured sediment concentration and rainfall over time at disturbed ground sites h) IC-L, i) CH-C

Reproduced with permission of the copyright owner. Further reproduction prohibited without permission.

j)

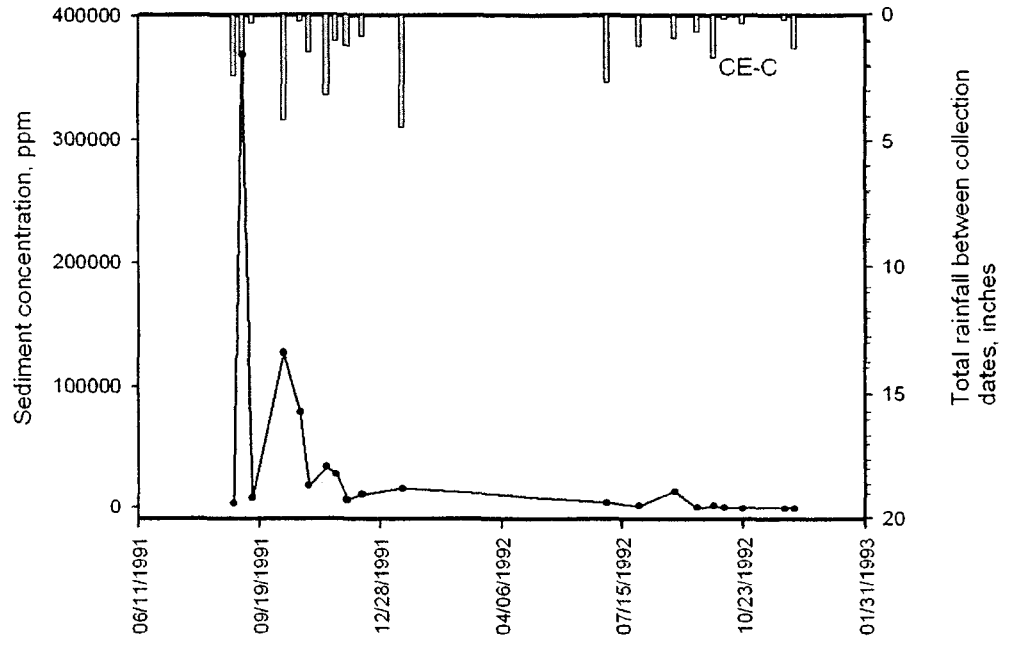

k)

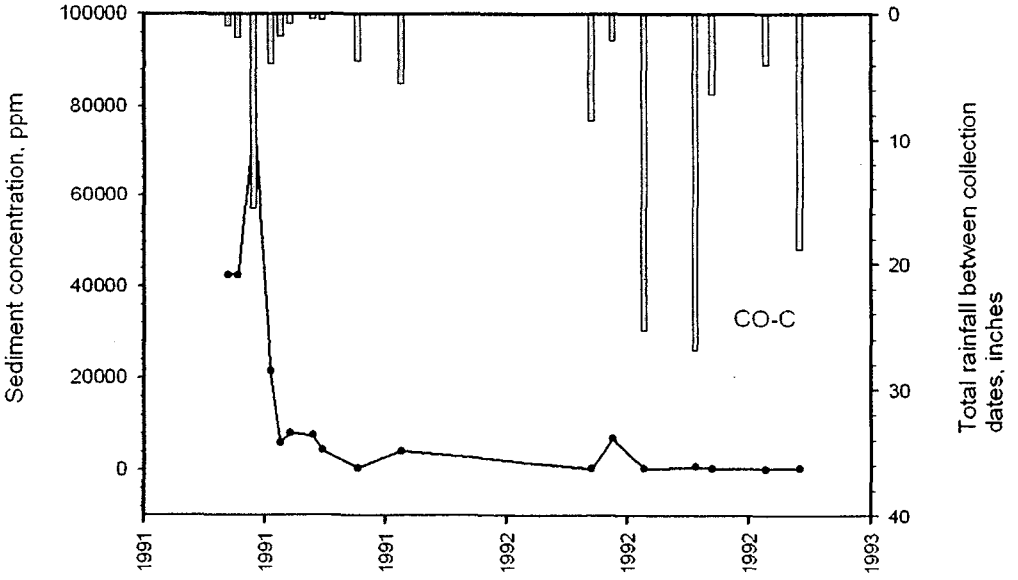

Figure 9.3. Concluded. Relation of measured sediment concentration and rainfall over time at disturbed ground sites j) CE-C, k) CO-C.

Reproduced with permission of the copyright owner. Further reproduction prohibited without permission.

Construction sites, CH-C, CE-C and CO-C, were instrumented on bare soil and were noted to have an increase in vegetation over time. Therefore, an increase in vegetation and a decrease in erosion over time were likely to have occurred at all disturbed land sites. Spikes in sheetwash erosion also are observed on cropland and pasture sites. The cropland sites went through periods of plowing and harvesting that can effect sediment concentration. Increased erosion at pasture sites may be caused by intensive grazing and natural factors, such as intense rainfall.

A plot of drainage area versus sheetwash erosion per day (g/day) for all traps shows a weak, inverse relationship (fig. 9.4a). Typically, sediment yield decreases with an increase in contributing area as more sites are available for sediment storage (Schumm, 1977; Walling, 1983). Although this relationship was derived at the basin scale, it is interesting that it is observed at the sediment trap scale. No relationship was found for slope versus sheetwash erosion (fig. 9.4b). Larsen (1997) also observed a poor relationship of sheetwash erosion to slope and attributed this poor relationship to the small scale of the traps. The sediment concentration per day (ppm/day) and sediment yield per day (grams/ft^2/day) at each trap were averaged to produce a value for each land-cover site (fig. 9.5). The highest average sediment concentration (ppm) and highest sediment yield per day are for construction sites (43,600 ppm; 0.126 g/ft^2/day), followed by cropland (20,600 ppm; 0.023 g/ft^2/day), landslide (4,100 ppm; 0.010 g/ft^2/day), forest (400 ppm; 0.007 g/ft^2/day), and pasture (3,500 ppm. 0.001 g/ft^2/day) (fig.(fig. 9.5).

Statistical results of sediment analysis for the four streamflow stations indicated that the runoff between events was significant in explaining sediment characteristics. Several sediment trap sites were installed in or near the basins draining to some of the streamflow-gaging stations used in this study (CO-C and EN-A in Quebrada Salvatierra; DO-A near Rio Caguitas) and provided

Reproduced with permission of the copyright owner. Further reproduction prohibited without permission.

a)

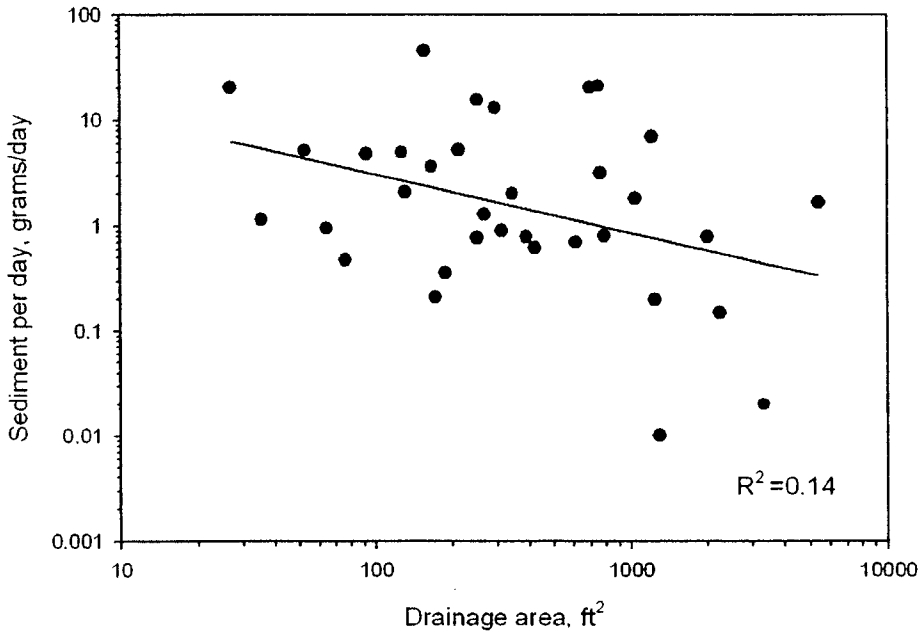

b)

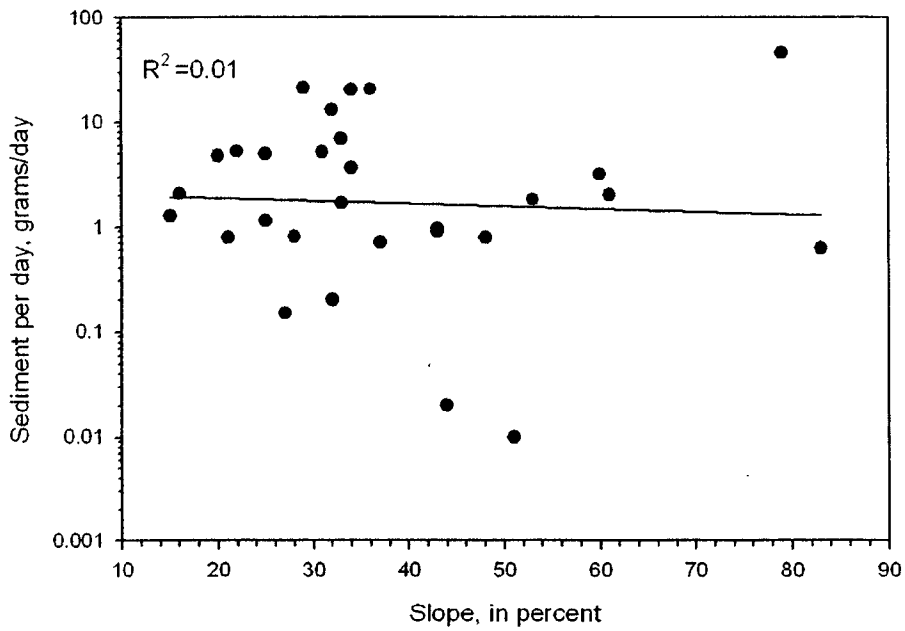

Figure 9.4. a) Relationship of drainage area and sediment per day for all sediment traps. B) Slope versus sediment per day for all sediment traps.

Reproduced with permission of the copyright owner. Further reproduction prohibited without permission.

a)

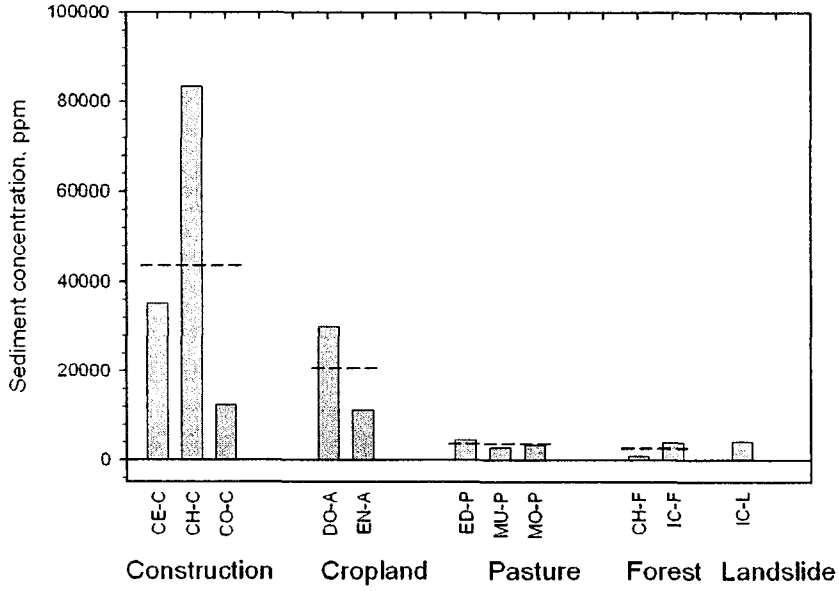

b)

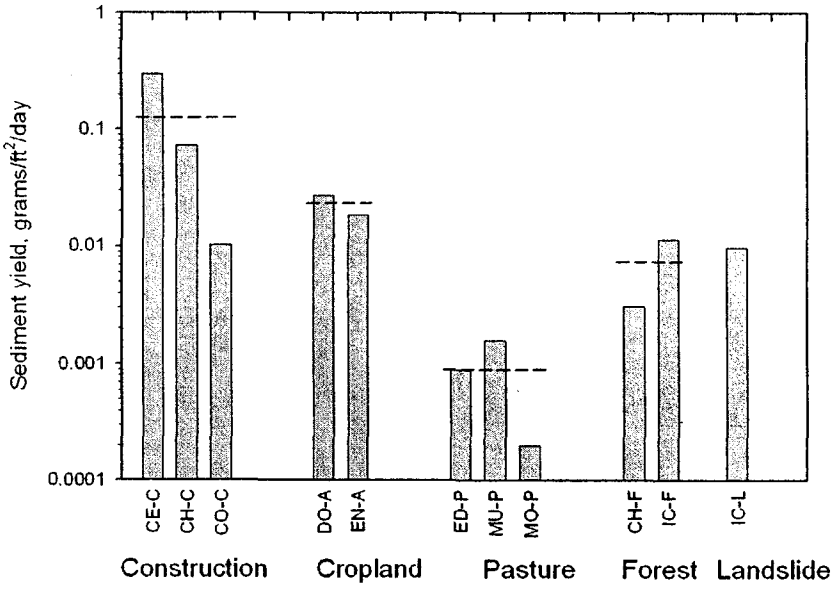

Figure 9.5. a) Average sediment concentration (ppm) for all land-cover sites. b) Average sediment yield (g/ft²/day) for all land-cover sites.

Reproduced with permission of the copyright owner. Further reproduction prohibited without permission.

a rare opportunity to investigate sheetwash erosion between runoff events (fig. 9.6). Plots of sheetwash erosion at these traps indicated that sediment was eroded and transported on hillslopes between high flow events. The sediment measured between events was similar to erosion rate measured at the traps during high flow events recorded at the streamflow-gaging station. For reasons, related possibly to the localized nature of rainfall or the duration of rainfall, runoff that contributed to sheetwash erosion at these sites did not cause a high flow event in the basin. The ultimate fate of this eroded hillslope sediment is not known. The eroded sediment may remain on the hillslope or be transported to the nearest low-order channel or to the main channel. If sediment is deposited in the channel, it may be an immediate source for the next event. Suspended-sediment samples classified as non-storm runoff or base flow showed low suspended-sediment concentrations (fig. 8.6d and other stations), and therefore little suspended sediment may be transported past the streamflow-gaging station during these minor events.

The plots on sheetwash in Chapter 9 (figs. 9.3. 9.4, 9.6) illustrate that the processes controlling overland flow are complex and incorporate many factors, including slope angle, degree of concavity, soil moisture, soil thickness, infiltration properties, vegetation, rainfall, rainfall intensity, etc. (Kirkby and Chorley, 1967). The sheetwash erosion results presented here on hillslopes of different land use were meant to describe general relationships of erosion and land use and not to present an in-depth analysis on the controls of overland flow generation. Results of sheetwash measurements presented here showed the highest sediment concentrations for disturbed land (construction and cropland) compared to forest and pasture. Basins that contain large areas of disturbed land may therefore have higher sediment loads and suspended-sediment concentrations. Many studies on basin-scale sediment yield do not have the benefit of the type of sheetwash data presented here. However,

Reproduced with permission of the copyright owner. Further reproduction prohibited without permission.

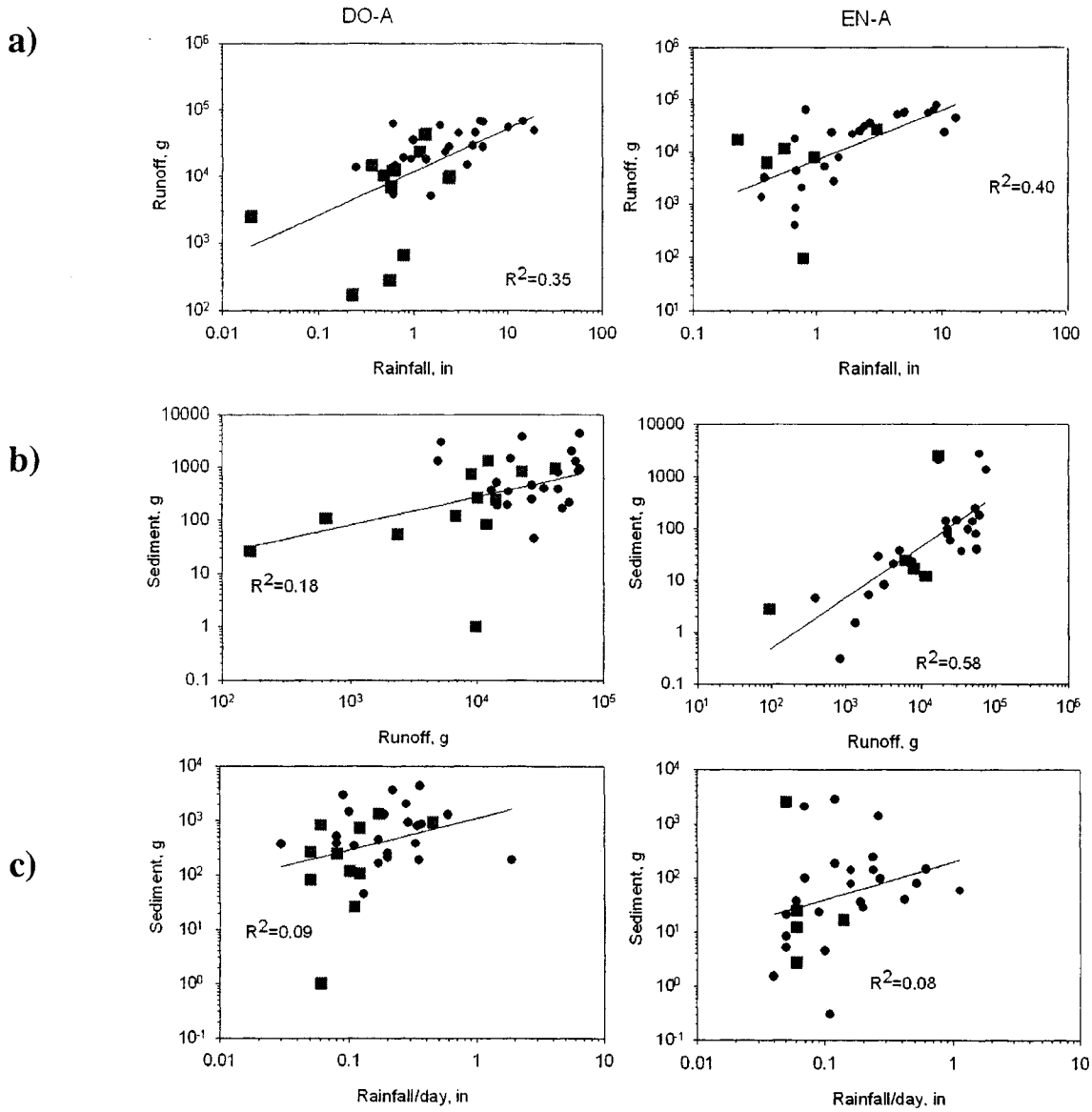

Figure 9.6. Sediment trap relations between runoff events at the streamflow stations (shown as squares) for cropland site DO-A and EN-A in a) relation of runoff to total sediment, b) runoff to sediment, and c) rainfall per day to total sediment.

Reproduced with permission of the copyright owner. Further reproduction prohibited without permission.

a)

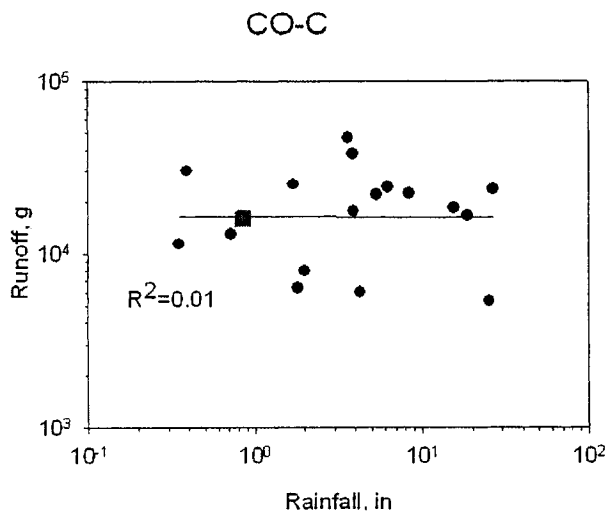

b)

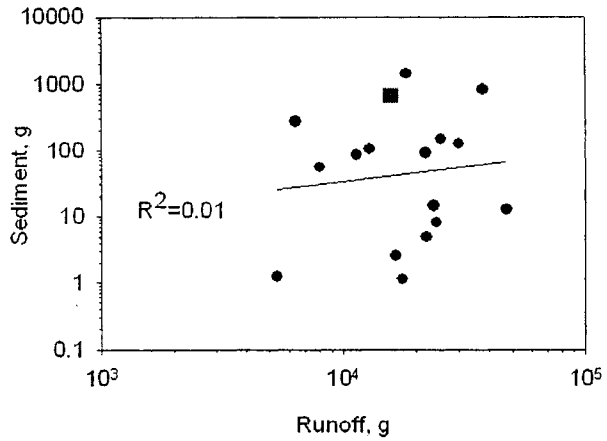

c)

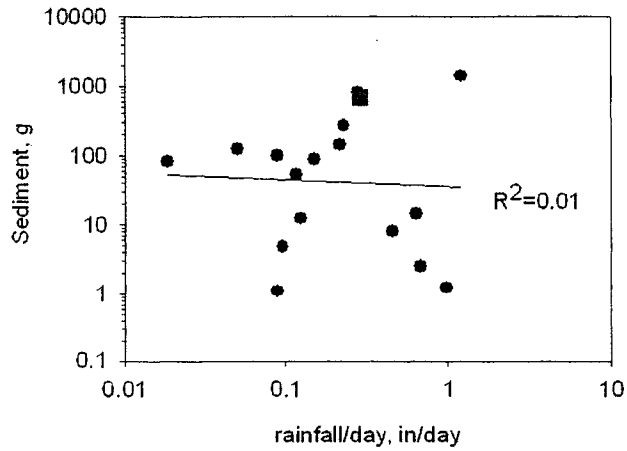

Figure 9.6. Continued. Sediment trap relations between runoff events at the streamflow stations (shown as squares) for construction site CO-C in a) relation of runoff to total sediment, b) runoff to sediment, and c) rainfall per day to total sediment.

Reproduced with permission of the copyright owner. Further reproduction prohibited without permission.

it is important to note that because of problems in the design and collection frequency of sediment traps, the data shown here provided minimum values. Problems with the sediment traps included cows stepping on the traps and disconnecting hoses, and other animals making the traps their homes. Ideally the traps should be visited after each rainfall event. At times it was noted that the collection buckets were completely filled and thus, some runoff and sediment were possibly lost.

Reproduced with permission of the copyright owner. Further reproduction prohibited without permission.

CHAPTER X

SUMMARY

Suspended-sediment transport in most river systems accounts for over 90% of the total annual sediment load (Meade and others, 1990). Most rivers transport 80 to 90% of their load during 10% of the year (Meade and others, 1990). Understanding the significant factors controlling suspended-sediment concentrations and suspended-sediment loads during storm events is therefore important for our understanding of how geomorphic systems operate. Comparing these significant factors in basins varying from undisturbed to disturbed informs us of the human impact on the fluvial system.

In this PhD dissertation, over three thousand (3,096) suspended-sediment samples and 754 storm-generated runoff events were examined using a variety of hydrological and statistical operations to determine the significant controls on storm generated suspended-sediment loads and sediment concentrations for four basins of differing land use in humid-tropical Puerto Rico. The factors thought to control storm-generated suspended-sediment loads and concentrations were separated into three time categories: 1) previous-event factors, 2) factors between events, and 3) current-event factors.

The suspended-sediment samples were collected by the USGS Caribbean District as part of their sediment collection program. Samples were collected with manual samplers and with automatic samplers. The automatic samplers were designed to collect sediment during storm-generated runoff events. Ideally the automatic samples should be calibrated with cross-sectional

Reproduced with permission of the copyright owner. Further reproduction prohibited without permission.

manual samples. Because of the flashy nature of most storm events, this was rarely performed and it is understood that not calibrating many of the suspended-sediment samples may introduce some error. However, it is observed that most of the streams are very turbid during high flows and the cross section is well mixed, therefore limiting some of this error.

A graphical separation technique was used to separate the hydrograph into quickflow and base flow. The quickflow portion includes storm overland flow, saturated overland flow, and throughflow. The location on each hydrograph where quickflow ends was defined by an inflection point on the hydrograph recession limb, which was determined by taking the second derivative of a 3rd order best-fit regression line fit to the hydrograph recession limb. The quickflow volume was computed as the area under the hydrograph, defined by a line drawn from the start of the event to the inflection point. Complex events are closely-spaced storms where the recession portions of the storm hydrograph approach but never reach base flow. Complex events were separated into quickflow and base flow by determining whether the hydrograph recession met threshold discharge and threshold slope criteria based on examination of recession curves. If these criteria were met, the end of the event was selected just before the next hydrograph rise. The final recession limb of the complex event had to meet the criteria established for a single event.

The quickflow portion of the hydrograph and the runoff hydrograph (which includes base flow) were statistically analyzed for two portions of the storm-generated hydrograph: (1) the entire hydrograph, and to (2) determine whether statistical factors controlling sediment are more sensitive on the rising limb of the hydrograph, variables to the highest peak flow were examined. Storms were classified by their hysteresis loops (clockwise or counterclockwise) and significant controls on the amount of sediment exhaustion or increase of the hysteresis loops were examined.

Reproduced with permission of the copyright owner. Further reproduction prohibited without permission.

Sheetwash Erosion

The four basins studied are representative of the major land uses on Puerto Rico: forest (Rio Icacos), cropland (Rio Caguitas), pasture (Quebrada Blanca, Rio Caguitas), and urbanizing-construction (Rio Piedras). To obtain a better understanding of upland erosion rates in different land-use settings, sheetwash erosion was measured using sediment traps. The average sediment concentration (ppm) and average sediment yield per day are highest for construction sites (43,600 ppm; 0.126 g/ft^2/day), followed by cropland (20,600 ppm; 0.023 g/ft^2/day), forest (400 ppm; 0.007 g/ft^2/day), and pasture (3,500 ppm0.001 g/ft^2/day) (fig. 9.5). A landslide instrumented by Larsen (1997) in the Rio Icacos basin showed an average sediment concentration and an average sediment yield per day of 4,100 ppm and 0.010 g/ft^2/day, respectively. Based on the sediment trap data, basins draining urbanizing watersheds, such as Rio Piedras which have construction activities also have high rates of sheetwash erosion. Although the sediment concentrations and yields in forested basins are low, findings indicate that sheetwash erosion is an active geomorphic process in forested settings. Average sheetwash sediment yields from this study are lower than sheetwash measurements obtained from the literature (fig. 10.1). In this study it was often noted that the traps were damaged, overflowed, or missed an event. Therefore, the sheetwash erosion measurements presented here should be considered minimum values. However, if we assume that all the traps operated with the same errors, then the sheetwash erosion rates can be used to determine relative differences in erosion under varying land use settings.

Reproduced with permission of the copyright owner. Further reproduction prohibited without permission.

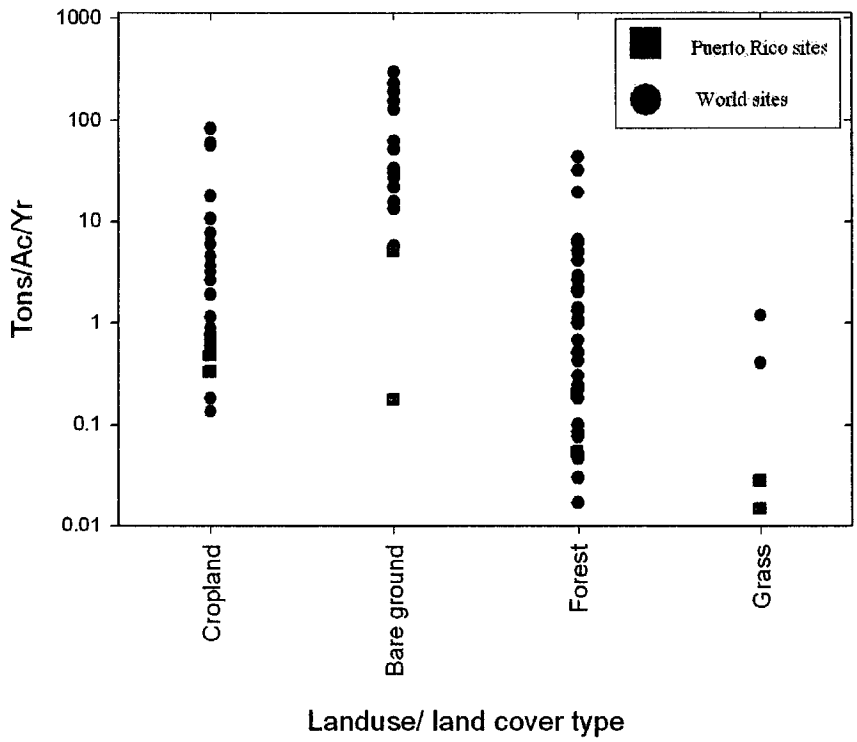

Figure 10.1. Comparison of average sheetwash erosion measurements for each instrumented site compared to world sheetwash erosion See Table 2.1 for references on the world sheetwash erosion rates.

Processes controlling overland flow are complex and incorporate many factors including, slope angle, degree of concavity, soil moisture, soil thickness, infiltration properties, vegetation, rainfall, rainfall intensity, etc. (Kirkby and Chorley, 1967). The sheetwash erosion results presented here on hillslopes under varying land use were meant to describe general relationships between erosion and land use and were not intended to provide an in-depth analysis on the controls of overland flow generation. Several sediment trap sites were installed in or near the basins draining to some of the streamflow-gaging stations used in this study (CO-C and EN-A in Quebrada Salvatierra; DO-A near Rio Caguitas) and indicated that sediment was eroded and transported on hillslopes between high flow events

Reproduced with permission of the copyright owner. Further reproduction prohibited without permission.

recorded at the streamflow-gaging stations. The localized nature of rainfall may contribute to sheetwash erosion between major runoff events. Sediment eroded during these 'between-event' rainstorms may remain on the hillslope or be transported to the nearest channel. If this sediment is deposited in the channel network it may become an immediate source for the next event.

Hydrology and sediment characteristics at the four study basins

A plot of mean annual precipitation versus mean daily discharge for the four basins is shown in figure (10.2). Rio Icacos is situated at a higher elevation and thus, higher rainfall and runoff volumes are expected (fig. 10.2). The lower relative discharge at Quebrada Blanca may reflect high infiltration rates caused by the sandy texture of the overlying soils created by weathering of the underlying granodiorite (Table 3.1).

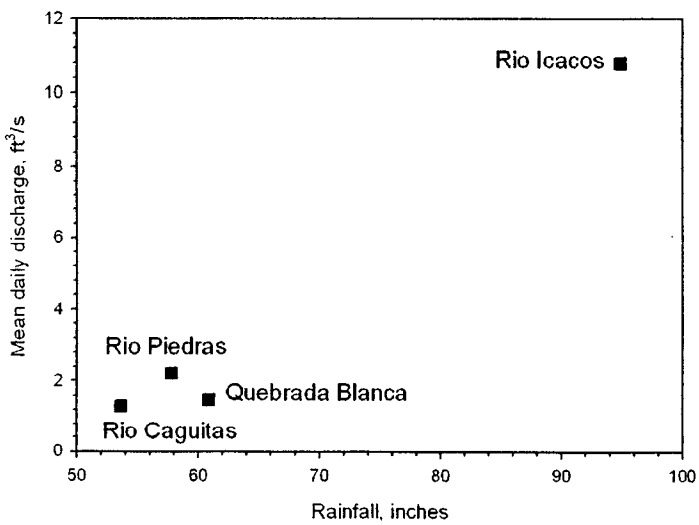

Figure 10.2. Graph showing average daily rainfall versus mean daily discharge for period of study at each basin.

Reproduced with permission of the copyright owner. Further reproduction prohibited without permission.

The median grain diameter (d_{50}) on the bed of the river varies for the four study basins (fig. 10.3). The variability in d_{50} may be related to lithology and land use. Intrusive rocks weather to fine sand and volcaniclastic rocks weather to clay. Higher soil erosion in the clay-rich hillslopes draining volcaniclastic rocks can lead to finer material found in the bed of the channel.

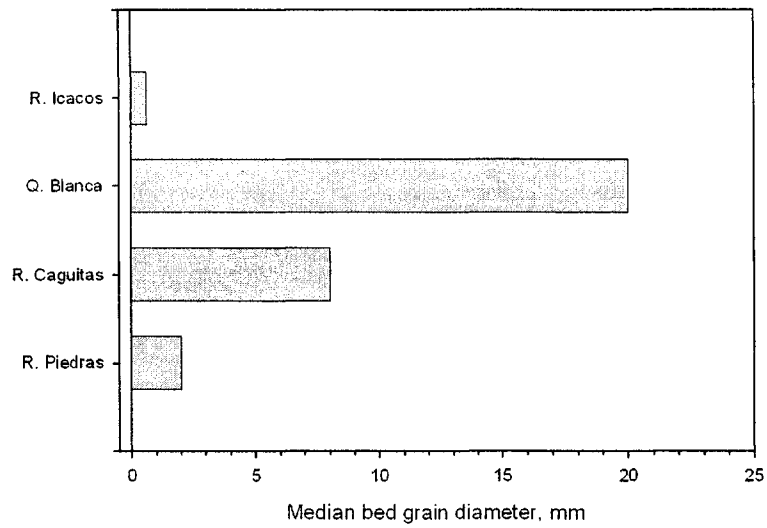

Figure 10.3. Median bed grain diameter (d_{50}) (mm) measured at the streamflow-gaging station for the four study basins.

Larsen (1997) attributed the fine sand of the Rio Icacos (d_{50}=0.6 mm) to weathering of intrusive rocks and to frequent exceedence of the critical shear stress needed to transport sand. The largest median size bed material was sampled in Quebrada Blanca (d_{50}=20mm), which drains approximately 50% volcaniclastic rocks and 50% granodiorite, followed by Rio Caguitas (d_{50}=8mm), which drains close to 100% volcaniclastic rocks. Rio Piedras drains primarily volcaniclastic rocks and its finer bed material with respect to Quebrada Blanca and Rio Caguitas may reflect the influence of hillslope disturbance from housing constructions, which has introduced finer material to the channel.

Reproduced with permission of the copyright owner. Further reproduction prohibited without permission.

Sediment Yields

Average annual sediment yield for each study basin during their study period showed the highest sediment yield for the urbanizing basin (Rio Piedras), followed by the forested basin (Rio Icacos), cropland (Rio Caguitas), and pasture (Quebrada Blanca) (fig. 10.4a). Normalizing by average annual runoff to produce a discharge-weighted sediment concentration showed Rio Piedras with the highest concentration followed by Rio Caguitas, Quebrada Blanca, and Rio Icacos (fig. 10.4b). Figure 10.4 illustrates the importance of normalizing suspended-sediment loads by runoff rather than basin area. If climatic conditions vary, as was the case for the 4 basins studied here, sediment load per unit area is not comparable between stations and therefore a better normalization procedure is to divide suspended-sediment load by runoff.

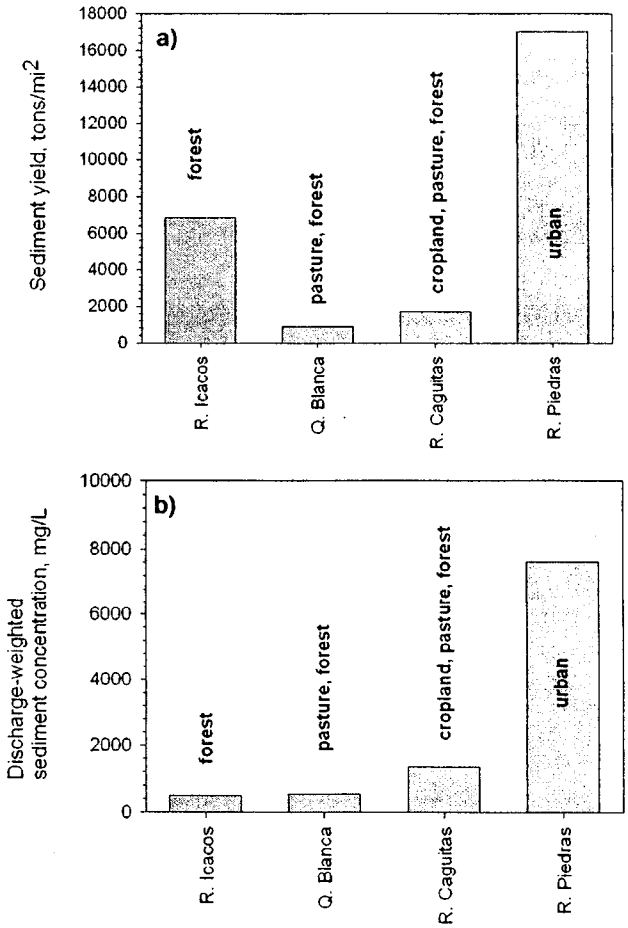

Figure 10.4. a) Average annual sediment yield and (b) average annual discharge-weighted sediment concentration, for the four study basins.

Reproduced with permission of the copyright owner. Further reproduction prohibited without permission.

A comparison of average annual sediment yields and concentrations for the four study basins to other stations operating in Puerto Rico are shown in figure 10.5. The sediment yield and discharge-weighted sediment concentration of Rio Piedras is the highest for the Island. Comparison of Puerto Rican sediment yields (including the four study basins) to other tropical rivers show they have similar magnitudes of sediment yields with respect to drainage area (fig. 10.6a). World tropical rivers show a decrease in sediment yield as drainage area increases, although the R^2 value is low (fig. 10.6a). The relation of sediment yield to drainage area for Puerto Rican streams is especially poor (fig. 10.5). Drainage areas of world tropical rivers plotted against their discharge-weighted sediment concentration also shows a poor relationship (fig. 10.6b). Compared to world tropical rivers, Rio Piedras has the seventh highest discharge-weighted sediment concentration for those rivers in the data set (fig. 10.6b).

Sediment yields of the four study basins plotted on the sediment yield models developed by Langbein and Schumm (1958) and Fournier (1960) show Puerto Rican rivers to have relatively high sediment yields (fig. 10.7a,b). Using the sediment yield database compiled by the Food and Agriculture Organization of the United Nations (2003), combined with Puerto Rican streams and two stations from the Rio Puerco Basin, United States, and categorizing rivers by the Koppen classification system into tropical, temperate, and dry climates, show tropical rivers to have sediment yields similar to semi-arid regions (fig. 10.8a). Temperate climates have the lowest sediment yields (fig. 10.8a). The higher sediment yields in semi-arid regions and tropical regions support the models of Langbein and Schumm (1958) and Fournier (1960). Semi-arid rivers have the highest discharge-weighted sediment concentrations, followed by tropical rivers and temperate rivers (fig. 10.8b). Puerto Rican streams appear to have low sediment concentrations per drainage

Reproduced with permission of the copyright owner. Further reproduction prohibited without permission.

area compared to other world rivers. The world rivers in figures 10.6 and 10.8 have drainage areas that are larger than the streams in Puerto Rico, which may explain some of this difference.

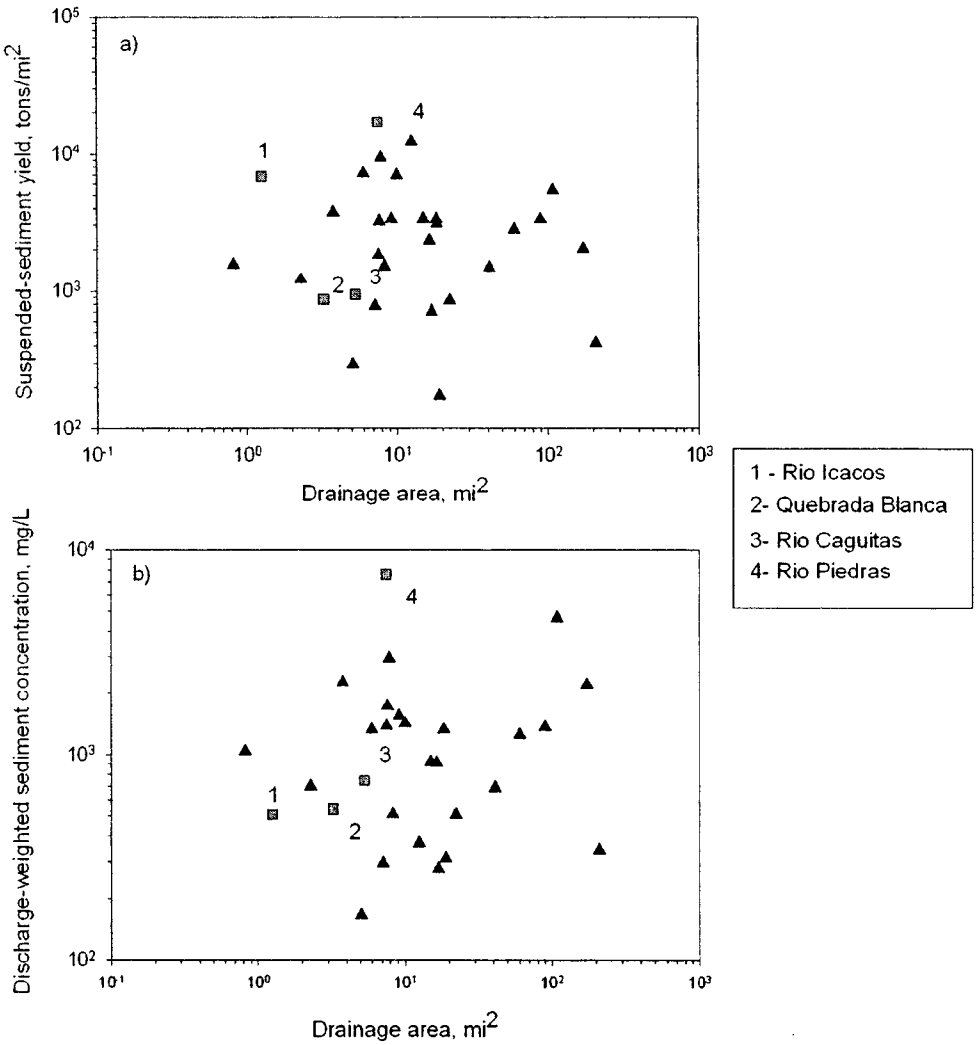

Figure 10.5. Comparison of a) average annual sediment yield and b) average annual discharge-weighted sediment concentration of the four study basins to other stations operating in Puerto Rico.

Reproduced with permission of the copyright owner. Further reproduction prohibited without permission.

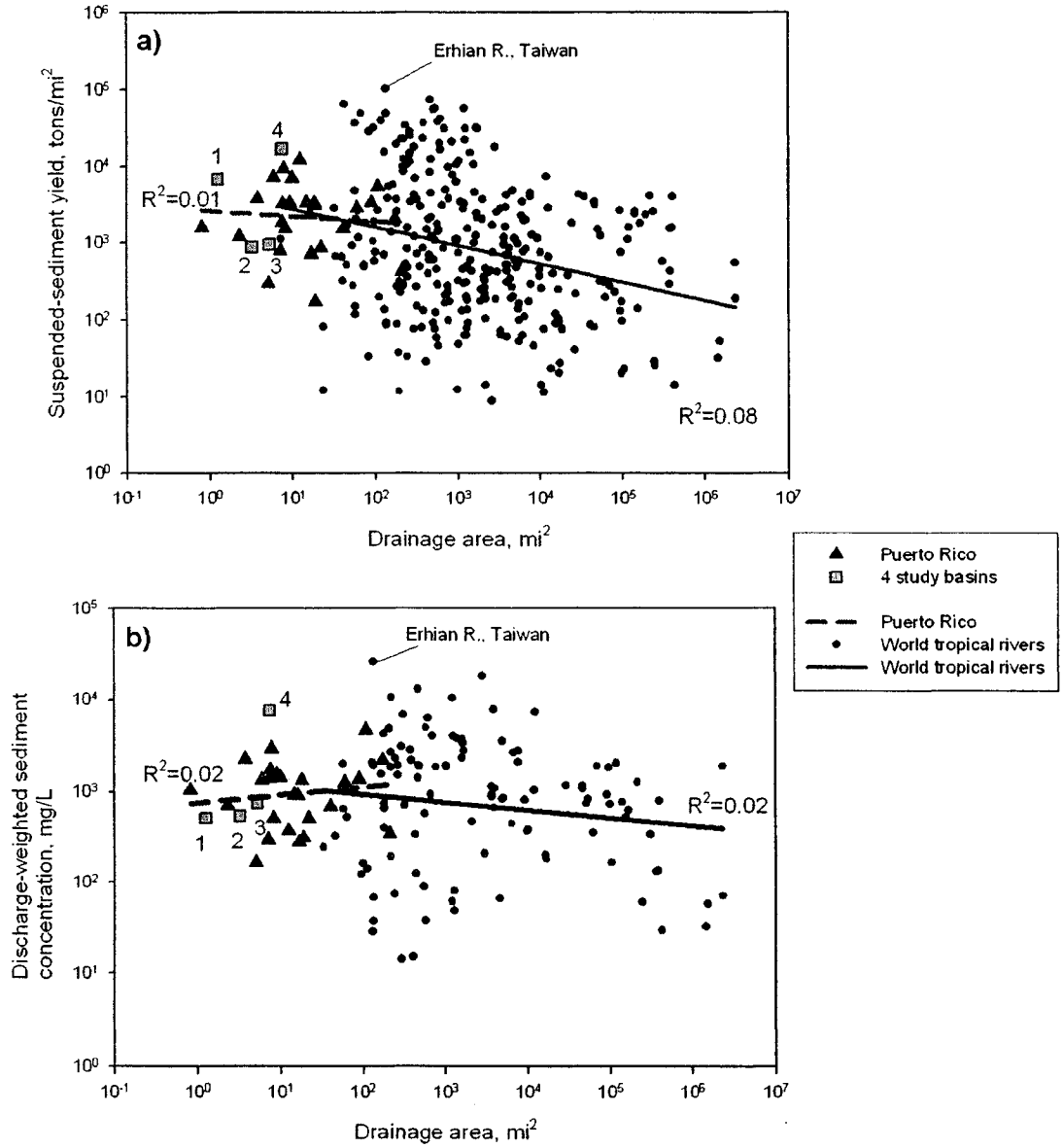

Figure 10.6. Comparison of Puerto Rican stations, including the four study basins to world tropical rivers a) average annual sediment yield and b) average annual discharge-weighted sediment concentration Refer back to figure 10.5 for names of the four study basins Data on tropical rivers was obtained from the Food and Agriculture Organization of the United Nations (2003).

Figure 10.8 also illustrates the problems in comparing sediment yields between different climatic regions. Normalizing by drainage area does not take into account a significant aspect of

Reproduced with permission of the copyright owner. Further reproduction prohibited without permission.

sediment transport, which is flow. The difference in discharge-weighted sediment concentrations between the three climatic types reflect sediment availability. Semi-arid regions have low-vegetation density and significant sources of sediment. In many areas of the world, including the western United States, semi-arid regions have high relief, which increases erosion and sediment delivery. Tropical areas have high vegetation density as a result of increased rainfall but also have increased chemical weathering, resulting in deep weathered soils. Rainfall in many tropical areas is delivered to the ground during intense storms, which can cause masswasting and large floods, all contributing to significant sources of sediment. Many tropical areas, including Puerto Rico, are in areas of high relief. Temperate areas can have high vegetation density and deeply weathered soils, but the lower sediment concentration may reflect lower relief and less frequent, intense rainfall events. Additional research will be needed to fully support this conclusion.

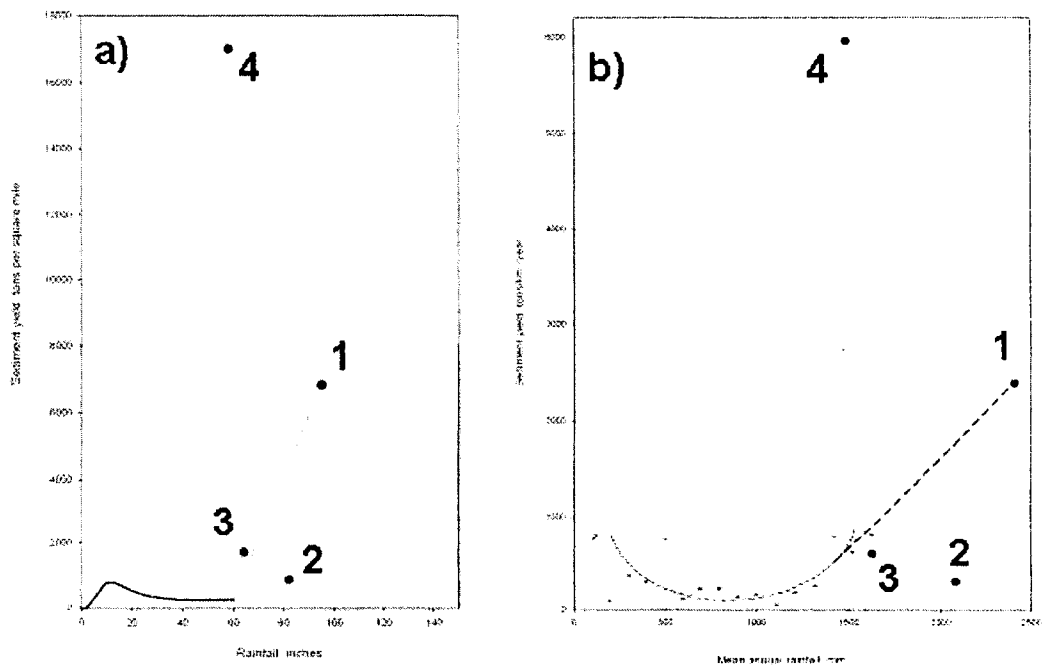

Figure 10.7. The four study basins plotted on the sediment yield model of a) Langbein and Schumm (1958) and b Fournier (1960) Refer to figure 10.5 for names of the four study basins.

Reproduced with permission of the copyright owner. Further reproduction prohibited without permission.

The data set on world rivers does not distinguish between another important factor controlling sediment yields, that of land use. Wolman (1967) characterized sediment yield and its relation to changing land-use for a fixed area in the humid-temperate northeastern U.S., from forest to agriculture in the 1800's, with reforestation following abandonment of cropland in around 1940, to urbanization after the 1950's (fig. 10.9). Agriculture increased sediment yields 60 times above

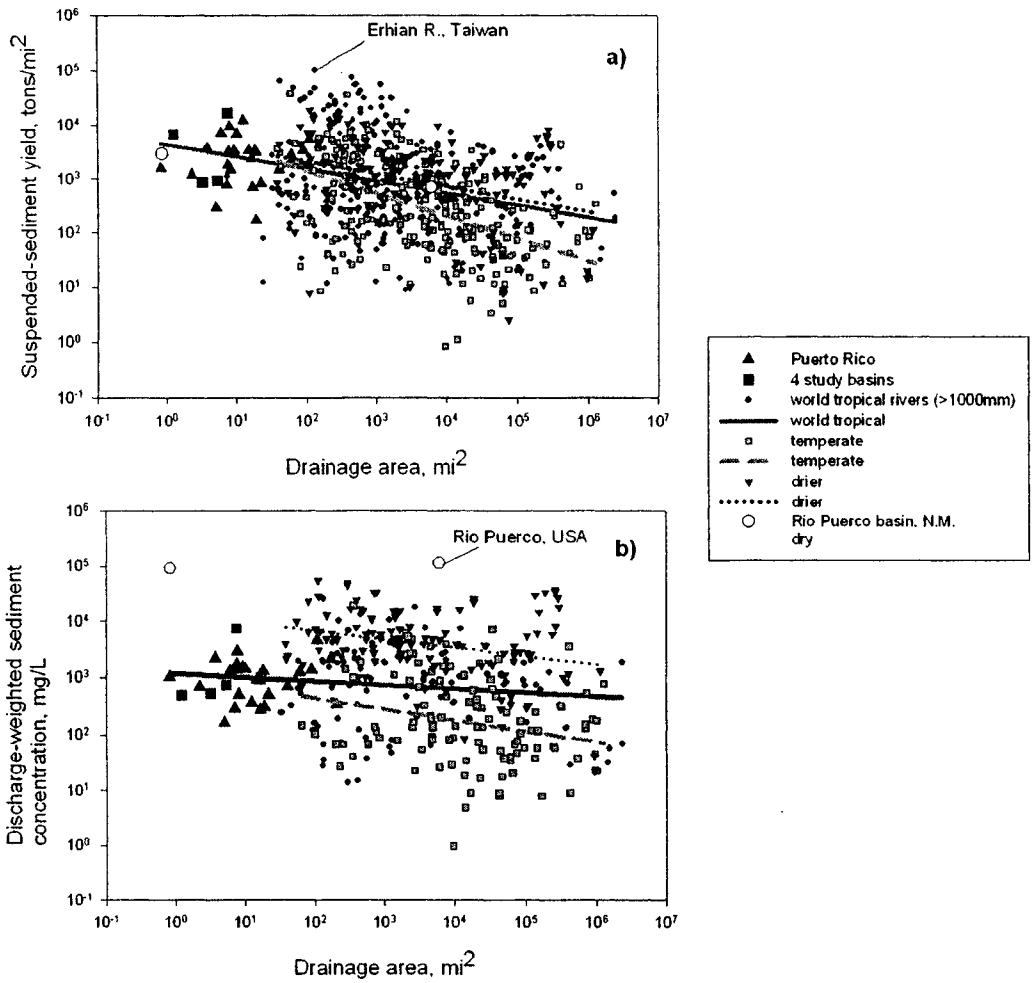

Figure 10.8. Classification of world rivers into tropical, temperate, and dry, including the four study basins, and two stations in the Rio Puerco Basin, United States (Gellis and others, 2001) for a) average annual sediment yield and b) average annual discharge-weighted sediment concentration Sediment data for world rivers was obtained by the Food and Agriculture Organization of the United Nations (2003), refer back to figure 10.5 for names of the four study basins.

Reproduced with permission of the copyright owner. Further reproduction prohibited without permission.

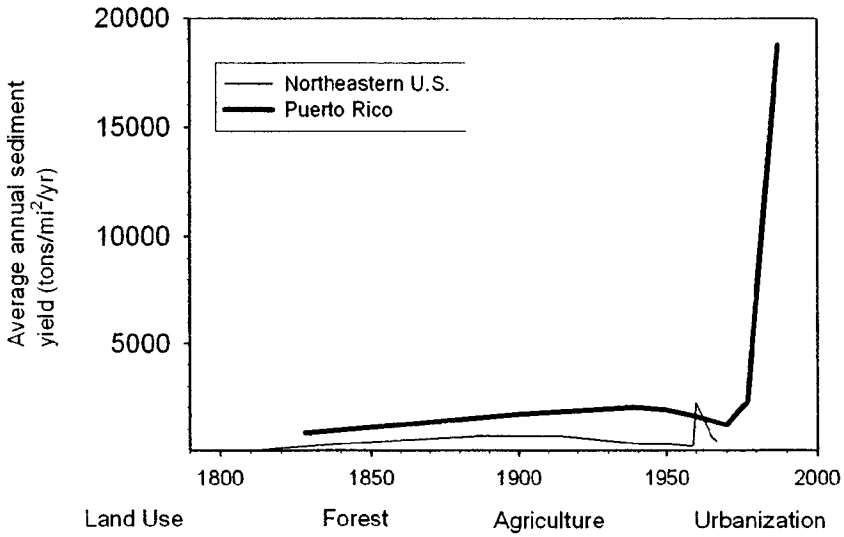

Figure 10.9. a) Hypothetical plot of sediment yield response to land-use changes northeastern U.S. (after Wolman, 1967) compared with data from Puerto Rico (USGS, 1989-2000).

Table 10.1 Sediment yields from drainage basins under diverse land use, Puerto Rico (USGS, 1989-95).

Station	Years	Drainage area (mi^2)	Sediment yield ($tons/mi^2/yr$)	Land use
Rio Icacos near Naguabo	1995-2000	1.26	6,830	forest
Rio Canovanos near Campo Rico	1991-95	9.85	405	forest
Rio Mameyes near Sabana	1991-95	6.87	334	forest
Rio Grande de Loiza near San Lorenzo	1991-93	40.9	1,900	cropland, pasture
Rio Caguitas near Aguas Buenas	1991-96	5.29	1,720	cropland, pasture
Rio Piedras at El Senorial	1989-95	7.49	17,000	urbanized

Reproduced with permission of the copyright owner. Further reproduction prohibited without permission.

background levels and urbanization increased sediment yields 200 times above background levels. Although the timing of land-use change is different in Puerto Rico compared to the northeastern U.S., the sequence of land-use change in Puerto Rico is similar. Using USGS Water-Resources Data Reports for stations in the Lago Loiza basin, Puerto Rico and surrounding areas (USGS, 1989-1995), sediment yield values for dominantly cropland, forest, and urbanized basins were identified (table 10.1) and compared to Wolman's (1967) hypothetical curve (fig. 10.9). Sediment yields in the Lago Loiza basin and surrounding areas increased from deforestation for agriculture in the 1900s at higher rates than reported for the northeastern U.S. Average annual sediment yields during the agricultural period in Puerto Rico may have been 3 times higher than sediment yields reported for the northeastern United States. Sediment yield in an urbanizing basin in Puerto Rico (Rio Piedras) is 17,000 tons/mi^2 (5,950 metric tons/ km^2), which is over eight times higher than sediment yields reported by Wolman (1967) for an urbanizing basin (2,200 tons/mi^2; 2000 metric tons/km^2) in the northeastern U.S. Wolman's (1967) curve depicts a decrease in sediment yield after 1960 when urbanization was almost complete. The curve for Puerto Rico does not show this decrease, because at the time of this study, urbanization and housing projects were still on the increase.

The higher sediment yields as a result of land disturbance reported for Puerto Rico may again reflect differences in climate and topography. The humid-tropical climate of Puerto Rico produces deeply weathered soils, in areas up to 6 feet deep (1.8 m). The thick soils in Puerto Rico combined with steeper slopes and higher rainfall amounts, typically of high intensity and duration, may produce higher sediment yields in disturbed basins compared to disturbed basins in the humid temperate northeastern U.S.

Reproduced with permission of the copyright owner. Further reproduction prohibited without permission.

Suspended-Sediment Transport

In most fluvial settings, a significant portion of average annual suspended-sediment is transported in a few days (Meade and others, 1990; Walling, 1996). In the four basins being investigated, 90% of the annual suspended sediment was transported in 12 to 28 days and 75% in 5 to 11 days, (fig. 10.10a, b). Of particular interest is that the basins with the two highest sediment yields, Rio Piedras and Rio Icacos, showed the most days to transport sediment. The percent of annual suspended-sediment load transported in one day for the four stations, averaged for all years, ranged from 25 to 50%. At Quebrada Blanca, on September 20, 1994, 84% of the annual suspended-sediment load (2,260 tons; 2,050 metric tons) was transported in one day! The differences in percent of suspended-sediment load transported between the four study basins may reflect the occurrence of large storm events in one basin, such as hurricanes, rather than a

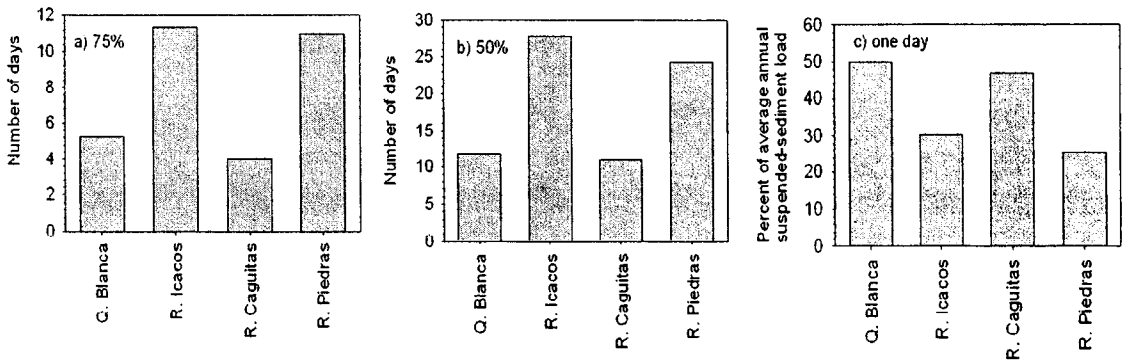

Figure 10.10. The number of days annual suspended-sediment load was transported at the four study basins for a) 75% of the average annual load and b) for 90% of the average annual load c) The average annual percentage of suspended-sediment transported load in one day.

Reproduced with permission of the copyright owner. Further reproduction prohibited without permission.

difference in land use. Figure 10.10 illustrates the importance of obtaining suspended-sediment samples during large storm events to adequately define annual suspended-sediment loads.

Box plots of suspended-sediment concentrations for each basin show that the mean and median concentrations for the Rio Piedras basin were an order of magnitude higher than the other 3 basins (fig. 10.11). Rio Caguitas drains a large area of cropland (23%), an erosive land use, but showed percentiles of suspended-sediment concentrations only a little higher than pasture and forest. This may be caused in part by the large number of base flow samples taken, which would give a higher weight to the lower discharges. The mean of suspended-sediment concentrations may be a better way to represent the data rather than the median.

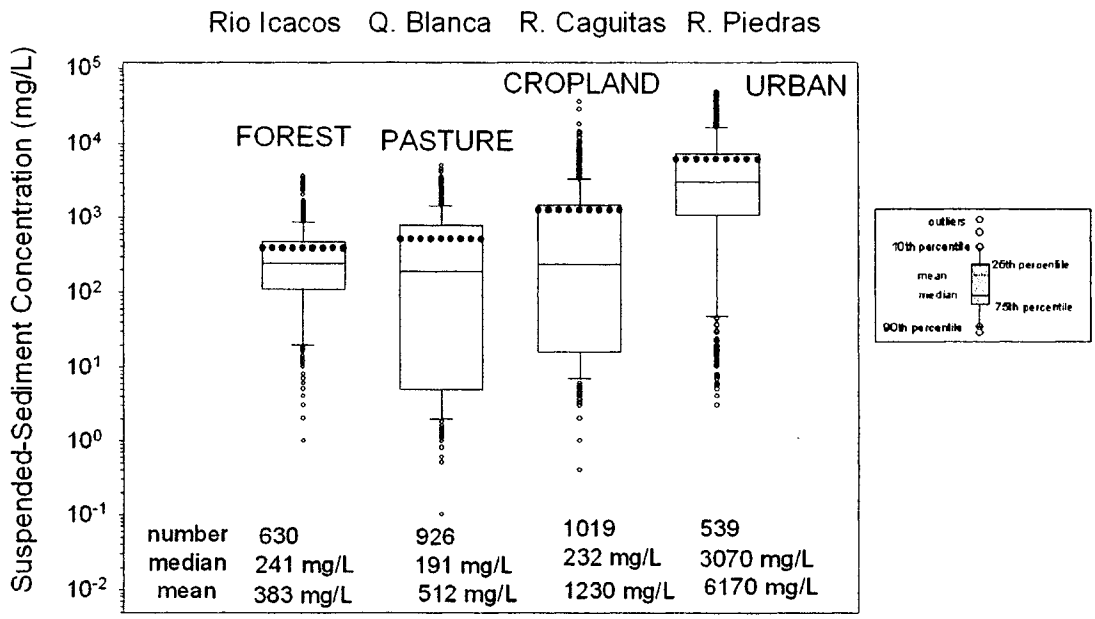

Figure 10.11. Box plots of suspended-sediment concentrations for the four study basins.

Reproduced with permission of the copyright owner. Further reproduction prohibited without permission.

Sediment-Transport Curves

The best-fit lines for the sediment-transport curves normalized by area for all samples, rising samples, falling samples, and base flow samples all showed that Rio Piedras and Rio Caguitas at a given discharge have the two highest suspended-sediment concentrations, followed by Quebrada Blanca, and Rio Icacos (fig. 10.12a,b,c). For all samples, at a discharge per unit area of 60 $ft^3/s/mi^2$(1.7 $m^3/s/km^2$), Rio Caguitas' suspended-sediment concentration (8,260 mg/L) was the highest followed by Rio Piedras (6,370 mg/L), Quebrada Blanca (1,770 mg/L), and Rio Icacos (217 mg/L) (fig.10.12a).

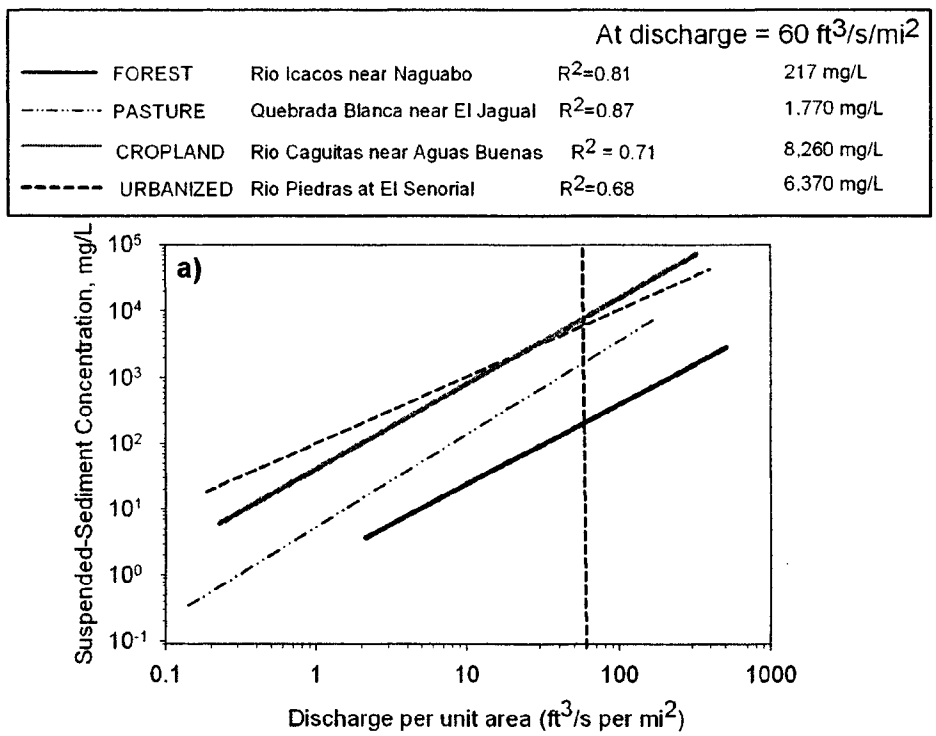

Figure 10.12. a) Sediment transport curves, using all samples, for the four study basins, normalized by area.

Reproduced with permission of the copyright owner. Further reproduction prohibited without permission.

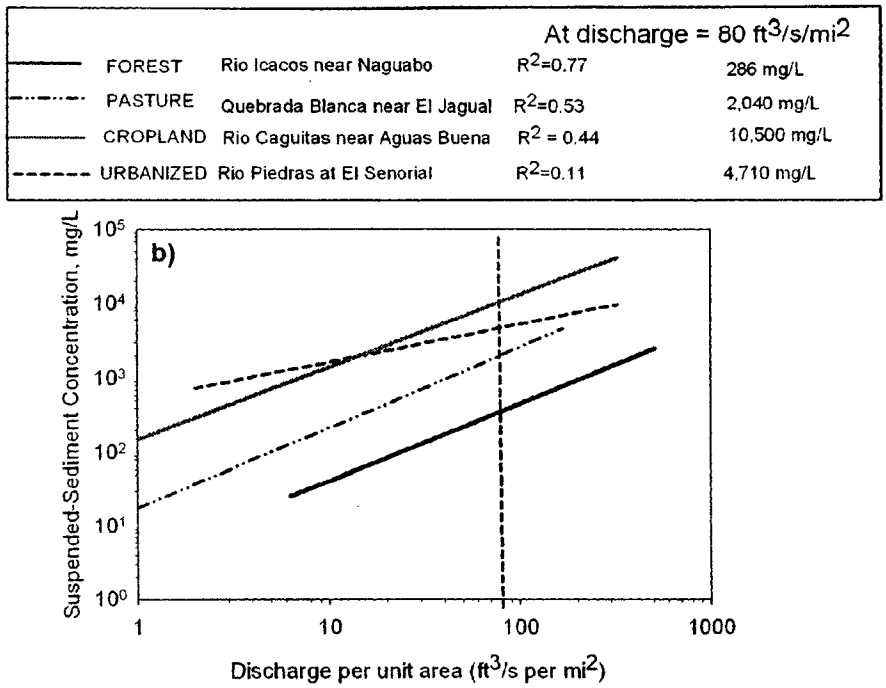

Figure 10.12. b) Sediment transport curves, for samples rising to the highest peak flow, for the four study basins, normalized by area.

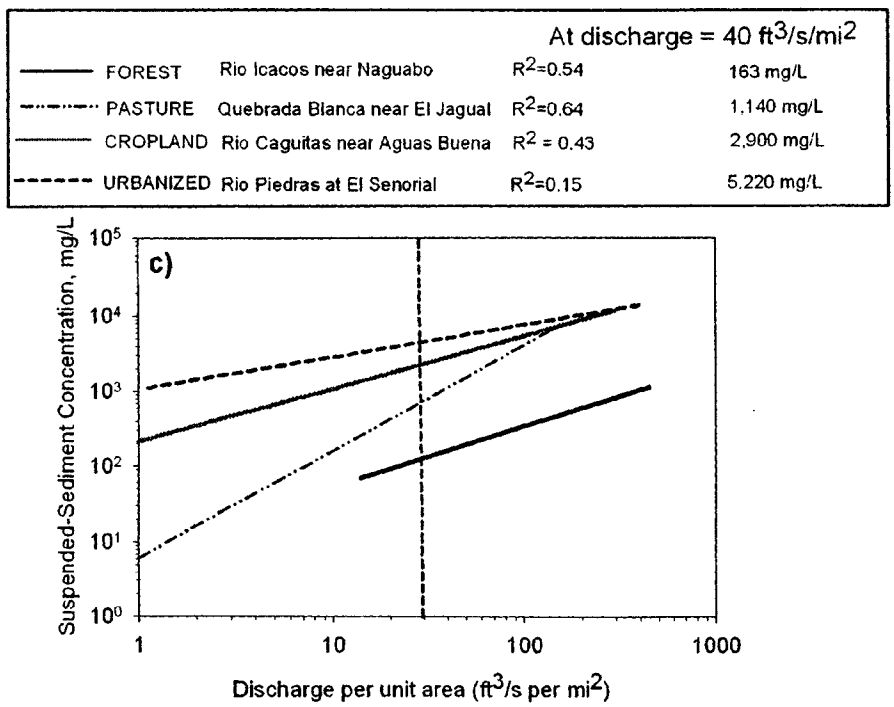

Figure 10.12. c) Sediment transport curves, for samples falling from the highest peak flow, for the four study basins, normalized by area.

Reproduced with permission of the copyright owner. Further reproduction prohibited without permission.

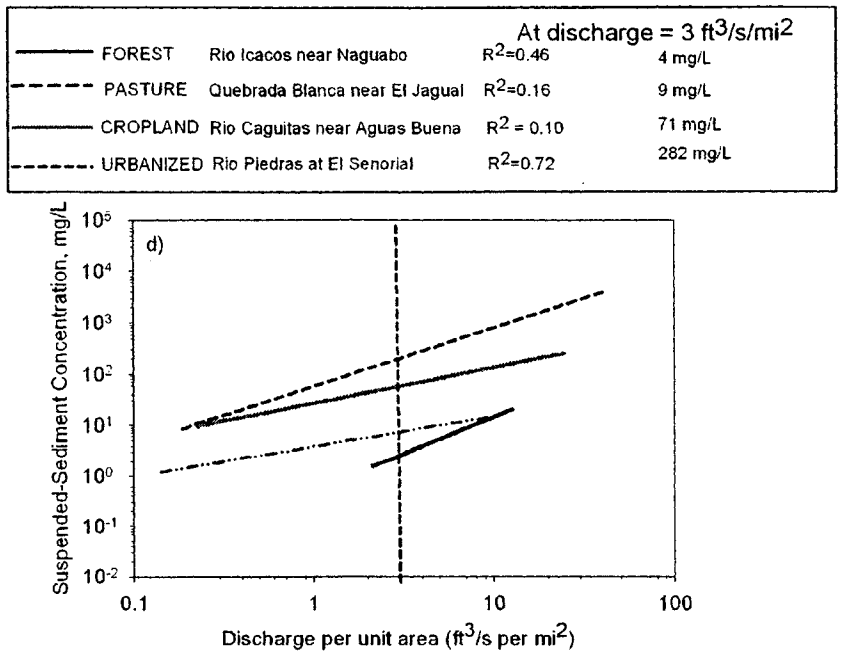

Figure 10.12. d) Sediment transport curves, for samples taken at base flow, for the four study basins, normalized by area.

For samples collected on the rising limb, Rio Caguitas shows the steepest slope for the best-fit regression line, indicating a large sediment supply available for transport (fig. 10.12b). For samples collected on the falling limb, Rio Piedras has the highest suspended-sediment concentrations which matches the high occurrence of counterclockwise hysteresis (Type-3) loops. Quebrada Blanca, on the falling limb, has the steepest slope of the best-fit regression lines, indicating rapid sediment exhaustion (fig. 10.12c). R^2 values did not improve at any of the four stations by separating sediment samples into rising, falling, or base flow either relative to the highest peak flow or relative to any peak. An exception was at Rio Piedras which showed a higher R^2 (0.72) for base flow samples (fig. 10.12d). Sidle and Campbell (1985) also found that for nine storms sampled in Alaska, separating samples into rising and falling did not improve the correlation.

Reproduced with permission of the copyright owner. Further reproduction prohibited without permission.

Previous runoff events decrease sediment availability for the current event by flushing sediment from channel and hillslope storage (Wood, 1977; Walling and Webb, 1982). Sediment-transport curves generated to show the effects of previous runoff events indicated that at the four stations, samples collected after a large recent runoff event have low suspended-sediment concentrations for some or all flows (fig. 10.13). For Rio Icacos and Rio Caguitas high, recent previous events only reduced the suspended-sediment concentration at low flows. At Quebrada Blanca high previous flows had low concentrations (fig. 10.13). For the most disturbed basin, Rio Piedras, low sediment concentrations were observed after recent high flow events (fig. 10.13). Sediment samples taken after previous peaks in the current event showed both high and low suspended-sediment concentrations for the four stations (fig. 10.14). At Rio Piedras, at all flows, higher previous peaks in the current event led to low suspended-sediment concentrations (fig.10.14d). At Quebrada Blanca the opposite was observed, where larger previous peaks in the current event led to higher suspended-sediment concentrations (fig. 10.14b). This may indicate that large peak flows make sediment available for transport. Previous peaks showed no effect on sediment concentrations at Rio Caguitas (fig 10.14a), and at Rio Icacos, low flows showed lower sediment concentrations after high peak flows (fig 10.14c). In summary, the most disturbed basin, Rio Piedras, shows the effect of previous events and previous peaks flushing sediment from the system (fig. 10.14d, 10.15).

There are two seasons in Puerto Rico, a wet season from May through December associated with tropical waves and hurricanes, and a drier season from January through April. Separating samples by seasons did not improve the R^2 values (figs. 5.7, 6.8, 7.7, 8.7). Generally, sediment concentrations were higher for Rio Icacos, Rio Caguitas, and Rio Piedras for rising limb

Reproduced with permission of the copyright owner. Further reproduction prohibited without permission.

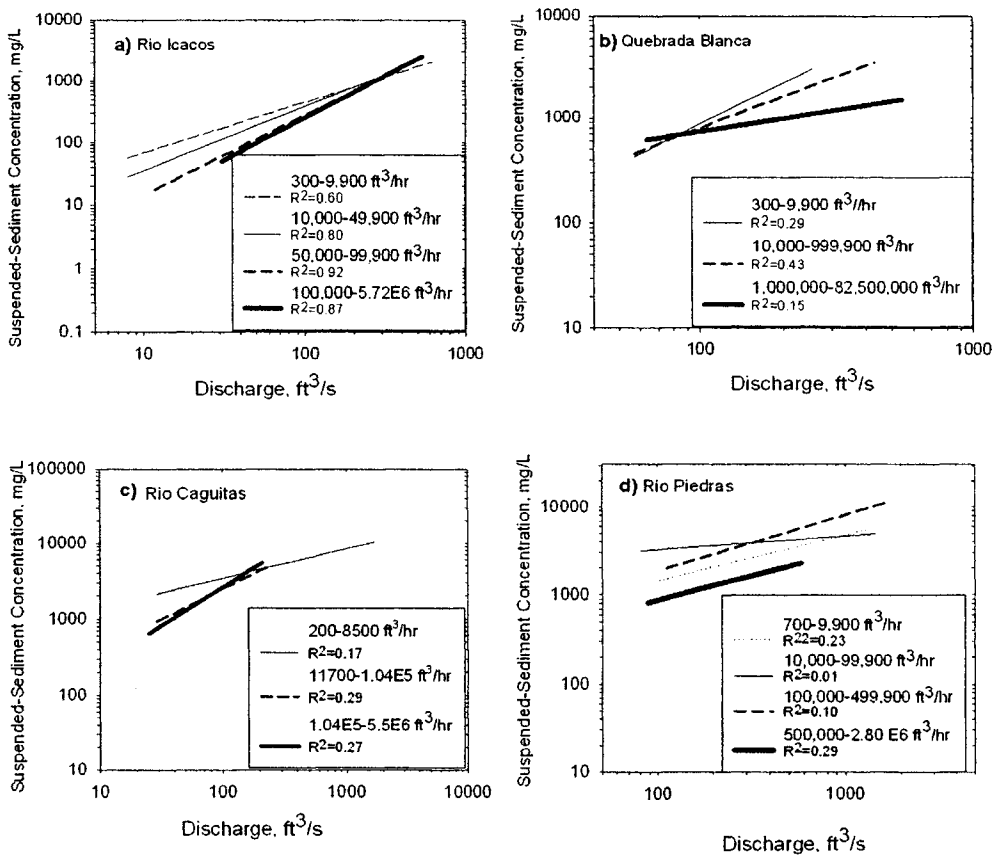

Figure 10.13. Comparison of effect of previous runoff events on suspended-sediment concentrations for just the rising limb at the four study basins: a) Rio Icacos, b) Quebrada Blanca, c) Rio Caguitas, and d) Rio Piedras.

samples taken from May to December (figs. 5.7, 7.7, 8.7). The higher sediment concentration from May through December may reflect more frequent storms, some of large magnitude, that increase erosion and suspended-sediment transport.

Walling (1996) reported that in most rivers the amount of sand in suspension is controlled by hydraulic variables and increases with increased discharge. Sediment-transport curves developed to show the percent of sand in suspension versus flow showed different results for each basin (figs. 10.16, 5.8, 6.8, 7.8, 8.8). At Quebrada Blanca no relation was observed. For Rio

Reproduced with permission of the copyright owner. Further reproduction prohibited without permission.

Icacos, Rio Caguitas, and Rio Piedras as flow increased the percent of sand in suspension increased. The average amount of sand in suspension at Rio Icacos, Quebrada Blanca, Rio Caguitas, and Rio Piedras was 52.4% (ranging from 19 to 82%), 7.6% (0-31%), 6.4% (1 - 36%), and 13.5% (1 - 52%), respectively (figs. 5.8, 6.8, 7.8, 8.8, 10.16). The high proportion of fines in suspension at Rio Piedras and Rio Caguitas reflects fine-grained soil textures in the basin and

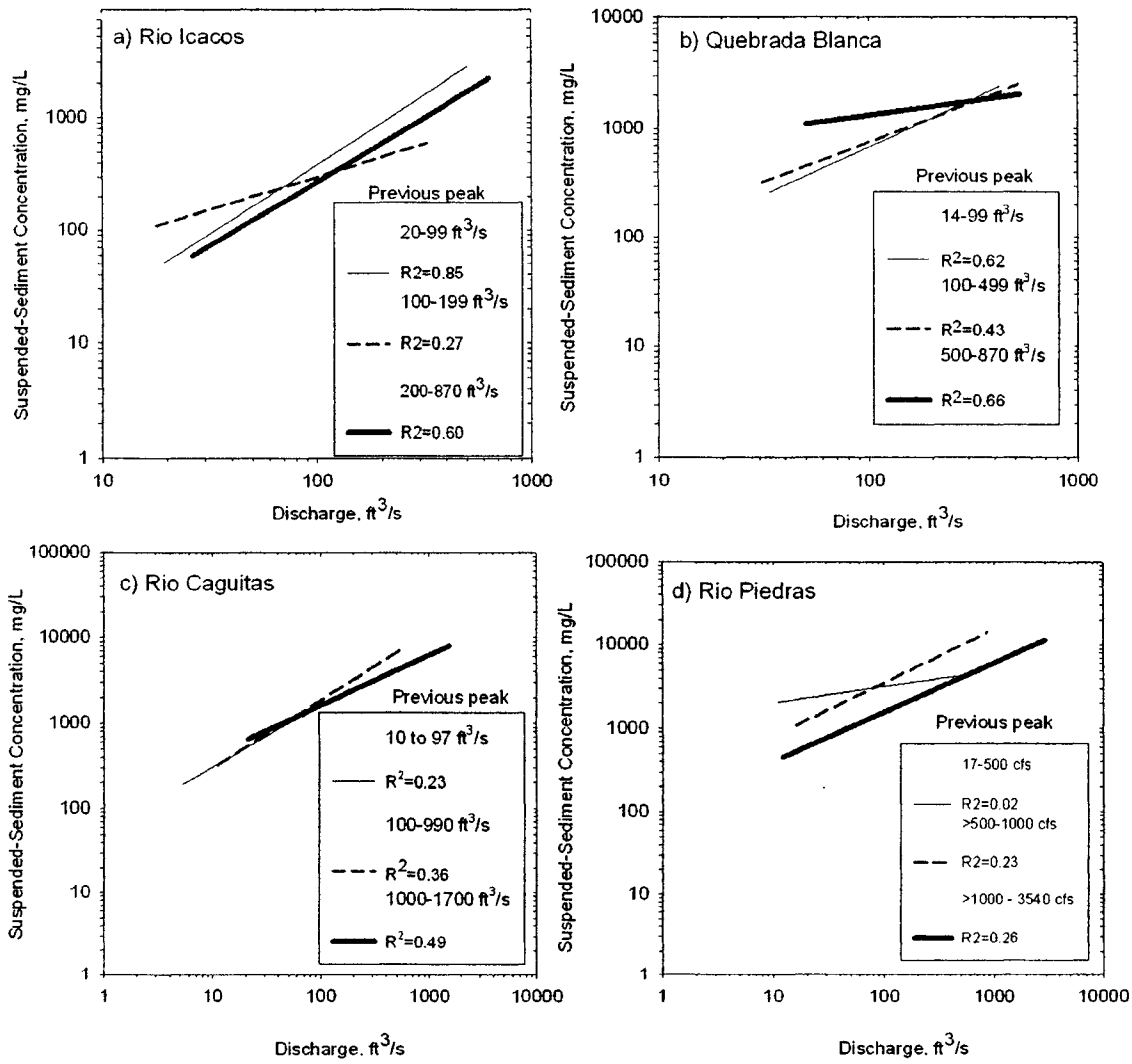

Figure 10.14. Comparison of effect of previous peak flows of current event on suspended-sediment concentrations for the four study basins: a) Rio Icacos, b) Quebrada Blanca, c) Rio Caguitas, and d) Rio Piedras.

Reproduced with permission of the copyright owner. Further reproduction prohibited without permission.

human disturbance leading to erosion of fine material from hillslopes. Rio Icacos has the highest percent sand in suspension, reflecting the underlying intrusive bedrock of the basin which weathers to medium quartz sand. At high flows with increased stream power a steep slope to the best-fit regression line is observed for the sand transport curve at Rio Icacos (figs. 10.15, 5.8). This may point to the channel as a source of sand. The small percent of sand in suspension at Quebrada Blanca reflects the lack of sampling at high flows (figs. 10.16, 6.8).

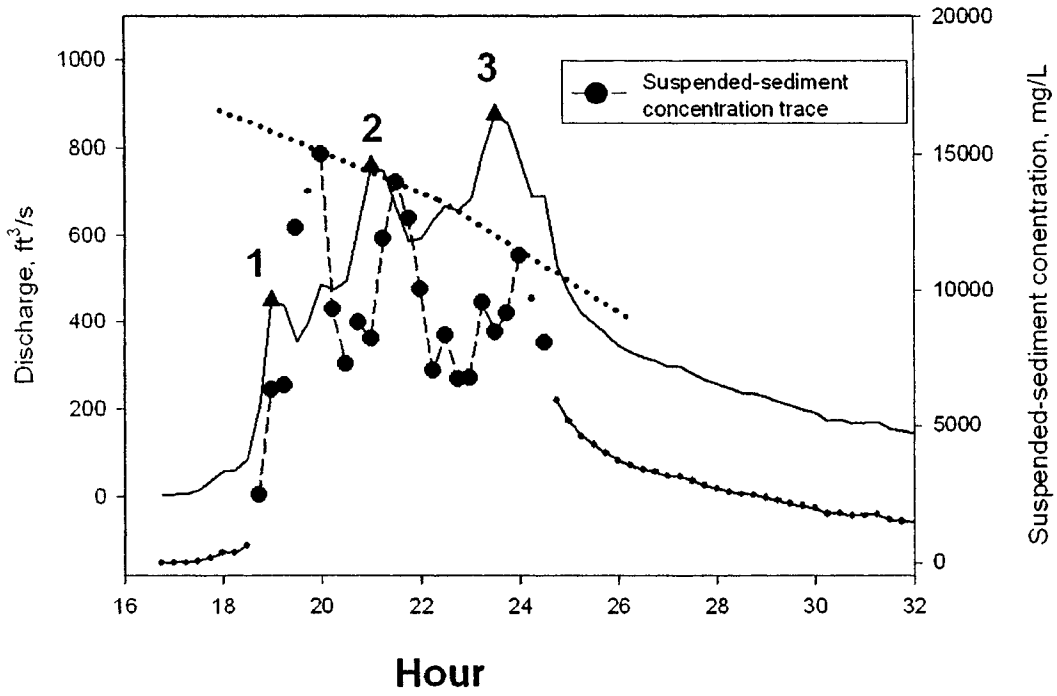

Figure 10.15. Example of a decrease in suspended-sediment concentrations decreasing after previous peaks, Rio Piedras May 1-3, 1992. The dashed line illustrates the decrease in peak suspended-sediment concentration after each peak Also note that suspended-sediment concentrations peak after each peak flow

There is a general lack of association between the percent of sand in suspension and the median grain size (d_{50}) of material on the bed of the channel (figs. 10.3, 10.16). Quebrada Blanca has the largest median bed material size (20 mm) but does not have the highest percent sand in

Reproduced with permission of the copyright owner. Further reproduction prohibited without permission.

suspension (figs. 10.3,10.16). Rio Icacos has the highest percent sand in suspension which matches the median size of the bed material (figs. 10.3, 10.16). The association of sand sized bed material in the channel and sand in suspension at Rio Icacos points to the channel as a source for suspended-sediment. The lack of an association of bed material to percent sand in suspension at the other sites may reflect different sources of sediment (bed material and upland sediment). Very coarse channel bed material may have its source as colluvium and other mass wasting activity. Simon and Guzman-Rios (1990) attributed the coarse material found in Puerto Rican stream beds and in the deposits in Lago Loiza to landslide activity. The large number of corestones observed in and around the channel at Quebrada Blanca may reflect groundwater weathering and incision of the channel over geologic time into these corestone fields. The finer material in suspension at Rio Caguitas and Rio Piedras reflects an upland supply of sediment from soil erosion.

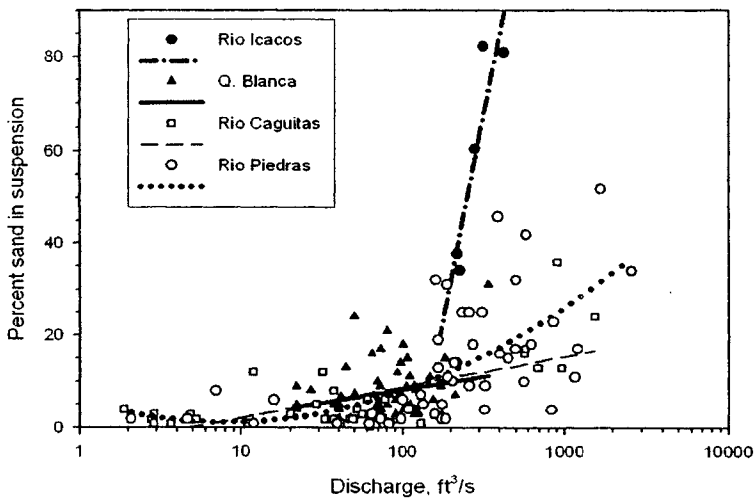

Figure 10.16. Comparison of percent sand in suspension for the four study basins.

Reproduced with permission of the copyright owner. Further reproduction prohibited without permission.

Results of Statistical Analysis

Several statistical approaches were used to determine the significant controls on suspended-sediment concentrations and loads. The storm hydrograph was separated into runoff and quickflow, each examined for the entire event and to the highest peak flow, to determine whether this improved statistical relationships.

Walling (1974) Sediment-Transport Curve Approach

Walling (1974) used four variables to describe suspended-sediment relations for rivers in the United Kingdom: 1) discharge minus base flow, 2) time relation of sample to the highest peak flow, 3) base flow at start of storm, and 4) index of flood intensity. These same variables were used in this research to determine if they improved the relationship of suspended-sediment concentrations to discharge for the four study basins. Results using Walling's (1974) four independent variables to describe suspended-sediment concentrations for the four stations indicated that results were similar with and without base flow for three stations (Quebrada Blanca, Rio Caguitas, Rio Icacos). At these three stations the most important factor explaining suspended-sediment concentrations during all flows, rising flows, and falling flows (with and without base flow) was discharge. At Rio Piedras, discharge was significant in the first step for all samples with base flow. For all samples without base flow and rising limb samples without base flow, the most significant variable at Rio Piedras was base flow at the start of the event. The slope of the best-fit regression line was positive, indicating that an increase in base flow at the start of the event was not diluting but increasing suspended-sediment concentrations. For falling limb samples at Rio Piedras, the time of the sample was most significant and had a negative slope for the best-fit line, indicating

Reproduced with permission of the copyright owner. Further reproduction prohibited without permission.

that samples collected later in the event have low sediment concentrations. Although Rio Piedras showed the highest sediment concentrations on the falling limb, eventually as time proceeds in the storm, sediment concentrations become lower.

The findings reported here (except for Rio Piedras) agree with Walling's (1974) results, that discharge was significant in explaining suspended-sediment concentrations in the first step of forward stepwise regression. The significant variable in the second step of forward stepwise regression was different for each basin. Base flow at the start of the event was significant in the second step for Rio Caguitas (all samples and falling samples) with and without base flow and the slope of the best-fit line is negative, indicating an inverse relation of base flow to suspended-sediment concentration. This would indicate a dilution effect from base flow at Rio Caguitas. For Quebrada Blanca (all samples, rising, and falling samples) with and without base flow, the time relation of the sediment was significant and the slopes of the best-fit regression lines at both stations were negative, indicating that for samples collected later in the event the suspended-sediment concentrations decreased. This would point to Type-1 hysteresis loops being more common. Flood intensity was significant in the second step of forward stepwise regression for rising samples at Rio Caguitas, with and without base flow, and for Rio Icacos (rising, and falling samples) with and without base flow. The slope of the best-fit regression line at both stations was positive, indicating that faster rising flows are increasing suspended-sediment concentrations. In summary, the four variables Walling (1974) used to describe sediment concentrations were shown to be significant for the four basins being studied in Puerto Rico.

Reproduced with permission of the copyright owner. Further reproduction prohibited without permission.

Storm-Generated Suspended-Sediment Loads and Concentrations

The significant controlling factors on storm generated suspended-sediment loads and sediment concentrations were examined using the statistical operations of multiple regression analysis and principal components analysis. A significant portion of this statistical analysis involved developing definitions of storms and developing techniques to separate quickflow from base flow.

Event definition

Storms were defined in each basin by a threshold peak flow determined as the 95th percentile of hourly discharges for the period of study (Table 7.1). In a multi-peaked event, a minimum difference in discharge of each peak minus the preceding trough was used to separate peaks over a range of discharges for each station (Table 7.1b).

Events that are closely spaced in time are termed complex events (fig4.2). A definition involving recession limb slope and threshold discharge was used to define when closely spaced events were separate events, part of the same event, or events that make up a complex event (Table 7.5). A plot of rainfall with the hydrograph was used to help determine when complex events should be separated into discrete events (fig7.3).

Hydrograph separation

Quickflow and runoff were calculated for each storm-generated hydrograph. Hydrograph separation was accomplished with a graphical technique using the break in maximum curvature of the recession curve or inflection point to define the point where storm-water flow ceases and base flow begins. The start of the event was selected where there was an abrupt rise in the hydrograph.

Reproduced with permission of the copyright owner. Further reproduction prohibited without permission.

Four graphical techniques were examined to define the end of a runoff event and develop a consistent methodology. A method using the 2nd derivative of a 3rd order best-fit regression to the recession curve was used in this research to determine the end of a runoff event because it provided a consistent methodology and consistent results.

The portion of the falling limb chosen to define the inflection point might affect the location of the inflection point. Different portions of the recession curves were selected to determine how the location of the inflection point might change and how that would affect the amount of quickflow derived from a straight line drawn from the beginning of the event to the inflection point. The differences in quickflow ranged from 7 to13% for the three basins analyzed. Therefore, the selection of the portion of the recession curve used to define the end of the event is subjective and the errors involved are approximately 10%. Selection of the beginning of the hydrograph recession curve immediately below the peak flow provided the most consistent results.

The determination of whether base flow is increasing or decreasing under the flood hydrograph assumes a-priori knowledge of groundwater characteristics. Base flow in this study was separated by a straight line drawn from the beginning of the event to the inflection point. This assumes a constant rate of base flow change. The quickflow computed by drawing a straight line from the beginning of the event to the inflection point was compared to a base flow rise under the storm hydrograph and a base flow decline under the hydrograph. The straight line separation compared to a base flow rise showed a difference up to 27%, while a 13% difference was found with a base flow decline. The straight line method was used in this study. It is understood that there is subjectivity in many of the steps used to separate out the quickflow portion of the

Reproduced with permission of the copyright owner. Further reproduction prohibited without permission.

hydrograph and every effort was made to reduce this through a consistent methodology developed over the first 6 months of this research.

The reliability of the graphical methods developed in this study to determine quickflow was tested by comparing the hypothetical amount of runoff generated for each rainfall event to the calculated volume of quickflow. The hypothetical runoff generated for each storm event was computed by assuming that the entire basin area is impervious, and therefore all rainfall is quickflow. Owing to infiltration and evaporation, the range of quickflow should be less than runoff. The range and average of calculated quickflow to computed runoff was: Quebrada Blanca 4 to 98%, averaged 22%; Rio Piedras 9 to 71%, averaged 35%; Rio Caguitas 3 to 41%, averaged 18%; Rio Icacos 7 to 66%, averaged 42%. Woodruff and Hewlett (1970) showed that for rivers in the humid temperate northeastern U.S., 10% of rainfall on average appears as quickflow under the storm hydrograph. In the humid-tropical Senegal River basin, Africa, quickflow accounted for 34% of mean annual runoff (Kattan and others, 1987). In the Luquillo Experimental Forest, Puerto Rico, hydrograph separation of 31 storms gave a mean quickflow/precipitation ratio of 9% (Fred Scatena, University of Pennsylvania, written communication, April 16, 2003). Recent advances in tracers to determine the ratio of base flow to storm flow contributions in humid environments confirm that a large majority of the volume of the hydrograph in forested areas is base flow (Ogunkoya and Jenkins, 1993). The average values in this study are higher than 10% for humid-temperate regions and possibly higher than other values reported for Puerto Rico. Differences between the quickflow values generated in this study and humid temperate regions may be related to geology, soil conditions, higher rainfall amounts, and disturbance in the four study basins. The differences in the volume of quickflow to rainfall also reflect the impreciseness of measuring rainfall.

Reproduced with permission of the copyright owner. Further reproduction prohibited without permission.

Multiple regression and principal components analysis

Dependent variables used to describe storm-generated sediment were suspended-sediment load and discharge-weighted sediment concentration. Suspended-sediment load was computed by developing a continuous trace of suspended-sediment on the hydrograph and using the subdivision method to compute suspended-sediment load. Suspended-sediment samples collected during the storm were used to develop the continuous trace. Samples between collection times were linearly interpreted or a sediment transport curve was used to estimate the suspended-sediment concentration. Several transport curves were developed to estimate the sediment concentration, including transport curves from all samples or samples from the select event. The transport curves were often separated into rising and falling samples. At least two samples had to be collected on the rising limb and at least 50% of the total suspended-sediment load had to be calculated between the first and last sample for it to be used in the statistical analysis.

The second dependent variable, discharge-weighted sediment concentration, is the total suspended-sediment load, computed by subdivision, divided by the runoff of the event. The entire storm hydrograph was examined, as well as the portion to the highest peak flow. Variables selected as important controls on storm-generated sediment were separated into three categories: 1) previous-event factors, 2) factors between events, and 3) current-event factors . Hydrologic variables included quickflow and runoff, peak flows, rainfall, rainfall intensity, hysteresis type, and rate of hydrograph rise.

Sediment characteristics were analyzed using several statistical tests. First, the independent variables were tested for normality and if necessary were transformed. At this point, two distinct approaches to reducing the number of variables were used to assess potential analytical and

Reproduced with permission of the copyright owner. Further reproduction prohibited without permission.

interpretive advantages. The first approach was an inspection of the Pearson's product-moment correlation matrix to remove highly correlated (R>0.80) variables. The second approach was a more involved principal component analysis of the correlation matrix. The variables resulting from the two approaches were then subjected to forward-stepwise multiple regression. Varimax rotation of the principal components was performed to determine whether this improved interpretations. A summary of all statistical results is shown in figures 10.17, 10.18, 10.19, and 10.20.

Rio Icacos

At Rio Icacos, statistical results for both the entire event or to the highest peak flow indicated that separating out the quickflow portion of the hydrograph did not improve or in most cases change multiple-regression and principal components interpretations (figs. 10.17, 10.18, 10.19, 10.20). Higher R^2 values were observed using suspended-sediment load as a dependent variable (fig. 10.17, 10.18) and may be related to the use of discharge to compute sediment loads. Discharge is highly correlated to many of the hydrological variables used in this statistical analysis. Analyzing variables to the highest peak flow only slightly improved R^2 values but did not change which variables were significant (fig. 10.18, 10.20).

Whether using runoff or quickflow for the entire event or to the highest peak flow, statistical results were always the same at Rio Icacos, making this the most consistent basin for interpretations (fig. 10.19a; 10.20a). Current-event characteristics were positively correlated to the dependent variables (sediment load and sediment concentration), between-event characteristics were inversely correlated, and the previous event and the sum of the 3 previous events were positively correlated

Reproduced with permission of the copyright owner. Further reproduction prohibited without permission.

Reproduced with permission of the copyright owner. Further reproduction prohibited without permission.

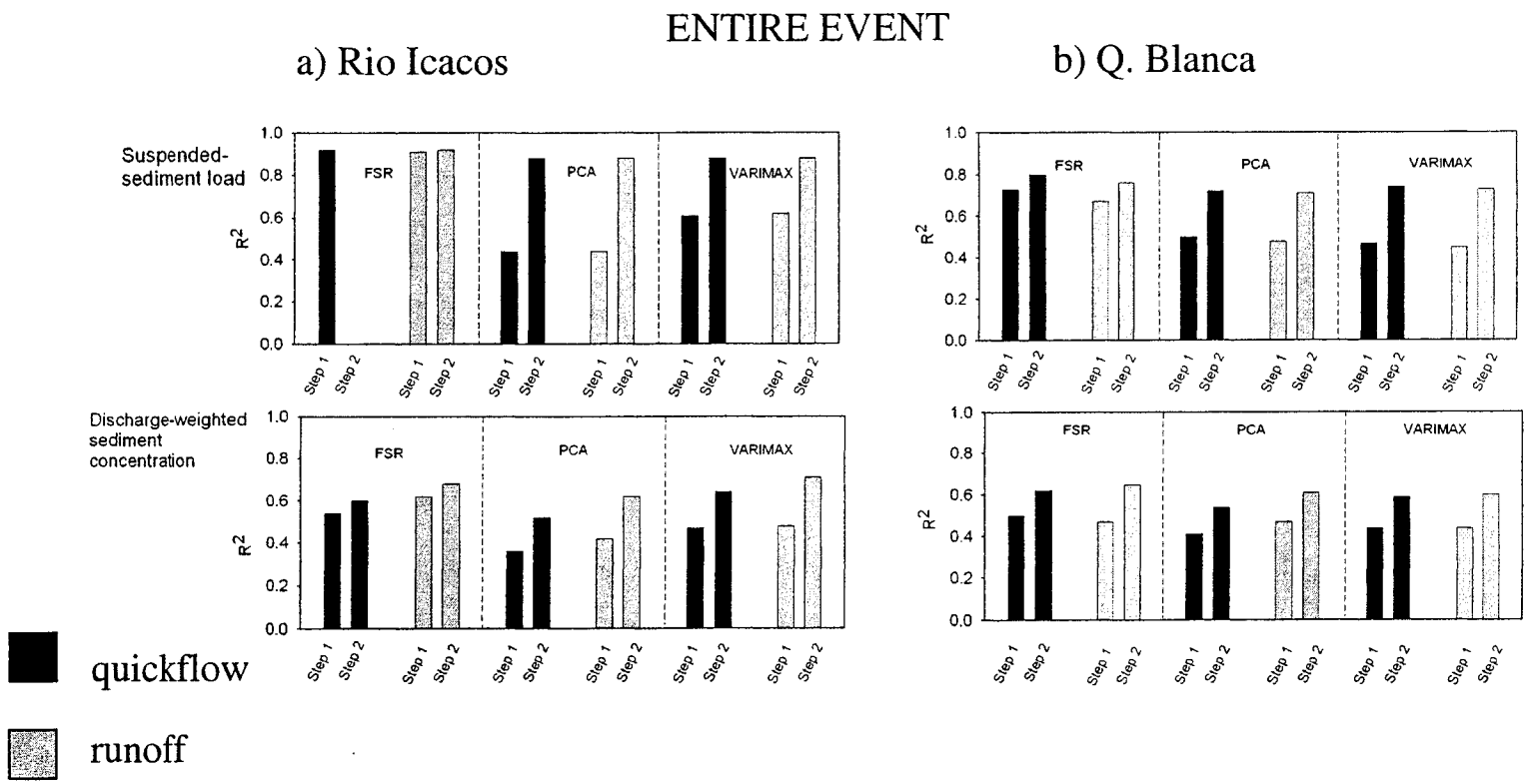

Figure 10.17. Summary of correlation coefficient (R^2) values for forward stepwise regression (FSR) on the independent variables and principal components analysis (PCA), including varimax rotation (VARIMAX) for the entire storm generated hydrograph at: a) Rio Icacos, b) Quebrada Blanca.

Reproduced with permission of the copyright owner. Further reproduction prohibited without permission.

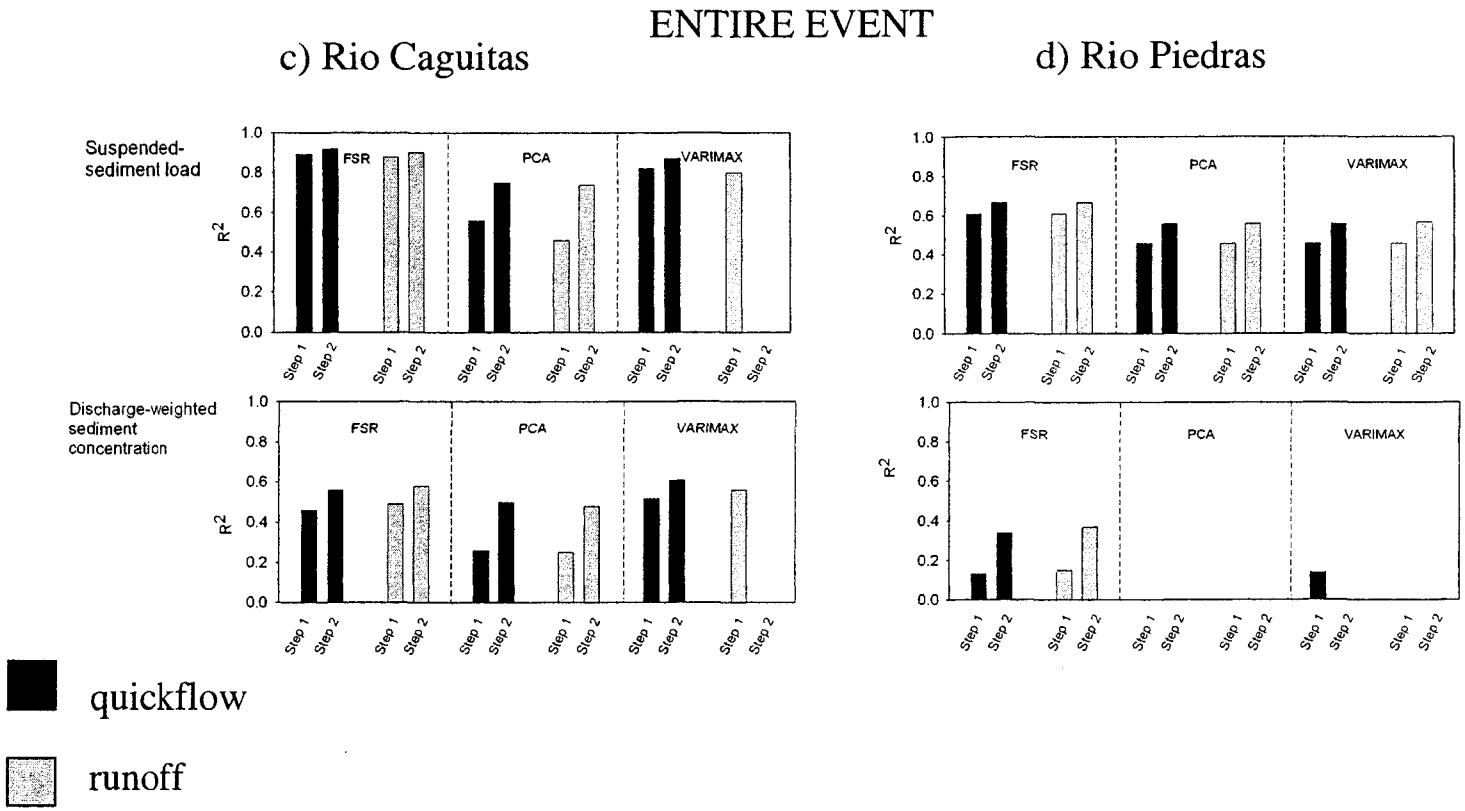

Figure 10.17. Continued. c) Rio Caguitas, and d) Rio Piedras.

Reproduced with permission of the copyright owner. Further reproduction prohibited without permission.

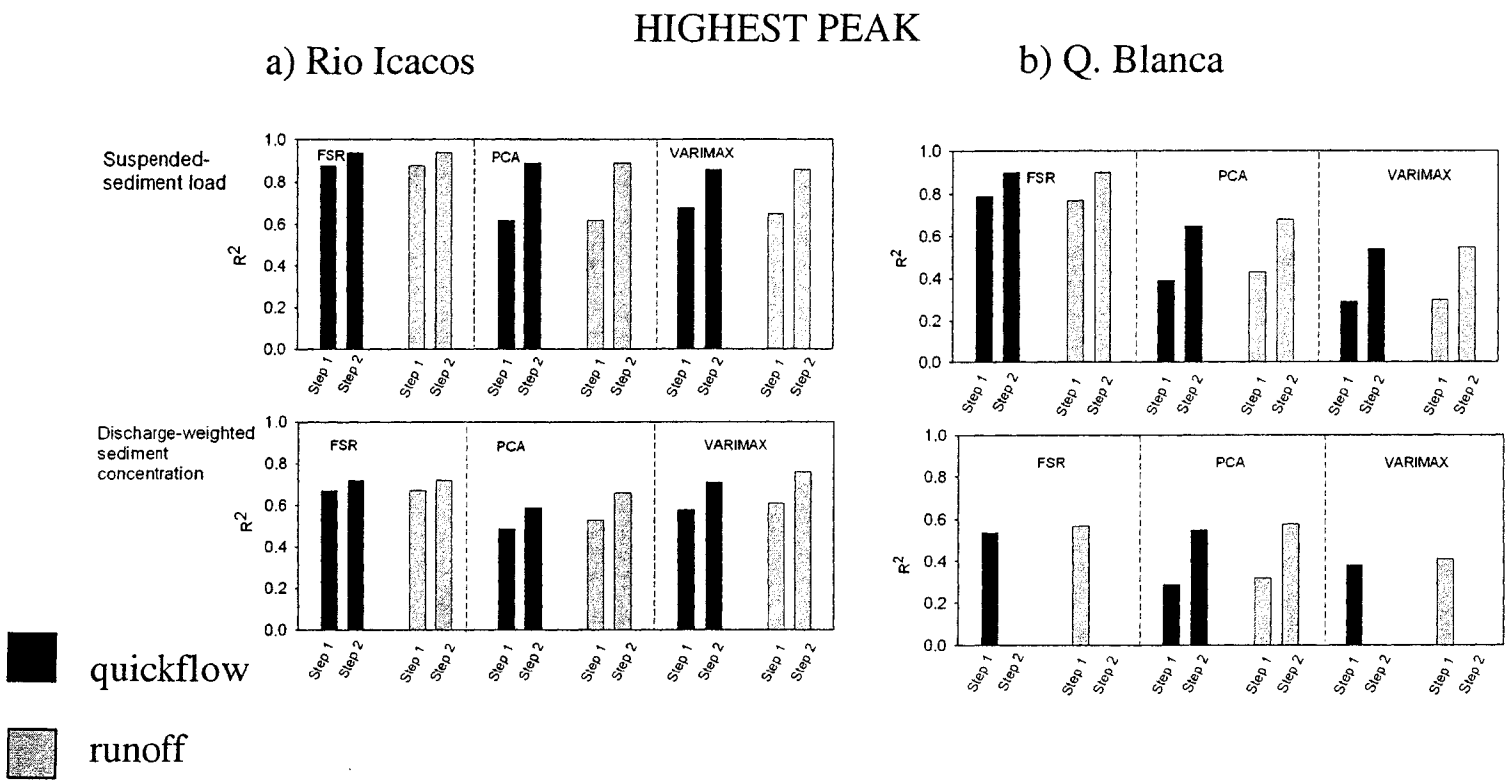

Figure 10.18. Summary of correlation coefficient (R^2) values for forward stepwise regression (FSR) on the independent variables and principal components analysis (PCA), including varimax (VARIMAX) rotation to the highest peak flow at: a) Rio Icacos, b) Quebrada Blanca.

Reproduced with permission of the copyright owner. Further reproduction prohibited without permission.

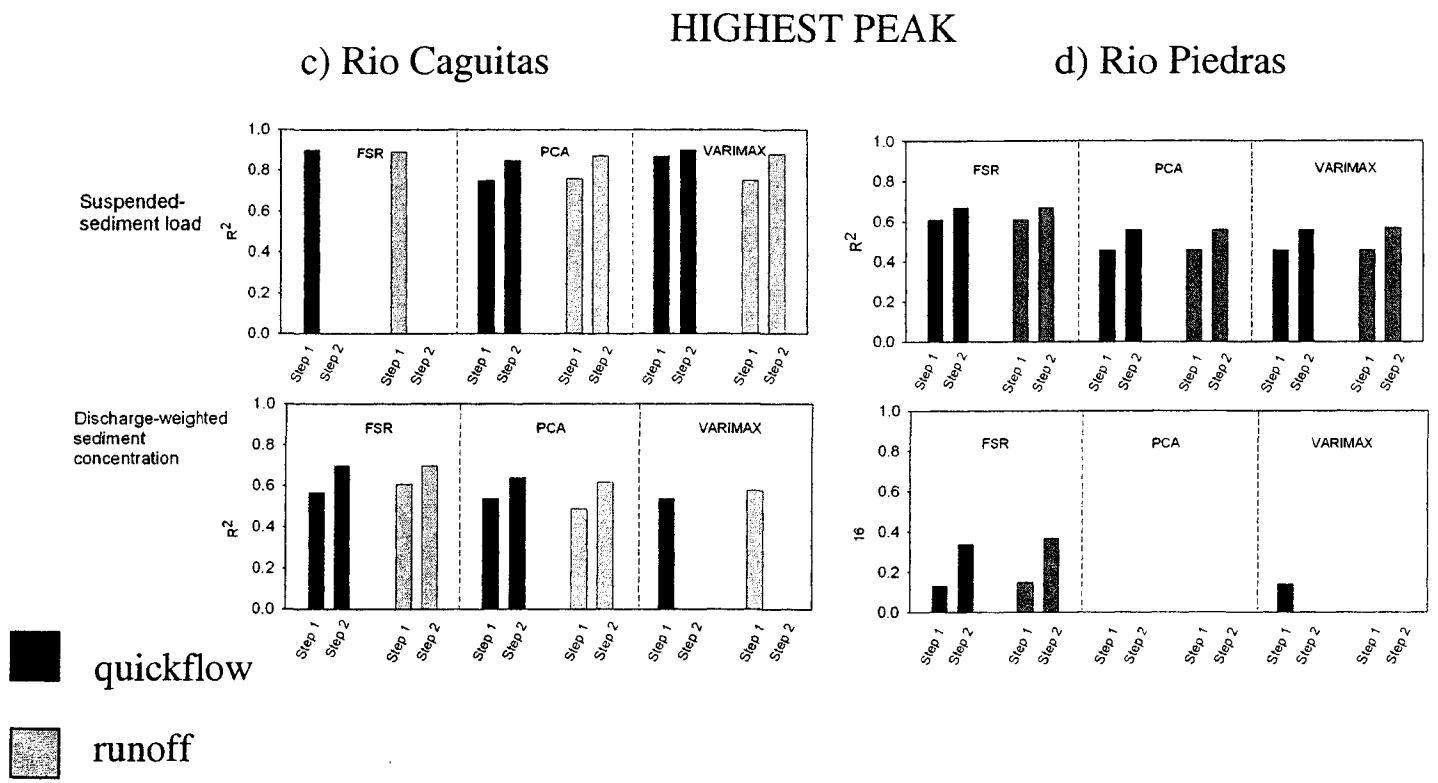

Figure 10.18. Continued. c) Rio Caguitas, and d) Rio Piedras.

Figure 10.19. Statistical summary of significant variables by time category for forward stepwise regression (FSR) on the independent variables and principal components analysis (PCA), including varimax rotation (VARIMAX) for the entire event using: a) suspended-sediment load at the four study basins. The correlation sign is '+' for direct correlation and '-' for inverse correlation.

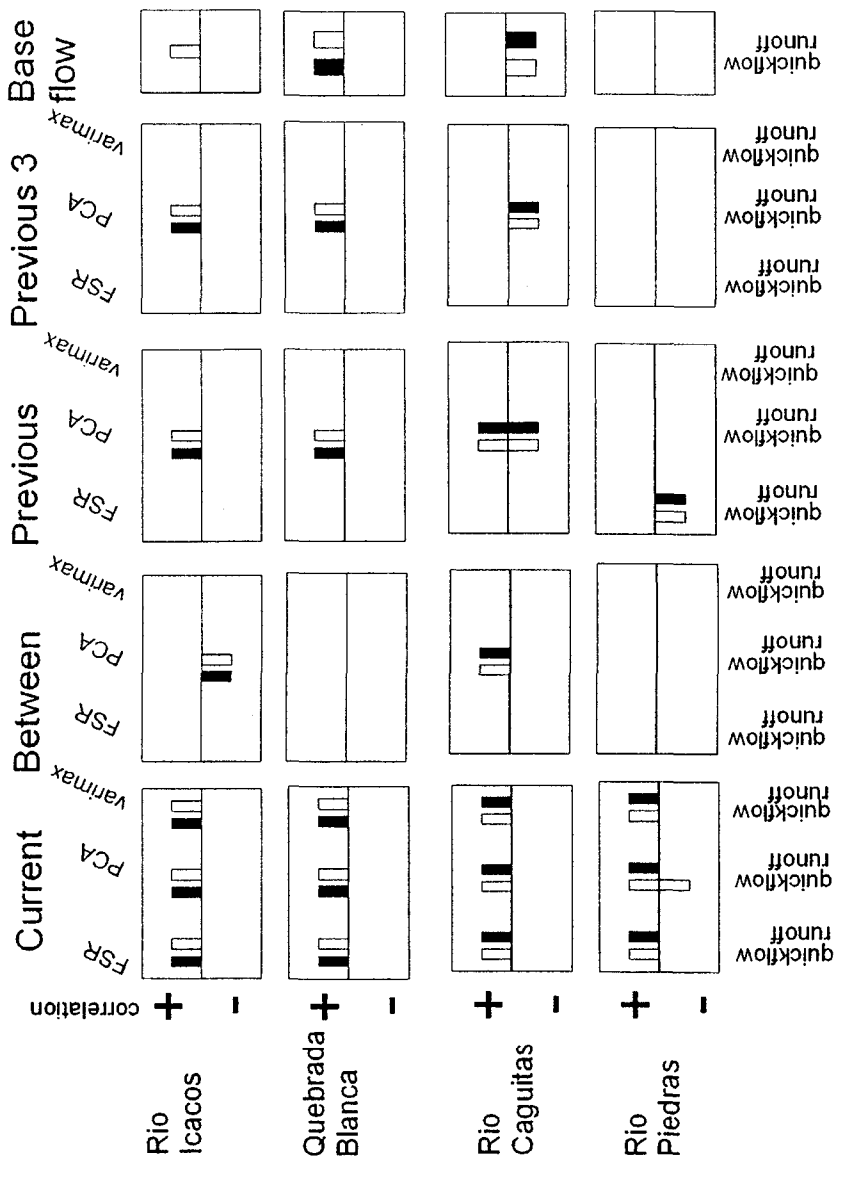

Reproduced with permission of the copyright owner. Further reproduction prohibited without permission.

Figure 10.19. Contined. b) Discharge-weighted sediment concentration as a dependent variable for the entire event at the four study basins.

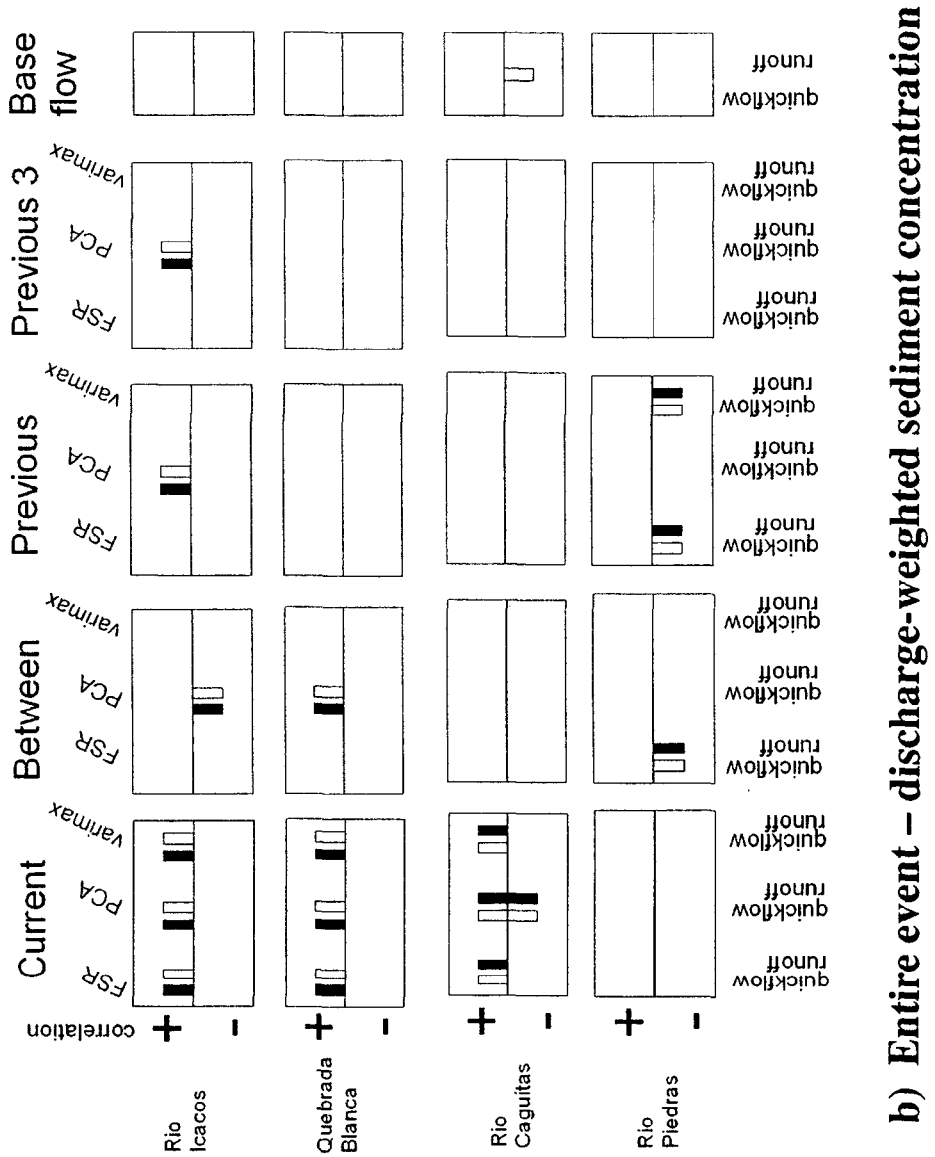

Reproduced with permission of the copyright owner. Further reproduction prohibited without permission.

Figure 10.20. Statistical summary of significant variables by time category for forward stepwise regression (FSR) on the independent variables and principal components analysis (PCA), including varimax rotation (VARIMAX) to the highest peak flow using: a) suspended-sediment load at the four study basins. The correlation sign is '+' for direct correlation and '-' for inverse correlation.

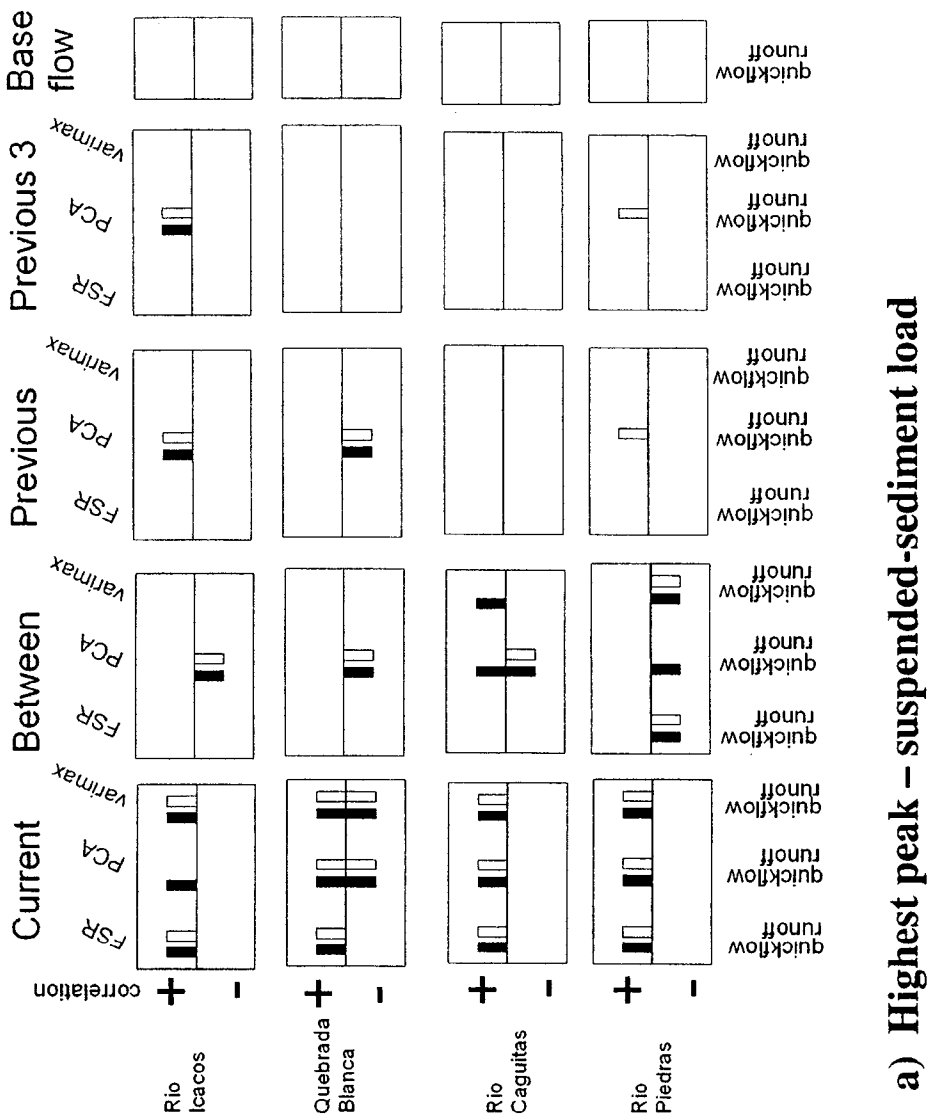

Reproduced with permission of the copyright owner. Further reproduction prohibited without permission.

Figure 10.20. b) Discharge-weighted sediment concentration as a dependent variable to the highest peak flow at the four study basins.

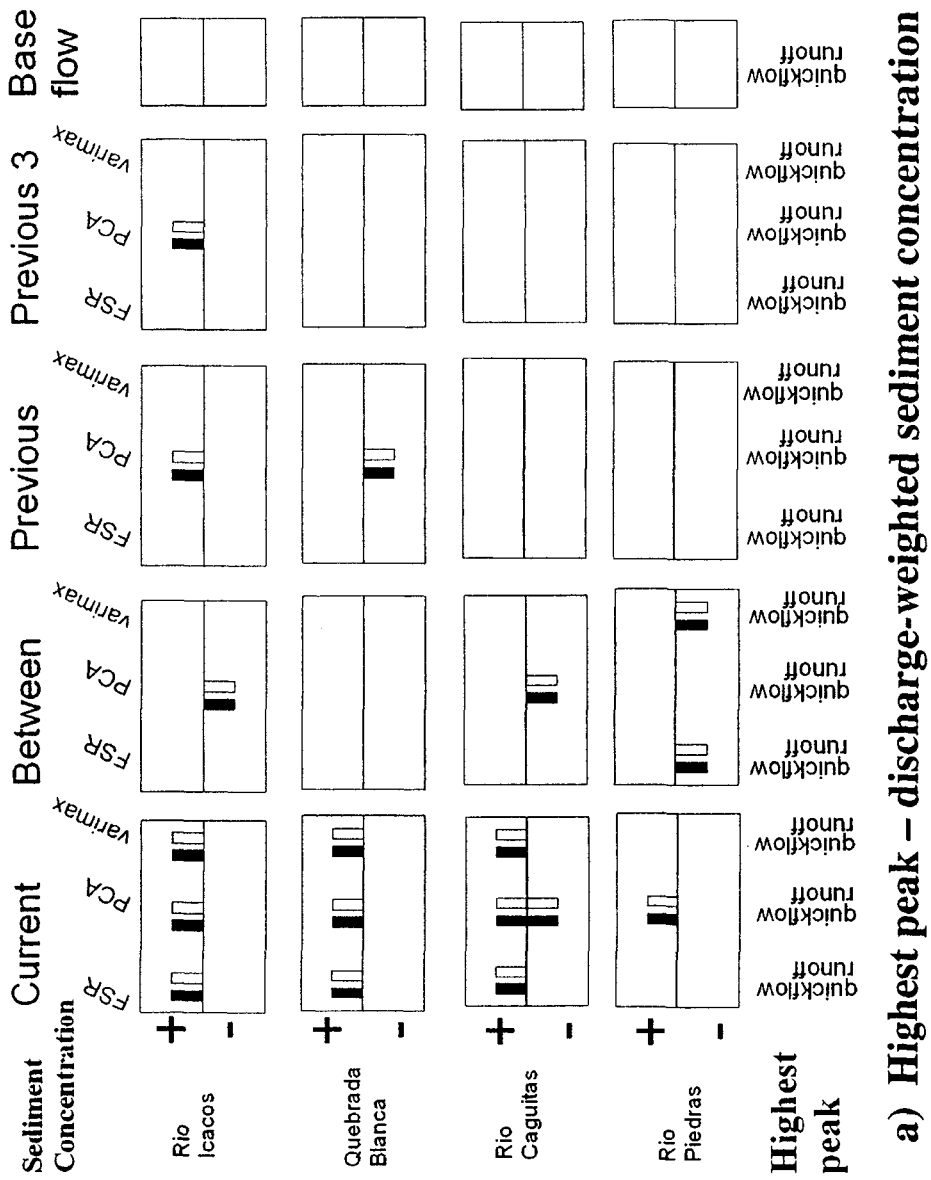

Reproduced with permission of the copyright owner. Further reproduction prohibited without permission.

to the dependent variables. Current-event characteristics that were significant in transport of suspended-sediment loads for the entire event and to the highest peak flow included total rainfall, rainfall intensity, runoff (quickflow), peak flow, and the sum of peak flows (Table 5.25a). Using the discharge-weighted sediment concentration as a dependent variable for the entire event and to the highest peak flow showed peak flow, the sum of peak flows, total rainfall, rainfall intensity, and the maximum rate of hydrograph rise were significant (Table 5.25a). Using runoff characteristics for the entire event showed base flow was significant in the second step of forward stepwise regression analysis and positively correlated with suspended-sediment load, indicating that increases in base flow before the storm event increased sediment loads (fig. 10.19a; Table 5.25a). Base flow was also found to be significant using Walling's (1974) four variables, who noted that higher base flows were correlated with a decrease in sediment concentration as sediment was diluted. In Rio Icacos, quickflow added to the high base flow increases the depth of flow, causing increased shear stress on the channel bed and sediment resuspension. Higher base flow at the start of the event also indicates wetter antecedent conditions in the basin which would increase saturated overland flow, runoff (quickflow), and sediment transport. This suggests the channel as a source of sediment at Rio Icacos. Kattan and others (1987) also acknowledged the importance of base flow contribution in sediment transport during floods and between events in the humid-tropical Senegal River Basin, Africa.

Interpretations of sediment generation and delivery in the forested Rio Icacos basin suggest that large previous storm events provide more sediment for transport to the current event. Large storm events in Rio Icacos may trigger landslides and stream bank failures (Matt Larsen, USGS, personnel communication, 2003). Large events may also mobilize stored sediment in first and

Reproduced with permission of the copyright owner. Further reproduction prohibited without permission.

second order channels. Brown and others (1995) determined that 55% of channel sands in the Rio Icacos basin is from landslides and 45% from sheetwash. The sediment that is mobilized by these large events is deposited in the channel and becomes an immediate source of sediment for the next event. The increased sediment delivered to the channel by large previous events is flushed by runoff and rainfall between events.

Quebrada Blanca

At Quebrada Blanca, statistical results for both the entire event or to the highest peak flow indicated that separating out the quickflow portion of the hydrograph did not improve or in most cases change multiple-regression and principal-components interpretations (figs. 10.17b, 10.18b, 10.19b, 10.20b). Higher R^2 values were observed using suspended-sediment load as a dependent variable (fig. 10.17b, 10.18b).

For the entire event at Quebrada Blanca, using quickflow and runoff, current-storm characteristics were significant and were positively correlated to the dependent variables of suspended-sediment load and discharge-weighted sediment concentration in either forward stepwise regression, principal components analysis, or varimax rotation of the principal components (fig. 10.19b). Between-event characteristics that were significant included peak flow, the sum of peak flows, runoff, quickflow, and total rainfall (Table 6.24a). For the discharge-weighted sediment concentration, significant current-event variables included peak flow, the highest rate of rise for any peak, total rainfall, rainfall intensity, and rainfall on the rising limb (Table 6.24a).

For the entire event at Quebrada Blanca, previous-event characteristics (peak flow, quickflow, rainfall, the sum of the 3 previous rainfall, runoff and quickflow) were significant in

Reproduced with permission of the copyright owner. Further reproduction prohibited without permission.

principal components analysis using suspended-sediment load as a dependent variable (fig. 10.19b; Table 6.24a). The principal components were positively correlated with the dependent variables of suspended-sediment load, indicating that larger previous events increased the current sediment load. Using the discharge-weighted sediment concentration as a dependent variable in principal components analysis indicated that between-event characteristics of rainfall and runoff were significant and positively correlated. This indicates that larger rainfall and runoff amounts between events can increase sediment concentration. Base flow is also significant in principal components analysis and was positively correlated with sediment load using quickflow and runoff. Base flow was significant in the statistical analysis using Walling's (1974) four variables (Table 6.2). Similar to the results at Rio Icacos, the positive correlation of base flow to sediment load suggests the channel as a source of sediment at Quebrada Blanca.

For analysis to the highest peak flow at Quebrada Blanca, current-event characteristics were significant for both dependent variables in each of the statistical operations, but the current-event characteristic of rainfall intensity showed an inverse relation to suspended-sediment load in principal components analysis with and without varimax rotation (fig.10.20a, Table 6.24b). Typically, high rainfall intensities will increase hillslope erosion and suspended-sediment concentrations. Depending on the timing of the maximum rainfall intensity, there may be lag between sediment generated by intense rainfall, and delivery and transport to the sampling station before the highest peak flow occurs.

For analysis to the highest peak flow at Quebrada Blanca, between-event characteristics of rainfall and runoff and previous-event characteristics of rainfall intensity were significant in principal components analysis and showed an inverse relation to suspended-sediment load as a

Reproduced with permission of the copyright owner. Further reproduction prohibited without permission.

dependent variable, indicating these processes flush sediment to the highest peak flow (fig. 10.20; Table 6.24b). Using the discharge-weighted sediment concentration as a dependent variable also showed an inverse relationship to rainfall intensity of the previous event. At Quebrada Blanca the correlation of variables to sediment loads and sediment concentrations were different when comparing the entire storm hydrograph to the highest peak flow. For the entire event, between-event characteristics (flow and rainfall) and previous-event characteristics (runoff and rainfall) were directly correlated to the dependent variables, but to the highest peak flow, between-event and previous-event characteristics were inversely correlated to the dependent variables. Since one analysis is for the entire event and the other is to the highest peak flow, a hypothesis is that the observed differences were occurring on the falling limb. Sediment generated by between event and previous events may not be transported to the monitoring station before the highest peak flow. This may reflect slow sediment delivery processes and the abrupt, quick rise in flow. Interpretations from this analysis would suggest that previous-event rainfall intensity in this relatively undisturbed basin is increasing sediment loads for the current event but not before the highest peak flow.

A possible explanation for the observed increase in suspended-sediment loads from previous events may be related to increases in saturated areas in the basin. Increases in previous-event rainfall and runoff indicate that more saturated areas exist in the basin for the current rain event. Rain falling on these saturated areas would increase runoff. Even if upland erosion was not increased during the event, sediment loads would increase because runoff increased. Therefore, previous wetter periods may increase sediment loads to the current event.

Reproduced with permission of the copyright owner. Further reproduction prohibited without permission.

Rio Caguitas

Analysis of the entire event at Rio Caguitas showed current-storm characteristics to be significant and positively correlated to the dependent variables of sediment load and discharge-weighted sediment concentration in either forward stepwise regression, principal components analysis, or varimax rotation of the principal components (fig. 10.19; 10.20; Table 7.25a). Current-event characteristics that were significant in transport of both dependent variables included total rainfall, rainfall intensity, runoff (quickflow), the rate of hydrograph rise, peak flow, and the sum of peak flows (Table 7.25a). Rainfall intensity was positively correlated to the discharge-weighted sediment concentration on PC2 and negatively correlated on PC4. Because rainfall intensity has higher loadings on PC2, rainfall intensity was considered positively correlated to the discharge-weighted sediment concentration. However, in some storm events, increases in rainfall intensity were associated with decreasing sediment concentrations; possibly as a result of increases in runoff compared to sediment. Base flow was significant for the entire event and indicated an inverse relation to both dependent variables, implying that increased base flow decreased sediment loads and concentrations (fig. 10.19), although the slope of the best-fit line was low (Tables 7.4, 7.7).

For the entire event at Rio Caguitas, previous-event rainfall and rainfall intensity were directly correlated to suspended-sediment load, and previous-event quickflow and the sum of three previous events (rainfall and runoff), were inversely correlated to suspended-sediment load (fig.10.19; Table 7.25a). This suggests that higher amounts of previous-event rainfall and rainfall intensity were supplying sediment from hillslopes and higher previous-event quickflow and peak flows flush sediment. To the highest peak flow, rainfall and rainfall intensity between events was

Reproduced with permission of the copyright owner. Further reproduction prohibited without permission.

correlated directly with suspended-sediment load and was supplying sediment to the system. For the entire event and to the highest peak flow, runoff between events was inversely correlated with sediment loads and flushed sediment.(fig. 10.19; 10.20). Previous rainstorms with high intensity were supplying sediment and delivering sediment to the channel where it was being flushed by previous high flows. Between-event characteristics were acting in the same fashion; rainfall between events supplied sediment, whereas high runoff between events flushed sediment.

Rio Piedras

For the entire-event analysis at Rio Piedras, current-storm characteristics were significant for only suspended-sediment load using all three statistical tests (fig. 10.19a). Current-event characteristics (runoff, quickflow, rainfall, peak flows, and rainfall intensity) were positively correlated to suspended-sediment load (fig.10.19a; Table 8.19). The sum of the previous-event peak flows was inversely correlated to suspended-sediment load, implying a flushing mechanism.

Using the discharge-weighted sediment concentration as a dependent variable for the entire event at Rio Piedras only showed significant variables in the multiple regression analysis (fig. 10.19b; Table 8.24a). Rainfall since the previous-event and the sum of the previous-event peak flows were significant using an alpha of 0.10 and were negatively correlated to the discharge-weighted sediment concentration, implying a flushing mechanism. In general, statistical results for the entire event at Rio Piedras showed only a few significant variables and the R^2 values were low.

Results to the highest peak flow for Rio Piedras showed more significant variables compared to the entire event (fig. 10.20, Table 8.24b). Current-event characteristics were significant and positively correlated to the dependent variable, suspended-sediment loads in all

Reproduced with permission of the copyright owner. Further reproduction prohibited without permission.

three statistical tests. Using the discharge-weighted sediment concentration as a dependent variable only showed a positive correlation to current-event characteristics in principal components analysis (fig. 10.20b; Table 8.24b). For both dependent variables, between-event characteristics were negatively correlated and previous-event characteristics were positively correlated (fig. 10.20a,b).

In summary, statistical results (R^2 values) at Rio Piedras were generally lower compared to the other three stations. This may indicate that in disturbed basins such as Rio Piedras, strong statistical relations to many hydrologic functions are absent. Results to the highest peak flow showed more significant variables than for entire event analysis, but R^2 values were low. At Rio Piedras, previous events effect on sediment loads and concentrations showed differences when comparing the entire storm hydrograph to the highest peak flow. For the entire event, previous-event characteristics (rainfall, rainfall intensity, peakflow, quickflow, runoff) were inversely correlated to the dependent variables but to the highest peak flow, previous-event characteristics (rainfall intensity, peakflow, quickflow, runoff) were directly correlated to the dependent variables. Sediment-transport curves developed for preceding runoff events (fig. 10.13) also showed that large previous runoff events were reducing suspended-sediment concentrations. The prevalence of bare ground in the basin and counterclockwise hysteresis loops indicate that upland sediment is an important source of sediment in this basin. This sediment is fine grained and as flow decreases concentrations remain high leading to counterclockwise hysteresis. If previous events are flushing sediment, the effect may be most noticeable on the falling limb. Thus the entire event shows low sediment loads and concentrations. Previous events can supply sediment to the channel, which caused sediment loads and concentrations to increase to the highest peak flow. Thirty-three of the events showed clockwise loops (fig. 8.15a).

Reproduced with permission of the copyright owner. Further reproduction prohibited without permission.

Hysteresis Results

The different types of hysteresis loops, their characteristics, and controls on the amount of sediment exhaustion and increase were examined in this PhD dissertation for the four basins being studied. There is a certain fascination about hysteresis because it illustrates a variety of geomorphic processes operating during a storm event. Comparison of hysteresis types between basins may provide useful information on basin characteristics. Most of the literature on hysteresis loops has focused on small-scale basins and has attributed Type-1 loops (clockwise loops) to a channel sediment source (Sidle and Campbell, 1985; Kattan and others, 1987). This readily available bed sediment becomes the "first flush", as it is often called (Irvine and Drake, 1987), and sediment concentration peaks before peak flow Type-3 loops (counterclockwise loops) which have sediment concentration peaking after peak flow are less common in the literature and have been attributed to tributary input, bank collapse on the recession limb, and wave celerity (Guy, 1969; Marcus, 1989; Asselman and Middelkoop, 1998). In large scale basins, the suspended-sediment peak travels with the mean flow velocity, a phenomenon known as "wave celerity" and over large distances mean flow velocity and peak sediment concentration lag behind peak flow and Type-3 hysteresis occurs (Heidel, 1956; Marcus, 1989; Brasington and Richards, 2000), although Bull and others (1995) showed that sediment waves both lagged behind and were faster than the peak flow traveling downstream in the Severn River (8.7-355 km^2), United Kingdom. The basins studied in Puerto Rico are at a relatively small scale and thus, wave celerity may have a minor effect.

The highest percentage of storm events in Quebrada Blanca (39%), Rio Icacos (67%), and Rio Caguitas (39%) have the suspended sediment concentration peak 0 to 30 minutes before peak discharge (fig. 10.21). Rio Piedras has the highest percentage of events (38%) peaking 0 to 30

Reproduced with permission of the copyright owner. Further reproduction prohibited without permission.

minutes after the peak discharge (fig, 10.21). Rio Caguitas has 22% of its events peaking more than 60 minutes after peak discharge. In summary, for all stations over 30% of the suspended-sediment concentration peaks are within +/- 15 minutes of the peak flow and over 70% are +/- 30 minutes of the peak flow.

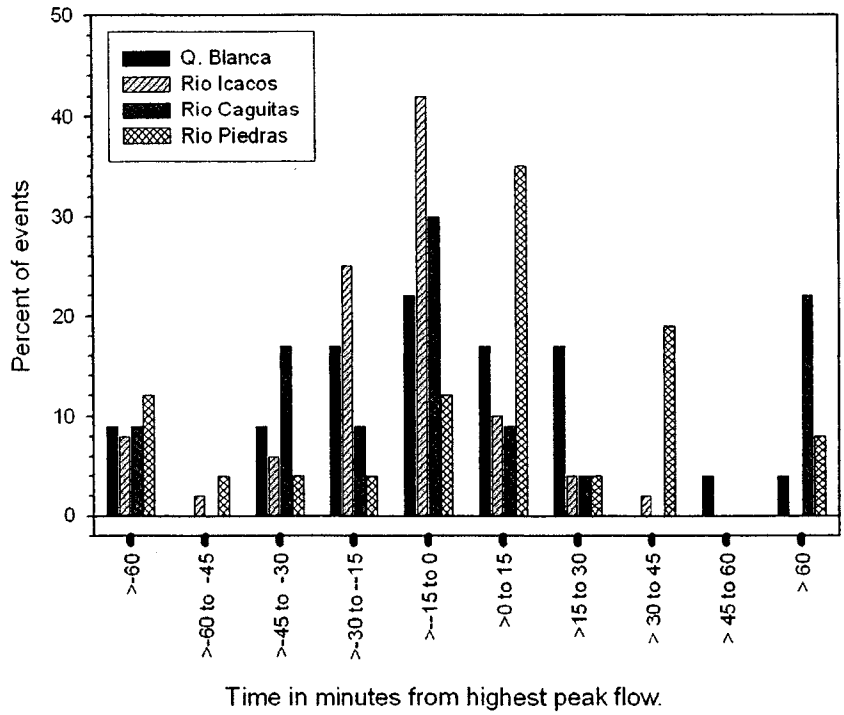

Figure 10.21. Relation of the timing of the suspended-sediment concentration peak relative to peak flow. Negative numbers indicate the peak suspended-sediment concentration occurred before peak flow.

Rio Icacos had the highest percentage of events (84%) classified as Type-1 loops (fig. 10.22) Quebrada Blanca and Rio Caguitas were split between the number of Type-1 and Type-3 events and Rio Piedras had 56 % of its events classified as Type-3. Type-4 events, which have a counterclockwise hysteresis shape around the highest peak flow, occurred 14% of the time in Quebrada Blanca.

Reproduced with permission of the copyright owner. Further reproduction prohibited without permission.

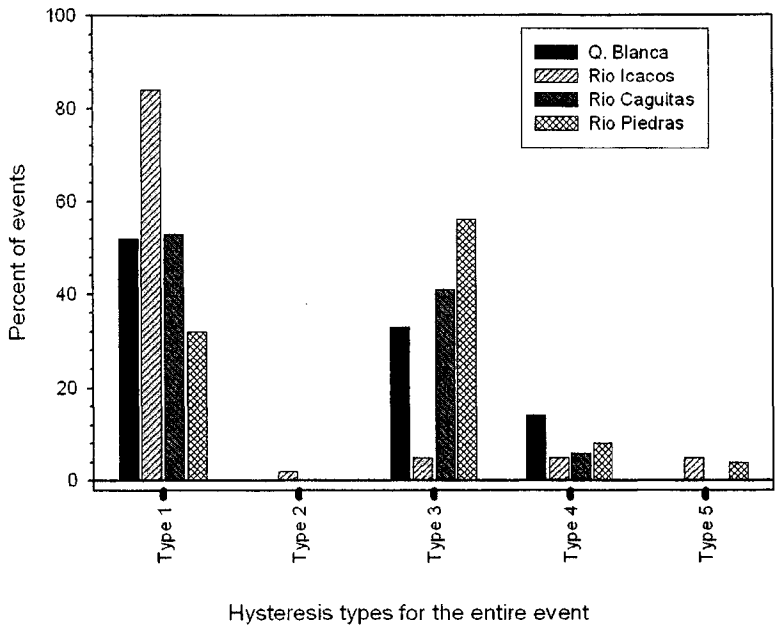

Figure 10.22. Hysteresis types for the entire event for each of the four study basins.

In the supply-limited Quebrada Blanca and Rio Icacos basins, the same magnitude of sediment exhaustion in Type-1 events and sediment increases in Type-3 events occurs. Rio Piedras showed higher sediment concentrations and higher sediment increases on Type-3 loops, reflecting an upland source of sediment (fig. 10.23). Rio Caguitas showed a wider sediment exhaustion in Type-1 loops and higher sediment concentrations and loads in Type-1 events, which may reflect a channel source of sediment in these events (fig. 10.23). Larger runoff events led to Type-1 hysteresis in Rio Caguitas and Rio Piedras (fig.10.23). This may indicate a channel source of sediment in the larger events or that the large storms reach a point where they exhaust upland and channel sediment so that any sediment generated travels to the streamflow station before peak flow. Sidle and Campbell (1985) concluded that wider hysteresis loops occurring in Type-1 events were related to an increase in the supply of sediment. The supply of sediment increased during the

Reproduced with permission of the copyright owner. Further reproduction prohibited without permission.

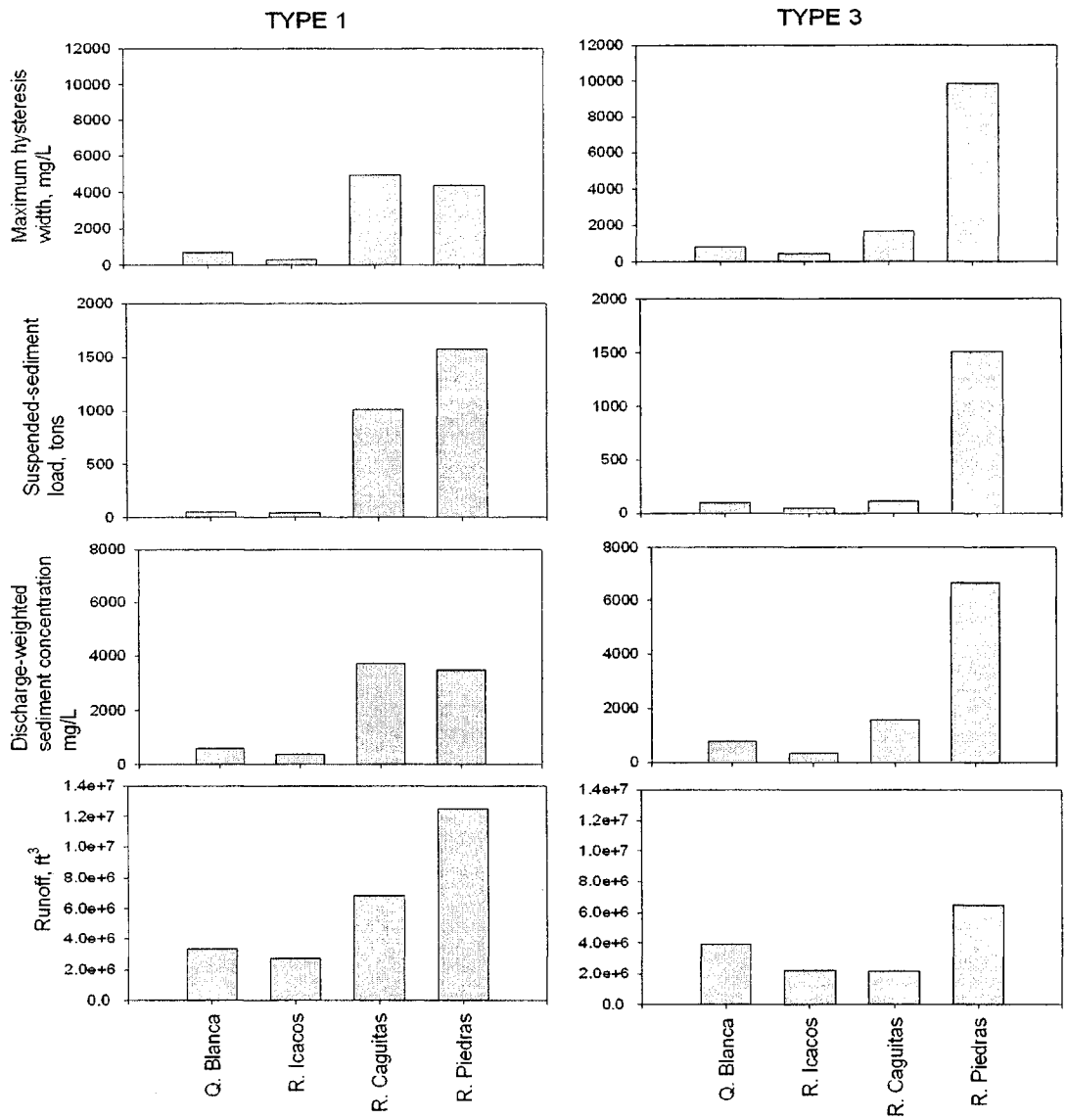

Figure 10.23. Type-1 and Type-3 hysteresis widths around the highest peak flow with corresponding average suspended-sediment loads, discharge-weighted sediment concentration, and runoff values.

early wet season and during large storm events. Wood (1977) indicated that the longer the duration of a storm event, the more sediment exhaustion in Type-1 hysteresis would occur. In Quebrada Blanca, runoff in Type-3 storms was 17% higher than Type-1 storms (fig. 10.23),

Reproduced with permission of the copyright owner. Further reproduction prohibited without permission.

indicating that upland sediment may be generated late in the event and not reach the station before peak flow. In Rio Icacos, Type-1 events are most common for a range of flows.

Significant factors affecting the amount of sediment exhaustion in Type-1 events and sediment increases in Type-3 events were tested using multiple regression with forward stepwise regression. The small number of storms classified as Type-3 for Rio Icacos did not permit statistical analysis for this group. Results for Type-1 storms showed that at three of the basins (Rio Icacos, Rio Caguitas, and Rio Piedras), current-event characteristics were most significant in explaining the amount of sediment exhaustion (fig. 10.24). At Rio Piedras, rainfall on the rising limb was significant and positively correlated to the amount of sediment exhaustion, implying that the higher the rainfall intensity, the more sediment exhaustion occurs. The time of the peak suspended-sediment concentration was positively correlated for Rio Caguitas and negatively correlated for Rio Icacos. A negative correlation at Rio Icacos implies that the earlier the peak of suspended sediment occurs relative to the highest peak flow, the higher the amount of sediment exhaustion. In Rio Icacos, Type-1 events are more prevalent, and therefore an inverse relation is expected.. Rio Caguitas has 41% of its events classified as Type-3, and therefore more sediment may be generated closer to the peak flow, and thus the positive relation of time of peak observed at Rio Caguitas . Quebrada Blanca showed the sum of the 3 previous runoff events as significant in controlling the width of Type-1 hysteresis loops. The slope of the line of best-fit is negative, indicating that as the sum of runoff of the previous events increases, the amount of sediment exhaustion decreases. This is in part related to a reduction in the amount of sediment available for transport.

Reproduced with permission of the copyright owner. Further reproduction prohibited without permission.

a)

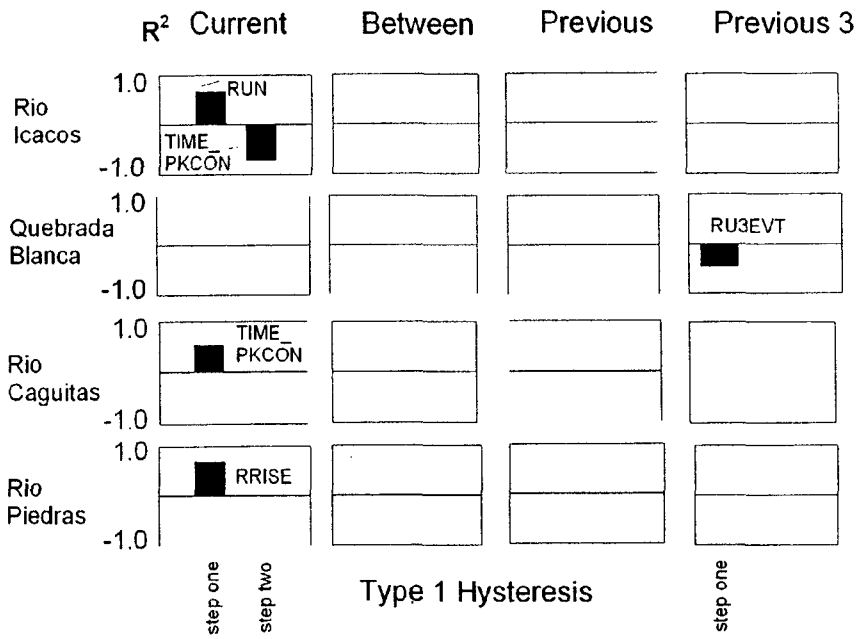

b)

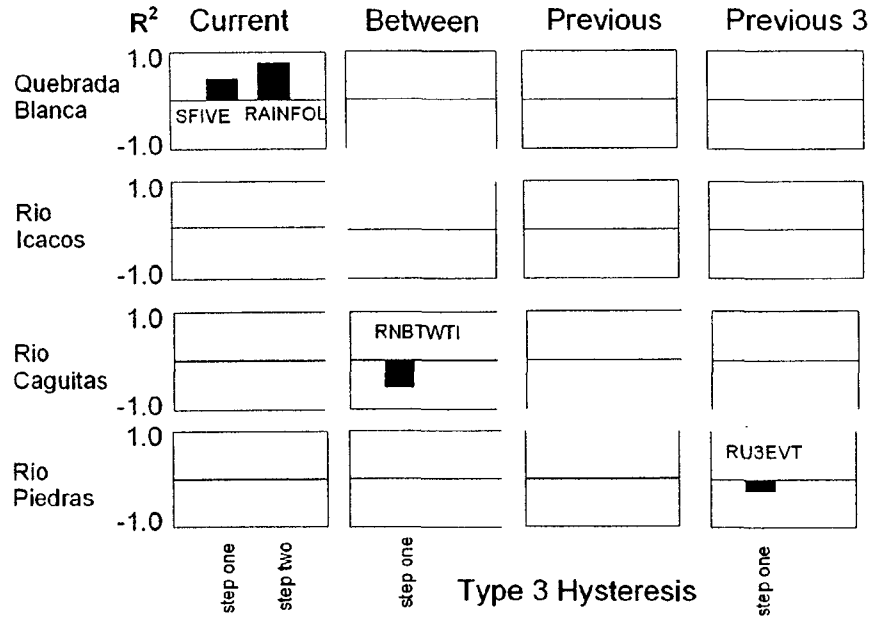

Figure 10.24. Significant factors effecting the width (exhaustion and increase) of a) Type-1 hysteresis loops and b) Type-3 hysteresis loops. See Table 4.9 for abbreviations.

Reproduced with permission of the copyright owner. Further reproduction prohibited without permission.

Factors thought to control the amount of sediment increase during Type-3 events for the three stations were analyzed and showed that current-event characteristics were important in Quebrada Blanca, between-event characteristics were significant in Rio Caguitas, and the three previous events were important in Rio Piedras (fig. 10.17). Current-event characteristics of rainfall intensity and rainfall on the falling limb of the hydrograph were shown to be significant at Quebrada Blanca and positively correlated to the amount of sediment increase, implying that higher rainfall intensity and amounts are increasing sediment that is getting to the station after the peak flow. Between-event runoff at Rio Caguitas was inversely correlated with the amount of sediment increase. In principal components analysis, between-event rainfall is positively correlated with sediment load (fig. 10.19a). Thus, between-event rainfall is supplying sediment and between-event runoff is removing sediment from the system. At Rio Piedras the sum of the 3 previous-events runoff was inversely correlated to the amount of sediment replenishment, indicating removal of sediment.

Discussion

Results of the statistical analysis in all four basins always indicated that current-event characteristics were significant and directly correlated to suspended-sediment load and the discharge-weighted sediment concentration. In multiple regression analysis and factor analysis, with and without varimax rotation, current-event characteristics were typically significant in the first step of forward stepwise regression. The peak flow and sum of the peak flows were also significant in the first or second step of forward stepwise regression. This result that peak flow is significant in describing suspended-sediment load and sediment concentrations has significant applications.

Reproduced with permission of the copyright owner. Further reproduction prohibited without permission.

Monitoring streamflow and sediment collection is expensive and labor intensive. Recording just the peak flow with a crest-stage gage is less costly and less labor intensive. Results from this study suggest that for most of the study basins, recording only the peak flow will provide a statistically significant suspended-sediment load and discharge-weighted sediment concentration.

Results of the statistical analysis for storm events at all four study basins showed that the rate of hydrograph rise to any peak or the highest peak flow was significant for both dependent variables (suspended-sediment load and discharge-weighted sediment concentration). Beschta (1987) had similar results and showed that on steeply rising hydrograph limbs, suspended-sediment was being supplied at a relatively high rate, thus leading to higher concentrations. Faster rates of hydrograph rise are the product of storm generated runoff being delivered faster to the channel. This can occur by a combination of higher rainfall intensity and/or more saturated areas in the basin. Dunne and Leopold (1978) showed that saturation overland flow contributes to faster rising hydrograph peaks. As the storm progresses, more areas of the basin become saturated and contribute to saturated overland flow. This will translate into more hillslope erosion, higher runoff amounts to the channel, with higher shear stress on the channel bed causing sediment resuspension, and increased sediment transport to the sampling station.

Forward stepwise regression and principal components analysis indicate some generalizations about sediment transport in the four study basins. For the entire event, previous-event rainfall and runoff were increasing the current sediment loads and concentrations at Rio Icacos, increasing loads at Quebrada Blanca, increasing and decreasing current sediment loads at Rio Caguitas and decreasing current sediment loads and concentrations at Rio Piedras. Between-event rainfall and runoff decreased current sediment loads and concentrations at Rio Icacos,

Reproduced with permission of the copyright owner. Further reproduction prohibited without permission.

increased sediment concentrations at Quebrada Blanca, and decreased sediment concentrations at Rio Piedras. At Rio Caguitas, an interesting coupling action is occurring where previous and between-event rainfall supply sediment that is flushed by previous and between-event flows.

To the highest peak flow, previous-event rainfall and runoff increased the current sediment loads and concentrations at Rio Icacos, decreased sediment loads and concentrations at Quebrada Blanca, having no effect at Rio Caguitas, and increased loads at Rio Piedras. Between-event rainfall and runoff were decreasing current sediment loads and concentrations at Rio Icacos, decreasing sediment loads at Quebrada Blanca, decreasing sediment concentrations at Rio Caguitas. Runoff between events (using quickflow and runoff) were decreasing sediment loads at Rio Caguitas whereas rainfall and rainfall intensity were increasing sediment loads. At Rio Piedras rainfall and rainfall intensity between events was decreasing sediment loads and concentrations to the highest peak flow.

When analyzing suspended-sediment load as a dependent variable it is important to remember that it is a product of water discharge and suspended-sediment concentration and increases in either will increase suspended-sediment loads. Therefore, for two storms of similar rainfall and equal amounts of material eroded off upland areas, if more saturated areas exist in the basin for the second storm, there would be higher sediment loads. More saturated areas in the basin would be expected to occur with more frequent, closely spaced storms.

The results from this study on factors controlling sediment characteristics in four humid-tropical streams of contrasting land use, indicated that in the forested and least disturbed basin, previous events supply sediment to the channel and between events flush sediment. Sediment concentration peaks before peak flow and most of the hysteresis loops are clockwise, implying a

Reproduced with permission of the copyright owner. Further reproduction prohibited without permission.

channel source of sediment in the events. Rio Piedras, the most disturbed basin from construction activities, had the highest suspended-sediment concentrations, sediment yields and discharge-weighted concentrations. When examining the entire event for sediment loads and sediment concentrations at Rio Piedras, between events and previous events flush sediment. When examining just sediment characteristics on the rising limb, between-event characteristics flush sediment and previous events increase sediment. This may indicate that on the rising limb at Rio Piedras, in-channel sediment is important and after the peak flow hillslope sediment is more important. This is verified by the hysteresis analysis which indicates that most events are Type-3, counterclockwise hysteresis loops. Quebrada Blanca and Rio Caguitas are basins that are between relatively undisturbed and disturbed and showed characteristics of each. The number of hysteresis loops defined as Type-1 and Type-3 were generally split. In Rio Caguitas, previous-event rainfall and between-event rainfall supplied sediment and previous-event runoff and between-event runoff flushed sediment.

Reproduced with permission of the copyright owner. Further reproduction prohibited without permission.

CHAPTER XI

CONCLUSIONS

The humid tropics is a climatic region undergoing dramatic worldwide land-use changes. Tropical forests make up one-half of the world's forests, and 42 million acres (17 million hectares) of deforestation occur annually. Puerto Rico is a microcosm of the developing humid tropics and may provide a model of land-use change and sediment yield. Changes in land use in Puerto Rico follow a sequence very similar to the northeastern United States; of 93% deforestation by the 1940s for agriculture, abandonment of agriculture and reforestation since 1949, and suburbanization and urbanization since the 1960s, which was continuing at the time period analyzed in this PhD dissertation (1989-1996). The major classes of land use (forest, cropland, pasture, and urban) are all present in Puerto Rico, and therefore the Island is an excellent natural laboratory to study suspended sediment in different land-use settings.

Suspended-sediment concentrations in streams are products of rock weathering, soil formation, normal and accelerated erosion, and subsequent delivery to the fluvial system. Identifying suspended-sediment sources and significant controls on the variability of suspended-sediment concentrations in natural systems is crucial to our understanding of how natural landscapes function. Suspended sediments are the "white blood cells" of the fluvial system, increasing in response to disturbance. Sediment is currently the leading pollutant in the United States. Understanding how land-use disturbance(s) affect suspended-sediment dynamics and cause a

Reproduced with permission of the copyright owner. Further reproduction prohibited without permission.

departure from natural settings is important in classifying disturbed systems and developing sound strategies to reduce erosion and suspended-sediment concentrations.

Compared to other tropical rivers, Puerto Rican rivers have a similar relation of drainage area to sediment yield. Discharge-weighted sediment concentrations were somewhat lower in Puerto Rican streams than in other tropical environments, although Rio Piedras had the 7th highest discharge-weighted sediment concentration for all tropical rivers (n=365) studied. Tropical rivers have average annual sediment yields and average annual sediment concentrations lower than those of semi-arid climates, but higher than those of temperate climates. Higher relief in tropical watersheds, which leads to mass wasting and a higher frequency and duration of intense rainfall events, may lead to higher erosion and sediment concentrations than those in temperate climates. Differences between sediment production in tropical and humid-temperate systems are highlighted when watersheds are disturbed by land-use activities. Sediment yields in the urbanizing Rio Piedras basin (17,000 tons/mi^2; 5,950 metric tons/ km^2) are eight times higher than sediment yields reported for an urbanizing area (2,200 tons/mi^2; 2000 metric tons/km^2) in the northeastern United States. The higher sediment yields in disturbed Puerto Rican watersheds reflect a substantial supply of available sediment, steep slopes, and frequent intense rainfall.

Contributions of this PhD research are the development of methodologies to address the voluminous suspended-sediment data gathered for select watersheds in Puerto Rico, and to extract significant information on hydrologic and geologic processes from those data. The first, more minor contribution was the development and testing of techniques to reduce the data by classifying events (i.e., what level of flow constitutes a runoff event, what level of complexity is necessary for a simple event to become a complex event), and for those events separating out quickflow from total runoff.

Reproduced with permission of the copyright owner. Further reproduction prohibited without permission.

A graphical technique was developed for hydrograph separation that determined the inflection point on the hydrograph recession limb by taking the second derivative of a 3rd order best-fit regression line fit to the hydrograph recession limb. Quickflow was separated from base flow by drawing a straight line from the beginning of the event to the inflection point.

A more significant contribution is the development of a statistical approach to determine the important factors controlling suspended-sediment concentrations and loads in tropical fluvial systems. To develop this statistical approach, four basins with different land use were selected to analyze storm-generated suspended-sediment loads and concentrations: forest (Rio Icacos), pasture (Quebrada Blanca), cropland and pasture (Rio Caguitas), and urbanizing (Rio Piedras). The independent variables used to understand storm-generated suspended-sediment loads, and concentrations were divided into three categories: 1) previous-event factors, 2) factors between events, and 3) current-event factors. Hydrologic factors for each of these categories included some or all of the following: peak flow, the rate of hydrograph rise, runoff (quickflow), hysteresis, and rainfall amounts and intensity. Two distinct approaches for reducing the number of independent variables were used to assess potential analytical and interpretive advantages. The first approach was an inspection of the Pearson's product-moment correlation matrix to remove highly correlated ($R > 0.80$) variables. The second approach was a more involved principal component analysis of the correlation matrix. Varimax rotation was used on the principal components to see if that improved interpretations of the results. Forward stepwise regression was performed on the independent variables and principal components with and without varimax rotation. The use of forward stepwise regression on the principal components was a unique

Reproduced with permission of the copyright owner. Further reproduction prohibited without permission.

approach to determine the significant controls on storm-generated sediment loads and concentrations.

From this analysis, several important points about the relationship between the variables were determined:

- Two dependent variables were used to describe storm-generated sediment loads, suspended-sediment load and the discharge-weighted sediment concentration, determined by normalizing storm suspended-sediment load by runoff. The discharge-weighted sediment concentration may be a better variable to describe storm-generated sediment characteristics because it is representative of the overall suspended-sediment concentration for the event. However, suspended-sediment load often had higher correlation coefficients than the discharge-weighted sediment concentration because discharge is used in the calculation of suspended-sediment load and there may be a spurious relation between many of the independent variables thought to control sediment and discharge, such as peak flow, runoff, and rainfall.
- Separation of the storm hydrograph into quickflow did not improve the significance of the variables found to be important in controlling storm-generated sediment loads. The assumption that only the quickflow portion contributes to sediment transport may not apply to streams in Puerto Rico where a large amount of easily resuspended sediment is in the channel. Quickflow added to base flow increases the depth of flow and the shear stress on the bed, causing resuspension and sediment transport, so total storm runoff may be a better indicator of sediment transport than quickflow.

Reproduced with permission of the copyright owner. Further reproduction prohibited without permission.

- Examination of just the rising limb of the storm hydrograph to the highest peak flow only marginally improved regression coefficients and in some basins added or slightly changed the interpretation of significant variables controlling suspended-sediment concentrations. Examination of only suspended-sediment concentrations on the rising limb of the hydrograph was thought to improve the understanding of significant variables of previous and between-flow events. However, it is unclear whether isolating suspended-sediment characteristics on the rising limb of the hydrograph improves the understanding of how previous and between-event characteristics affect sediment concentrations.
- Four variables were shown to be statistically significant to suspended-sediment concentrations for a humid-temperate river, 1) discharge minus base flow, 2) time relation of sample to major peak, 3) base flow at start of storm, and 4) index of flood intensity, were also shown to be significant variables describing suspended-sediment concentrations for the four basins studied in Puerto Rico.
- Results of the statistical analysis always indicated that current-event characteristics were significant and directly correlated to suspended-sediment load and the discharge-weighted sediment concentration. The peak flow and sum of the peak flows were often significant in the first or second step of forward stepwise regression. Results from this study indicate that for most of the study basins, recording only the peak flow will provide a statistically significant suspended-sediment load and discharge-weighted sediment concentration. Recording only peak flows with a device, such as a crest-stage gage, is considerably less expensive and less labor-intensive than measuring streamflow.

Reproduced with permission of the copyright owner. Further reproduction prohibited without permission.

Considering the stochastic nature of many hydrologic and sediment variables, the basins tended to behave in a systematic fashion (fig. 11.1, 11.2). The forested basin (Rio Icacos) is representative of a relatively undisturbed basin and has a cycle of sediment production and delivery where previous events mobilize upland sediment through landsliding, transport of sediment in storage, and bank failures (fig. 11.1a, 11.2a). This mobilized sediment is deposited in the main channel and tributaries. In the next event, this recently deposited sediment becomes the first flush causing a clockwise (Type-1) hysteresis. Channel sources of sediment may be depleted rather quickly, as stream discharge increases, resulting in dilution so that suspended-sediment concentrations rapidly decline. In the forested basin, runoff and rainfall occurring between events flush some of this sediment in storage (fig. 11.1a, 11.2a). This pattern of sediment production and delivery in the forested basin was evident in both statistical analyses for the entire event and to the highest peak.

In Quebrada Blanca, draining dominantly pasture, sediment production and delivery results differed between the entire event and to the highest peak flow (fig. 11.1b, 11.2b). For the entire event, previous events and between events supply sediment to the system (fig. 11.1b). To the highest peak flow, previous events and between events flush sediment (fig. 11.2b). This leads to the interpretation that large previous events and rainfall between events increases sediment to the system, but the sediment does not reach the station before the highest peak flow. This model of sediment delivery is supported by examination of the hysteresis loops, which showed that 26 percent of the storm events in Quebrada Blanca were classified as counterclockwise (Type-3). Larger runoff events, which increase erosion and sediment transport, were correlated with Type-3 hysteresis. Large events deposit sediment on the bed of the channel. Eventually, as the previous

Reproduced with permission of the copyright owner. Further reproduction prohibited without permission.

Figure 11.1. Hypothetical model of sediment transport for the entire event showing statistically significant hydrologic characteristics of the previous events, between events, and the current event . A '+' and '-' indicates the hydrologic variable is increasing or reducing sediment transport, respectively. a) Rio Icacos.

Reproduced with permission of the copyright owner. Further reproduction prohibited without permission.

Reproduced with permission of the copyright owner. Further reproduction prohibited without permission.

Figure 11.1. b) Quebrada Blanca.

Reproduced with permission of the copyright owner. Further reproduction prohibited without permission.

Figure 11.1. c) Rio Caguitas.

Reproduced with permission of the copyright owner. Further reproduction prohibited without permission.

Figure 11.1. d) Rio Piedras.

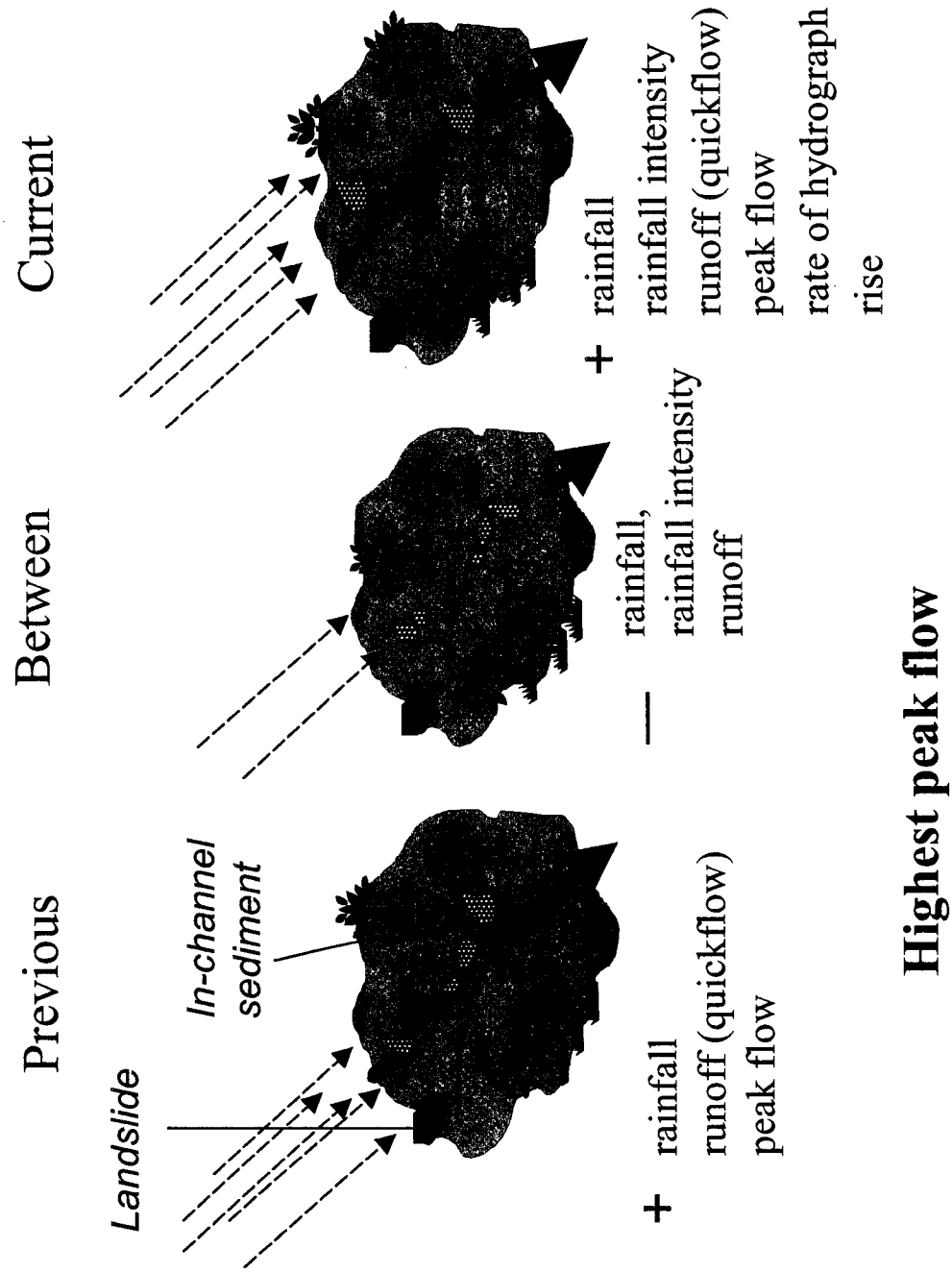

Figure 11.2. Hypothetical model of sediment transport to the highest peak flow showing statistically significant hydrologic characteristics of the previous events, between events, and the current event . A '+' and '-' indicates the hydrologic variable is increasing or reducing sediment transport, respectively. a) Rio Icacos.

Reproduced with permission of the copyright owner. Further reproduction prohibited without permission.

Reproduced with permission of the copyright owner. Further reproduction prohibited without permission.

Figure 11.2. b) Quebrada Blanca.

Reproduced with permission of the copyright owner. Further reproduction prohibited without permission.

Figure 11.2 c) Rio Caguitas.

Reproduced with permission of the copyright owner. Further reproduction prohibited without permission.

Figure 11.2 d) Rio Piedras.

events become large enough and occur closely spaced in time, there is an increased amount of sediment on the bed of the channel and Type-1 hysteresis occurs. The effect of large previous events was shown to be statistically important, as the sum of the 3 previous-events runoff was positively correlated to Type-1 hysteresis.

In Rio Caguitas, a mixed land-use basin with cropland as a major sediment source, results were similar for the entire event and to the highest peak flow (fig. 11.1c, 11.2c). For the entire event, previous rainfall and rainfall intensity supply sediment to the system and previous-event runoff and peak flow flush sediment (fig. 11.1c, 11.2c). Between-event rainfall and rainfall intensity supply sediment and high runoff between events flush sediment (fig. 11.1c, 11.2c). Sheetwash erosion between events measured at cropland sites (DO-A, EN-A) showed that sediment moves on hillslopes between events (fig. 9.2). In Type-3 hysteresis events, the runoff between events was significant in exhausting sediment. Statistical interpretations of the data at Rio Caguitas indicate that increases in rainfall and rainfall intensity between events supplied sediment, and increases in previous and between-event runoff flushed sediment.

In Rio Piedras, an urbanizing basin with significant sediment sources, a similar pattern emerged from the statistical analysis of the entire event and to the highest peak flow, where increases in previous events (rainfall intensity, runoff, and peak flow) and increases between events (rainfall) flush sediment (fig. 11.1d, 11.2d). Long dry periods are favorable for high sediment transport in the Rio Piedras basin. The large amount of fine-textured sediment in Rio Piedras leads to Type-3 hysteresis, where most of the sediment stays in suspension for the entire storm. Only during the largest storm events was most of the sediment transported before the highest peak flow, leading to Type-1 hysteresis. The limited amount of sediment deposited in the channel during an

Reproduced with permission of the copyright owner. Further reproduction prohibited without permission.

event enhances the flushing characteristics of this basin. The classification of disturbed basins in humid tropical environments by counterclockwise hysteresis is an original contribution of this PhD dissertation.

If we assume that the forested basin (Rio Icacos) represents undisturbed conditions and the urbanizing basin (Rio Piedras) represents disturbed conditions, hypothetical models of sediment transport can be developed (fig. 11.3, 11.4). In an undisturbed basin, storm events increase sediment availability to the fluvial system (fig. 11.3a). As time proceeds until the next storm, this available sediment is removed from storage. In the disturbed basin, sediment is made available between storm events through construction practices (fig. 11.3b). Storm events and runoff between events flush sediment and reduce sediment availability. As a basin proceeds from undisturbed to disturbed conditions, storm-generated hysteresis loops change from clockwise (Type 1) to counterclockwise (Type 3) and sediment flushing occurs (fig. 11.4).

The United States Environmental Protection Agency (USEPA) has identified fluvial sediment as the leading cause of impairment of surface waters in the United States. Every two years, States publish a priority list of impaired waters that is known as the 303(d) list. If sediment is the cause of impairment, States and tribes must develop a total maximum daily load (TMDL) for sediment. The sediment TMDL can be developed through sediment data collection, often from sediment samples collected at a regular frequency (i.e. biweekly). Results from this dissertation indicate that knowledge of the current storm-generated hydrograph variables, between-event characteristics, and previous-event characteristics can affect the current samples. Timing of a single sample relative to the peak flow is especially important. If the basin is disturbed and impaired by sediment, then the peak sediment concentration may occur after the peak flow. Samples taken on

Reproduced with permission of the copyright owner. Further reproduction prohibited without permission.

the rising limb may underestimate the predicted load. States report a maximum allowable TMDL level (mg/L) above naturally occurring background levels. Forested areas are often representative of background or natural rates. A model for an undisturbed watershed is presented in this study that is dominated by in-channel sediment having clockwise hysteresis loops. Previous events are supplying sediment to the channel and between-event characteristics are removing this sediment.

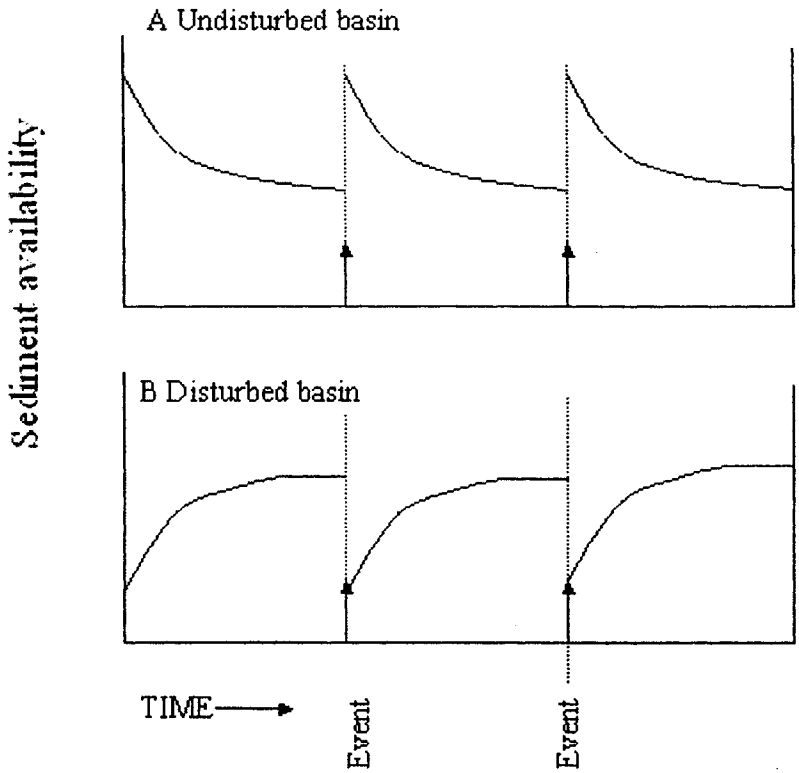

Figure 11.3. Hypothetical model of sediment availability through time in response to storm event and between storm events for a) an undisturbed basin and b) a disturbed basin.

Reproduced with permission of the copyright owner. Further reproduction prohibited without permission.

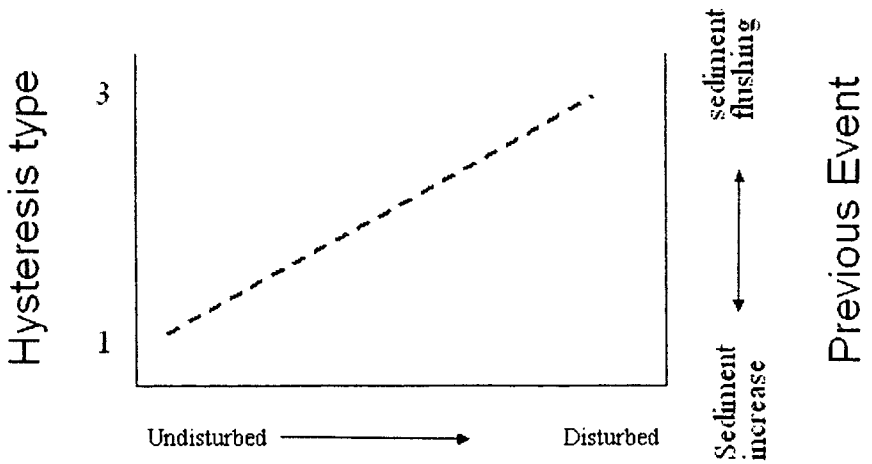

Figure 11.4. Hypothetical model showing changes in hysteresis types (clockwise Type 1, counterclockwise Type 3) and sediment flushing, as land use changes from undisturbed to disturbed.

This PhD research contributes to the understanding of suspended-sediment transport in humid tropical systems under various land-use settings. It should be emphasized that the statistical results shown here are most useful as exploratory tools in our knowledge of the fluvial system, and exemplify the need for more field research in understanding hydrologic variables shown in the research to be statistically significant. For example, measurement of upland sediment movement between events can be improved through better field measurements. This research points to a need for a better understanding of sediment storage and transport in first and second-order channels. An important next step in determining the causes for variability in storm-generated sediment concentrations is the development of a more quantitative approach, such as the sediment "fingerprinting" approach to identifying sediment sources through the course of the hydrograph.

Reproduced with permission of the copyright owner. Further reproduction prohibited without permission.

The fingerprinting approach involves collecting suspended sediment from stream-monitoring sites and comparing its characteristics to that of surface soil and sediment samples collected from potential contributing areas or sources within the watershed. Many characteristics can be used to fingerprint sediment, such as: total carbon, nitrogen, and phosphorous, stable isotopes (C-13, N-15, Al, Sr, Zn, etc.), clay mineralogy, radionuclides (Cesium-137, unsupported Lead-210, Beryllium-7, Beryllium-10), and magnetic susceptibility. Statistical methods consisting of cluster analysis and a mixing model are applied to determine sources. Understanding sediment sources during storms in humid-tropical settings and how these sources may change during the course of the hydrograph will validate or refute many of the statistical findings in this study.

The null hypothesis put forth in this PhD research was that land use does not affect upland erosion and suspended-sediment characteristics in a humid-tropical environment. The results of this research showed the impact that land use had on upland erosion, suspended-sediment transport (concentration, loads, and yields), and how previous storm events, between-event, and current-event processes operated in different land-use settings.

Reproduced with permission of the copyright owner. Further reproduction prohibited without permission.

CHAPTER XII

REFERENCES

Alberts, H.W., and Garcia-Molinari, O,. 1943, Pastures of Puerto Rico and their relation to soil conservation: U.S. Department of Agriculture Miscellaneous Publication no. 513, 43 p.

Asselman, N.E.M., and Middelkoop, H., 1998, temporal variability of contemporary floodplain sedimentation in the Rhine-Meuse Delta, the Netherlands: Earth Surface Processes and Landforms, v. 23, p. 595-609.

Asselman, N.E.M., 1999, Suspended sediment dynamics in a large drainage basin–The River Rhine: Hydrological Processes, v. 13, p. 1437-1450.

Barnes, B.S., 1939, The structure of discharge-recession curves: Transaction of the American Geophysical Union, Part IV, Reports and Papers-Hydrology, p. 721-725.

Barnett, A.P., Carreker, J.R., Abruna, F., and Dooley, A.E., 1971, Erodibility of selected tropical soils: Transactions of the American Society of Agricultural Engineers, Paper 70-738, p. 496-499.

Barnett, A.P., Carreker, J.R., and Abruna, F., 1972, Soil and nutrient losses in runoff with selected cropping treatments in tropical soils: Journal of Agronomy, v. 64, p. 391-395.

Beard, D., 1994, Despite monsoons, no end in sight to Puerto Rican drought: Albuquerque Journal, September 4, 1994.

Beschta, R.L., 1987, Conceptual models of sediment transport in streams: In Thorne, C.R., Bathurst, J.C., and hey, R.D., eds., Sediment transport in gravel-bed rivers, John Wiley, Chichester, p. 387-419.

Bhowmik, N.G., 1988. Sediment transport in streams and rivers: Journal of applied hydrology, v. 1, p. 25-62.

Bierman, P.R., and Steig, E., 1996, Estimating rates of denudation using cosmogenic isotope abundances in sediment: Earth Surface Processes, v. 21.

Birkeland, P.W., 1984, Soils and geomorphology: Oxford university Press, 372 p.

Reproduced with permission of the copyright owner. Further reproduction prohibited without permission.

Birot, P., 1960, Geographic physique generale de la zone intertropical, Paris: Center de Documentation Universitaire. 137 p.

Birot, P., 1966, General physical geography, London: Harrap, p. 209-213.

Boccheciamp, R.A., 1977, Soil survey of Humucao area of Eastern Puerto Rico: U.S. Department of Agriculture, Soil Conservation Service, 103 p.

Boccheciamp, R.A., 1978, Soil survey of San Juan area of Puerto Rico: U.S. Department of Agriculture, Soil Conservation Service, 141 p.

Bonnet, J.A. and Lugo-Lopez, M.A., 1950, Relative erosiveness of Puerto Rico soils: Journal of Agriculture of the University of Puerto Rico, v. 34, p. 294-307.

Bons, C.A., 1990, Accelerated erosion due to clearcutting of plantation fires and subsequent Taungya cultivation in upland West-Java, Indonesia: In, Research Needs and Applications to Reduce Erosion and Sedimentation in Tropical Steeplands, IAHS-AISH Publication No. 192, p. 279-288.

Brasington, J., and Richards, K., 2000, Turbidity and suspended sediment dynamics in small catchments in the Nepal Middle Hills: Hydrological Processes, v. 14, p. 2559-2574.

Bremer, H., 1980, Landform development in the humid tropics, German geomorphological research: Zeitschrift fur Geomorphologie, v. 36, p. 162-175.

Brenner, M., and Binford, M.W., 1988, A sedimentary record of human disturbance from Lake Miragoane, Haiti: Journal of Paleolimnology, v. 1, p. 85-97.

Briggs, R.P. and Akers, J.P., 1965, Hydrogeologic map of Puerto Rico and adjacent islands: U.S. Geological Survey Hydrogeologic Investigations Atlas HA-197, scale 1:240,000.

Brockman, V.W., 1952, The rural land classification program of Puerto Rico: Studies in Geography, Number 1, Department of Geography, Northwestern University, Evanston, Illinois, July 1952, 161 p.

Brooks, K.N., Ffolliott, P.F., Gregersen, H.M., and Thames, J.L., 1991, Hydrology and the management of watersheds: Iowa Sate University Press, Ames, Io, 392 p.

Brown, E., Stallard, R.F., Larsen, M.C., Raisbeck, G.M., and Yiou, F., 1995, Denudation rates determined from the accumulation of in situ produced 10Be in the Luquillo Experimental Forest, Puerto Rico: Earth and Planetary Science Letters, v. 129, p. 193-202.

Reproduced with permission of the copyright owner. Further reproduction prohibited without permission.

Brown, E., Stallard, R.F., Larsen, M.C., Bourles, D.L., Raisbeck, G.M., and Yiou, F., 1998, Determination of predevelopment denudation rates of an agricultural watershed (Cayaguas River, Puerto Rico) using in-situ produced 10Be in river-borne quartz: Earth and Planetary Science Letter, v. 160, p. 723-728.

Brunig, E.F., 1975, Tropical ecosystems--State and targets of research into the ecology of humid tropical ecosystems: Plant research and development, v. 1, p. 22-38.

Bryan R.B., 1991, Surface wash: in Field Experiments and Measurement Programs in Geomorphology, Slaymaker, O., ed, UBC Press, Vancouver, Canada, p. 107-167.

Budel, J., 1957, Die Doppelten Einebnungsflachen in den feuchten Tropen.: Zeitschrift fur Geomorphologie, NF 1, p. 201-288.

Budel, J., 1982, Climatic geomorphology, English translation by L. Fischer and D. Bushe. Princeton: Princeton University Press, 443 p.

Bull, L.J., Lawler, D.M., Leeks, G.J.L., and Marks, S., 1995, Downstream changes in suspended sediment fluxes in the River Severn, UK: Effect of Scale on Interpretation and Management of Sediment and Water Quality, Osterkamp, W.R., ed., IAHS Pub. No 226, p. 27-37.

Butcher, D.P., Claydon, J., Labadz, J.C., Pattinson, V.A., Potter, W.R., and White, P., 1992, Reservoir sedimentation and colour problems in Southern Pennine reservoirs: Journal of the Institution of Water and Environmental Management, v.6., no.4, p.418-431.

Carter, R.W., and Davidian, J., 1968, General procedures for gaging streams: U.S. Geological Survey Techniques of Water-Resources Investigations, book 3, chap. A6, 13 p.

Chang, R., 1981, Physical chemistry with applications to biological systems: MacMillan Publishing Co., New York, 657 p.

Chanson, H., 1998, Extreme reservoir sedimentation in Australia--A review: Water Resources Journal, v.199, p.96-102.

Chatterjea, K., 1989, Surface wash--The dominant geomorphic process in the surviving rainforest of Singapore: Singapore Journal of Tropical Geomorphology, v. 10, p. 95-109.

Chorley, R.J., Schumm, S.A., and Sugden, D.E., 1984, Morphogenetic landforms: Geomorphology, Methuen, London, p. 467-484.

Clapp, E.M., Bieman, P.R., and Caffee, M.L., 1997, Rates of erosion determined from in situ produced cosmogenic isotopes in a small arroyo basin, northwestern New Mex.: Geol. Society of America Abstracts with Program, 1997 GSA Annual Meeting Salt Lake City, UT. p. A-371.

Reproduced with permission of the copyright owner. Further reproduction prohibited without permission.

Clark, J. J., and Wilcock, P. W., 2000, Effects of Land Use Change on Channel Morphology and Hydraulic Geometry in Northeastern Puerto Rico: Geological Society of America Bulletin, v. 112, No 12, pp. 1763-1777.

Clifford, N., French, J.R. and Hardisty, J., 1993, eds., Turbulence: perspectives on flow and sediment transport. John Wiley and Sons.

Coch, N.K., 1994, Geologic effects of hurricanes: Geomorphology, v. 10, p. 37-63.

Collar, P.D., and Guzman-Rios, S, 1991, Sedimentation rates and capacity restoration options, Lago Loiza, Puerto Rico: Proceedings of the Fifth Federal Interagency Sedimentation Conference, Las Vegas, Nev., Chap. 15, p. 17-25.

Collins, A.L., Walling, D.E., and Leeks, J.L., 1998, Use of composite fingerprints to determine the provenance of the contemporary suspended sediment load transported by rivers: Earth Surface Processes and Landforms, v. 23, p. 31-52.

Costa, J.E., 1977, Sediment concentration and duration in stream channels: Journal of Soil and Water Conservation, v. 32, p.168-170.

CSA Architects and Engineers/Weston, Inc., 1999, Watershed Management Study of the San Juan Bay Estuarine System, Puerto Rico, Draft Report. Prepared for the San Juan Bay Estuarine Program, November, 1999.

Curtis, W.F., Flint, R.F., and George, F.H., 1978, Fluvial sediment study of Fishtrap and Dewey lakes drainage basins, Kentucky-Virginia: U.S. Geological Survey Open-File Report 77-123, 92 p.

Dana, J.D., 1850, On denudation in the Pacific: American Journal of Science, vol. 9, p. 48-62.

Dano, A.M., 1990, Effect of burning and reforestation on grassland watersheds in the Philippines: In, Research Needs and Applications to Reduce Erosion and Sedimentation in Tropical Steeplands, IAHS-AISH Publication No. 192, p. 53-61.

Daultrey, S., 1976, Principal components analysis: Concepts and Techniques in Modern Geography, No. 8, 51 p.

Davis, J.C., 1973, Statistics and data analysis in geology: John Wiley and Sons, First Edition, 550 p.

Davis, J.C., 1986, Statistics and data analysis in geology: John Wiley and Sons, Second Edition, 646 p.

Reproduced with permission of the copyright owner. Further reproduction prohibited without permission.

De La Torre, B., 1990, San Juan area may be facing a thirsty future: San Juan Star, February 25, 1990, p. 1.

Dietrich, W.E., Dunne, T., Humphrey, N.F., and Reid, L.M., 1982, Construction of sediment budgets for drainage basins: In Sediment Budgets and Routing in Forested Drainage Basin, U.S. Forest Service General Technical Report PAW-141, p. 5-23.

Donnelly, T.W., 1989, Geologic history of the Caribbean and Central America: in Bally, A.W., and Palmer, eds., The geology of North America--An overview, Boulder Colorado, Geological Society of America, p. 299-321.

Douglas, I., 1967, Natural and man-made erosion in the humid tropics of Australia, Malaysia, and Singapore: IAHS Pub., no., 75 p. 17-25.

Douglas, I., 1977, Humid landforms: MIT Press, Cambridge, Mass., 288 p.

Douglas, I., 1978, Tropical geomorphology-Present problems and future prospects, in Geomorphology---Present problems and future prospects, Embleton, C., Brunsden, D., and Jones, D.K.C., eds., Oxford University Press, p. 162-184.

Douglas, I., and Spencer, T., 1985a, The history of geomorphology in low latitudes: In Environmental Change and Tropical Geomorphology, Douglas, I., and Spencer, T., eds., George Allen and Unwin, p. 3-12.

Douglas, I., and Spencer, T., 1985b, Present-day processes as a key to the effect of environmental change: In Environmental Change and Tropical Geomorphology, Douglas, I., and Spencer, T., eds., George Allen and Unwin, p. 39-73.

Douglas, I., Greer, T., Meng, W.M., Spencer, T., and Sinun, W., 1990, The impact of commercial logging on a small rainforest catchment in Ull Segama, Sabah, Malaysia: In, Research Needs and Applications to Reduce Erosion and Sedimentation in Tropical Steeplands, IAHS-AISH Publication No. 192, p. 165-173.

Dunne, T., Moore, T.R., and Taylor, C.H., 1975, Recognition and prediction of runoff-producing zones in humid regions: Hydrological Sciences Bulletin, v. 20, p. 305-327.
Dunne, T., 1979, Sediment yield and land use in tropical catchments: Journal of Hydrology, v. 42, p. 281-300.

Dunne, T., and Leopold, L.B., 1978, Water in environmental planning: W.H. Freeman and company, New York, 818 p.

Edwards, T.K., and Glysson, G.D., 1988, Field methods for measurement of fluvial sediment: U.S. Geological Survey Open-File Report 86-531, 118 p.

Reproduced with permission of the copyright owner. Further reproduction prohibited without permission.

Ehlmann, A.J., 1968, Clay mineralogy of weathered products and of river sediments, Puerto Rico: Journal of Sedimentary Petrology, v. 38, p. 885-894.

El-Swaify, S.A., 1990, Research needs and applications to reduce erosion and sedimentation in the tropics: In, Research Needs and Applications to Reduce Erosion and Sedimentation in Tropical Steeplands, IAHS-AISH Publication No. 192, p 3-13.

Eyles, R.J. and Ho, R., 1970, Soil creep on a humid tropical slope: Journal of Tropical Geography, v. 31, p. 40-42.

Fleming, W., 1985, Phewa Tal catchment management program--Benefits and costs of forestry and soil conservation in Nepal: In, Hamilton, L.S., eds., Forest and Watershed Development and Conservation in Asia and the Pacific, Westview Press, Boulder, Co., p. 217-288.

Food and Agriculture Organization of the United Nations, 2003: Water Resources Development and Management Service, World Sediment Yields Database, compiled by HR Wallingford Ltd., United Kingdom, assessed March 13, 2003 at URL *http://www.fao.org/ag/agl/aglw/sediment/default.asp*.

Fournier, M.F., 1960, Climat et erosion: Paris, Presses Universitaires de France, 201 p.

Gellis, A.C., 1991, Construction effects on sediment for two basins, Puerto Rico: Proceedings of the Fifth Federal Interagency Sedimentation Conference, Las Vegas, Nev., chap. 4, p. 72-78.

Gellis, A.C., 1993, The effects of Hurricane Hugo on suspended-sediment loads, Lago Loíza basin, Puerto Rico: Earth Surface Processes and Landforms, v .18, no. 5. p. 505-517.

Gellis, A.C., Webb, R.M.T., Wolfe, W.J., and McIntyre, S.C.I., 1999, Effects of land use on upland erosion, sediment transport, and reservoir sedimentation, Lago Loiza basin, Puerto Rico: U.S. Geological Survey Water-Resources Investigations Report 99-4010, 60 p.

Gellis, A.C., Pavich, M.J., and Ellwein, A., 2001, Erosion and sediment yields in two subbasins of contrasting land use, Rio Puerco, New Mexico: Proceedings of the Seventh Federal Interagency Sedimentation Conference, Reno, Nevada, p. V83-V90.

Gerlach, T., 1967, Hillslope troughs for measuring sediment movement. Revue Geomorphologie Dynamique, v. 4, p. 173.

Glysson, G.D., 1987, Sediment-transport curves: U.S. Geological Survey Open-File Report 87-218, 47 p.

Golding, M.J., 1973, A short history of Puerto Rico: The New American Library, 174 p.

Reproduced with permission of the copyright owner. Further reproduction prohibited without permission.

Goodwin, P., and Denton, R.A., 1991, Seasonal influences on the sediment transport characteristics of the Sacramento River, California: In, Proceedings of the Institution of Civil Engineers, Part 2, Research and Theory, v. 91, p. 163-172.

Goudie, A., 1984, Nature of the environment--The Tropics: Blackwell, Oxford, UK, p. 161-185.

Gumbs, F.A., J.I. Lindsay, M. Nasir, A. Mohmmed. 1985. Soil erosion studies in the northern mountain range, Trinidad, under different crop and soil management. In: Soil Erosion and Conservation, pp. 90-98. Soil Conservation Society of America, Ankeny, Iowa.

Gupta, A., 1975, Stream characteristics in eastern Jamaica, an environment of seasonal flow and large floods: American Journal of Science, v. 275, p. 825-847.

Gupta, A., 1988, Large floods as geomorphic events in the humid tropics: In Baker, V.R., Kochel, R.C., and Patton, P.C., eds., Flood Geomorphology, John Wiley and Sons, New York, p. 301-315.

Guy, H.P., 1964, An analysis of some storm-period variables affecting stream sediment transport: U.S. Geological Survey Professional Paper 462-E, 46p.

Guy, H.P., 1969, Laboratory theory and methods for sediment analysis: U.S. Geological Survey Techniques of Water Resources Investigations, Book 5, Chap. C1, 58p.

Hall, A.J., 1971, Baseflow recessions and the baseflow hydrograph separation problem: Hydrology Papers, 1971, p. 159-170.

Hammermeister, D.P., Kling, G.F., and Vomocil, J.A., 1982, Perched water tables on hillsides in western Oregon, II, Preferential movement of water and anions: Journal of the Soil Science Society of America, v. 46, p. 811-818.

Hastenrath, S,M., 1976, Variations in low-latitude circulation and extreme climatic events in the tropical Americas: Journal of the Atmospheric Sciences, v. 33, p. 202-215.

Heidel, S.G., 1956, The progressive lag of sediment concentration with flood waves: Transactions of the American Geophysical Union, v. 37, p. 56-66.

Helsel, D.R. and Hirsch, R.M., 1992, Statistical Methods in Water Resources: Studies in Environmental Science 49, Elsevier Science Publishers B.V., Netherlands, 522 p.

Hewlett and Hibbert, 1967, Factors effecting the response of small watersheds to precipitation in humid areas: In, Sopper, W.E., and Lull, H.W., eds., International Symposium on Forest Hydrology, p. 275-290.

Reproduced with permission of the copyright owner. Further reproduction prohibited without permission.

Hornberger, G.M., Raffensperger, J.P., and Wiberg, P.L., 1998, Elements of physical hydrology: the John Hopkins University Press, 302 p.

Hotchkiss, R.H., 1995, Reservoir sedimentation; causes and consequences: In Espey, W.H., Jr., and Combs, P.G., eds., Proceedings of the First International Conference of Water Resources Engineering, San Antonio, Texas, p. 1188-1992.

Hughes-Hallett, D., 1994: Calculus, John Wiley and Sons, 685 p.

Irvine, K.N., and Drake, J.J., 1987, Process-oriented etimation of suspended sediment concentration: Water Resources Bulletin, v. 23, p. 1017-1025.

Jibson, R.W., 1989, Debris flows in southern Puerto Rico: Geological Society of America Special Paper 236, p. 29-55.

Jordan, J.M.J., 1989, The sediment problem in South Africa reservoirs: In Yang., S.S.Y, ed., Sediment Transport Modeling, Proceedings of the International Symposium, Hydraulics Division of the ASCE, New Orleans, Louisiana, August 14-18, p. 795-800.

Kattan, Z., Gac., J.Y., and Probst, J.L., 1987, Suspended sediment load and mechanical erosion in the Senegal Basin - Estimation of the surface runoff concentration and relative contributions of channel and slope erosion: Journal of Hydrology, v. 92, p. 59-76.

Kennedy, W.J., 1984, Discharge ratings at gaging stations: U.S. Geological Survey Techniques of Water-Resources Investigations: Book 3, Chap. A1, 58p.

Kesel, R.H., 1977, Slope runoff and denudation in the Rupununi Savanna, Guyana: Journal of Tropical Geography, v. 44, p. 33-42.

Kesel, R.H., 1985, Alluvial fan systems in a wet-tropical environment, Costa Rica: national Geographic Research, v. 1, p. 450-469.

Kirkby, M.J., and Chorley, R.J., 1967, Throughflow, overland flow, and erosion: Bulletin of the International Association of Scientific Hydrology, v.12, no.3, p. 5-21.

Knighton, D., 1996, Fluvial Forms and processes: Halsted Press, New York, 218 p.

Krishnaswamy, J., Richter, D.D, Halpin, P.N., and Hofmockel, M.S., 2001, Spatial patterns of suspended-sediment yields in a humid tropical watershed in Costa Rica: Hydrological Processes, v. 15, p. 2237-2257.

Kulandaiswamy, V.C., and Seetharaman, S., 1969, A note on Barnes' method of hydrograph separation" Journal of Hydrology, v. 9, p. 222-229.

Reproduced with permission of the copyright owner. Further reproduction prohibited without permission.

Kurashige, Y., 1994, Mechanisms of sediment supply in headwater rivers: Transactions, Japanese Geomorphological Union, v. 15A, p. 109-129.

Lal, R., 1981, Deforestation of tropical rainforest and hydrological problems: In, Tropical Agricultural Hydrology, Lal, R., and Russell, E.W., (eds)., p. 131-140.

Lal, R., 1990, Soil erosion in the tropics: McGraw-Hill, inc., 580p.b

Langbein, W.B., and Schumm, S.A., 1958, Yield of sediment in relation to mean annual precipitation: Transactions of the American Geophysical Union, v. 39, p. 1076-1084.

Larsen, M.C., and Simon, A., 1990, Landslide processes in saprolitic soils of a tropical rain forest, Puerto Rico: In LaRue, D.K., and Drapeer, G., eds., Transactions of the 12th Caribbean Geological Conference, St. Croix., U.S. Virgin Islands, Miami Geological Society, p. 217-222.

Larsen, M.C., and Torres-Sanchez, A.J., 1990, Rainfall-soil moisture relations in landslide-prone areas of a tropical rain forest, Puerto Rico: In Krishna, J.H., Quinones-Aponte, V., Gomez-Geomez, F., and Morris, G.L., eds., International Symposium on Tropical Hydrology and Fourth Caribbean Islands Water Resources Congress, San Juan, Puerto Rico, p. 121-130.

Larsen, M.C., Torres-Sanchez, A.J., 1992, Landslides triggered by Hurricane Hugo in eastern Puerto Rico, September 1989: Caribbean Journal of Science, v. 28, p. 113-125.

Larsen, M.C., and Simon, A., 1993, A rainfall intensity-duration threshold for landslides in a humid-tropical environment, Puerto Rico: Geographiska Annaler, v. 75A, p. 13.23.

Larsen, M.C., Torres-Sanchez, A.J., 1995, Climatologic, geographic, and geologic factors influencing the distribution and occurrence of landslides in the Blanco, Cibuco, and Coamo river basins, Puerto Rico: U.S. Geological Survey Water Resources Investigations Report 95-4029, 100 p.

Larsen, M.C., 1997, Tropical geomorphology and geomorphic work--A study of geomorphic processes and sediment and water budgets in montane humid-tropical forested and developed watersheds, Puerto Rico: Unpublished Ph.D. dissertation, University of Colorado, 341 p.

Larsen, M.C., and Torres-Sanchez, A.J., 1998, The frequency and distribution and recent landslides in three montane tropical regions of Puerto Rico: Geomorphology, v. 24, p. 309-331.

Larsen, M.C., and Santiago-Roman., A., 2001, Mass wasting and sediment storage in a small montane watershed–an extreme case of anthropogenic disturbance in the humid tropics: In Geomorphic Processes and Riverine Habitat, Dorova, J.M,, Montgomery, D.R., Palcsak, B.B., and Fitzpatrick, F.A., eds, American Geophysical Union, Water Science and Application, v. 4, p. 119-238.

Reproduced with permission of the copyright owner. Further reproduction prohibited without permission.

Larsen, M.C., Torres-Sanchez, A.J., and Concepcion, I.M., 1999, Slopewash, surface runoff and fine-litter transport in forest and landslide scars in humid-tropical steeplands. Luquillo Experimental Forest, Puerto Rico: Earth Surface Processes and Landforms, v. 24, 22 p.

Leigh, C., 1982, Sediment transport by surface wash and throughflow at the Pasoh Forest Reserve, Negri Sembilan, Peninsular Malaysia: Geografiska Annaler 64A, p. 171-180.

Lerman, A., 1985, Weathering rates and major transport processes--An Introduction: In Physical and chemical weathering in geochemical cycles, Lerman, A., and Meybeck, M., eds., Kluwer Press, p. 1-10.

Lewis, G.K., 1963, Puerto Rico--Freedom and power in the Caribbean: MR Press New York, 626 p.

Lewis, J.F., and Draper, G., 1990, Geology and tectonic evolution of the northern Caribbean margin: In Dengo, G., and Case, J.E., The Caribbean Region, Geological Society of America, The geology of North America Volume H, p. 77-140.

Lewis, L.A., 1974, Slow movement of earth under tropical rainforest conditions: Geology, v. 2, p. 9-10.

Lewis, L.A., 1975, Slow Slope movement in the dry tropics: Zeitschrift fur Geomorphologie, v. 19, no. 3., p. 334-339.

Linsley, R.K., Kohler, M.A., and Paulhus, J.L., 1982, Hydrology for engineers: McGraw Hill, 508 p.

Lopes, V.L., and Ffolliott, P.F., 1993, Sediment rating curves for a clearcut Ponderosa Pine watershed in northern Arizona: Water Resources Bulletin, v. 29, p. 369-382.

Loughran, R.J., 1989, The measurement of soil erosion: Progress in Physical Geography, v. 13, p. 216-233.

Lugo-Lopez, M.A., 1969, Prediction of the erosiveness of Puerto Rican soils on the basis of the percentage of silt and clay when aggregated: Journal of Agriculture of the University of Puerto Rico, v. 53, p. 187-190.

Mahmood, K., 1987, Reservoir sedimentation–Impact, extent, and mitigation: Worldbank Technical Paper No. 71, 118 p.

Malmer, A., 1990, Stream suspended sediment load after clear-felling and different forestry treatments in tropical rainforest, Sabah, Malaysia: In, Research Needs and Applications to Reduce Erosion and Sedimentation in Tropical Steeplands, IAHS-AISH Publication No. 92, p. 62-71.

Reproduced with permission of the copyright owner. Further reproduction prohibited without permission.

Marcus, W.A., 1989, Lag-time routing of suspended-sediment concentrations during unsteady flow: Bulletin of the Geological Society of America, v. 101, p. 644-651.

Mar-Lopez, T, Aide, T.M., and Scantena, F.N., 1998, The effect of land use on soil erosion in the Guadiana watershed in Puerto Rico: Carribean Journal of Science, v. 34, p. 298-307.

Masson, D.G., and Scanlon, K.M., 1991, The neotectonic setting of Puerto Rico: Geological Society of America Bulletin, v. 103, p. 144-154.

McLean, S.R., 1992, On the Calculation of suspended load for noncohesive sediments, Journal of Geophysical Research , v. 97(C4), p. 5759-5770.

Meade, R.H., Yuzyk, T.R. and Day, T.J. 1990. Movement and storage of sediment in rivers of the United States and Canada, in Wolman, M.G. and Riggs, H.C., editors, Surface Water Hydrology. Geological Society of America. The Geology of North America, v. O-1, p. 255-280.

Medina, J.L., 1989, Experts predict Carraizo will dry up in next decade: San Juan Star, October 5, 1989. p. 3

Milliman, J.D., and Meade, R.H., 1983, World-wide delivery of river sediment to the oceans: Journal of Geology, v. 91, p. 1-21.

Millington, A.C., 1981, Relationship between three scales of erosion measurement on two small basins in Sierra Leone: IAHS-AISH Publication No. 133.

Molinelli, J., 1982, Soil erosion, sediment sources, and sediment loadings in the Loiza and La Plata lake watersheds, Puerto Rico: Unpublished report prepared for the Puerto Rican Environmental Quality Board, 34 p.

Monroe, W.H, 1980a, Geology of the middle Tertiary Formations of Puerto Rico: U.S. Geological Survey Professional Paper 953, 93 p.

Monroe, W.H, 1980b, Some tropical landforms of Puerto Rico: U.S. Geological Survey Professional Paper 1159, 39 p.

Moore, R.J., 1984, A dynamic model of basin sediment yield: Water Resources Research v. 20, p. 89-103.

Murphy, L.S., 1916, Forests of Porto Rico -- past, present, and future: USDA Bulletin No 354, 98 p.

Nagle, G.N., Fahey, T.J., and Lassoie, J.P., 1999, Management of sedimentation in tropical watersheds: Environmental Management, v.23, p. 441-452.

Reproduced with permission of the copyright owner. Further reproduction prohibited without permission.

Nathan, R.J., and McMahon, T.A., 1990, Evaluation of automated techniques for base flow and recession analyses: Water Resources Research, v. 26, p. 1465-1473.

Nevares, R., Jr., and Dunlop, J.C., 1948, Some engineering and geologic data on reservoir sedimentation in Puerto Rico: U.S. Geological Survey Unpublished Report, 24 p.

Nordin, C.F, 1991, J.C. Stevens and the silt problem a review: International Symposium on Special Problems of Alluvial Rivers, Sept. 16-19, 1991, Seoul, Korea, p. 1-18.

Ogunkoya, O.O., and Jenkins, A., 1993, Analysis of storm hydrograph and flow pathways using a three-component hydrograph separation model: Journal of hydrology, v.142, p. 71-88.

Okunishi, K., Walling, D.E., and Saito, T., 2000, A hydrological model of the mobilization of fine suspended sediment from slopes: Transactions, Japanese Geomorphological Union, p. 243-260.

Ongkosongo, O.S.R., Sukardi, S., and Ilyas, M.A., 1992, Sedimentation in rivers and associated water bodies in Indonesia with a special note on the volcanic debris deposits: International Journal of Sediment Research, v.7, no.1, p.93-103.

Osterkamp, W.R., 2002, Geoindicators for river-valley monitoring in the humid tropics: Environmental Geology, v. 42, p. 725-735.

Palmeiri, A., Shah, F., and Dinar, A., 1998, Reservoir sedimentation and the sustainable management of dams: Paper presented at the World Congress of Environmental and Resource Economists, Venice, Italy, June 23-27, 1998.

Peart, M.R., and Walling, D.E., 1986, Fingerprinting sediment source–The example of a drainage basin in Devon, UK: IAHS Publication, No. 159, p. 41-55.

Pease, M.H., 1968, Geologic map of the Aguas Buenas quadrangle, Puerto Rico: U.S. Geological Survey Miscellaneous Geologic Investigations Map I-479.

Peltier, L.C., 1950, The geographic cycle in periglacial regions as it is related to climatic geomorphology: Annals of the Association of American Geographers, v. 40, p. 214-236.

Pettyjohn, W.A., and Henning, R.J., 1979, Preliminary estimate of regional effective ground-water recharge rates in Ohio: Ohio State University Water Resources Center Project Completion Report Number 552, 323 p.

Pickup, G., Higgins, R.J., and Warner, R.F., 1981, Erosion and sediment yield in Fly River drainage basins, Papua New Guinea: Publication of the International Association of Hydrological Sciences 132, p. 438-456.

Reproduced with permission of the copyright owner. Further reproduction prohibited without permission.

Picouet, C., Hingray, B., and Olivry, J.C., 2001, Empirical and conceptual modeling of the suspended sediment dynamics in a large tropical African river–the Upper Niger basin: Journal of Hydrology, v. 250 p. 19-39.

Porterfield, G., 1972, Computation of fluvial-sediment discharge: U.S. Geological Survey Techniques of Water-Resources Investigations Book3, Chapter C3, 66 p.

Puerto Rico Department of Natural and Environmental Resources, 1977, Unpublished land-use maps.

Pugh, J.C., 1966, The landforms of low latitudes: In Essays in Geomorphology, Dury, G.H., Ed., Elsevier, New York, p. 121-139.

Quinones, F., Green, B., and Santiago, L., 1989, Sedimentation survey of Lago Loiza, Puerto Rico, July 1985: U.S. Geological Survey Water-Resources Investigation Report 187-4019, 16 p.

Reid, L.M., 1991, Research and cumulative watershed effects: U.S. Department of Agriculture, Forest Service General Technical Report PSW-141, 118p.

Renwick, W.H., 1996, Continent-scale reservoir sedimentation patterns in the United States: In Walling, D.E., and Webb, B.W., eds., Erosion and Sediment Yield–Global and Regional Perspectives, IAHS Publ. 236, p. 513-522.

Richards, R., 1991, The use of the data-collection platforms to trigger automatic samplers, USGS-Water Resources Division Instrument News, 52, p. 8-9.

Rieger, W.A., and Olive, L.J., 1986, Sediment responses during storm events in small forested watersheds: In, Statistical Aspects of Water Quality Monitoring, Proceedings of the Workshop held at the Canada Centre for Inland Waters, October 7-10, 1985, El-Shaarawi, A.H., and Kwiatkowski, R.E., eds., p. 490-497.

Rietbergen, S., 1993, Tropical Forestry: Castlefield Press, 328 p.

Roose, E.J., 1986, Runoff and erosion before and after clearing depending on the type of crop in western Africa: In Lal, R., Sanchez, P.A., and Cummings, R.W., Land Clearing and Development in the tropics, A.A. Balkema, Rotterdam, p. 317-329.

Rooseboom, A., and Mulke, F.J., 1982, Erosion initiation Proceedings of the Exeter Symposium, IAHS, Publ no, 137, p. 59-66.

Ross, K., 1994, Island's 'Oases' become its water tanker trucks: The Washington Post, September 4, 1994, p 3.

Reproduced with permission of the copyright owner. Further reproduction prohibited without permission.

Ross, S.M., Thornes, J.B., and Nortcliff, S., 1990, Soil hydrology, nutrient and erosional response to the clearance of terra firme forest, Maraca Island, Roraima, northern Brazil: The Geographical Journal, v. 156, no. 3, p. 267-282.

Rouse, I., 1989, Peopling and repeopling of the West Indies: Biogeography of the West Indies--Past, present, and future: Sandhill Crane Press, Gainesville, Fla., p. 119-136.

Rutledge, A.T., 1997, Model-estimated ground-water recharge and hydrograph of ground-water discharge to a stream: U.S. Geological Survey Water-Resources Investigations Report 97-4253, 29 p.

Ruxton, B.P., and Berry, L., 1957, Weathering and associated erosional features in Hong Kong: Geological Society of America Bulletin, v. 68, p. 1263-1292.

Ruxton, B.P., and Berry, L., 1961, Weathering profiles and geomorphic position on granite in two tropical regions: Revue de geomorphologie Dynamique, v. 12, p. 16-31.

Sauer, V.B., and Meyer ,R.W., 1992, Determination of error in individual discharge measurements: U.S. Geological Survey Open-File Report 92-144, 21 p.

Scanlon, T.M., Raffesnperger, J.P., and Hornberger, G.M., 2001, Modeling transport of dissolved silica in a forested headwater catchments–Implications for defining the hydrochemical response of observed flow pathways: Water Resources Research, v. 37, p. 1071-1082.

Scatena, F.N., 1995, Relative scales of time and effectiveness of watershed processes in a tropical montane rain forest of Puerto Rico: In Costa, J.E., Miller, A.J., Potter, K.W., and Wilcock, P.R., eds., Natural and anthropogenic influences in fluvial geomorphology, The Wolman Volume, American Geophysical Union, Geophysical Monograph 89, p. 103-111.

Schumm, S.A., 1977, The fluvial system: John Wiley and sons, 338 pp.

Serrano, S.E., 1997, Hydrology for Engineers, Geologists, and Environmental Professionals: HydroScience, Inc., Lexington, Kentucky.

Shahin, M.M.A., 1993, An overview of reservoir sedimentation in some African river basins: AIHS Publ. no. 217, p. 93-100.

Sharma, H.S., 1987, Tropical geomorphology: Concept Publishing Co., New Delhi, India, 385 p.

Sharma, K.D., and Correia, J.F., 1989, Upland erosion in a mixed pine forest ecosystem: Proceedings Indian Academy of Science, Earth and Planetary Science, v. 98, p. 133-145.

Reproduced with permission of the copyright owner. Further reproduction prohibited without permission.

Sidle, R.C., and Campbell, A.J., 1985, Patterns of suspended-sediment transport in a coastal Alaska Stream: Water Resources Bulletin, v. 21, p. 909-917.

Simon, A., and Guzman-Rios, 1990, Sediment discharge from a montane basin, Puerto Rico--Implications of erosion processes and rates in the humid tropics, in Research Needs and Applications to Reduce Erosion and Sedimentation in Tropical Steeplands: International Association of Hydrologic Sciences Publication No. 192, p. 35-47.

Simon, A., Larsen, M.C., and Hupp, C.R., 1990, The role of soil processes in determining mechanisms of slope failure and hillslope development in a humid-tropical forest, eastern Puerto Rico: Geomorphology, v. 3., p. 263-286.

Skoklevski, Z., and Velickov, S., 1995, Total suspended load transport as a natural stochastic process: Effects of scale on Interpretation and Management of Sediment and Water Quality, Proceedings of a Boulder Symposium, July 1995, IAHS Pub., no. 226, p. 215-221.

Smith, R.M., and Abruna, F., 1955, Soil and water conservation research in Puerto Rico, 1938 to 1947: University of Puerto Rico Agricultural Experiment Station Bulletin 154, 51 p.

Soler-Lopez, L.R. and Webb, R.M.T., 1998, Sedimentation survey of Lago Dos Bocas, Puerto Rico: U.S. Geological Survey Water-Resources Investigation Report 98-4188, 14 p.

Soler-Lopez, L.R., Webb, R.M.T., and Perez-Blair, F., 1998, Sedimentation survey of Lago Yahuecas, Puerto Rico: U.S. Geological Survey Water-Resources Investigation Report 98-4259, 15 p.

Soler-Lopez, L.R. and Webb, R.M.T., 1999, Sedimentation survey of Lago Prieto, Puerto Rico: U.S. Geological Survey Water-Resources Investigation Report 99-4169, 11 p.

Soler-Lopez, L.R., Webb, R.M.T., and Perez-Blair, F., 1999a, Sedimentation survey of Lago Garzas, Puerto Rico: U.S. Geological Survey Water-Resources Investigation Report 99-4143, 20 p.

Soler-Lopez, L.R., Webb, R.M.T., and Perez-Blair, F., 1999b, Sedimentation survey of Lago Patillas, Puerto Rico: U.S. Geological Survey Water-Resources Investigation Report 99-4030, 14 p.

Spencer, T., Douglas, I.,Greer, T., and Sinun, W., 1990, Vegetation and fluvial geomorphic processes in south-east Asian tropical rain forests: In, Thornes, J.B., ed., Vegetation and Erosion, Wiley, Chichester, p. 420-436.

Reproduced with permission of the copyright owner. Further reproduction prohibited without permission.

Stallard, R.F., 1988, Weathering and erosion in the humid tropics: in Physical and chemical weathering in geochemical cycles, Lerman, A., and Meybeck, M., eds., Kluwer Academic Publishers, Netherlands, p. 225-246.

Stoddart, D.R., 1969, Climatic geomorphology-A review and re-assessment: Progress in Physical Geography, v. 1., p. 159-222.

Strahler, A.N., and Strahler, A.H., 1976, Elements of Physical Geography: John Wiley and Sons, 469 p.

Swan, A.R.H. and Sandilands, M., 1995, Introduction to geological data analysis: Blackwell Science, 446 p.

Swan, S.B., 1970, Piedmont slope studies in a humid tropical region, Johor, Southern Malaya: Zeitschrift fur Geomorphologie, v. 10, p. 30-39.

Swan, S.B., 1972, Land surface evolution and related problems with reference to a humid tropical region, Johore, Malaya: Zeitschrift fur Geomorphologie, v. 16, p. 160-181.

Swistock, B.R., Dewalle, D.R., and Sharpe, W.E., 1989, Sources of acidic storm flow in an Appalachian headwater stream: Water Resources Research, v. 25, p. 2139-2147.

SYSTAT, 1997, Statistics: SPSS, inc., 751 p.

Taggart, B.M., and Joyce, J., 1991, Radiometrically dated marine terraces on northwestern, Puerto Rico: In Larue, D.K., and Draper, G., eds., Transactions of the 12th Caribbean Conference, St. Croix, USVI, Miami Geological Society, p. 248-258.

Takeuchi, K., and Sakamoto, Y., 1986, Hydrograph separation using NO_3^- for identifying the interaction between surface and subsurface waters in a small mountainous basin: In Conjunctive Water Use, Proceedings of the Budapest Symposium, July 1986, IAHS-AISH Publ. No. 156, p.199-210.

Thomas, M.F., 1974, Tropical geomorphology: MacMillan Press, 332 p.

Thomas, M.F., 1994, Geomorphology in the tropics: John Wiley and sons, 460 p.

Thongmee, U., and Vannapraqsert, M., 1990, Soil and water losses on plots with different land uses in the Phu Wiang watershed: In, Research Needs and Applications to Reduce Erosion and Sedimentation in Tropical Steeplands, IAHS-AISH Publication No. 192, p. 48-52.

Thornbury, W.D., 1954, Principles of geomorphology: John Wiley and Sons, 618 p.

Reproduced with permission of the copyright owner. Further reproduction prohibited without permission.

Tricart, J., 1972, Landforms of the humid tropics, forests, and savannas: Longman Group Limited, London, 306 p.

Tricart, J., and Cailleux, A., 1972, Introduction to climatic geomorphology: St. Martins Press, New York, 295 p.

UNESCO, 1990, Water related issues and problems of the humid tropics and other warm humid regions: United Nations Environment Programme, 33 p.

U.S. Department of Commerce, 1938, Census of Puerto Rico--1935, population and agriculture:

U.S. Department of Commerce, Bureau of the Census, 150 p.

U.S. Department of Commerce, 1949, Census of Puerto Rico--1945, population and agriculture: U.S. Department of Commerce, Bureau of the Census.

U.S. Department of Commerce, 1959, Census of Puerto Rico--1955, population and agriculture: U.S. Department of Commerce, Bureau of the Census.

U.S. Department of Commerce, 1969, Census of Puerto Rico--1965, population and agriculture: U.S. Department of Commerce, Bureau of the Census.

U.S. Department of Commerce, 1973, Census of Housing--1970: U.S. Department of Commerce, Bureau of the Census, p. 53.56-53.75.

U.S. Department of Commerce, 1978, Census of Puerto Rico--1975, population and agriculture: U.S. Department of Commerce, Bureau of the Census.

U.S. Department of Commerce, 1982, Statistical Abstract of the United States 1982-82: U.S. Department of Commerce, Bureau of the Census, National Data Book and Guide to Sources, 103d Edition, 1008 p.

U.S. Department of Commerce, 1987, Census of Puerto Rico--1985, population and agriculture: U.S. Department of Commerce, Bureau of the Census.

U.S. Geological Survey Water Resources Data Reports, 1989-1995, Water Resources Data Puerto Rico and the U.S. Virgin Islands.

U.S. War Department, 1900, Census of Porto Rico, 1899, 353 p.

VanSickle, J., and Beschta, R.L., 1983, Supply-based models of suspended sediment transport in streams: Water Resources Research, v. 19. p. 768-778.

Reproduced with permission of the copyright owner. Further reproduction prohibited without permission.

Waide, R.B., and Lugo, A.E., 1992, A research perspective on disturbance and recovery of a tropical montane forest: In Goldammer, J.G., ed., Tropical Forests in Transition, Berkhauser-Verlag, Basel, Switzerland, p. 173-190.

Walling, D.E., 1974, Suspended sediment and solute yields from a small catchment prior to urbanization: in Gregory, K.J. and Walling, D.E., eds., Fluvial Processes in Instrumented Watersheds, Institute of British Geographers Special Publication No. 6, p.169-192.

Walling, D.E., and Webb, B.W., 1982, Sediment availability and the prediction of storm-period sediment yields: IAHS Publication No. 137, p. 327-337.

Walling, D.E., 1983, The sediment delivery problem: Journal of Hydrology, v.65, p.209-237.

Walling, D.E. and Woodward, J.C., 1992. Use of radiometric fingerprints to derive information on suspended sediment sources. Erosion and Sediment Transport Monitoring Programmes in River Basins, Proceedings of the Oslo Symposium, August 1992. IAHS Publication Number 210: 153-164.

Walling, D.E. and Woodward, J.C., 1995, Tracing sources of suspended sediment in river basins– A case study of the River Culm, Devon, UK: Marine and Freshwater Research, v. 46, p. 327-336.

Walling, D.E., 1996, Suspended sediment transport by rivers– A geomorphological and hydrological perspective: Archives for Hydrobiology Special Issues, Advances in Limnology, Kausch, H., and Winfried, L., eds., v. 47, p. 1-27.

Walling, D.E., Owens, P.N., and Leeks, G.J.L., 1999, Fingerprinting sediment sources in the catchment of the River Ouse, Yyorkshire, UK: Hydrological Processes, v. 13, p. 955-975.

Walsh, R.P.D., 1985, The influence of climate, lithology and time on drainage density and relief development in the tropical volcanic terrain of the Windward Islands: In Environmental Change and Tropical Geomorphology, Douglas, I., and Spencer, T., eds, p. 93-122.

Wang, Y., Ren, M., and Syvitski, J., 1998, Sediment transport and terrigenous fluxes: In, the Sea, Brink, K.H., and Robinson, A.R., eds., John Wiley and Sons, v. 10, p. 253-292.

Ward, P.R.B., 1980, Sediment transport and reservoir siltation formula for Zimbabwe-Rhodesia: Civ. Engr. S. Afr., January 1980, no. 1, p. 1-15.

Webb, R.M.T, and Soler-Lopez, L.R., 1996, Sedimentation survey of Lago Caonillas: U.S. Geological Survey Water-Resources Investigation Report 96-4153, 27 p.

Webb, R.M.T, and Soler-Lopez, L.R., 1997, Sedimentation survey of Lago Loiza: U.S. Geological Survey Water-Resources Investigation Report 97-4108, 18 p.

Reproduced with permission of the copyright owner. Further reproduction prohibited without permission.

Webb, R.M.T, and Gomez-Gomez, F., 1998, Synoptic survey of water quality and bottom sediments, San Juan Bay estuary system, Puerto Rico, December 1994-July 1995: U.S. Geological Survey Water Resources Investigation 97-4144, 69 p.

Wiersum, K.F., 1985, Effects of various vegetation layers in an Acacia auruculiformis forest plantation on surface erosion in Java, Indonesia: In, Soil Erosion and Conservation, El-Swaify, S.A., Moldenhauer, W.C., and Lo, A., eds., Soil Conservation Society of America, Arkeny, Iowa, p. 79-89.

Williams, M.A.J., 1973, The efficacy of creep and slopewash in tropical and temperate Australia: Australian Geographical Studies, v. 11, p. 62-68.

Williams, G.P., 1989, Sediment concentration versus water discharge during single hydrologic events: Journal of Hydrology, v. 111, p.89-106.

Williams, M.A.J., Dunkerley, D.L., Deckker, P. De, Kershaw, A.P., and Stokes, T., 1993, Quaternary Environments: Arnold, p. 218-221.

Wolman, M.G., 1967, A cycle of sedimentation and erosion in urban river channels: Geografiska Annaler, v. 49A, p. 385-395.

Wood, P.A., 1977, Controls of suspended sediment concentration in the River Rother, West Sussex, England: Sedimentology, v. 24, p. 437-445.

Woodruff, J.F., and Hewlett, J.D., 1970, Predicting and mapping the average and hydrologic response for the eastern United States: Water Resources Research, v. 6, p. 1312-1326.

World Resources Institute, 1996, World Resources 1996-97, A Guide to the Global Environment: Oxford University Press, 400 p.

Wulder, M, 2000, Multivariate statistics--A practical guide: Canadian Forest Service, Pacific Forestry Center, accessed March 5, 2000 at *URL http://www.pfc.cfs.nrcan.gc.ca/landscape/inventory/wulder/mvstats/multicol.html.*

Yang, C.T., 1973, Incipient motion and sediment transport: Journal of the Hydraulics Division of the American Society of Civil Engineers v. 99 (HY10), p. 1679-1704.

Yang, C.T., 1984, Unit stream power equation for gravel: Journal of the Hydraulics Division of the American Society of Civil Engineers v. 110 (HY12), p. 1783-1797.

Younger, M.S., 1979, Handbook for linear regression: Duxbury Press Massachusetts, 569 p.

Reproduced with permission of the copyright owner. Further reproduction prohibited without permission.

Reproduced with permission of the copyright owner. Further reproduction prohibited without permission.

DISSERTATION

SUSPENDED-SEDIMENT CHARACTERISTICS IN FOUR HUMID TROPICAL WATERSHEDS OF CONTRASTING LAND USE, PUERTO RICO

Volume II
Chapter 13

Submitted by

Allen C Gellis

Department of Geosciences

In partial fulfillment of the requirements

For the Degree of Doctor of Philosophy

Colorado State University

Fort Collins, Colorado

Fall, 2003

Reproduced with permission of the copyright owner. Further reproduction prohibited without permission.

Table of Contents Volume II

Table of Contents.....xi

XIII. APPENDIX.....490

Reproduced with permission of the copyright owner. Further reproduction prohibited without permission.

APPENDIX

Refer to Table 4.3 for abbreviations

Reproduced with permission of the copyright owner. Further reproduction prohibited without permission.

Appendix 5.1. Relation of calculated quickflow to estimated quickflow. Estimated quickflow is calculated from rain falling on impervious basin Rio Icacos basin area = 1.26 sq.mi.

Start Date	Hour	End Date	Hour	Rainfall amount, in	Estimated volume of quickflow corresponding to impervious contributing area, ft3)	Calculated quickflow, ft3	Percent ratio: calculated quickflow/ estimated quickflow
5/23/1992	0.25	5/23/1992	15.25	0.92	2693203	1282186	48
6/1/1992	11.00	6/2/1992	3.00	3.52	10304438	2320200	23
7/8/1992	4.00	7/8/1992	9.25	0.48	1405140	369900	26
7/16/1992	22.75	7/17/1992	3.50	0.78	2283372	631777	28
7/24/1992	2.75	7/24/1992	7.00	0.16	468677	198900	42
7/26/1992	21.25	7/27/1992	3.00	0.13	380562	191340	50
8/5/1992	1.25	8/5/1992	9.75	1.58	4625291	1539000	33
8/14/1992	10.50	8/14/1992	22.50	0.54	1583723	614700	39
8/30/1992	23.50	8/31/1992	8.75	0.77	2254099	718920	32
9/4/1992	14.25	9/4/1992	20.00	0.47	1375881	213300	16
9/16/1992	2.00	9/16/1992	9.50	0.76	2224825	460800	21
9/18/1992	21.25	9/19/1992	4.25	0.17	497653	272475	55
9/23/1992	18.25	9/24/1992	2.00	0.39	1141684	308250	27
9/30/1992	13.00	9/30/1992	17.75	1.17	3425058	232200	7
10/22/1992	16.50	10/22/1992	23.50	0.61	1785716	655335	37
11/2/1992	21.25	11/3/1992	7.00	0.79	2312649	725400	31
11/3/1992	14.50	11/4/1992	12.50	5.09	14915073	4026249	27
11/12/1992	15.00	11/12/1992	20.50	0.68	1990633	405360	20
11/16/1992	8.50	11/16/1992	22.00	1.23	3600690	1628460	45
11/18/1992	2.00	11/18/1992	10.50	0.64	1873534	953691	51
11/20/1992	13.50	11/20/1992	22.75	0.54	1580799	1030320	65
11/22/1992	6.76	11/23/1992	7.25	2.94	8606563	3691476	43
12/6/1992	4.25	12/6/1992	14.00	1.64	4800957	1205820	25
12/25/1992	19.25	12/26/1992	9.75	1.37	4010524	2150594	54
12/26/1992	9.76	12/26/1992	20.75	1.91	5591300	2996772	54
12/29/1992	12.50	12/30/1992	16.00	4.81	14080832	7810560	55
1/22/1993	4.00	1/23/1993	4.50	2.52	7377061	3505500	48
2/20/1993	12.50	2/21/1993	17.50	4.03	11797464	4639950	39
4/30/1993	9.76	4/30/1993	18.75	1.64	4800934	2796813	58
5/1/1993	11.75	5/2/1993	5.25	4.98	14578451	4328772	30
5/2/1993	12.51	5/2/1993	23.25	0.92	2693208	1606286	60
5/8/1993	17.00	5/9/1993	7.75	1.03	3015230	1137510	38
5/9/1993	12.75	5/9/1993	19.75	1.01	2956669	1336590	45
7/7/1993	12.00	7/7/1993	20.50	1.46	4288608	1625670	38
7/22/1993	16.01	7/22/1993	23.00	0.79	2312649	1189743	51
9/15/1993	19.00	9/16/1993	10.75	2.12	6212940	3641498	59
9/16/1993	11.00	9/16/1993	23.00	0.71	2088210	2698740	129
10/7/1993	1.50	10/7/1993	12.25	1.68	4918033	1439712	29
10/22/1993	16.50	10/22/1993	22.75	0.58	1697896	1013838	60
12/19/1993	20.25	12/20/1993	1.00	0.46	1348065	870882	65
2/19/1994	5.50	2/19/1994	20.00	3.34	9777527	6341562	65
2/19/1994	20.01	2/20/1994	19.75	6.11	17886416	9677284	54
6/17/1994	9.00	6/18/1994	2.50	1.07	3132320	2066111	66
7/17/1994	23.00	7/18/1994	19.00	2.40	7011127	2544940	36
8/18/1994	19.75	8/19/1994	7.25	1.73	5049781	2612138	52
8/23/1994	17.00	8/24/1994	2.00	1.21	3542158	1298856	37
9/7/1994	18.50	9/8/1994	5.75	1.18	3461668	1754910	51
9/20/1994	5.26	9/20/1994	22.75	2.12	6206090	3567650	57

Reproduced with permission of the copyright owner. Further reproduction prohibited without permission.

Reproduced with permission of the copyright owner. Further reproduction prohibited without permission.

Appendix 5.2. Summary of dependent and independent variables used in the statistical analysis for quickflow characteristics of the entire event at Rio Icacos near Naguabo.

(D indicates dependent variable; L indicates data was log transformed for final statistical operations; SQRT indicates data was transformed by the square root for final statistical operations)

Start Date	Start Time hour	Start Discharge ft3/s	End Date	End Time hour	DL Suspended-sediment load tons	DL Discharge-weighted sediment concentration mg/L	L 1-QUICK	3-BASE	SQRT 4-PKBS	L 7-MXTRP
5/23/1992	0.25	9.0	5/23/1992	15.25	45.0	1125	1.28E+006	9.0	96.8	0.4667
6/1/1992	11.00	15.0	6/2/1992	3.00	99.0	1367	2.32E+006	15.0	490	5.4222
7/8/1992	4.00	9.8	7/8/1992	9.25	3.9	338	3.70E+005	9.8	65.3	0.4904
7/16/1992	22.75	9.4	7/17/1992	3.50	5.8	294	6.32E+005	9.4	79.9	0.8956
7/24/1992	2.75	9.0	7/24/1992	7.00	1.6	262	1.99E+005	9.0	38.3	0.6500
7/26/1992	21.25	7.4	7/27/1992	3.00	0.9	153	1.91E+005	7.4	33.3	0.7467
8/5/1992	*1.25*	*12.0*	*8/5/1992*	*9.75*	*53.9*	*1123*	*1.54E+006*	*12.0*	*239*	*5.3333*
8/14/1992	10.50	12.0	8/14/1992	22.50	4.0	210	6.15E+005	12.0	54.0	0.5600
8/30/1992	23.50	9.4	8/31/1992	8.75	5.0	221	7.19E+005	9.4	72.2	0.5378
9/4/1992	14.25	8.4	9/4/1992	20.00	0.7	105	2.13E+005	8.4	22.6	0.3767
9/16/1992	2.00	6.0	9/16/1992	9.50	4.8	333	4.61E+005	6.0	57.7	0.7867
9/18/1992	21.25	6.9	9/19/1992	4.25	1.1	126	2.72E+005	6.9	29.3	0.2867
9/23/1992	18.25	7.9	9/24/1992	2.00	1.1	117	3.08E+005	7.9	35.9	0.6017
9/30/1992	13.00	5.6	9/30/1992	17.75	1.5	206	2.32E+005	5.6	37.5	0.6400
10/22/1992	16.50	2.9	10/22/1992	23.50	7.7	378	6.55E+005	2.9	102	1.1456
11/2/1992	21.25	4.8	11/3/1992	7.00	6.1	269	7.25E+005	4.8	77.7	0.7448
11/3/1992	14.50	4.8	11/4/1992	12.50	31.3	249	4.03E+006	4.8	165	1.4667
11/12/1992	15.00	3.6	11/12/1992	20.50	1.9	152	4.05E+005	3.6	66.8	0.7600
11/16/1992	8.50	5.6	11/16/1992	22.00	19.2	377	1.63E+006	5.6	168	0.5944
11/18/1992	2.00	9.8	11/18/1992	10.50	4.0	134	9.54E+005	9.8	54.0	0.2258
11/20/1992	13.50	7.9	11/20/1992	22.75	18.0	559	1.03E+006	7.9	154	1.4676
11/22/1992	6.76	20.0	11/23/1992	7.25	16.3	141	3.69E+006	7.9	173	0.8964
12/6/1992	4.25	9.8	12/6/1992	14.00	17.1	455	1.21E+006	9.8	133	0.5633
12/25/1992	19.25	10.0	12/26/1992	9.75	22.0	328	2.15E+006	10.0	166	1.4381
12/26/1992	9.76	20.0	12/26/1992	20.75	67.7	724	3.00E+006	12.8	330	2.7007
12/29/1992	12.50	8.4	12/30/1992	16.00	177	727	7.81E+006	8.4	399	1.5444
1/22/1993	4.00	11.0	1/23/1993	4.50	24.0	220	3.51E+006	11.0	178	0.2791
2/20/1993	12.50	9.0	2/21/1993	17.50	31.9	220	4.64E+006	9.0	151	1.2000
4/30/1993	9.76	27.0	4/30/1993	18.75	45.4	520	2.80E+006	12.3	278	2.0381
5/1/1993	11.75	16.0	5/2/1993	5.25	150	1106	4.33E+006	16.0	223	3.1333
5/2/1993	12.51	24.0	5/2/1993	23.25	18.9	377	1.61E+006	16.7	190	2.4531
5/8/1993	17.00	5.6	5/9/1993	7.75	8.3	235	1.14E+006	5.6	130	0.4413
5/9/1993	12.75	9.4	5/9/1993	19.75	14.2	340	1.34E+006	9.4	182	3.0433
7/7/1993	12.00	7.4	7/7/1993	20.50	27.6	543	1.63E+006	7.4	227	1.0886
7/22/1993	16.01	9.4	7/22/1993	23.00	15.4	415	1.19E+006	8.6	189	2.5282
9/15/1993	19.00	3.9	9/16/1993	10.75	47.6	419	3.64E+006	3.9	323	5.5778
9/16/1993	11.00	11.0	9/16/1993	23.00	44.7	531	2.70E+006	9.0	327	3.6222
10/7/1993	1.50	6.4	10/7/1993	12.25	19.5	434	1.44E+006	6.4	224	1.3630
10/22/1993	16.50	6.0	10/22/1993	22.75	13.7	433	1.01E+006	6.0	163	1.5737
12/19/1993	20.25	10.6	12/20/1993	1.00	11.5	422	8.71E+005	10.6	141	2.3450
2/19/1994	5.50	5.2	2/19/1994	20.00	404	2042	6.34E+006	5.2	865	12.8345
2/19/1994	20.01	14.1	2/20/1994	19.75	368	1218	9.68E+006	7.4	554	6.8604
6/17/1994	9.00	6.4	6/18/1994	2.50	13.0	202	2.07E+006	6.4	161	1.3509
7/17/1994	23.00	5.1	7/18/1994	19.00	15.3	192	2.54E+006	5.1	160	0.4191
8/18/1994	19.75	10.0	8/19/1994	7.25	45.8	561	2.61E+006	10.0	329	2.7459
8/23/1994	17.00	3.1	8/24/1994	2.00	8.3	205	1.30E+006	3.1	185	1.5534
9/7/1994	18.50	3.5	9/8/1994	5.75	17.0	311	1.75E+006	3.5	222	2.1330
9/20/1994	5.26	10.7	9/20/1994	22.75	28.3	255	3.57E+006	7.5	232	1.1798

Reproduced with permission of the copyright owner. Further reproduction prohibited without permission.

Appendix 5.2. Continued.

Start Date	Start Time hour	End Date	End Time hour	L 6-MXTMJPK	L 8-SMPKBS	L 10-RAIN	L 11-INT15	L 12-SFIVE	L 13-RRISE	L 14-RAINFOL
5/23/1992	0.25	5/23/1992	15.25	0.4667	96.8	0.92	0.34	0.0022	0.64	0.28
6/1/1992	11.00	6/2/1992	3.00	5.4222	523	3.52	1.13	0.0060	3.47	0.04
7/8/1992	4.00	7/8/1992	9.25	0.4904	65.3	0.48	0.08	0.0031	0.44	0.04
7/16/1992	22.75	7/17/1992	3.50	0.8956	79.9	0.78	0.29	0.0064	0.77	0.01
7/24/1992	2.75	7/24/1992	7.00	0.6500	38.3	0.16	0.14	0.0050	0.16	0.00
7/26/1992	21.25	7/27/1992	3.00	0.7467	33.3	0.13	0.09	0.0033	0.13	0.00
8/5/1992	1.25	8/5/1992	9.75	5.3333	239	1.58	0.74	0.0173	1.30	0.28
8/14/1992	10.50	8/14/1992	22.50	0.5600	77.0	0.54	0.34	0.0014	0.54	0.00
8/30/1992	23.50	8/31/1992	8.75	0.5378	72.2	0.77	0.13	0.0018	0.58	0.19
9/4/1992	14.25	9/4/1992	20.00	0.3767	22.6	0.47	0.19	0.0031	0.37	0.10
9/16/1992	2.00	9/16/1992	9.50	0.7867	57.7	0.76	0.50	0.0112	0.72	0.04
9/18/1992	21.25	9/19/1992	4.25	0.2867	29.3	0.17	0.16	0.0107	0.17	0.00
9/23/1992	18.25	9/24/1992	2.00	0.6017	35.9	0.39	0.29	0.0123	0.37	0.02
9/30/1992	13.00	9/30/1992	17.75	0.6400	37.5	1.17	0.47	0.0098	1.15	0.02
10/22/1992	16.50	10/22/1992	23.50	1.1456	102	0.61	0.21	0.0034	0.61	0.00
11/2/1992	21.25	11/3/1992	7.00	0.7448	77.7	0.79	0.25	0.0030	0.63	0.16
11/3/1992	14.50	11/4/1992	12.50	1.4667	203	5.09	0.58	0.0045	4.08	1.01
11/12/1992	15.00	11/12/1992	20.50	0.7600	66.8	0.68	0.32	0.0120	0.68	0.00
11/16/1992	8.50	11/16/1992	22.00	0.5944	168	1.23	0.34	0.0038	1.15	0.08
11/18/1992	2.00	11/18/1992	10.50	0.2258	54.0	0.64	0.11	0.0015	0.43	0.21
11/20/1992	13.50	11/20/1992	22.75	1.4676	154	0.54	0.25	0.0020	0.39	0.15
11/22/1992	6.76	11/23/1992	7.25	0.8964	173	2.94	0.19	0.0037	1.31	1.63
12/6/1992	4.25	12/6/1992	14.00	0.5633	133	1.64	0.32	0.0052	1.64	0.00
12/25/1992	19.25	12/26/1992	9.75	1.4381	205	1.37	0.35	0.0025	1.23	0.14
12/26/1992	9.76	12/26/1992	20.75	2.7007	330	1.91	0.45	0.0076	1.48	0.43
12/29/1992	12.50	12/30/1992	16.00	1.4091	716	4.81	0.55	0.0060	1.91	2.90
1/22/1993	4.00	1/23/1993	4.50	0.2791	262	2.52	0.16	0.0022	1.71	0.81
2/20/1993	12.50	2/21/1993	17.50	1.2000	331	4.03	0.36	0.0045	2.68	1.35
4/30/1993	9.76	4/30/1993	18.75	2.0381	387	1.64	0.28	0.0047	1.55	0.09
5/1/1993	11.75	5/2/1993	5.25	3.1333	423	4.98	0.58	0.0062	2.71	2.27
5/2/1993	12.51	5/2/1993	23.25	2.4531	190	0.92	0.27	0.0109	0.83	0.09
5/8/1993	17.00	5/9/1993	7.75	0.4413	130	1.03	0.26	0.0025	0.83	0.20
5/9/1993	12.75	5/9/1993	19.75	3.0433	182	1.01	0.34	0.0127	0.90	0.11
7/7/1993	12.00	7/7/1993	20.50	1.0886	227	1.46	0.42	0.0024	1.42	0.04
7/22/1993	16.01	7/22/1993	23.00	2.5282	189	0.79	0.50	0.0099	0.78	0.01
9/15/1993	19.00	9/16/1993	10.75	5.5778	528	2.12	0.48	0.0033	1.07	1.05
9/16/1993	11.00	9/16/1993	23.00	3.6222	327	0.71	0.18	0.0039	0.55	0.16
10/7/1993	1.50	10/7/1993	12.25	1.3630	224	1.68	0.51	0.0067	1.49	0.19
10/22/1993	16.50	10/22/1993	22.75	1.5737	163	0.58	0.31	0.0038	0.58	0.01
12/19/1993	20.25	12/20/1993	1.00	2.3450	141	0.42	0.16	0.0071	0.45	-0.02
2/19/1994	5.50	2/19/1994	20.00	12.8345	1405	3.34	0.58	0.0047	3.08	0.26
2/19/1994	20.01	2/20/1994	19.75	4.1599	1264	6.11	0.63	0.0170	4.90	1.21
6/17/1994	9.00	6/18/1994	2.50	1.3509	161	1.07	0.21	0.0031	0.53	0.54
7/17/1994	23.00	7/18/1994	19.00	0.4191	160	2.40	0.51	0.0047	2.05	0.34
8/18/1994	19.75	8/19/1994	7.25	2.7459	329	1.73	0.33	0.0049	1.59	0.14
8/23/1994	17.00	8/24/1994	2.00	1.5534	185	1.21	0.33	0.0067	1.15	0.06
9/7/1994	18.50	9/8/1994	5.75	2.1330	222	1.18	0.39	0.0059	0.94	0.24
9/20/1994	5.26	9/20/1994	22.75	1.1798	232	2.12	0.37	0.0036	1.47	0.65

Reproduced with permission of the copyright owner. Further reproduction prohibited without permission.

Appendix 5.2. Continued.

Start Date	Start Time hour	End Date	End Time hour	16-HYSTER 1=normal 0=reverse	17-RNBTWTI	SQRT 18-PPTBTW	SQRT 19-INTBET	L 20-LSPKBTI	L 22-SMLSPKBS	L 24-QULST
5/23/1992	0.25	5/23/1992	15.25	1	36672	0.12	0.05	2.74	0.65	1.81E+004
6/1/1992	11.00	6/2/1992	3.00	0	41323	0.02	0.01	0.88	28.7	1.67E+004
7/8/1992	4.00	7/8/1992	9.25	1	28005	0.92	0.11	0.10	0.19	7.90E+002
7/16/1992	22.75	7/17/1992	3.50	1	32283	0.61	0.06	0.31	0.39	1.80E+003
7/24/1992	2.75	7/24/1992	7.00	0	36864	1.26	0.20	0.10	0.27	8.75E+002
7/26/1992	21.25	7/27/1992	3.00	0	28704	0.02	0.02	0.31	0.83	4.27E+003
8/5/1992	1.25	8/5/1992	9.75	1	30803	1.83	0.24	0.14	1.12	8.93E+002
8/14/1992	10.50	8/14/1992	22.50	0	38034	0.52	0.15	1.78	3.18	1.76E+004
8/30/1992	23.50	8/31/1992	8.75	0	20798	3.19	0.29	0.13	0.19	1.60E+003
9/4/1992	14.25	9/4/1992	20.00	1	22894	0.71	0.24	0.55	0.22	7.08E+003
9/16/1992	2.00	9/16/1992	9.50	1	22280	0.86	0.24	0.16	0.37	2.78E+003
9/18/1992	21.25	9/19/1992	4.25	1	46507	0.38	0.11	0.71	1.48	1.07E+004
9/23/1992	18.25	9/24/1992	2.00	0	33411	0.07	0.03	1.40	4.22	2.18E+004
9/30/1992	13.00	9/30/1992	17.75	1	22825	0.52	0.14	0.20	0.24	1.99E+003
10/22/1992	16.50	10/22/1992	23.50	1	14646	2.71	0.14	0.07	0.19	4.41E+002
11/2/1992	21.25	11/3/1992	7.00	1	11911	2.01	0.25	0.36	0.30	2.50E+003
11/3/1992	14.50	11/4/1992	12.50	1	20362	0.00	0.00	2.12	27.1	9.67E+004
11/12/1992	15.00	11/12/1992	20.50	0	18580	0.00	0.00	2.17	1.36	3.17E+004
11/16/1992	8.50	11/16/1992	22.00	1	26854	1.57	0.32	0.65	2.00	4.83E+003
11/18/1992	2.00	11/18/1992	10.50	1	41390	0.40	0.06	3.71	1.93	5.82E+004
11/20/1992	13.50	11/20/1992	22.75	1	30803	0.17	0.07	0.34	4.66	6.86E+003
11/22/1992	6.76	11/23/1992	7.25	1	0	0.02	0.01	3.07	25922	2.65E+008
12/6/1992	4.25	12/6/1992	14.00	1	48428	0.63	0.20	0.70	3.14	1.27E+004
12/25/1992	19.25	12/26/1992	9.75	1	50170	0.83	0.09	0.84	8.84	3.00E+004
12/26/1992	9.76	12/26/1992	20.75	1	0	0.12	0.10	5.92	49465	3.23E+008
12/29/1992	12.50	12/30/1992	16.00	1	31716	0.20	0.05	0.95	48.5	3.80E+004
1/22/1993	4.00	1/23/1993	4.50	1	39340	1.14	0.11	0.09	1.31	9.97E+002
2/20/1993	12.50	2/21/1993	17.50	1	31898	0.58	0.10	0.08	1.72	5.63E+002
4/30/1993	9.76	4/30/1993	18.75	1	0	0.04	0.02	2.85	57991	2.52E+008
5/1/1993	11.75	5/2/1993	5.25	0	58977	0.01	0.01	1.32	51.22	6.71E+004
5/2/1993	12.51	5/2/1993	23.25	1	0	0.00	0.00	8.23	28540	1.43E+008
5/8/1993	17.00	5/9/1993	7.75	1	25686	1.15	0.35	0.56	1.09	8.33E+003
5/9/1993	12.75	5/9/1993	19.75	1	39947	0.00	0.00	4.10	36.3	2.28E+005
7/7/1993	12.00	7/7/1993	20.50	1	15161	0.09	0.04	0.46	2.40	5.56E+003
7/22/1993	16.01	7/22/1993	23.00	1	0	0.00	0.00	3.81	28348	8.34E+007
9/15/1993	19.00	9/16/1993	10.75	1	35792	3.96	0.61	0.61	2.44	3.25E+003
9/16/1993	11.00	9/16/1993	23.00	1	0	0.00	0.00	9.95	1310	1.46E+007
10/7/1993	1.50	10/7/1993	12.25	1	20956	0.70	0.07	0.31	2.52	2.51E+003
10/22/1993	16.50	10/22/1993	22.75	0	24321	1.36	0.67	0.30	2.87	8.62E+003
12/19/1993	20.25	12/20/1993	1.00	1	18053	0.68	0.09	0.08	0.43	6.23E+002
2/19/1994	5.50	2/19/1994	20.00	1	15052	2.15	0.24	0.10	4.01	9.00E+002
2/19/1994	20.01	2/20/1994	19.75	1	0	0.00	0.00	73.61	189526	9.51E+008
6/17/1994	9.00	6/18/1994	2.50	1	18687	1.51	0.14	0.17	1.26	4.30E+003
7/17/1994	23.00	7/18/1994	19.00	1	18682	1.09	0.15	0.09	0.59	1.03E+003
8/18/1994	19.75	8/19/1994	7.25	1	35880	0.00	0.00	2.57	82.2	1.12E+005
8/23/1994	17.00	8/24/1994	2.00	1	15541	0.41	0.08	2.44	1.75	2.47E+004
9/7/1994	18.50	9/8/1994	5.75	1	18561	0.04	0.02	1.93	9.66	5.38E+004
9/20/1994	5.26	9/20/1994	22.75	1	0	0.00	0.00	2.93	34856	1.88E+008

Reproduced with permission of the copyright owner. Further reproduction prohibited without permission.

Appendix 5.2. Continued.

Start Date	Start Time hour	End Date	End Time hour	L 26-PPTLSTI	L 27-INTLST	L 28-LS75OTI	29-SUM3PPTI	30-QU3EVT
5/23/1992	0.25	5/23/1992	15.25	0.0461	0.0080	0.0002	-5.24	11.9
6/1/1992	11.00	6/2/1992	3.00	0.0142	0.0071	0.0002	-5.05	12.8
7/8/1992	4.00	7/8/1992	9.25	0.0022	0.0008	0.0000	-8.81	8.4
7/16/1992	22.75	7/17/1992	3.50	0.0023	0.0004	0.0000	-9.11	8.3
7/24/1992	2.75	7/24/1992	7.00	0.0013	0.0008	0.0000	-8.15	10.0
7/26/1992	21.25	7/27/1992	3.00	0.0035	0.0015	0.0000	-7.12	10.8
8/5/1992	1.25	8/5/1992	9.75	0.0006	0.0004	0.0000	-9.32	8.6
8/14/1992	10.50	8/14/1992	22.50	0.0227	0.0181	0.0012	-6.11	11.9
8/30/1992	23.50	8/31/1992	8.75	0.0014	0.0009	0.0000	-8.54	9.6
9/4/1992	14.25	9/4/1992	20.00	0.0076	0.0013	0.0000	-8.07	9.8
9/16/1992	2.00	9/16/1992	9.50	0.0021	0.0005	0.0000	-7.89	9.7
9/18/1992	21.25	9/19/1992	4.25	0.0167	0.0071	0.0000	-6.50	11.2
9/23/1992	18.25	9/24/1992	2.00	0.0200	0.0082	0.0003	-4.76	13.0
9/30/1992	13.00	9/30/1992	17.75	0.0025	0.0019	0.0001	-7.40	10.5
10/22/1992	16.50	10/22/1992	23.50	0.0022	0.0009	0.0000	-9.52	7.7
11/2/1992	21.25	11/3/1992	7.00	0.0023	0.0008	0.0000	-8.85	8.4
11/3/1992	14.50	11/4/1992	12.50	0.1053	0.0333	0.0004	-6.48	10.8
11/12/1992	15.00	11/12/1992	20.50	0.0339	0.0063	0.0001	-6.56	11.3
11/16/1992	8.50	11/16/1992	22.00	0.0081	0.0038	0.0001	-6.65	10.9
11/18/1992	2.00	11/18/1992	10.50	0.0439	0.0121	0.0001	-5.66	12.2
11/20/1992	13.50	11/20/1992	22.75	0.0088	0.0018	0.0000	-5.64	12.7
11/22/1992	6.76	11/23/1992	7.25	288	42.0	0.2939	-1.72	16.4
12/6/1992	4.25	12/6/1992	14.00	0.0139	0.0042	0.0000	-6.40	12.1
12/25/1992	19.25	12/26/1992	9.75	0.0374	0.0082	0.0001	-5.73	12.1
12/26/1992	9.76	12/26/1992	20.75	205	52.5	0.3821	-1.26	16.9
12/29/1992	12.50	12/30/1992	16.00	0.0292	0.0108	0.0001	-5.04	13.1
1/22/1993	4.00	1/23/1993	4.50	0.0008	0.0003	0.0000	-9.28	8.6
2/20/1993	12.50	2/21/1993	17.50	0.0018	0.0006	0.0000	-8.11	9.5
4/30/1993	9.76	4/30/1993	18.75	458	73.5	0.7387	-2.99	14.5
5/1/1993	11.75	5/2/1993	5.25	0.0909	0.0097	0.0003	-2.99	14.9
5/2/1993	12.51	5/2/1993	23.25	84.0	28.5	0.4200	0.12	18.2
5/8/1993	17.00	5/9/1993	7.75	0.0067	0.0018	0.0000	-6.77	11.8
5/9/1993	12.75	5/9/1993	19.75	0.2060	0.0520	0.0005	-5.16	13.2
7/7/1993	12.00	7/7/1993	20.50	0.0069	0.0015	0.0000	-7.18	10.3
7/22/1993	16.01	7/22/1993	23.00	117	37.5	0.5583	-1.40	16.2
9/15/1993	19.00	9/16/1993	10.75	0.0047	0.0022	0.0000	-7.75	10.0
9/16/1993	11.00	9/16/1993	23.00	8.4894	1.9200	0.0131	-3.75	14.3
10/7/1993	1.50	10/7/1993	12.25	0.0032	0.0015	0.0000	-7.70	11.0
10/22/1993	16.50	10/22/1993	22.75	0.0136	0.0023	0.0000	-6.30	11.3
12/19/1993	20.25	12/20/1993	1.00	0.0004	0.0003	0.0000	-8.89	9.3
2/19/1994	5.50	2/19/1994	20.00	0.0017	0.0004	0.0000	-8.54	9.0
2/19/1994	20.01	2/20/1994	19.75	501	87.0	0.7000	-2.89	15.1
6/17/1994	9.00	6/18/1994	2.50	0.0069	0.0016	0.0000	-7.28	10.5
7/17/1994	23.00	7/18/1994	19.00	0.0012	0.0004	0.0000	-8.29	9.9
8/18/1994	19.75	8/19/1994	7.25	0.2575	0.0850	0.0006	-5.81	11.9
8/23/1994	17.00	8/24/1994	2.00	0.0163	0.0031	0.0000	-6.34	11.5
9/7/1994	18.50	9/8/1994	5.75	0.0500	0.0130	0.0001	-6.54	11.3
9/20/1994	5.26	9/20/1994	22.75	186	66.8	0.3500	-2.79	15.3

**to eliminate zero values a value of 0.0002 was added to the precipitation between events and a value of 5000 was added to the runoff between events.

Reproduced with permission of the copyright owner. Further reproduction prohibited without permission.

Appendix 5.3. Pearson correlation matrix for the dependent and independent variables using quickflow characteristics at Rio Icacos for the entire event.

	SED	QU_SEDCONC	BASE	QUICK
SED	1.000			
QU_SEDCONC	0.830	1.000		
BASE	0.244	0.321	1.000	
QUICK	0.923	0.551	0.144	1.000
PKBS	0.919	0.767	0.125	0.846
LSPKBTI	0.282	0.134	0.205	0.330
RNBTWTI	-0.252	-0.101	-0.029	-0.307
QULST	0.337	0.141	0.301	0.408
QU3EVT	0.313	0.163	0.436	0.356
MXTMJPK	0.705	0.719	0.168	0.558
MXTRP	0.720	0.729	0.162	0.574
SUMPKBS	0.960	0.733	0.156	0.931
SMLSPKBSTI	0.507	0.289	0.359	0.560
TOTRAIN	0.813	0.485	0.108	0.882
INT15	0.611	0.571	0.021	0.520
SFIVE	0.083	0.183	0.051	-0.003
RRISE	0.789	0.523	0.107	0.819
RFALL	0.615	0.287	0.138	0.722
LSTPPTI	0.344	0.149	0.288	0.411
LST3PPTI	0.324	0.180	0.426	0.360
LSTINT	0.328	0.141	0.302	0.394
LST75OTI	0.303	0.168	0.341	0.338
PPTBTW	-0.127	-0.055	-0.323	-0.152
INTBET	-0.175	-0.066	-0.299	-0.217
HYSTER	0.278	0.099	-0.202	0.346

	PKBS	LSPKBTI	RNBTWTI	QULST	QU3EVT
PKBS	1.000				
LSPKBTI	0.286	1.000			
RNBTWTI	-0.336	-0.494	1.000		
QULST	0.354	0.847	-0.799	1.000	
QU3EVT	0.304	0.805	-0.588	0.899	1.000
MXTMJPK	0.804	0.243	-0.307	0.302	0.274
MXTRP	0.817	0.273	-0.323	0.324	0.286
SUMPKBS	0.959	0.280	-0.298	0.349	0.308
SMLSPKBSTI	0.529	0.762	-0.778	0.963	0.880
TOTRAIN	0.720	0.228	-0.177	0.273	0.233
INT15	0.588	0.213	-0.051	0.151	0.203
SFIVE	0.169	0.234	-0.206	0.248	0.239
RRISE	0.724	0.222	-0.180	0.254	0.197
RFALL	0.510	0.199	-0.206	0.254	0.223
LSTPPTI	0.352	0.829	-0.795	0.994	0.887
LST3PPTI	0.304	0.821	-0.607	0.913	0.990
LSTINT	0.345	0.815	-0.801	0.989	0.884
LST75OTI	0.315	0.809	-0.782	0.971	0.885

Reproduced with permission of the copyright owner. Further reproduction prohibited without permission.

Appendix 5.3. Continued.

PPTBTW	-0.122	-0.704	0.333	-0.651	-0.696
INTBET	-0.173	-0.586	0.346	-0.564	-0.545

	MXTMJPK	MXTRP	SUMPKBS	SMLSPKBSTI	TOTRAIN
MXTMJPK	1.000				
MXTRP	0.997	1.000			
SUMPKBS	0.757	0.772	1.000		
SMLSPKBSTI	0.454	0.475	0.533	1.000	
TOTRAIN	0.448	0.465	0.807	0.410	1.000
INT15	0.569	0.575	0.593	0.272	0.686
SFIVE	0.394	0.411	0.119	0.283	0.106
RRISE	0.474	0.491	0.791	0.395	0.968
RFALL	0.307	0.316	0.583	0.328	0.713
LSTPPTI	0.298	0.319	0.352	0.962	0.275
LST3PPTI	0.282	0.294	0.309	0.891	0.237
LSTINT	0.299	0.320	0.340	0.964	0.258
LST75OTI	0.303	0.324	0.307	0.946	0.227
PPTBTW	-0.138	-0.150	-0.115	-0.616	-0.127
INTBET	-0.189	-0.201	-0.175	-0.557	-0.182
HYSTER	0.069	0.074	0.256	0.168	0.296

Reproduced with permission of the copyright owner. Further reproduction prohibited without permission.

Appendix 5.3. Continued.

	INTI5	SFIVE	RRISE	RFALL	LSTPPTI
INTI5	1.000				
SFIVE	0.437	1.000			
RRISE	0.746	0.188	1.000		
RFALL	0.342	-0.104	0.592	1.000	
LSTPPTI	0.145	0.222	0.258	0.239	1.000
LST3PPTI	0.208	0.232	0.205	0.224	0.909
LSTINT	0.144	0.234	0.245	0.218	0.994
LST75OTI	0.174	0.255	0.226	0.173	0.976
PPTBTW	-0.156	-0.316	-0.151	-0.050	-0.640
INTBET	-0.087	-0.293	-0.198	-0.090	-0.561
HYSTER	0.080	0.034	0.271	0.399	0.163

	LST3PPTI	LSTINT	LST75OTI	PPTBTW	INTBET
LST3PPTI	1.000				
LSTINT	0.902	1.000			
LST75OTI	0.908	0.986	1.000		
PPTBTW	-0.707	-0.622	-0.637	1.000	
INTBET	-0.562	-0.553	-0.557	0.880	1.000
HYSTER	-0.008	0.152	0.099	0.052	-0.037

	HYSTER
HYSTE R	1.000

Reproduced with permission of the copyright owner. Further reproduction prohibited without permission.

Appendix 5.4. Results of principal component analysis on the independent variables using quickflow characteristics for the entire event at Rio Icacos.

Component loadings

	1	2	3	4	5
BASE	0.345	-0.157	-0.192	-0.539	0.459
QUICK	0.686	0.609	0.267	-0.128	0.068
PKBS	0.666	0.643	-0.071	0.105	0.166
LSPKBTI	0.785	-0.355	0.005	-0.069	-0.123
RNBTWTI	-0.698	0.245	-0.212	-0.489	-0.030
QULST	0.904	-0.378	0.120	0.104	0.025
QU3EVT	0.846	-0.397	-0.016	-0.120	0.106
MXTMJPK	0.584	0.506	-0.459	0.268	0.220
MXTRP	0.605	0.504	-0.451	0.271	0.203
SMPKBS	0.673	0.678	0.012	0.004	0.157
SMLSPKBS	0.959	-0.194	0.062	0.084	0.083
RAIN	0.579	0.679	0.203	-0.267	-0.165
INT15	0.456	0.580	-0.326	-0.092	-0.285
SFIVE	0.330	0.004	-0.632	0.235	-0.461
RRISE	0.568	0.676	0.091	-0.234	-0.221
RFOL	0.454	0.498	0.462	-0.211	0.011
PPTLSTI	0.899	-0.376	0.136	0.113	0.030
SUM3PPTI	0.860	-0.402	-0.008	-0.108	0.095
INTLST	0.892	-0.385	0.120	0.127	0.046
LGLS75OTI	0.879	-0.409	0.052	0.105	0.054
PPTBTW	-0.637	0.435	0.216	0.354	0.320
INTBET	-0.595	0.322	0.180	0.320	0.343
HYSTER	0.205	0.252	0.539	0.335	-0.405

	6
BASE	-0.177
QUICK	-0.040
PKBS	-0.112
LSPKBTI	0.085
RNBTWTI	0.013
QULST	0.063
QU3EVT	0.136
MXTMJPK	-0.188
MXTRP	-0.177
SUMPKBS	-0.081
SMLSPKBSTI	0.022
RAIN	0.154
INT15	0.386
SFIVE	0.068
RRISE	0.175
RFOL	-0.080
PPTLSTI	0.061
SUM3PPTI	0.129

	6
INTLST	0.070
LS75OTI	0.097
PPTBTW	0.223
INTBET	0.447
HYSTER	-0.357

Reproduced with permission of the copyright owner. Further reproduction prohibited without permission.

Appendix 5.5. Results of principal component analysis on the independent variables using quickflow characteristics for the entire event (without the variable-QUICK) at Rio Icacos.

Component loadings

	1	2	3	4	5
BASE	0.355	-0.133	-0.256	-0.495	0.488
PKBS	0.620	0.686	-0.021	0.100	0.167
LSPKBTI	0.806	-0.303	-0.003	-0.074	-0.120
RNBTWTI	-0.714	0.196	-0.269	-0.460	-0.014
QULST	0.926	-0.321	0.129	0.092	0.025
QU3EVT	0.870	-0.342	-0.036	-0.110	0.113
MXTMJPK	0.559	0.576	-0.391	0.306	0.197
MXTRP	0.579	0.575	-0.382	0.307	0.181
SUMPKBS	0.622	0.710	0.049	-0.007	0.166
SMLSPKBSTI	0.968	-0.134	0.076	0.077	0.084
TOTRAIN	0.526	0.697	0.229	-0.325	-0.125
INT15	0.425	0.637	-0.268	-0.108	-0.272
SFIVE	0.345	0.078	-0.572	0.263	-0.492
RRISE	0.518	0.704	0.126	-0.286	-0.186
RFALL	0.410	0.498	0.480	-0.285	0.058
LSTPPTI	0.921	-0.320	0.145	0.099	0.030
LST3PPTI	0.884	-0.346	-0.026	-0.100	0.102
LSTINT	0.915	-0.329	0.130	0.115	0.044
LST75OTI	0.905	-0.347	0.062	0.100	0.052
PPTBTW	-0.666	0.385	0.258	0.338	0.314
INTBET	-0.615	0.279	0.217	0.308	0.340
HYSTER	0.183	0.248	0.609	0.236	-0.392

	6		6
BASE	-0.204	LSTPPTI	0.061
PKBS	-0.111	LST3PPTI	0.127
LSPKBTI	0.091	LSTINT	0.069
RNBTWTI	0.014	LST75OTI	0.095
QULST	0.062	PPTBTW	0.214
QU3EVT	0.133	INTBET	0.437
MXTMJPK	-0.187	HYSTER	-0.372
MXTRP	-0.176		
SUMPKBS	-0.082		
SMLSPKBSTI	0.020		
TOTRAIN	0.144		
INT15	0.380		
SFIVE	0.067		
RRISE	0.167		
RFALL	-0.101		

Reproduced with permission of the copyright owner. Further reproduction prohibited without permission.

Appendix 5.6. Results of principal component analysis on the independent variables using quickflow characteristics after varimax rotation for the entire event at Rio Icacos.

Rotated Loading Matrix (VARIMAX, Gamma = 1.0000)

	1	2	3	4	5
BASE	0.251	0.093	-0.336	-0.600	0.173
QUICK	0.259	0.856	-0.135	0.100	0.326
PKBS	0.204	0.654	0.019	0.056	0.663
LSPKBTI	0.806	0.151	0.146	-0.041	-0.006
RNBTWTI	-0.796	-0.008	0.010	-0.359	-0.243
QULST	0.968	0.134	0.017	0.047	0.107
QU3EVT	0.897	0.141	0.030	-0.223	0.057
MXTMJPK	0.164	0.317	0.196	-0.049	0.891
MXTRP	0.184	0.331	0.209	-0.039	0.883
SUMPKBS	0.195	0.753	-0.028	0.033	0.582
SMLSPKBSTI	0.904	0.265	0.013	0.012	0.259
TOTRAIN	0.121	0.957	0.104	0.043	0.122
INT15	0.050	0.661	0.612	-0.142	0.230
SFIVE	0.171	-0.064	0.775	0.049	0.301
RRISE	0.100	0.914	0.221	0.029	0.154
RAINFOL	0.134	0.764	-0.279	0.176	0.071
LSTPPTI	0.968	0.135	0.005	0.058	0.105
LST3PPTI	0.911	0.141	0.032	-0.204	0.059
LSTINT	0.970	0.114	0.011	0.046	0.115
LST75OTI	0.963	0.082	0.050	-0.016	0.117
PPTBTW	-0.572	-0.033	-0.194	0.113	0.051
INTBET	-0.447	-0.056	-0.100	-0.031	-0.060
HYSTER	0.068	0.296	-0.120	0.827	0.027

	6		6
BASE	0.372	RAINFOL	0.050
QUICK	0.033	LSTPPTI	0.131
PKBS	-0.012	LST3PPTI	0.205
LSPKBTI	0.270	LSTINT	0.116
RNBTWTI	0.104	LST75OTI	0.124
QULST	0.141	PPTBTW	-0.733
QU3EVT	0.201	INTBET	-0.832
MXTMJPK	0.033	HYSTER	0.088
MXTRP	0.033		
SUMPKBS	-0.001		
SMLSPKBSTI	0.145		
TOTRAIN	0.044		
INT15	-0.039		
SFIVE	0.229		
RRISE	0.058		

Reproduced with permission of the copyright owner. Further reproduction prohibited without permission.

Appendix 5.7. Results of principal component analysis on the independent variables (without the variable QUICK) after varimax rotation for the entire event at Rio Icacos.

Rotated Loading Matrix (VARIMAX, Gamma = 1.0000)

	1	2	3	4	5
BASE	0.248	0.062	-0.412	-0.536	0.199
PKBS	0.214	0.581	-0.026	0.093	0.716
LSPKBTI	0.807	0.153	0.136	-0.035	0.004
RNBTWTI	-0.796	0.036	-0.026	-0.358	-0.239
QULST	0.969	0.107	0.014	0.060	0.118
QU3EVT	0.897	0.130	0.000	-0.206	0.074
MXTMJPK	0.166	0.263	0.173	-0.037	0.914
MXTRP	0.186	0.277	0.186	-0.028	0.907
SUMPKBS	0.206	0.676	-0.083	0.077	0.644
SMLSPKBSTI	0.906	0.223	-0.003	0.034	0.281
TOTRAIN	0.135	0.942	0.001	0.087	0.204
INT15	0.058	0.720	0.510	-0.155	0.284
SFIVE	0.163	-0.001	0.778	-0.001	0.287
RRISE	0.113	0.914	0.118	0.063	0.231
RAINFOL	0.145	0.713	-0.360	0.246	0.142
LSTPPTI	0.968	0.106	0.004	0.072	0.116
LST3PPTI	0.911	0.130	0.004	-0.188	0.075
LSTINT	0.970	0.086	0.010	0.058	0.125
LST75OTI	0.962	0.065	0.043	-0.008	0.126
PPTBTW	-0.569	-0.051	-0.191	0.095	0.052
INTBET	-0.443	-0.045	-0.114	-0.062	-0.058
HYSTER	0.069	0.246	-0.092	0.857	0.045

	6		6
BASE	0.415	LSTPPTI	0.135
PKBS	-0.012	LST3PPTI	0.222
LSPKBTI	0.274	LSTINT	0.121
RNBTWTI	0.114	LST75OTI	0.133
QULST	0.146	PPTBTW	-0.737
QU3EVT	0.219	INTBET	-0.829
MXTMJPK	0.040	HYSTER	0.058
MXTRP	0.040		
SUMPKBS	0.001		
SMLSPKBSTI	0.153		
TOTRAIN	0.048		
INT15	-0.026		
SFIVE	0.234		
RRISE	0.063		
RAINFOL	0.052		

Reproduced with permission of the copyright owner. Further reproduction prohibited without permission.

Appendix 5.8. Summary of dependent and independent variables used in the statistical analysis for runoff characteristics of the entire event at Rio Icacos near Naguabo.

(D indicates dependent variable; L indicates log transformed; SQRT indicates square root)

Start Date	Start Time hour	Start Discharge ft3/s	End Date	End Time hour	DL Suspended-sediment load tons	DL Discharge-weighted sediment concentration mg/L	DL Time-weighted sediment concentration mg/L	L 2-RUN	3-BASE	SQRT 5-PK
5/23/1992	0.25	9.0	5/23/1992	15.25	45.0	758	85.9	1.90E+006	9.0	107
6/1/1992	11.00	15.0	6/2/1992	3.00	99.0	996	266	3.18E+006	15.0	505
7/8/1992	4.00	9.8	7/8/1992	9.25	3.9	217	147	5.76E+005	9.8	76.0
7/16/1992	22.75	9.4	7/17/1992	3.50	5.8	228	168	8.12E+005	9.4	90.0
7/24/1992	2.75	9.0	7/24/1992	7.00	1.6	145	105	3.60E+005	9.0	48.0
7/26/1992	21.25	7.4	7/27/1992	3.00	0.9	79.4	49.0	3.69E+005	7.4	41.0
8/5/1992	1.25	12.0	8/5/1992	9.75	53.9	865	341	2.00E+006	12.0	252
8/14/1992	10.50	12.0	8/14/1992	22.50	4.0	114	85.4	1.13E+006	12.0	66.0
8/30/1992	23.50	9.4	8/31/1992	8.75	5.0	150	91.9	1.06E+006	9.4	82.0
9/4/1992	14.25	8.4	9/4/1992	20.00	0.7	58.0	45.3	3.87E+005	8.4	31.0
9/16/1992	2.00	6.0	9/16/1992	9.50	4.8	210	146	7.31E+005	6.0	65.0
9/18/1992	21.25	6.9	9/19/1992	4.25	1.1	70.8	60.2	4.85E+005	6.9	37.0
9/23/1992	18.25	7.9	9/24/1992	2.00	1.1	65.0	41.9	5.55E+005	7.9	44.0
9/30/1992	13.00	5.6	9/30/1992	17.75	1.5	131	90.1	3.64E+005	5.6	44.0
10/22/1992	16.50	2.9	10/22/1992	23.50	7.7	323	163	7.67E+005	2.9	106
11/2/1992	21.25	4.8	11/3/1992	7.00	6.1	208	111	9.40E+005	4.8	83.0
11/3/1992	14.50	4.8	11/4/1992	12.50	31.3	223	93.2	4.50E+006	4.8	171
11/12/1992	15.00	3.6	11/12/1992	20.50	1.9	116	61.9	5.34E+005	3.6	72.0
11/16/1992	8.50	5.6	11/16/1992	22.00	19.2	308	137	1.99E+006	5.6	175
11/18/1992	2.00	9.8	11/18/1992	10.50	4.0	101	83.3	1.26E+006	9.8	64.0
11/20/1992	13.50	7.9	11/20/1992	22.75	18.0	434	182	1.33E+006	7.9	162
11/22/1992	6.76	20.0	11/23/1992	7.25	16.3	114	56.0	4.57E+006	7.9	181
12/6/1992	4.25	9.8	12/6/1992	14.00	17.1	338	196	1.62E+006	9.8	145
12/25/1992	19.25	10.0	12/26/1992	9.75	22.0	257	135	2.75E+006	10.0	177
12/26/1992	9.76	20.0	12/26/1992	20.75	67.7	612	242	3.55E+006	12.8	343
12/29/1992	12.50	8.4	12/30/1992	16.00	177	613	330	9.27E+006	8.4	410
1/22/1993	4.00	11.0	1/23/1993	4.50	24.0	165	81.5	4.65E+006	11.0	191
2/20/1993	12.50	9.0	2/21/1993	17.50	31.9	172	111	5.94E+006	9.0	162
4/30/1993	9.76	27.0	4/30/1993	18.75	45.4	419	295	3.47E+006	12.3	292
5/1/1993	11.75	16.0	5/2/1993	5.25	150	895	626	5.35E+006	16.0	239
5/2/1993	12.51	24.0	5/2/1993	23.25	18.9	268	158	2.26E+006	16.7	207
5/8/1993	17.00	5.6	5/9/1993	7.75	8.3	167	62.0	1.60E+006	5.6	138
5/9/1993	12.75	9.4	5/9/1993	19.75	14.2	274	136	1.66E+006	9.4	192
7/7/1993	12.00	7.4	7/7/1993	20.50	27.6	459	220	1.92E+006	7.4	236
7/22/1993	16.01	9.4	7/22/1993	23.00	15.4	344	146	1.44E+006	8.6	198
9/15/1993	19.00	3.9	9/16/1993	10.75	47.6	381	172	4.01E+006	3.9	328
9/16/1993	11.00	11.0	9/16/1993	23.00	44.7	451	156	3.17E+006	9.0	337
10/7/1993	1.50	6.4	10/7/1993	12.25	19.5	350	124	1.79E+006	6.4	231
10/22/1993	16.50	6.0	10/22/1993	22.75	13.7	356	183	1.23E+006	6.0	171
12/19/1993	20.25	10.6	12/20/1993	1.00	11.5	350	192	1.05E+006	10.6	151
2/19/1994	5.50	5.2	2/19/1994	20.00	404	1941	597	6.67E+006	5.2	872
2/19/1994	20.01	14.1	2/20/1994	19.75	368	1126	396	1.05E+007	7.4	562
6/17/1994	9.00	6.4	6/18/1994	2.50	13.0	155	74.9	2.68E+006	6.4	169
7/17/1994	23.00	5.1	7/18/1994	19.00	15.3	150	88.0	3.27E+006	5.1	169
8/18/1994	19.75	10.0	8/19/1994	7.25	45.8	474	145	3.09E+006	10.0	340
8/23/1994	17.00	3.1	8/24/1994	2.00	8.3	176	67.3	1.51E+006	3.1	190
9/7/1994	18.50	3.5	9/8/1994	5.75	17.0	256	90.2	2.13E+006	3.5	228
9/20/1994	5.26	10.7	9/20/1994	22.75	28.3	221	116	4.12E+006	7.5	240

Reproduced with permission of the copyright owner. Further reproduction prohibited without permission.

Appendix 5.8. Continued.

Start Date	Start Time hour	End Date	End Time hour	L 7-MXTRP	L 6-MXTMJPK	L 9-SMPK	L 10-RAIN	L 11-INT15	L 12-SFIVE	L 13-RRISE	L 14-RAINFOL
5/23/1992	0.25	9.0	5/23/1992	0.4667	0.4667	107	0.92	0.34	0.0022	0.64	0.28
6/1/1992	11.00	15.0	6/2/1992	5.4222	5.4222	553	3.52	1.13	0.0060	3.47	0.04
7/8/1992	4.00	9.8	7/8/1992	0.4904	0.4904	76	0.48	0.08	0.0031	0.44	0.04
7/16/1992	22.75	9.4	7/17/1992	0.8956	0.8956	90	0.78	0.29	0.0064	0.77	0.01
7/24/1992	2.75	9.0	7/24/1992	0.6500	0.6500	48	0.16	0.14	0.0050	0.16	0.00
7/26/1992	21.25	7.4	7/27/1992	0.7467	0.7467	41	0.13	0.09	0.0033	0.13	0.00
8/5/1992	1.25	12.0	8/5/1992	5.3333	5.3333	252	1.58	0.74	0.0173	1.30	0.28
8/14/1992	10.50	12.0	8/14/1992	0.5600	0.5600	101	0.54	0.34	0.0014	0.54	0.00
8/30/1992	23.50	9.4	8/31/1992	0.5378	0.5378	82	0.77	0.13	0.0018	0.58	0.19
9/4/1992	14.25	8.4	9/4/1992	0.3767	0.3767	31	0.47	0.19	0.0031	0.37	0.10
9/16/1992	2.00	6.0	9/16/1992	0.7867	0.7867	65	0.76	0.50	0.0112	0.72	0.04
9/18/1992	21.25	6.9	9/19/1992	0.2867	0.2867	37	0.17	0.16	0.0107	0.17	0.00
9/23/1992	18.25	7.9	9/24/1992	0.6017	0.6017	44	0.39	0.29	0.0123	0.37	0.02
9/30/1992	13.00	5.6	9/30/1992	0.6400	0.6400	44	1.17	0.47	0.0098	1.15	0.02
10/22/1992	16.50	2.9	10/22/1992	1.1456	1.1456	106	0.61	0.21	0.0034	0.61	0.00
11/2/1992	21.25	4.8	11/3/1992	0.7448	0.7448	83	0.79	0.25	0.0030	0.63	0.16
11/3/1992	14.50	4.8	11/4/1992	1.4667	1.4667	526	5.09	0.58	0.0045	4.08	1.01
11/12/1992	15.00	3.6	11/12/1992	0.7600	0.7600	72	0.68	0.32	0.0120	0.68	0.00
11/16/1992	8.50	5.6	11/16/1992	0.5944	0.5944	175	1.23	0.34	0.0038	1.15	0.08
11/18/1992	2.00	9.8	11/18/1992	0.2258	0.2258	64	0.64	0.11	0.0015	0.43	0.21
11/20/1992	13.50	7.9	11/20/1992	1.4676	1.4676	162	0.54	0.25	0.0020	0.39	0.15
11/22/1992	6.76	20.0	11/23/1992	0.8964	0.8964	181	2.94	0.19	0.0037	1.31	1.63
12/6/1992	4.25	9.8	12/6/1992	0.5633	0.5633	145	1.64	0.32	0.0052	1.64	0.00
12/25/1992	19.25	10.0	12/26/1992	1.4381	1.4381	227	1.37	0.35	0.0025	1.23	0.14
12/26/1992	9.76	20.0	12/26/1992	2.7007	2.7007	343	1.91	0.45	0.0076	1.48	0.43
12/29/1992	12.50	8.4	12/30/1992	1.5444	1.4091	756	4.81	0.55	0.0060	1.91	2.90
1/22/1993	4.00	11.0	1/23/1993	0.2791	0.2791	288	2.52	0.16	0.0022	1.71	0.81
2/20/1993	12.50	9.0	2/21/1993	1.2000	1.2000	364	4.03	0.36	0.0045	2.68	1.35
4/30/1993	9.76	27.0	4/30/1993	2.0381	2.0381	413	1.64	0.28	0.0047	1.55	0.09
5/1/1993	11.75	16.0	5/2/1993	3.1333	3.1333	471	4.98	0.58	0.0062	2.71	2.27
5/2/1993	12.51	24.0	5/2/1993	2.4531	2.4531	207	0.92	0.27	0.0109	0.83	0.09
5/8/1993	17.00	5.6	5/9/1993	0.4413	0.4413	138	1.03	0.26	0.0025	0.83	0.20
5/9/1993	12.75	9.4	5/9/1993	3.0433	3.0433	192	1.01	0.34	0.0127	0.90	0.11
7/7/1993	12.00	7.4	7/7/1993	1.0886	1.0886	236	1.46	0.42	0.0024	1.42	0.04
7/22/1993	16.01	9.4	7/22/1993	2.5282	2.5282	198	0.79	0.50	0.0099	0.78	0.01
9/15/1993	19.00	3.9	9/16/1993	5.5778	5.5778	543	2.12	0.48	0.0033	1.07	1.05
9/16/1993	11.00	11.0	9/16/1993	3.6222	3.6222	337	0.71	0.18	0.0039	0.55	0.16
10/7/1993	1.50	6.4	10/7/1993	1.3630	1.3630	231.3	1.68	0.51	0.0067	1.49	0.19
10/22/1993	16.50	6.0	10/22/1993	1.5737	1.5737	171.2	0.58	0.31	0.0038	0.58	0.01
12/19/1993	20.25	10.6	12/20/1993	2.3450	2.3450	151.3	0.42	0.16	0.0071	0.45	-0.02
2/19/1994	5.50	5.2	2/19/1994	12.8345	12.8345	1423	3.34	0.58	0.0047	3.08	0.26
2/19/1994	20.01	14.1	2/20/1994	6.8604	4.1599	1287.7	6.11	0.63	0.0170	4.90	1.21
6/17/1994	9.00	6.4	6/18/1994	1.3509	1.3509	168.5	1.07	0.21	0.0031	0.53	0.54
7/17/1994	23.00	5.1	7/18/1994	0.4191	0.4191	168.5	2.40	0.51	0.0047	2.05	0.34
8/18/1994	19.75	10.0	8/19/1994	2.7459	2.7459	339.5	1.73	0.33	0.0049	1.59	0.14
8/23/1994	17.00	3.1	8/24/1994	1.5534	1.5534	189.5	1.21	0.33	0.0067	1.15	0.06
9/7/1994	18.50	3.5	9/8/1994	2.1330	2.1330	227.5	1.18	0.39	0.0059	0.94	0.24
9/20/1994	5.26	10.7	9/20/1994	1.1798	1.1798	240.3	2.12	0.37	0.0036	1.47	0.65

Reproduced with permission of the copyright owner. Further reproduction prohibited without permission.

Appendix 5.8. Continued.

Start Date	Start Time hour	End Date	16-HYSTER 1=normal 0=reverse	17-RNBTWTI	SQRT 18-PPTBTW	SQRT 19-INTBET	L 21-LSPKTI	L 23-SMLSPKT	L 25-RULST	L 26-PPTLSTI
5/23/1992	0.25	5/23/1992	1	36672	0.12	0.05	2.81	0.71	2.09E+004	0.0461
6/1/1992	11.00	6/2/1992	0	41323	0.02	0.01	1.12	30.3	3.15E+004	0.0142
7/8/1992	4.00	7/8/1992	1	28005	0.92	0.11	0.13	0.22	1.47E+003	0.0022
7/16/1992	22.75	7/17/1992	1	32283	0.61	0.06	0.36	0.44	2.80E+003	0.0023
7/24/1992	2.75	7/24/1992	0	36864	1.26	0.20	0.18	0.33	2.83E+003	0.0013
7/26/1992	21.25	7/27/1992	0	28704	0.02	0.02	0.45	1.02	9.87E+003	0.0035
8/5/1992	1.25	8/5/1992	1	30803	1.83	0.24	0.17	1.18	1.72E+003	0.0006
8/14/1992	10.50	8/14/1992	0	38034	0.52	0.15	2.03	4.16	2.72E+004	0.0227
8/30/1992	23.50	8/31/1992	0	20798	3.19	0.29	0.16	0.21	2.94E+003	0.0014
9/4/1992	14.25	9/4/1992	1	22894	0.71	0.24	0.62	0.31	1.04E+004	0.0076
9/16/1992	2.00	9/16/1992	1	22280	0.86	0.24	0.19	0.41	4.53E+003	0.0021
9/18/1992	21.25	9/19/1992	1	46507	0.38	0.11	0.89	1.87	2.01E+004	0.0167
9/23/1992	18.25	9/24/1992	0	33411	0.07	0.03	2.03	5.18	5.09E+004	0.0200
9/30/1992	13.00	9/30/1992	1	22825	0.52	0.14	0.24	0.28	3.58E+003	0.0025
10/22/1992	16.50	10/22/1992	1	14646	2.71	0.14	0.08	0.2	6.91E+002	0.0022
11/2/1992	21.25	11/3/1992	1	11911	2.01	0.25	0.37	0.32	2.93E+003	0.0023
11/3/1992	14.50	11/4/1992	1	20362	0.00	0.00	2.26	70.13	1.25E+005	0.1053
11/12/1992	15.00	11/12/1992	0	18580	0.00	0.00	2.28	1.46	3.79E+004	0.0339
11/16/1992	8.50	11/16/1992	1	26854	1.57	0.32	0.7	2.08	6.36E+003	0.0081
11/18/1992	2.00	11/18/1992	1	41390	0.40	0.06	3.87	2.29	7.12E+004	0.0439
11/20/1992	13.50	11/20/1992	1	30803	0.17	0.07	0.52	4.91	1.48E+004	0.0088
11/22/1992	6.76	11/23/1992	1	0	0.02	0.01	3.42	27150	3.35E+008	288
12/6/1992	4.25	12/6/1992	1	48428	0.63	0.20	0.86	3.41	2.33E+004	0.0139
12/25/1992	19.25	12/26/1992	1	50170	0.83	0.09	1.07	9.76	5.48E+004	0.0374
12/26/1992	9.76	12/26/1992	1	0	0.12	0.10	6.32	51450	4.12E+008	205
12/29/1992	12.50	12/30/1992	1	31716	0.20	0.05	1.31	51.25	7.24E+004	0.0292
1/22/1993	4.00	1/23/1993	1	39340	1.14	0.11	0.17	1.44	3.90E+003	0.0008
2/20/1993	12.50	2/21/1993	1	31898	0.58	0.10	0.15	1.9	1.61E+003	0.0018
4/30/1993	9.76	4/30/1993	1	0	0.04	0.02	3.25	61950	3.24E+008	458
5/1/1993	11.75	5/2/1993	0	58977	0.01	0.01	1.79	57.09	1.28E+005	0.0909
5/2/1993	12.51	5/2/1993	1	0	0.00	0.00	9.89	31050	2.34E+008	84.0
5/8/1993	17.00	5/9/1993	1	25686	1.15	0.35	0.64	1.16	1.16E+004	0.0067
5/9/1993	12.75	5/9/1993	1	39947	0.00	0.00	4.35	38.4	3.21E+005	0.2060
7/7/1993	12.00	7/7/1993	1	15161	0.09	0.04	0.54	2.5	8.27E+003	0.0069
7/22/1993	16.01	7/22/1993	1	0	0.00	0.00	4.28	29700	1.13E+008	117
9/15/1993	19.00	9/16/1993	1	35792	3.96	0.61	0.63	2.51	3.84E+003	0.0047
9/16/1993	11.00	9/16/1993	1	0	0.00	0.00	10.09	1348	1.60E+007	8.4894
10/7/1993	1.50	10/7/1993	1	20956	0.70	0.07	0.38	2.61	5.00E+003	0.0032
10/22/1993	16.50	10/22/1993	0	24321	1.36	0.67	0.39	3.02	1.62E+004	0.0136
12/19/1993	20.25	12/20/1993	1	18053	0.68	0.09	0.1	0.46	1.21E+003	0.0004
2/19/1994	5.50	2/19/1994	1	15052	2.15	0.24	0.11	4.07	1.29E+003	0.0017
2/19/1994	20.01	2/20/1994	1	0	0.00	0.00	74.16	193159.4	1.00E+009	501
6/17/1994	9.00	6/18/1994	1	18687	1.51	0.14	0.21	1.31	6.92E+003	0.0069
7/17/1994	23.00	7/18/1994	1	18682	1.09	0.15	0.11	0.62	1.74E+003	0.0012
8/18/1994	19.75	8/19/1994	1	35880	0.00	0.00	3.12	84.88	1.85E+005	0.2575
8/23/1994	17.00	8/24/1994	1	15541	0.41	0.08	2.51	1.79	2.92E+004	0.0163
9/7/1994	18.50	9/8/1994	1	18561	0.04	0.02	2.1	9.89	6.92E+004	0.0500
9/20/1994	5.26	9/20/1994	1	0	0.00	0.00	3.16	36046.67	2.32E+008	186

Reproduced with permission of the copyright owner. Further reproduction prohibited without permission.

Appendix 5.8. Continued.

Start Date	Start Time hour	End Date	L 27-INTLST	L 28-LS75OTI	29-SUM3PPTI	31-RU3EVT
5/23/1992	0.25	5/23/1992	0.0080	0.0002	0.0755	12.3
6/1/1992	11.00	6/2/1992	0.0071	0.0002	0.0761	13.3
7/8/1992	4.00	7/8/1992	0.0008	0.0000	0.0046	9.3
7/16/1992	22.75	7/17/1992	0.0004	0.0000	0.0039	9.2
7/24/1992	2.75	7/24/1992	0.0008	0.0000	0.0063	10.9
7/26/1992	21.25	7/27/1992	0.0015	0.0000	0.0163	11.7
8/5/1992	1.25	8/5/1992	0.0004	0.0000	0.0027	9.6
8/14/1992	10.50	8/14/1992	0.0181	0.0012	0.0374	12.4
8/30/1992	23.50	8/31/1992	0.0009	0.0000	0.0044	10.2
9/4/1992	14.25	9/4/1992	0.0013	0.0000	0.0098	10.5
9/16/1992	2.00	9/16/1992	0.0005	0.0000	0.0077	10.4
9/18/1992	21.25	9/19/1992	0.0071	0.0000	0.0324	11.9
9/23/1992	18.25	9/24/1992	0.0082	0.0003	0.1172	13.8
9/30/1992	13.00	9/30/1992	0.0019	0.0001	0.0207	11.3
10/22/1992	16.50	10/22/1992	0.0009	0.0000	0.0030	8.5
11/2/1992	21.25	11/3/1992	0.0008	0.0000	0.0042	8.9
11/3/1992	14.50	11/4/1992	0.0333	0.0004	0.1091	11.2
11/12/1992	15.00	11/12/1992	0.0063	0.0001	0.0405	11.8
11/16/1992	8.50	11/16/1992	0.0038	0.0001	0.0231	11.3
11/18/1992	2.00	11/18/1992	0.0121	0.0001	0.0604	12.5
11/20/1992	13.50	11/20/1992	0.0018	0.0000	0.0533	13.3
11/22/1992	6.76	11/23/1992	42.0	0.2939	288	17.0
12/6/1992	4.25	12/6/1992	0.0042	0.0000	0.0307	12.6
12/25/1992	19.25	12/26/1992	0.0082	0.0001	0.0592	12.6
12/26/1992	9.76	12/26/1992	52.5	0.3821	206	17.4
12/29/1992	12.50	12/30/1992	0.0108	0.0001	0.0886	13.8
1/22/1993	4.00	1/23/1993	0.0003	0.0000	0.0030	10.3
2/20/1993	12.50	2/21/1993	0.0006	0.0000	0.0069	10.3
4/30/1993	9.76	4/30/1993	73.5	0.7387	458	15.1
5/1/1993	11.75	5/2/1993	0.0097	0.0003	0.6586	15.3
5/2/1993	12.51	5/2/1993	28.5	0.4200	458	18.7
5/8/1993	17.00	5/9/1993	0.0018	0.0000	0.0183	12.3
5/9/1993	12.75	5/9/1993	0.0520	0.0005	0.2194	13.7
7/7/1993	12.00	7/7/1993	0.0015	0.0000	0.0157	10.9
7/22/1993	16.01	7/22/1993	37.5	0.5583	117	16.5
9/15/1993	19.00	9/16/1993	0.0022	0.0000	0.0107	10.4
9/16/1993	11.00	9/16/1993	1.9200	0.0131	8.4993	14.5
10/7/1993	1.50	10/7/1993	0.0015	0.0000	0.0091	11.4
10/22/1993	16.50	10/22/1993	0.0023	0.0000	0.0291	11.9
12/19/1993	20.25	12/20/1993	0.0003	0.0000	0.0042	9.9
2/19/1994	5.50	2/19/1994	0.0004	0.0000	0.0044	9.5
2/19/1994	20.01	2/20/1994	87.0	0.7000	501	15.4
6/17/1994	9.00	6/18/1994	0.0016	0.0000	0.0134	11.0
7/17/1994	23.00	7/18/1994	0.0004	0.0000	0.0055	10.4
8/18/1994	19.75	8/19/1994	0.0850	0.0006	0.2633	12.3
8/23/1994	17.00	8/24/1994	0.0031	0.0000	0.0291	11.9
9/7/1994	18.50	9/8/1994	0.0130	0.0001	0.0553	11.7
9/20/1994	5.26	9/20/1994	66.8	0.3500	186	15.9

Reproduced with permission of the copyright owner. Further reproduction prohibited without permission.

Appendix 5.9. Pearson correlation matrix for the dependent and independent variables using runoff characteristics at Rio Icacos for the entire event.

	SED	QU_SEDRONC	BASE	RUN
SED	1.000			
QU_SEDCONC	0.886	1.000		
BASE	0.244	0.253	1.000	
RUN	0.912	0.618	0.192	1.000
PK	0.920	0.828	0.145	0.827
LSPKTI	0.281	0.154	0.242	0.340
RNBTWTI	-0.252	-0.159	-0.029	-0.286
RULST	0.333	0.175	0.331	0.411
RU3EVT	0.295	0.156	0.467	0.364
MXTMJPK	0.705	0.757	0.168	0.527
MXTRP	0.720	0.766	0.162	0.544
SUMPK	0.955	0.786	0.156	0.925
SMLSPKTI	0.499	0.325	0.360	0.560
TOTRAIN	0.813	0.566	0.108	0.878
INT15	0.611	0.594	0.021	0.512
SFIVE	0.083	0.178	0.051	-0.017
RRISE	0.789	0.597	0.107	0.809
RFALL	0.615	0.354	0.138	0.730
LSTPPTI	0.344	0.192	0.288	0.413
LST3PPTI	0.324	0.195	0.426	0.376
LSTINT	0.328	0.179	0.302	0.398
LST75OTI	0.303	0.193	0.341	0.344
PPTBTW	-0.127	-0.054	-0.323	-0.168
INTBET	-0.175	-0.085	-0.299	-0.222
HYSTER	0.278	0.177	-0.202	0.312

	PK	LSPKTI	RNBTWTI	RULST	RU3EVT
PK	1.000				
LSPKTI	0.283	1.000			
RNBTWTI	-0.333	-0.479	1.000		
RULST	0.352	0.839	-0.791	1.000	
RU3EVT	0.290	0.801	-0.584	0.906	1.000
MXTMJPK	0.804	0.234	-0.307	0.295	0.250
MXTRP	0.816	0.265	-0.323	0.318	0.262
SUMPK	0.941	0.294	-0.278	0.345	0.282
SMLSPKTI	0.521	0.777	-0.775	0.970	0.881
TOTRAIN	0.717	0.225	-0.177	0.268	0.223
INT15	0.585	0.201	-0.051	0.141	0.179
SFIVE	0.168	0.240	-0.206	0.254	0.247
RRISE	0.722	0.215	-0.180	0.249	0.185
RFALL	0.510	0.197	-0.206	0.249	0.215
LSTPPTI	0.354	0.832	-0.795	0.992	0.883
LST3PPTI	0.309	0.836	-0.607	0.918	0.985

Reproduced with permission of the copyright owner. Further reproduction prohibited without permission.

Appendix 5.9. Continued.

LSTINT	0.347	0.818	-0.801	0.989	0.881
LST75OTI	0.319	0.813	-0.782	0.970	0.883
PPTBTW	-0.127	-0.730	0.333	-0.659	-0.698
INTBET	-0.176	-0.608	0.346	-0.571	-0.549
HYSTER	0.236	0.042	-0.277	0.136	-0.028

	MXTMJPK	MXTRP	SUMPK	SMLSPKTI	TOTRAIN
MXTMJPK	1.000				
MXTRP	0.997	1.000			
SUMPK	0.747	0.762	1.000		
SMLSPKTI	0.447	0.468	0.527	1.000	
TOTRAIN	0.448	0.465	0.830	0.409	1.000
INT15	0.569	0.575	0.606	0.271	0.686
SFIVE	0.394	0.411	0.110	0.281	0.106
RRISE	0.474	0.491	0.816	0.395	0.968
RFALL	0.307	0.316	0.595	0.327	0.713
LSTPPTI	0.298	0.319	0.351	0.963	0.275
LST3PPTI	0.282	0.294	0.304	0.892	0.237
LSTINT	0.299	0.320	0.340	0.965	0.258
LST75OTI	0.303	0.324	0.309	0.948	0.227
PPTBTW	-0.138	-0.150	-0.141	-0.624	-0.127
INTBET	-0.189	-0.201	-0.199	-0.563	-0.182
HYSTER	0.069	0.074	0.245	0.165	0.296

	INT15	SFIVE	RRISE	RFALL	LSTPPTI
INT15	1.000				
SFIVE	0.437	1.000			
RRISE	0.746	0.188	1.000		
RFALL	0.342	-0.104	0.592	1.000	
LSTPPTI	0.145	0.222	0.258	0.239	1.000
LST3PPTI	0.208	0.232	0.205	0.224	0.909
LSTINT	0.144	0.234	0.245	0.218	0.994
LST75OTI	0.174	0.255	0.226	0.173	0.976
PPTBTW	-0.156	-0.316	-0.151	-0.050	-0.640
INTBET	-0.087	-0.293	-0.198	-0.090	-0.561
HYSTER	0.080	0.034	0.271	0.399	0.163

	LST3PPTI	LSTINT	LST75OTI	PPTBTW	INTBET
LST3PPTI	1.000				
LSTINT	0.902	1.000			
LST75OTI	0.908	0.986	1.000		
PPTBTW	-0.707	-0.622	-0.637	1.000	
INTBET	-0.562	-0.553	-0.557	0.880	1.000
HYSTER	-0.008	0.152	0.099	0.052	-0.037

	HYSTER
HYSTER	1.000

Reproduced with permission of the copyright owner. Further reproduction prohibited without permission.

Appendix 5.10. Results of principal component analysis on the independent variables using runoff characteristics for the entire event at Rio Icacos.

Component loadings

	1	2	3	4	5
BASE	0.359	-0.152	-0.156	-0.560	0.427
RUN	0.683	0.593	0.282	-0.165	0.077
PK	0.660	0.641	-0.079	0.091	0.181
LSPKTI	0.791	-0.358	-0.007	-0.102	-0.117
RNBTWTI	-0.693	0.244	-0.191	-0.511	-0.055
RULST	0.905	-0.380	0.108	0.096	0.042
RU3EVT	0.841	-0.408	-0.005	-0.136	0.102
MXTMJPK	0.576	0.508	-0.470	0.247	0.240
MXTRP	0.597	0.506	-0.463	0.251	0.224
SUMPK	0.671	0.685	0.018	-0.032	0.126
SMLSPKTI	0.960	-0.194	0.063	0.086	0.078
TOTRAIN	0.577	0.688	0.214	-0.229	-0.179
INT15	0.450	0.588	-0.324	-0.075	-0.281
SFIVE	0.329	0.002	-0.645	0.237	-0.437
RRISE	0.565	0.685	0.099	-0.197	-0.231
RFALL	0.453	0.505	0.472	-0.171	-0.004
LSTPPTI	0.900	-0.369	0.133	0.128	0.034
LST3PPTI	0.863	-0.395	-0.000	-0.104	0.086
LSTINT	0.894	-0.378	0.116	0.140	0.051
LST75OTI	0.881	-0.401	0.050	0.116	0.059
PPTBTW	-0.645	0.426	0.202	0.340	0.345
INTBET	-0.602	0.314	0.169	0.300	0.368
HYSTER	0.196	0.250	0.516	0.395	-0.392

	6
BASE	-0.151
RUN	-0.029
PK	-0.124
LSPKTI	0.051
RNBTWTI	0.002
RULST	0.060
RU3EVT	0.133
MXTMJPK	-0.198
MXTRP	-0.187
SUMPK	-0.085
SMLSPKTI	0.030
TOTRAIN	0.157
INT15	0.386
SFIVE	0.103
RRISE	0.180
RFALL	-0.081
LSTPPTI	0.062
LST3PPTI	0.129
LSTINT	0.073
LST75OTI	0.101
PPTBTW	0.226
INTBET	0.447
HYSTER	-0.340

Reproduced with permission of the copyright owner. Further reproduction prohibited without permission.

Appendix 5.11. Results of principal component analysis on the independent variables using runoff characteristics for the entire event (without the variable RUN) at Rio Icacos.

Component loadings

	1	2	3	4	5
BASE	0.365	-0.136	-0.247	-0.504	0.469
PK	0.616	0.682	-0.029	0.088	0.182
LSPKTI	0.812	-0.308	-0.023	-0.105	-0.112
RNBTWTI	-0.710	0.192	-0.269	-0.474	-0.028
RULST	0.926	-0.324	0.118	0.082	0.040
RU3EVT	0.864	-0.358	-0.034	-0.123	0.112
MXTMJPK	0.552	0.578	-0.393	0.303	0.210
MXTRP	0.573	0.577	-0.385	0.305	0.194
SUMPK	0.620	0.714	0.050	-0.050	0.140
SMLSPKTI	0.969	-0.136	0.080	0.076	0.078
TOTRAIN	0.524	0.704	0.233	-0.309	-0.131
INT15	0.420	0.643	-0.267	-0.091	-0.268
SFIVE	0.346	0.077	-0.572	0.283	-0.480
RRISE	0.516	0.711	0.130	-0.268	-0.190
RFALL	0.409	0.502	0.484	-0.273	0.052
LSTPPTI	0.921	-0.314	0.148	0.108	0.031
LST3PPTI	0.886	-0.342	-0.022	-0.095	0.094
LSTINT	0.916	-0.322	0.133	0.125	0.046
LST75OTI	0.906	-0.340	0.065	0.109	0.055
PPTBTW	-0.673	0.377	0.250	0.325	0.333
INTBET	-0.621	0.271	0.209	0.292	0.359
HYSTER	0.176	0.250	0.607	0.262	-0.385

	6		6
BASE	-0.170	LST75OTI	0.099
PK	-0.124	PPTBTW	0.221
LSPKTI	0.056	INTBET	0.441
RNBTWTI	0.001	HYSTER	-0.349
RULST	0.059		
RU3EVT	0.130		
MXTMJPK	-0.197		
MXTRP	-0.185		
SUMPK	-0.086		
SMLSPKTI	0.029		
TOTRAIN	0.150		
INT15	0.383		
SFIVE	0.106		
RRISE	0.173		
RFALL	-0.096		
LSTPPTI	0.062		
LST3PPTI	0.127		
LSTINT	0.073		

Reproduced with permission of the copyright owner. Further reproduction prohibited without permission.

Appendix 5.12. Results of principal component analysis on the independent variables using runoff characteristics after varimax rotation for the entire event at Rio Icacos.

Rotated Loading Matrix (VARIMAX, Gamma = 1.0000)

	1	2	3	4	5
BASE	0.268	0.107	-0.309	-0.622	0.158
RUN	0.265	0.870	-0.147	0.044	0.283
PK	0.203	0.658	0.017	0.040	0.658
LSPKTI	0.797	0.149	0.128	-0.074	-0.001
RNBTWTI	-0.799	-0.011	0.007	-0.365	-0.240
RULST	0.968	0.134	0.013	0.022	0.105
RU3EVT	0.896	0.133	0.030	-0.238	0.038
MXTMJPK	0.161	0.322	0.197	-0.046	0.893
MXTRP	0.181	0.335	0.210	-0.037	0.885
SUMPK	0.186	0.783	-0.010	0.020	0.543
SMLSPKTI	0.908	0.273	0.024	0.007	0.242
TOTRAIN	0.118	0.957	0.119	0.049	0.113
INT15	0.043	0.653	0.626	-0.120	0.228
SFIVE	0.177	-0.068	0.779	0.055	0.295
RRISE	0.097	0.912	0.236	0.037	0.147
RFALL	0.135	0.768	-0.271	0.173	0.066
LSTPPTI	0.967	0.139	0.011	0.059	0.103
LST3PPTI	0.910	0.144	0.044	-0.203	0.054
LSTINT	0.970	0.120	0.016	0.047	0.113
LST75OTI	0.963	0.087	0.058	-0.014	0.116
PPTBTW	-0.569	-0.034	-0.186	0.120	0.043
INTBET	-0.445	-0.058	-0.088	-0.017	-0.068
HYSTER	0.068	0.295	-0.132	0.821	0.027

	6
BASE	0.323
RUN	0.043
PK	-0.006
LSPKTI	0.319
RNBTWTI	0.107
RULST	0.152
RU3EVT	0.205
MXTMJPK	0.030
MXTRP	0.031
SUMPK	0.027
SMLSPKTI	0.145
TOTRAIN	0.038
INT15	-0.037
SFIVE	0.222
RRISE	0.054
RFALL	0.041
LSTPPTI	0.130
LST3PPTI	0.201
LSTINT	0.113
LST75OTI	0.119
PPTBTW	-0.740
INTBET	-0.837
HYSTER	0.093

Reproduced with permission of the copyright owner. Further reproduction prohibited without permission.

Appendix 5.13. Results of principal component analysis on the independent variables using runoff characteristics after varimax rotation for the entire event)without the variable RUN) at Rio Icacos

Rotated Loading Matrix (VARIMAX, Gamma = 1.0000)

	1	2	3	4	5
BASE	0.268	0.076	-0.372	-0.585	0.184
PK	0.213	0.592	-0.028	0.068	0.707
LSPKTI	0.798	0.147	0.118	-0.066	0.009
RNBTWTI	-0.798	0.027	-0.022	-0.365	-0.237
RULST	0.968	0.107	0.010	0.034	0.116
RU3EVT	0.897	0.120	0.007	-0.226	0.052
MXTMJPK	0.163	0.275	0.179	-0.038	0.912
MXTRP	0.183	0.289	0.191	-0.029	0.905
SUMPK	0.199	0.717	-0.069	0.055	0.604
SMLSPKTI	0.910	0.234	0.010	0.024	0.263
TOTRAIN	0.134	0.948	0.015	0.077	0.186
INT15	0.051	0.715	0.532	-0.134	0.269
SFIVE	0.168	-0.003	0.789	0.015	0.275
RRISE	0.111	0.919	0.132	0.058	0.215
RFALL	0.148	0.723	-0.357	0.219	0.132
LSTPPTI	0.968	0.111	0.009	0.070	0.114
LST3PPTI	0.912	0.131	0.022	-0.192	0.069
LSTINT	0.971	0.093	0.016	0.057	0.123
LST75OTI	0.963	0.070	0.053	-0.008	0.123
PPTBTW	-0.565	-0.048	-0.184	0.108	0.043
INTBET	-0.441	-0.046	-0.099	-0.039	-0.069
HYSTER	0.070	0.257	-0.124	0.841	0.044

	6		
BASE	0.353	LST75OTI	0.126
PK	-0.003	PPTBTW	-0.745
LSPKTI	0.324	INTBET	-0.837
RNBTWTI	0.112	HYSTER	0.077
RULST	0.158		
RU3EVT	0.219		
MXTMJPK	0.033		
MXTRP	0.035		
SUMPK	0.031		
SMLSPKTI	0.152		
TOTRAIN	0.044		
INT15	-0.030		
SFIVE	0.222		
RRISE	0.059		
RFALL	0.047		
LSTPPTI	0.135		
LST3PPTI	0.213		
LSTINT	0.119		

Reproduced with permission of the copyright owner. Further reproduction prohibited without permission.

Appendix 5.14. Summary of dependent and independent variables used in the statistical analysis for quickflow characteristics to the hihgest peak flow at Rio Icacos near Naguabo

(D indicates dependent variable; L indicates data was log transformed for final statistical operations; SQRT indicates data was transformed by th

Start Date	Start Time hour	Start Discharge ft3/s	End Date	End Time hour	DL Suspended-sediment load tons	DL Discharge-weighted sediment concentration mg/L	L 1-QUICK	3-BASE	SQRT 4-PKBS
5/23/1992	0.25	9.0	5/23/1992	15.25	3.65	465	251079	9.0	96.8
6/1/1992	11.00	15.0	6/2/1992	3.00	37.0	1342	883800	15.0	490
7/8/1992	4.00	9.8	7/8/1992	9.25	1.57	291	173211	9.8	65.3
7/16/1992	22.75	9.4	7/17/1992	3.50	1.47	291	162084	9.4	79.9
7/24/1992	2.75	9.0	7/24/1992	7.00	0.62	324	61279	9.0	38.3
7/26/1992	21.25	7.4	7/27/1992	3.00	0.28	260	34677	7.4	33.3
8/5/1992	1.25	12.0	8/5/1992	9.75	13.3	1647	258485	12.0	239
8/14/1992	10.50	12.0	8/14/1992	22.50	2.04	186	350100	12.0	54.0
8/30/1992	23.50	9.4	8/31/1992	8.75	1.21	183	211811	9.4	72.2
9/4/1992	14.25	8.4	9/4/1992	20.00	0.23	169	43290	8.4	22.6
9/16/1992	2.00	6.0	9/16/1992	9.50	1.57	470	107250	6.0	57.7
9/18/1992	21.25	6.9	9/19/1992	4.25	0.35	129	87154	6.9	29.3
9/23/1992	18.25	7.9	9/24/1992	2.00	0.43	209	66634	7.9	35.9
9/30/1992	13.00	5.6	9/30/1992	17.75	0.84	355	75705	5.6	37.5
10/22/1992	16.50	2.9	10/22/1992	23.50	3.36	493	218751	2.9	102
11/2/1992	21.25	4.8	11/3/1992	7.00	2.81	507	177360	4.8	77.7
11/3/1992	14.50	4.8	11/4/1992	12.50	12.4	234	1693788	4.8	165
11/12/1992	15.00	3.6	11/12/1992	20.50	0.82	174	151159	3.6	66.8
11/16/1992	8.50	5.6	11/16/1992	22.00	3.79	225	539188	5.6	168
11/18/1992	2.00	9.8	11/18/1992	10.50	3.17	167	609886	9.8	54.0
11/20/1992	13.50	7.9	11/20/1992	22.75	8.43	912	296334	7.9	154
11/22/1992	6.76	20.0	11/23/1992	7.25	5.76	226	817290	7.9	173
12/6/1992	4.25	9.8	12/6/1992	14.00	12.9	719	574934	9.8	133
12/25/1992	19.25	10.0	12/26/1992	9.75	13.9	462	962581	10.0	166
12/26/1992	9.76	20.0	12/26/1992	20.75	18.5	958	617392	12.8	330
12/29/1992	12.50	8.4	12/30/1992	16.00	50.0	1191	1343632	8.4	399
1/22/1993	4.00	11.0	1/23/1993	4.50	7.10	196	1158539	11.0	178
2/20/1993	12.50	9.0	2/21/1993	17.50	15.2	236	2060678	9.0	151
4/30/1993	9.76	27.0	4/30/1993	18.75	32.0	598	1714682	12.3	278
5/1/1993	11.75	16.0	5/2/1993	5.25	29.1	1016	918133	16.0	223
5/2/1993	12.51	24.0	5/2/1993	23.25	7.07	576	393011	16.7	190
5/8/1993	17.00	5.6	5/9/1993	7.75	3.30	419	252365	5.6	130
5/9/1993	12.75	9.4	5/9/1993	19.75	6.18	583	339493	9.4	182
7/7/1993	12.00	7.4	7/7/1993	20.50	10.2	526	621217	7.4	227
7/22/1993	16.01	9.4	7/22/1993	23.00	10.3	709	464081	8.6	189
9/15/1993	19.00	3.9	9/16/1993	10.75	20.5	718	915739	3.9	323
9/16/1993	11.00	11.0	9/16/1993	23.00	16.6	629	843655	9.0	327
10/7/1993	1.50	6.4	10/7/1993	12.25	11.3	744	485600	6.4	224
10/22/1993	16.50	6.0	10/22/1993	22.75	5.72	481	380453	6.0	163
12/19/1993	20.25	10.6	12/20/1993	1.00	2.52	360	224220	10.6	141
2/19/1994	5.50	5.2	2/19/1994	20.00	268	2697	3180265	5.2	865
2/19/1994	20.01	14.1	2/20/1994	19.75	173	1390	3989457	7.4	554
6/17/1994	9.00	6.4	6/18/1994	2.50	4.51	369	391597	6.4	161
7/17/1994	23.00	5.1	7/18/1994	19.00	5.93	220	862492	5.1	160
8/18/1994	19.75	10.0	8/19/1994	7.25	25.4	943	864636	10.0	329
8/23/1994	17.00	3.1	8/24/1994	2.00	5.32	418	407572	3.1	185
9/7/1994	18.50	3.5	9/8/1994	5.75	8.52	516	529475	3.5	222
9/20/1994	5.26	10.7	9/20/1994	22.75	9.72	331	940930	7.5	232

Reproduced with permission of the copyright owner. Further reproduction prohibited without permission.

Appendix 5.14. Continued.

Start Date	Start Time hour	End Date	End Time hour	L 6-MXTMJPK	L 11-INT15	L 13-RRISE	17-RNBTWTI	SQRT 18-PPTBTW	SQRT 19-INTBET
5/23/1992	0.25	5/23/1992	15.25	0.4667	0.34	0.64	36672	0.12	0.05
6/1/1992	11.00	6/2/1992	3.00	5.4222	1.13	3.47	41323	0.02	0.01
7/8/1992	4.00	7/8/1992	9.25	0.4904	0.08	0.44	28005	0.92	0.11
7/16/1992	22.75	7/17/1992	3.50	0.8956	0.29	0.77	32283	0.61	0.06
7/24/1992	2.75	7/24/1992	7.00	0.6500	0.14	0.16	36864	1.26	0.20
7/26/1992	21.25	7/27/1992	3.00	0.7467	0.09	0.13	28704	0.02	0.02
8/5/1992	1.25	8/5/1992	9.75	5.3333	0.74	1.30	30803	1.83	0.24
8/14/1992	10.50	8/14/1992	22.50	0.5600	0.34	0.54	38034	0.52	0.15
8/30/1992	23.50	8/31/1992	8.75	0.5378	0.13	0.58	20798	3.19	0.29
9/4/1992	14.25	9/4/1992	20.00	0.3767	0.19	0.37	22894	0.71	0.24
9/16/1992	2.00	9/16/1992	9.50	0.7867	0.50	0.72	22280	0.86	0.24
9/18/1992	21.25	9/19/1992	4.25	0.2867	0.16	0.17	46507	0.38	0.11
9/23/1992	18.25	9/24/1992	2.00	0.6017	0.29	0.37	33411	0.07	0.03
9/30/1992	13.00	9/30/1992	17.75	0.6400	0.47	1.15	22825	0.52	0.14
10/22/1992	16.50	10/22/1992	23.50	1.1456	0.21	0.61	14646	2.71	0.14
11/2/1992	21.25	11/3/1992	7.00	0.7448	0.25	0.63	11911	2.01	0.25
11/3/1992	14.50	11/4/1992	12.50	1.4667	0.58	4.08	20362	0.00	0.00
11/12/1992	15.00	11/12/1992	20.50	0.7600	0.32	0.68	18580	0.00	0.00
11/16/1992	8.50	11/16/1992	22.00	0.5944	0.34	1.15	26854	1.57	0.32
11/18/1992	2.00	11/18/1992	10.50	0.2258	0.11	0.43	41390	0.40	0.06
11/20/1992	13.50	11/20/1992	22.75	1.4676	0.25	0.39	30803	0.17	0.07
11/22/1992	6.76	11/23/1992	7.25	0.8964	0.19	1.31	0	0.02	0.01
12/6/1992	4.25	12/6/1992	14.00	0.5633	0.32	1.64	48428	0.63	0.20
12/25/1992	19.25	12/26/1992	9.75	1.4381	0.35	1.23	50170	0.83	0.09
12/26/1992	9.76	12/26/1992	20.75	2.7007	0.45	1.48	0	0.12	0.10
12/29/1992	12.50	12/30/1992	16.00	1.4091	0.30	1.91	31716	0.20	0.05
1/22/1993	4.00	1/23/1993	4.50	0.2791	0.16	1.71	39340	1.14	0.11
2/20/1993	12.50	2/21/1993	17.50	1.2000	0.36	2.68	31898	0.58	0.10
4/30/1993	9.76	4/30/1993	18.75	2.0381	0.28	1.55	0	0.04	0.02
5/1/1993	11.75	5/2/1993	5.25	3.1333	0.58	2.71	58977	0.01	0.01
5/2/1993	12.51	5/2/1993	23.25	2.4531	0.27	0.83	0	0.00	0.00
5/8/1993	17.00	5/9/1993	7.75	0.4413	0.26	0.83	25686	1.15	0.35
5/9/1993	12.75	5/9/1993	19.75	3.0433	0.34	0.90	39947	0.00	0.00
7/7/1993	12.00	7/7/1993	20.50	1.0886	0.42	1.42	15161	0.09	0.04
7/22/1993	16.01	7/22/1993	23.00	2.5282	0.50	0.78	0	0.00	0.00
9/15/1993	19.00	9/16/1993	10.75	5.5778	0.38	1.07	35792	3.96	0.61
9/16/1993	11.00	9/16/1993	23.00	3.6222	0.14	0.55	0	0.00	0.00
10/7/1993	1.50	10/7/1993	12.25	1.3630	0.51	1.49	20956	0.70	0.07
10/22/1993	16.50	10/22/1993	22.75	1.5737	0.31	0.58	24321	1.36	0.67
12/19/1993	20.25	12/20/1993	1.00	2.3450	0.16	0.45	18053	0.68	0.09
2/19/1994	5.50	2/19/1994	20.00	12.8345	0.58	3.08	15052	2.15	0.24
2/19/1994	20.01	2/20/1994	19.75	4.1599	0.63	4.90	0	0.00	0.00
6/17/1994	9.00	6/18/1994	2.50	1.3509	0.21	0.53	18687	1.51	0.14
7/17/1994	23.00	7/18/1994	19.00	0.4191	0.51	2.05	18682	1.09	0.15
8/18/1994	19.75	8/19/1994	7.25	2.7459	0.33	1.59	35880	0.00	0.00
8/23/1994	17.00	8/24/1994	2.00	1.5534	0.33	1.15	15541	0.41	0.08
9/7/1994	18.50	9/8/1994	5.75	2.1330	0.39	0.94	18561	0.04	0.02
9/20/1994	5.26	9/20/1994	22.75	1.1798	0.37	1.47	0	0.00	0.00

Reproduced with permission of the copyright owner. Further reproduction prohibited without permission.

Appendix 5.14. Continued.

Start Date	Start Time hour	End Date	End Time hour	L 20-LSPKBTI	L 22-SMLSPKBS	L 24-QULST	L 26-PPTLSTI
5/23/1992	0.25	5/23/1992	15.25	2.74	0.65	18097	0.0461
6/1/1992	11.00	6/2/1992	3.00	0.88	28.7	16718	0.0142
7/8/1992	4.00	7/8/1992	9.25	0.10	0.19	790	0.0022
7/16/1992	22.75	7/17/1992	3.50	0.31	0.39	1800	0.0023
7/24/1992	2.75	7/24/1992	7.00	0.10	0.27	875	0.0013
7/26/1992	21.25	7/27/1992	3.00	0.31	0.83	4266	0.0035
8/5/1992	1.25	8/5/1992	9.75	0.14	1.12	893	0.0006
8/14/1992	10.50	8/14/1992	22.50	1.78	3.18	17564	0.0227
8/30/1992	23.50	8/31/1992	8.75	0.13	0.19	1597	0.0014
9/4/1992	14.25	9/4/1992	20.00	0.55	0.22	7083	0.0076
9/16/1992	2.00	9/16/1992	9.50	0.16	0.37	2777	0.0021
9/18/1992	21.25	9/19/1992	4.25	0.71	1.48	10686	0.0167
9/23/1992	18.25	9/24/1992	2.00	1.40	4.22	21812	0.0200
9/30/1992	13.00	9/30/1992	17.75	0.20	0.24	1989	0.0025
10/22/1992	16.50	10/22/1992	23.50	0.07	0.19	441	0.0022
11/2/1992	21.25	11/3/1992	7.00	0.36	0.30	2504	0.0023
11/3/1992	14.50	11/4/1992	12.50	2.12	27.1	96720	0.1053
11/12/1992	15.00	11/12/1992	20.50	2.17	1.36	31720	0.0339
11/16/1992	8.50	11/16/1992	22.00	0.65	2.00	4826	0.0081
11/18/1992	2.00	11/18/1992	10.50	3.71	1.93	58159	0.0439
11/20/1992	13.50	11/20/1992	22.75	0.34	4.66	6858	0.0088
11/22/1992	6.76	11/23/1992	7.25	3.07	25922	264830211	288
12/6/1992	4.25	12/6/1992	14.00	0.70	3.14	12729	0.0139
12/25/1992	19.25	12/26/1992	9.75	0.84	8.84	29981	0.0374
12/26/1992	9.76	12/26/1992	20.75	5.92	49465	322589118	205
12/29/1992	12.50	12/30/1992	16.00	0.95	48.5	37953	0.0292
1/22/1993	4.00	1/23/1993	4.50	0.09	1.31	997	0.0008
2/20/1993	12.50	2/21/1993	17.50	0.08	1.72	563	0.0018
4/30/1993	9.76	4/30/1993	18.75	2.85	57991	251822976	458
5/1/1993	11.75	5/2/1993	5.25	1.32	51.22	67114	0.0909
5/2/1993	12.51	5/2/1993	23.25	8.23	28540	142608075	84.0
5/8/1993	17.00	5/9/1993	7.75	0.56	1.09	8331	0.0067
5/9/1993	12.75	5/9/1993	19.75	4.10	36.3	227502	0.2060
7/7/1993	12.00	7/7/1993	20.50	0.46	2.40	5555	0.0069
7/22/1993	16.01	7/22/1993	23.00	3.81	28348	83376931	117
9/15/1993	19.00	9/16/1993	10.75	0.61	2.44	3245	0.0047
9/16/1993	11.00	9/16/1993	23.00	9.95	1310	14565994	8.4894
10/7/1993	1.50	10/7/1993	12.25	0.31	2.52	2507	0.0032
10/22/1993	16.50	10/22/1993	22.75	0.30	2.87	8623	0.0136
12/19/1993	20.25	12/20/1993	1.00	0.08	0.43	623	0.0004
2/19/1994	5.50	2/19/1994	20.00	0.10	4.01	900	0.0017
2/19/1994	20.01	2/20/1994	19.75	73.61	189526	951234271	501
6/17/1994	9.00	6/18/1994	2.50	0.17	1.26	4299	0.0069
7/17/1994	23.00	7/18/1994	19.00	0.09	0.59	1027	0.0012
8/18/1994	19.75	8/19/1994	7.25	2.57	82.2	111521	0.2575
8/23/1994	17.00	8/24/1994	2.00	2.44	1.75	24701	0.0163
9/7/1994	18.50	9/8/1994	5.75	1.93	9.66	53788	0.0500
9/20/1994	5.26	9/20/1994	22.75	2.93	34856	188300016	186

Reproduced with permission of the copyright owner. Further reproduction prohibited without permission.

Appendix 5.14. Continued.

Start Date	Start Time hour	End Date	End Time hour	L 27-INTLST	L 28-LS75OTI	29-SUM3PPTI	30-QU3EVT
5/23/1992	0.25	5/23/1992	15.25	0.0080	0.0002	-5.24	11.9
6/1/1992	11	6/2/1992	3	0.0071	0.0002	-5.05	12.8
7/8/1992	4	7/8/1992	9.25	0.0008	0.0000	-8.81	8.4
7/16/1992	22.75	7/17/1992	3.5	0.0004	0.0000	-9.11	8.3
7/24/1992	2.75	7/24/1992	7	0.0008	0.0000	-8.15	10.0
7/26/1992	21.25	7/27/1992	3	0.0015	0.0000	-7.12	10.8
8/5/1992	1.25	8/5/1992	9.75	0.0004	0.0000	-9.32	8.6
8/14/1992	10.5	8/14/1992	22.5	0.0181	0.0012	-6.11	11.9
8/30/1992	23.5	8/31/1992	8.75	0.0009	0.0000	-8.54	9.6
9/4/1992	14.25	9/4/1992	20	0.0013	0.0000	-8.07	9.8
9/16/1992	2	9/16/1992	9.5	0.0005	0.0000	-7.89	9.7
9/18/1992	21.25	9/19/1992	4.25	0.0071	0.0000	-6.50	11.2
9/23/1992	18.25	9/24/1992	2	0.0082	0.0003	-4.76	13.0
9/30/1992	13	9/30/1992	17.75	0.0019	0.0001	-7.40	10.5
10/22/1992	16.5	10/22/1992	23.5	0.0009	0.0000	-9.52	7.7
11/2/1992	21.25	11/3/1992	7	0.0008	0.0000	-8.85	8.4
11/3/1992	14.5	11/4/1992	12.5	0.0333	0.0004	-6.48	10.8
11/12/1992	15	11/12/1992	20.5	0.0063	0.0001	-6.56	11.3
11/16/1992	8.5	11/16/1992	22	0.0038	0.0001	-6.65	10.9
11/18/1992	2	11/18/1992	10.5	0.0121	0.0001	-5.66	12.2
11/20/1992	13.5	11/20/1992	22.75	0.0018	0.0000	-5.64	12.7
11/22/1992	6.7566667	11/23/1992	7.25	42.0	0.2939	-1.72	16.4
12/6/1992	4.25	12/6/1992	14	0.0042	0.0000	-6.40	12.1
12/25/1992	19.25	12/26/1992	9.75	0.0082	0.0001	-5.73	12.1
12/26/1992	9.7566667	12/26/1992	20.75	52.5	0.3821	-1.26	16.9
12/29/1992	12.5	12/30/1992	16	0.0108	0.0001	-5.04	13.1
1/22/1993	4	1/23/1993	4.5	0.0003	0.0000	-9.28	8.6
2/20/1993	12.5	2/21/1993	17.5	0.0006	0.0000	-8.11	9.5
4/30/1993	9.7566667	4/30/1993	18.75	73.5	0.7387	-2.99	14.5
5/1/1993	11.75	5/2/1993	5.25	0.0097	0.0003	-2.99	14.9
5/2/1993	12.506667	5/2/1993	23.25	28.5	0.4200	0.12	18.2
5/8/1993	17	5/9/1993	7.75	0.0018	0.0000	-6.77	11.8
5/9/1993	12.75	5/9/1993	19.75	0.0520	0.0005	-5.16	13.2
7/7/1993	12	7/7/1993	20.5	0.0015	0.0000	-7.18	10.3
7/22/1993	16.006667	7/22/1993	23	37.5	0.5583	-1.40	16.2
9/15/1993	19	9/16/1993	10.75	0.0022	0.0000	-7.75	10.0
9/16/1993	11	9/16/1993	23	1.9200	0.0131	-3.75	14.3
10/7/1993	1.5	10/7/1993	12.25	0.0015	0.0000	-7.70	11.0
10/22/1993	16.5	10/22/1993	22.75	0.0023	0.0000	-6.30	11.3
12/19/1993	20.25	12/20/1993	1	0.0003	0.0000	-8.89	9.3
2/19/1994	5.5	2/19/1994	20	0.0004	0.0000	-8.54	9.0
2/19/1994	20.006667	2/20/1994	19.75	87.0	0.7000	-2.89	15.1
6/17/1994	9	6/18/1994	2.5	0.0016	0.0000	-7.28	10.5
7/17/1994	23	7/18/1994	19	0.0004	0.0000	-8.29	9.9
8/18/1994	19.75	8/19/1994	7.25	0.0850	0.0006	-5.81	11.9
8/23/1994	17	8/24/1994	2	0.0031	0.0000	-6.34	11.5
9/7/1994	18.5	9/8/1994	5.75	0.0130	0.0001	-6.54	11.3
9/20/1994	5.2566667	9/20/1994	22.75	66.8	0.3500	-2.79	15.3

**to eliminate zero values a value of 0.0002 was added to the precipitation between events and a value of 5000 was added to the runoff between events.

Reproduced with permission of the copyright owner. Further reproduction prohibited without permission.

Appendix 5.15. Pearson correlation matrix for the dependent and independent variables using quickflow characteristics to the highest peak.

	SED	QU_SEDCONC	BASE	QUICK
SED	1.000			
QU_SEDCONC	0.774	1.000		
BASE	0.184	0.204	1.000	
QUICK	0.915	0.452	0.128	1.000
PKBS	0.936	0.790	0.125	0.815
LSPKBTI	0.306	0.168	0.205	0.325
RNBTWTI	-0.280	-0.172	-0.029	-0.284
QULST	0.365	0.201	0.301	0.386
QU3EVT	0.326	0.234	0.436	0.310
MXTMJPK	0.725	0.816	0.168	0.500
SMLSPKBSTI	0.538	0.350	0.359	0.535
INT15	0.570	0.564	0.029	0.443
RRISE	0.807	0.488	0.107	0.825
LSTPPTI	0.373	0.196	0.288	0.400
LST3PPTI	0.331	0.227	0.426	0.321
LSTINT	0.360	0.189	0.302	0.386
LST75OTI	0.330	0.205	0.341	0.334
PPTBTW	-0.132	-0.066	-0.323	-0.145
INTBET	-0.186	-0.072	-0.299	-0.216

	PKBS	LSPKBTI	RNBTWTI	QULST	QU3EVT
PKBS	1.000				
LSPKBTI	0.286	1.000			
RNBTWTI	-0.336	-0.494	1.000		
QULST	0.354	0.847	-0.799	1.000	
QU3EVT	0.304	0.805	-0.588	0.899	1.000
MXTMJPK	0.804	0.243	-0.307	0.302	0.274
SMLSPKBSTI	0.529	0.762	-0.778	0.963	0.880
INT15	0.542	0.200	-0.057	0.147	0.189
RRISE	0.724	0.222	-0.180	0.254	0.197
LSTPPTI	0.352	0.829	-0.795	0.994	0.887
LST3PPTI	0.304	0.821	-0.607	0.913	0.990
LSTINT	0.345	0.815	-0.801	0.989	0.884
LST75OTI	0.315	0.809	-0.782	0.971	0.885
PPTBTW	-0.122	-0.704	0.333	-0.651	-0.696
INTBET	-0.173	-0.586	0.346	-0.564	-0.545

Reproduced with permission of the copyright owner. Further reproduction prohibited without permission.

Appendix 5.15. Continued.

	MXTMJPK	SMLSPKBSTI	INT15	RRISE	LSTPPTI
MXTMJPK	1.000				
SMLSPKBSTI	0.454	1.000			
INT15	0.546	0.260	1.000		
RRISE	0.474	0.395	0.734	1.000	
LSTPPTI	0.298	0.962	0.144	0.258	1.000
LST3PPTI	0.282	0.891	0.197	0.205	0.909
LSTINT	0.299	0.964	0.142	0.245	0.994
LST75OTI	0.303	0.946	0.176	0.226	0.976
PPTBTW	-0.138	-0.616	-0.162	-0.151	-0.640
INTBET	-0.189	-0.557	-0.094	-0.198	-0.561

	LST3PPTI	LSTINT	LST75OTI	PPTBTW	INTBET
LST3PPT	1.000				
I					
LSTINT	0.902	1.000			
LST75OT	0.908	0.986	1.000		
I					
PPTBTW	-0.707	-0.622	-0.637	1.000	
INTBET	-0.562	-0.553	-0.557	0.880	1.000

Reproduced with permission of the copyright owner. Further reproduction prohibited without permission.

Appendix 5.16. Results of principal component analysis on the independent variables using quickflow characterisitcs to the highest peak at Rio Icacos.

Component loadings

	1	2	3	4	5	6
BASE	0.371	-0.082	-0.515	0.740	0.068	-0.039
QUICK	0.513	0.695	0.040	0.007	0.335	-0.304
PKBS	0.505	0.777	0.076	0.091	-0.140	-0.185
LSPKBTI	0.845	-0.166	-0.075	-0.196	0.057	0.130
RNBTWTI	-0.735	0.091	-0.523	0.048	0.134	0.134
QULST	0.966	-0.172	0.157	0.002	0.041	0.014
QU3EVT	0.913	-0.201	-0.069	0.121	0.045	0.174
MXTMJPK	0.445	0.641	0.016	0.160	-0.579	0.005
SMLSPKBSTI	0.978	0.023	0.121	0.081	0.011	-0.041
INT15	0.305	0.700	-0.212	-0.196	-0.034	0.531
RRISE	0.408	0.795	-0.132	-0.130	0.326	-0.010
LSTPPTI	0.963	-0.167	0.170	-0.003	0.054	0.002
LST3PPTI	0.928	-0.201	-0.059	0.100	0.042	0.166
LSTINT	0.959	-0.173	0.180	0.022	0.044	0.009
LST75OTI	0.951	-0.189	0.135	0.042	0.009	0.072
PPTBTW	-0.716	0.270	0.512	0.300	0.101	0.070
INTBET	-0.647	0.185	0.508	0.323	0.158	0.342

Reproduced with permission of the copyright owner. Further reproduction prohibited without permission.

Appendix 5.17. Results of principal component analysis on the independent variables using quickflow characterisitcs to the major peak (after removal of the variable - QUICK) at Rio Icacos.

Component loadings

	1	2	3	4	5	6
BASE	0.375	0.060	-0.517	0.739	0.021	-0.156
PKBS	0.464	-0.782	0.088	0.093	-0.228	0.010
LSPKBTI	0.852	0.127	-0.075	-0.196	0.130	0.251
RNBTWTI	-0.739	-0.051	-0.525	0.047	0.185	0.235
QULST	0.973	0.131	0.157	0.002	0.039	-0.026
QU3EVT	0.923	0.150	-0.068	0.121	0.155	0.156
MXTMJPK	0.422	-0.710	0.038	0.164	-0.396	0.312
SMLSPKBSTI	0.975	-0.060	0.123	0.081	-0.021	-0.070
INT15	0.280	-0.771	-0.189	-0.192	0.364	0.101
RRISE	0.364	-0.780	-0.124	-0.131	0.224	-0.366
LSTPPTI	0.968	0.129	0.169	-0.003	0.039	-0.041
LST3PPTI	0.938	0.150	-0.059	0.100	0.148	0.146
LSTINT	0.965	0.134	0.179	0.022	0.037	-0.047
LST75OTI	0.960	0.137	0.136	0.043	0.059	-0.022
PPTBTW	-0.730	-0.219	0.514	0.301	0.121	-0.023
INTBET	-0.655	-0.154	0.511	0.324	0.356	0.167

Reproduced with permission of the copyright owner. Further reproduction prohibited without permission.

Appendix 5.18. Results of principal component analysis on the independent variables using quickflow characterisitcs after varimax rotation to the highest peak at Rio Icacos.

Rotated Loading Matrix (VARIMAX, Gamma = 1.0000)

	1	2	3	4	5	6
BASE	0.203	0.049	0.129	0.948	0.065	-0.029
QUICK	0.241	0.933	0.038	0.046	0.145	-0.000
PKBS	0.210	0.722	0.010	0.036	0.592	0.096
LSPKBTI	0.776	0.102	0.389	0.015	-0.031	0.203
RNBTWTI	-0.819	-0.113	0.019	0.234	-0.264	0.227
QULST	0.955	0.149	0.213	0.065	0.077	-0.002
QU3EVT	0.869	0.056	0.246	0.283	0.035	0.165
MXTMJPK	0.176	0.326	0.049	0.077	0.883	0.211
SMLSPKBSTI	0.890	0.301	0.192	0.134	0.207	0.009
INT15	0.059	0.436	0.039	-0.038	0.279	0.822
RRISE	0.097	0.886	0.076	0.011	0.106	0.358
LSTPPTI	0.954	0.162	0.206	0.054	0.070	-0.014
LST3PPTI	0.882	0.062	0.258	0.262	0.038	0.162
LSTINT	0.957	0.148	0.186	0.068	0.080	-0.019
LST75OTI	0.947	0.095	0.194	0.106	0.094	0.039
PPTBTW	-0.494	0.010	-0.819	-0.132	0.019	-0.142
INTBET	-0.365	-0.102	-0.892	-0.084	-0.076	0.068

Reproduced with permission of the copyright owner. Further reproduction prohibited without permission.

Appendix 5.19. Results of principal component analysis on the independent variables (without the variable - QUICK) after varimax rotation to the highest peak at Rio Icacos.

Rotated Loading Matrix (VARIMAX, Gamma = 1.0000)

	1	2	3	4	5	6
BASE	0.203	0.012	0.135	0.958	0.066	0.017
PKBS	0.227	0.507	0.010	0.045	0.750	-0.146
LSPKBTI	0.788	0.114	0.373	-0.039	0.064	0.295
RNBTWTI	-0.802	0.015	-0.017	0.171	-0.203	0.451
QULST	0.956	0.080	0.223	0.069	0.109	-0.061
QU3EVT	0.875	0.078	0.241	0.249	0.082	0.211
MXTMJPK	0.175	0.268	0.047	0.056	0.924	0.061
SMLSPKBSTI	0.893	0.192	0.205	0.148	0.260	-0.121
INT15	0.072	0.852	0.029	-0.047	0.280	0.275
RRISE	0.122	0.914	0.081	0.062	0.235	-0.204
LSTPPTI	0.955	0.083	0.217	0.061	0.104	-0.078
LST3PPTI	0.888	0.083	0.254	0.230	0.083	0.197
LSTINT	0.957	0.073	0.199	0.077	0.106	-0.089
LST75OTI	0.945	0.076	0.206	0.112	0.098	-0.044
PPTBTW	-0.490	-0.070	-0.818	-0.117	0.021	-0.152
INTBET	-0.356	-0.047	-0.904	-0.105	-0.073	0.107

Reproduced with permission of the copyright owner. Further reproduction prohibited without permission.

Appendix 5.20. Summary of dependent and independent variables used in the statistical analysis for quickflow characteristics to the hihgest peak flow at Rio Icacos near Naguabo

(D indicates dependent variable; L indicates data was log transformed for final statistical operations; SQRT indicates data was transformed by the

Start Date	Start Time hour	Start Discharge ft3/s	End Date	End Time hour	DL Suspended-sediment load tons	DL Discharge-weighted sediment concentration mg/L	L 2-RUN	3-BASE	SQRT 5-PK
5/23/1992	0.25	9.0	5/23/1992	15.25	3.65	314	371880	9.0	107
6/1/1992	11.00	15.0	6/2/1992	3	37.0	893	1329300	15.0	505
7/8/1992	4.00	9.8	7/8/1992	9.25	1.57	196	256410	9.8	76.0
7/16/1992	22.75	9.4	7/17/1992	3.5	1.47	220	214830	9.4	90.0
7/24/1992	2.75	9.0	7/24/1992	7	0.62	209	94950	9.0	48.0
7/26/1992	21.25	7.4	7/27/1992	3	0.28	164	55080	7.4	41.0
8/5/1992	1.25	12.0	8/5/1992	9.75	13.3	1460	291600	12.0	252
8/14/1992	10.50	12.0	8/14/1992	22.5	2.04	103	630900	12.0	66.0
8/30/1992	23.50	9.4	8/31/1992	8.75	1.21	134	289586	9.4	82.0
9/4/1992	14.25	8.4	9/4/1992	20	0.23	100	73530	8.4	31.0
9/16/1992	2.00	6.0	9/16/1992	9.5	1.57	367	137250	6.0	65.0
9/18/1992	21.25	6.9	9/19/1992	4.25	0.35	84.6	133065	6.9	37.0
9/23/1992	18.25	7.9	9/24/1992	2	0.43	144	96255	7.9	44.0
9/30/1992	13.00	5.6	9/30/1992	17.75	0.84	278	96840	5.6	44.0
10/22/1992	16.50	2.9	10/22/1992	23.5	3.36	456	236205	2.9	106
11/2/1992	21.25	4.8	11/3/1992	7	2.81	430	209070	4.8	83.0
11/3/1992	14.50	4.8	11/4/1992	12.5	12.4	204	1940670	4.8	171
11/12/1992	15.00	3.6	11/12/1992	20.5	0.82	151	174870	3.6	72.0
11/16/1992	8.50	5.6	11/16/1992	22	3.79	188	646380	5.6	175
11/18/1992	2.00	9.8	11/18/1992	10.5	3.17	135	752310	9.8	64.0
11/20/1992	13.50	7.9	11/20/1992	22.75	8.43	778	347355	7.9	162
11/22/1992	6.76	20.0	11/23/1992	7.25	5.76	200	925050	7.9	181
12/6/1992	4.25	9.8	12/6/1992	14	12.9	568	728460	9.8	145
12/25/1992	19.25	10.0	12/26/1992	9.75	13.9	377	1181250	10.0	177
12/26/1992	9.76	20.0	12/26/1992	20.75	18.5	832	710958	12.8	343
12/29/1992	12.50	8.4	12/30/1992	16	50.0	1063	1505880	8.4	410
1/22/1993	4.00	11.0	1/23/1993	4.5	7.10	141	1618200	11.0	191
2/20/1993	12.50	9.0	2/21/1993	17.5	15.2	206	2357550	9.0	162
4/30/1993	9.76	27.0	4/30/1993	18.75	32.0	529	1935534	12.3	292
5/1/1993	11.75	16.0	5/2/1993	5.25	29.1	878	1062450	16.0	239
5/2/1993	12.51	24.0	5/2/1993	23.25	7.07	484	467826	16.7	207
5/8/1993	17.00	5.6	5/9/1993	7.75	3.30	284	372690	5.6	138
5/9/1993	12.75	9.4	5/9/1993	19.75	6.18	528	375030	9.4	192
7/7/1993	12.00	7.4	7/7/1993	20.5	10.2	450	726390	7.4	236
7/22/1993	16.01	9.4	7/22/1993	23	10.3	653	503473	8.6	198
9/15/1993	19.00	3.9	9/16/1993	10.75	20.5	689	954495	3.9	328
9/16/1993	11.00	11.0	9/16/1993	23	16.6	594	893700	9.0	337
10/7/1993	1.50	6.4	10/7/1993	12.25	11.3	650	555671	6.4	231
10/22/1993	16.50	6.0	10/22/1993	22.75	5.72	431	424854	6.0	171
12/19/1993	20.25	10.6	12/20/1993	1	2.52	308	262404	10.6	151
2/19/1994	5.50	5.2	2/19/1994	20	268	2558	3353689	5.2	872
2/19/1994	20.01	14.1	2/20/1994	19.75	173	1350	4108004	7.4	562
6/17/1994	9.00	6.4	6/18/1994	2.5	4.51	328	440392	6.4	169
7/17/1994	23.00	5.1	7/18/1994	19	5.93	187	1018712	5.1	169
8/18/1994	19.75	10.0	8/19/1994	7.25	25.4	868	938605	10.0	340
8/23/1994	17.00	3.1	8/24/1994	2	5.32	391	435647	3.1	190
9/7/1994	18.50	3.5	9/8/1994	5.75	8.52	490	557394	3.5	228
9/20/1994	5.26	10.7	9/20/1994	22.75	9.72	302	1030838	7.5	240

Reproduced with permission of the copyright owner. Further reproduction prohibited without permission.

Appendix 5.20. Continued.

Start Date	Start Time hour	End Date	End Time hour	L 6-MXTMJPK	L 11-INT15	L 13-RRISE	17-RNBTWTI	SQRT 18-PPTBTW	SQRT 19-INTBET
5/23/1992	0.25	5/23/1992	15.25	0.4667	0.34	0.64	36672	0.12	0.05
6/1/1992	11.00	6/2/1992	3.00	5.4222	1.13	3.47	41323	0.02	0.01
7/8/1992	4.00	7/8/1992	9.25	0.4904	0.08	0.44	28005	0.92	0.11
7/16/1992	22.75	7/17/1992	3.50	0.8956	0.29	0.77	32283	0.61	0.06
7/24/1992	2.75	7/24/1992	7.00	0.6500	0.14	0.16	36864	1.26	0.20
7/26/1992	21.25	7/27/1992	3.00	0.7467	0.09	0.13	28704	0.02	0.02
8/5/1992	1.25	8/5/1992	9.75	5.3333	0.74	1.30	30803	1.83	0.24
8/14/1992	10.50	8/14/1992	22.50	0.5600	0.34	0.54	38034	0.52	0.15
8/30/1992	23.50	8/31/1992	8.75	0.5378	0.13	0.58	20798	3.19	0.29
9/4/1992	14.25	9/4/1992	20.00	0.3767	0.19	0.37	22894	0.71	0.24
9/16/1992	2.00	9/16/1992	9.50	0.7867	0.50	0.72	22280	0.86	0.24
9/18/1992	21.25	9/19/1992	4.25	0.2867	0.16	0.17	46507	0.38	0.11
9/23/1992	18.25	9/24/1992	2.00	0.6017	0.29	0.37	33411	0.07	0.03
9/30/1992	13.00	9/30/1992	17.75	0.6400	0.47	1.15	22825	0.52	0.14
10/22/1992	16.50	10/22/1992	23.50	1.1456	0.21	0.61	14646	2.71	0.14
11/2/1992	21.25	11/3/1992	7.00	0.7448	0.25	0.63	11911	2.01	0.25
11/3/1992	14.50	11/4/1992	12.50	1.4667	0.58	4.08	20362	0.00	0.00
11/12/1992	15.00	11/12/1992	20.50	0.7600	0.32	0.68	18580	0.00	0.00
11/16/1992	8.50	11/16/1992	22.00	0.5944	0.34	1.15	26854	1.57	0.32
11/18/1992	2.00	11/18/1992	10.50	0.2258	0.11	0.43	41390	0.40	0.06
11/20/1992	13.50	11/20/1992	22.75	1.4676	0.25	0.39	30803	0.17	0.07
11/22/1992	6.76	11/23/1992	7.25	0.8964	0.19	1.31	0	0.02	0.01
12/6/1992	4.25	12/6/1992	14.00	0.5633	0.32	1.64	48428	0.63	0.20
12/25/1992	19.25	12/26/1992	9.75	1.4381	0.35	1.23	50170	0.83	0.09
12/26/1992	9.76	12/26/1992	20.75	2.7007	0.45	1.48	0	0.12	0.10
12/29/1992	12.50	12/30/1992	16.00	1.4091	0.30	1.91	31716	0.20	0.05
1/22/1993	4.00	1/23/1993	4.50	0.2791	0.16	1.71	39340	1.14	0.11
2/20/1993	12.50	2/21/1993	17.50	1.2000	0.36	2.68	31898	0.58	0.10
4/30/1993	9.76	4/30/1993	18.75	2.0381	0.28	1.55	0	0.04	0.02
5/1/1993	11.75	5/2/1993	5.25	3.1333	0.58	2.71	58977	0.01	0.01
5/2/1993	12.51	5/2/1993	23.25	2.4531	0.27	0.83	0	0.00	0.00
5/8/1993	17.00	5/9/1993	7.75	0.4413	0.26	0.83	25686	1.15	0.35
5/9/1993	12.75	5/9/1993	19.75	3.0433	0.34	0.90	39947	0.00	0.00
7/7/1993	12.00	7/7/1993	20.50	1.0886	0.42	1.42	15161	0.09	0.04
7/22/1993	16.01	7/22/1993	23.00	2.5282	0.50	0.78	0	0.00	0.00
9/15/1993	19.00	9/16/1993	10.75	5.5778	0.38	1.07	35792	3.96	0.61
9/16/1993	11.00	9/16/1993	23.00	3.6222	0.14	0.55	0	0.00	0.00
10/7/1993	1.50	10/7/1993	12.25	1.3630	0.51	1.49	20956	0.70	0.07
10/22/1993	16.50	10/22/1993	22.75	1.5737	0.31	0.58	24321	1.36	0.67
12/19/1993	20.25	12/20/1993	1.00	2.3450	0.16	0.45	18053	0.68	0.09
2/19/1994	5.50	2/19/1994	20.00	12.8345	0.58	3.08	15052	2.15	0.24
2/19/1994	20.01	2/20/1994	19.75	4.1599	0.63	4.90	0	0.00	0.00
6/17/1994	9.00	6/18/1994	2.50	1.3509	0.21	0.53	18687	1.51	0.14
7/17/1994	23.00	7/18/1994	19.00	0.4191	0.51	2.05	18682	1.09	0.15
8/18/1994	19.75	8/19/1994	7.25	2.7459	0.33	1.59	35880	0.00	0.00
8/23/1994	17.00	8/24/1994	2.00	1.5534	0.33	1.15	15541	0.41	0.08
9/7/1994	18.50	9/8/1994	5.75	2.1330	0.39	0.94	18561	0.04	0.02
9/20/1994	5.26	9/20/1994	22.75	1.1798	0.37	1.47	0	0.00	0.00

Reproduced with permission of the copyright owner. Further reproduction prohibited without permission.

Appendix 5.20. Continued.

Start Date	Start Time hour	End Date	End Time hour	L 21-LSPKTI	L 23-SMLSPK	L 25-RULST	L 26-PPTLSTI
5/23/1992	0.25	5/23/1992	15.25	2.81	0.71	2.09E+004	0.0461
6/1/1992	11.00	6/2/1992	3.00	1.12	30.3	3.15E+004	0.0142
7/8/1992	4.00	7/8/1992	9.25	0.13	0.22	1.47E+003	0.0022
7/16/1992	22.75	7/17/1992	3.50	0.36	0.44	2.80E+003	0.0023
7/24/1992	2.75	7/24/1992	7.00	0.18	0.33	2.83E+003	0.0013
7/26/1992	21.25	7/27/1992	3.00	0.45	1.02	9.87E+003	0.0035
8/5/1992	1.25	8/5/1992	9.75	0.17	1.18	1.72E+003	0.0006
8/14/1992	10.50	8/14/1992	22.50	2.03	4.16	2.72E+004	0.0227
8/30/1992	23.50	8/31/1992	8.75	0.16	0.21	2.94E+003	0.0014
9/4/1992	14.25	9/4/1992	20.00	0.62	0.31	1.04E+004	0.0076
9/16/1992	2.00	9/16/1992	9.50	0.19	0.41	4.53E+003	0.0021
9/18/1992	21.25	9/19/1992	4.25	0.89	1.87	2.01E+004	0.0167
9/23/1992	18.25	9/24/1992	2.00	2.03	5.18	5.09E+004	0.0200
9/30/1992	13.00	9/30/1992	17.75	0.24	0.28	3.58E+003	0.0025
10/22/1992	16.50	10/22/1992	23.50	0.08	0.2	6.91E+002	0.0022
11/2/1992	21.25	11/3/1992	7.00	0.37	0.32	2.93E+003	0.0023
11/3/1992	14.50	11/4/1992	12.50	2.26	70.1	1.25E+005	0.1053
11/12/1992	15.00	11/12/1992	20.50	2.28	1.46	3.79E+004	0.0339
11/16/1992	8.50	11/16/1992	22.00	0.70	2.08	6.36E+003	0.0081
11/18/1992	2.00	11/18/1992	10.50	3.87	2.29	7.12E+004	0.0439
11/20/1992	13.50	11/20/1992	22.75	0.52	4.91	1.48E+004	0.0088
11/22/1992	6.76	11/23/1992	7.25	3.42	27150	3.35E+008	288
12/6/1992	4.25	12/6/1992	14.00	0.86	3.41	2.33E+004	0.0139
12/25/1992	19.25	12/26/1992	9.75	1.07	9.76	5.48E+004	0.0374
12/26/1992	9.76	12/26/1992	20.75	6.32	51450	4.12E+008	205
12/29/1992	12.50	12/30/1992	16.00	1.31	51.3	7.24E+004	0.0292
1/22/1993	4.00	1/23/1993	4.50	0.17	1.44	3.90E+003	0.0008
2/20/1993	12.50	2/21/1993	17.50	0.15	1.9	1.61E+003	0.0018
4/30/1993	9.76	4/30/1993	18.75	3.25	61950	3.24E+008	458
5/1/1993	11.75	5/2/1993	5.25	1.79	57.09	1.28E+005	0.0909
5/2/1993	12.51	5/2/1993	23.25	9.89	31050	2.34E+008	84.0
5/8/1993	17.00	5/9/1993	7.75	0.64	1.16	1.16E+004	0.0067
5/9/1993	12.75	5/9/1993	19.75	4.35	38.4	3.21E+005	0.2060
7/7/1993	12.00	7/7/1993	20.50	0.54	2.5	8.27E+003	0.0069
7/22/1993	16.01	7/22/1993	23.00	4.28	29700	1.13E+008	117
9/15/1993	19.00	9/16/1993	10.75	0.63	2.51	3.84E+003	0.0047
9/16/1993	11.00	9/16/1993	23.00	10.09	1348	1.60E+007	8.4894
10/7/1993	1.50	10/7/1993	12.25	0.38	2.61	5.00E+003	0.0032
10/22/1993	16.50	10/22/1993	22.75	0.39	3.02	1.62E+004	0.0136
12/19/1993	20.25	12/20/1993	1.00	0.10	0.46	1.21E+003	0.0004
2/19/1994	5.50	2/19/1994	20.00	0.11	4.07	1.29E+003	0.0017
2/19/1994	20.01	2/20/1994	19.75	74.16	193159	1.00E+009	501
6/17/1994	9.00	6/18/1994	2.50	0.21	1.31	6.92E+003	0.0069
7/17/1994	23.00	7/18/1994	19.00	0.11	0.62	1.74E+003	0.0012
8/18/1994	19.75	8/19/1994	7.25	3.12	84.9	1.85E+005	0.2575
8/23/1994	17.00	8/24/1994	2.00	2.51	1.79	2.92E+004	0.0163
9/7/1994	18.50	9/8/1994	5.75	2.10	9.89	6.92E+004	0.0500
9/20/1994	5.26	9/20/1994	22.75	3.16	36047	2.32E+008	186

Reproduced with permission of the copyright owner. Further reproduction prohibited without permission.

Appendix 5.20. Continued.

Start Date	Start Time hour	End Date	End Time hour	L 27-INTLST	L 28-LS75OTI	29-SUM3PPTI	31-RU3EVT
5/23/1992	0.25	5/23/1992	15.25	0.0080	0.0002	-5.24	12.3
6/1/1992	11	6/2/1992	3	0.0071	0.0002	-5.05	13.3
7/8/1992	4	7/8/1992	9.25	0.0008	0.0000	-8.81	9.3
7/16/1992	22.75	7/17/1992	3.5	0.0004	0.0000	-9.11	9.2
7/24/1992	2.75	7/24/1992	7	0.0008	0.0000	-8.15	10.9
7/26/1992	21.25	7/27/1992	3	0.0015	0.0000	-7.12	11.7
8/5/1992	1.25	8/5/1992	9.75	0.0004	0.0000	-9.32	9.6
8/14/1992	10.5	8/14/1992	22.5	0.0181	0.0012	-6.11	12.4
8/30/1992	23.5	8/31/1992	8.75	0.0009	0.0000	-8.54	10.2
9/4/1992	14.25	9/4/1992	20	0.0013	0.0000	-8.07	10.5
9/16/1992	2	9/16/1992	9.5	0.0005	0.0000	-7.89	10.4
9/18/1992	21.25	9/19/1992	4.25	0.0071	0.0000	-6.50	11.9
9/23/1992	18.25	9/24/1992	2	0.0082	0.0003	-4.76	13.8
9/30/1992	13	9/30/1992	17.75	0.0019	0.0001	-7.40	11.3
10/22/1992	16.5	10/22/1992	23.5	0.0009	0.0000	-9.52	8.5
11/2/1992	21.25	11/3/1992	7	0.0008	0.0000	-8.85	8.9
11/3/1992	14.5	11/4/1992	12.5	0.0333	0.0004	-6.48	11.2
11/12/1992	15	11/12/1992	20.5	0.0063	0.0001	-6.56	11.8
11/16/1992	8.5	11/16/1992	22	0.0038	0.0001	-6.65	11.3
11/18/1992	2	11/18/1992	10.5	0.0121	0.0001	-5.66	12.5
11/20/1992	13.5	11/20/1992	22.75	0.0018	0.0000	-5.64	13.3
11/22/1992	6.7566667	11/23/1992	7.25	42.0	0.2939	-1.72	17.0
12/6/1992	4.25	12/6/1992	14	0.0042	0.0000	-6.40	12.6
12/25/1992	19.25	12/26/1992	9.75	0.0082	0.0001	-5.73	12.6
12/26/1992	9.7566667	12/26/1992	20.75	52.5	0.3821	-1.26	17.4
12/29/1992	12.5	12/30/1992	16	0.0108	0.0001	-5.04	13.8
1/22/1993	4	1/23/1993	4.5	0.0003	0.0000	-9.28	10.3
2/20/1993	12.5	2/21/1993	17.5	0.0006	0.0000	-8.11	10.3
4/30/1993	9.7566667	4/30/1993	18.75	73.5	0.7387	-2.99	15.1
5/1/1993	11.75	5/2/1993	5.25	0.0097	0.0003	-2.99	15.3
5/2/1993	12.506667	5/2/1993	23.25	28.5	0.4200	0.12	18.7
5/8/1993	17	5/9/1993	7.75	0.0018	0.0000	-6.77	12.3
5/9/1993	12.75	5/9/1993	19.75	0.0520	0.0005	-5.16	13.7
7/7/1993	12	7/7/1993	20.5	0.0015	0.0000	-7.18	10.9
7/22/1993	16.006667	7/22/1993	23	37.5	0.5583	-1.40	16.5
9/15/1993	19	9/16/1993	10.75	0.0022	0.0000	-7.75	10.4
9/16/1993	11	9/16/1993	23	1.9200	0.0131	-3.75	14.5
10/7/1993	1.5	10/7/1993	12.25	0.0015	0.0000	-7.70	11.4
10/22/1993	16.5	10/22/1993	22.75	0.0023	0.0000	-6.30	11.9
12/19/1993	20.25	12/20/1993	1	0.0003	0.0000	-8.89	9.9
2/19/1994	5.5	2/19/1994	20	0.0004	0.0000	-8.54	9.5
2/19/1994	20.006667	2/20/1994	19.75	87.0	0.7000	-2.89	15.4
6/17/1994	9	6/18/1994	2.5	0.0016	0.0000	-7.28	11.0
7/17/1994	23	7/18/1994	19	0.0004	0.0000	-8.29	10.4
8/18/1994	19.75	8/19/1994	7.25	0.0850	0.0006	-5.81	12.3
8/23/1994	17	8/24/1994	2	0.0031	0.0000	-6.34	11.9
9/7/1994	18.5	9/8/1994	5.75	0.0130	0.0001	-6.54	11.7
9/20/1994	5.2566667	9/20/1994	22.75	66.8	0.3500	-2.79	15.9

**to eliminate zero values a value of 0.0002 was added to the precipitation between events and a value of 5000 was added to the runoff between events.

Reproduced with permission of the copyright owner. Further reproduction prohibited without permission.

Appendix 5.21. Pearson correlation matrix for the dependent and independent variables using runoff characteristics to the highest peak.

	SED	RUSEDCONC	BASE	RUN
SED	1.000			
RUSEDCONC	0.774	1.000		
BASE	0.184	0.204	1.000	
RUN	0.895	0.419	0.174	1.000
PK	0.936	0.791	0.145	0.794
LSPKTI	0.305	0.163	0.242	0.320
RNBTWTI	-0.280	-0.172	-0.029	-0.246
RULST	0.361	0.197	0.331	0.368
RU3EVT	0.304	0.216	0.467	0.286
MXTMJPK	0.725	0.816	0.168	0.453
SMLSPKTI	0.530	0.337	0.360	0.516
INT15	0.570	0.564	0.029	0.428
RRISE	0.807	0.488	0.107	0.819
LSTPPTI	0.373	0.196	0.288	0.384
LST3PPTI	0.331	0.227	0.426	0.313
LSTINT	0.360	0.189	0.302	0.371
LST75OTI	0.330	0.205	0.341	0.324
PPTBTW	-0.132	-0.066	-0.323	-0.146
INTBET	-0.186	-0.072	-0.299	-0.208

	PK	LSPKTI	RNBTWTI	RULST	RU3EVT
PK	1.000				
LSPKTI	0.283	1.000			
RNBTWTI	-0.333	-0.479	1.000		
RULST	0.352	0.839	-0.791	1.000	
RU3EVT	0.290	0.801	-0.584	0.906	1.000
MXTMJPK	0.804	0.234	-0.307	0.295	0.250
SMLSPKTI	0.521	0.777	-0.775	0.970	0.881
INT15	0.539	0.187	-0.057	0.137	0.166
RRISE	0.722	0.215	-0.180	0.249	0.185
LSTPPTI	0.354	0.832	-0.795	0.992	0.883
LST3PPTI	0.309	0.836	-0.607	0.918	0.985
LSTINT	0.347	0.818	-0.801	0.989	0.881
LST75OTI	0.319	0.813	-0.782	0.970	0.883
PPTBTW	-0.127	-0.730	0.333	-0.659	-0.698
INTBET	-0.176	-0.608	0.346	-0.571	-0.549

Reproduced with permission of the copyright owner. Further reproduction prohibited without permission.

Appendix 5.21. Continued.

	MXTMJPK	SMLSPKTI	INT15	RRISE	LSTPPTI
MXTMJPK	1.000				
SMLSPKTI	0.447	1.000			
INT15	0.546	0.259	1.000		
RRISE	0.474	0.395	0.734	1.000	
LSTPPTI	0.298	0.963	0.144	0.258	1.000
LST3PPTI	0.282	0.892	0.197	0.205	0.909
LSTINT	0.299	0.965	0.142	0.245	0.994
LST75OTI	0.303	0.948	0.176	0.226	0.976
PPTBTW	-0.138	-0.624	-0.162	-0.151	-0.640
INTBET	-0.189	-0.563	-0.094	-0.198	-0.561

	LST3PPTI	LSTINT	LST75OTI	PPTBTW	INTBET
LST3PPTI	1.000				
LSTINT	0.902	1.000			
LST75OTI	0.908	0.986	1.000		
PPTBTW	-0.707	-0.622	-0.637	1.000	
INTBET	-0.562	-0.553	-0.557	0.880	1.000

Reproduced with permission of the copyright owner. Further reproduction prohibited without permission.

Appendix 5.22. Results of principal component analysis on the independent variables using runoff characteristics to the highest peakflow, at Rio Icacos.

Component loadings

	1	2	3	4	5	6
BASE	0.385	-0.062	-0.504	0.740	0.000	-0.008
RUN	0.494	0.687	-0.001	0.065	0.445	-0.207
PK	0.500	0.777	0.080	0.094	-0.094	-0.226
LSPKTI	0.852	-0.170	-0.115	-0.167	0.054	0.108
RNBTWTI	-0.729	0.093	-0.538	0.072	0.092	0.154
RULST	0.968	-0.173	0.145	0.022	0.041	0.018
RU3EVT	0.911	-0.214	-0.073	0.145	0.000	0.173
MXTMJPK	0.436	0.639	0.044	0.110	-0.578	-0.145
SMLSPKTI	0.980	0.024	0.126	0.063	0.019	-0.029
INT15	0.298	0.705	-0.188	-0.224	-0.169	0.510
RRISE	0.402	0.802	-0.121	-0.124	0.302	0.077
LSTPPTI	0.962	-0.159	0.178	-0.009	0.052	0.017
LST3PPTI	0.931	-0.191	-0.051	0.094	-0.010	0.174
LSTINT	0.959	-0.165	0.189	0.015	0.040	0.021
LST75OTI	0.952	-0.180	0.146	0.031	-0.011	0.075
PPTBTW	-0.722	0.260	0.508	0.307	0.072	0.086
INTBET	-0.652	0.177	0.503	0.330	0.067	0.360

Reproduced with permission of the copyright owner. Further reproduction prohibited without permission.

Appendix 5.23. Factor loadings scores for the first 6 principal components for runoff characteristics to the highest peakflow (without the variable- RUN) at Rio Icacos.

Component loadings

	1	2	3	4	5	6
BASE	0.386	0.057	-0.504	0.739	0.010	0.168
PK	0.462	-0.782	0.080	0.104	-0.228	0.007
LSPKTI	0.858	0.136	-0.115	-0.170	0.109	-0.243
RNBTWTI	-0.735	-0.045	-0.538	0.067	0.170	-0.229
RULST	0.974	0.133	0.146	0.019	0.038	0.031
RU3EVT	0.920	0.167	-0.073	0.147	0.147	-0.130
MXTMJPK	0.416	-0.714	0.043	0.154	-0.411	-0.297
SMLSPKTI	0.976	-0.059	0.126	0.063	-0.010	0.064
INT15	0.274	-0.773	-0.189	-0.189	0.365	-0.128
RRISE	0.360	-0.782	-0.121	-0.131	0.242	0.358
LSTPPTI	0.968	0.122	0.178	-0.012	0.041	0.031
LST3PPTI	0.939	0.144	-0.051	0.097	0.140	-0.156
LSTINT	0.965	0.126	0.189	0.012	0.040	0.037
LST75OTI	0.960	0.129	0.146	0.033	0.060	0.009
PPTBTW	-0.735	-0.214	0.508	0.304	0.117	0.025
INTBET	-0.659	-0.149	0.503	0.333	0.345	-0.182

Reproduced with permission of the copyright owner. Further reproduction prohibited without permission.

Appendix 5.24. Results of principal component analysis on the independent variables using runoff characteristics to the highest peak after varimax rotation at Rio Icacos.

Rotated Loading Matrix (VARIMAX, Gamma = 1.0000)

	1	2	3	4	5	6
BASE	0.209	0.066	0.126	0.940	0.071	-0.036
RUN	0.225	0.942	0.039	0.080	0.126	0.011
PK	0.210	0.703	0.013	0.047	0.614	0.107
LSPKTI	0.763	0.111	0.423	0.065	-0.042	0.176
RNBTWTI	-0.823	-0.090	0.022	0.254	-0.277	0.200
RULST	0.952	0.143	0.221	0.089	0.079	-0.005
RU3EVT	0.865	0.046	0.250	0.314	0.018	0.142
MXTMJPK	0.174	0.289	0.051	0.076	0.891	0.224
SMLSPKTI	0.893	0.290	0.203	0.121	0.207	0.026
INT15	0.056	0.404	0.043	-0.041	0.288	0.841
RRISE	0.099	0.865	0.076	-0.011	0.142	0.386
LSTPPTI	0.954	0.158	0.209	0.045	0.077	-0.005
LST3PPTI	0.881	0.062	0.263	0.262	0.036	0.161
LSTINT	0.958	0.144	0.189	0.058	0.086	-0.010
LST75OTI	0.948	0.092	0.197	0.098	0.098	0.047
PPTBTW	-0.492	0.008	-0.821	-0.133	0.021	-0.138
INTBET	-0.365	-0.097	-0.891	-0.076	-0.085	0.064

Reproduced with permission of the copyright owner. Further reproduction prohibited without permission.

Appendix 5.25. Results of principal component analysis on the independent variables using runoff characteristics to the highest peak after varimax rotation (without the variable RUN) at Rio Icacos.

Rotated Loading Matrix (VARIMAX, Gamma = 1.0000)

	1	2	3	4	5	6
BASE	0.211	0.011	0.132	0.956	0.071	-0.017
PK	0.226	0.504	0.012	0.067	0.750	0.147
LSPKTI	0.778	0.106	0.404	0.004	0.060	-0.292
RNBTWTI	-0.804	0.014	-0.013	0.183	-0.205	-0.442
RULST	0.953	0.074	0.230	0.096	0.107	0.062
RU3EVT	0.871	0.067	0.244	0.279	0.061	-0.191
MXTMJPK	0.172	0.266	0.047	0.048	0.926	-0.062
SMLSPKTI	0.896	0.195	0.213	0.138	0.251	0.109
INT15	0.068	0.851	0.030	-0.056	0.284	-0.283
RRISE	0.121	0.914	0.082	0.065	0.236	0.208
LSTPPTI	0.955	0.084	0.217	0.053	0.108	0.071
LST3PPTI	0.888	0.084	0.256	0.222	0.085	-0.203
LSTINT	0.958	0.074	0.199	0.068	0.110	0.081
LST75OTI	0.946	0.077	0.206	0.101	0.103	0.035
PPTBTW	-0.490	-0.070	-0.818	-0.113	0.019	0.154
INTBET	-0.356	-0.047	-0.903	-0.104	-0.073	-0.112

Reproduced with permission of the copyright owner. Further reproduction prohibited without permission.

Appendix 5.26. Summary of dependent and independent variables used in the statistical analysis for hysteresis.
(A) Type 1 storms and (B) Type 3 storms.
(D indicates dependent variable; L indicates log transformed; IR indicates negative inverse square root transformed)

A. Start Date	Start Time hour	End Date	End Time hour	Width of clockwise loop, mg/L D L	Discharge used in width analysis, ft3/s	Sediment load, tons SED L	Discharge-weighted sediment concentration, mg/L CONC L	Runoff ft3 2-RUN L	L Sum of peak flows 9-SMPK L	Maximum rate of hydrograph rise to the highest peak, cfs/min 6-MXTMJPK L	Runoff of the previous event divided by the time since the previous event, fts/hour 25-RULST L
5/23/1992	0.25	5/23/1992	15.25	98	86.8	45.0	758	1.90E+006	107	0.4667	2.09E+004
7/8/1992	4.00	7/8/1992	9.25	78	60.8	3.9	217	5.76E+005	76	0.4904	1.47E+003
7/16/1992	22.75	7/17/1992	3.5	141	76.5	5.8	228	8.12E+005	90	0.8956	2.80E+003
7/24/1992	2.75	7/24/1992	7	47	43.9	1.6	145	3.60E+005	48	0.6500	2.83E+003
8/5/1992	1.25	8/5/1992	9.75	761	158.0	53.9	865	2.00E+006	252	5.3333	1.72E+003
8/14/1992	10.50	8/14/1992	22.5	56	43.2	4.0	114	1.13E+006	101	0.5600	2.72E+004
9/4/1992	14.25	9/4/1992	20	27	30.3	0.7	58.0	3.87E+005	31	0.3767	1.04E+004
9/16/1992	2.00	9/16/1992	9.5	188	44.7	4.8	210	7.31E+005	65	0.7867	4.53E+003
9/18/1992	21.25	9/19/1992	4.25	40	34.0	1.1	70.8	4.85E+005	37	0.2867	2.01E+004
9/30/1992	13.00	9/30/1992	17.75	192	42.7	1.5	131	3.64E+005	44	0.6400	3.58E+003
10/22/1992	16.50	10/22/1992	23.5	187	63.3	7.7	323	7.67E+005	106	1.1456	6.91E+002
11/2/1992	21.25	11/3/1992	7	162	64.5	6.1	208	9.40E+005	83	0.7448	2.93E+003
11/3/1992	14.50	11/4/1992	12.5	110	123.9	31.3	223	4.50E+006	526	1.4667	1.25E+005
11/18/1992	2.00	11/18/1992	10.5	85	61.8	4.0	101	1.26E+006	64	0.2258	7.12E+004
11/20/1992	13.50	11/20/1992	22.75	472	82.6	18.0	434	1.33E+006	162	1.4676	1.48E+004
11/22/1992	6.76	11/23/1992	7.25	94	125.4	16.3	114	4.57E+006	181	0.8964	3.35E+008
12/6/1992	4.25	12/6/1992	14	935	94.3	17.1	338	1.62E+006	145	0.5633	2.33E+004
12/25/1992	19.25	12/26/1992	9.75	452	105.5	22.0	257	2.75E+006	227	1.4381	5.48E+004
12/26/1992	9.76	12/26/1992	20.75	369	190.2	67.7	612	3.55E+006	343	2.7007	4.12E+008
12/29/1992	12.50	12/30/1992	16	955	291.0	177	613	9.27E+006	756	1.4091	7.24E+004
1/22/1993	4.00	1/23/1993	4.5	90	177.6	24.0	165	4.65E+006	288	0.2791	3.90E+003
2/20/1993	12.50	2/21/1993	17.5	82	102.9	31.9	172	5.94E+006	364	1.2000	1.61E+003
4/30/1993	9.76	4/30/1993	18.75	452	228.4	45.4	419	3.47E+006	413	2.0381	3.24E+008
5/2/1993	12.51	5/2/1993	23.25	300	180.0	18.9	268	2.26E+006	207	2.4531	2.34E+008
7/7/1993	12.00	7/7/1993	20.5	584	171.0	27.6	459	1.92E+006	236	1.0886	8.27E+003
7/22/1993	16.01	7/22/1993	23	203	191.0	15.4	344	1.44E+006	198	2.5282	1.13E+008
9/15/1993	19.00	9/16/1993	10.75	681	210.5	47.6	381	4.01E+006	543	5.5778	3.84E+003
9/16/1993	11.00	9/16/1993	23	156	264.8	44.7	451	3.17E+006	337	3.6222	1.60E+007
10/7/1993	1.50	10/7/1993	12.25	462	188.0	19.5	350	1.79E+006	231.3	1.3630	5.00E+003
12/19/1993	20.25	12/20/1993	1	238	153.4	11.5	350	1.05E+006	151.3	2.3450	1.21E+003
2/19/1994	5.50	2/19/1994	20	1548	511.0	404	1941	6.67E+006	1423	12.8345	1.29E+003
2/19/1994	20.01	2/20/1994	19.75	841	538.0	368	1126	1.05E+007	1287.7	4.1599	1.00E+009
6/17/1994	9.00	6/18/1994	2.5	110	155.0	13.0	155	2.68E+006	168.5	1.3509	6.92E+003
8/18/1994	19.75	8/19/1994	7.25	439	316.0	45.8	474	3.09E+006	339.5	2.7459	1.85E+005
8/23/1994	17.00	8/24/1994	2	108	177.0	8.3	176	1.51E+006	189.5	1.5534	2.92E+004
9/7/1994	18.50	9/8/1994	5.75	150	201.0	17.0	256	2.13E+006	227.5	2.1330	6.92E+004
9/20/1994	5.26	9/20/1994	22.75	183	220.0	28.3	220.5	4.12E+006	240.3	1.1798	2.32E+008
			AVERAGE	326	157	45	371	2694101	278	2	72092194

Reproduced with permission of the copyright owner. Further reproduction prohibited without permission.

Appendix 5.26. Continued.

Start Date	Start Time hour	End Date	End Time hour	Runoff of the 3 previous events divided by the time since the 3 events 31-RU3EVT L	Sediment transport curve slope on falling limb, cfs/(mg/L) 33-RATE_FALL L	Rainfall on the rising limb to the highest peak, in 13-RRISE L	Rainfall on the falling limb after the highest peak, in 14-RAINFOL L	Seventy five percent rainfall intensity of current event, in/min 12-SFIVE L	Runoff since the previous event over time since the previous event ft3/hour 17-RNBTWTI	Sediment transport curve slope on rising limb, cfs/(mg/L 32-RATE_RISE	Time of peak sediment concentration relative to peak flow (minutes) 34-TIME_PKCON
5/23/1992	0.25	5/23/1992	15.25	12.3	3.83	0.64	0.28	0.0022	41672	4.95	-10
7/8/1992	4.00	7/8/1992	9.25	9.3	5.27	0.44	0.04	0.0031	33005	4.77	0
7/16/1992	22.75	7/17/1992	3.5	9.2	5.14	0.77	0.01	0.0064	37283	1.05	-10
7/24/1992	2.75	7/24/1992	7	10.9	3.31	0.16	0.00	0.0050	41864	7.39	-10
8/5/1992	1.25	8/5/1992	9.75	9.6	6.42	1.30	0.28	0.0173	35803	0.96	-0
8/14/1992	10.50	8/14/1992	22.5	12.4	3.46	0.54	0.00	0.0014	43034	3.42	15
9/4/1992	14.25	9/4/1992	20	10.5	20.45	0.37	0.10	0.0031	27894	2.43	0
9/16/1992	2.00	9/16/1992	9.5	10.4	5.29	0.72	0.04	0.0112	27280	4.63	-16
9/18/1992	21.25	9/19/1992	4.25	11.9	1.48	0.17	0.01	0.0107	51507	4.04	-30
9/30/1992	13.00	9/30/1992	17.75	11.3	5.59	1.15	0.02	0.0098	27825	8.45	-19
10/22/1992	16.50	10/22/1992	23.5	8.5	5.32	0.61	0.01	0.0034	19646	3.78	-11
11/2/1992	21.25	11/3/1992	7	8.9	5.20	0.63	0.16	0.0030	16911	-4.49	-40
11/3/1992	14.50	11/4/1992	12.5	11.2	5.89	4.08	1.01	0.0045	25362	5.91	-15
11/18/1992	2.00	11/18/1992	10.5	12.5	1.51	0.43	0.21	0.0015	46390	3.53	-183
11/20/1992	13.50	11/20/1992	22.75	13.3	5.68	0.39	0.15	0.0020	35803	1.34	0
11/22/1992	6.76	11/23/1992	7.25	17.0	2.18	1.31	1.63	0.0037	5000	2.97	-23
12/6/1992	4.25	12/6/1992	14	12.6	3.32	1.64	0.01	0.0052	53428	-9.09	-75
12/25/1992	19.25	12/26/1992	9.75	12.6	2.42	1.23	0.14	0.0025	55170	3.40	-80
12/26/1992	9.76	12/26/1992	20.75	17.4	3.95	1.48	0.43	0.0076	5000	2.23	0
12/29/1992	12.50	12/30/1992	16	13.8	3.32	1.91	2.90	0.0060	36716	5.58	-50
1/22/1993	4.00	1/23/1993	4.5	10.3	3.35	1.71	0.81	0.0022	44340	4.24	-8
2/20/1993	12.50	2/21/1993	17.5	10.3	3.00	2.68	1.35	0.0045	36898	1.89	2
4/30/1993	9.76	4/30/1993	18.75	15.1	1.90	1.55	0.09	0.0047	5000	4.16	-37
5/2/1993	12.51	5/2/1993	23.25	18.7	1.82	0.83	0.09	0.0109	5000	3.73	-1
7/7/1993	12.00	7/7/1993	20.5	10.9	3.68	1.42	0.04	0.0024	20161	6.12	-6
7/22/1993	16.01	7/22/1993	23	16.5	2.86	0.78	0.01	0.0099	5000	3.45	-15
9/15/1993	19.00	9/16/1993	10.75	10.4	2.09	1.07	1.05	0.0033	40792	-1.40	-21
9/16/1993	11.00	9/16/1993	23	14.5	3.70	0.55	0.16	0.0039	5000	2.66	9
10/7/1993	1.50	10/7/1993	12.25	11.4	2.58	1.49	0.19	0.0067	25956	-3.91	-20
12/19/1993	20.25	12/20/1993	1	9.9	4.07	0.45	0.01	0.0071	23053	5.49	-20
2/19/1994	5.50	2/19/1994	20	9.5	3.77	3.08	0.26	0.0047	20052	-1.12	-90
2/19/1994	20.01	2/20/1994	19.75	15.4	3.11	4.90	1.21	0.0170	5000	5.07	-20
6/17/1994	9.00	6/18/1994	2.5	11.0	2.98	0.53	0.54	0.0031	23687	-6.42	-15
8/18/1994	19.75	8/19/1994	7.25	12.3	2.43	1.59	0.14	0.0049	40880	3.15	-21
8/23/1994	17.00	8/24/1994	2	11.9	2.21	1.15	0.06	0.0067	20541	-3.34	-25
9/7/1994	18.50	9/8/1994	5.75	11.7	2.84	0.94	0.24	0.0059	23561	1.24	-25
9/20/1994	5.26	9/20/1994	22.75	15.9	1.87	1.47	0.65	0.0036	5000	2.71	-10
			AVERAGE	11	4	1	0.3411	0.0050	24793	**Average negative slope = -20.5**	-21
										Average positive slope = 3.67	

Reproduced with permission of the copyright owner. Further reproduction prohibited without permission.

Appendix 5.26. Continued.

B.

Start Date	Start Time hour	End Date	End Time hour	Width of counter-clockwise loop. mg/L D IR	Discharge used in width analysis, ft3/s	Sediment load tons	Discharge-weighted sediment concentration, mg/L	Runoff ft3 2-RUN	Sum of peak flows 9-SMPK	Maximum rate of hydrograph rise to the highest peak, cfs/min 6-MXTMJPK
8/30/1992	23.5	8/31/1992	8.75	280	68.2	5.0	150	1058580	82	0.5378
11/12/1992	15	11/12/1992	20.5	36	67.6	2	116	534060	72	0.7600
11/16/1992	8.5	11/16/1992	22	48	172.0	19.2	308	1992959.9955	175	0.5944
5/1/1993	11.75	5/2/1993	5.25	1420	219.0	150	895	5352300.00000001	471	3.1333
			AVERAGE	**446**	**132**	**44**	**367**	**2234475**	**200**	**1**

Start Date	Start Time hour	End Date	End Time hour	Runoff of the 3 previous events divided by the time since the 3 events 31-'RU3EVT	Sediment transport cu slope on falling limb, cfs/(mg/L) 32-RATE_FALL	Rainfall on the rising limb to the highest peak, in 13-RRISE	Rainfall on the falling limb after the highest peak, in 14-RAINFOL L	Seventy five percent rainfall intensity of current event, in/min 12-SFIVE	Runoff since the previous event over time since the previous event ft3/hour 17-RNBTWTI	Sediment transport curve slope on rising limb, cfs/(mg/L 32-RATE_RISE
8/30/1992	23.5	8/31/1992	8.75	10.2	5.83	0.58	0.19	0.0018	25798	4.22
11/12/1992	15	11/12/1992	20.5	11.8	4.70	0.68	0.00	0.0120	23580	7.16
11/16/1992	8.5	11/16/1992	22	11.3	3.40	1.15	0.08	0.0038	31854	2.73
5/1/1993	11.75	5/2/1993	5.25	15.3	25.02	2.71	2.27	0.0062	63977	21.07
			AVERAGE	**12**	**10**	**1.2800**	**0.6350**	**0.0060**	**36302**	**8.79**

Reproduced with permission of the copyright owner. Further reproduction prohibited without permission.

Appendix 6.1. Relation of calculated quickflow to estimated quickflow. Estimated quickflow is calculated from rain falling on impervious basin Quebrada Blanca basin area = 3.24 sq.mi.

Start Date	Hour	End Date	Hour	Rainfall amount, in	Estimated volume of quickflow corresponding to impervious contributing area, ft3)	Calculated quickflow, ft3	Percent ratio: calculated quickflow/ estimated quickflow
8/11/1989	16.00	8/12/1989	5.75	1.06	7.97E+006	7.43E+005	9
8/18/1989	22.00	8/19/1989	23.25	1.84	1.39E+007	2.08E+006	15
9/13/1989	21.50	9/14/1989	20.00	1.56	1.17E+007	1.03E+006	9
9/18/1989	2.75	9/20/1989	7.75	7.22	5.44E+007	1.11E+007	21
9/22/1989	9.00	9/22/1989	21.50	1.46	1.10E+007	1.54E+006	14
10/1/1989	13.75	10/2/1989	1.25	0.52	3.93E+006	4.03E+005	10
5/9/1990	19.25	5/10/1990	20.00	2.02	1.52E+007	1.45E+006	10
6/14/1990	14.00	6/15/1990	11.50	4.09	3.08E+007	1.26E+006	4
8/7/1990	17.00	8/9/1990	13.50	1.86	1.40E+007	1.79E+006	13
8/9/1990	13.75	8/12/1990	21.75	3.02	2.27E+007	6.22E+006	27
10/16/1990	12.00	10/17/1990	14.75	1.12	8.44E+006	1.73E+006	20
10/24/1990	18.75	10/25/1990	15.25	1.39	1.04E+007	2.31E+006	22
11/4/1990	12.25	11/5/1990	14.50	1.48	1.11E+007	2.82E+006	25
12/30/1990	19.25	1/2/1991	6.75	2.14	1.61E+007	4.61E+006	29
7/15/1991	13.25	7/16/1991	2.75	1.55	1.17E+007	1.56E+006	13
8/27/1991	10.00	8/28/1991	15.25	2.06	1.55E+007	3.05E+006	20
9/17/1991	2.42	9/18/1991	10.75	2.74	2.06E+007	3.94E+006	19
9/22/1991	8.50	9/23/1991	17.75	1.21	9.10E+006	3.37E+006	37
11/28/1991	12.25	12/1/1991	11.75	0.52	3.93E+006	3.86E+006	98
5/16/1992	4.00	5/17/1992	8.75	1.89	1.42E+007	1.45E+006	10
6/4/1992	8.50	6/5/1992	13.50	1.31	9.83E+006	2.38E+006	24
7/22/1993	16.00	7/23/1993	2.75	2.31	1.74E+007	2.69E+006	16
8/15/1993	21.50	8/17/1993	17.00	2.26	1.70E+007	6.48E+006	38

Reproduced with permission of the copyright owner. Further reproduction prohibited without permission.

Appendix 6.2 Summary of dependent and independent variables used in the statistical analysis for quickflow characteristics of the entire event at Quebrada Blanca near El Jagual (D indicates dependent variable; L indicates data was log transformed for final statistical operations; IR indicates data had negative inverse square root transformed)

Start Date	Start Time hour	Start Discharge ft3/s	End Date	End Time hour	Hours since End of Last Event	DL Suspended-sediment load tons	DL Discharge-weighted sediment concentration mg/L	L Quickflow, ft3 1-QUICK	L Previous event peak flow minus baseflow over time since last peak, ft3/s/hour 20-LSPKBTI	L Previous event quickflow over the time since previous event, ft3/hour 24-QULST
08/11/1989	16	0.98	08/12/1989	5.75	151.0	6.5	282	742990	0.13	1725
08/18/1989	22	3.1	08/19/1989	23.25	14.0	63	966	2079900	1.46	72270
09/13/1989	21.5	3.1	09/14/1989	20	30.5	12	382	1027890	0.45	9626
09/18/1989	2.75	7.3	09/20/1989	7.75	0.3	376	1081	11147630	2.70	1745442
09/22/1989	9	4.4	09/22/1989	21.5	49.3	52	1086	1537030	5.54	226348
10/01/1989	13.75	7	10/02/1989	1.25	31.2	5.2	411	403070	2.60	48444
05/09/1990	19.25	0.73	05/10/1990	20	321.5	34	753	1452430	0.03	757
06/14/1990	14	1.4	06/15/1990	11.5	798.5	36	912	1257480	0.02	638
08/07/1990	17	3.3	08/09/1990	13.5	1255.0	7.9	141	1788130	0.01	101
08/09/1990	13.75	12	08/12/1990	21.75	0.2	99	509	6219530	2.02	7152518
10/16/1990	12	2.1	10/17/1990	14.75	22.7	19	358	1727660	0.24	14085
10/24/1990	18.75	7	10/25/1990	15.25	26.0	16	215	2314490	14.70	300208
11/04/1990	12.25	4.1	11/05/1990	14.5	105.5	48	547	2815080	0.32	62196
12/30/1990	19.25	2	01/02/1991	6.75	374.3	34	237	4610390	0.09	2191
07/15/1991	13.25	0.65	07/16/1991	2.75	294.8	16	331	1564080	0.41	24832
08/27/1991	10	0.75	08/28/1991	15.25	94.2	49	518	3048940	0.47	11659
09/17/1991	2.42	0.98	09/18/1991	10.75	467.2	75	610	3940770	0.51	6526
09/22/1991	8.5	3.2	09/23/1991	17.75	8.5	49	462	3372600	1.29	30547
11/28/1991	12.25	24	12/01/1991	11.75	0.2	23	187	3861880	2.03	3115179
05/16/1992	4	2	05/17/1992	8.75	3114.2	55	1218	1449420	2.22	7211
06/04/1992	8.5	4.3	06/05/1992	13.5	34.2	115	1553	2377040	1.02	29466
07/22/1993	16	5.9	07/23/1993	2.75	222.0	97	1153	2694810	13.96	86642
08/15/1993	21.5	5.3	08/17/1993	17	464.5	152	751	6476630	0.10	1944

Reproduced with permission of the copyright owner. Further reproduction prohibited without permission.

Appendix 6.2 Continued.

Start Date	Start Time hour	End Date	End Time hour	L Previous event rainfall over time since previous event, in/hour 26-PPTLSTI	L Previous event maximum 15-minute rainfall intensity over the time since the previous event, in/min/hour 27-INTLST	L Previous event 75% rainfall intensity over time since previous event, in/min/hour 28-LS75OTI	Sum of 3 previous rainfall events over the time since these events in/hour 29-SUM3PPTI	Sum of 3 previous quickflow events over the time since these events ft3/hour 30-QU3EVT	Runoff since the previous event over time since the previous event ft3/hour 17-RNBTWTI	L Rainfall since the previous event over time since the previous event in/hour 18-PPTBTW
08/11/1989	16	08/12/1989	5.75	0.005	0.0016	0.000021	-8.618	9.12	8420	0.0009
08/18/1989	22	08/19/1989	23.25	0.107	0.0485	0.000375	-5.917	11.43	18371	0.0007
09/13/1989	21.5	09/14/1989	20	0.014	0.0058	0.000207	-6.037	11.33	18760	0.0014
09/18/1989	2.75	09/20/1989	7.75	0.817	0.5615	0.011072	-4.032	13.71	5000	0.0002
09/22/1989	9	09/22/1989	21.5	0.154	0.0096	0.000221	-5.299	12.74	26441	0.0063
10/01/1989	13.75	10/02/1989	1.25	0.048	0.0119	0.000394	-5.649	12.47	35970	0.0004
05/09/1990	19.25	05/10/1990	20	0.003	0.001	0.000015	-8.683	8.56	8596	0.0023
06/14/1990	14	06/15/1990	11.5	0.001	0.0008	0.000036	-8.689	8.36	8532	0.0048
08/07/1990	17	08/09/1990	13.5	0.0004	0.0002	0.000006	-9.316	7.38	14733	0.0093
08/09/1990	13.75	08/12/1990	21.75	3.717	0.5844	0.003064	-5.100	11.82	5000	0.0002
10/16/1990	12	10/17/1990	14.75	0.023	0.0069	0.000132	-6.074	11.43	14135	0.0081
10/24/1990	18.75	10/25/1990	15.25	0.12	0.0168	0.000124	-5.069	13.86	38110	0.0115
11/04/1990	12.25	11/05/1990	14.5	0.015	0.0022	0.00001	-6.211	12.97	25256	0.0007
12/30/1990	19.25	01/02/1991	6.75	0.002	0.0006	0.000004	-9.253	9.35	14209	0.0025
07/15/1991	13.25	07/16/1991	2.75	0.006	0.0013	0.00001	-7.548	11.23	11386	0.0014
08/27/1991	10	08/28/1991	15.25	0.012	0.0028	0.000019	-7.751	10.56	10186	0.0022
09/17/1991	2.42	09/18/1991	10.75	0.004	0.0014	0.000009	-8.327	9.63	11270	0.0025
09/22/1991	8.5	09/23/1991	17.75	0.055	0.0261	0.001232	-5.294	12.82	18182	0.0052
11/28/1991	12.25	12/01/1991	11.75	0.081	0.0581	0.000147	-3.901	16.89	5000	0.0002
05/16/1992	4	05/17/1992	8.75	0.003	0.0003	0.000003	-10.373	8.26	13264	0.0030
06/04/1992	8.5	06/05/1992	13.5	0.017	0.0099	0.000214	-6.798	11.60	23042	0.0062
07/22/1993	16	07/23/1993	2.75	0.017	0.0022	0.000018	-8.068	10.71	23916	0.0030
08/15/1993	21.5	08/17/1993	17	0.001	0.0003	0.000002	-8.847	10.08	19489	0.0014

Reproduced with permission of the copyright owner. Further reproduction prohibited without permission.

Appendix 6.2 Continued.

Start Date	Start Time hour	End Date	End Time hour	L Maximum 15-minute rainfall intensity since the previous event over the time since the previous event, in/miln/hour 19-INTBET	L Rainfall of current event, in 10-RAIN	Maximum 15-minute rainfall of current event, in/min 11-INT15	L Seventy five percent rainfall intensity of current event, in/min 12-SFIVE	L Baseflow at start of event, ft3/s 3-BASE	L Peakflow minus baseflow ft3/s 4-PKBS	L Rainfall on the rising limb of the hydrograph to the highest peak flow, in 13-RRISE
08/11/1989	16	08/12/1989	5.75	0.0007	1.06	0.64	0.0309	1	85.0	1.05
08/18/1989	22	08/19/1989	23.25	0.0005	1.84	0.73	0.0045	3.1	228	1.28
09/13/1989	21.5	09/14/1989	20	0.0013	1.56	0.51	0.0051	3.1	111	1.36
09/18/1989	2.75	09/20/1989	7.75	0.0001	7.22	0.45	0.0104	7.3	532	5.27
09/22/1989	9	09/22/1989	21.5	0.0045	1.46	0.64	0.0119	4.4	331	1.38
10/01/1989	13.75	10/02/1989	1.25	0.0003	0.52	0.19	0.008	7	48	0.50
05/09/1990	19.25	05/10/1990	20	0.0006	2.02	0.45	0.0106	0.7	506	1.68
06/14/1990	14	06/15/1990	11.5	0.0005	4.09	0.9	0.0106	1.4	224	2.08
08/07/1990	17	08/09/1990	13.5	0.0004	1.86	0.29	0.0015	3.3	58	1.66
08/09/1990	13.75	08/12/1990	21.75	0.0001	3.02	0.36	0.0019	12	833	1.94
10/16/1990	12	10/17/1990	14.75	0.0018	1.12	0.41	0.0121	2.1	107	1.06
10/24/1990	18.75	10/25/1990	15.25	0.0019	1.39	0.34	0.0093	7	111	0.99
11/04/1990	12.25	11/05/1990	14.5	0.0002	1.48	0.4	0.0034	4.1	106	0.91
12/30/1990	19.25	01/02/1991	6.75	0.0003	2.14	0.22	0.0024	2	88	1.03
07/15/1991	13.25	07/16/1991	2.75	0.0003	1.55	0.49	0.0038	0.65	96	1.49
08/27/1991	10	08/28/1991	15.25	0.0007	2.06	0.67	0.0042	0.8	253	1.51
09/17/1991	2.42	09/18/1991	10.75	0.0004	2.74	0.5	0.0062	1	338	2.51
09/22/1991	8.5	09/23/1991	17.75	0.0021	1.21	0.54	0.0022	3.2	127	0.93
11/28/1991	12.25	12/01/1991	11.75	0.0001	0.52	0.26	0.0045	24	120	0.43
05/16/1992	4	05/17/1992	8.75	0.0002	1.89	0.39	0.0031	2	124	1.71
06/04/1992	8.5	06/05/1992	13.5	0.0020	1.31	0.41	0.0143	4.3	343	1.12
07/22/1993	16	07/23/1993	2.75	0.0007	2.31	0.43	0.0158	5.9	495	1.35
08/15/1993	21.5	08/17/1993	17	0.0004	2.26	0.25	0.0025	5.3	227	1.82

Reproduced with permission of the copyright owner. Further reproduction prohibited without permission.

Appendix 6.2 Continued.

Start Date	Start Time hour	End Date	End Time hour	Rainfall amount after highest peak flow, in 14-RAINFOL	L Maximum rate for any peak of hydrograph rise from trough to peak flow, ft3/min 7-MXTRP	L Maximum rate of hydrograph rise from start of event to the highest peak flow. ft3/min 6-MXTMJPK	L Sum of current peak flows minus baseflow, ft3/s 8-SMPKBS	Hysteresis of current event 1=clockwise 0=other than clockwise 16-HYSTER	L Sum of peak flows in previous event minus baseflow over time since the previous event, ft3/s/hour 22-SMLSPKBS
08/11/1989	16	08/12/1989	5.75	0.01	1.1	1.1	85	1	0.14
08/18/1989	22	08/19/1989	23.25	0.56	1.7	1.7	227	1	5.68
09/13/1989	21.5	09/14/1989	20	0.2	3.0	3.0	175	1	0.65
09/18/1989	2.75	09/20/1989	7.75	1.95	2.3	2.3	775	1	135
09/22/1989	9	09/22/1989	21.5	0.08	4.9	4.4	465	0	15.8
10/01/1989	13.75	10/02/1989	1.25	0.02	0.8	0.8	48	1	9.19
05/09/1990	19.25	05/10/1990	20	0.34	3.4	3.4	506	0	0.03
06/14/1990	14	06/15/1990	11.5	2.01	2.5	2.5	224	1	0.02
08/07/1990	17	08/09/1990	13.5	0.2	0.1	0.1	58	0	0.01
08/09/1990	13.75	08/12/1990	21.75	1.08	3.3	0.8	1103	0	233
10/16/1990	12	10/17/1990	14.75	0.07	0.9	0.9	107	0	0.44
10/24/1990	18.75	10/25/1990	15.25	0.4	1.8	1.8	225	1	67.9
11/04/1990	12.25	11/05/1990	14.5	0.57	1.7	0.6	191	1	0.65
12/30/1990	19.25	01/02/1991	6.75	1.1	0.6	0.6	166	0	0.09
07/15/1991	13.25	07/16/1991	2.75	0.06	2.3	2.3	96	1	1.32
08/27/1991	10	08/28/1991	15.25	0.55	1.7	0.8	372	1	0.80
09/17/1991	2.42	09/18/1991	10.75	0.23	1.7	1.7	553	0	0.80
09/22/1991	8.5	09/23/1991	17.75	0.28	2.4	2.4	270	1	2.62
11/28/1991	12.25	12/01/1991	11.75	0.09	1.0	1.0	120	0	97.4
05/16/1992	4	05/17/1992	8.75	0.18	1.4	1.4	137	1	3.91
06/04/1992	8.5	06/05/1992	13.5	0.19	4.6	4.6	343	1	1.82
07/22/1993	16	07/23/1993	2.75	0.96	4.7	4.7	495	1	19.4
08/15/1993	21.5	08/17/1993	17	0.44	3.9	3.9	1136	1	0.10

**to eliminate zero values a value of 0.0002 was added to the precipitation between events. 0.0001 was added to the rainfall intensity between events, and a value of 5000 was added to the runoff between events.

Reproduced with permission of the copyright owner. Further reproduction prohibited without permission.

Appendix 6.3. Pearson correlation matrix for the entire runoff event using quickflow characteristics of the entire runoff event, Quebrada Blanca near El Jagual.

Pearson correlation matrix

	LGSED	LGSEDCONC	LGLSPKBTI	LGPPTBTW
LGSED	1.000			
LGSEDCONC	0.716	1.000		
LGLSPKBTI	0.264	0.270	1.000	
LGPPTBTW	-0.165	0.001	-0.185	1.000
LGQUICK	0.784	0.128	0.136	-0.236
LGRAIN	0.661	0.443	-0.167	-0.006
INT15	0.102	0.386	-0.113	0.181
LGSFIVE	-0.072	0.309	0.201	0.119
LGBASE	0.189	-0.059	0.531	-0.382
LGPKBS	0.795	0.671	0.238	-0.164
LGRRISE	0.596	0.454	-0.171	0.017
RAINFOL	0.528	0.313	-0.071	-0.214
LGPPTLSTI	0.308	0.152	0.736	-0.478
LGINTLST	0.303	0.101	0.600	-0.532
RNBTWTI	-0.231	0.025	0.430	0.347
LMXTMJPK	0.509	0.695	0.388	0.057
HYSTER	0.080	0.326	0.245	-0.057
LGINTBET	-0.163	0.105	0.083	0.746
SUM3PPTI	0.102	-0.069	0.589	-0.403
LGLS75OTI	0.209	0.143	0.488	-0.369
QU3EVT	0.117	-0.111	0.660	-0.415
LGSMPKBS	0.853	0.581	0.209	-0.123
LGSMLSPKS	0.317	0.162	0.914	-0.448
LGQULST	0.349	0.121	0.806	-0.538
LGMXTRP	0.595	0.706	0.422	-0.080

Reproduced with permission of the copyright owner. Further reproduction prohibited without permission.

Appendix 6.3. Continued.

	LGQUICK	LG_RAIN	INT15	LGSFIVE	LGBASE
LGQUICK	1.000				
LGRAIN	0.542	1.000			
INT15	-0.199	0.327	1.000		
LGSFIVE	-0.375	-0.071	0.349	1.000	
LGBASE	0.324	-0.205	-0.488	-0.140	1.000
LGPKBS	0.532	0.624	0.279	0.188	0.081
LGRRISE	0.440	0.935	0.327	-0.004	-0.292
RAINFOL	0.470	0.782	0.269	0.017	0.112
LGPPTLSTI	0.305	0.002	-0.020	0.088	0.592
LGINTLST	0.344	0.025	0.018	0.093	0.591
RNBTWTI	-0.350	-0.408	-0.251	0.139	0.277
LMXTMJPK	0.106	0.160	0.283	0.507	0.130
HYSTER	-0.179	0.048	0.274	0.177	-0.060
LGINTBET	-0.325	-0.234	0.324	0.379	-0.231
SUM3PPTI	0.211	-0.230	-0.058	0.097	0.644
LGLS75OTI	0.173	0.043	0.117	0.165	0.510
QU3EVT	0.269	-0.374	-0.213	0.061	0.682
LGSMPKBS	0.694	0.630	0.133	-0.016	0.138
LGSMLSPKS	0.309	-0.078	-0.173	0.074	0.668
LGQULST	0.391	-0.074	-0.151	0.038	0.687
LGMXTRP	0.216	0.222	0.285	0.382	0.190

Reproduced with permission of the copyright owner. Further reproduction prohibited without permission.

Appendix 6.3. Continued.

	LGPKBS	LGRRISE	RAINFOL	LGPPTLSTI	LGINTLST
LGPKBS	1.000				
LGRRISE	0.599	1.000			
RAINFOL	0.462	0.565	1.000		
LGPPTLSTI	0.404	-0.016	0.162	1.000	
LGINTLST	0.385	0.003	0.236	0.954	1.000
RNBTWTI	-0.317	-0.434	-0.313	0.076	-0.054
LMXTMJPK	0.569	0.140	0.175	0.234	0.219
HYSTER	-0.128	0.026	0.137	-0.015	-0.003
LGINTBET	-0.048	-0.171	-0.360	-0.081	-0.129
SUM3PPTI	0.131	-0.236	0.030	0.858	0.892
LGLS75OTI	0.312	0.054	0.249	0.859	0.935
QU3EVT	0.028	-0.408	-0.072	0.735	0.742
LGSMPKBS	0.894	0.588	0.437	0.330	0.294
LGSMLSPKS	0.324	-0.090	0.076	0.891	0.808
LGQULST	0.359	-0.118	0.131	0.928	0.869
LGMXTRP	0.692	0.166	0.247	0.390	0.339

	RNBTWTI	LMXTMJPK	HYSTER	LGINTBET	SUM3PPTI
RNBTWTI	1.000				
LMXTMJPK	0.180	1.000			
HYSTER	0.324	0.262	1.000		
LGINTBET	0.487	0.395	0.066	1.000	
SUM3PPTI	0.182	0.176	0.000	0.045	1.000
LGLS75OTI	0.006	0.254	0.055	0.042	0.848
QU3EVT	0.232	0.186	0.057	-0.034	0.913
LGSMPKBS	-0.180	0.604	-0.051	-0.001	0.113
LGSMLSPKS	0.168	0.244	0.088	-0.187	0.741
LGQULST	0.074	0.212	0.005	-0.223	0.831
LGMXTRP	0.124	0.932	0.229	0.283	0.252

Reproduced with permission of the copyright owner. Further reproduction prohibited without permission.

Appendix 6.3. Continued.

	LGLS75OTI	QU3EVT	LGSMPKBS	LGSMLSPKS	LGQULST
LGLS75OTI	1.000				
QU3EVT	0.615	1.000			
LGSMPKBS	0.207	0.068	1.000		
LGSMLSPKS	0.659	0.766	0.263	1.000	
LGQULST	0.696	0.847	0.306	0.957	1.000
LGMXTRP	0.318	0.237	0.732	0.339	0.357

	LGMXTRP
LGMXTRP	1.000

Reproduced with permission of the copyright owner. Further reproduction prohibited without permission.

Appendix 6.4. Component loadings from principal component analysis on the independent variables using quickflow characteristics of the entire event.

Component loadings

	1	2	3	4	5
LGLSPKBTI	0.770	0.244	0.266	0.146	-0.211
LGPPTBTW	-0.514	-0.001	0.530	0.284	0.260
LGQUICK	0.437	-0.510	-0.426	0.415	0.050
LGRAIN	0.045	-0.923	-0.146	-0.037	-0.114
INT15	-0.071	-0.435	0.461	-0.604	0.113
LGSFIVE	0.115	-0.040	0.663	-0.346	0.042
LGBASE	0.703	0.310	-0.220	0.305	-0.126
LGPKBS	0.485	-0.758	0.139	0.150	0.171
LGRRISE	-0.000	-0.876	-0.101	-0.081	-0.016
RAINFOL	0.246	-0.684	-0.196	-0.200	-0.266
LGPPTLSTI	0.944	0.075	-0.029	-0.135	0.132
LGINTLST	0.927	0.038	-0.096	-0.251	0.167
RNBTWTI	0.083	0.525	0.509	0.344	-0.305
LMXTMJPK	0.406	-0.353	0.704	0.193	-0.097
HYSTER	0.064	0.003	0.369	-0.274	-0.792
LGINTBET	-0.128	0.141	0.827	0.124	0.368
SUM3PPTI	0.859	0.312	0.001	-0.170	0.194
LGLS75OTI	0.813	0.031	0.043	-0.356	0.206
QU3EVT	0.812	0.427	-0.028	0.017	0.030
LGSMPKBS	0.456	-0.747	0.118	0.399	0.054
LGSMLSPKBS	0.913	0.174	-0.043	0.035	-0.104
LGQULST	0.952	0.147	-0.122	0.001	-0.006
LGMXTRP	0.526	-0.415	0.590	0.203	-0.087

Reproduced with permission of the copyright owner. Further reproduction prohibited without permission.

Appendix 6.4. Continued.

	6
LGLSPKBTI	0.077
LGPPTBTW	0.472
LGQUICK	0.147
LGRAIN	0.285
INT15	0.083
LGSFIVE	-0.296
LGBASE	0.040
LGPKBS	-0.178
LGRRISE	0.244
RAINFOL	0.216
LGPPTLSTI	0.093
LGINTLST	0.081
RNBTWTI	0.335
LMXTMJPK	-0.286
HYSTER	0.166
LGINTBET	0.295
SUM3PPTI	0.143
LGLS75OTI	0.212
QU3EVT	-0.006
LGSMPKBS	-0.076
LGSMLSPKBS	0.028
LGQULST	-0.024
LGMXTRP	-0.294

Reproduced with permission of the copyright owner. Further reproduction prohibited without permission.

Appendix 6.5. Component loadings from principal component analysis on the independent variables using quickflow characteristics of the entire event without the variable QUICKFLOW.

Component loadings

	1	2	3	4	5
LGLSPKBTI	0.789	-0.168	0.277	0.150	-0.198
LGPPTBTW	-0.507	0.021	0.591	0.113	0.248
LGRAIN	-0.015	0.892	-0.267	0.020	-0.114
INT15	-0.070	0.521	0.339	-0.644	0.040
LGSFIVE	0.145	0.163	0.595	-0.346	0.016
LGBASE	0.707	-0.314	-0.173	0.338	-0.090
LGPKBS	0.443	0.790	0.025	0.218	0.209
LGRRISE	-0.054	0.855	-0.223	-0.027	-0.018
RAINFOL	0.202	0.670	-0.311	-0.127	-0.282
LGPPTLSTI	0.950	-0.018	-0.073	-0.116	0.122
LGINTLST	0.928	0.009	-0.148	-0.242	0.143
RNBTWTI	0.125	-0.457	0.598	0.276	-0.293
LMXTMJPK	0.405	0.462	0.646	0.198	-0.070
HYSTER	0.080	0.063	0.338	-0.266	-0.837
LGINTBET	-0.100	-0.047	0.869	-0.067	0.341
SUM3PPTI	0.876	-0.260	0.003	-0.222	0.164
LGLS75OTI	0.822	0.038	-0.023	-0.365	0.166
QU3EVT	0.828	-0.396	0.019	-0.038	0.019
LGSMPKBS	0.404	0.753	0.048	0.429	0.104
LGSMLSPKBS	0.920	-0.128	-0.055	0.075	-0.093
LGQULST	0.954	-0.113	-0.136	0.031	0.001
LGMXTRP	0.518	0.515	0.518	0.233	-0.053

Reproduced with permission of the copyright owner. Further reproduction prohibited without permission.

Appendix 6.5. Continued.

	6
LGLSPKBTI	0.098
LGPPTBTW	0.483
LGRAIN	0.312
INT15	-0.015
LGSFIVE	-0.340
LGBASE	0.092
LGPKBS	-0.113
LGRRISE	0.276
RAINFOL	0.204
LGPPTLSTI	0.106
LGINTLST	0.067
RNBTWTI	0.360
LMXTMJPK	-0.280
HYSTER	0.059
LGINTBET	0.269
SUM3PPTI	0.110
LGLS75OTI	0.190
QU3EVT	-0.046
LGSMPKBS	-0.012
LGSMLSPKBS	0.053
LGQULST	-0.011
LGMXTRP	-0.275

Reproduced with permission of the copyright owner. Further reproduction prohibited without permission.

Appendix 6.6. Component loadings from principal component analysis after varimax rotation on the independent variables using quickflow characteristics of the entire event.

Rotated Loading Matrix (VARIMAX, Gamma = 1.0000)

	1	2	3	4	5
LGLSPKBTI	0.725	-0.121	-0.108	-0.168	0.322
LGPPTBTW	-0.422	-0.022	-0.857	0.057	-0.020
LGQUICK	0.263	0.639	0.115	-0.503	-0.244
LG_RAIN	-0.140	0.965	0.051	0.052	0.018
INT15	-0.071	0.314	-0.131	0.806	0.080
LSFIVE	0.069	-0.212	-0.075	0.619	0.130
LGBASE	0.681	-0.106	0.103	-0.500	0.078
LGPKBS	0.214	0.599	0.078	0.063	-0.261
LGRRISE	-0.160	0.886	0.023	0.133	-0.056
RAINFOL	0.102	0.787	0.227	0.084	0.185
LGPPTLSTI	0.950	0.110	0.068	0.023	-0.047
LGINTLST	0.948	0.152	0.140	0.107	-0.090
RNBTWTI	0.156	-0.408	-0.568	-0.252	0.528
LMXTMJPK	0.154	0.083	-0.157	0.173	0.163
HYSTER	0.016	0.059	0.031	0.195	0.905
LGINTBET	-0.037	-0.232	-0.863	0.308	-0.022
LSUM3PPTI	0.953	-0.095	-0.029	0.046	-0.049
LGLS75OTI	0.882	0.168	-0.020	0.266	-0.042
QU3EVT	0.860	-0.254	0.063	-0.160	0.041
LGSMPKBS	0.155	0.631	-0.022	-0.191	-0.171
LGSMLSPKS	0.876	0.006	0.128	-0.186	0.134
LGQULST	0.917	0.025	0.194	-0.165	0.012
LGMXTRP	0.253	0.174	-0.070	0.115	0.112

Reproduced with permission of the copyright owner. Further reproduction prohibited without permission.

Appendix 6.6. Continued.

	6
LGLSPKBTI	0.334
LGPPTBTW	-0.017
LGQUICK	0.159
LGRAIN	0.113
INT15	0.123
LGSFIVE	0.456
LGBASE	0.083
LGPKBSE	0.655
LGRRISE	0.106
RAINFOL	0.044
LGPPTLSTI	0.145
LGINTLST	0.075
RNBTWTI	0.095
LMXTMJPK	0.896
HYSTER	0.087
LGINTBET	0.250
LSUM3PPTI	0.003
LGLS75OTI	0.010
QU3EVT	0.090
LGSMPKBS	0.677
LGSMLSPKS	0.204
LGQULST	0.190
LGMXTRP	0.898

Reproduced with permission of the copyright owner. Further reproduction prohibited without permission.

Appendix 6.7. Component loadings from principal component analysis after varimax rotation on the independent variables using quickflow characteristics of the entire event without the variable QUICKFLOW.

Rotated Loading Matrix (VARIMAX, Gamma = 1.0000)

	1	2	3	4	5
LGLSPKBTI	0.725	-0.122	0.332	-0.181	0.315
LGPPTBTW	-0.423	-0.008	-0.021	0.062	-0.040
LGRAIN	-0.125	0.969	0.134	0.035	-0.005
INT15	-0.072	0.318	0.108	0.815	0.101
LGSFIVE	0.063	-0.200	0.428	0.613	0.155
LGBASE	0.683	-0.118	0.096	-0.506	0.064
LGPKBS	0.223	0.584	0.670	0.067	-0.272
LGRRISE	-0.145	0.898	0.123	0.108	-0.080
RAINFOL	0.113	0.785	0.060	0.073	0.175
LGPPTLSTI	0.953	0.103	0.150	0.013	-0.051
LGINTLST	0.950	0.132	0.078	0.116	-0.084
RNBTWTI	0.153	-0.373	0.089	-0.298	0.501
LMXTMJPK	0.151	0.063	0.892	0.200	0.172
HYSTER	0.011	0.063	0.076	0.196	0.922
LGINTBET	-0.045	-0.233	0.236	0.335	-0.022
LSUM3PPTI	0.949	-0.123	0.003	0.075	-0.037
LGLS75OTI	0.884	0.168	0.009	0.252	-0.043
QU3EVT	0.852	-0.304	0.090	-0.097	0.065
LGSMPKBS	0.163	0.595	0.700	-0.155	-0.183
LGSMLSPKS	0.879	-0.003	0.209	-0.196	0.129
LGQULST	0.918	0.001	0.196	-0.152	0.015
LGMXTRP	0.252	0.154	0.900	0.136	0.117

Reproduced with permission of the copyright owner. Further reproduction prohibited without permission.

Appendix 6.7. Continued.

	6
LGLSPKBTI	-0.130
LGPPTBTW	-0.854
LGRAIN	0.060
INT15	-0.122
LGSFIVE	-0.099
LGBASE	0.097
LGPKBSE	0.085
LGRRISE	0.026
RAINFOL	0.234
LGPPTLSTI	0.061
LGINTLST	0.145
RNBTWTI	-0.603
LMXTMJPK	-0.157
HYSTER	0.020
LGINTBET	-0.857
LSUM3PPTI	-0.018
LGLS75OTI	-0.023
QU3EVT	0.083
LGSMPKBS	0.001
LGSMLPKS	0.114
LGQULST	0.194
LGMXTRP	-0.069

Reproduced with permission of the copyright owner. Further reproduction prohibited without permission.

Appendix 6.8. Summary of dependent and independent variables used in the statistical analysis for runoff characteristics of the entire event at Quebrada Blanca near El Jagual
(D indicates dependent variable; L indicates log transformed; IR indicates negative inverse square root transformed)

Start Date	Start Time hour	Start Discharge ft3/s	End Date	End Time hour	D Suspended-sediment load tons	D Discharge-weighted suspended-sediment concentration mg/L	L Runoff, ft3/s 2-RUN	L Previous event peak flow over time since last peak flow, ft3/s/hour 21-LSPKTI	L Previous event runoff over the time since previous event, ft3/hour 25-RULST	L Previous event rainfall over time since previous event, in/hour 26-PPTLSTI
08/11/1989	16	0.98	08/12/1989	5.75	6.5	282	858820	0.13	2358	0.005
08/18/1989	22	3.1	08/19/1989	23.25	63	966	2588940	1.57	95670	0.107
09/13/1989	21.5	3.1	09/14/1989	20	12	382	1481490	0.59	20690	0.014
09/18/1989	2.75	7.3	09/20/1989	7.75	376	1081	12330270	3.04	2678760	0.817
09/22/1989	9	4.4	09/22/1989	21.5	52	1086	1752210	5.59	250360	0.154
10/01/1989	13.75	7	10/02/1989	1.25	5.2	411	740480	2.69	77430	0.048
05/09/1990	19.25	0.73	05/10/1990	20	34	753	1537050	0.03	1159	0.003
06/14/1990	14	1.4	06/15/1990	11.5	36	912	1814760	0.02	874	0.001
08/07/1990	17	3.3	08/09/1990	13.5	7.9	141	2436800	0.02	385	0
08/09/1990	13.75	12	08/12/1990	21.75	99	509	7984940	2.16	9747180	3.717
10/16/1990	12	2.1	10/17/1990	14.75	19	358	1996250	0.29	22450	0.023
10/24/1990	18.75	7	10/25/1990	15.25	16	215	2841050	14.78	390640	0.12
11/04/1990	12.25	4.1	11/05/1990	14.5	48	547	3290810	0.35	93510	0.015
12/30/1990	19.25	2	01/02/1991	6.75	34	237	5820620	0.10	3209	0.002
07/15/1991	13.25	0.65	07/16/1991	2.75	16	331	1619200	0.42	28400	0.006
08/27/1991	10	0.75	08/28/1991	15.25	49	518	3614930	0.48	13940	0.012
09/17/1991	2.42	0.98	09/18/1991	10.75	75	610	4370280	0.52	7738	0.004
09/22/1991	8.5	3.2	09/23/1991	17.75	49	462	4162620	1.45	47149	0.055
11/28/1991	12.25	24	12/01/1991	11.75	23	187	6840670	2.83	4860920	0.081
05/16/1992	4	2	05/17/1992	8.75	55	1218	1966920	2.28	7450	0.003
06/04/1992	8.5	4.3	06/05/1992	13.5	115	1553	3019100	1.08	42500	0.017
07/22/1993	16	5.9	07/23/1993	2.75	97	1153	2946110	13.97	92050	0.017
08/15/1993	21.5	5.3	08/17/1993	17	152	751	7831220	0.12	3682	0.001

Reproduced with permission of the copyright owner. Further reproduction prohibited without permission.

Appendix 6.8. Continued.

Start Date	Start Time hour	End Date	End Time hour	L Previous event maximum 15-minute rainfall intensity over the time since the previous event, in/min/hour 27-INTLST	L Previous event 75% rainfall intensity over time since previous event, in/min/hour 28-LS75OTI	Sum of 3 previous rainfall events over the time since these events in/hour 29-SUM3PPTI	Sum of 3 previous quickflow events over the time since these events ft3/hour 31-RU3EVT	Runoff since the previous event over time since the previous event ft3/hour 17-RNBTWTI	L Rainfall since the previous event over time since the previous event in/hour 18-PPTBTW
08/11/1989	16	08/12/1989	5.75	0.0016	2.10E-005	-8.618	9.66	8420	0.0009
08/18/1989	22	08/19/1989	23.25	0.0485	3.75E-004	-5.917	11.75	18371	0.0007
09/13/1989	21.5	09/14/1989	20	0.0058	2.07E-004	-6.037	12.06	18760	0.0014
09/18/1989	2.75	09/20/1989	7.75	0.5615	1.11E-002	-4.032	14.38	5000	0.0002
09/22/1989	9	09/22/1989	21.5	0.0096	2.21E-004	-5.299	13.13	26441	0.0063
10/01/1989	13.75	10/02/1989	1.25	0.0119	3.94E-004	-5.649	12.91	35970	0.0004
05/09/1990	19.25	05/10/1990	20	0.001	1.50E-005	-8.683	9.22	8596	0.0023
06/14/1990	14	06/15/1990	11.5	0.0008	3.60E-005	-8.689	8.71	8532	0.0048
08/07/1990	17	08/09/1990	13.5	0.0002	6.00E-006	-9.316	8.26	14733	0.0093
08/09/1990	13.75	08/12/1990	21.75	0.5844	3.06E-003	-5.100	12.70	5000	0.0002
10/16/1990	12	10/17/1990	14.75	0.0069	1.32E-004	-6.074	11.95	14135	0.0081
10/24/1990	18.75	10/25/1990	15.25	0.0168	1.24E-004	-5.069	14.22	38110	0.0115
11/04/1990	12.25	11/05/1990	14.5	0.0022	1.00E-005	-6.211	13.30	25256	0.0007
12/30/1990	19.25	01/02/1991	6.75	0.0006	4.00E-006	-9.253	9.97	14209	0.0025
07/15/1991	13.25	07/16/1991	2.75	0.0013	1.00E-005	-7.548	11.41	11386	0.0014
08/27/1991	10	08/28/1991	15.25	0.0028	1.90E-005	-7.751	10.78	10186	0.0022
09/17/1991	2.42	09/18/1991	10.75	0.0014	9.00E-006	-8.327	9.86	11270	0.0025
09/22/1991	8.5	09/23/1991	17.75	0.0261	1.23E-003	-5.294	13.13	18182	0.0052
11/28/1991	12.25	12/01/1991	11.75	0.0581	1.47E-004	-3.901	17.35	5000	0.0002
05/16/1992	4	05/17/1992	8.75	0.0003	3.00E-006	-10.373	8.89	13264	0.0030
06/04/1992	8.5	06/05/1992	13.5	0.0099	2.14E-004	-6.798	12.49	23042	0.0062
07/22/1993	16	07/23/1993	2.75	0.0022	1.80E-005	-8.068	11.63	23916	0.0030
08/15/1993	21.5	08/17/1993	17	0.0003	2.00E-006	-8.847	10.76	19489	0.0014

Reproduced with permission of the copyright owner. Further reproduction prohibited without permission.

Appendix 6.8. Continued.

Start Date	Start Time hour	End Date	End Time hour	L Maximum 15-minute rainfall intensity since the previous event over the time since the previous event, in/miln/hour 19-INTBET	L Rainfall of current event, in 10-RAIN	Maximum 15-minute rainfall of current event, in/min 11-INT15	L Seventy five percent rainfall intensity of current event, in/min 12-SFIVE	L Baseflow at start of event, ft3/s 3-BASE	L Peakflow, ft3/s 5-PK
08/11/1989	16	08/12/1989	5.75	0.0007	1.06	0.64	0.031	1	86
08/18/1989	22	08/19/1989	23.25	0.0005	1.84	0.73	0.005	3.1	231
09/13/1989	21.5	09/14/1989	20	0.0013	1.56	0.51	0.005	3.1	115
09/18/1989	2.75	09/20/1989	7.75	0.0001	7.22	0.45	0.010	7.3	537
09/22/1989	9	09/22/1989	21.5	0.0045	1.46	0.64	0.012	4.4	335
10/01/1989	13.75	10/02/1989	1.25	0.0003	0.52	0.19	0.008	7	55
05/09/1990	19.25	05/10/1990	20	0.0006	2.02	0.45	0.011	0.7	507
06/14/1990	14	06/15/1990	11.5	0.0005	4.09	0.9	0.011	1.4	226
08/07/1990	17	08/09/1990	13.5	0.0004	1.86	0.29	0.002	3.3	62
08/09/1990	13.75	08/12/1990	21.75	0.0001	3.02	0.36	0.002	12	838
10/16/1990	12	10/17/1990	14.75	0.0018	1.12	0.41	0.012	2.1	109
10/24/1990	18.75	10/25/1990	15.25	0.0019	1.39	0.34	0.009	7	118
11/04/1990	12.25	11/05/1990	14.5	0.0002	1.48	0.4	0.003	4.1	110
12/30/1990	19.25	01/02/1991	6.75	0.0003	2.14	0.22	0.002	2	91
07/15/1991	13.25	07/16/1991	2.75	0.0003	1.55	0.49	0.004	0.65	97
08/27/1991	10	08/28/1991	15.25	0.0007	2.06	0.67	0.004	0.8	255
09/17/1991	2.42	09/18/1991	10.75	0.0004	2.74	0.5	0.006	1	340
09/22/1991	8.5	09/23/1991	17.75	0.0021	1.21	0.54	0.002	3.2	132
11/28/1991	12.25	12/01/1991	11.75	0.0001	0.52	0.26	0.005	24	130
05/16/1992	4	05/17/1992	8.75	0.0002	1.89	0.39	0.003	2	128
06/04/1992	8.5	06/05/1992	13.5	0.0020	1.31	0.41	0.014	4.3	347
07/22/1993	16	07/23/1993	2.75	0.0007	2.31	0.43	0.016	5.9	501
08/15/1993	21.5	08/17/1993	17	0.0004	2.26	0.25	0.003	5.3	234

Reproduced with permission of the copyright owner. Further reproduction prohibited without permission.

Appendix 6.8. Continued.

Start Date	Start Time hour	End Date	End Time hour	L Rainfall on the rising limb of the hydrograph to the highest peak flow, in 13-RRISE	Rainfall amount after highest peak flow, in 14-RAINFOL	L Maximum rate for any peak of hydrograph rise from trough to peak flow, ft3/min 7-MXTRP	L Maximum rate of hydrograph rise from start of event to the highest peak flow, ft3/min 6-MXTMJPK	L Sum of current peak flows, ft3/s 9-SMPK	Hysteresis of current event: 1=clockwise 0=other than clockwise 16-HYSTER 0=reverse	L Sum of peak flows in previous event over time since the previous event, ft3/s/hour 23-SMLSPK
08/11/1989	16	08/12/1989	5.75	1.05	0.01	1.13	1.13	86	1	0.15
08/18/1989	22	08/19/1989	23.25	1.28	0.56	1.69	1.69	231	1	6.00
09/13/1989	21.5	09/14/1989	20	1.36	0.20	3	3.00	180	1	0.85
09/18/1989	2.75	09/20/1989	7.75	5.27	1.95	2.33	2.33	791	1	152
09/22/1989	9	09/22/1989	21.5	1.38	0.08	4.87	4.41	471	0	16.1
10/01/1989	13.75	10/02/1989	1.25	0.50	0.02	0.8	0.80	55	1	9.41
05/09/1990	19.25	05/10/1990	20	1.68	0.34	3.38	3.38	507	0	0.03
06/14/1990	14	06/15/1990	11.5	2.08	2.01	2.5	2.50	226	1	0.03
08/07/1990	17	08/09/1990	13.5	1.66	0.20	0.06	0.06	62	0	0.02
08/09/1990	13.75	08/12/1990	21.75	1.94	1.08	3.27	0.79	1112	0	248
10/16/1990	12	10/17/1990	14.75	1.06	0.07	0.89	0.89	109	0	0.53
10/24/1990	18.75	10/25/1990	15.25	0.99	0.40	1.84	1.84	233	1	68.4
11/04/1990	12.25	11/05/1990	14.5	0.91	0.57	1.67	0.64	197	1	0.72
12/30/1990	19.25	01/02/1991	6.75	1.03	1.10	0.62	0.62	171	0	0.10
07/15/1991	13.25	07/16/1991	2.75	1.49	0.06	2.27	2.27	349	1	1.34
08/27/1991	10	08/28/1991	15.25	1.51	0.55	1.73	0.79	376	1	0.83
09/17/1991	2.42	09/18/1991	10.75	2.51	0.23	1.66	1.66	558	0	0.81
09/22/1991	8.5	09/23/1991	17.75	0.93	0.28	2.37	2.37	277	1	2.94
11/28/1991	12.25	12/01/1991	11.75	0.43	0.09	1.01	1.01	130	0	136
05/16/1992	4	05/17/1992	8.75	1.71	0.18	1.35	1.35	142	1	3.49
06/04/1992	8.5	06/05/1992	13.5	1.12	0.19	4.57	4.57	347	1	1.93
07/22/1993	16	07/23/1993	2.75	1.35	0.96	4.72	4.72	501	1	19.4
08/15/1993	21.5	08/17/1993	17	1.82	0.45	3.87	3.87	1151	1	0.13

**to eliminate zero values a value of 0.0002 was added to the precipitation between events. 0.0001 was added to the rainfall intensity between events, and a value of 5000 was added to the runoff between events.

Reproduced with permission of the copyright owner. Further reproduction prohibited without permission.

Appendix 6.9. Pearson correlation matrix for the entire runoff event using runoff characteristics of the entire runoff event, Quebrada Blanca near El Jagual.

Pearson correlation matrix

	LGSEDCORU	LGSED	LGLSPKTI	LGPPTBTW
LGSEDCORU	1.000			
LGSED	0.743	1.000		
LGLSPKTI	0.212	0.254	1.000	
LGPPTBTW	0.057	-0.165	-0.193	1.000
LGRUN	0.091	0.734	0.163	-0.303
LGRAIN	0.510	0.661	-0.182	-0.006
INT15	0.414	0.102	-0.136	0.181
LGSFIVE	0.323	-0.072	0.182	0.119
LGBASE	-0.157	0.189	0.564	-0.382
LGPK	0.704	0.794	0.233	-0.172
LGRRISE	0.531	0.596	-0.183	0.017
RAINFOL	0.308	0.529	-0.083	-0.214
LGPPTLSTI	0.131	0.308	0.739	-0.478
LGINTLST	0.068	0.303	0.609	-0.532
RNBTWTI	-0.007	-0.231	0.428	0.347
LMXTMJPK	0.671	0.509	0.372	0.057
HYSTER	0.299	0.080	0.234	-0.057
LGINTBET	0.152	-0.163	0.075	0.746
SUM3PPTI	-0.107	0.102	0.607	-0.403
LGLS75OTI	0.098	0.209	0.497	-0.369
RU3EVT	-0.145	0.139	0.688	-0.426
LGSMPK	0.613	0.819	0.195	-0.150
LGSMLSPK	0.122	0.317	0.920	-0.448
LGRULST	0.039	0.328	0.789	-0.551
LGMXTRP	0.688	0.595	0.403	-0.080

Reproduced with permission of the copyright owner. Further reproduction prohibited without permission.

Appendix 6.9. Continued.

	LGRUN	LGRAIN	INT15	LGSFIVE	LGBASE
LGRUN	1.000				
LGRAIN	0.466	1.000			
INT15	-0.268	0.327	1.000		
LGSFIVE	-0.435	-0.071	0.349	1.000	
LGBASE	0.441	-0.205	-0.488	-0.140	1.000
LGPK	0.467	0.612	0.260	0.184	0.103
LGRRISE	0.347	0.935	0.327	-0.004	-0.292
RAINFOL	0.474	0.783	0.269	0.016	0.112
LGPPTLSTI	0.325	0.002	-0.020	0.088	0.592
LGINTLST	0.383	0.025	0.018	0.093	0.591
RNBTWTI	-0.336	-0.408	-0.251	0.139	0.277
LMXTMJPK	0.075	0.160	0.283	0.507	0.130
HYSTER	-0.185	0.048	0.274	0.177	-0.060
LGINTBET	-0.397	-0.234	0.324	0.379	-0.231
SUM3PPTI	0.261	-0.230	-0.058	0.097	0.644
LGLS75OTI	0.212	0.043	0.117	0.165	0.510
RU3EVT	0.355	-0.361	-0.262	0.063	0.735
LGSMPK	0.597	0.626	0.133	-0.059	0.047
LGSMLSPKS	0.348	-0.078	-0.173	0.074	0.668
LGRULST	0.448	-0.085	-0.191	0.002	0.730
LGMXTRP	0.187	0.222	0.285	0.382	0.190

Reproduced with permission of the copyright owner. Further reproduction prohibited without permission.

Appendix 6.9. Continued.

	LGPK	LGRRISE	RAINFOL	LGPPTLSTI	LGINTLST
LGPK	1.000				
LGRRISE	0.585	1.000			
RAINFOL	0.461	0.566	1.000		
LGPPTLSTI	0.413	-0.016	0.161	1.000	
LGINTLST	0.393	0.003	0.235	0.954	1.000
RNBTWTI	-0.304	-0.434	-0.313	0.076	-0.054
LMXTMJPK	0.570	0.140	0.175	0.234	0.219
HYSTER	-0.132	0.026	0.138	-0.015	-0.003
LGINTBET	-0.056	-0.171	-0.360	-0.081	-0.129
SUM3PPTI	0.141	-0.236	0.029	0.858	0.892
LGLS75OTI	0.320	0.054	0.248	0.859	0.935
RU3EVT	0.070	-0.397	-0.059	0.748	0.758
LGSMPK	0.856	0.609	0.394	0.313	0.269
LGSMLSPK	0.336	-0.090	0.075	0.891	0.808
LGRULST	0.344	-0.126	0.125	0.929	0.883
LGMXTRP	0.695	0.166	0.247	0.390	0.339

	RNBTWTI	LMXTMJPK	HYSTER	LGINTBET	SUM3PPTI
RNBTWTI	1.000				
LMXTMJPK	0.180	1.000			
HYSTER	0.324	0.262	1.000		
LGINTBET	0.487	0.395	0.066	1.000	
SUM3PPTI	0.182	0.176	0.000	0.045	1.000
LGLS75OTI	0.006	0.254	0.055	0.042	0.848
RU3EVT	0.229	0.200	0.041	-0.047	0.914
LGSMPK	-0.213	0.506	-0.005	-0.044	0.106
LGSMLSPK	0.168	0.244	0.088	-0.187	0.741
LGRULST	0.073	0.175	-0.016	-0.235	0.856
LGMXTRP	0.124	0.932	0.229	0.283	0.252

Reproduced with permission of the copyright owner. Further reproduction prohibited without permission.

Appendix 6.9. Continued.

	LGLS75OTI	RU3EVT	LGSMPK	LGSMLSPK	LGRULST
LGLS75OTI	1.000				
RU3EVT	0.634	1.000			
LGSMPK	0.167	0.096	1.000		
LGSMLSPK	0.659	0.781	0.276	1.000	
LGRULST	0.719	0.877	0.302	0.946	1.000
LGMXTRP	0.318	0.253	0.627	0.339	0.320

	LGMXTRP
LGMXTRP	1.000

Reproduced with permission of the copyright owner. Further reproduction prohibited without permission.

Appendix 6.10. Component loadings from principal component analysis on the independent variables using runoff characteristics of the entire event.

Component loadings

	1	2	3	4	5
LGLSPKTI	0.772	0.300	0.262	0.171	-0.161
LGPPTBTW	-0.530	0.017	0.498	0.280	0.280
LGRUN	0.484	-0.428	-0.484	0.404	0.029
LGRAIN	0.078	-0.920	-0.111	-0.022	-0.098
INT15	-0.080	-0.437	0.496	-0.580	0.063
LG_SFIVE	0.084	-0.022	0.683	-0.317	0.012
LGBASE	0.703	0.331	-0.224	0.307	-0.125
LGPK	0.518	-0.717	0.172	0.165	0.208
LGRRISE	0.033	-0.873	-0.062	-0.074	0.004
RAINFOL	0.263	-0.692	-0.164	-0.162	-0.296
LGPPTLSTI	0.950	0.104	0.019	-0.153	0.130
LGINTLST	0.929	0.057	-0.045	-0.266	0.136
RNBTWTI	0.054	0.551	0.482	0.372	-0.284
LMXTMJPK	0.369	-0.328	0.713	0.256	-0.098
HYSTER	0.051	-0.003	0.378	-0.187	-0.821
LGINTBET	-0.167	0.168	0.815	0.126	0.356
SUM3PPTI	0.858	0.318	0.146	-0.214	0.136
LGLS75OTI	0.811	0.050	0.094	-0.363	0.156
RU3EVT	0.955	0.183	-0.168	0.008	0.045
LGSMPK	0.442	-0.715	0.090	0.367	0.076
LGSMLSPK	0.920	0.199	-0.011	0.039	-0.076
LGRULST	0.957	0.186	-0.129	0.001	0.021
LGMXTRP	0.502	-0.382	0.606	0.252	-0.077

Reproduced with permission of the copyright owner. Further reproduction prohibited without permission.

Appendix 6.10. Continued.

	6
LGLSPKTI	0.088
LGPPTBTW	0.479
LGRUN	0.119
LGRAIN	0.292
INT15	0.086
LGSFIVE	-0.318
LGBASE	0.023
LGPK	-0.169
LGRRISE	0.256
RAINFOL	0.198
LGPPTLSTI	0.085
LGINTLST	0.063
RNBTWTI	0.327
LMXTMJPK	-0.304
HYSTER	0.156
LGINTBET	0.287
SUM3PPTI	0.156
LGLS75OTI	0.188
RU3EVT	0.008
LGSMPK	-0.039
LGSMLSPK	0.028
LGRULST	-0.005
LGMXTRP	- 0.302

Reproduced with permission of the copyright owner. Further reproduction prohibited without permission.

Appendix 6.11. Component loadings from principal component analysis on the independent variables using runoff characteristics of the entire event without the variable RUNOFF.

Component loadings

	1	2	3	4	5
LGLSPKTI	0.793	-0.228	0.284	0.165	-0.152
LGPPTBTW	-0.519	0.022	0.566	0.120	0.274
LGRAIN	0.029	0.892	-0.254	0.031	-0.098
INT15	-0.068	0.531	0.362	-0.624	0.019
LGSFIVE	0.122	0.154	0.613	-0.326	-0.004
LGBASE	0.699	-0.351	-0.159	0.315	-0.106
LGPK	0.489	0.752	0.044	0.229	0.231
LGRRISE	-0.008	0.857	-0.210	-0.014	0.005
RAINFOL	0.224	0.669	-0.289	-0.115	-0.306
LGPPTLSTI	0.959	-0.053	-0.029	-0.136	0.122
LGINTLST	0.932	-0.018	-0.101	-0.261	0.119
RNBTWTI	0.094	-0.477	0.591	0.294	-0.275
LMXTMJPK	0.376	0.442	0.660	0.234	-0.081
HYSTER	0.069	0.072	0.350	-0.201	-0.842
LGINTBET	-0.132	-0.054	0.865	-0.054	0.340
SUM3PPTI	0.881	-0.249	0.133	-0.248	0.117
LGLS75OTI	0.823	0.012	0.027	-0.384	0.129
RU3EVT	0.953	-0.171	-0.176	0.033	0.048
LGSMPK	0.402	0.720	0.000	0.410	0.106
LGSMLSPK	0.927	-0.160	-0.023	0.073	-0.069
LGRULST	0.958	-0.167	-0.140	0.030	0.025
LGMXTRP	0.503	0.485	0.537	0.254	-0.057

Reproduced with permission of the copyright owner. Further reproduction prohibited without permission.

Appendix 6.11. Continued.

	6
LGLSPKTI	0.113
LGPPTBTW	0.483
LGRAIN	0.318
INT15	0.002
LGSFIVE	-0.361
LGBASE	0.049
LGPK	-0.117
LGRRISE	0.289
RAINFOL	0.180
LGPPTLSTI	0.086
LGINTLST	0.036
RNBTWTI	0.352
LMXTMJPK	-0.300
HYSTER	0.095
LGINTBET	0.258
SUM3PPTI	0.130
LGLS75OTI	0.145
RU3EVT	0.019
LGSMPK	0.025
LGSMLSPK	0.051
LGRULST	0.007
LGMXTRP	-0.288

Reproduced with permission of the copyright owner. Further reproduction prohibited without permission.

Appendix 6.12 Component loadings from principal component analysis after varimax rotation on the independent variables using runoff characteristics of the entire event.

Rotated Loading Matrix (VARIMAX, Gamma = 1.0000)

	1	2	3	4	5
LGLSPKTI	0.733	-0.140	-0.113	-0.172	0.305
LGPPTBTW	-0.420	-0.021	-0.858	0.062	-0.027
LGRUN	0.313	0.552	0.178	-0.583	-0.209
LGRAIN	-0.137	0.965	0.047	0.023	0.008
INT15	-0.075	0.346	-0.125	0.791	0.069
LGSFIVE	0.069	-0.200	-0.069	0.642	0.122
LGBASE	0.692	-0.126	0.097	-0.496	0.095
LGPK	0.225	0.584	0.078	0.032	-0.268
LGRRISE	-0.158	0.888	0.020	0.106	-0.070
RAINFOL	0.107	0.793	0.223	0.054	0.184
LGPPTLSTI	0.948	0.106	0.068	0.028	-0.048
LGINTLST	0.950	0.151	0.144	0.103	-0.087
RNBTWTI	0.155	-0.414	-0.573	-0.218	0.531
LMXTMJPK	0.155	0.085	-0.159	0.181	0.165
HYSTER	0.011	0.072	0.034	0.199	0.906
LGINTBET	-0.037	-0.225	-0.857	0.325	-0.023
SUM3PPTI	0.952	-0.095	-0.023	0.046	-0.041
LGLS75OTI	0.888	0.175	-0.017	0.260	-0.041
RU3EVT	0.866	-0.253	0.077	-0.193	0.041
LGSMPK	0.141	0.626	0.010	-0.203	-0.154
LGSMLSPKS	0.871	-0.003	0.123	-0.181	0.129
LGRULST	0.929	0.014	0.189	-0.193	-0.007
LGMXTRP	0.253	0.173	-0.072	0.122	0.115

Reproduced with permission of the copyright owner. Further reproduction prohibited without permission.

Appendix 6.12. Continued.

	6
LGLSPKTI	0.324
LGPPTBTW	-0.022
LGRUN	0.122
LGRAIN	0.119
INT15	0.115
LGSFIVE	0.446
LGBASE	0.074
LGPK	0.666
LGRRISE	0.117
RAINFOL	0.038
LGPPTLSTI	0.147
LGINTLST	0.074
RNBTWTI	0.090
LMXTMJPK	0.888
HYSTER	0.092
LGINTBET	0.243
SUM3PPTI	0.006
LGLS75OTI	0.004
RU3EVT	0.121
LGSMPK	0.620
LGSMLSPKS	0.216
LGRULST	0.156
LGMXTRP	0.890

Reproduced with permission of the copyright owner. Further reproduction prohibited without permission.

Appendix 6.13.Component loadings from principal component analysis after varimax rotation on the independent variables using runoff characteristics of the entire event without the variable RUNOFF.

Rotated Loading Matrix (VARIMAX, Gamma = 1.0000)

	1	2	3	4	5
LGLSPKTI	0.739	-0.116	0.320	-0.209	0.285
LGPPTBTW	-0.423	-0.011	-0.026	0.057	-0.039
LGRAIN	-0.126	0.971	0.103	0.044	0.004
INT15	-0.093	0.316	0.120	0.808	0.104
LGSFIVE	0.053	-0.203	0.455	0.605	0.143
LGBASE	0.702	-0.127	0.072	-0.470	0.078
LGPK	0.235	0.601	0.654	0.041	-0.278
LGRRISE	-0.147	0.904	0.102	0.104	-0.076
RAINFOL	0.112	0.770	0.032	0.105	0.195
LGPPTLSTI	0.951	0.110	0.143	0.030	-0.053
LGINTLST	0.948	0.132	0.072	0.141	-0.078
RNBTWTI	0.159	-0.375	0.094	-0.294	0.497
LMXTMJPK	0.151	0.082	0.891	0.190	0.167
HYSTER	0.005	0.059	0.102	0.180	0.920
LGINTBET	-0.049	-0.229	0.245	0.327	-0.023
SUM3PPTI	0.948	-0.121	0.008	0.093	-0.033
LGLS75OTI	0.883	0.157	0.003	0.287	-0.030
RU3EVT	0.864	-0.283	0.123	-0.134	0.047
LGSMPK	0.155	0.640	0.605	-0.176	-0.170
LGSMLSPK	0.879	0.012	0.211	-0.197	0.115
LGRULST	0.935	0.013	0.152	-0.174	-0.014
LGMXTRP	0.252	0.175	0.890	0.130	0.113

Reproduced with permission of the copyright owner. Further reproduction prohibited without permission.

Appendix 6.13. Continued.

	6
LGLSPKTI	-0.140
LGPPTBTW	-0.855
LGRAIN	0.059
INT15	-0.125
LGSFIVE	-0.096
LGBASE	0.108
LGPK	0.081
LGRRISE	0.021
RAINFOL	0.246
LGPPTLSTI	0.059
LGINTLST	0.148
RNBTWTI	-0.599
LMXTMJPK	-0.158
HYSTER	0.019
LGINTBET	-0.857
SUM3PPTI	-0.014
LGLS75OTI	-0.014
RU3EVT	0.089
LGSMPK	0.023
LGSMLSPK	0.105
LGRULST	0.187
LGMXTRP	-0.071

Reproduced with permission of the copyright owner. Further reproduction prohibited without permission.

Appendix 6.14-- Summary of dependent and independent variables used in statistical analysis for quickflow characteristics to highest peak for Quebrada Blanca near El Jagual. (D-indicates dependent variable; L-indicated data was log transformed) (D indicates dependent variable; L indicates log transformed; IR indicates negative inverse square root transformed)

Start Date	Start Time	Start discharge cfs	End Date	End Time	End discharge ft3/s	DL Total suspended-sediment load tons	DL Discharge-weighted sediment concentration mg/L	L Quickflow, ft3 1-QUICK	L Previous event peak flow minus baseflow over time since last peak, ft3/s/hour 20-LSPKBTI
8/11/1989	16.00	0.98	8/11/1989	17.25	86	1.3	708	57750	0.13
8/18/1989	22.00	3.10	8/19/1989	0.25	231	9.3	1703	174640	1.46
9/13/1989	21.50	3.10	9/14/1989	0.75	115	4.7	660	229640	0.45
9/18/1989	2.75	7.30	9/18/1989	9.00	537	154	1016	4849670	2.70
9/22/1989	9.00	4.40	9/22/1989	10.25	335	20.2	1706	379980	5.54
5/9/1990	19.25	0.73	5/9/1990	21.75	507	6.54	774	270540	0.03
6/14/1990	14.00	1.40	6/14/1990	15.50	226	5.3	1237	136860	0.02
8/9/1990	13.75	12.00	8/10/1990	7.50	838	30.7	580	1694040	2.02
10/16/1990	12.00	2.10	10/16/1990	14.00	109	2.5	420	188670	0.24
10/24/1990	18.75	7.00	10/24/1990	20.25	118	3.0	722	131580	14.7
12/30/1990	19.25	2.00	12/31/1990	4.75	91	14.3	604	758210	0.09
9/17/1991	2.42	0.98	9/17/1991	9.33	340	21.9	631	1113560	0.51
9/22/1991	8.5	3.2	9/23/1991	17.75	10.00	25.9	914	908150	1.29
11/16/1991	13.25	5.10	11/16/1991	14.50	154	9.3	1371	217200	3.51
11/21/1991	15.50	3.60	11/21/1991	22.00	101	3.0	259	367370	1.23
11/28/1991	12.25	24.00	11/28/1991	14.00	130	9.3	826	362500	2.03
5/16/1992	4.00	2.00	5/16/1992	13.25	128	30.6	1976	495980	2.22
6/4/1992	8.50	4.30	6/4/1992	9.75	347	47.0	3007	500240	1.02
7/22/1993	16.00	5.90	7/22/1993	17.75	501	47.7	1555	982320	14.0
8/15/1993	21.50	5.3	8/16/1993	9	234	101	1348	2391130	0.10

Reproduced with permission of the copyright owner. Further reproduction prohibited without permission.

Appendix 6.14. Continued.

Start Date	Start Time	End Date	End Time	Sum of 3 previous quickflow events over the time since these events ft3/hour 30-QU3EVT	Previous event rainfall over time since previous event, in/hour 26-PPTLSTI	Previous event maximum 15-minute rainfall intensity over the time since the previous event, in/min/hour 27-INTLST	Rainfall since the previous event over time since the previous event in/hour 18-PPTBTW	Maximum 15-minute rainfall intensity since the previous event over the time since the previous event, in/miln/hour 19-INTBET	Sum of 3 previous rainfall events over the time since these events in/hour 29-SUM3PPTI	Rainfall on the rising limb of the hydrograph to the highest peak flow, in 13-RRISE
8/11/1989	16.00	8/11/1989	17.25	9.12	0.005	0.0016	0.0009	0.0007	-8.618	1.05
8/18/1989	22.00	8/19/1989	0.25	11.43	0.107	0.0485	0.0007	0.0005	-5.917	1.28
9/13/1989	21.50	9/14/1989	0.75	11.33	0.014	0.0058	0.0014	0.0012	-6.037	1.36
9/18/1989	2.75	9/18/1989	9.00	13.71	0.817	0.5615	0.1402	0.0001	-4.032	5.27
9/22/1989	9.00	9/22/1989	10.25	12.74	0.154	0.0096	0.0063	0.0045	-5.299	1.38
5/9/1990	19.25	5/9/1990	21.75	8.56	0.003	0.0010	0.0023	0.0006	-8.683	1.68
6/14/1990	14.00	6/14/1990	15.50	8.36	0.001	0.0008	0.0048	0.0005	-8.689	2.08
8/9/1990	13.75	8/10/1990	7.50	11.82	3.717	0.5844	0.0002	0.0001	-5.100	1.94
10/16/1990	12.00	10/16/1990	14.00	11.43	0.023	0.0069	0.0082	0.0018	-6.074	1.05
10/24/1990	18.75	10/24/1990	20.25	13.86	0.120	0.0168	0.0115	0.0019	-5.069	0.99
12/30/1990	19.25	12/31/1990	4.75	9.35	0.002	0.0006	0.0025	0.0003	-9.253	1.03
9/17/1991	2.42	9/17/1991	9.33	9.63	0.006	0.0013	0.0015	0.0003	-8.327	2.51
9/22/1991	8.5	9/23/1991	17.75	12.82	0.012	0.0028	0.0022	0.0007	-5.294	0.41
11/16/1991	13.25	11/16/1991	14.50	12.84	0.004	0.0014	0.0025	0.0004	-6.430	0.63
11/21/1991	15.50	11/21/1991	22.00	13.34	0.055	0.0261	0.0053	0.0021	-5.940	0.74
11/28/1991	12.25	11/28/1991	14.00	16.89	0.081	0.0581	0.0002	0.0001	-3.901	0.43
5/16/1992	4.00	5/16/1992	13.25	8.26	0.003	0.0003	0.0029	0.0002	-10.373	1.71
6/4/1992	8.50	6/4/1992	9.75	11.60	0.017	0.0099	0.0062	0.0020	-6.798	1.12
7/22/1993	16.00	7/22/1993	17.75	10.71	0.017	0.0022	0.0030	0.0007	-8.068	1.35
8/15/1993	21.50	8/16/1993	9	10.08	0.001	0.0003	0.0014	0.0004	-8.847	1.82

Reproduced with permission of the copyright owner. Further reproduction prohibited without permission.

Appendix 6.14. Continued.

Start Date	Start Time	End Date	End Time	Maximum 15-minute rainfal of current event, in/min 11-INT15	Baseflow at start of event, ft3/s 3-BASE	Peakflow minus baseflow ft3/s 4-PKBS	Previous event quickflow over the time since previous event, ft3/hour 24-QULST	Previous event 75% rainfall intensity over time since previous event, in/min/hour 28-LS75OTI	Maximum rate of hydrograph rise from start of event to the highest peak flow. ft3/min 6-MXTMJPK	Sum of peak flows in previous event minus baseflow over time since the previous event, ft3/s/hour 22-SMLSPKBS	Runoff since the previous event over time since the previous event ft3/hour 17-RNBTWTI
8/11/1989	16.00	8/11/1989	17.25	0.64	0.98	85	1725	2.09E-005	1.13	0.14	6420
8/18/1989	22.00	8/19/1989	0.25	0.73	3.10	227	72270	3.75E-004	1.69	5.7	16370
9/13/1989	21.50	9/14/1989	0.75	0.51	3.10	111	9626	2.07E-004	3.00	0.65	16760
9/18/1989	2.75	9/18/1989	9.00	0.28	7.30	532	1745440	1.11E-002	2.33	135	3000
9/22/1989	9.00	9/22/1989	10.25	0.64	4.40	331	226350	2.21E-004	4.41	15.7	24440
5/9/1990	19.25	5/9/1990	21.75	0.45	0.73	506	757	1.49E-005	3.38	0.0	6596
6/14/1990	14.00	6/14/1990	15.50	0.90	1.40	224	638	3.63E-005	2.50	0.0	6532
8/9/1990	13.75	8/10/1990	7.50	0.36	12.0	833	7152520	3.06E-003	0.79	233	3000
10/16/1990	12.00	10/16/1990	14.00	0.41	2.10	107	14090	1.32E-004	0.89	0.44	12135
10/24/1990	18.75	10/24/1990	20.25	0.34	7.00	111	300210	1.24E-004	1.84	67.9	36110
12/30/1990	19.25	12/31/1990	4.75	0.19	2.00	88	2191	3.94E-006	0.62	0.09	12209
9/17/1991	2.42	9/17/1991	9.33	0.51	0.98	338	6388	1.01E-005	0.79	0.80	9270
9/22/1991	8.5	9/23/1991	17.75	0.54	3.20	127	30550	1.91E-005	0.11	2.6	16180
11/16/1991	13.25	11/16/1991	14.50	0.39	5.10	149	175940	9.09E-006	1.66	12.1	33440
11/21/1991	15.50	11/21/1991	22.00	0.16	3.60	97	25460	1.23E-003	2.37	1.6	24270
11/28/1991	12.25	11/28/1991	14.00	0.26	24.00	120	3115180	1.47E-004	1.01	97.3	3000
5/16/1992	4.00	5/16/1992	13.25	0.39	2.00	124	7211	2.64E-006	1.35	3.9	11264
6/4/1992	8.50	6/4/1992	9.75	0.41	4.30	343	29470	2.14E-004	4.57	1.8	21040
7/22/1993	16.00	7/22/1993	17.75	0.39	5.90	495	86640	1.77E-005	4.72	19.4	21920
8/15/1993	21.50	8/16/1993	9	0.32	5.30	227	1944	2.40E-006	3.87	0.10	17490

**to eliminate zero values a value of 0.0002 was added to the precipitation between events. 0.0001 was added to the rainfall intensity between events, and a value of 5000 was added to the runoff between events.

Reproduced with permission of the copyright owner. Further reproduction prohibited without permission.

Appendix 6.15. Pearson correlation matrix using quickflow characteristics to the highest peak in the event , Quebrada Blanca near El Jagual.

Pearson correlation matrix

	LGSED	LGSEDCOQU	LGLSPKBTI	LG_QULST
LGSED	1.000			
LGSEDCOQU	0.532	1.000		
LGLSPKBTI	0.255	0.219	1.000	
LG_QULST	0.282	0.027	0.777	1.000
LGPPTBTW	-0.333	0.060	-0.025	-0.460
LGQUICK	0.891	0.091	0.183	0.317
INT15	-0.232	0.356	-0.279	-0.331
LGBASE	0.356	0.111	0.654	0.858
LGPKBS	0.617	0.327	0.127	0.308
LGRRISE	0.430	0.144	-0.170	-0.087
LGPPTLSTI	0.156	-0.153	0.620	0.877
LGINTLST	0.107	-0.198	0.470	0.828
RNBTWTI	-0.133	0.167	0.506	0.080
LMXTMJPK	0.443	0.733	0.070	-0.101
LGINTBET	-0.411	-0.036	0.046	-0.279
SUM3PPTI	0.001	-0.186	0.541	0.815
LGLS75OTI	0.020	-0.229	0.346	0.659
LGQU3EVT	0.030	-0.141	0.626	0.806
LSMLSPKBS	0.319	0.116	0.892	0.965

Reproduced with permission of the copyright owner. Further reproduction prohibited without permission.

Appendix 6.15. Continued.

	LGPPTBTW	LGQUICK	INT15	LGBASE	LGPKBS
LGPPTBTW	1.000				
LGQUICK	-0.422	1.000			
INT15	0.136	-0.465	1.000		
LGBASE	-0.384	0.360	-0.446	1.000	
LGPKBS	-0.319	0.549	0.104	0.148	1.000
LGRRISE	-0.219	0.426	0.147	-0.223	0.612
LGPPTLSTI	-0.418	0.264	-0.209	0.639	0.389
LGINTLST	-0.510	0.232	-0.203	0.630	0.342
RNBTWTI	0.654	-0.244	-0.118	0.170	-0.254
LMXTMJPK	0.141	0.129	0.418	-0.023	0.464
LGINTBET	0.801	-0.464	0.204	-0.253	-0.251
SUM3PPTI	-0.304	0.102	-0.167	0.695	0.092
LGLS75OTI	-0.339	0.146	-0.094	0.464	0.320
LGQU3EVT	-0.251	0.113	-0.394	0.810	-0.089
LSMLSPKBS	-0.378	0.314	-0.327	0.808	0.278

	LGRRISE	LGPPTLSTI	LGINTLST	RNBTWTI	LMXTMJPK
LGRRISE	1.000				
LGPPTLSTI	0.129	1.000			
LGINTLST	0.116	0.951	1.000		
RNBTWTI	-0.378	-0.050	-0.155	1.000	
LMXTMJPK	0.265	-0.189	-0.233	0.180	1.000
LGINTBET	-0.271	-0.113	-0.176	0.635	0.188
SUM3PPTI	-0.230	0.803	0.847	0.122	-0.087
LGLS75OTI	0.215	0.872	0.943	-0.125	-0.197
LGQU3EVT	-0.433	0.643	0.684	0.251	-0.153
LSMLSPKBS	-0.053	0.827	0.735	0.174	-0.047

Reproduced with permission of the copyright owner. Further reproduction prohibited without permission.

Appendix 6.15. Continued.

	LGINTBET	SUM3PPTI	LGLS75OTI	LGQU3EVT	LSMLSPKBS
LGINTBET	1.000				
SUM3PPTI	0.046	1.000			
LGLS75OTI	0.015	0.783	1.000		
LGQU3EVT	0.001	0.906	0.568	1.000	
LSMLSPKBS	-0.263	0.714	0.564	0.737	1.000

Reproduced with permission of the copyright owner. Further reproduction prohibited without permission.

Appendix 6.16. Results of principal component analysis to the major peak using quickflow characteristics for the independent variables after removal due to multicollinearity.

Component loadings

	1	2	3	4	5
LGLSPKBTI	0.714	0.376	0.248	0.335	-0.043
LG_QULST	0.973	0.047	0.026	0.080	-0.113
LGPPTBTW	-0.501	0.658	0.346	0.042	0.326
LGQUICK	0.375	-0.556	0.061	0.554	0.270
INT15	-0.380	-0.080	0.474	-0.523	-0.510
LG_BASE	0.847	0.139	-0.078	0.293	-0.170
LGPKBSE	0.309	-0.620	0.597	0.106	0.058
LGRRISE	-0.029	-0.738	0.432	-0.046	0.337
LGPPTLSTI	0.919	-0.063	0.130	-0.252	0.151
LGINTLST	0.908	-0.118	0.024	-0.368	0.117
RNBTWTI	0.022	0.812	0.345	0.311	0.134
LMXTMJPK	-0.146	-0.101	0.790	0.264	-0.391
LGINTBET	-0.255	0.709	0.444	-0.256	0.291
LSUM3PPTI	0.866	0.245	0.038	-0.276	-0.092
LGLS75OTI	0.773	-0.087	0.142	-0.518	0.260
LGQU3EVT	0.831	0.398	-0.150	0.006	-0.132
LSMLSPKBS	0.923	0.090	0.091	0.195	-0.104

Reproduced with permission of the copyright owner. Further reproduction prohibited without permission.

Appendix 6.16. Continued.

	6
LGLSPKBTI	-0.364
LG_QULST	-0.114
LGPPTBTW	-0.031
LGQUICK	0.257
INT15	-0.151
LG_BASE	0.145
LGPKBSE	0.045
LGRRISE	-0.161
LGPPTLSTI	-0.131
LGINTLST	0.023
RNBTWTI	-0.084
LMXTMJPK	0.275
LGINTBET	0.192
LSUM3PPTI	0.258
LG75OTI	0.081
LGQU3EVT	0.263
LSMLSPKBS	-0.275

Reproduced with permission of the copyright owner. Further reproduction prohibited without permission.

Appendix 6.17. Results of principal component analysis to the major peak using quickflow characteristics for the independent variables after removal due to multicollinearity without quickflow.

Component loadings

	1	2	3	4	5
LGLSPKBTI	0.722	0.390	0.229	-0.349	0.126
LGQULST	0.974	0.012	0.025	-0.151	-0.032
LGPPTBTW	-0.478	0.698	0.329	0.145	0.262
INT15	-0.363	-0.166	0.506	0.298	-0.569
LGBASE	0.844	0.145	-0.092	-0.315	-0.110
LGPKBS	0.276	-0.587	0.600	-0.196	0.141
LGRRISE	-0.063	-0.712	0.443	0.007	0.415
LGPPTLSTI	0.921	-0.129	0.146	0.226	0.134
LGINTLST	0.911	-0.202	0.046	0.335	0.040
RNBTWTI	0.047	0.859	0.315	-0.173	0.174
LMXTMJPK	-0.158	-0.045	0.778	-0.380	-0.342
LGINTBET	-0.224	0.700	0.442	0.439	0.093
LSUM3PPTI	0.880	0.174	0.050	0.277	-0.239
LGLS75OTI	0.779	-0.178	0.170	0.532	0.113
LGQU3EVT	0.847	0.362	-0.155	0.025	-0.213
LSMLSPKBS	0.923	0.072	0.084	-0.270	0.044

Reproduced with permission of the copyright owner. Further reproduction prohibited without permission.

Appendix 6.17. Continued.

	6
LGLSPKBTI	0.322
LGQULST	0.090
LGPPTBTW	0.013
INT15	0.391
LGBASE	-0.187
LGPKBS	-0.160
LGRRISE	0.008
LGPPTLSTI	0.119
LGINTLST	-0.016
RNBTWTI	0.034
LMXTMJPK	-0.264
LGINTBET	-0.130
LSUM3PPTI	-0.145
LGLS75OTI	-0.065
LGQU3EVT	-0.202
LSMLSPKBS	0.230

Reproduced with permission of the copyright owner. Further reproduction prohibited without permission.

Appendix 6.18. Component loadings from principal component analysis after varimax rotation on the independent variables using quickflow characteristics of the entire event.

Rotated Loading Matrix (VARIMAX, Gamma = 1.0000)

	1	2	3	4	5
LGLSPKBTI	0.344	-0.187	-0.029	0.116	0.047
LGQULST	0.704	0.216	-0.038	0.173	0.038
LGPPTBTW	-0.329	-0.887	-0.070	-0.095	-0.025
INT15	-0.095	-0.011	0.127	-0.871	0.337
LGBASE	0.554	0.191	-0.259	0.386	0.187
LGPKBS	0.230	0.204	0.729	0.089	0.454
LGRRISE	-0.013	0.173	0.908	0.010	0.070
LGPPTLSTI	0.855	0.102	0.227	0.046	-0.123
LGINTLST	0.930	0.192	0.148	0.050	-0.118
RNBTWTI	-0.071	-0.787	-0.251	0.078	0.108
LMXTMJPK	-0.153	-0.152	0.222	-0.136	0.914
LGINTBET	0.089	-0.925	-0.119	-0.182	0.083
SUM3PPTI	0.914	0.002	-0.242	0.064	0.110
LGLS75OTI	0.942	0.011	0.247	-0.020	-0.135
QU3EVT	0.732	0.001	-0.471	0.260	0.079
LGSMLSPKBS	0.570	0.154	0.017	0.149	0.018
LGQUICK	0.090	0.325	0.423	0.732	0.242

Reproduced with permission of the copyright owner. Further reproduction prohibited without permission.

Appendix 6.18. Continued.

	6
LGLSPKBTI	0.889
LGQULST	0.638
LGPPTBTW	-0.062
INT15	-0.183
LGBASE	0.533
LGPKBSE	0.114
LGRRISE	-0.116
LGPPTLSTI	0.397
LGINTLST	0.217
RNBTWTI	0.441
LMXTMJPK	0.071
LGINTBET	-0.184
SUM3PPTI	0.229
LGLS75OTI	0.038
QU3EVT	0.358
LGSMLSPKBS	0.788
LGQUICK	0.113

Reproduced with permission of the copyright owner. Further reproduction prohibited without permission.

Appendix 6.19. Component loadings from principal component analysis after varimax rotation on the independent variables using quickflow characteristics of the entire event without the variable QUICKFLOW.

Rotated Loading Matrix (VARIMAX, Gamma = 1.0000)

	1	2	3	4	5
LGLSPKBTI	0.320	-0.185	-0.035	0.905	0.094
LGQULST	0.684	0.223	-0.033	0.657	0.165
LGPPTBTW	-0.325	-0.891	-0.069	-0.076	-0.047
INT15	-0.088	-0.054	0.059	-0.178	-0.941
LGBASE	0.536	0.208	-0.231	0.545	0.388
LGPKBS	0.229	0.212	0.740	0.129	-0.012
LGRRISE	-0.005	0.178	0.910	-0.111	-0.061
LGPPTLSTI	0.845	0.105	0.217	0.424	0.032
LGINTLST	0.925	0.196	0.144	0.240	0.055
RNBTWTI	-0.082	-0.786	-0.236	0.430	0.132
LMXTMJPK	-0.155	-0.156	0.232	0.072	-0.228
LGINTBET	0.096	-0.933	-0.126	-0.185	-0.141
SUM3PPTI	0.905	0.006	-0.249	0.260	0.047
LGLS75OTI	0.942	0.013	0.240	0.061	-0.013
QU3EVT	0.718	0.013	-0.457	0.379	0.279
LGSMLSPKBS	0.548	0.159	0.018	0.805	0.134

Reproduced with permission of the copyright owner. Further reproduction prohibited without permission.

Appendix 6.19. Continued.

	6
LGLSPKBTI	0.041
LGQULST	0.055
LGPPTBTW	-0.030
INT15	0.221
LGBASE	0.238
LGPKBS	0.449
LGRRISE	0.055
LGPPTLSTI	-0.129
LGINTLST	-0.111
RNBTWTI	0.129
LMXTMJPK	0.896
LGINTBET	0.071
SUM3PPTI	0.110
LGLS75OTI	-0.136
QU3EVT	0.114
LGSMLSPKBS	0.024

Reproduced with permission of the copyright owner. Further reproduction prohibited without permission.

Appendix 6.20. Summary of dependent and independent variables used in statistical analysis for runoff characteristics to highest peak for Quebrada Blanca near El Jagual. (D-indicates dependent variable; L-indicated data was log transformed) (D indicates dependent variable; L indicates log transformed; IR indicates negative inverse square root transformed)

Start Date	Start Time hour	Start discharge ft3/s	End Date	End Time hour	End discharge ft3/s	DL Total sediment load current event, tons	DL Discharge-weighted sediment concentration (mg/L)	L Runoff, ft3/s 2-RUN	L Previous event peak flow over time since last peak flow, ft3/s/hour 21-LSPKTI
8/11/1989	16.00	0.98	8/11/1989	17.25	86	1.3	652	62720	0.13
8/18/1989	22.00	3.10	8/19/1989	0.25	231	9.3	1475	201560	1.57
9/13/1989	21.50	3.10	9/14/1989	0.75	115	4.7	561	270140	0.59
9/18/1989	2.75	7.30	9/18/1989	9.00	537	154	993	4963370	3.04
9/22/1989	9.00	4.40	9/22/1989	10.25	335	20.2	1621	399960	5.59
5/9/1990	19.25	0.73	5/9/1990	21.75	507	6.5	755	277320	0.03
6/14/1990	14.00	1.40	6/14/1990	15.50	226	5.3	1155	146610	0.02
8/9/1990	13.75	12.00	8/10/1990	7.50	838	30.7	488	2015100	2.16
10/16/1990	12.00	2.10	10/16/1990	14.00	109	2.5	388	204170	0.29
10/24/1990	18.75	7.00	10/24/1990	20.25	118	3.0	561	169390	14.8
12/30/1990	19.25	2.00	12/31/1990	4.75	91	14.3	541	846540	0.10
9/17/1991	2.42	0.98	9/17/1991	9.33	340	21.9	610	1152390	0.52
9/22/1991	8.5	3.2	9/23/1991	17.75	10	25.9	727	1142220	1.45
11/16/1991	13.25	5.10	11/16/1991	14.50	154	9.3	1236	240800	3.60
11/21/1991	15.50	3.60	11/21/1991	22.00	101	3.0	209	454680	1.27
11/28/1991	12.25	24.00	11/28/1991	14.00	130	9.3	702	426600	2.83
5/16/1992	4.00	2.00	5/16/1992	13.25	128	30.6	1648	594720	2.28
6/4/1992	8.50	4.30	6/4/1992	9.75	347	47.0	2893	519950	1.08
7/22/1993	16.00	5.90	7/22/1993	17.75	501	47.7	1497	1020110	14.0
8/15/1993	21.50	5.3	8/16/1993	9	234	101	1217	2647220	0.12

Reproduced with permission of the copyright owner. Further reproduction prohibited without permission.

Appendix 6.20. Continued.

Start Date	Start Time hour	End Date	End Time hour	Sum of 3 previous runoff events over the time since these events ft3/hour 31-RU3EVT	Previous event rainfall over time since previous event, in/hour 26-PPTLSTI	Previous event maximum 15-minute rainfall intensity over the time since the previous event, in/min/hour 27-INTLST	Rainfall since the previous event over time since the previous event in/hour 18-PPTBTW	Maximum 15-minute rainfall intensity since the previous event over the time since the previous event, in/miln/hour 19-INTBET	Sum of 3 previous rainfall events over the time since these events in/hour 29-SUM3PPTI	Rainfall on the rising limb of the hydrograph to the highest peak flow, in 13-RRISE	Maximum 15-minute rainfall of current event, in/min 11-INT15
8/11/1989	16.00	8/11/1989	17.25	9.66	0.005	0.0016	0.0009	0.0007	-8.618	1.05	0.64
8/18/1989	22.00	8/19/1989	0.25	11.75	0.107	0.0485	0.0007	0.0005	-5.917	1.28	0.73
9/13/1989	21.50	9/14/1989	0.75	12.06	0.014	0.0058	0.0014	0.0012	-6.037	1.36	0.51
9/18/1989	2.75	9/18/1989	9.00	14.38	0.817	0.5615	0.1402	0.0001	-4.032	5.27	0.28
9/22/1989	9.00	9/22/1989	10.25	13.13	0.154	0.0096	0.0063	0.0045	-5.299	1.38	0.64
5/9/1990	19.25	5/9/1990	21.75	9.22	0.003	0.0010	0.0023	0.0006	-8.683	1.68	0.45
6/14/1990	14.00	6/14/1990	15.50	8.71	0.001	0.0008	0.0048	0.0005	-8.689	2.08	0.90
8/9/1990	13.75	8/10/1990	7.50	12.70	3.717	0.5844	0.0002	0.0001	-5.100	1.94	0.36
10/16/1990	12.00	10/16/1990	14.00	11.95	0.023	0.0069	0.0082	0.0018	-6.074	1.05	0.41
10/24/1990	18.75	10/24/1990	20.25	14.22	0.120	0.0168	0.0115	0.0019	-5.069	0.99	0.34
12/30/1990	19.25	12/31/1990	4.75	9.97	0.002	0.0006	0.0025	0.0003	-9.253	1.03	0.19
9/17/1991	2.42	9/17/1991	9.33	9.86	0.006	0.0013	0.0015	0.0003	-8.327	2.51	0.51
9/22/1991	8.5	9/23/1991	17.75	13.13	0.012	0.0028	0.0022	0.0007	-5.294	0.41	0.54
11/16/1991	13.25	11/16/1991	14.50	13.89	0.004	0.0014	0.0025	0.0004	-6.430	0.63	0.39
11/21/1991	15.50	11/21/1991	22.00	14.38	0.055	0.0261	0.0053	0.0021	-5.940	0.74	0.16
11/28/1991	12.25	11/28/1991	14.00	17.35	0.081	0.0581	0.0002	0.0001	-3.901	0.43	0.26
5/16/1992	4.00	5/16/1992	13.25	8.89	0.003	0.0003	0.0029	0.0002	-10.373	1.71	0.39
6/4/1992	8.50	6/4/1992	9.75	12.49	0.017	0.0099	0.0062	0.0020	-6.798	1.12	0.41
7/22/1993	16.00	7/22/1993	17.75	11.63	0.017	0.0022	0.0030	0.0007	-8.068	1.35	0.39
8/15/1993	21.50	8/16/1993	9	10.76	0.001	0.0003	0.0014	0.0004	-8.847	1.82	0.32

Reproduced with permission of the copyright owner. Further reproduction prohibited without permission.

Appendix 6.20. Continued.

Start Date	Start Time hour	End Date	End Time hour	Baseflow at start of event, ft3/s 3-BASE	Peakflow, ft3/s 5-PK	Previous event runoff over the time since previous event, ft3/hour 25-RULST	Previous event 75% rainfall intensity over time since previous event, in/min/hour 28-LS75OTI	Maximum rate of hydrograph rise from start of event to the highest peak flow. ft3/min 6-MXTMJPK	Sum of peak flows in previous event over time since the previous event, ft3/s/hour 23-SMLSPK	Runoff since the previous event over time since the previous event ft3/hour 17-RNBTWTI
8/11/1989	16.00	8/11/1989	17.25	0.98	86	2350	2.09E-005	1.13	0.15	6420
8/18/1989	22.00	8/19/1989	0.25	3.10	231	95660	3.75E-004	1.69	6.00	16370
9/13/1989	21.50	9/14/1989	0.75	3.10	115	20680	2.07E-004	3.00	0.85	16760
9/18/1989	2.75	9/18/1989	9.00	7.30	537	2678750	1.11E-002	2.33	152	3000
9/22/1989	9.00	9/22/1989	10.25	4.40	335	250360	2.21E-004	4.41	16.1	24440
5/9/1990	19.25	5/9/1990	21.75	0.73	507	1150	1.49E-005	3.38	0.03	6596
6/14/1990	14.00	6/14/1990	15.50	1.40	226	870	3.63E-005	2.50	0.03	6532
8/9/1990	13.75	8/10/1990	7.50	12.00	838	9747180	3.06E-003	0.79	248	3000
10/16/1990	12.00	10/16/1990	14.00	2.10	109	22450	1.32E-004	0.89	0.53	12135
10/24/1990	18.75	10/24/1990	20.25	7.00	118	390630	1.24E-004	1.84	68.4	36110
12/30/1990	19.25	12/31/1990	4.75	2.00	91	3200	3.94E-006	0.62	0.10	12209
9/17/1991	2.42	9/17/1991	9.33	0.98	340	7730	1.01E-005	0.79	0.80	9270
9/22/1991	8.5	9/23/1991	17.75	3.20	132	47140	1.91E-005	0.11	2.94	16180
11/16/1991	13.25	11/16/1991	14.50	5.10	154	242550	9.09E-006	1.66	12.3	33440
11/21/1991	15.50	11/21/1991	22.00	3.60	101	35470	1.23E-003	2.37	1.67	24270
11/28/1991	12.25	11/28/1991	14.00	24.0	130	4860920	1.47E-004	1.01	136	3000
5/16/1992	4.00	5/16/1992	13.25	2.00	128	7450	2.64E-006	1.35	3.49	11264
6/4/1992	8.50	6/4/1992	9.75	4.30	347	42490	2.14E-004	4.57	1.93	21040
7/22/1993	16.00	7/22/1993	17.75	5.90	501	92040	1.77E-005	4.72	19.4	21920
8/15/1993	21.50	8/16/1993	9	5.30	234	3680	2.40E-006	3.87	0.12	17490

**to eliminate zero values a value of 0.0002 was added to the precipitation between events and a value of 3000 was added to the runoff between events.

Reproduced with permission of the copyright owner. Further reproduction prohibited without permission.

Appendix 6.21. Pearson correlation matrix for the event to the highest peak in the event using runoff characteristics, Quebrada Blanca near El Jagual.

Pearson correlation matrix

	LGSED	LGSEDCONC	LGLSPKTI	LGRUNLST
LGSED	1.000			
LGSEDCONC	0.544	1.000		
LGLSPKTI	0.257	0.164	1.000	
LGRUNLST	0.278	-0.025	0.768	1.000
LGPPTBTW	-0.333	0.055	-0.047	-0.479
LGRUN	0.880	0.080	0.212	0.344
INT15	-0.232	0.371	-0.291	-0.344
LGBASE	0.356	0.065	0.678	0.871
LGPK	0.622	0.376	0.129	0.310
LGRRISE	0.430	0.202	-0.182	-0.093
LGPPTLSTI	0.156	-0.171	0.627	0.876
LGINTLST	0.107	-0.208	0.483	0.840
RNBTWTI	-0.133	0.126	0.492	0.070
LMXTMJPK	0.443	0.756	0.070	-0.101
LGINTBET	-0.411	-0.032	0.035	-0.282
SUM3PPTI	0.001	-0.212	0.563	0.836
LGLS75OTI	0.020	-0.227	0.355	0.673
RU3EVT	0.046	-0.181	0.660	0.831
LGSMLSPK	0.317	0.065	0.894	0.960

Reproduced with permission of the copyright owner. Further reproduction prohibited without permission.

Appendix 6.21. Continued.

	LGPPTBTW	LGRUN	INT15	LGBASE	LGPEAK
LGPPTBTW	1.000				
LGRUN	-0.424	1.000			
INT15	0.136	-0.484	1.000		
LGBASE	-0.384	0.386	-0.446	1.000	
LGPK	-0.326	0.524	0.093	0.167	1.000
LGRRISE	-0.219	0.394	0.147	-0.223	0.604
LGPPTLSTI	-0.418	0.281	-0.209	0.639	0.398
LGINTLST	-0.510	0.245	-0.203	0.630	0.351
RNBTWTI	0.654	-0.227	-0.118	0.170	-0.250
LMXTMJPK	0.141	0.099	0.418	-0.023	0.463
LGINTBET	0.801	-0.469	0.204	-0.253	-0.257
SUM3PPTI	-0.304	0.123	-0.167	0.695	0.104
LGLS75OTI	-0.339	0.152	-0.094	0.464	0.324
RU3EVT	-0.250	0.159	-0.448	0.829	-0.054
LGSMLSPK	-0.393	0.339	-0.332	0.822	0.287

	LGRRISE	LGPPTLSTI	LGINTLST	RNBTWTI	LMXTMJPK
LGRRISE	1.000				
LGPPTLSTI	0.129	1.000			
LGINTLST	0.116	0.951	1.000		
RNBTWTI	-0.378	-0.050	-0.155	1.000	
LMXTMJPK	0.265	-0.189	-0.233	0.180	1.000
LGINTBET	-0.271	-0.113	-0.176	0.635	0.188
SUM3PPTI	-0.230	0.803	0.847	0.122	-0.087
LGLS75OTI	0.215	0.872	0.943	-0.125	-0.197
RU3EVT	-0.431	0.642	0.686	0.274	-0.165
LGSMLSPK	-0.061	0.831	0.744	0.163	-0.047

Reproduced with permission of the copyright owner. Further reproduction prohibited without permission.

Appendix 6.21. Continued.

	LGINTBET	SUM3PPTI	LGLS75OTI	RU3EVT	LGSMLSPK
LGINTBET	1.000				
SUM3PPTI	0.046	1.000			
LGLS75OTI	0.015	0.783	1.000		
RU3EVT	-0.002	0.891	0.577	1.000	
LGSMLSPK	-0.268	0.730	0.572	0.758	1.000

Reproduced with permission of the copyright owner. Further reproduction prohibited without permission.

Appendix 6.22. Component loadings from principal component analysis on the independent variables using runoff characteristics to the highest peak.

Component loadings

	1	2	3	4	5
LGLSPKTI	0.725	0.377	0.205	0.335	-0.061
LG_RUNLST	0.978	0.043	0.012	0.062	-0.118
LGPPTBTW	-0.505	0.662	0.327	0.058	0.329
LGRUN	0.402	-0.521	-0.008	0.568	0.290
INT15	-0.391	-0.090	0.517	-0.477	-0.505
LG_BASE	0.852	0.142	-0.089	0.287	-0.169
LOGPEAK	0.320	-0.606	0.586	0.163	0.067
LGRRISE	-0.033	-0.734	0.434	-0.010	0.351
LGPPTLSTI	0.914	-0.065	0.154	-0.251	0.147
LGINTLST	0.906	-0.119	0.059	-0.370	0.112
RNBTWTI	0.022	0.819	0.310	0.324	0.134
LMXTMJPK	-0.147	-0.092	0.776	0.339	-0.369
LGINTBET	-0.258	0.715	0.452	-0.227	0.292
SUM3PPTI	0.866	0.243	0.070	-0.272	-0.093
LGL75OTI	0.771	-0.086	0.185	-0.510	0.256
RU3EVT	0.843	0.400	-0.150	0.025	-0.094
LGSMLSPK	0.928	0.087	0.071	0.183	-0.117

Reproduced with permission of the copyright owner. Further reproduction prohibited without permission.

Appendix 6.22. Continued.

	6
LGLSPKTI	-0.365
LGRUNLST	-0.076
LGPPTBTW	-0.039
LGRUN	0.224
INT15	-0.132
LGBASE	0.130
LGPK	0.062
LGRRISE	-0.180
LGPPTLSTI	-0.138
LGINTLST	0.021
RNBTWTI	-0.103
LMXTMJPK	0.263
LGINTBET	0.185
SUM3PPTI	0.246
LGLS75OTI	0.081
RU3EVT	0.249
LGSMLSPK	-0.267

Reproduced with permission of the copyright owner. Further reproduction prohibited without permission.

Appendix 6.23. Component loadings from principal component analysis on the independent variables using runoff characteristics to the highest peak without the variable RUNOFF.

Component loadings

	1	2	3	4	5
LGLSPKTI	0.733	0.385	0.207	-0.337	0.102
LG_RUNLST	0.979	0.007	0.012	-0.133	-0.048
LGPPTBTW	-0.483	0.696	0.329	0.150	0.259
INT_15	-0.372	-0.175	0.513	0.280	-0.590
LG_BASE	0.849	0.147	-0.087	-0.321	-0.091
LOGPEAK	0.288	-0.583	0.586	-0.212	0.161
LG_RRISE	-0.066	-0.713	0.433	0.012	0.431
LGPPTLSTI	0.917	-0.131	0.152	0.235	0.121
LG_INT_LST	0.910	-0.202	0.056	0.337	0.030
RNBTW_TI	0.046	0.858	0.314	-0.169	0.177
LMXTMJPK	-0.158	-0.048	0.778	-0.416	-0.299
LGINT_BET	-0.226	0.699	0.452	0.430	0.086
SUM3PPTI	0.881	0.173	0.068	0.264	-0.238
LGL75_OTI	0.778	-0.177	0.181	0.533	0.099
RU3EVT	0.858	0.369	-0.150	-0.007	-0.150
LGSMLSPK	0.929	0.066	0.072	-0.255	0.025

Reproduced with permission of the copyright owner. Further reproduction prohibited without permission.

Appendix 6.23. Continued.

	6
LGLSPKTI	0.336
LG_RUNLST	0.060
LGPPTBTW	0.022
INT_15	0.346
LG_BASE	-0.164
LOGPEAK	-0.167
LG_RRISE	0.047
LGPPTLSTI	0.132
LG_INT_LST	-0.014
RNBTW_TI	0.060
LMXTMJPK	-0.255
LGINT_BET	-0.133
SUM3PPTI	-0.147
LGL75_OTI	-0.067
RU3EVT	-0.224
LGSMLSPK	0.234

Reproduced with permission of the copyright owner. Further reproduction prohibited without permission.

Appendix 6.24. Component loadings from principal component analysis after varimax rotation on the independent variables using runoff characteristics to the highest peak.

Rotated Loading Matrix (VARIMAX, Gamma = 1.0000)

	1	2	3	4	5
LGLSPKTI	0.569	-0.183	0.071	0.160	0.083
LGRUNLST	0.859	0.205	0.101	0.216	0.065
LGPPTBTW	-0.355	-0.878	0.039	-0.100	-0.033
LGRUN	0.140	0.319	-0.336	0.760	0.266
INT15	-0.137	0.002	-0.114	-0.872	0.344
LGBASE	0.666	0.168	0.319	0.407	0.169
LGPK	0.306	0.210	-0.581	0.148	0.595
LGRRISE	-0.035	0.195	-0.932	0.016	0.153
LGPPTLSTI	0.943	0.086	-0.196	0.076	-0.070
LGINTLST	0.963	0.173	-0.131	0.059	-0.096
RNBTWTI	0.020	-0.792	0.244	0.082	0.087
LMXTMJPK	-0.140	-0.148	-0.129	-0.139	0.924
LGINTBET	0.019	-0.928	0.115	-0.202	0.059
SUM3PPTI	0.931	-0.111	0.168	-0.033	0.091
LGLS75OTI	0.923	-0.004	-0.248	-0.023	-0.115
RU3EVT	0.881	0.177	0.145	0.266	0.029
LGSMLSPK	0.765	0.149	0.027	0.190	0.055

Reproduced with permission of the copyright owner. Further reproduction prohibited without permission.

Appendix 6.24. Continued.

	6
LGLSPKTI	0.750
LGRUNLST	0.380
LGPPTBTW	0.028
LGRUN	0.062
INT15	-0.123
LGBASE	0.342
LGPK	-0.044
LGRRISE	-0.068
LGPPTLSTI	0.144
LGINTLST	-0.030
RNBTWTI	0.449
LMXTMJPK	0.096
LGINTBET	-0.200
SUM3PPTI	0.179
LGLS75OTI	-0.190
RU3EVT	0.290
LGSMLSPK	0.587

Reproduced with permission of the copyright owner. Further reproduction prohibited without permission.

Appendix 6.25. Component loadings from principal component analysis after varimax rotation on the independent variables using runoff characteristics to the highest peak with the variable RUNOFF.

Rotated Loading Matrix (VARIMAX, Gamma = 1.0000)

	1	2	3	4	5
LGLSPKTI	0.347	-0.170	-0.043	0.895	0.103
LGRUNLST	0.714	0.231	-0.051	0.615	0.185
LGPPTBTW	-0.327	-0.892	-0.062	-0.078	-0.045
INT15	-0.090	-0.054	0.050	-0.181	-0.939
LGBASE	0.538	0.205	-0.233	0.551	0.384
LGPK	0.248	0.219	0.711	0.111	0.008
LGRRISE	-0.002	0.181	0.913	-0.115	-0.068
LGPPTLSTI	0.854	0.104	0.219	0.407	0.030
LGINTLST	0.930	0.196	0.140	0.225	0.055
RNBTWTI	-0.079	-0.789	-0.229	0.434	0.131
LMXTMJPK	-0.159	-0.156	0.212	0.080	-0.231
LGINTBET	0.092	-0.932	-0.131	-0.188	-0.141
SUM3PPTI	0.903	0.004	-0.254	0.258	0.046
LGLS75OTI	0.947	0.014	0.232	0.044	-0.012
RU3EVT	0.709	-0.003	-0.436	0.388	0.339
LGSMLSPK	0.572	0.167	0.011	0.785	0.139

Reproduced with permission of the copyright owner. Further reproduction prohibited without permission.

Appendix 6.25. Continued.

	6
LGLSPKTI	0.045
LGRUNLST	0.069
LGPPTBTW	-0.032
INT15	0.225
LGBASE	0.228
LGPK	0.488
LGRRISE	0.072
LGPPTLSTI	-0.120
LGINTLST	-0.103
RNBTWTI	0.118
LMXTMJPK	0.898
LGINTBET	0.070
SUM3PPTI	0.103
LGL75OTI	-0.122
RU3EVT	0.097
LGSMLSPK	0.032

Reproduced with permission of the copyright owner. Further reproduction prohibited without permission.

Appendix 6.26. Summary of dependent and independent variables used in the statistical analysis for hysteresis.
(A) Type 1 storms and (B) Type 3 storms.
(D indicates dependent variable; L indicates log transformed; IR indicates negative inverse square root transformed)

Appendix 6.26A.

Start Date	Start Time hour	End Date	End Time hour	Width of clockwise clockwise loop, mg/L D L	Discharge used in width analysis, ft3/s	Sediment load, tons SED	Discharge-weighted sediment concentration, mg/L CONC	Runoff ft3 2-RUN L	Sum of peak flows 9-SMPK	Maximum rate of hydrograph rise to the highest peak, ft3/s//min 6-MXTMJPK	Runoff of the previous event divided by the time since the previous event, fts/hour 25-RULST
8/11/1989	16.00	8/12/1989	5.75	509	76	6.5	282	8.59E+005	86	1.69	2.36E+003
9/13/1989	21.50	9/14/1989	20.00	492	55	12	382	2.59E+006	231	2.33	2.07E+004
10/24/1990	18.75	10/25/1990	15.25	486	88	16	215	1.23E+007	791	0.64	3.91E+005
11/4/1990	12.25	11/5/1990	14.50	680	102	48	547	1.75E+006	471	0.16	9.35E+004
12/30/1990	19.25	1/2/1991	6.75	620	75	34	237	7.40E+005	55	0.62	3.21E+003
7/15/1991	13.25	7/16/1991	2.75	1200	77	16	331	1.54E+006	507	0.26	2.84E+004
9/22/1991	8.50	9/23/1991	17.75	201	114	49	462	1.81E+006	226	2.37	4.71E+004
11/28/1991	12.25	12/1/1991	11.75	95	122	23	187	2.44E+006	62	1.01	4.86E+006
5/16/1992	4.00	5/17/1992	8.75	1530	107	55	1218	7.98E+006	1112	1.35	7.45E+003
6/4/1992	8.50	6/5/1992	13.50	1580	201	115	1553	2.00E+006	109	4.57	4.25E+004
7/22/1993	16.00	7/23/1993	2.75	386	276	97	1153	2.84E+006	233	0.21	9.21E+004
8/15/1993	21.50	8/17/1993	17.00	534	142	152	751	3.29E+006	197	3.87	3.68E+003
			AVERAGE	**693**	**120**	**52**	**610**	**3.35E+006**	**340**	**1.59**	**4.66E+005**

Start Date	Start Time hour	End Date	End Time hour	Runoff of the 3 previous events divided by the time since the 3 events 31-RU3EVT	Sediment transport curve slope on falling limb, ft3/s/(mg/L) 33-RATE_FALL	Rainfall on the rising limb to the highest peak, in., 13-RRISE	Rainfall on the falling limb after the highest peak, in 14-RAINFOL L	75% rainfall intensity of current event, in/min, 12-SFIVE L	Runoff since the previous event over time since the previous event ft3/hour 17-RNBTWTI	Sediment transport curve slope on rising limb, ft3/s/(mg/L) 32-RATE_RISE	Time of peak sediment concentration relative to peak flow (minutes) 34-TIME_PKCON
8/11/1989	16.00	8/12/1989	5.75	9.66	34.2	1.05	0.01	0.0309	8420	15.05	-1
9/13/1989	21.50	9/14/1989	20.00	12.06	5.1	1.36	0.20	0.0051	18760	-8.01	-32
10/24/1990	18.75	10/25/1990	15.25	14.22	7.7	0.99	0.40	0.0093	38110	-1.34	-10
11/4/1990	12.25	11/5/1990	14.50	13.30	10.3	0.91	0.57	0.0034	25256	15.40	1
12/30/1990	19.25	1/2/1991	6.75	9.97	21.9	1.03	1.10	0.0024	14209	3.01	-27
7/15/1991	13.25	7/16/1991	2.75	11.41	8.0	1.49	0.06	0.0038	11386	-43.90	365
9/22/1991	8.50	9/23/1991	17.75	13.13	4.5	0.93	0.28	0.0022	18182	-6.84	-61
11/28/1991	12.25	12/1/1991	11.75	17.35	14.8	0.43	0.09	0.0045	5000	9.92	-20
5/16/1992	4.00	5/17/1992	8.75	8.89	20.1	1.71	0.18	0.0031	13264	-46.86	-32
6/4/1992	8.50	6/5/1992	13.50	12.49	9.2	1.12	0.19	0.0143	23042	-7.57	-20
7/22/1993	16.00	7/23/1993	2.75	11.63	2.7	1.35	0.96	0.0158	23916	2.82	-9
8/15/1993	21.50	8/17/1993	17.00	10.76	8.0	1.82	0.44	0.0025	19489	4.91	-456
			AVERAGE	**12.07**	**Average positive slope = 12.21**	**1.18**	**0.37**	**0.0081**	**18253**	**Average negative slope = -19.09 Average positive slope = 8.52**	**-25**

Reproduced with permission of the copyright owner. Further reproduction prohibited without permission.

Appendix 6.26B.

Start Date	Start Time hour	End Date	End Time hour	Width of counter-clockwise loop. mg/L D IR	Discharge used in width analysis, ft3/s	Sediment load tons	Discharge-weighted sediment concentration, mg/L	Runoff ft3 2-RUN	Sum of peak flows 9-SMPK	Maximum rate of hydrograph rise to the highest peak, cfs/min 6-MXTMJPK	Runoff of the previous event divided by the time since the previous event, fts/hour 25-RULST
8/18/1989	22.00	8/19/1989	23.25	624	195	63	966	5.82E+006	171	3.00	9.57E+004
9/18/1989	2.75	9/20/1989	7.75	893	314	376	1081	1.62E+006	349	4.41	2.68E+006
9/22/1989	9.00	9/22/1989	21.50	553	282	52	1086	3.61E+006	376	0.80	2.50E+005
5/9/1990	19.25	5/10/1990	20.00	726	245	34	753	4.37E+006	558	2.50	1.16E+003
6/14/1990	14.00	6/15/1990	11.50	1990	157	36	912	4.16E+006	277	0.06	8.74E+002
8/9/1990	13.75	8/12/1990	21.75	360	366	99	509	6.84E+006	130	0.89	9.75E+006
10/16/1990	12.00	10/17/1990	14.75	782	81	19	358	1.97E+006	142	1.84	2.25E+004
9/17/1991	2.42	9/18/1991	10.75	400	100	75	610	3.02E+006	347	1.66	7.74E+003
			AVERAGE	**791**	**218**	**94**	**784**	**3.93E+006**	**294**	**1.89**	**1.60E+006**

Start Date	Start Time hour	End Date	End Time hour	Runoff of the 3 previous events divided by the time since the 3 events 31-RU3EVT	Sediment transport curve slope on falling limb, ft3/s/(mg/L) 32-RATE_FALL	Rainfall on the rising limb to the highest peak, in, 13-RRISE	Rainfall on the falling limb after the highest peak, in 14-RAINFOL L	Seventy five percent rainfall intensity of current event, in/min 12-SFIVE	Runoff since the previous event over time since the previous event ft3/hour 17-RNBTWTI	Sediment transport curve slope on rising limb, cfs/(mg/L 32-RATE_RISE	Time of peak sediment concentration relative to peak flow (minutes) 34-TIME_PKCON
8/18/1989	22.00	8/19/1989	23.25	11.75	11.2	1.28	0.56	0.0045	18371	-6.95	-10
9/18/1989	2.75	9/20/1989	7.75	14.38	4.3	5.27	1.95	0.0104	5000	1.86	24
9/22/1989	9.00	9/22/1989	21.50	13.13	6.8	1.38	0.08	0.0119	26441	-0.55	-22
5/9/1990	19.25	5/10/1990	20.00	9.22	-1.5	1.68	0.34	0.0106	8596	2.22	50
6/14/1990	14.00	6/15/1990	11.50	8.71	16.1	2.08	2.01	0.0106	8532	11.61	11
8/9/1990	13.75	8/12/1990	21.75	12.70	3.1	1.94	1.08	0.0019	5000	2.25	7
10/16/1990	12.00	10/17/1990	14.75	11.95	-8.5	1.06	0.07	0.0121	14135	7.50	17
9/17/1991	2.42	9/18/1991	10.75	9.86	5.6	2.51	0.23	0.0062	11270	6.96	13
			AVERAGE	**11.46**	**4.6**	**2.15**	**0.79**	**0.0085**	**12168**		**11.2500**
					Average negative slope = -5.02					**Average negative slope = -3.75**	
					Average positive slope = 7.83					**Average positive slope = 5.40**	

Reproduced with permission of the copyright owner. Further reproduction prohibited without permission.

Appendix 7.1 . Relation of calculated quickflow to estimated quickflow. Estimated quickflow is calculated from rain falling on impervious basin Rio Caguitas basin area = 5.30 sq.mi.

Start Date	Hour	End Date	Hour	Rainfall amount, in	Estimated volume of quickflow corresponding to impervious contributing area, ft3	Calculated quickflow, ft3	Percent ratio: calculated quickflow/ estimated quickflow
1/5/1992	15.75	1/7/1992	6	5.76	7.10E+007	2.88E+007	41
9/22/1992	13.75	9/23/1992	9.75	0.52	6.40E+006	1.18E+006	18
12/1/1992	12.5	12/1/1992	22	0.30	3.69E+006	3.11E+005	8
12/29/1992	12.25	12/30/1992	4	0.78	9.60E+006	5.99E+005	6
1/7/1993	13.25	1/8/1993	5.75	0.65	8.00E+006	1.72E+006	21
5/1/1993	14.75	5/2/1993	16	0.95	1.17E+007	2.26E+006	19
5/6/1993	14.25	5/7/1993	1.25	0.29	3.57E+006	9.81E+005	27
5/26/1993	13.5	5/26/1993	23.5	0.64	7.88E+006	1.49E+006	19
7/3/1993	10.75	7/4/1993	0.75	0.50	6.16E+006	3.49E+005	6
7/13/1993	16.75	7/14/1993	4.25	0.27	3.32E+006	1.35E+006	41
7/22/1993	13.75	7/23/1993	2	0.84	1.03E+007	2.33E+006	23
8/15/1993	23.75	8/16/1993	7.75	1.37	1.69E+007	5.92E+005	4
8/18/1995	11.25	8/19/1995	9	2.61	3.21E+007	4.95E+006	15
9/6/1995	2.25	9/7/1995	3.75	3.16	3.89E+007	1.17E+007	30
9/7/1995	11.5	9/8/1995	6.5	0.63	7.76E+006	1.63E+006	21
9/15/1995	21.75	9/17/1995	8.25	2.87	3.53E+007	1.08E+007	30
9/27/1995	14.25	9/27/1995	21.5	0.25	3.08E+006	5.75E+005	19
10/27/1995	14.75	10/28/1995	2	0.89	1.10E+007	2.04E+006	19
11/4/1995	13.75	11/5/1995	6	1.34	1.65E+007	2.29E+006	14
12/25/1995	16.25	12/25/1995	23.5	0.66	8.13E+006	1.25E+006	15
3/15/1996	13.5	3/16/1996	1.25	1.53	1.88E+007	8.47E+005	4
4/3/1996	14.5	4/3/1996	22	2.71	3.34E+007	8.54E+005	3
5/23/1996	1.75	5/23/1996	13.25	0.82	1.01E+007	7.16E+005	7

Reproduced with permission of the copyright owner. Further reproduction prohibited without permission.

Appendix 7.2. Summary of dependent and independent variables used in the statistical analysis for quickf characteristics of the entire event at Rio Caguitas near Aguas Buenas.
(D indicates dependent variable; L indicates data was log transformed for final statistical operations; IR indicates data had negative inverse square root transformed)

Start Date	Start Time hour	Start Discharge ft3/s	End Date	End Time hour	DL Suspended-sediment load tons	DL Discharge-weighted sediment concentration mg/L	L QUICK	L LSPKBTI	L QULST
01/05/1992	15.75	6.4	1/7/1992	6	3800	4236	28759860	0.03	643
09/22/1992	13.75	6.4	9/23/1992	9.75	38.2	1036	1182780	0.42	8635
12/01/1992	12.5	11.0	12/1/1992	22	8.47	873	310950	16.03	257630
12/29/1992	12.25	13.0	12/30/1992	4	21.0	1125	598560	20.12	1034911
01/07/1993	13.25	8.6	1/8/1993	5.75	139	2592	1718550	0.29	2974
05/01/1993	14.75	9.3	5/2/1993	16	71.6	1015	2259778	1.28	15659
05/06/1993	14.25	8.9	5/7/1993	1.25	73.5	2401	981315	1.19	20632
05/26/1993	13.5	8.2	5/26/1993	23.5	109	2344	1488780	1.37	15869
07/03/1993	10.75	7.3	7/4/1993	0.75	5.43	499	348840	0.26	2591
07/13/1993	16.75	11.0	7/14/1993	4.25	51.9	1228	1353150	15.55	409791
07/22/1993	13.75	8.9	7/23/1993	2	191	2631	2330263	0.36	3281
08/15/1993	23.75	13.0	8/16/1993	7.75	21	1120	591730	0.34	5294
08/18/1995	11.25	6.2	8/19/1995	9	351	2272	4950059	0.10	1617
09/06/1995	2.25	8.9	9/7/1995	3.75	3500	9562	11717552	14.23	1022691
09/07/1995	11.5	9.9	9/8/1995	6.5	50	981	1626211	49.95	1511942
09/15/1995	21.75	8.3	9/17/1995	8.42	1030	3050	10778128	19.97	3929288
09/27/1995	14.25	2.7	9/27/1995	21.5	97	5379	574983	0.32	7894
10/27/1995	14.75	2.6	10/28/1995	2	452	7080	2043728	0.12	1302
11/04/1995	13.75	2.6	11/5/1995	6	147	2057	2288244	2.35	11370
12/25/1995	16.25	1.7	12/25/1995	23.5	250	6411	1248920	0.52	5811
03/15/1996	13.5	1.9	3/16/1996	1.25	46.1	1744	846691	0.05	160
04/03/1996	14.5	1.4	4/3/1996	22	166	6220	854160	0.14	1902
05/23/1996	1.75	1.8	5/23/1996	13.25	64.2	2872	715826	0.06	359

Reproduced with permission of the copyright owner. Further reproduction prohibited without permission.

Appendix 7.2. Continued.

Start Date	Start Time hour	End Date	End Time hour	L PPTLSTI	L INTLST	L L75OTI	SUM3PPTI	QU3EVT	RNBTWTI
01/05/1992	15.75	6.4	1/7/1992	0.0014	0.0003	0.00001	-9.68	7.15	18441
09/22/1992	13.75	6.4	9/23/1992	0.0071	0.0056	0.00029	-5.23	13.52	27283
12/01/1992	12.5	11.0	12/1/1992	0.0656	0.0253	0.00041	-5.49	13.64	42935
12/29/1992	12.25	13.0	12/30/1992	1.8000	0.5800	0.02163	-3.69	14.93	0
01/07/1993	13.25	8.6	1/8/1993	0.0039	0.0031	0.00001	-7.31	11.18	36553
05/01/1993	14.75	9.3	5/2/1993	0.0276	0.0085	0.00022	-6.74	10.94	39051
05/06/1993	14.25	8.9	5/7/1993	0.0087	0.0049	0.00015	-6.23	12.28	38222
05/26/1993	13.5	8.2	5/26/1993	0.0248	0.0114	0.00033	-6.67	12.51	33598
07/03/1993	10.75	7.3	7/4/1993	0.0026	0.0012	0.00003	-6.83	10.35	25687
07/13/1993	16.75	11.0	7/14/1993	0.0631	0.0034	0.00008	-6.31	11.30	45677
07/22/1993	13.75	8.9	7/23/1993	0.0032	0.0018	0.00003	-7.49	12.04	34867
08/15/1993	23.75	13.0	8/16/1993	0.0009	0.0003	0.00001	-8.70	11.08	38656
08/18/1995	11.25	6.2	8/19/1995	0.0028	0.0018	0.00005	-8.27	9.47	11259
09/06/1995	2.25	8.9	9/7/1995	4.4400	0.8800	0.01259	-4.35	14.00	0
09/07/1995	11.5	9.9	9/8/1995	0.4077	0.0594	0.00066	-4.69	13.95	37593
09/15/1995	21.75	8.3	9/17/1995	7.8000	2.5500	0.08000	-3.39	15.29	0
09/27/1995	14.25	2.7	9/27/1995	0.0025	0.0014	0.00001	-7.26	11.51	16840
10/27/1995	14.75	2.6	10/28/1995	0.0070	0.0018	0.00002	-8.84	9.29	7897
11/04/1995	13.75	2.6	11/5/1995	0.0050	0.0012	0.00003	-8.56	9.43	10265
12/25/1995	16.25	1.7	12/25/1995	0.0209	0.0120	0.00067	-7.08	9.73	6685
03/15/1996	13.5	1.9	3/16/1996	0.0008	0.0005	0.00002	-10.00	6.30	6829
04/03/1996	14.5	1.4	4/3/1996	0.0034	0.0006	0.00001	-9.69	7.04	4502
05/23/1996	1.75	1.8	5/23/1996	0.0011	0.0006	0.00003	-10.20	6.25	7555

Reproduced with permission of the copyright owner. Further reproduction prohibited without permission.

Appendix 7.2. Continued.

Start Date	Start Time hour	End Date	End Time hour	L PPTBTW	L INTBET	L RAIN	L INT15	L SFIVE	BASE
01/05/1992	15.75	6.4	1/7/1992	0.86	0.09	5.76	0.64	0.0096	17.0
09/22/1992	13.75	6.4	9/23/1992	0.01	0.01	0.52	0.20	0.0024	10.0
12/01/1992	12.5	11.0	12/1/1992	0.00	0.00	0.30	0.14	0.0036	12.0
12/29/1992	12.25	13.0	12/30/1992	0.00	0.00	0.78	0.62	0.0023	15.0
01/07/1993	13.25	8.6	1/8/1993	0.82	0.14	0.65	0.20	0.0030	15.0
05/01/1993	14.75	9.3	5/2/1993	0.21	0.07	0.95	0.31	0.0022	18.0
05/06/1993	14.25	8.9	5/7/1993	0.08	0.05	0.29	0.19	0.0073	16.0
05/26/1993	13.5	8.2	5/26/1993	0.37	0.05	0.64	0.30	0.0040	18.0
07/03/1993	10.75	7.3	7/4/1993	0.59	0.15	0.50	0.25	0.0024	9.3
07/13/1993	16.75	11.0	7/14/1993	0.01	0.01	0.27	0.22	0.0036	18.0
07/22/1993	13.75	8.9	7/23/1993	0.19	0.05	0.84	0.29	0.0038	19.0
08/15/1993	23.75	13.0	8/16/1993	0.94	0.31	1.37	0.33	0.0067	24.0
08/18/1995	11.25	6.2	8/19/1995	1.01	0.15	2.61	0.34	0.0047	27.7
09/06/1995	2.25	8.9	9/7/1995	0.00	0.00	3.16	0.46	0.0051	12.8
09/07/1995	11.5	9.9	9/8/1995	0.01	0.01	0.63	0.19	0.0023	12.8
09/15/1995	21.75	8.3	9/17/1995	0.01	0.01	2.87	0.39	0.0031	19.8
09/27/1995	14.25	2.7	9/27/1995	0.60	0.16	0.25	0.08	0.0012	9.5
10/27/1995	14.75	2.6	10/28/1995	0.06	0.01	0.89	0.22	0.0047	8.6
11/04/1995	13.75	2.6	11/5/1995	1.12	0.19	1.34	0.32	0.0043	9.2
12/25/1995	16.25	1.7	12/25/1995	0.01	0.01	0.66	0.16	0.0076	10.9
03/15/1996	13.5	1.9	3/16/1996	1.49	0.13	1.53	0.27	0.0059	3.9
04/03/1996	14.5	1.4	4/3/1996	0.46	0.04	2.71	1.07	0.0231	8.9
05/23/1996	1.75	1.8	5/23/1996	1.76	0.25	0.82	0.16	0.0021	6.5

Reproduced with permission of the copyright owner. Further reproduction prohibited without permission.

Appendix 7.2. Continued.

Start Date	Start Time hour	End Date	End Time hour	L PKBS	L RRISE	L RAINFOL	L MXTRP	L MXTMJPK	L SMPKBS	L SMLSPKBS	HYSTER 1=clockwise 0=other than clockwise
01/05/1992	15.75	6.4	1/7/1992	1723.0	3.15	2.62	14.36333333	14.363333	3895.8288	12.70740741	1
09/22/1992	13.75	6.4	9/23/1992	59.2	0.43	0.09	0.397333333	0.3973333	59.15	15.42604423	0
12/01/1992	12.5	11.0	12/1/1992	29.7	0.30	0.00	0.833333333	0.8333333	59.552632	560.9645692	0
12/29/1992	12.25	13.0	12/30/1992	65.7	0.71	0.07	1.066666667	0.2888889	105.383	20.11881188	1
01/07/1993	13.25	8.6	1/8/1993	152.0	0.64	0.01	0.73047619	0.7304762	152.04242	105.3829954	1
05/01/1993	14.75	9.3	5/2/1993	92.4	0.69	0.26	1.166666667	0.7725	185.79663	139.4285714	1
05/06/1993	14.25	8.9	5/7/1993	88.4	0.28	0.01	0.43190481	0.4319048	88.440919	129.7457721	0
05/26/1993	13.5	8.2	5/26/1993	227.6	0.58	0.06	3.050666653	3.0506667	227.575	115.668	1
07/03/1993	10.75	7.3	7/4/1993	26.2	0.49	0.01	0.118666667	0.1186667	26.164286	20.88125	1
07/13/1993	16.75	11.0	7/14/1993	133.2	0.27	0.00	1.786666667	1.7866667	133.23913	1588.542748	0
07/22/1993	13.75	8.9	7/23/1993	349.4	0.82	0.02	1.45875	1.45875	349.37805	65.09677419	0
08/15/1993	23.75	13.0	8/16/1993	80.5	1.33	0.04	0.9	0.9	80.460674	185.8285292	1
08/18/1995	11.25	6.2	8/19/1995	607.5	2.17	0.44	2.513017917	2.5130179	607.48254	69.8816278	1
09/06/1995	2.25	8.9	9/7/1995	1473.6	2.50	0.66	4.093740289	4.0937403	1473.5774	48.50718023	1
09/07/1995	11.5	9.9	9/8/1995	86.2	0.62	0.01	0.276308813	0.2763088	86.21161	1473.577425	0
09/15/1995	21.75	8.3	9/17/1995	591.1	1.78	1.09	3.518053	3.518053	1217.3414	19.97081652	0
09/27/1995	14.25	2.7	9/27/1995	80.8	0.18	0.07	0.688905483	0.6889055	80.787558	80.76491098	0
10/27/1995	14.75	2.6	10/28/1995	481.5	0.88	0.01	6.429110253	6.4291103	481.52097	9.929994941	1
11/04/1995	13.75	2.6	11/5/1995	233.5	1.20	0.14	2.230336848	2.2303368	233.47706	481.520966	1
12/25/1995	16.25	1.7	12/25/1995	206.3	0.64	0.02	2.313439533	2.3134395	206.29743	33.1618812	1
03/15/1996	13.5	1.9	3/16/1996	64.2	1.25	0.28	0.391749915	0.3917499	64.155652	26.75196	1
04/03/1996	14.5	1.4	4/3/1996	142.2	2.01	0.70	2.386931383	2.3869314	211.53549	66.51311	1
05/23/1996	1.75	1.8	5/23/1996	96.2	0.28	0.54	2.143826489	2.1438265	130.39384	26.30632	1

**to eliminate zero values a value of 0.0002 was added to the precipitation between events and a value of 5000 was added to the runoff between events.

Reproduced with permission of the copyright owner. Further reproduction prohibited without permission.

Appendix 7.3. Pearson correlation matrix for the entire runoff event using quickflow characteristics of the entire event, Rio Caguitas near Aguas Buenas.

	Sediment Load	QU_SEDCONC	BASE	QUICK
SED	1.000			
QU_SEDCONC	0.798	1.000		
BASE	0.187	-0.146	1.000	
QUICK	0.907	0.470	0.376	1.000
PKBS	0.961	0.699	0.346	0.918
LSPKBTI	-0.130	-0.270	0.168	-0.002
RNBTWTI	-0.135	-0.281	0.150	-0.002
QULST	0.000	-0.175	0.253	0.122
QU3EVT	-0.114	-0.263	0.343	0.016
HYSTER	0.171	0.208	-0.084	0.105
MXTMJPK	0.817	0.713	0.205	0.699
MXTRP	0.795	0.680	0.236	0.689
SUMPKBS	0.944	0.644	0.355	0.932
SMLSPKBSTI	-0.319	-0.355	0.218	-0.220
TOTRAIN	0.683	0.397	0.211	0.722
INT15	0.363	0.140	0.243	0.434
SFIVE	0.353	0.405	0.062	0.234
RRISE	0.634	0.341	0.284	0.690
RFALL	0.617	0.393	0.051	0.629
LSTPPTI	0.207	0.025	0.161	0.285
LST3PPTI	-0.078	-0.251	0.223	0.061
LSTINT	0.184	0.025	0.159	0.251
LST75OTI	0.143	-0.017	0.145	0.221
PPTBTW	0.016	0.051	0.010	-0.012
INTBET	-0.059	-0.038	0.074	-0.060

	PKBS	LSPKBTI	RNBTWTI	QULST	QU3EVT
PKBS	1.000				
LSPKBTI	-0.104	1.000			
RNBTWTI	-0.113	0.200	1.000		
QULST	0.014	0.970	0.175	1.000	
QU3EVT	-0.084	0.814	0.356	0.855	1.000
HYSTER	0.219	-0.455	-0.282	-0.473	-0.544
MXTMJPK	0.851	-0.203	-0.167	-0.121	-0.290
MXTRP	0.838	-0.131	-0.219	-0.044	-0.223
SUMPKBS	0.969	-0.066	-0.096	0.064	-0.071
SMLSPKBSTI	-0.264	0.541	0.145	0.407	0.237
TOTRAIN	0.705	-0.258	-0.338	-0.149	-0.306
INT15	0.425	-0.029	-0.174	0.045	-0.116
SFIVE	0.358	-0.294	-0.154	-0.274	-0.428
RRISE	0.687	-0.172	-0.272	-0.080	-0.198
RFALL	0.553	-0.282	-0.341	-0.156	-0.337

Reproduced with permission of the copyright owner. Further reproduction prohibited without permission.

Appendix 7.3. **Continued.**

LSTPPTI	0.199	0.868	0.103	0.925	0.764
LST3PPTI	-0.083	0.852	0.327	0.900	0.948
LSTINT	0.163	0.810	0.122	0.873	0.805
LST75OTI	0.128	0.757	0.065	0.818	0.739
PPTBTW	0.024	-0.761	-0.210	-0.786	-0.724
INTBET	-0.049	-0.684	-0.165	-0.712	-0.637

	HYSTER	MXTMJPK	MXTRP	SUMPKBS	SMLSPKBSTI
HYSTER	1.000				
MXTMJPK	0.251	1.000			
MXTRP	0.313	0.969	1.000		
SUMPKBS	0.207	0.866	0.878	1.000	
SMLSPKBSTI	-0.368	-0.192	-0.243	-0.291	1.000
TOTRAIN	0.508	0.580	0.597	0.751	-0.397
INT15	0.451	0.324	0.422	0.494	-0.247
SFIVE	0.327	0.445	0.401	0.354	-0.086
RRISE	0.495	0.510	0.527	0.704	-0.305
RFALL	0.347	0.512	0.536	0.645	-0.441
LSTPPTI	-0.262	0.027	0.128	0.257	0.123
LST3PPTI	-0.492	-0.309	-0.228	-0.050	0.164
LSTINT	-0.259	-0.039	0.063	0.217	0.014
LST75OTI	-0.220	-0.038	0.072	0.191	-0.064
PPTBTW	0.353	0.096	-0.003	-0.026	-0.087
INTBET	0.295	-0.006	-0.104	-0.102	-0.014

	TOTRAIN	INT15	SFIVE	RRISE	RFALL
TOTRAIN	1.000				
INT15	0.764	1.000			
SFIVE	0.515	0.597	1.000		
RRISE	0.956	0.791	0.586	1.000	
RFALL	0.834	0.581	0.274	0.663	1.000
LSTPPTI	0.063	0.187	-0.201	0.105	0.045
LST3PPTI	-0.260	-0.065	-0.416	-0.178	-0.237
LSTINT	0.036	0.117	-0.265	0.073	0.037
LST75OTI	0.063	0.156	-0.214	0.078	0.100
PPTBTW	0.177	-0.020	0.138	0.101	0.205
INTBET	0.104	-0.103	0.042	0.026	0.152

	LSTPPTI	LST3PPTI	LSTINT	LST75OTI	PPTBTW
LSTPPTI	1.000				
LST3PPTI	0.869	1.000			
LSTINT	0.973	0.898	1.000		
LST75OTI	0.937	0.857	0.970	1.000	
PPTBTW	-0.814	-0.804	-0.802	-0.792	1.000
INTBET	-0.783	-0.724	-0.762	-0.752	0.976

	INTBET
INTBET	1.000

Reproduced with permission of the copyright owner. Further reproduction prohibited without permission.

Appendix 7.4. Component loadings from principal component analysis on the independent variables using quickflow characteristics of the entire event.

Component loadings

	1	2	3	4	5
BASE	-0.036	0.334	0.683	0.282	0.342
QUICK	0.337	0.789	0.298	-0.172	0.197
PKBS	0.446	0.772	0.280	-0.254	0.004
LSPKBTI	-0.855	0.369	0.132	0.141	-0.110
RNBTWTI	-0.336	-0.490	0.678	0.175	-0.033
QULST	-0.820	0.499	0.122	0.101	-0.022
QU3EVT	-0.863	0.324	0.139	0.035	0.193
HYSTER	0.618	0.111	-0.348	0.262	-0.012
MXTMJPK	0.538	0.604	0.294	-0.362	-0.293
MXTRP	0.480	0.681	0.208	-0.316	-0.273
SUMPKBS	0.428	0.829	0.248	-0.229	0.012
SMLSPKBSTI	-0.413	-0.227	0.616	0.275	-0.263
TOTRAIN	0.624	0.682	-0.095	0.253	0.147
INT15	0.368	0.602	-0.135	0.598	-0.053
SFIVE	0.533	0.259	0.047	0.425	-0.550
RRISE	0.539	0.683	-0.033	0.389	0.074
RFALL	0.556	0.568	-0.205	0.006	0.278
LSTPPTI	-0.682	0.697	-0.100	0.020	-0.001
LST3PPTI	-0.881	0.400	-0.027	0.026	0.177
LSTINT	-0.697	0.662	-0.172	-0.025	0.109
LST75OTI	-0.653	0.656	-0.253	-0.005	0.104
PPTBTW	0.748	-0.465	0.199	0.038	0.311
INTBET	0.650	-0.510	0.240	0.061	0.403

	6
BASE	-0.309
QUICK	0.030
PKBS	-0.044
LSPKBTI	0.264
RNBTWTI	-0.156
QULST	0.180
QU3EVT	-0.191
HYSTER	0.035
MXTMJPK	0.033
MXTRP	0.004
SUMPKBS	-0.021
SMLSPKBSTI	0.478
TOTRAIN	0.087
INT15	-0.055
SFIVE	-0.173
RRISE	-0.019
RFALL	0.270

	6
LSTPPTI	0.129
LST3PPTI	-0.106
LSTINT	0.031
LST75OTI	0.001
PPTBTW	0.170

Reproduced with permission of the copyright owner. Further reproduction prohibited without permission.

Appendix 7.5. Results of principal component analysis on the independent variables using quickflow characteristics for the entire event (without the variable quickflow).

Component loadings

	1	2	3	4	5
BASE	-0.093	0.298	0.711	0.253	0.393
PKBS	0.313	0.805	0.291	-0.285	0.074
LSPKBTI	-0.903	0.229	0.152	0.114	-0.116
RNBTWTI	-0.261	-0.571	0.654	0.142	-0.039
QULST	-0.889	0.360	0.141	0.083	-0.019
QU3EVT	-0.905	0.175	0.132	0.048	0.202
HYSTER	0.599	0.237	-0.298	0.262	-0.033
MXTMJPK	0.433	0.669	0.324	-0.444	-0.183
MXTRP	0.366	0.744	0.249	-0.396	-0.163
SUMPKBS	0.287	0.862	0.265	-0.260	0.080
SMLSPKBSTI	-0.376	-0.307	0.632	0.204	-0.269
TOTRAIN	0.509	0.775	-0.048	0.260	0.124
INT15	0.273	0.675	-0.048	0.574	-0.112
SFIVE	0.490	0.361	0.134	0.333	-0.586
RRISE	0.425	0.762	0.026	0.383	0.034
RFALL	0.460	0.650	-0.189	0.043	0.274
LSTPPTI	-0.783	0.585	-0.077	0.016	0.003
LST3PPTI	-0.934	0.250	-0.035	0.053	0.166
LSTINT	-0.792	0.549	-0.160	-0.009	0.115
LST75OTI	-0.747	0.556	-0.235	0.013	0.106
PPTBTW	0.809	-0.358	0.173	0.070	0.312
INTBET	0.719	-0.420	0.207	0.103	0.401

	6
BASE	-0.289
PKBS	-0.040
LSPKBTI	0.265
RNBTWTI	-0.160
QULST	0.181
QU3EVT	-0.187
HYSTER	0.055
MXTMJPK	0.042
MXTRP	0.018
SUMPKBS	-0.017
SMLSPKBSTI	0.477
TOTRAIN	0.085
INT15	-0.058
SFIVE	-0.188
RRISE	-0.023
RFALL	0.268

	6
LSTPPTI	0.132
LST3PPTI	-0.106
LSTINT	0.036
LST75OTI	0.006
PPTBTW	0.176
INTBET	0.204

Reproduced with permission of the copyright owner. Further reproduction prohibited without permission.

Appendix 7.6. Results of principal component analysis on the independent variables using quickflow characteristics after varimax rotation for the entire event.

Rotated Loading Matrix (VARIMAX, Gamma = 1.0000)

	1	2	3	4	5
BASE	0.121	0.266	0.868	0.129	0.045
QUICK	0.135	0.835	0.215	0.300	0.194
PKBS	0.045	0.921	0.122	0.253	0.011
LSPKBTI	0.879	-0.089	0.047	-0.100	0.043
RNBTWTI	-0.116	-0.303	0.582	-0.455	-0.156
QULST	0.925	0.012	0.110	-0.055	0.081
QU3EVT	0.851	-0.133	0.376	-0.229	0.085
HYSTER	-0.364	0.074	-0.219	0.597	-0.059
MXTMJPK	-0.124	0.944	-0.085	0.111	-0.179
MXTRP	-0.019	0.915	-0.094	0.179	-0.181
SUMPKBS	0.099	0.928	0.105	0.302	0.025
SMLSPKBSTI	0.109	-0.164	0.173	-0.220	-0.040
TOTRAIN	-0.079	0.540	0.012	0.795	0.095
INT15	0.102	0.219	0.107	0.875	-0.207
SFIVE	-0.247	0.262	-0.008	0.542	-0.658
RRISE	-0.014	0.466	0.129	0.819	-0.049
RFALL	-0.090	0.508	-0.179	0.610	0.355
LSTPPTI	0.964	0.152	-0.032	0.092	0.092
LST3PPTI	0.936	-0.139	0.217	-0.150	0.124
LSTINT	0.963	0.099	-0.000	0.058	0.148
LST75OTI	0.939	0.072	-0.038	0.107	0.124
PPTBTW	-0.908	0.016	0.101	0.123	0.300
INTBET	-0.865	-0.060	0.167	0.081	0.387

	6
BASE	-0.119
QUICK	0.065
PKBS	0.106
LSPKBTI	-0.439
RNBTWTI	-0.439
QULST	-0.317
QU3EVT	-0.010
HYSTER	0.200
MXTMJPK	-0.016
MXTRP	0.041
SUMPKBS	0.106
SMLSPKBSTI	-0.926
TOTRAIN	0.135
INT15	0.032
SFIVE	-0.100
RRISE	0.093
RFALL	0.167

	6
LSTPPTI	-0.085
LST3PPTI	0.025
LSTINT	0.064
LST75OTI	0.128
PPTBTW	-0.057
INTBET	-0.097

Reproduced with permission of the copyright owner. Further reproduction prohibited without permission.

Appendix 7.7. Results of principal component analysis on the independent variables without quickflow after varimax rotation for the entire event.

Rotated Loading Matrix (VARIMAX, Gamma = 1.0000)

	1	2	3	4	5
BASE	0.124	0.235	0.894	0.138	0.046
PKBS	0.058	0.884	0.158	0.311	0.023
LSPKBTI	0.877	-0.093	0.045	-0.108	0.044
RNBTWTI	-0.121	-0.297	0.552	-0.491	-0.175
QULST	0.925	-0.001	0.115	-0.054	0.082
QU3EVT	0.850	-0.150	0.373	-0.233	0.084
HYSTER	-0.364	0.070	-0.210	0.598	-0.056
MXTMJPK	-0.111	0.959	-0.040	0.155	-0.118
MXTRP	-0.006	0.931	-0.047	0.220	-0.116
SUMPKBS	0.112	0.890	0.144	0.361	0.037
SMLSPKBSTI	0.106	-0.146	0.163	-0.245	-0.042
TOTRAIN	-0.072	0.479	0.039	0.834	0.050
INT15	0.104	0.176	0.114	0.868	-0.264
SFIVE	-0.244	0.270	-0.019	0.505	-0.693
RRISE	-0.007	0.405	0.144	0.841	-0.107
RFALL	-0.082	0.455	-0.141	0.668	0.332
LSTPPTI	0.966	0.131	-0.022	0.106	0.095
LST3PPTI	0.934	-0.165	0.210	-0.150	0.111
LSTINT	0.965	0.074	0.010	0.075	0.152
LST75OTI	0.940	0.050	-0.027	0.121	0.129
PPTBTW	-0.908	0.002	0.114	0.145	0.290
INTBET	-0.866	-0.078	0.181	0.104	0.375

	6		6
BASE	0.121	LSTPPTI	0.087
PKBS	-0.112	LST3PPTI	-0.024
LSPKBTI	0.440	LSTINT	-0.062
RNBTWTI	0.435	LST75OTI	-0.125
QULST	0.317	PPTBTW	0.060
QU3EVT	0.010	INTBET	0.100
HYSTER	-0.185		
MXTMJPK	0.007		
MXTRP	-0.047		
SUMPKBS	-0.111		
SMLSPKBSTI	0.925		
TOTRAIN	-0.132		
INT15	-0.026		
SFIVE	0.096		
RRISE	-0.089		
RFALL	-0.166		

Reproduced with permission of the copyright owner. Further reproduction prohibited without permission.

Appendix 7.8. Summary of dependent and independent variables used in the statistical analysis for runoff c of the entire event at Rio Caguitas near Aguas Buenas.
(D indicates dependent variable; L indicates data was log transformed for final statistical operations; IR indicates data had negative inverse square root transformed)

Start Date	Start Time hour	Start Discharge ft3/s	End Date	End Time hour	DL Suspended-sediment lo: tons	DL Discharge-weighted sediment concentration mg/L	L RUN	L LSPKTI	L RULST
01/05/1992	15.75	6.4	1/7/1992	6	3800	4012	3.04E+007	0.06	1846
09/22/1992	13.75	6.4	9/23/1992	9.75	38.2	691	1.77E+006	0.68	25105
12/01/1992	12.5	11.0	12/1/1992	22	8.47	385	7.04E+005	16.3	310014
12/29/1992	12.25	13.0	12/30/1992	4	21.0	499	1.35E+006	2.86	2434500
01/07/1993	13.25	8.6	1/8/1993	5.75	139	1841	2.42E+006	0.35	6709
05/01/1993	14.75	9.3	5/2/1993	16	71.6	700	3.28E+006	1.42	24804
05/06/1993	14.25	8.9	5/7/1993	1.25	73.5	1598	1.47E+006	1.31	33902
05/26/1993	13.5	8.2	5/26/1993	23.5	109	1780	1.96E+006	1.46	22229
07/03/1993	10.75	7.3	7/4/1993	0.75	5.43	227	7.67E+005	0.37	6573
07/13/1993	16.75	11.0	7/14/1993	4.25	51.9	851	1.95E+006	15.7	466423
07/22/1993	13.75	8.9	7/23/1993	2	191	2212	2.77E+006	0.42	5400
08/15/1993	23.75	13.0	8/16/1993	7.75	21	658	1.01E+006	0.37	8308
08/18/1995	11.25	6.2	8/19/1995	9	351	2012	5.59E+006	0.10	2112
09/06/1995	2.25	8.9	9/7/1995	3.75	3500	8844	1.27E+007	0.95	2323698
09/07/1995	11.5	9.9	9/8/1995	6.5	50	664	2.40E+006	50.3	1634718
09/15/1995	21.75	8.3	9/17/1995	8.42	1030	2825	1.16E+007	1.25	5620100
09/27/1995	14.25	2.7	9/27/1995	21.5	97	4211	7.34E+005	0.36	11881
10/27/1995	14.75	2.6	10/28/1995	2	452	6372	2.27E+006	0.16	2473
11/04/1995	13.75	2.6	11/5/1995	6	147	1787	2.63E+006	2.37	12632
12/25/1995	16.25	1.7	12/25/1995	23.5	250	5668	1.41E+006	0.55	7365
03/15/1996	13.5	1.9	3/16/1996	1.25	46.1	1523	9.70E+005	0.06	245
04/03/1996	14.5	1.4	4/3/1996	22	166	5353	9.93E+005	0.15	2178
05/23/1996	1.75	1.8	5/23/1996	13.25	64.2	2318	8.87E+005	0.07	484

Reproduced with permission of the copyright owner. Further reproduction prohibited without permission.

Appendix 7.8. Continued.

Start Date	Start Time hour	End Date	End Time hour	L PPTLSTI	L INTLST	L L75OTI	SUM3PPTI	RU3EVT	RNBTWTI	L PPTBTW
01/05/1992	15.75	6.4	1/7/1992	0.0014	0.0003	0.00001	-9.68	8.639111202	18441	0.86
09/22/1992	13.75	6.4	9/23/1992	0.0071	0.0056	0.00029	-5.23	14.17123716	27283	0.01
12/01/1992	12.5	11.0	12/1/1992	0.0656	0.0253	0.00041	-5.49	14.21438592	42935	0.00
12/29/1992	12.25	13.0	12/30/1992	1.8000	0.5800	0.02163	-3.69	15.73679961	0	0.00
01/07/1993	13.25	8.6	1/8/1993	0.0039	0.0031	0.00001	-7.31	11.9456374	36553	0.82
05/01/1993	14.75	9.3	5/2/1993	0.0276	0.0085	0.00022	-6.74	11.86301102	39051	0.21
05/06/1993	14.25	8.9	5/7/1993	0.0087	0.0049	0.00015	-6.23	12.85499447	38222	0.08
05/26/1993	13.5	8.2	5/26/1993	0.0248	0.0114	0.00033	-6.67	12.8700731	33598	0.37
07/03/1993	10.75	7.3	7/4/1993	0.0026	0.0012	0.00003	-6.83	11.39730749	25687	0.59
07/13/1993	16.75	11.0	7/14/1993	0.0631	0.0034	0.00008	-6.31	12.28908959	45677	0.01
07/22/1993	13.75	8.9	7/23/1993	0.0032	0.0018	0.00003	-7.49	12.46956312	34867	0.19
08/15/1993	23.75	13.0	8/16/1993	0.0009	0.0003	0.00001	-8.70	11.48549554	38656	0.94
08/18/1995	11.25	6.2	8/19/1995	0.0028	0.0018	0.00005	-8.27	9.898973644	11259	1.01
09/06/1995	2.25	8.9	9/7/1995	4.4400	0.8800	0.01259	-4.35	14.50602869	0	0.00
09/07/1995	11.5	9.9	9/8/1995	0.4077	0.0594	0.00066	-4.69	14.43927481	37593	0.01
09/15/1995	21.75	8.3	9/17/1995	7.8000	2.5500	0.08000	-3.39	15.64783079	0	0.01
09/27/1995	14.25	2.7	9/27/1995	0.0025	0.0014	0.00001	-7.26	11.87571053	16840	0.60
10/27/1995	14.75	2.6	10/28/1995	0.0070	0.0018	0.00002	-8.84	9.854315738	7897	0.06
11/04/1995	13.75	2.6	11/5/1995	0.0050	0.0012	0.00003	-8.56	9.864671657	10265	1.12
12/25/1995	16.25	1.7	12/25/1995	0.0209	0.0120	0.00067	-7.08	10.15031598	6685	0.01
03/15/1996	13.5	1.9	3/16/1996	0.0008	0.0005	0.00002	-10.00	7.128811762	6829	1.49
04/03/1996	14.5	1.4	4/3/1996	0.0034	0.0006	0.00001	-9.69	7.573665475	4502	0.46
05/23/1996	1.75	1.8	5/23/1996	0.0011	0.0006	0.00003	-10.20	6.804397525	7555	1.76

Reproduced with permission of the copyright owner. Further reproduction prohibited without permission.

Appendix 7.8. Continued.

Start Date	Start Time hour	End Date	End Time hour	L INTBET	L RAIN	L INT15	L SFIVE	BASE	L PK	L RRISE
01/05/1992	15.75	6.4	1/7/1992	0.09	5.76	0.64	0.0096	17.0	1730	3.15
09/22/1992	13.75	6.4	9/23/1992	0.01	0.52	0.20	0.0024	10.0	66	0.43
12/01/1992	12.5	11.0	12/1/1992	0.00	0.30	0.14	0.0036	12.0	41	0.30
12/29/1992	12.25	13.0	12/30/1992	0.00	0.78	0.62	0.0023	15.0	78	0.71
01/07/1993	13.25	8.6	1/8/1993	0.14	0.65	0.20	0.0030	15.0	162	0.64
05/01/1993	14.75	9.3	5/2/1993	0.07	0.95	0.31	0.0022	18.0	102	0.69
05/06/1993	14.25	8.9	5/7/1993	0.05	0.29	0.19	0.0073	16.0	100	0.28
05/26/1993	13.5	8.2	5/26/1993	0.05	0.64	0.30	0.0040	18.0	237	0.58
07/03/1993	10.75	7.3	7/4/1993	0.15	0.50	0.25	0.0024	9.3	34	0.49
07/13/1993	16.75	11.0	7/14/1993	0.01	0.27	0.22	0.0036	18.0	145	0.27
07/22/1993	13.75	8.9	7/23/1993	0.05	0.84	0.29	0.0038	19.0	359	0.82
08/15/1993	23.75	13.0	8/16/1993	0.31	1.37	0.33	0.0067	24.0	94	1.33
08/18/1995	11.25	6.2	8/19/1995	0.15	2.61	0.34	0.0047	27.7	615	2.17
09/06/1995	2.25	8.9	9/7/1995	0.00	3.16	0.46	0.0051	12.8	1483	2.50
09/07/1995	11.5	9.9	9/8/1995	0.01	0.63	0.19	0.0023	12.8	97	0.62
09/15/1995	21.75	8.3	9/17/1995	0.01	2.87	0.39	0.0031	19.8	597	1.78
09/27/1995	14.25	2.7	9/27/1995	0.16	0.25	0.08	0.0012	9.5	85	0.18
10/27/1995	14.75	2.6	10/28/1995	0.01	0.89	0.22	0.0047	8.6	485	0.88
11/04/1995	13.75	2.6	11/5/1995	0.19	1.34	0.32	0.0043	9.2	237	1.20
12/25/1995	16.25	1.7	12/25/1995	0.01	0.66	0.16	0.0076	10.9	210	0.64
03/15/1996	13.5	1.9	3/16/1996	0.13	1.53	0.27	0.0059	3.9	67	1.25
04/03/1996	14.5	1.4	4/3/1996	0.04	2.71	1.07	0.0231	8.9	145	2.01
05/23/1996	1.75	1.8	5/23/1996	0.25	0.82	0.16	0.0021	6.5	98	0.28

Reproduced with permission of the copyright owner. Further reproduction prohibited without permission.

Appendix 7.8. Continued.

Start Date	Start Time hour	End Date	End Time hour	L INTBET	L RAIN	L INT15	L SFIVE	BASE	L PK	L RRISE
01/05/1992	15.75	6.4	1/7/1992	0.09	5.76	0.64	0.0096	17.0	1730	3.15
09/22/1992	13.75	6.4	9/23/1992	0.01	0.52	0.20	0.0024	10.0	66	0.43
12/01/1992	12.5	11.0	12/1/1992	0.00	0.30	0.14	0.0036	12.0	41	0.30
12/29/1992	12.25	13.0	12/30/1992	0.00	0.78	0.62	0.0023	15.0	78	0.71
01/07/1993	13.25	8.6	1/8/1993	0.14	0.65	0.20	0.0030	15.0	162	0.64
05/01/1993	14.75	9.3	5/2/1993	0.07	0.95	0.31	0.0022	18.0	102	0.69
05/06/1993	14.25	8.9	5/7/1993	0.05	0.29	0.19	0.0073	16.0	100	0.28
05/26/1993	13.5	8.2	5/26/1993	0.05	0.64	0.30	0.0040	18.0	237	0.58
07/03/1993	10.75	7.3	7/4/1993	0.15	0.50	0.25	0.0024	9.3	34	0.49
07/13/1993	16.75	11.0	7/14/1993	0.01	0.27	0.22	0.0036	18.0	145	0.27
07/22/1993	13.75	8.9	7/23/1993	0.05	0.84	0.29	0.0038	19.0	359	0.82
08/15/1993	23.75	13.0	8/16/1993	0.31	1.37	0.33	0.0067	24.0	94	1.33
08/18/1995	11.25	6.2	8/19/1995	0.15	2.61	0.34	0.0047	27.7	615	2.17
09/06/1995	2.25	8.9	9/7/1995	0.00	3.16	0.46	0.0051	12.8	1483	2.50
09/07/1995	11.5	9.9	9/8/1995	0.01	0.63	0.19	0.0023	12.8	97	0.62
09/15/1995	21.75	8.3	9/17/1995	0.01	2.87	0.39	0.0031	19.8	597	1.78
09/27/1995	14.25	2.7	9/27/1995	0.16	0.25	0.08	0.0012	9.5	85	0.18
10/27/1995	14.75	2.6	10/28/1995	0.01	0.89	0.22	0.0047	8.6	485	0.88
11/04/1995	13.75	2.6	11/5/1995	0.19	1.34	0.32	0.0043	9.2	237	1.20
12/25/1995	16.25	1.7	12/25/1995	0.01	0.66	0.16	0.0076	10.9	210	0.64
03/15/1996	13.5	1.9	3/16/1996	0.13	1.53	0.27	0.0059	3.9	67	1.25
04/03/1996	14.5	1.4	4/3/1996	0.04	2.71	1.07	0.0231	8.9	145	2.01
05/23/1996	1.75	1.8	5/23/1996	0.25	0.82	0.16	0.0021	6.5	98	0.28

Reproduced with permission of the copyright owner. Further reproduction prohibited without permission.

7.9. Pearson correlation matrix for the entire runoff event using runoff characteristics of the entire event, Rio Caguitas near Aguas Bueanas.

	SED	RU_SEDCONC	BASE	RUN
SED	1.000			
RU_SEDCONC	0.841	1.000		
BASE	0.187	-0.121	1.000	
RUN	0.841	0.413	0.436	1.000
PK	0.953	0.722	0.365	0.880
LSPKTI	-0.339	-0.471	0.128	-0.100
RNBTWTI	-0.467	-0.566	0.331	-0.220
RULST	0.015	-0.221	0.251	0.246
RU3EVT	-0.119	-0.349	0.344	0.150
HYSTER	0.171	0.205	-0.084	0.082
MXTMJPK	0.817	0.746	0.205	0.629
MXTRP	0.795	0.698	0.236	0.638
SUMPK	0.936	0.664	0.369	0.909
SMLSPKTI	-0.321	-0.375	0.250	-0.164
TOTRAIN	0.683	0.454	0.211	0.694
INT15	0.363	0.152	0.243	0.459
SFIVE	0.353	0.410	0.062	0.184
RRISE	0.634	0.391	0.284	0.675
RFALL	0.617	0.449	0.051	0.588
LSTPPTI	0.207	-0.008	0.161	0.357
LST3PPTI	-0.078	-0.297	0.223	0.165
LSTINT	0.184	-0.013	0.159	0.322
LST75OTI	0.143	-0.047	0.145	0.287
PPTBTW	0.016	0.126	0.010	-0.098
INTBET	-0.059	0.033	0.074	-0.132

	PK	LSPKTI	RNBTWTI	RULST	RU3EVT
PK	1.000				
LSPKTI	-0.280	1.000			
RNBTWTI	-0.385	0.475	1.000		
RULST	0.053	0.793	0.078	1.000	
RU3EVT	-0.059	0.710	0.267	0.885	1.000
HYSTER	0.211	-0.538	-0.429	-0.457	-0.536
MXTMJPK	0.846	-0.316	-0.339	-0.133	-0.302
MXTRP	0.835	-0.281	-0.408	-0.048	-0.228
SUMPK	0.970	-0.266	-0.394	0.095	-0.046
SMLSPKTI	-0.253	0.771	0.675	0.380	0.285
TOTRAIN	0.703	-0.489	-0.567	-0.133	-0.300
INT15	0.430	-0.214	-0.372	0.067	-0.091
SFIVE	0.356	-0.314	-0.186	-0.291	-0.433
RRISE	0.691	-0.379	-0.480	-0.064	-0.193
RFALL	0.542	-0.516	-0.607	-0.143	-0.329
LSTPPTI	0.218	0.624	-0.191	0.931	0.766
LST3PPTI	-0.059	0.709	0.105	0.924	0.956

Reproduced with permission of the copyright owner. Further reproduction prohibited without permission.

Appendix 7.9. Continued.

LSTINT	0.180	0.549	-0.221	0.887	0.800
LST75OTI	0.144	0.494	-0.281	0.830	0.734
PPTBTW	-0.003	-0.620	0.061	-0.807	-0.734
INTBET	-0.073	-0.546	0.126	-0.732	-0.648

	HYSTER	MXTMJPK	MXTRP	SUMPK	SMLSPKTI
HYSTER	1.000				
MXTMJPK	0.251	1.000			
MXTRP	0.313	0.969	1.000		
SUMPK	0.203	0.858	0.871	1.000	
SMLSPKTI	-0.412	-0.217	-0.262	-0.284	1.000
TOTRAIN	0.508	0.580	0.597	0.751	-0.423
INT15	0.451	0.324	0.422	0.501	-0.239
SFIVE	0.327	0.445	0.401	0.353	-0.088
RRISE	0.495	0.510	0.527	0.707	-0.321
RFALL	0.347	0.512	0.536	0.639	-0.469
LSTPPTI	-0.262	0.027	0.128	0.267	0.140
LST3PPTI	-0.492	-0.309	-0.228	-0.035	0.216
LSTINT	-0.259	-0.039	0.063	0.225	0.032
LST75OTI	-0.220	-0.038	0.072	0.198	-0.048
PPTBTW	0.353	0.096	-0.003	-0.038	-0.121
INTBET	0.295	-0.006	-0.104	-0.111	-0.042

	TOTRAIN	INT15	SFIVE	RRISE	RFALL
TOTRAIN	1.000				
INT15	0.764	1.000			
SFIVE	0.515	0.597	1.000		
RRISE	0.956	0.791	0.586	1.000	
RFALL	0.834	0.581	0.274	0.663	1.000
LSTPPTI	0.063	0.187	-0.201	0.105	0.045
LST3PPTI	-0.260	-0.065	-0.416	-0.178	-0.237
LSTINT	0.036	0.117	-0.265	0.073	0.037
LST75OTI	0.063	0.156	-0.214	0.078	0.100
PPTBTW	0.177	-0.020	0.138	0.101	0.205
INTBET	0.104	-0.103	0.042	0.026	0.152

	LSTPPTI	LST3PPTI	LSTINT	LST75OTI	PPTBTW
LSTPPTI	1.000				
LST3PPTI	0.869	1.000			
LSTINT	0.973	0.898	1.000		
LST75OTI	0.937	0.857	0.970	1.000	
PPTBTW	-0.814	-0.804	-0.802	-0.792	1.000
INTBET	-0.783	-0.724	-0.762	-0.752	0.976

	INTBET
INTBET	1.000

Reproduced with permission of the copyright owner. Further reproduction prohibited without permission.

Appendix 7.10. Results of principal component analysis on the independent variables using runoff characteristics for the entire event with the variable runoff.

Component loadings

	1	2	3	4	5
BASE	0.002	0.347	0.680	0.215	0.369
RUN	0.338	0.776	0.318	-0.119	0.227
PK	0.524	0.715	0.285	-0.263	-0.003
LSPKTI	-0.844	0.177	0.299	0.133	-0.214
RNBTWTI	-0.430	-0.423	0.691	0.132	0.004
RULST	-0.737	0.629	0.072	0.086	0.014
RU3EVT	-0.808	0.458	0.113	0.044	0.209
HYSTER	0.640	0.023	-0.303	0.272	-0.023
MXTMJPK	0.610	0.514	0.285	-0.397	-0.296
MXTRP	0.566	0.600	0.204	-0.347	-0.277
SUMPK	0.522	0.769	0.254	-0.237	0.013
SMLSPKTI	-0.497	-0.161	0.651	0.234	-0.236
TOTRAIN	0.720	0.587	-0.061	0.254	0.130
INT15	0.453	0.547	-0.069	0.604	-0.065
SFIVE	0.561	0.175	0.107	0.421	-0.554
RRISE	0.634	0.600	0.011	0.389	0.059
RFALL	0.641	0.480	-0.196	0.016	0.256
LSTPPTI	-0.570	0.783	-0.124	0.024	-0.011
LST3PPTI	-0.814	0.528	-0.053	0.035	0.176
LSTINT	-0.585	0.752	-0.206	-0.016	0.098
LST75OTI	-0.541	0.739	-0.283	0.010	0.088
PPTBTW	0.672	-0.571	0.209	0.022	0.310
INTBET	0.569	-0.601	0.244	0.040	0.406

	6
BASE	-0.355
RUN	0.076
PK	-0.049
LSPKTI	0.242
RNBTWTI	-0.121
RULST	0.128
RU3EVT	-0.170
HYSTER	-0.170
MXTMJPK	0.000
MXTRP	-0.052
SUMPK	-0.000
SMLSPKTI	0.372
TOTRAIN	0.128
INT15	-0.014
SFIVE	-0.118
RRISE	0.011
RFALL	0.355

	6
LSTPPTI	0.107
LST3PPTI	-0.069
LSTINT	0.012
LST75OTI	-0.010
PPTBTW	0.142
INTBET	0.156

Reproduced with permission of the copyright owner. Further reproduction prohibited without permission.

Appendix 7.11. Results of principal component analysis on the independent variables using runoff characteristics for the entire event with the variable runoff.

Component loadings

	1	2	3	4	5
BASE	-0.058	0.310	0.695	0.216	0.439
PK	0.402	0.761	0.308	-0.282	0.070
LSPKTI	-0.863	0.036	0.311	0.097	-0.215
RNBTWTI	-0.368	-0.525	0.657	0.118	0.006
RULST	-0.826	0.505	0.094	0.079	0.022
RU3EVT	-0.872	0.316	0.109	0.062	0.217
HYSTER	0.633	0.145	-0.267	0.270	-0.052
MXTMJPK	0.521	0.591	0.329	-0.456	-0.183
MXTRP	0.467	0.677	0.257	-0.404	-0.167
SUMPK	0.393	0.815	0.280	-0.253	0.082
SMLSPKTI	-0.471	-0.259	0.659	0.182	-0.226
TOTRAIN	0.621	0.689	-0.021	0.261	0.112
INT15	0.367	0.626	0.003	0.582	-0.115
SFIVE	0.531	0.278	0.188	0.337	-0.575
RRISE	0.534	0.689	0.060	0.384	0.029
RFALL	0.559	0.573	-0.181	0.048	0.251
LSTPPTI	-0.682	0.693	-0.091	0.018	-0.000
LST3PPTI	-0.886	0.392	-0.055	0.057	0.170
LSTINT	-0.692	0.662	-0.183	-0.005	0.109
LST75OTI	-0.645	0.663	-0.255	0.021	0.094
PPTBTW	0.748	-0.480	0.171	0.056	0.312
INTBET	0.651	-0.528	0.198	0.085	0.406

	6
BASE	-0.307
PK	-0.045
LSPKTI	0.254
RNBTWTI	-0.135
RULST	0.138
RU3EVT	-0.171
HYSTER	-0.098
MXTMJPK	0.025
MXTRP	-0.013
SUMPK	0.003
SMLSPKTI	0.391
TOTRAIN	0.123
INT15	-0.019
SFIVE	-0.160
RRISE	0.001
RFALL	0.350
LSTPPTI	0.126
LST3PPTI	-0.072
LSTINT	0.031

	6
LST75OTI	0.009
PPTBTW	0.163
INTBET	0.184

Reproduced with permission of the copyright owner. Further reproduction prohibited without permission.

Appendix 7.12. Results of principal component analysis on the independent variables using runoff characteristics after varimax rotation for the entire event.

Rotated Loading Matrix (VARIMAX, Gamma = 1.0000)

	1	2	3	4	5	6
BASE	0.105	0.277	-0.188	0.134	0.021	0.866
RUN	0.227	0.773	0.037	0.235	0.318	0.287
PK	0.069	0.914	0.133	0.222	0.079	0.157
LSPKTI	0.633	-0.202	-0.690	-0.184	-0.068	0.014
RNBTWTI	-0.143	-0.279	-0.635	-0.306	-0.223	0.478
RULST	0.922	0.020	-0.308	-0.042	0.101	0.101
RU3EVT	0.849	-0.128	-0.159	-0.214	0.005	0.376
HYSTER	-0.337	0.067	0.438	0.537	-0.037	-0.067
MXTMJPK	-0.131	0.949	0.049	0.139	-0.116	-0.089
MXTRP	-0.020	0.921	0.119	0.194	-0.124	-0.074
SUMPK	0.113	0.921	0.134	0.262	0.133	0.132
SMLSPKTI	0.083	-0.153	-0.945	-0.101	-0.027	0.100
TOTRAIN	-0.068	0.534	0.266	0.700	0.336	0.033
INT15	0.110	0.232	0.103	0.888	0.079	0.089
SFIVE	-0.254	0.288	-0.092	0.728	-0.395	-0.112
RRISE	-0.005	0.467	0.191	0.778	0.197	0.135
RFALL	-0.078	0.490	0.308	0.437	0.563	-0.154
LSTPPTI	0.957	0.154	-0.086	0.059	0.118	-0.024
LST3PPTI	0.934	-0.135	-0.096	-0.171	0.071	0.214
LSTINT	0.964	0.096	0.055	-0.003	0.131	0.033
LST75OTI	0.944	0.068	0.123	0.042	0.118	-0.002
PPTBTW	-0.911	-0.006	0.051	0.034	0.296	0.127
INTBET	-0.871	-0.084	0.010	-0.027	0.357	0.201

Reproduced with permission of the copyright owner. Further reproduction prohibited without permission.

Appendix 7.13. Results of principal component analysis on the independent variables using runoff characteristics for the entire event with the variable runoff after varimax rotation..

Rotated Loading Matrix (VARIMAX, Gamma = 1.0000)

	1	2	3	4	5
BASE	0.115	0.245	-0.178	0.151	0.040
PK	0.086	0.883	0.133	0.279	0.067
LSPKTI	0.629	-0.200	-0.687	-0.225	-0.058
RNBTWTI	-0.145	-0.285	-0.594	-0.366	-0.224
RULST	0.925	-0.000	-0.309	-0.032	0.096
RU3EVT	0.851	-0.154	-0.135	-0.211	0.009
HYSTER	-0.344	0.066	0.377	0.547	-0.040
MXTMJPK	-0.116	0.962	0.039	0.157	-0.073
MXTRP	-0.007	0.933	0.101	0.213	-0.076
SUMPK	0.130	0.888	0.132	0.327	0.114
SMLSPKTI	0.081	-0.145	-0.946	-0.149	-0.020
TOTRAIN	-0.060	0.488	0.235	0.776	0.239
INT15	0.108	0.193	0.068	0.903	-0.048
SFIVE	-0.259	0.290	-0.099	0.661	-0.508
RRISE	0.000	0.417	0.165	0.829	0.080
RFALL	-0.067	0.455	0.277	0.545	0.507
LSTPPTI	0.960	0.135	-0.099	0.084	0.116
LST3PPTI	0.935	-0.162	-0.081	-0.158	0.066
LSTINT	0.967	0.075	0.046	0.029	0.138
LST75OTI	0.946	0.050	0.111	0.073	0.123
PPTBTW	-0.908	-0.007	0.039	0.077	0.311
INTBET	-0.868	-0.087	-0.001	0.023	0.381

	6		6
BASE	0.887	LST75OTI	-0.009
PK	0.183	PPTBTW	0.130
LSPKTI	0.018	INTBET	0.202
RNBTWTI	0.485		
RULST	0.105		
RU3EVT	0.375		
HYSTER	-0.116		
MXTMJPK	-0.047		
MXTRP	-0.040		
SUMPK	0.160		
SMLSPKTI	0.120		
TOTRAIN	0.037		
INT15	0.083		
SFIVE	-0.094		
RRISE	0.134		
RFALL	-0.140		
LSTPPTI	-0.025		
LST3PPTI	0.206		
LSTINT	0.027		

Reproduced with permission of the copyright owner. Further reproduction prohibited without permission.

Appendix 7.14. Summary of dependent and independent variables used in the statistical analysis for quickf characteristics to the major peak at Rio Caguitas near Aguas Buenas.
(D indicates dependent variable; L indicates data was log transformed for final statistical operations; IR indicates data had negative inverse square root transformed)

Start Date	Start Time hour	Start Discharge ft3/s	End Date	End Time hour	DL Suspended-sediment load tons	DL Discharge-weighted sediment concentration mg/L	L QUICK	L LSPKBTI	L QULST
01/05/1992	15.75	6.4	1/5/1992	17.75	1390	9785	2.88E+007	0.0321097	643
09/22/1992	13.75	6.4	9/22/1992	16.25	3.39	768	1.18E+006	0.4169201	8635
12/01/1992	12.5	11.0	12/1/1992	15.5	1.95	524	3.11E+005	16.027559	257630
12/29/1992	12.25	13.0	12/29/1992	16	3.30	1024	5.99E+005	20.118812	1034911
01/07/1993	13.25	8.6	1/7/1993	16.75	37.6	2673	1.72E+006	0.2911546	2974
05/01/1993	14.75	9.3	5/1/1993	16.75	20.2	3517	2.26E+006	1.2769679	15659
05/06/1993	14.25	8.9	5/6/1993	17.75	15.3	1389	9.81E+005	1.1876043	20632
05/26/1993	13.5	8.2	5/26/1993	14.75	NOT ENOUGH SAMPLES		1.49E+006	1.3688521	15869
07/03/1993	10.75	7.3	7/3/1993	14.5	1.83	671	3.49E+005	0.2577932	2591
07/13/1993	16.75	11.0	7/13/1993	18	8.2	1202	1.35E+006	15.552446	409791
07/22/1993	13.75	8.9	7/22/1993	17.75	38.3	2705	2.33E+006	0.3616487	3281
08/15/1993	23.75	13.0	8/16/1993	1.25	7.1	1648	5.92E+005	0.3391032	5294
08/18/1995	11.25	6.2	8/18/1995	19.25	243	4656	4.95E+006	0.0953702	1617
09/06/1995	2.25	8.9	9/6/1995	8.25	1560	14061	1.17E+007	14.228868	1022691
09/07/1995	11.5	9.9	9/7/1995	16.75	24.0	1301	1.63E+006	49.951777	1511942
09/15/1995	21.75	8.3	9/16/1995	4.25	415	4626	1.08E+007	19.970817	3929288
09/27/1995	14.25	2.7	9/27/1995	16.25	36.3	5600	5.75E+005	0.3204957	7894
10/27/1995	14.75	2.6	10/27/1995	16	175	9837	2.04E+006	0.1199999	1302
11/04/1995	13.75	2.6	11/4/1995	15.5	70.7	3415	2.29E+006	2.3546258	11370
12/25/1995	16.25	1.7	12/25/1995	17.75	101	8564	1.25E+006	0.5222344	5811
03/15/1996	13.5	1.9	3/15/1996	16.25	11.0	2324	8.47E+005	0.0504664	160
04/03/1996	14.5	1.4	4/3/1996	15.5	71.9	21454	8.54E+005	0.1412342	1902
05/23/1996	1.75	1.8	5/23/1996	2.5	NOT ENOUGH SAMPLES		7.16E+005	0.0633116	359

Reproduced with permission of the copyright owner. Further reproduction prohibited without permission.

Appendix 7.14. Continued.

Start Date	Start Time hour	End Date	End Time hour	L PPTLSTI	L INTLST	L L75OTI	SUM3PPTI	QU3EVT	L INTBET
01/05/1992	15.75	6.4	1/7/1992	0.0014	0.0003	0.00001	-9.68	7.15	0.09
09/22/1992	13.75	6.4	9/23/1992	0.0071	0.0056	0.00029	-5.23	13.52	0.01
12/01/1992	12.5	11.0	12/1/1992	0.0656	0.0253	0.00041	-5.49	13.64	0.00
12/29/1992	12.25	13.0	12/30/1992	1.8000	0.5800	0.02163	-3.69	14.93	0.00
01/07/1993	13.25	8.6	1/8/1993	0.0039	0.0031	0.00001	-7.31	11.18	0.14
05/01/1993	14.75	9.3	5/2/1993	0.0276	0.0085	0.00022	-6.74	10.94	0.07
05/06/1993	14.25	8.9	5/7/1993	0.0087	0.0049	0.00015	-6.23	12.28	0.05
05/26/1993	13.5	8.2	5/26/1993	0.0248	0.0114	0.00033	-6.67	12.51	0.05
07/03/1993	10.75	7.3	7/4/1993	0.0026	0.0012	0.00003	-6.83	10.35	0.15
07/13/1993	16.75	11.0	7/14/1993	0.0631	0.0034	0.00008	-6.31	11.30	0.01
07/22/1993	13.75	8.9	7/23/1993	0.0032	0.0018	0.00003	-7.49	12.04	0.05
08/15/1993	23.75	13.0	8/16/1993	0.0009	0.0003	0.00001	-8.70	11.08	0.31
08/18/1995	11.25	6.2	8/19/1995	0.0028	0.0018	0.00005	-8.27	9.47	0.15
09/06/1995	2.25	8.9	9/7/1995	4.4400	0.8800	0.01259	-4.35	14.00	0.00
09/07/1995	11.5	9.9	9/8/1995	0.4077	0.0594	0.00066	-4.69	13.95	0.01
09/15/1995	21.75	8.3	9/17/1995	7.8000	2.5500	0.08000	-3.39	15.29	0.01
09/27/1995	14.25	2.7	9/27/1995	0.0025	0.0014	0.00001	-7.26	11.51	0.16
10/27/1995	14.75	2.6	10/28/1995	0.0070	0.0018	0.00002	-8.84	9.29	0.01
11/04/1995	13.75	2.6	11/5/1995	0.0050	0.0012	0.00003	-8.56	9.43	0.19
12/25/1995	16.25	1.7	12/25/1995	0.0209	0.0120	0.00067	-7.08	9.73	0.01
03/15/1996	13.5	1.9	3/16/1996	0.0008	0.0005	0.00002	-10.00	6.30	0.13
04/03/1996	14.5	1.4	4/3/1996	0.0034	0.0006	0.00001	-9.69	7.04	0.04
05/23/1996	1.75	1.8	5/23/1996	0.0011	0.0006	0.00003	-10.20	6.25	0.25

Reproduced with permission of the copyright owner. Further reproduction prohibited without permission.

Appendix 7.14. Continued.

Start Date	Start Time hour	End Date	End Time hour	L INT15	BASE	L PKBS	L RRISE	RNBTWTI	L PPTBTW
01/05/1992	15.75	6.4	1/7/1992	0.64	17.0	1720	3.15	18441	0.86
09/22/1992	13.75	6.4	9/23/1992	0.20	10.0	59.2	0.43	27283	0.01
12/01/1992	12.5	11.0	12/1/1992	0.14	12.0	29.7	0.30	42935	0.00
12/29/1992	12.25	13.0	12/30/1992	0.62	15.0	65.7	0.71	0	0.00
01/07/1993	13.25	8.6	1/8/1993	0.20	15.0	152	0.64	36553	0.82
05/01/1993	14.75	9.3	5/2/1993	0.31	18.0	92.4	0.69	39051	0.21
05/06/1993	14.25	8.9	5/7/1993	0.19	16.0	88.4	0.28	38222	0.08
05/26/1993	13.5	8.2	5/26/1993	0.30	18.0	228	0.58	33598	0.37
07/03/1993	10.75	7.3	7/4/1993	0.25	9.3	26.2	0.49	25687	0.59
07/13/1993	16.75	11.0	7/14/1993	0.22	18.0	133	0.27	45677	0.01
07/22/1993	13.75	8.9	7/23/1993	0.29	19.0	349	0.82	34867	0.19
08/15/1993	23.75	13.0	8/16/1993	0.33	24.0	80.5	1.33	38656	0.94
08/18/1995	11.25	6.2	8/19/1995	0.34	27.7	607	2.17	11259	1.01
09/06/1995	2.25	8.9	9/7/1995	0.46	12.8	1470	2.50	0	0.00
09/07/1995	11.5	9.9	9/8/1995	0.19	12.8	86.2	0.62	37593	0.01
09/15/1995	21.75	8.3	9/17/1995	0.39	19.8	591	1.78	0	0.01
09/27/1995	14.25	2.7	9/27/1995	0.08	9.5	80.8	0.18	16840	0.60
10/27/1995	14.75	2.6	10/28/1995	0.22	8.6	482	0.88	7897	0.06
11/04/1995	13.75	2.6	11/5/1995	0.32	9.2	233	1.20	10265	1.12
12/25/1995	16.25	1.7	12/25/1995	0.16	10.9	206	0.64	6685	0.01
03/15/1996	13.5	1.9	3/16/1996	0.27	3.9	64.2	1.25	6829	1.49
04/03/1996	14.5	1.4	4/3/1996	1.07	8.9	142	2.01	4502	0.46
05/23/1996	1.75	1.8	5/23/1996	0.16	6.5	96.2	0.28	7555	1.76

Reproduced with permission of the copyright owner. Further reproduction prohibited without permission.

Appendix 7.14. Continued.

Start Date	Start Time hour	End Date	End Time hour	L MXTMJPK	L SMLSPKBS
01/05/1992	15.75	6.4	1/7/1992	14.36	13
09/22/1992	13.75	6.4	9/23/1992	0.40	15
12/01/1992	12.5	11.0	12/1/1992	0.83	561
12/29/1992	12.25	13.0	12/30/1992	0.29	20
01/07/1993	13.25	8.6	1/8/1993	0.73	105
05/01/1993	14.75	9.3	5/2/1993	0.77	139
05/06/1993	14.25	8.9	5/7/1993	0.43	130
05/26/1993	13.5	8.2	5/26/1993	3.05	116
07/03/1993	10.75	7.3	7/4/1993	0.12	21
07/13/1993	16.75	11.0	7/14/1993	1.79	1589
07/22/1993	13.75	8.9	7/23/1993	1.46	65
08/15/1993	23.75	13.0	8/16/1993	0.90	186
08/18/1995	11.25	6.2	8/19/1995	2.51	70
09/06/1995	2.25	8.9	9/7/1995	4.09	49
09/07/1995	11.5	9.9	9/8/1995	0.28	1474
09/15/1995	21.75	8.3	9/17/1995	3.52	20
09/27/1995	14.25	2.7	9/27/1995	0.69	81
10/27/1995	14.75	2.6	10/28/1995	6.43	10
11/04/1995	13.75	2.6	11/5/1995	2.23	482
12/25/1995	16.25	1.7	12/25/1995	2.31	33
03/15/1996	13.5	1.9	3/16/1996	0.39	27
04/03/1996	14.5	1.4	4/3/1996	2.39	67
05/23/1996	1.75	1.8	5/23/1996	2.14	26

**to eliminate zero values a value of 0.0002 was added to the precipitation between events and a

Reproduced with permission of the copyright owner. Further reproduction prohibited without permission.

7.15. Pearson correlation matrix to the highest peak using quickflow characteristics, Rio Caguitas near Aguas Buenas.

	SED	QU_SEDCONC	BASE	QUICK
SED	1.000			
QU_SEDCONC	0.856	1.000		
BASE	0.187	-0.047	1.000	
QUICK	0.877	0.576	0.355	1.000
PKBS	0.948	0.741	0.328	0.923
LSPKBTI	-0.165	-0.353	0.097	-0.045
RNBTWTI	-0.525	-0.605	0.278	-0.328
QULST	0.092	0.265	-0.255	-0.002
QU3EVT	-0.210	-0.445	0.249	-0.048
MXTMJPK	0.837	0.756	0.227	0.744
SMLSPKBSTI	-0.278	-0.338	0.176	-0.251
INT15	0.348	0.395	0.194	0.417
RRISE	0.683	0.603	0.240	0.682
LSTPPTI	0.169	-0.027	0.104	0.262
LST3PPTI	-0.165	-0.392	0.136	0.008
LSTINT	0.141	-0.065	0.103	0.229
LST75OTI	0.094	-0.094	0.107	0.209
PPTBTW	0.112	0.229	0.064	0.028
INTBET	0.041	0.122	0.149	-0.020

	PKBS	LSPKBTI	RNBTWTI	QULST	QU3EVT
PKBS	1.000				
LSPKBTI	-0.138	1.000			
RNBTWTI	-0.448	0.131	1.000		
QULST	0.061	-0.924	-0.161	1.000	
QU3EVT	-0.143	0.804	0.172	-0.868	1.000
MXTMJPK	0.874	-0.192	-0.366	0.107	-0.299
SMLSPKBSTI	-0.290	0.523	0.620	-0.437	0.187
INT15	0.414	-0.088	-0.439	0.095	-0.225
RRISE	0.700	-0.259	-0.558	0.289	-0.338
LSTPPTI	0.182	0.861	-0.249	-0.819	0.759
LST3PPTI	-0.127	0.841	0.039	-0.867	0.945
LSTINT	0.144	0.801	-0.282	-0.775	0.807
LST75OTI	0.114	0.758	-0.329	-0.727	0.757
PPTBTW	0.040	-0.757	0.090	0.727	-0.733
INTBET	-0.030	-0.667	0.174	0.620	-0.618

	MXTMJPK	SMLSPKBSTI	INT15	RRISE	LSTPPTI	
MXTMJPK	1.000					
SMLSPKBSTI	-0.193	1.000				
INT15	0.356	-0.292	1.000			
RRISE	0.591	-0.363	0.786	1.000		
LSTPPTI	0.047	0.090	0.148	0.051	1.000	
LST3PPTI	-0.303	0.117	-0.149	-0.299	0.866	
LSTINT	-0.029	-0.021	0.077	0.025	0.972	
LST75OTI	-0.041	-0.089	0.134	0.056		0.942

Reproduced with permission of the copyright owner. Further reproduction prohibited without permission.

Appendix 7.15. **Continued.**

PPTBTW	0.052	-0.061	0.026	0.191	-0.816
INTBET	-0.047	0.023	-0.055	0.109	-0.775

	LST3PPTI	LSTINT	LST75OTI	PPTBTW	INTBET
LST3PPTI	1.000				
LSTINT	0.902	1.000			
LST75OTI	0.877	0.973	1.000		
PPTBTW	-0.804	-0.808	-0.812	1.000	
INTBET	-0.705	-0.758	-0.761	0.977	1.000

Reproduced with permission of the copyright owner. Further reproduction prohibited without permission.

Appendix 7.16. Results of principal component analysis to the major peak using quickflow characteristics.

Component loadings

	1	2	3	4	5	6
BASE	0.102	0.242	0.772	0.340	0.317	-0.214
QUICK	0.058	0.854	0.322	-0.181	0.148	0.125
PKBS	-0.029	0.900	0.255	-0.289	0.099	0.049
LSPKBTI	0.915	-0.162	0.202	-0.005	-0.257	0.141
RNBTWTI	-0.056	-0.669	0.606	-0.039	0.025	-0.281
QULST	0.951	-0.022	0.201	0.021	-0.132	0.114
QU3EVT	0.891	-0.190	0.143	0.078	0.283	-0.020
MXTMJPK	-0.142	0.793	0.234	-0.459	-0.100	-0.121
SMLSPKBSTI	0.183	-0.489	0.635	-0.108	-0.513	0.166
INT15	-0.040	0.689	-0.054	0.537	-0.382	-0.204
RRISE	-0.184	0.878	0.034	0.286	-0.181	0.028
LSTPPTI	0.950	0.246	-0.013	0.016	-0.073	0.116
LST3PPTI	0.955	-0.117	0.006	0.081	0.217	0.043
LSTINT	0.947	0.220	-0.091	0.053	0.094	0.126
LST75OTI	0.923	0.241	-0.153	0.118	0.096	0.069
PPTBTW	-0.897	-0.008	0.194	0.171	0.092	0.325
INTBET	-0.826	-0.100	0.279	0.228	0.156	0.379

Reproduced with permission of the copyright owner. Further reproduction prohibited without permission.

Appendix 7.17. Results of principal component analysis to the major peak using quickflow characteristics without the variable quickflow.

Component loadings

	1	2	3	4	5
BASE	0.097	0.166	0.821	0.358	0.296
PKBS	-0.041	0.836	0.323	-0.274	0.243
LSPKBTI	0.917	-0.169	0.195	-0.093	-0.242
RNBTWTI	-0.050	-0.750	0.506	-0.031	0.039
QULST	0.951	-0.032	0.207	-0.032	-0.123
QU3EVT	0.893	-0.201	0.113	0.167	0.242
MXTMJPK	-0.152	0.747	0.307	-0.516	0.145
SMLSPKBSTI	0.187	-0.550	0.588	-0.287	-0.434
INT15	-0.047	0.728	0.096	0.345	-0.490
RRISE	-0.194	0.879	0.167	0.177	-0.221
LSTPPTI	0.947	0.255	0.020	-0.014	-0.071
LST3PPTI	0.956	-0.117	-0.020	0.161	0.157
LSTINT	0.945	0.235	-0.066	0.082	0.065
LST75OTI	0.920	0.268	-0.117	0.143	0.049
PPTBTW	-0.897	-0.048	0.182	0.199	0.007
INTBET	-0.825	-0.149	0.256	0.274	0.048

	6
BASE	-0.142
PKBS	0.103
LSPKBTI	0.128
RNBTWTI	-0.316
QULST	0.115
QU3EVT	-0.007
MXTMJPK	-0.042
SMLSPKBSTI	0.153
INT15	-0.252
RRISE	0.020
LSTPPTI	0.116
LST3PPTI	0.034
LSTINT	0.132
LST75OTI	0.074
PPTBTW	0.318
INTBET	0.376

Reproduced with permission of the copyright owner. Further reproduction prohibited without permission.

Appendix 7.18. Results of principal component analysis to the major peak after varimax rotation using quickflow characteristics.

Rotated Loading Matrix (VARIMAX, Gamma = 1.0000)

	1	2	3	4	5	6
BASE	0.101	0.261	0.898	0.134	0.105	0.105
QUICK	0.121	0.891	0.163	0.185	-0.117	0.153
PKBS	0.025	0.955	0.077	0.181	-0.141	0.039
LSPKBTI	0.883	-0.094	-0.010	-0.030	0.447	-0.022
RNBTWTI	-0.163	-0.345	0.534	-0.401	0.523	-0.187
QULST	0.935	0.007	0.066	-0.004	0.312	-0.007
QU3EVT	0.877	-0.163	0.291	-0.238	0.010	-0.017
MXTMJPK	-0.130	0.925	-0.033	0.143	0.005	-0.209
SMLSPKBSTI	0.099	-0.153	0.111	-0.151	0.953	0.045
INT15	0.005	0.227	0.066	0.940	-0.107	-0.069
RRISE	-0.105	0.568	0.027	0.731	-0.185	0.136
LSTPPTI	0.967	0.159	-0.063	0.120	0.057	-0.015
LST3PPTI	0.954	-0.149	0.143	-0.162	-0.038	-0.001
LSTINT	0.978	0.105	-0.029	0.053	-0.101	0.034
LST75OTI	0.956	0.065	-0.025	0.120	-0.168	0.000
PPTBTW	-0.848	0.034	0.102	0.039	0.013	0.503
INTBET	-0.776	-0.035	0.196	-0.021	0.056	0.587

Reproduced with permission of the copyright owner. Further reproduction prohibited without permission.

Appendix 7.19. Results of principal component analysis to the major peak after varimax rotation using quickflow characteristics for the independent variables after removal of quickflow.

Rotated Loading Matrix (VARIMAX, Gamma = 1.0000)

	1	2	3	4	5
PKBS	0.048	-0.911	-0.171	0.151	0.237
LSPKBTI	0.881	0.097	0.450	-0.016	-0.040
RNBTWTI	-0.182	0.360	0.545	0.483	-0.393
QULST	0.935	0.009	0.313	0.071	-0.008
QU3EVT	0.869	0.192	0.020	0.287	-0.244
MXTMJPK	-0.101	-0.953	-0.025	0.026	0.176
SMLSPKBSTI	0.096	0.120	0.957	0.094	-0.165
INT15	0.011	-0.169	-0.108	0.065	0.956
RRISE	-0.092	-0.504	-0.201	0.069	0.765
LSTPPTI	0.972	-0.130	0.051	-0.046	0.126
LST3PPTI	0.946	0.194	-0.030	0.138	-0.162
LSTINT	0.980	-0.069	-0.105	-0.010	0.056
LST75OTI	0.958	-0.029	-0.170	-0.012	0.120
PPTBTW	-0.852	0.001	0.008	0.128	0.051
INTBET	-0.783	0.077	0.053	0.223	-0.013
BASE	0.104	-0.210	0.109	0.924	0.138

	6
PKBS	0.096
LSPKBTI	-0.016
RNBTWTI	-0.275
QULST	0.001
QU3EVT	-0.045
MXTMJPK	-0.116
SMLSPKBSTI	0.048
INT15	-0.076
RRISE	0.160
LSTPPTI	0.003
LST3PPTI	-0.031
LSTINT	0.045
LST75OTI	0.009
PPTBTW	0.487
INTBET	0.562
BASE	0.092

Reproduced with permission of the copyright owner. Further reproduction prohibited without permission.

Appendix 7.20. Summary of dependent and independent variables used in the statistical analysis for runof characteristics to the major peak at Rio Caguitas near Aguas Buenas.
(D indicates dependent variable; L indicates data was log transformed for final statistical operations; IR indicates data had negative inverse square root transformed)

Start Date	Start Time hour	Start Discharge ft3/s	End Date	End Time hour	DL Suspended-sediment load tons	DL Discharge-weighted sediment concentration mg/L	L RUNOFF	L LSPKTI	L RULST
01/05/1992	15.75	6.4	1/5/1992	17.75	1390	9683	2.88E+007	0.056	1846
09/22/1992	13.75	6.4	9/22/1992	16.25	3.39	540	1.18E+006	0.676	25105
12/01/1992	12.5	11.0	12/1/1992	15.5	1.95	260	3.11E+005	16.34	310014
12/29/1992	12.25	13.0	12/29/1992	16	3.30	400	5.99E+005	2.857	2434500
01/07/1993	13.25	8.6	1/7/1993	16.75	37.6	2123	1.72E+006	0.346	6709
05/01/1993	14.75	9.3	5/1/1993	16.75	20.2	2561	2.26E+006	1.420	24804
05/06/1993	14.25	8.9	5/6/1993	17.75	15.3	1022	9.81E+005	1.309	33902
07/03/1993	10.75	7.3	7/3/1993	14.5	1.83	309	3.49E+005	0.370	6573
07/13/1993	16.75	11.0	7/13/1993	18	8.2	975	1.35E+006	15.74	466423
07/22/1993	13.75	8.9	7/22/1993	17.75	38.3	2004	2.33E+006	0.422	5400
08/15/1993	23.75	13.0	8/16/1993	1.25	7.1	1137	5.92E+005	0.369	8308
08/18/1995	11.25	6.2	8/18/1995	19.25	243	4158	4.95E+006	0.103	2112
09/06/1995	2.25	8.9	9/6/1995	8.25	1560	13374	1.17E+007	0.948	2323698
09/07/1995	11.5	9.9	9/7/1995	16.75	24.0	980	1.63E+006	50.26	1634718
09/15/1995	21.75	8.3	9/16/1995	4.25	415	4395	1.08E+007	1.250	5620100
09/27/1995	14.25	2.7	9/27/1995	16.25	36.3	4972	5.75E+005	0.359	11881
10/27/1995	14.75	2.6	10/27/1995	16	175	9613	2.04E+006	0.155	2473
11/04/1995	13.75	2.6	11/4/1995	15.5	70.7	3322	2.29E+006	2.371	12632
12/25/1995	16.25	1.7	12/25/1995	17.75	101	8256	1.25E+006	0.550	7365
03/15/1996	13.5	1.9	3/15/1996	16.25	11.0	2043	8.47E+005	0.056	245
04/03/1996	14.5	1.4	4/3/1996	15.5	71.9	20189	8.54E+005	0.146	2178

Reproduced with permission of the copyright owner. Further reproduction prohibited without permission.

Appendix 7.20. Continued.

Start Date	Start Time hour	End Date	End Time hour	L PPTLSTI	L INTLST	L L75OTI	SUM3PPTI	RU3EVT	L INTBET
01/05/1992	15.75	6.4	1/7/1992	0.0014	0.0003	0.00001	-9.68	8.6	0.09
09/22/1992	13.75	6.4	9/23/1992	0.0071	0.0056	0.00029	-5.23	14.2	0.01
12/01/1992	12.5	11.0	12/1/1992	0.0656	0.0253	0.00041	-5.49	14.2	0.00
12/29/1992	12.25	13.0	12/30/1992	1.8000	0.5800	0.02163	-3.69	15.7	0.00
01/07/1993	13.25	8.6	1/8/1993	0.0039	0.0031	0.00001	-7.31	11.9	0.14
05/01/1993	14.75	9.3	5/2/1993	0.0276	0.0085	0.00022	-6.74	11.9	0.07
05/06/1993	14.25	8.9	5/7/1993	0.0087	0.0049	0.00015	-6.23	12.9	0.05
07/03/1993	10.75	7.3	7/4/1993	0.0026	0.0012	0.00003	-6.83	11.4	0.15
07/13/1993	16.75	11.0	7/14/1993	0.0631	0.0034	0.00008	-6.31	12.3	0.01
07/22/1993	13.75	8.9	7/23/1993	0.0032	0.0018	0.00003	-7.49	12.5	0.05
08/15/1993	23.75	13.0	8/16/1993	0.0009	0.0003	0.00001	-8.70	11.5	0.31
08/18/1995	11.25	6.2	8/19/1995	0.0028	0.0018	0.00005	-8.27	9.9	0.15
09/06/1995	2.25	8.9	9/7/1995	4.4400	0.8800	0.01259	-4.35	14.5	0.00
09/07/1995	11.5	9.9	9/8/1995	0.4077	0.0594	0.00066	-4.69	14.4	0.01
09/15/1995	21.75	8.3	9/17/1995	7.8000	2.5500	0.08000	-3.39	15.6	0.01
09/27/1995	14.25	2.7	9/27/1995	0.0025	0.0014	0.00001	-7.26	11.9	0.16
10/27/1995	14.75	2.6	10/28/1995	0.0070	0.0018	0.00002	-8.84	9.9	0.01
11/04/1995	13.75	2.6	11/5/1995	0.0050	0.0012	0.00003	-8.56	9.9	0.19
12/25/1995	16.25	1.7	12/25/1995	0.0209	0.0120	0.00067	-7.08	10.2	0.01
03/15/1996	13.5	1.9	3/16/1996	0.0008	0.0005	0.00002	-10.00	7.1	0.13
04/03/1996	14.5	1.4	4/3/1996	0.0034	0.0006	0.00001	-9.69	7.6	0.04

Reproduced with permission of the copyright owner. Further reproduction prohibited without permission.

Appendix 7.20. Continued.

Start Date	Start Time hour	End Date	End Time hour	L INT15	BASE	L PK	L RRISE	RNBTWTI	L PPTBTW
01/05/1992	15.75	6.4	1/7/1992	0.64	17.0	1730	3.15	18441	0.86
09/22/1992	13.75	6.4	9/23/1992	0.20	10.0	66.0	0.43	27283	0.01
12/01/1992	12.5	11.0	12/1/1992	0.14	12.0	41.0	0.30	42935	0.00
12/29/1992	12.25	13.0	12/30/1992	0.62	15.0	78.0	0.71	0	0.00
01/07/1993	13.25	8.6	1/8/1993	0.20	15.0	162	0.64	36553	0.82
05/01/1993	14.75	9.3	5/2/1993	0.31	18.0	102	0.69	39051	0.21
05/06/1993	14.25	8.9	5/7/1993	0.19	16.0	99.6	0.28	38222	0.08
07/03/1993	10.75	7.3	7/4/1993	0.25	9.3	34.0	0.49	25687	0.59
07/13/1993	16.75	11.0	7/14/1993	0.22	18.0	145	0.27	45677	0.01
07/22/1993	13.75	8.9	7/23/1993	0.29	19.0	359	0.82	34867	0.19
08/15/1993	23.75	13.0	8/16/1993	0.33	24.0	94.0	1.33	38656	0.94
08/18/1995	11.25	6.2	8/19/1995	0.34	27.7	615	2.17	11259	1.01
09/06/1995	2.25	8.9	9/7/1995	0.46	12.8	1483	2.50	0	0.00
09/07/1995	11.5	9.9	9/8/1995	0.19	12.8	96.9	0.62	37593	0.01
09/15/1995	21.75	8.3	9/17/1995	0.39	19.8	597	1.78	0	0.01
09/27/1995	14.25	2.7	9/27/1995	0.08	9.5	85.4	0.18	16840	0.60
10/27/1995	14.75	2.6	10/28/1995	0.22	8.6	485	0.88	7897	0.06
11/04/1995	13.75	2.6	11/5/1995	0.32	9.2	237	1.20	10265	1.12
12/25/1995	16.25	1.7	12/25/1995	0.16	10.9	210	0.64	6685	0.01
03/15/1996	13.5	1.9	3/16/1996	0.27	3.9	66.5	1.25	6829	1.49
04/03/1996	14.5	1.4	4/3/1996	1.07	8.9	145	2.01	4502	0.46

Reproduced with permission of the copyright owner. Further reproduction prohibited without permission.

Appendix 7.20. Continued.

Start Date	Start Time hour	End Date	End Time hour	L MXTMJPK	L SMLSPK
01/05/1992	15.75	6.4	1/7/1992	14.4	22.0
09/22/1992	13.75	6.4	9/23/1992	0.40	25.0
12/01/1992	12.5	11.0	12/1/1992	0.83	572
12/29/1992	12.25	13.0	12/30/1992	0.29	30.0
01/07/1993	13.25	8.6	1/8/1993	0.73	119
05/01/1993	14.75	9.3	5/2/1993	0.77	151
05/06/1993	14.25	8.9	5/7/1993	0.43	237
07/03/1993	10.75	7.3	7/4/1993	0.12	30.0
07/13/1993	16.75	11.0	7/14/1993	1.79	1605
07/22/1993	13.75	8.9	7/23/1993	1.46	76.0
08/15/1993	23.75	13.0	8/16/1993	0.90	202
08/18/1995	11.25	6.2	8/19/1995	2.51	73.7
09/06/1995	2.25	8.9	9/7/1995	4.09	56.6
09/07/1995	11.5	9.9	9/8/1995	0.28	1483
09/15/1995	21.75	8.3	9/17/1995	3.52	23.7
09/27/1995	14.25	2.7	9/27/1995	0.69	90.4
10/27/1995	14.75	2.6	10/28/1995	6.43	12.8
11/04/1995	13.75	2.6	11/5/1995	2.23	485
12/25/1995	16.25	1.7	12/25/1995	2.31	35.0
03/15/1996	13.5	1.9	3/16/1996	0.39	24.2
04/03/1996	14.5	1.4	4/3/1996	2.39	64.2

**to eliminate zero values a value of 0.0002 was added to the precipitation between events and a value of 5000 was added to the runoff between events.

Reproduced with permission of the copyright owner. Further reproduction prohibited without permission.

7.21. Pearson correlation matrix to the highest peak using runoff characteristics, Rio Caguitas near Aguas Buenas.

	SED	RU_SEDCONC	BASE	RUN
SED	1.000			
RU_SEDCONC	0.874	1.000		
BASE	0.187	-0.044	1.000	
RUN	0.820	0.439	0.397	1.000
PK	0.941	0.736	0.344	0.874
LSPKTI	-0.378	-0.518	0.042	-0.091
RNBTWTI	-0.525	-0.569	0.278	-0.301
RULST	-0.039	-0.285	0.186	0.262
RU3EVT	-0.227	-0.496	0.250	0.164
MXTMJPK	0.837	0.776	0.227	0.635
SMLSPKTI	-0.298	-0.341	0.198	-0.152
INT15	0.348	0.340	0.194	0.244
RRISE	0.683	0.589	0.240	0.571
LSTPPTI	0.169	-0.055	0.104	0.377
LST3PPTI	-0.165	-0.414	0.136	0.181
LSTINT	0.141	-0.096	0.103	0.372
LST75OTI	0.094	-0.125	0.107	0.321
PPTBTW	0.112	0.267	0.064	-0.107
INTBET	0.041	0.163	0.149	-0.116

	PK	LSPKTI	RNBTWTI	RULST	RU3EVT
PK	1.000				
LSPKTI	-0.334	1.000			
RNBTWTI	-0.434	0.442	1.000		
RULST	0.021	0.778	0.026	1.000	
RU3EVT	-0.124	0.677	0.200	0.881	1.000
MXTMJPK	0.873	-0.320	-0.366	-0.106	-0.308
SMLSPKTI	-0.290	0.758	0.664	0.341	0.221
INT15	0.417	-0.293	-0.439	0.005	-0.201
RRISE	0.700	-0.489	-0.558	-0.161	-0.342
LSTPPTI	0.198	0.601	-0.249	0.931	0.762
LST3PPTI	-0.108	0.680	0.039	0.918	0.953
LSTINT	0.159	0.522	-0.282	0.887	0.804
LST75OTI	0.128	0.481	-0.329	0.843	0.755
PPTBTW	0.017	-0.611	0.090	-0.799	-0.742
INTBET	-0.050	-0.521	0.174	-0.712	-0.628

Reproduced with permission of the copyright owner. Further reproduction prohibited without permission.

Appendix 7.21. Continued.

	MXTMJPK	SMLSPKTI	INT15	RRISE	LSTPPTI
MXTMJPK	1.000				
SMLSPKTI	-0.213	1.000			
INT15	0.356	-0.298	1.000		
RRISE	0.591	-0.400	0.786	1.000	
LSTPPTI	0.047	0.098	0.148	0.051	1.000
LST3PPTI	-0.303	0.156	-0.149	-0.299	0.866
LSTINT	-0.029	-0.013	0.077	0.025	0.972
LST75OTI	-0.041	-0.079	0.134	0.056	0.942
PPTBTW	0.052	-0.083	0.026	0.191	-0.816
INTBET	-0.047	0.008	-0.055	0.109	-0.775

	LST3PPTI	LSTINT	LST75OTI	PPTBTW	INTBET
LST3PPTI	1.000				
LSTINT	0.902	1.000			
LST75OTI	0.877	0.973	1.000		
PPTBTW	-0.804	-0.808	-0.812	1.000	
INTBET	-0.705	-0.758	-0.761	0.977	1.000

Reproduced with permission of the copyright owner. Further reproduction prohibited without permission.

Appendix 7.22. Results of principal component analysis to the major peak after varimax rotation using runoff characteristics.

Component loadings

	1	2	3	4	5	6
BASE	0.119	0.252	0.789	0.328	0.217	-0.289
RUN	0.262	0.756	0.387	-0.260	0.207	0.175
PK	0.034	0.906	0.270	-0.281	0.018	-0.004
RNBTWTI	-0.068	-0.669	0.622	0.006	-0.139	-0.211
RULST	0.953	-0.035	0.158	0.069	-0.082	0.164
RU3EVT	0.898	-0.223	0.185	0.061	0.225	-0.061
MXTMJPK	-0.109	0.803	0.206	-0.399	-0.246	-0.142
SMLSPKTI	0.154	-0.494	0.607	-0.009	-0.491	0.318
INT15	-0.022	0.677	-0.118	0.621	-0.311	-0.057
RRISE	-0.161	0.890	-0.004	0.304	-0.087	0.084
LSTPPTI	0.946	0.206	-0.031	0.040	-0.054	0.169
LST3PPTI	0.957	-0.160	0.034	0.056	0.201	0.043
LST75OTI	0.926	0.197	-0.154	0.107	0.122	0.061
PPTBTW	-0.910	0.029	0.191	0.124	0.214	0.230
INTBET	-0.844	-0.062	0.284	0.165	0.292	0.271

Reproduced with permission of the copyright owner. Further reproduction prohibited without permission.

Appendix 7.23. Results of principal component analysis to the major peak after varimax rotation using runoff characteristics without the variable runoff.

Component loadings

	1	2	3	4	5	6
BASE	0.090	0.174	0.855	0.256	0.284	-0.171
PK	-0.044	0.836	0.331	-0.323	0.170	0.075
RNBTWTI	-0.026	-0.744	0.537	-0.062	-0.100	-0.274
RULST	0.951	0.019	0.184	0.025	-0.095	0.169
RU3EVT	0.909	-0.185	0.165	0.113	0.213	-0.039
MXTMJPK	-0.175	0.753	0.281	-0.536	0.005	-0.029
SMLSPKTI	0.184	-0.546	0.563	-0.172	-0.482	0.266
INT15	-0.065	0.731	0.074	0.458	-0.427	-0.162
RRISE	-0.227	0.879	0.135	0.230	-0.148	0.040
LSTPPTI	0.928	0.279	0.023	0.011	-0.062	0.186
LST3PPTI	0.964	-0.100	0.023	0.117	0.164	0.059
LST75OTI	0.910	0.285	-0.099	0.132	0.092	0.095
PPTBTW	-0.914	-0.072	0.158	0.192	0.130	0.250
INTBET	-0.842	-0.170	0.238	0.253	0.190	0.305

Reproduced with permission of the copyright owner. Further reproduction prohibited without permission.

Appendix 7.24. Results of principal component analysis to the major peak after varimax rotation using runoff characteristics.

Rotated Loading Matrix (VARIMAX, Gamma = 1.0000)

	1	2	3	4	5
BASE	0.080	0.267	0.144	0.140	0.902
RUN	0.248	0.871	-0.081	0.069	0.185
PK	0.016	0.943	-0.152	0.225	0.105
RNBTWTI	-0.132	-0.326	0.606	-0.400	0.472
RULST	0.947	0.039	0.259	0.010	0.064
RU3EVT	0.886	-0.125	0.060	-0.235	0.295
MXTMJPK	-0.145	0.895	-0.038	0.197	-0.025
SMLSPKTI	0.107	-0.125	0.959	-0.149	0.083
INT15	0.013	0.169	-0.127	0.950	0.078
RRISE	-0.131	0.538	-0.228	0.741	0.049
LSTPPTI	0.955	0.176	0.050	0.135	-0.067
LST3PPTI	0.959	-0.114	0.004	-0.168	0.133
LST75OTI	0.946	0.077	-0.172	0.121	-0.012
PPTBTW	-0.894	0.004	0.000	0.045	0.116
INTBET	-0.828	-0.054	0.053	-0.019	0.207

	6
BASE	0.072
RUN	0.255
PK	0.007
RNBTWTI	-0.172
RULST	0.069
RU3EVT	0.053
MXTMJPK	-0.274
SMLSPKTI	0.050
INT15	-0.067
RRISE	0.126
LSTPPTI	0.062
LST3PPTI	0.099
LST75OTI	0.070
PPTBTW	0.406
INTBET	0.497

Reproduced with permission of the copyright owner. Further reproduction prohibited without permission.

Appendix 7.25. Results of principal component analysis to the major peak after varimax rotation using runoff characteristics without the variable runoff.

Rotated Loading Matrix (VARIMAX, Gamma = 1.0000)

	1	2	3	4	5	6
BASE	0.091	0.214	0.921	0.138	0.142	0.061
PK	0.057	0.905	0.179	0.237	-0.173	0.095
RNBTWTI	-0.156	-0.338	0.433	-0.373	0.616	-0.295
RULST	0.950	-0.010	0.077	0.008	0.254	0.068
RU3EVT	0.875	-0.201	0.296	-0.219	0.058	-0.026
MXTMJPK	-0.098	0.954	0.021	0.175	-0.050	-0.102
SMLSPKTI	0.106	-0.118	0.080	-0.158	0.960	0.062
INT15	0.016	0.168	0.066	0.955	-0.123	-0.064
RRISE	-0.111	0.495	0.090	0.757	-0.240	0.151
LSTPPTI	0.965	0.134	-0.045	0.129	0.042	0.094
LST3PPTI	0.950	-0.187	0.139	-0.157	0.000	0.041
LST75OTI	0.950	0.028	0.002	0.117	-0.177	0.079
PPTBTW	-0.890	-0.017	0.151	0.045	-0.007	0.406
INTBET	-0.826	-0.093	0.247	-0.019	0.044	0.484

Reproduced with permission of the copyright owner. Further reproduction prohibited without permission.

Appendix 7.26. Summary of dependent and independent variables used in the statistical analysis for hysteresis.
(A) Type 1 storms and (B) Type 3 storms.
(D indicates dependent variable; L indicates log transformed; LN indicates natural log transform; IR indicates negative inverse square root transformed)

Appendix 7.26A.

Start Date	Start Time hour	End Date	End Time hour	Width of clockwise loop, mg/L D L	Discharge used in width analysis, ft3/s	Sediment load tons SED	Discharge-weighted sediment concentration, mg/L CONC	Runoff ft3 2-RUN L	Sum of peak flows 9-SMPK L	Maximum rate of hydrograph rise to the highest peak, cfs/min 6-MXTMJPK L	Runoff of the previous event divided by the time since the previous event, fts/hour 25-RULST L
1/5/1992	15.75	1/7/1992	6	5260	1354	3800	4012	3.04E+007	3905	14.36	1846
1/7/1993	13.25	1/8/1993	5.75	900	129	139	1841	2.42E+006	162	0.73	6710
5/1/1993	14.75	5/2/1993	16	2460	64	71.6	700	3.28E+006	196	0.77	24800
9/6/1995	2.25	9/7/1995	3.75	7400	902	3500	8844	1.27E+007	1483	4.09	2.32E+006
11/4/1995	13.75	11/5/1995	6	2182	154	147	1787	2.63E+006	237	2.23	1.26E+004
12/25/1995	16.25	12/25/1995	23.5	3920	138	250	5668	1.41E+006	210	2.31	7365
3/15/1996	13.5	3/16/1996	1.25	695	53	46.1	1523	9.70E+005	67	0.39	245
4/3/1996	14.5	4/3/1996	22	16735	85	166	5353	9.93E+005	217	2.39	2180
			AVERAGE	**4944**	**360**	**1015**	**3716**	**6.84E+006**	**809**	**3.41**	**297435**

Start Date	Start Time hour	End Date	End Time hour	Runoff of the 3 previous events divided by the time since the 3 e 31-RU3EVT L	Sediment transport surve slope on falling limb, ft3/s/(mg/L) 33-RATE_FALL	Rainfall on the rising limb to the highest peak, in 13-RRISE	Rainfall on the falling limb after the highest peak, in 14-RAINFOL L	75% rainfall intensity of current event, in/min 12-SFIVE L	Runoff since the previous event over time since the previous event ft3/hour 17-RNBTWTI	Sediment transport surve slope on rising limb, ft3/s/(mg/L) 32-RATE_RISE	Time of peak sediment concentration relative to peak flow (minutes) 34-TIME_PKCON
1/5/1992	15.75	1/7/1992	6	8.64	2.84	3.15	2.62	0.0096	23441	3.49	-3
1/7/1993	13.25	1/8/1993	5.75	11.95	18.90	0.64	0.01	0.0030	41553	8.08	-43
5/1/1993	14.75	5/2/1993	16	11.86	44.91	0.69	0.26	0.0022	44051	-11.26	-15
9/6/1995	2.25	9/7/1995	3.75	14.51	11.93	2.50	0.66	0.0051	5000	19.6	-24
11/4/1995	13.75	11/5/1995	6	9.86	15.38	1.20	0.14	0.0043	15265	-15.1	-43
12/25/1995	16.25	12/25/1995	23.5	10.15	26.82	0.64	0.02	0.0076	11685	-36.1	-28
3/15/1996	13.5	3/16/1996	1.25	7.13	28.01	1.25	0.28	0.0059	11829	25.6	-44
4/3/1996	14.5	4/3/1996	22	7.57	13.41	2.01	0.70	0.0231	9502	-194.4	-14
			AVERAGE	**9.84**	**Average positive slo**	**1.52**	**0.36**	**0.0092**	**10656**	**Average negative slope = -(Average positive slope = 14.19**	**-30.6**

Reproduced with permission of the copyright owner. Further reproduction prohibited without permission.

Appendix 7.26B. Type 3 storms.

Start Date	Start Time hour	End Date	End Time hour	Width of counter-clockwise loop. mg/L D LN	Discharge used in width analysis, ft3/s	Sediment load tons	Discharge-weighted sediment concentration, mg/L	Runoff ft3 2-RUNL	Sum of peak flows 9-SMPKIR	Maximum rate of hydrograph rise to the highest peak, cfs/min 6-MXTMJPK	Runoff of the previous event divided by the time since the previous event, fts/hour 25-RULSTIR
9/22/1992	13.75	9/23/1992	9.75	894	46	38.2	691	1.77E+006	66	0.40	25105
12/1/1992	12.5	12/1/1992	22	266	23	8.47	385	7.04E+005	71	0.83	310014
5/6/1993	14.25	5/7/1993	1.25	670	70	73.5	1598	1.47E+006	99.6	0.43	33902
7/13/1993	16.75	7/14/1993	4.25	993	56	51.9	851	1.95E+006	145	1.79	466423
7/22/1993	13.75	7/23/1993	2	1350	247	191	2212	2.77E+006	359	1.46	5400
8/18/1995	11.25	8/19/1995	9	1900	431	351	2012	5.59E+006	615	2.51	2112
9/7/1995	11.5	9/8/1995	6.5	670	53	50	664	2.40E+006	96.9	0.28	1634718
9/27/1995	14.25	9/27/1995	21.5	6590	61	97	4211	7.34E+005	85.4	0.69	11881
			AVERAGE	1667	123	108	1578	2.18E+006	192	1.05	311194

Start Date	Start Time hour	End Date	End Time hour	previous events divided by the time since the 3 events 31-RU3EVT LN	Sediment transport surve slope on falling limb, ft3/s/(mg/L) 33-RATE_FALL	Rainfall on the rising limb to the highest peak, in 13-RRISE	Rainfall on the falling limb after the highest peak, in 14-RAINFOL	75% rainfall intensity of current event, in/min 12-SFIVE	Runoff since the previous event over time since the previous event ft3/hour 17-RNBTWTI	Sediment transport surve slope on rising limb, ft3/s/(mg/L) 32-RATE_RISE	Time of peak sediment concentration relative to peak flow (minutes) 34-TIME_PKCON
9/22/1992	13.75	9/23/1992	9.75	14.17	9.23	0.43	0.09	0.0024	32283	15.7	176
12/1/1992	12.5	12/1/1992	22	14.21	-28.0	0.30	0.00	0.0036	47935	13.1	152
5/6/1993	14.25	5/7/1993	1.25	12.85	19.4	0.28	0.01	0.0073	43222	31.6	75
7/13/1993	16.75	7/14/1993	4.25	12.29	11.0	0.27	0.00	0.0036	50677	4.24	92
7/22/1993	13.75	7/23/1993	2	12.47	9.19	0.82	0.02	0.0038	39867	5.43	22
8/18/1995	11.25	8/19/1995	9	9.90	10.7	2.17	0.44	0.0047	16259	-37.3	-83
9/7/1995	11.5	9/8/1995	6.5	14.44	8.0	0.62	0.01	0.0023	42593	14.7	-40
9/27/1995	14.25	9/27/1995	21.5	11.88	-6.14	0.18	0.07	0.0012	21840	76.7	-8
			AVERAGE	**12.78**	**Average negative slc**	**0.63**	**0.08**	**0.0036**	**36834**	**Average positive slope = 23.1**	
					Average positive slope = 11.3						

Appendix 8.1. Relation of calculated quickflow to estimated quickflow. Estimated quickflow is calculated from rain falling on an impervious basin. Rio Piedras basin area = 7.49 square miles.

Start Date	Hour	End Date	Hour	Rainfall amount, in	Estimate volume of quickflow corresponding to impervious contributing area, ft3	Calculated quickflow, ft3	Percent ratio: calculated quickflow/ estimated quickflow
3/28/1992	15.25	3/29/1992	4.00	1.28	22203412	7286203	33
4/19/1992	12.00	4/20/1992	6.00	1.11	19400242	3870608	20
4/29/1992	17.25	4/30/1992	16.75	3.11	54131341	12340215	23
5/1/1992	16.75	5/3/1992	14.50	2.26	39334832	24788070	63
5/16/1992	11.00	5/17/1992	9.00	0.93	16149786	8409330	52
7/20/1992	10.75	7/21/1992	6.00	2.25	39070686	3499830	9
8/5/1992	2.00	8/6/1992	10.50	1.09	18901461	13428000	71
9/6/1992	13.25	9/6/1992	21.50	0.71	12355418	2924535	24
9/23/1992	10.50	9/23/1992	21.00	0.91	15833766	2762820	17
6/9/1993	11.25	6/9/1993	23.00	0.35	6090269	2871330	47
6/29/1993	17.00	6/30/1993	2.50	0.32	5510241	1424283	26
9/6/1993	17.00	9/7/1993	6.00	1.29	22446984	6763784	30
1/11/1994	0.50	1/11/1994	19.25	0.53	9309400	3680422	40
1/23/1994	14.25	1/24/1994	3.00	0.33	5742251	2663274	46
4/10/1994	7.50	4/10/1994	19.50	0.54	9417584	6304760	67
7/2/1994	8.83	7/2/1994	23.25	0.62	10853230	2661619	25
11/19/199	16.17	11/20/1994	2.50	1.53	26602476	5661957	21
12/1/1994	14.75	12/2/1994	3.75	0.47	8178393	2061697	25
12/2/1994	11.25	12/3/1994	15.25	1.10	19140845	7339530	38
2/25/1995	15.00	2/26/1995	23.75	3.90	67862889	17727461	26
5/15/1995	18.00	5/16/1995	2.75	1.30	22597785	2438436	11
6/10/1995	11.50	6/10/1995	22.50	1.09	18897576	3249718	17
6/15/1995	11.50	6/15/1995	21.25	0.74	12876568	1926114	15
6/16/1995	12.50	6/16/1995	23.75	0.43	7556877	4170431	55
7/21/1995	17.50	7/22/1995	4.25	0.51	8874392	5183263	58
9/6/1995	3.75	9/7/1995	2.50	2.91	50653502	27415546	54

Reproduced with permission of the copyright owner. Further reproduction prohibited without permission.

Reproduced with permission of the copyright owner. Further reproduction prohibited without permission.

Appendix 8.2 Summary of dependent and independent variables used in the statistical analysis for quickflow characteristi of the entire event at Rio Piedras at El Senorial
(D indicates dependent variable; L indicates log transformed)

Start Date	Start Time hour	Start Discharge ft3/s	End Date	End Time hour	DL Suspended-sediment load tons	DL Discharge-weighted sediment concentration mg/L	L 1-QUICK ft3	3-BASE ft3/s	L 4-PKBS ft3/s	L 7-MXTRP ft3/s/min
3/28/1992	15.25	3.5	3/29/1992	4.00	4302	18915	7.29E+006	3.5	1796.1	29.94
4/19/1992	12.00	4.1	4/20/1992	6.00	2051	16972	3.87E+006	4.1	591.7	13.15
4/29/1992	17.25	2.1	4/30/1992	16.75	3696	9594	1.23E+007	2.1	841.0	8.84
5/1/1992	16.75	2.6	5/3/1992	14.50	4679	6046	2.48E+007	2.6	870.3	4.83
5/16/1992	11.00	2.8	5/17/1992	9.00	2960	11276	8.41E+006	2.8	915.6	12.22
7/20/1992	10.75	6.4	7/21/1992	6.00	457	4180	3.50E+006	6.4	423.8	24.47
8/5/1992	2.00	8.0	8/6/1992	10.50	3306	7886	1.34E+007	8.0	1291.8	43.07
9/6/1992	13.25	6.8	9/6/1992	21.50	398	4354	2.92E+006	6.8	584.6	18.27
9/23/1992	10.50	6.4	9/23/1992	21.00	349	4045	2.76E+006	6.4	709.1	4.31
6/9/1993	11.25	7.6	6/9/1993	23.00	1348	15038	2.87E+006	7.6	411.4	59.00
6/29/1993	17.00	8.4	6/30/1993	2.50	283	6355	1.42E+006	8.4	193.4	4.30
9/6/1993	17.00	8.9	9/7/1993	6.00	888	4206	6.76E+006	8.9	1051.0	23.36
1/11/1994	0.50	4.3	1/11/1994	19.25	526	4580	3.68E+006	4.3	209.3	4.86
1/23/1994	14.25	6.0	1/24/1994	3.00	1187	14274	2.66E+006	6.0	262.5	6.74
4/10/1994	7.50	3.2	4/10/1994	19.50	244	1237	6.30E+006	3.2	1286.9	7.16
7/2/1994	8.83	3.7	7/2/1994	23.25	354	4266	2.66E+006	3.7	542.9	10.89
11/19/1994	16.17	6.2	11/20/1994	2.50	489	2766	5.66E+006	6.2	1075.5	30.73
12/1/1994	14.75	9.9	12/2/1994	3.75	80	1245	2.06E+006	9.9	238.4	7.96
12/2/1994	11.25	13.3	12/3/1994	15.25	769	3358	7.34E+006	13.3	727.9	13.23
2/25/1995	15.00	2.8	2/26/1995	23.75	3358	6067	1.77E+007	2.8	2496.5	41.62
5/15/1995	18.00	2.8	5/16/1995	2.75	453	5955	2.44E+006	2.8	764.3	10.19
6/10/1995	11.50	1.5	6/10/1995	22.50	198	1949	3.25E+006	1.5	469.0	5.22
6/15/1995	11.50	1.4	6/15/1995	21.25	186	3099	1.93E+006	1.4	386.2	12.88
6/16/1995	12.50	2.0	6/16/1995	23.75	483	3712	4.17E+006	2.0	1132.2	18.87
7/21/1995	17.50	1.5	7/22/1995	4.25	497	3073	5.18E+006	1.5	1035.0	10.71
9/6/1995	3.75	3.9	9/7/1995	2.50	3721	4348	2.74E+007	3.9	2959.4	16.45

Reproduced with permission of the copyright owner. Further reproduction prohibited without permission.

Appendix 8.2. Continued.

Start Date	Start Time hour	End Date	End Time hour	L 6-MXTMJPK ft3/s/min	L 8-SMPKBS ft3/s	L 10-RAIN inches	L 11-INT15 in/min	L 12-SFIVE in/min	L 13-RRISE inches	L 14-RAINFOL inches	16-HYSTER 1=normal 0=reverse
3/28/1992	15.25	3/29/1992	4.00	29.94	1796.1	1.28	0.56	0.0206	1.23	0.05	0
4/19/1992	12.00	4/20/1992	6.00	13.15	693.2	1.11	0.36	0.0128	0.62	0.50	0
4/29/1992	17.25	4/30/1992	16.75	3.74	1217.5	3.11	0.37	0.0093	2.28	0.83	0
5/1/1992	16.75	5/3/1992	14.50	2.15	2072.1	2.26	0.22	0.0045	1.98	0.28	1
5/16/1992	11.00	5/17/1992	9.00	12.22	915.6	0.93	0.39	0.0127	0.86	0.07	0
7/20/1992	10.75	7/21/1992	6.00	1.14	793.5	2.25	0.27	0.0048	1.49	0.76	0
8/5/1992	2.00	8/6/1992	10.50	43.07	1291.8	1.09	0.59	0.0244	0.77	0.32	0
9/6/1992	13.25	9/6/1992	21.50	6.46	1066.7	0.71	0.34	0.0128	0.71	0.00	0
9/23/1992	10.50	9/23/1992	21.00	4.31	744.5	0.91	0.55	0.0054	0.90	0.01	0
6/9/1993	11.25	6/9/1993	23.00	3.93	613.4	0.35	0.07	0.0024	0.26	0.09	1
6/29/1993	17.00	6/30/1993	2.50	4.30	193.4	0.32	0.10	0.0007	0.26	0.06	0
9/6/1993	17.00	9/7/1993	6.00	23.36	1051.0	1.29	0.53	0.0077	0.57	0.72	1
1/11/1994	0.50	1/11/1994	19.25	1.08	557.6	0.53	0.08	0.0007	0.16	0.38	0
1/23/1994	14.25	1/24/1994	3.00	3.50	456.4	0.33	0.02	0.0040	0.30	0.03	1
4/10/1994	7.50	4/10/1994	19.50	7.16	1286.9	0.54	0.54	0.0092	0.54	0.00	1
7/2/1994	8.83	7/2/1994	23.25	6.39	863.2	0.62	0.25	0.0060	0.57	0.05	0
11/19/1994	16.17	11/20/1994	2.50	30.73	1075.5	1.53	0.44	0.0227	1.36	0.17	0
12/1/1994	14.75	12/2/1994	3.75	7.96	238.4	0.47	0.20	0.0010	0.17	0.30	0
12/2/1994	11.25	12/3/1994	15.25	6.07	1225.4	1.10	0.64	0.0007	0.21	0.89	1
2/25/1995	15.00	2/26/1995	23.75	41.62	2496.5	3.90	0.77	0.0005	2.10	1.80	1
5/15/1995	18.00	5/16/1995	2.75	10.19	764.3	1.30	0.50	0.0121	1.07	0.22	0
6/10/1995	11.50	6/10/1995	22.50	5.22	469.0	1.09	0.17	0.0050	0.34	0.75	0
6/15/1995	11.50	6/15/1995	21.25	12.88	593.5	0.74	0.06	0.0040	0.14	0.60	0
6/16/1995	12.50	6/16/1995	23.75	18.87	1132.2	0.39	0.33	0.0110	0.38	0.01	0
7/21/1995	17.50	7/22/1995	4.25	5.76	1159.2	0.51	0.26	0.0015	0.34	0.17	1
9/6/1995	3.75	9/7/1995	2.50	16.45	4120.1	2.91	0.49	0.0067	1.66	1.25	1

Reproduced with permission of the copyright owner. Further reproduction prohibited without permission.

Appendix 8.2. Continued.

Start Date	Start Time hour	End Date	End Time hour	17-RNBTWTI ft3/hour	L 18-PPTBTW in/hour	L 19-INTBET in/hour	L 20-LSPKBTI ft3/s/hour	L 22-SMLSPKBS ft3/s/hour	L 24-QULST ft3/hour	L 26-PPTLSTI in/hour	L 27-INTLST in/hour
3/28/1992	15.25	3/29/1992	4.00	17481	0.00111	0.00006	0.10	0.10	596	0.0004	0.00022
4/19/1992	12.00	4/20/1992	6.00	13951	0.00246	0.00016	0.52	0.54	2649	0.0019	0.00047
4/29/1992	17.25	4/30/1992	16.75	17106	0.00004	0.00010	2.31	3.05	17032	0.0049	0.00159
5/1/1992	16.75	5/3/1992	14.50	23125	0.00036	0.00378	13.79	50.73	514176	0.1296	0.01533
5/16/1992	11.00	5/17/1992	9.00	11581	0.00101	0.00122	0.36	0.41	1640	0.0007	0.00041
7/20/1992	10.75	7/21/1992	6.00	21798	0.00381	0.00087	0.54	0.68	4117	0.0059	0.00113
8/5/1992	2.00	8/6/1992	10.50	37774	0.00506	0.00117	3.92	11.14	99073	0.0180	0.00580
9/6/1992	13.25	9/6/1992	21.50	27984	0.00038	0.00111	1.01	3.80	17501	0.0036	0.00224
9/23/1992	10.50	9/23/1992	21.00	35138	0.00274	0.00007	0.89	2.33	100359	0.0126	0.00220
6/9/1993	11.25	6/9/1993	23.00	32930	0.00004	0.00027	7.17	18.47	130378	0.0361	0.00605
6/29/1993	17.00	6/30/1993	2.50	29401	0.00181	0.00078	2.80	7.44	93552	0.0142	0.00070
9/6/1993	17.00	9/7/1993	6.00	35694	0.00009	0.00015	4.71	15.66	116313	0.0033	0.00082
1/11/1994	0.50	1/11/1994	19.25	20509	0.00065	0.00003	0.14	0.15	482	0.0010	0.00055
1/23/1994	14.25	1/24/1994	3.00	22305	0.00008	0.01017	2.27	5.57	33507	0.0061	0.00271
4/10/1994	7.50	4/10/1994	19.50	12907	0.00203	0.00033	1.91	3.37	13752	0.0058	0.00217
7/2/1994	8.83	7/2/1994	23.25	10887	0.00141	0.00012	2.25	3.46	14931	0.0165	0.00294
11/19/1994	16.17	11/20/1994	2.50	18243	0.00069	0.00001	3.32	3.69	20996	0.0060	0.00161
12/1/1994	14.75	12/2/1994	3.75	41003	0.01192	0.00308	4.53	75.36	629209	0.1813	0.01543
12/2/1994	11.25	12/3/1994	15.25	53485	0.00031	0.01572	6.86	31.79	274893	0.0627	0.02667
2/25/1995	15.00	2/26/1995	23.75	10540	0.00004	0.00368	9.09	14.40	92926	0.0017	0.00098
5/15/1995	18.00	5/16/1995	2.75	10988	0.00612	0.00008	0.79	0.89	3912	0.0044	0.00098
6/10/1995	11.50	6/10/1995	22.50	11249	0.00682	0.00000	1.48	2.19	6641	0.0068	0.00126
6/15/1995	11.50	6/15/1995	21.25	7377	0.00015	0.00000	3.61	4.30	29814	0.0100	0.00159
6/16/1995	12.50	6/16/1995	23.75	9128	0.00017	0.00000	10.73	38.92	126303	0.0243	0.00393
7/21/1995	17.50	7/22/1995	4.25	6189	0.00412	0.00090	1.67	1.90	7861	0.0013	0.00115
9/6/1995	3.75	9/7/1995	2.50	16681	0.00099	0.04273	2.97	19.97	141721	0.0867	0.02493

Reproduced with permission of the copyright owner. Further reproduction prohibited without permission.

Appendix 8.2. Continued.

Start Date	Start Time hour	End Date	End Time hour	L 28-LS75OTI	29-SUM3PPTI	30-QU3EVT
3/28/1992	15.25	3/29/1992	4.00	0.000002	-10.70	7.89
4/19/1992	12.00	4/20/1992	6.00	0.000021	-8.94	10.14
4/29/1992	17.25	4/30/1992	16.75	0.000057	-8.14	11.31
5/1/1992	16.75	5/3/1992	14.50	0.000386	-6.38	12.91
5/16/1992	11.00	5/17/1992	9.00	0.000023	-7.97	11.45
7/20/1992	10.75	7/21/1992	6.00	0.000017	-7.64	10.89
8/5/1992	2.00	8/6/1992	10.50	0.000107	-6.22	14.51
9/6/1992	13.25	9/6/1992	21.50	0.000096	-9.35	13.02
9/23/1992	10.50	9/23/1992	21.00	0.000017	-7.40	12.53
6/9/1993	11.25	6/9/1993	23.00	0.000360	-7.35	13.42
6/29/1993	17.00	6/30/1993	2.50	0.000009	-8.21	11.52
9/6/1993	17.00	9/7/1993	6.00	0.000054	-12.69	13.54
1/11/1994	0.50	1/11/1994	19.25	0.000015	-9.02	9.44
1/23/1994	14.25	1/24/1994	3.00	0.000068	-7.77	11.90
4/10/1994	7.50	4/10/1994	19.50	0.000073	-9.92	9.10
7/2/1994	8.83	7/2/1994	23.25	0.000062	-8.70	9.93
11/19/1994	16.17	11/20/1994	2.50	0.000073	-7.31	12.16
12/1/1994	14.75	12/2/1994	3.75	0.000104	-4.48	14.25
12/2/1994	11.25	12/3/1994	15.25	0.000140	-4.03	14.53
2/25/1995	15.00	2/26/1995	23.75	0.000035	-7.41	14.07
5/15/1995	18.00	5/16/1995	2.75	0.000045	-8.62	9.44
6/10/1995	11.50	6/10/1995	22.50	0.000084	-8.60	12.27
6/15/1995	11.50	6/15/1995	21.25	0.000046	-8.35	4.63
6/16/1995	12.50	6/16/1995	23.75	0.000262	-6.24	12.64
7/21/1995	17.50	7/22/1995	4.25	0.000015	-9.25	10.95
9/6/1995	3.75	9/7/1995	2.50	0.000560	-5.26	14.10

**to eliminate zero values a value of 0.001 was added to RFOL, and a value of 0.00004 was added to PPTBTW.

Appendix 8.3. Pearson correlation matrix for the entire runoff event using quickflow characteristics of the entire runoff event, Rio Piedras at El Senorial.

	LGSED	LGQU_SEDCONC	LGQUICK	BASE
LGSED	1.000			
LGQU_SEDCONC	0.734	1.000		
LGQUICK	0.784	0.153	1.000	
BASE	-0.163	-0.068	-0.176	1.000
LGPKBS	0.572	0.057	0.779	-0.286
LGMXTMJPK	0.260	0.071	0.313	-0.039
LGMXTRP	0.375	0.293	0.277	0.158
LGSMPKBS	0.664	0.116	0.859	-0.288
LGRAIN	0.552	0.092	0.718	-0.205
LGINT15	0.369	-0.019	0.554	0.085
LGSFIVE	0.278	0.253	0.172	-0.184
LGRRISE	0.516	0.241	0.530	-0.164
LGRFOL	0.288	0.080	0.346	-0.061
HYSTER	0.173	-0.042	0.290	0.201
RNBTWTI	-0.052	-0.039	-0.040	0.934
LGPPTBTW	-0.399	-0.363	-0.249	0.023
LGINTBET	0.399	0.183	0.413	0.453
LGLSPKBTI	-0.019	-0.278	0.226	0.207
LGSMLSPKBSTI	-0.073	-0.332	0.198	0.375
LGQULST	-0.055	-0.279	0.175	0.457
LGPPTLSTI	-0.184	-0.351	0.054	0.396
LGINTLST	-0.025	-0.333	0.268	0.387
LGLS75OTI	0.044	-0.255	0.298	0.117
SUM3PPTI	0.025	-0.166	0.189	0.314
QU3EVT	0.219	-0.061	0.374	0.533

	LGPKBS	LGMXTMJPK	LGMXTRP	LGSMPKBS	LGRAIN
LGPKBS	1.000				
LGMXTMJPK	0.657	1.000			
LGMXTRP	0.477	0.582	1.000		
LGSMPKBS	0.905	0.388	0.420	1.000	
LGRAIN	0.620	0.235	0.259	0.677	1.000
LGINT15	0.775	0.543	0.283	0.630	0.561
LGSFIVE	0.326	0.303	0.214	0.265	0.277
LGRRISE	0.484	0.065	0.108	0.513	0.702
LGRFOL	0.142	0.148	0.223	0.169	0.521
HYSTER	0.309	0.104	0.239	0.323	-0.030
RNBTWTI	-0.242	-0.112	0.058	-0.207	-0.123
LGPPTBTW	-0.123	-0.061	-0.312	-0.270	-0.119
LGINTBET	0.164	-0.088	0.063	0.263	0.159
LGLSPKBTI	0.140	0.194	0.166	0.125	0.032
LGSMLSPKBSTI	0.081	0.154	0.099	0.072	-0.032
LGQULST	0.061	0.126	0.050	0.044	-0.007
LGPPTLSTI	-0.129	-0.139	-0.116	-0.062	-0.063
LGINTLST	0.071	-0.081	0.001	0.197	0.022
LGLS75OTI	0.136	0.018	0.120	0.242	0.055
SUM3PPTI	-0.023	-0.050	-0.003	0.037	0.080
QU3EVT	0.198	0.114	0.209	0.169	0.160

Reproduced with permission of the copyright owner. Further reproduction prohibited without permission.

Appendix 8.3. Continued.

	LGINT15	LGSFIVE	LGRRISE	LGRFOL	HYSTER
LGINT15	1.000				
LGSFIVE	0.347	1.000			
LGRRISE	0.531	0.684	1.000		
LGRFOL	-0.007	-0.301	-0.033	1.000	
HYSTER	0.155	-0.293	-0.195	0.051	1.000
RNBTWTI	0.089	-0.160	-0.085	-0.050	0.140
LGPPTBTW	0.126	0.207	0.133	-0.159	-0.395
LGINTBET	0.323	-0.124	0.284	-0.055	0.478
LGLSPKBTI	-0.007	-0.349	-0.196	0.252	0.367
LGSMLSPKBSTI	0.017	-0.372	-0.199	0.171	0.349
LGQULST	0.047	-0.345	-0.128	0.129	0.308
LGPPTLSTI	-0.141	-0.250	-0.073	0.120	0.069
LGINTLST	0.029	-0.220	-0.038	0.096	0.282
LGLS75OTI	-0.040	-0.067	-0.033	0.128	0.278
SUM3PPTI	0.016	-0.352	-0.085	0.290	-0.014
QU3EVT	0.353	-0.212	0.100	0.165	0.313

	RNBTWTI	LGPPTBTW	LGINTBET	LGLSPKBTI
RNBTWTI	1.000			
LGPPTBTW	-0.008	1.000		
LGINTBET	0.432	-0.010	1.000	
LGLSPKBTI	0.237	-0.394	0.147	1.000
LGSMLSPKBSTI	0.424	-0.280	0.289	0.943
LGQULST	0.534	-0.242	0.328	0.890
LGPPTLSTI	0.476	0.034	0.247	0.706
LGINTLST	0.481	-0.057	0.416	0.681
LGLS75OTI	0.186	-0.267	0.177	0.739
SUM3PPTI	0.363	0.080	0.352	0.464
QU3EVT	0.581	-0.086	0.562	0.510

	LGQULST	LGPPTLSTI	LGINTLST	LGLS75OTI	SUM3PPTI
LGQULST	1.000				
LGPPTLSTI	0.835	1.000			
LGINTLST	0.787	0.912	1.000		
LGLS75OTI	0.666	0.751	0.822	1.000	
SUM3PPTI	0.570	0.729	0.768	0.535	1.000
QU3EVT	0.634	0.468	0.559	0.523	0.495

	QU3EVT
QU3EVT	1.000

Reproduced with permission of the copyright owner. Further reproduction prohibited without permission.

Appendix 8.4. Results of principal component analysis on the independent variables using quickflow characteristics for the entire event.

Component loadings

	1	2	3	4	5
LGQUICK	0.429	0.778	-0.011	-0.285	-0.094
BASE	0.478	-0.404	0.648	0.067	0.338
LGPKBS	0.227	0.921	-0.029	0.108	0.057
LGMXTMJPK	0.118	0.561	0.009	0.521	0.315
LGMXTRP	0.194	0.482	0.065	0.280	0.519
LGSMPKBS	0.283	0.876	-0.101	-0.114	0.001
LGRAIN	0.168	0.771	0.118	-0.266	-0.281
LGINT15	0.140	0.710	0.436	0.231	-0.100
LGSFIVE	-0.255	0.485	0.004	0.614	-0.116
LGRRISE	0.067	0.821	0.133	-0.076	-0.222
LGRFOL	0.179	0.158	-0.033	-0.432	-0.200
HYSTER	0.554	0.145	-0.233	-0.482	0.380
RNBTWTI	0.549	-0.366	0.616	0.028	0.223
LGPPTBTW	-0.258	-0.139	0.494	0.233	-0.566
LGINTBET	0.527	0.094	0.455	-0.448	0.094
LGLSPKBTI	0.830	-0.070	-0.403	0.139	0.093
LGSMLSPKBSTI	0.914	-0.168	-0.220	0.169	0.049
LGQULST	0.906	-0.188	-0.096	0.147	0.037
LGPPTLSTI	0.813	-0.339	-0.078	0.178	-0.352
LGINTLST	0.891	-0.166	-0.053	0.075	-0.260
LGLS75OTI	0.781	-0.027	-0.375	0.192	-0.160
SUM3PPTI	0.687	-0.179	0.106	0.025	-0.431
QU3EVT	0.767	0.054	0.347	-0.001	0.086

	6
LGQUICK	-0.058
BASE	0.085
LGPKBS	-0.077
LGMXTMJPK	0.308
LGMXTRP	0.295
LGSMPKBS	-0.191
LGRAIN	0.261
LGINT15	0.026
LGSFIVE	-0.251
LGRRISE	-0.139
LGRFOL	0.787
HYSTER	-0.263
RNBTWTI	0.030
LGPPTBTW	-0.035
LGINTBET	-0.340
LGLSPKBTI	0.133
LGSMLSPKBSTI	0.041
LGQULST	0.042
LGPPTLSTI	0.000
LGINTLST	-0.137
LGLS75OTI	-0.152
SUM3PPTI	0.167
QU3EVT	-0.054

Reproduced with permission of the copyright owner. Further reproduction prohibited without permission.

Appendix 8.5. Results of principal component analysis on the independent variables without quickflow characteristics for the entire event.

Component loadings

	1	2	3	4	5
BASE	0.535	-0.315	-0.647	-0.036	0.350
LGPKBS	0.095	0.947	0.033	0.028	0.050
LGMXTMJPK	0.047	0.615	-0.001	0.341	0.436
LGMXTRP	0.132	0.545	-0.059	0.040	0.543
LGSMPKBS	0.152	0.889	0.102	-0.153	-0.069
LGRAIN	0.052	0.768	-0.119	-0.217	-0.403
LGINT15	0.042	0.742	-0.432	0.204	-0.054
LGSFIVE	-0.315	0.475	0.003	0.609	0.095
LGRRISE	-0.051	0.818	-0.132	-0.050	-0.274
LGRFOL	0.148	0.150	0.029	-0.373	-0.365
HYSTER	0.522	0.193	0.230	-0.596	0.187
RNBTWTI	0.596	-0.282	-0.616	-0.027	0.235
LGPPTBTW	-0.233	-0.166	-0.494	0.426	-0.443
LGINTBET	0.501	0.136	-0.459	-0.455	-0.062
LGLSPKBTI	0.835	0.064	0.406	0.071	0.112
LGSMLSPKBSTI	0.932	-0.022	0.222	0.126	0.090
LGQULST	0.927	-0.043	0.098	0.109	0.071
LGPPTLSTI	0.855	-0.213	0.080	0.284	-0.273
LGINTLST	0.904	-0.042	0.054	0.156	-0.220
LGLS75OTI	0.778	0.088	0.377	0.225	-0.091
SUM3PPTI	0.703	-0.087	-0.106	0.163	-0.403
QU3EVT	0.751	0.161	-0.346	-0.043	0.071

	6
BASE	0.098
LGPKBS	-0.086
LGMXTMJPK	0.329
LGMXTRP	0.308
LGSMPKBS	-0.208
LGRAIN	0.228
LGINT15	0.020
LGSFIVE	-0.228
LGRRISE	-0.164
LGRFOL	0.761
HYSTER	-0.282
RNBTWTI	0.042
LGPPTBTW	-0.034
LGINTBET	-0.362
LGLSPKBTI	0.133
LGSMLSPKBSTI	0.044
LGQULST	0.044
LGPPTLSTI	-0.000
LGINTLST	-0.140
LGLS75OTI	-0.149
SUM3PPTI	0.160
QU3EVT	-0.057

Reproduced with permission of the copyright owner. Further reproduction prohibited without permission.

Appendix 8.6. Results of principal component analysis on the independent variables after varimax rotation for the entire event.

Rotated Loading Matrix (VARIMAX, Gamma = 1.0000)

	1	2	3	4	5	6
LGQUICK	0.182	0.873	0.034	0.036	0.249	0.150
BASE	0.213	-0.274	0.891	0.146	-0.048	0.026
LGPKBS	0.050	0.854	-0.098	0.390	0.128	-0.103
LGMXTMJPK	0.044	0.309	-0.049	0.831	-0.040	-0.033
LGMXTRP	-0.016	0.258	0.147	0.760	0.204	0.043
LGSMPKBS	0.084	0.889	-0.102	0.157	0.264	-0.077
LGRAIN	-0.019	0.814	-0.049	0.078	-0.060	0.422
LGINT15	-0.044	0.713	0.209	0.353	-0.311	-0.052
LGSFIVE	-0.110	0.348	-0.307	0.359	-0.369	-0.511
LGRRISE	-0.084	0.865	-0.070	0.056	-0.077	-0.031
LGRFOL	0.076	0.157	-0.037	0.049	0.020	0.932
HYSTER	0.278	0.255	0.222	-0.140	0.786	-0.007
RNBTWTI	0.299	-0.184	0.858	0.053	-0.061	0.025
LGPPTBTW	-0.113	-0.005	0.107	-0.232	-0.790	-0.063
LGINTBET	0.156	0.383	0.689	-0.327	0.255	-0.037
LGLSPKBTI	0.848	-0.018	0.014	0.221	0.350	0.104
LGSMLSPKBSTI	0.905	-0.039	0.203	0.145	0.247	0.027
LGQULST	0.864	-0.033	0.304	0.117	0.187	0.042
LGPPTLSTI	0.928	-0.091	0.180	-0.144	-0.120	0.052
LGINTLST	0.902	0.106	0.255	-0.159	0.033	-0.024
LGLS75OTI	0.879	0.118	-0.062	0.002	0.181	-0.123
SUM3PPTI	0.719	0.070	0.236	-0.157	-0.229	0.272
QU3EVT	0.520	0.253	0.611	0.080	0.084	0.013

Reproduced with permission of the copyright owner. Further reproduction prohibited without permission.

Appendix 8.7. Results of PCA analysis after varimax rotation on quickflow characteristics of the entire event without quickflow.

Rotated Loading Matrix (VARIMAX, Gamma = 1.0000)

	1	2	3	4	5	6
BASE	0.206	-0.268	0.894	-0.053	0.143	0.017
LGPKBS	0.063	0.854	-0.099	0.164	0.378	-0.078
LGMXTMJPK	0.046	0.321	-0.043	-0.038	0.828	-0.030
LGMXTRP	-0.015	0.268	0.150	0.211	0.753	0.051
LGSMPKBS	0.099	0.870	-0.107	0.303	0.150	-0.052
LGRAIN	-0.005	0.812	-0.051	-0.018	0.061	0.449
LGINT15	-0.033	0.744	0.213	-0.273	0.329	-0.030
LGSFIVE	-0.104	0.381	-0.301	-0.362	0.353	-0.506
LGRRISE	-0.069	0.884	-0.072	-0.027	0.031	0.001
LGRFOL	0.079	0.119	-0.037	0.021	0.058	0.934
HYSTER	0.282	0.210	0.212	0.803	-0.135	0.004
RNBTWTI	0.294	-0.194	0.860	-0.067	0.056	0.015
LGPPTBTW	-0.112	0.039	0.113	-0.783	-0.248	-0.062
LGINTBET	0.162	0.365	0.682	0.287	-0.337	-0.021
LGLSPKBTI	0.847	-0.043	0.014	0.348	0.225	0.104
LGSMLSPKBSTI	0.903	-0.061	0.203	0.246	0.149	0.026
LGQULST	0.862	-0.050	0.305	0.190	0.117	0.042
LGPPTLSTI	0.926	-0.101	0.181	-0.119	-0.144	0.050
LGINTLST	0.904	0.084	0.254	0.042	-0.156	-0.021
LGLS75OTI	0.880	0.093	-0.063	0.184	0.010	-0.120
SUM3PPTI	0.721	0.054	0.238	-0.224	-0.156	0.273
QU3EVT	0.522	0.239	0.611	0.101	0.076	0.020

Reproduced with permission of the copyright owner. Further reproduction prohibited without permission.

Reproduced with permission of the copyright owner. Further reproduction prohibited without permission.

Appendix 8.8. Summary of dependent and independent variables used in the statistical analysis for runoff characteristics of the entire event at Rio Piedras at El Senorial
(D indicates dependent variable; L indicates log transformed)

Start Date	Start Time hour	Start Discharge ft3/s	End Date	End Time hour	DL Suspended-sediment load tons	DL Discharge-weighted sediment concentration mg/L	L 2-RUN	3-BASE	L 5-PK	L 7-MXTRP
3/28/1992	15.25	3.5	3/29/1992	4.00	4302	18221	7.56E+006	3.5	1800	29.94
4/19/1992	12.00	4.1	4/20/1992	6.00	2051	15405	4.26E+006	4.1	596	13.15
4/29/1992	17.25	2.1	4/30/1992	16.75	3696	9273	1.28E+007	2.1	844	8.84
5/1/1992	16.75	2.6	5/3/1992	14.50	4679	5807	2.58E+007	2.6	874	4.83
5/16/1992	11.00	2.8	5/17/1992	9.00	2960	10495	9.04E+006	2.8	919	12.22
7/20/1992	10.75	6.4	7/21/1992	6.00	457	3367	4.35E+006	6.4	434	24.47
8/5/1992	2.00	8.0	8/6/1992	10.50	3306	6931	1.53E+007	8.0	1300	43.07
9/6/1992	13.25	6.8	9/6/1992	21.50	398	3906	3.26E+006	6.8	593	18.27
9/23/1992	10.50	6.4	9/23/1992	21.00	349	3507	3.19E+006	6.4	718	4.31
6/9/1993	11.25	7.6	6/9/1993	23.00	1348	12974	3.33E+006	7.6	420	59.00
6/29/1993	17.00	8.4	6/30/1993	2.50	283	5140	1.76E+006	8.4	202	4.30
9/6/1993	17.00	8.9	9/7/1993	6.00	888	3935	7.23E+006	8.9	1060	23.36
1/11/1994	0.50	4.3	1/11/1994	19.25	526	4065	4.15E+006	4.3	214	4.86
1/23/1994	14.25	6.0	1/24/1994	3.00	1187	12657	3.00E+006	6.0	269	6.74
4/10/1994	7.50	3.2	4/10/1994	19.50	244	1187	6.57E+006	3.2	1292	7.16
7/2/1994	8.83	3.7	7/2/1994	23.25	354	3930	2.89E+006	3.7	547	10.89
11/19/1994	16.17	6.2	11/20/1994	2.50	489	2635	5.94E+006	6.2	1082	30.73
12/1/1994	14.75	9.9	12/2/1994	3.75	80	944	2.72E+006	9.9	249	7.96
12/2/1994	11.25	13.3	12/3/1994	15.25	769	2721	9.06E+006	13.3	742	13.23
2/25/1995	15.00	2.8	2/26/1995	23.75	3358	5811	1.85E+007	2.8	2500	41.62
5/15/1995	18.00	2.8	5/16/1995	2.75	453	5708	2.54E+006	2.8	767	10.19
6/10/1995	11.50	1.5	6/10/1995	22.50	198	1870	3.39E+006	1.5	471	5.22
6/15/1995	11.50	1.4	6/15/1995	21.25	186	2942	2.03E+006	1.4	388	12.88
6/16/1995	12.50	2.0	6/16/1995	23.75	483	3611	4.29E+006	2.0	1134	18.87
7/21/1995	17.50	1.5	7/22/1995	4.25	497	2959	5.38E+006	1.5	1039	10.71
9/6/1995	3.75	3.9	9/7/1995	2.50	3721	4236	2.81E+007	3.9	2965	16.45

Reproduced with permission of the copyright owner. Further reproduction prohibited without permission.

Appendix 8.8. Continued.

Start Date	Start Time hour	End Date	End Time hour	L 6-MXTMJPK	L 9-SMPK	L 10-RAIN	L 11-INT15	L 12-SFIVE	L 13-RRISE	L 14-RAINFOL
3/28/1992	15.25	3/29/1992	4.00	29.94	1800	1.28	0.56	0.0206	1.23	0.05
4/19/1992	12.00	4/20/1992	6.00	13.15	703	1.11	0.36	0.0128	0.62	0.50
4/29/1992	17.25	4/30/1992	16.75	3.74	1223	3.11	0.37	0.0093	2.28	0.83
5/1/1992	16.75	5/3/1992	14.50	2.15	2082	2.26	0.22	0.0045	1.98	0.28
5/16/1992	11.00	5/17/1992	9.00	12.22	919	0.93	0.39	0.0127	0.86	0.07
7/20/1992	10.75	7/21/1992	6.00	1.14	829	2.25	0.27	0.0048	1.49	0.76
8/5/1992	2.00	8/6/1992	10.50	43.07	1300	1.09	0.59	0.0244	0.77	0.32
9/6/1992	13.25	9/6/1992	21.50	6.46	1083	0.71	0.34	0.0128	0.71	0.00
9/23/1992	10.50	9/23/1992	21.00	4.31	760	0.91	0.55	0.0054	0.90	0.01
6/9/1993	11.25	6/9/1993	23.00	3.93	630	0.35	0.07	0.0024	0.26	0.09
6/29/1993	17.00	6/30/1993	2.50	4.30	202	0.32	0.10	0.0007	0.26	0.06
9/6/1993	17.00	9/7/1993	6.00	23.36	1060	1.29	0.53	0.0077	0.57	0.72
1/11/1994	0.50	1/11/1994	19.25	1.08	576	0.53	0.08	0.0007	0.16	0.38
1/23/1994	14.25	1/24/1994	3.00	3.50	469	0.33	0.02	0.0040	0.30	0.03
4/10/1994	7.50	4/10/1994	19.50	7.16	1292	0.54	0.54	0.0092	0.54	0.00
7/2/1994	8.83	7/2/1994	23.25	6.39	875	0.62	0.25	0.0060	0.57	0.05
11/19/1994	16.17	11/20/1994	2.50	30.73	1082	1.53	0.44	0.0227	1.36	0.17
12/1/1994	14.75	12/2/1994	3.75	7.96	249	0.47	0.20	0.0010	0.17	0.30
12/2/1994	11.25	12/3/1994	15.25	6.07	1268	1.10	0.64	0.0007	0.21	0.89
2/25/1995	15.00	2/26/1995	23.75	41.62	2500	3.90	0.77	0.0005	2.10	1.80
5/15/1995	18.00	5/16/1995	2.75	10.19	767	1.30	0.50	0.0121	1.07	0.22
6/10/1995	11.50	6/10/1995	22.50	5.22	471	1.09	0.17	0.0050	0.34	0.75
6/15/1995	11.50	6/15/1995	21.25	12.88	597	0.74	0.06	0.0040	0.14	0.60
6/16/1995	12.50	6/16/1995	23.75	18.87	1134	0.39	0.33	0.0110	0.38	0.01
7/21/1995	17.50	7/22/1995	4.25	5.76	1165	0.51	0.26	0.0015	0.34	0.17
9/6/1995	3.75	9/7/1995	2.50	16.45	4132	2.91	0.49	0.0067	1.66	1.25

Reproduced with permission of the copyright owner. Further reproduction prohibited without permission.

Appendix 8.8. Continued.

Start Date	Start Time hour	End Date	End Time hour	16-HYSTER 1=normal 0=reverse	17-RNBTWTI	L 18-PPTBTW	L 19-INTBET	L 21-LSPKTI	L 23-SMLSPK	L 25-RULST
3/28/1992	15.25	3/29/1992	4.00	0	17481	0.00111	0.00006	0.11	0.11	1166
4/19/1992	12.00	4/20/1992	6.00	0	13951	0.00246	0.00016	0.53	0.55	3192
4/29/1992	17.25	4/30/1992	16.75	0	17106	0.00004	0.00010	2.32	3.09	18765
5/1/1992	16.75	5/3/1992	14.50	1	23125	0.00036	0.00378	13.84	50.96	531977
5/16/1992	11.00	5/17/1992	9.00	0	11581	0.00101	0.00122	0.38	0.44	2091
7/20/1992	10.75	7/21/1992	6.00	0	21798	0.00381	0.00087	0.59	0.74	5968
8/5/1992	2.00	8/6/1992	10.50	0	37774	0.00506	0.00117	3.99	11.34	107047
9/6/1992	13.25	9/6/1992	21.50	0	27984	0.00038	0.00111	1.05	4.02	22497
9/23/1992	10.50	9/23/1992	21.00	0	35138	0.00274	0.00007	0.95	2.51	115694
6/9/1993	11.25	6/9/1993	23.00	1	32930	0.00004	0.00027	7.40	19.04	154158
6/29/1993	17.00	6/30/1993	2.50	0	29401	0.00181	0.00078	2.83	7.60	103219
9/6/1993	17.00	9/7/1993	6.00	1	35694	0.00009	0.00015	4.86	16.16	150616
1/11/1994	0.50	1/11/1994	19.25	0	20509	0.00065	0.00003	0.16	0.16	706
1/23/1994	14.25	1/24/1994	3.00	1	22305	0.00008	0.01017	2.42	5.93	47596
4/10/1994	7.50	4/10/1994	19.50	1	12907	0.00203	0.00033	1.94	3.45	15312
7/2/1994	8.83	7/2/1994	23.25	0	10887	0.00141	0.00012	2.30	3.53	17574
11/19/1994	16.17	11/20/1994	2.50	0	18243	0.00069	0.00001	3.35	3.73	23295
12/1/1994	14.75	12/2/1994	3.75	0	41003	0.01192	0.00308	4.74	81.14	812104
12/2/1994	11.25	12/3/1994	15.25	1	53485	0.00031	0.01572	7.16	33.15	362386
2/25/1995	15.00	2/26/1995	23.75	1	10540	0.00004	0.00368	9.14	14.48	97647
5/15/1995	18.00	5/16/1995	2.75	0	10988	0.00612	0.00008	0.80	0.90	4414
6/10/1995	11.50	6/10/1995	22.50	0	11249	0.00682	0.00000	1.51	2.24	7619
6/15/1995	11.50	6/15/1995	21.25	0	7377	0.00015	0.00000	3.62	4.32	31079
6/16/1995	12.50	6/16/1995	23.75	0	9128	0.00017	0.00000	10.77	39.17	133017
7/21/1995	17.50	7/22/1995	4.25	1	6189	0.00412	0.00090	1.69	1.91	8484
9/6/1995	3.75	9/7/1995	2.50	1	16681	0.00099	0.04273	3.12	20.99	182621

Reproduced with permission of the copyright owner. Further reproduction prohibited without permission.

Appendix 8.8. Continued.

Start Date	Start Time hour	End Date	End Time hour	L 26-PPTLSTI	L 27-INTLST	L 28-LS75OTI	29-SUM3PPTI	31-RU3EVT
3/28/1992	15.25	3/29/1992	4.00	0.0004	0.00022	0.000002	-10.70	8.77
4/19/1992	12.00	4/20/1992	6.00	0.0019	0.00047	0.000021	-8.94	10.53
4/29/1992	17.25	4/30/1992	16.75	0.0049	0.00159	0.000057	-8.14	11.45
5/1/1992	16.75	5/3/1992	14.50	0.1296	0.01533	0.000386	-6.38	13.05
5/16/1992	11.00	5/17/1992	9.00	0.0007	0.00041	0.000023	-7.97	11.73
7/20/1992	10.75	7/21/1992	6.00	0.0059	0.00113	0.000017	-7.64	11.36
8/5/1992	2.00	8/6/1992	10.50	0.0180	0.00580	0.000107	-6.22	14.69
9/6/1992	13.25	9/6/1992	21.50	0.0036	0.00224	0.000096	-9.35	13.27
9/23/1992	10.50	9/23/1992	21.00	0.0126	0.00220	0.000017	-7.40	12.75
6/9/1993	11.25	6/9/1993	23.00	0.0361	0.00605	0.000360	-7.35	13.74
6/29/1993	17.00	6/30/1993	2.50	0.0142	0.00070	0.000009	-8.21	11.84
9/6/1993	17.00	9/7/1993	6.00	0.0033	0.00082	0.000054	-12.69	13.88
1/11/1994	0.50	1/11/1994	19.25	0.0010	0.00055	0.000015	-9.02	9.81
1/23/1994	14.25	1/24/1994	3.00	0.0061	0.00271	0.000068	-7.77	12.29
4/10/1994	7.50	4/10/1994	19.50	0.0058	0.00217	0.000073	-9.92	9.38
7/2/1994	8.83	7/2/1994	23.25	0.0165	0.00294	0.000062	-8.70	10.13
11/19/1994	16.17	11/20/1994	2.50	0.0060	0.00161	0.000073	-7.31	12.35
12/1/1994	14.75	12/2/1994	3.75	0.1813	0.01543	0.000104	-4.48	14.79
12/2/1994	11.25	12/3/1994	15.25	0.0627	0.02667	0.000140	-4.03	15.10
2/25/1995	15.00	2/26/1995	23.75	0.0017	0.00098	0.000035	-7.41	14.18
5/15/1995	18.00	5/16/1995	2.75	0.0044	0.00098	0.000045	-8.62	9.60
6/10/1995	11.50	6/10/1995	22.50	0.0068	0.00126	0.000084	-8.60	12.38
6/15/1995	11.50	6/15/1995	21.25	0.0100	0.00159	0.000046	-8.35	4.65
6/16/1995	12.50	6/16/1995	23.75	0.0243	0.00393	0.000262	-6.24	12.74
7/21/1995	17.50	7/22/1995	4.25	0.0013	0.00115	0.000015	-9.25	11.05
9/6/1995	3.75	9/7/1995	2.50	0.0867	0.02493	0.000560	-5.26	14.24

**to eliminate zero values a value of 0.001 was added to RFOL, and a value of 0.00004 was added to PPTBTW.

Appendix 8.9. Pearson correlation matrix for the entire runoff event using runoff characteristics of the entire runoff event, Rio Piedras at El Senorial.

	LGSED	LGRU_SEDCONC	BASE	LGRUN
LGSED	1.000			
LGRU_SEDCONC	0.759	1.000		
BASE	-0.165	-0.144	1.000	
LGRUN	0.779	0.183	-0.110	1.000
LGPK	0.571	0.115	-0.277	0.752
LGLSPKTI	-0.018	-0.275	0.217	0.238
RNBTWTI	-0.052	-0.108	0.934	0.026
LGRULST	-0.045	-0.290	0.492	0.211
RU3EVT	0.224	-0.072	0.573	0.407
HYSTER	0.173	-0.034	0.200	0.293
LGMXTMJPK	0.260	0.107	-0.036	0.290
LGMXTRP	0.375	0.299	0.160	0.279
LGSUMPK	0.665	0.172	-0.277	0.838
LGSMLSPK	-0.074	-0.347	0.385	0.222
LGTOTRAIN	0.552	0.125	-0.204	0.713
LGINT15	0.369	0.005	0.087	0.553
LGSFIVE	0.278	0.285	-0.182	0.145
LGRRISE	0.516	0.264	-0.163	0.525
LGRFALL	0.288	0.085	-0.063	0.354
LGLSTPPTI	-0.184	-0.381	0.397	0.090
SUM3PPTI	0.025	-0.202	0.314	0.233
LGLSTINT	-0.025	-0.353	0.388	0.302
LGLST75OTI	0.044	-0.244	0.118	0.302
LGPPTBTW	-0.399	-0.382	0.023	-0.234
LGINTBET	0.399	0.147	0.453	0.461

	LGPK	LGLSPKTI	RNBTWTI	LGRULST	RU3EVT
LGPK	1.000				
LGLSPKTI	0.138	1.000			
RNBTWTI	-0.235	0.247	1.000		
LGRULST	0.062	0.874	0.567	1.000	
RU3EVT	0.190	0.480	0.618	0.630	1.000
HYSTER	0.311	0.371	0.140	0.318	0.314
LGMXTMJPK	0.658	0.189	-0.112	0.121	0.108
LGMXTRP	0.479	0.167	0.058	0.060	0.218
LGSUMPK	0.901	0.126	-0.197	0.049	0.162
LGSMLSPK	0.081	0.942	0.433	0.961	0.615
LGTOTRAIN	0.620	0.031	-0.123	-0.009	0.149
LGINT15	0.777	-0.009	0.089	0.052	0.361
LGSFIVE	0.322	-0.355	-0.160	-0.345	-0.210
LGRRISE	0.484	-0.199	-0.085	-0.125	0.101
LGRFALL	0.142	0.254	-0.050	0.124	0.152
LGLSTPPTI	-0.126	0.711	0.476	0.836	0.455
SUM3PPTI	-0.019	0.470	0.363	0.572	0.489
LGLSTINT	0.074	0.687	0.481	0.793	0.547
LGLST75OTI	0.135	0.742	0.186	0.653	0.486
LGPPTBTW	-0.122	-0.398	-0.008	-0.244	-0.075
LGINTBET	0.171	0.155	0.432	0.353	0.584

Reproduced with permission of the copyright owner. Further reproduction prohibited without permission.

Appendix 8.9. Continued.

	HYSTER	LGMXTMJPK	LGMXTRP	LGSUMPK	LGSMLSPK
HYSTER	1.000				
LGMXTMJPK	0.104	1.000			
LGMXTRP	0.239	0.582	1.000		
LGSUMPK	0.327	0.381	0.421	1.000	
LGSMLSPK	0.350	0.149	0.097	0.072	1.000
LGTOTRAIN	-0.030	0.235	0.259	0.678	-0.035
LGINT15	0.155	0.543	0.283	0.630	0.016
LGSFIVE	-0.293	0.303	0.214	0.259	-0.376
LGRRISE	-0.195	0.065	0.108	0.513	-0.200
LGRFALL	0.051	0.148	0.223	0.170	0.169
LGLSTPPTI	0.069	-0.139	-0.116	-0.056	0.827
SUM3PPTI	-0.014	-0.050	-0.003	0.043	0.565
LGLSTINT	0.282	-0.081	0.001	0.203	0.808
LGLST75OTI	0.278	0.018	0.120	0.243	0.768
LGPPTBTW	-0.395	-0.061	-0.312	-0.270	-0.279
LGINTBET	0.478	-0.088	0.063	0.273	0.295

	LGTOTRAIN	LGINT15	LGSFIVE	LGRRISE	LGRFALL
LGTOTRAIN	1.000				
LGINT15	0.561	1.000			
LGSFIVE	0.277	0.347	1.000		
LGRRISE	0.702	0.531	0.684	1.000	
LGRFALL	0.521	-0.007	-0.301	-0.033	1.000
LGLSTPPTI	-0.063	-0.141	-0.250	-0.073	0.120
SUM3PPTI	0.080	0.016	-0.352	-0.085	0.290
LGLSTINT	0.022	0.029	-0.220	-0.038	0.096
LGLST75OTI	0.055	-0.040	-0.067	-0.033	0.128
LGPPTBTW	-0.119	0.126	0.207	0.133	-0.159
LGINTBET	0.159	0.323	-0.124	0.284	-0.055

	LGLSTPPTI	SUM3PPTI	LGLSTINT	LGLST75OTI	LGPPTBTW
LGLSTPPTI	1.000				
SUM3PPTI	0.729	1.000			
LGLSTINT	0.912	0.768	1.000		
LGLST75OTI	0.751	0.535	0.822	1.000	
LGPPTBTW	0.034	0.080	-0.057	-0.267	1.000
LGINTBET	0.247	0.352	0.416	0.177	-0.010

	LGINTBET
LGINTBET	1.000

Reproduced with permission of the copyright owner. Further reproduction prohibited without permission.

Appendix 8.10. Results of principal component analysis on the independent variables using runoff characteristics for the entire event.

Component loadings

	1	2	3	4	5
BASE	0.494	-0.393	-0.645	0.097	0.320
LGRUN	0.470	0.746	-0.032	-0.298	-0.090
LGPK	0.230	0.918	0.042	0.113	0.056
LGLSPKTI	0.824	-0.080	0.414	0.130	0.094
RNBTWTI	0.564	-0.357	-0.613	0.052	0.208
LGRULST	0.908	-0.195	0.079	0.140	0.048
RU3EVT	0.760	0.047	-0.389	0.005	0.101
HYSTER	0.555	0.142	0.228	-0.470	0.394
LGMXTMJPK	0.115	0.559	0.008	0.530	0.299
LGMXTRP	0.197	0.485	-0.050	0.296	0.506
LGSUMPK	0.290	0.871	0.110	-0.117	0.004
LGSMLSPK	0.910	-0.177	0.228	0.167	0.045
LGTOTRAIN	0.169	0.774	-0.102	-0.268	-0.278
LGINT15	0.143	0.716	-0.416	0.240	-0.114
LGSFIVE	-0.259	0.482	0.014	0.612	-0.129
LGRRISE	0.068	0.824	-0.118	-0.076	-0.220
LGRFALL	0.180	0.160	0.036	-0.439	-0.194
LGLSTPPTI	0.810	-0.341	0.101	0.173	-0.360
SUM3PPTI	0.688	-0.176	-0.084	0.021	-0.440
LGLSTINT	0.890	-0.168	0.077	0.076	-0.267
LGLST75OTI	0.771	-0.034	0.398	0.187	-0.163
LGPPTBTW	-0.255	-0.133	-0.487	0.228	-0.579
LGINTBET	0.540	0.102	-0.456	-0.429	0.095

Reproduced with permission of the copyright owner. Further reproduction prohibited without permission.

Appendix 8.10. Continued.

	6
BASE	-0.091
LGRUN	0.049
LGPK	0.079
LGLSPKTI	-0.130
RNBTWTI	-0.037
LGRULST	-0.037
RU3EVT	0.050
HYSTER	0.264
LGMXTMJPK	-0.311
LGMXTRP	-0.299
LGSUMPK	0.194
LGSMLSPK	-0.038
LGTOTRAIN	-0.256
LGINT15	-0.026
LGSFIVE	0.249
LGRRISE	0.144
LGRFALL	-0.784
LGLSTPPTI	0.000
SUM3PPTI	-0.167
LGLSTINT	0.136
LGLST75OTI	0.151
LGPPTBTW	0.035
LGINTBET	0.339

Reproduced with permission of the copyright owner. Further reproduction prohibited without permission.

Appendix 8.11. Results of principal component analysis on the independent variables using runoff characteristics for the entire event with the variable runoff.

Component loadings

	1	2	3	4	5
BASE	0.550	-0.304	0.649	-0.038	0.327
LGPK	0.094	0.947	-0.033	0.029	0.052
LGLSPKTI	0.833	0.062	-0.407	0.070	0.121
RNBTWTI	0.609	-0.274	0.614	-0.030	0.213
LGRULST	0.931	-0.044	-0.074	0.097	0.084
RU3EVT	0.743	0.153	0.391	-0.059	0.077
HYSTER	0.522	0.196	-0.237	-0.593	0.184
LGMXTMJPK	0.043	0.614	0.012	0.337	0.439
LGMXTRP	0.134	0.547	0.065	0.038	0.539
LGSUMPK	0.154	0.887	-0.108	-0.153	-0.071
LGSMLSPK	0.930	-0.024	-0.221	0.127	0.094
LGTOTRAIN	0.048	0.769	0.099	-0.209	-0.409
LGINT15	0.040	0.744	0.428	0.203	-0.065
LGSFIVE	-0.319	0.471	0.004	0.610	0.105
LGRRISE	-0.056	0.818	0.121	-0.046	-0.277
LGRFALL	0.146	0.151	-0.047	-0.365	-0.372
LGLSTPPTI	0.854	-0.209	-0.098	0.294	-0.271
SUM3PPTI	0.704	-0.082	0.083	0.174	-0.408
LGLSTINT	0.904	-0.037	-0.075	0.167	-0.221
LGLST75OTI	0.770	0.089	-0.392	0.235	-0.081
LGPPTBTW	-0.232	-0.165	0.489	0.426	-0.452
LGINTBET	0.510	0.144	0.445	-0.453	-0.083

Reproduced with permission of the copyright owner. Further reproduction prohibited without permission.

Appendix 8.11. Continued.

	6
BASE	0.101
LGPK	-0.086
LGLSPKTI	0.132
RNBTWTI	0.045
LGRULST	0.039
RU3EVT	-0.053
HYSTER	-0.281
LGMXTMJPK	0.330
LGMXTRP	0.310
LGSUMPK	-0.209
LGSMLSPK	0.042
LGTOTRAIN	0.228
LGINT15	0.020
LGSFIVE	-0.228
LGRRISE	-0.165
LGRFALL	0.762
LGLSTPPTI	-0.000
SUM3PPTI	0.160
LGLSTINT	-0.139
LGLST75OTI	-0.148
LGPPTBTW	-0.036
LGINTBET	-0.360

Reproduced with permission of the copyright owner. Further reproduction prohibited without permission.

Appendix 8.12. Results of principal component analysis on the independent variables using runoff characteristics after varimax rotation for the entire event.

Rotated Loading Matrix (VARIMAX, Gamma = 1.0000)

	1	2	3	4	5
BASE	0.209	-0.261	0.895	0.139	-0.047
LGPK	0.049	0.850	-0.097	0.396	0.130
LGLSPKTI	0.845	-0.019	0.033	0.219	0.356
RNBTWTI	0.293	-0.173	0.864	0.044	-0.059
LGRULST	0.846	-0.029	0.352	0.114	0.195
RU3EVT	0.476	0.251	0.664	0.077	0.080
HYSTER	0.275	0.256	0.217	-0.141	0.787
LGMXTMJPK	0.040	0.303	-0.043	0.834	-0.039
LGMXTRP	-0.019	0.258	0.147	0.759	0.206
LGSUMPK	0.087	0.886	-0.102	0.158	0.268
LGSMLSPK	0.899	-0.038	0.224	0.141	0.248
LGTOTRAIN	-0.020	0.815	-0.060	0.082	-0.057
LGINT15	-0.051	0.714	0.204	0.353	-0.308
LGSFIVE	-0.105	0.341	-0.308	0.366	-0.369
LGRRISE	-0.086	0.865	-0.080	0.061	-0.073
LGRFALL	0.076	0.160	-0.037	0.049	0.020
LGLSTPPTI	0.929	-0.086	0.187	-0.142	-0.117
SUM3PPTI	0.721	0.078	0.239	-0.156	-0.227
LGLSTINT	0.904	0.111	0.257	-0.156	0.036
LGLST75OTI	0.879	0.116	-0.059	0.009	0.182
LGPPTBTW	-0.112	-0.002	0.105	-0.233	-0.791
LGINTBET	0.151	0.393	0.680	-0.332	0.258
LGRUN	0.198	0.863	0.095	0.024	0.238

Reproduced with permission of the copyright owner. Further reproduction prohibited without permission.

Appendix 8.12. Continued.

	6
BASE	0.024
LGPK	-0.105
LGLSPKTI	0.106
RNBTWTI	0.026
LGRULST	0.040
RU3EVT	0.013
HYSTER	-0.009
LGMXTMJPK	-0.032
LGMXTRP	0.044
LGSUMPK	-0.077
LGSMLSPK	0.027
LGTOTRAIN	0.418
LGINT15	-0.056
LGSFIVE	-0.511
LGRRISE	-0.036
LGRFALL	0.932
LGLSTPPTI	0.052
SUM3PPTI	0.272
LGLSTINT	-0.024
LGLST75OTI	-0.121
LGPPTBTW	-0.064
LGINTBET	-0.040
LGRUN	0.169

Reproduced with permission of the copyright owner. Further reproduction prohibited without permission.

Appendix 8.13. Results of principal component analysis on the independent variables using runoff characteristics after varimax rotation for the entire event without the variable runoff.

Rotated Loading Matrix (VARIMAX, Gamma = 1.0000)

	1	2	3	4	5
BASE	0.203	-0.267	0.894	-0.054	0.141
LGPK	0.062	0.854	-0.088	0.164	0.379
LGLSPKTI	0.843	-0.043	0.032	0.355	0.223
RNBTWTI	0.289	-0.194	0.862	-0.066	0.052
LGRULST	0.844	-0.049	0.352	0.197	0.116
RU3EVT	0.479	0.229	0.667	0.094	0.074
HYSTER	0.279	0.212	0.214	0.803	-0.137
LGMXTMJPK	0.042	0.320	-0.036	-0.037	0.829
LGMXTRP	-0.017	0.268	0.152	0.212	0.753
LGSUMPK	0.102	0.871	-0.095	0.304	0.147
LGSMLSPK	0.897	-0.062	0.223	0.248	0.145
LGTOTRAIN	-0.006	0.812	-0.051	-0.019	0.062
LGINT15	-0.040	0.744	0.215	-0.274	0.326
LGSFIVE	-0.100	0.379	-0.301	-0.362	0.358
LGRRISE	-0.072	0.884	-0.070	-0.028	0.032
LGRFALL	0.080	0.120	-0.037	0.021	0.058
LGLSTPPTI	0.928	-0.099	0.187	-0.116	-0.140
SUM3PPTI	0.723	0.056	0.241	-0.222	-0.153
LGLSTINT	0.906	0.086	0.258	0.044	-0.153
LGLST75OTI	0.881	0.093	-0.059	0.186	0.015
LGPPTBTW	-0.111	0.038	0.110	-0.784	-0.249
LGINTBET	0.158	0.367	0.681	0.286	-0.340

Reproduced with permission of the copyright owner. Further reproduction prohibited without permission.

Appendix 8.13. Continued.

	6
BASE	0.015
LGPK	-0.078
LGLSPKTI	0.106
RNBTWTI	0.016
LGRULST	0.040
RU3EVT	0.020
HYSTER	0.003
LGMXTMJPK	-0.029
LGMXTRP	0.051
LGSUMPK	-0.049
LGSMLSPK	0.025
LGTOTRAIN	0.448
LGINT15	-0.030
LGSFIVE	-0.506
LGRRISE	-0.000
LGRFALL	0.934
LGLSTPPTI	0.050
SUM3PPTI	0.273
LGLSTINT	-0.021
LGLST75OTI	-0.120
LGPPTBTW	-0.061
LGINTBET	-0.022

Reproduced with permission of the copyright owner. Further reproduction prohibited without permission.

Reproduced with permission of the copyright owner. Further reproduction prohibited without permission.

Appendix 8.14. Summary of dependent and independent variables used in statistical analysis for quickflow characteristics to major peak for Rio Piedras at El Senorial. (D-indicates dependent variable; L indicates data was log transformed for final statistical operations

Start Date	Start Time	Start discharge ft3/s	End Date	End Time	End discharge ft3/s	DL Total suspended-sediment load tons	DL Discharge-weighted sediment concentration mg/l	L QUICK	L LSPKBTI	L QU3EVT
3/28/1992	15.25	3.5	3/28/1992	16.25	1800	244	6263	1.25E+006	0.098	1.37E+003
4/19/1992	12.00	4.1	4/19/1992	12.75	596	84.2	6659	4.05E+005	0.516	1.72E+004
4/29/1992	17.25	2.1	4/29/1992	21.00	844	419	4020	3.34E+006	2.307	4.48E+005
5/1/1992	16.75	2.6	5/1/1992	23.50	874	2939	9266	1.02E+007	13.786	5.29E+005
5/16/1992	11.00	2.8	5/16/1992	12.25	919	506	10191	1.59E+006	0.356	3.25E+004
7/20/1992	10.75	6.4	7/20/1992	17.00	434	113	2936	1.23E+006	0.545	1.58E+004
8/5/1992	2.00	8.0	8/6/1992	2.5	1300	376	10355	1.16E+006	3.916	2.54E+005
9/6/1992	13.24	7.0	9/6/1992	14.75	593	220	4317	1.63E+006	1.006	1.80E+005
9/23/1992	10.50	6.4	9/23/1992	13.25	718	121	3702	1.05E+006	0.892	1.12E+005
6/9/1993	11.25	7.6	6/9/1993	13.00	420	495	21337	7.43E+005	7.174	3.47E+006
6/29/1993	17.00	8.4	6/29/1993	17.75	202	26.8	3686	2.33E+005	2.803	9.75E+004
9/6/1993	17.00	8.9	9/6/1993	17.75	1060	257	6470	1.27E+006	4.708	1.79E+005
1/11/1994	0.50	4.3	1/11/1994	3.75	214	11.6	1783	2.09E+005	0.140	6.84E+003
1/23/1994	14.25	6.0	1/23/1994	15.50	269	248	11173	7.12E+005	2.271	4.83E+004
4/10/1994	7.50	3.2	4/10/1994	10.50	1292	139	1535	2.91E+006	1.913	1.44E+004
7/2/1994	8.83	3.7	7/2/1994	10.25	547	120	4066	9.43E+005	2.250	1.65E+004
11/19/1994	16.17	6.2	11/19/1994	16.75	1082	84.9	2399	1.13E+006	3.320	3.93E+004
12/1/1994	14.75	9.9	12/1/1994	15.25	249	14.9	1541	3.09E+005	4.531	6.75E+005
12/2/1994	11.25	13.3	12/2/1994	13.25	742	255	3855	2.12E+006	6.861	4.97E+005
2/25/1995	15.00	2.8	2/25/1995	16.00	2500	2549	29650	2.75E+006	9.087	1.76E+005
5/15/1995	18.00	2.8	5/15/1995	19.25	767	167	14282	3.74E+005	0.790	6.09E+003
6/10/1995	11.50	1.5	6/10/1995	13.00	471	70.4	1988	1.13E+006	1.480	4.18E+004
6/15/1995	11.50	1.4	6/15/1995	12.00	388	49.9	3871	4.13E+005	3.608	4.23E+004
6/16/1995	12.50	2.0	6/16/1995	13.50	1134	169	3277	1.65E+006	10.727	1.52E+005
7/21/1995	17.50	1.5	7/21/1995	20.50	1039	198	3385	1.87E+006	1.675	1.65E+004
9/6/1995	3.75	3.9	9/6/1995	7.00	2874	1310	6623	6.33E+006	2.965	2.60E+005

Reproduced with permission of the copyright owner. Further reproduction prohibited without permission.

Appendix 8.14. Continued.

Start Date	Start Time	End Date	End Time	L PPTLSTI	L INTLST	L PPTBTW	L INTBET	L SUM3PPTI	L RRISE	INT15
3/28/1992	15.25	3/28/1992	16.25	0.0004	0.00022	0.00111	0.00006	0.00086	1.23	0.56
4/19/1992	12.00	4/19/1992	12.75	0.0019	0.00047	0.00246	0.00016	0.00459	0.62	0.35
4/29/1992	17.25	4/29/1992	21.00	0.0049	0.00159	0.00004	0.00010	0.00747	2.28	0.37
5/1/1992	16.75	5/1/1992	23.50	0.1296	0.01533	0.00036	0.00378	0.13447	1.98	0.22
5/16/1992	11.00	5/16/1992	12.25	0.0007	0.00041	0.00101	0.00122	0.00835	0.86	0.35
7/20/1992	10.75	7/20/1992	17.00	0.0059	0.00113	0.00381	0.00087	0.00991	1.49	0.24
8/5/1992	2.00	8/6/1992	2.5	0.0180	0.00580	0.00506	0.00117	0.03233	0.77	0.50
9/6/1992	13.24	9/6/1992	14.75	0.0036	0.00224	0.00038	0.00111	0.00434	0.71	0.34
9/23/1992	10.50	9/23/1992	13.25	0.0126	0.00220	0.00274	0.00007	0.01615	0.90	0.55
6/9/1993	11.25	6/9/1993	13.00	0.0361	0.00605	0.00004	0.00027	0.03835	0.26	0.05
6/29/1993	17.00	6/29/1993	17.75	0.0142	0.00070	0.00181	0.00078	0.01562	0.26	0.10
9/6/1993	17.00	9/6/1993	17.75	0.0033	0.00082	0.00009	0.00015	0.00327	0.57	0.52
1/11/1994	0.50	1/11/1994	3.75	0.0010	0.00055	0.00065	0.00003	0.00344	0.16	0.07
1/23/1994	14.25	1/23/1994	15.50	0.0061	0.00271	0.00008	0.01017	0.00911	0.30	0.05
4/10/1994	7.50	4/10/1994	10.50	0.0058	0.00217	0.00203	0.00033	0.00611	0.54	0.54
7/2/1994	8.83	7/2/1994	10.25	0.0165	0.00294	0.00141	0.00012	0.01737	0.57	0.25
11/19/1994	16.17	11/19/1994	16.75	0.0060	0.00161	0.00069	0.00001	0.01176	1.36	0.44
12/1/1994	14.75	12/1/1994	15.25	0.1813	0.01543	0.01192	0.00308	0.21813	0.17	0.23
12/2/1994	11.25	12/2/1994	13.25	0.0627	0.02667	0.00031	0.01572	0.14870	0.21	0.10
2/25/1995	15.00	2/25/1995	16.00	0.0017	0.00098	0.00004	0.00368	0.01308	2.10	0.77
5/15/1995	18.00	5/15/1995	19.25	0.0044	0.00098	0.00612	0.00008	0.00598	1.07	0.53
6/10/1995	11.50	6/10/1995	13.00	0.0068	0.00126	0.00682	0.00000	0.00735	0.34	0.14
6/15/1995	11.50	6/15/1995	12.00	0.0100	0.00159	0.00015	0.00000	0.01192	0.14	0.06
6/16/1995	12.50	6/16/1995	13.50	0.0243	0.00393	0.00017	0.00000	0.05809	0.38	0.33
7/21/1995	17.50	7/21/1995	20.50	0.0013	0.00115	0.00412	0.00090	0.00273	0.34	0.10
9/6/1995	3.75	9/6/1995	7.00	0.0867	0.02493	0.00099	0.04273	0.10636	1.66	0.56

Reproduced with permission of the copyright owner. Further reproduction prohibited without permission.

Appendix 8.14. Continued.

Start Date	Start Time	End Date	End Time	BASE	L PKBS	L QULST	L L75OTI	L MXTMJPK	L SMLSPKBS	RNBTWTI
3/28/1992	15.25	3/28/1992	16.25	3.50	1796.1	596	0.000002	29.94	0.10	17481
4/19/1992	12.00	4/19/1992	12.75	4.10	591.7	2649	0.000021	13.15	0.54	13951
4/29/1992	17.25	4/29/1992	21.00	2.10	841.0	17032	0.000057	3.74	3.05	17106
5/1/1992	16.75	5/1/1992	23.50	2.60	870.3	514176	0.000386	2.15	50.73	23125
5/16/1992	11.00	5/16/1992	12.25	2.80	915.6	1640	0.000023	12.22	0.41	11581
7/20/1992	10.75	7/20/1992	17.00	6.40	423.8	4117	0.000017	1.14	0.68	21798
8/5/1992	2.00	8/6/1992	2.5	8.00	1291.8	99073	0.000107	43.07	11.14	37774
9/6/1992	13.24	9/6/1992	14.75	6.97	584.6	17501	0.000096	6.46	3.80	27984
9/23/1992	10.50	9/23/1992	13.25	6.40	709.1	100359	0.000017	4.31	2.33	35138
6/9/1993	11.25	6/9/1993	13.00	7.60	411.4	130378	0.000360	3.93	18.47	32930
6/29/1993	17.00	6/29/1993	17.75	8.40	193.4	93552	0.000009	4.30	7.44	29401
9/6/1993	17.00	9/6/1993	17.75	8.90	1051.0	116313	0.000054	23.36	15.66	35694
1/11/1994	0.50	1/11/1994	3.75	4.25	209.3	482	0.000015	1.08	0.15	20509
1/23/1994	14.25	1/23/1994	15.50	5.97	262.5	33507	0.000068	3.50	5.57	22305
4/10/1994	7.50	4/10/1994	10.50	3.25	1286.9	13752	0.000073	7.16	3.37	12907
7/2/1994	8.83	7/2/1994	10.25	3.72	542.9	14931	0.000062	6.39	3.46	10887
11/19/1994	16.17	11/19/1994	16.75	6.22	1075.5	20996	0.000073	30.73	3.69	18243
12/1/1994	14.75	12/1/1994	15.25	9.93	238.4	629209	0.000104	7.96	75.36	41003
12/2/1994	11.25	12/2/1994	13.25	13.28	727.9	274893	0.000140	6.07	31.79	53485
2/25/1995	15.00	2/25/1995	16.00	2.82	2496.5	92926	0.000035	41.62	14.40	10540
5/15/1995	18.00	5/15/1995	19.25	2.82	764.3	3912	0.000045	10.19	0.89	10988
6/10/1995	11.50	6/10/1995	13.00	1.47	469.0	6641	0.000084	5.22	2.19	11249
6/15/1995	11.50	6/15/1995	12.00	1.40	386.2	29814	0.000046	12.88	4.30	7377
6/16/1995	12.50	6/16/1995	13.50	2.01	1132.2	126303	0.000262	18.87	38.92	9128
7/21/1995	17.50	7/21/1995	20.50	1.47	1035.0	7861	0.000015	5.76	1.90	6189
9/6/1995	3.75	9/6/1995	7.00	3.89	2959.4	141721	0.000560	16.45	19.97	16681

Appendix 8.15. Pearson correlation matrix to the highest peak using quickflow characteristics, Rio Piedras at El Senorial.

	LGSED	LGQU_SEDCONC	LGQUICK	BASE
LGSED	1.000			
LGQU_SEDCONC	0.714	1.000		
LGQUICK	0.820	0.185	1.000	
BASE	-0.191	-0.054	-0.224	1.000
LGMXTMJPK	0.274	0.317	0.126	-0.037
INT15	0.429	0.282	0.371	-0.137
LGRRISE	0.486	0.190	0.528	-0.162
RNBTWTI	-0.080	-0.027	-0.090	0.934
LGPPTBTW	-0.447	-0.436	-0.271	0.022
LGINTBET	0.446	0.346	0.344	0.453
LGSMLSPKBS	0.299	0.114	0.326	0.376
LGQULST	0.289	0.136	0.295	0.458
LGPPTLSTI	0.086	-0.086	0.191	0.395
LGLS75OTI	0.378	0.130	0.424	0.119
SUM3PPTI	0.128	0.017	0.166	0.312
QU3EVT	0.383	0.222	0.356	0.533
LGINTLST	0.272	-0.017	0.395	0.388
LGPKBS	0.712	0.332	0.729	-0.285
LSPKBTI	0.374	0.201	0.361	0.207

	LGMXTMJPK	INT15	LGRRISE	RNBTWTI	LGPPTBTW
LGMXTMJPK	1.000				
INT15	0.637	1.000			
LGRRISE	0.065	0.544	1.000		
RNBTWTI	-0.112	-0.123	-0.085	1.000	
LGPPTBTW	-0.061	0.034	0.133	-0.008	1.000
LGINTBET	-0.088	0.127	0.284	0.432	-0.010
LGSMLSPKBS	0.154	-0.052	-0.199	0.424	-0.280
LGQULST	0.126	-0.004	-0.128	0.534	-0.242
LGPPTLSTI	-0.139	-0.217	-0.073	0.476	0.034
LGLS75OTI	0.018	-0.091	-0.033	0.186	-0.267
SUM3PPTI	-0.050	-0.160	-0.085	0.363	0.080
QU3EVT	0.114	0.167	0.100	0.581	-0.086
LGINTLST	-0.081	-0.150	-0.038	0.481	-0.057
LGPKBS	0.657	0.777	0.484	-0.242	-0.123
LSPKBTI	0.194	-0.056	-0.196	0.237	-0.394

Reproduced with permission of the copyright owner. Further reproduction prohibited without permission.

Appendix 8.15. Continued.

	LGINTBET	LGSMLSPKBS	LGQULST	LGPPTLSTI	LGLS75OTI
LGINTBET	1.000				
LGSMLSPKBS	0.289	1.000			
LGQULST	0.328	0.965	1.000		
LGPPTLSTI	0.247	0.825	0.835	1.000	
LGLS75OTI	0.177	0.769	0.666	0.751	1.000
SUM3PPTI	0.352	0.561	0.570	0.729	0.535
QU3EVT	0.562	0.633	0.634	0.468	0.523
LGINTLST	0.416	0.805	0.787	0.912	0.822
LGPKBS	0.164	0.081	0.061	-0.129	0.136
LSPKBTI	0.147	0.943	0.890	0.706	0.739

	SUM3PPTI	QU3EVT	LGINTLST	LGPKBS	LSPKBTI
SUM3PPTI	1.000				
QU3EVT	0.495	1.000			
LGINTLST	0.768	0.559	1.000		
LGPKBS	-0.023	0.198	0.071	1.000	
LSPKBTI	0.464	0.510	0.681	0.140	1.000

Reproduced with permission of the copyright owner. Further reproduction prohibited without permission.

Appendix 8.16. Results of principal component analysis to the major peak using quickflow characteristics for the independent variables after removal due to multicollinearity.

Component loadings

	1	2	3	4	5	6
LGQUICK	0.378	0.727	-0.112	0.369	-0.234	0.053
BASE	0.524	-0.416	0.641	-0.269	-0.105	0.029
LGMXTMJPK	0.039	0.604	0.090	-0.640	0.347	-0.255
INT15	-0.066	0.827	0.340	-0.189	0.187	0.167
LGRRISE	-0.037	0.818	0.197	0.307	-0.094	0.240
RNBTWTI	0.594	-0.374	0.597	-0.177	-0.133	0.136
LGPPTBTW	-0.201	-0.194	0.342	0.316	0.774	0.177
LGINTBET	0.470	0.132	0.575	0.355	-0.260	-0.276
LGSMLSPKBS	0.934	0.037	-0.205	-0.204	0.008	0.068
LGQULST	0.930	0.015	-0.078	-0.205	0.009	0.151
LGPPTLSTI	0.882	-0.202	-0.164	0.139	0.246	0.161
LGLS75OTI	0.798	0.107	-0.389	0.103	0.021	-0.006
SUM3PPTI	0.720	-0.117	0.009	0.289	0.321	-0.350
QU3EVT	0.748	0.161	0.385	0.001	-0.099	0.006
LGINTLST	0.919	-0.052	-0.099	0.226	0.140	-0.065
LGPKBS	0.082	0.943	0.068	-0.038	0.093	-0.117
LSPKBTI	0.830	0.125	-0.379	-0.254	-0.059	0.066

Reproduced with permission of the copyright owner. Further reproduction prohibited without permission.

Appendix 8.17. Results of principal component analysis to the major peak using quickflow characteristics for the independent variables after removal of quickflow.

Component loadings

	1	2	3	4	5	6
BASE	0.560	-0.315	0.641	0.334	0.119	0.012
LGMXTMJPK	0.014	0.709	0.008	0.330	0.531	-0.267
INT15	-0.114	0.878	0.279	0.011	0.146	0.181
LGRRISE	-0.100	0.779	0.179	-0.278	-0.340	0.277
RNBTWTI	0.623	-0.293	0.604	0.272	0.063	0.114
LGPPTBTW	-0.183	-0.178	0.351	-0.622	0.580	0.158
LGINTBET	0.455	0.142	0.591	-0.181	-0.421	-0.255
LGSMLSPKBS	0.931	0.113	-0.228	0.145	0.064	0.072
LGQULST	0.930	0.098	-0.100	0.153	0.075	0.156
LGPPTLSTI	0.893	-0.148	-0.160	-0.250	0.133	0.162
LGLS75OTI	0.784	0.130	-0.395	-0.139	-0.096	-0.004
SUM3PPTI	0.727	-0.068	0.014	-0.428	0.092	-0.328
QU3EVT	0.737	0.229	0.371	0.034	-0.119	0.022
LGINTLST	0.915	-0.021	-0.091	-0.271	0.007	-0.077
LGPKBS	0.013	0.934	0.022	-0.063	0.030	-0.135
LSPKBTI	0.820	0.185	-0.406	0.210	0.011	0.074

Reproduced with permission of the copyright owner. Further reproduction prohibited without permission.

Appendix 8.18. Results of principal component analysis to the major peak after varimax rotation using quickflow characteristics for the independent variables.

Rotated Loading Matrix (VARIMAX, Gamma = 1.0000)

	1	2	3	4	5	6
LGQUICK	0.349	0.809	-0.121	-0.041	0.225	0.186
BASE	0.179	-0.252	0.919	0.018	-0.031	0.057
LGMXTMJPK	0.044	0.162	-0.028	0.968	0.040	-0.039
INT15	-0.131	0.706	0.078	0.582	-0.129	-0.160
LGRRISE	-0.095	0.923	-0.056	0.076	-0.031	-0.020
RNBTWTI	0.266	-0.151	0.903	-0.078	-0.041	0.014
LGPPTBTW	-0.151	-0.062	0.014	-0.017	-0.947	0.038
LGINTBET	0.097	0.363	0.576	-0.129	0.060	0.587
LGSMLSPKBS	0.919	0.007	0.261	0.118	0.183	-0.010
LGQULST	0.874	0.036	0.379	0.096	0.122	-0.059
LGPPTLSTI	0.910	-0.072	0.211	-0.163	-0.204	0.071
LGLS75OTI	0.869	0.109	-0.039	-0.055	0.141	0.138
SUM3PPTI	0.651	-0.078	0.147	-0.006	-0.241	0.576
QU3EVT	0.487	0.293	0.607	0.081	0.051	0.208
LGINTLST	0.871	0.056	0.220	-0.113	-0.082	0.321
LGPKBS	0.060	0.751	-0.158	0.556	0.079	0.128
LSPKBTI	0.887	0.028	0.083	0.147	0.312	-0.083

Reproduced with permission of the copyright owner. Further reproduction prohibited without permission.

Appendix 8.19 Results of principal component analysis to the major peak after varimax rotation using quickflow characteristics for the independent variables after removal of quickflow.

Rotated Loading Matrix (VARIMAX, Gamma = 1.0000)

	1	2	3	4	5	6
BASE	0.166	-0.204	0.931	-0.038	0.015	0.113
LGMXTMJPK	0.042	0.241	-0.002	0.030	0.947	-0.090
INT15	-0.098	0.810	0.044	-0.078	0.485	-0.084
LGRRISE	-0.044	0.941	-0.138	0.035	-0.011	0.104
RNBTWTI	0.254	-0.127	0.913	-0.045	-0.075	0.086
LGPPTBTW	-0.157	-0.010	0.031	-0.953	-0.028	0.008
LGINTBET	0.129	0.305	0.474	0.077	-0.128	0.703
LGSMLSPKBS	0.918	-0.016	0.266	0.181	0.120	-0.007
LGQULST	0.874	0.034	0.384	0.127	0.083	-0.037
LGPPTLSTI	0.909	-0.104	0.208	-0.205	-0.158	0.071
LGLS75OTI	0.877	0.034	-0.065	0.144	-0.035	0.143
SUM3PPTI	0.660	-0.140	0.099	-0.259	0.021	0.548
QU3EVT	0.506	0.292	0.559	0.071	0.054	0.295
LGINTLST	0.874	-0.042	0.190	-0.095	-0.065	0.334
LGPKBS	0.085	0.704	-0.201	0.089	0.562	0.170
LSPKBTI	0.886	0.002	0.094	0.311	0.147	-0.093

Reproduced with permission of the copyright owner. Further reproduction prohibited without permission.

Reproduced with permission of the copyright owner. Further reproduction prohibited without permission.

Appendix 8.20 Summary of dependent and independent variables used in statistical analysis for runoff characteristics to major peak for Rio Piedras at El Senorial. (D-indicates dependent variable; L-indicated data was log transformed)

						DL	DL	L	L	
Start Date	Start Time	Start discharge ft3/s	End Date	End Time	End discharge ft3/s	Total suspended-sediment load tons	Discharge-weighted sediment concentration mg/L	RUNOFF ft3	LSPKTI ft3/s/hour	RU3EVT ft3
3/28/1992	15.25	3.50	3/28/1992	16.25	1800	244	6197	1.26E+006	0.107	8.77
4/19/1992	12.00	4.10	4/19/1992	12.75	596	84.2	6470	4.17E+005	0.532	10.53
4/29/1992	17.25	2.10	4/29/1992	21.00	844	419	3979	3.38E+006	2.324	11.45
5/1/1992	16.75	2.60	5/1/1992	23.50	874	2939	9171	1.03E+007	13.84	13.05
5/16/1992	11.00	2.80	5/16/1992	12.25	919	506	10102	1.61E+006	0.384	11.73
7/20/1992	10.75	6.40	7/20/1992	17.00	434	113	2550	1.42E+006	0.592	11.36
8/5/1992	2.00	8.00	8/6/1992	2.5	1300	376	10226	1.18E+006	3.986	14.69
9/6/1992	13.24	6.97	9/6/1992	14.75	593	220	4208	1.67E+006	1.047	13.27
9/23/1992	10.50	6.40	9/23/1992	13.25	718	121	3452	1.12E+006	0.946	12.75
6/9/1993	11.25	7.60	6/9/1993	13.00	420	495	19970	7.94E+005	7.396	13.74
6/29/1993	17.00	8.40	6/29/1993	17.75	202	26.8	3355	2.56E+005	2.831	11.84
9/6/1993	17.00	8.90	9/6/1993	17.75	1060	257	6349	1.30E+006	4.859	13.88
1/11/1994	0.50	4.25	1/11/1994	3.75	214	11.6	1411	2.64E+005	0.156	9.81
1/23/1994	14.25	5.97	1/23/1994	15.50	269	248	10757	7.39E+005	2.418	12.29
4/10/1994	7.50	3.25	4/10/1994	10.50	1292	139	1513	2.95E+006	1.944	9.38
7/2/1994	8.83	3.72	7/2/1994	10.25	547	120	3985	9.62E+005	2.297	10.13
11/19/1994	16.17	6.22	11/19/1994	16.75	1082	84.9	2371	1.15E+006	3.351	12.35
12/1/1994	14.75	9.93	12/1/1994	15.25	249	14.9	1455	3.28E+005	4.737	14.79
12/2/1994	11.25	13.28	12/2/1994	13.25	742	255	3685	2.21E+006	7.155	15.10
2/25/1995	15.00	2.82	2/25/1995	16.00	2500	2549	16508	4.95E+006	9.139	14.18
5/15/1995	18.00	2.82	5/15/1995	19.25	767	167	19641	3.87E+005	0.800	9.60
6/10/1995	11.50	1.47	6/10/1995	13.00	471	70.4	1971	1.14E+006	1.512	12.38
6/15/1995	11.50	1.40	6/15/1995	12.00	388	49.9	3847	4.15E+005	3.623	4.65
6/16/1995	12.50	2.01	6/16/1995	13.50	1134	169	3262	1.65E+006	10.770	12.74
7/21/1995	17.50	1.47	7/21/1995	20.50	1039	198	3337	1.90E+006	1.687	11.05
9/6/1995	3.75	3.89	9/6/1995	7.00	2874	1310	6567	6.39E+006	3.117	14.24

Reproduced with permission of the copyright owner. Further reproduction prohibited without permission.

Appendix 8.20. Continued.

Start Date	Start Time	End Date	End Time	L PPTLSTI	L INTLST	L PPTBTW	L INTBET	SUM3PPTI	L RRISE	INT15
3/28/1992	15.25	3/28/1992	16.25	0.0004	0.00022	0.00111	0.00006	-10.70	1.23	0.56
4/19/1992	12.00	4/19/1992	12.75	0.0019	0.00047	0.00246	0.00016	-8.94	0.62	0.35
4/29/1992	17.25	4/29/1992	21.00	0.0049	0.00159	0.00004	0.00010	-8.14	2.28	0.37
5/1/1992	16.75	5/1/1992	23.50	0.1296	0.01533	0.00036	0.00378	-6.38	1.98	0.22
5/16/1992	11.00	5/16/1992	12.25	0.0007	0.00041	0.00101	0.00122	-7.97	0.86	0.35
7/20/1992	10.75	7/20/1992	17.00	0.0059	0.00113	0.00381	0.00087	-7.64	1.49	0.24
8/5/1992	2.00	8/6/1992	2.5	0.0180	0.00580	0.00506	0.00117	-6.22	0.77	0.50
9/6/1992	13.24	9/6/1992	14.75	0.0036	0.00224	0.00038	0.00111	-9.35	0.71	0.34
9/23/1992	10.50	9/23/1992	13.25	0.0126	0.00220	0.00274	0.00007	-7.40	0.90	0.55
6/9/1993	11.25	6/9/1993	13.00	0.0361	0.00605	0.00004	0.00027	-7.35	0.26	0.05
6/29/1993	17.00	6/29/1993	17.75	0.0142	0.00070	0.00181	0.00078	-8.21	0.26	0.10
9/6/1993	17.00	9/6/1993	17.75	0.0033	0.00082	0.00009	0.00015	-12.69	0.57	0.52
1/11/1994	0.50	1/11/1994	3.75	0.0010	0.00055	0.00065	0.00003	-9.02	0.16	0.07
1/23/1994	14.25	1/23/1994	15.50	0.0061	0.00271	0.00008	0.01017	-7.77	0.30	0.05
4/10/1994	7.50	4/10/1994	10.50	0.0058	0.00217	0.00203	0.00033	-9.92	0.54	0.54
7/2/1994	8.83	7/2/1994	10.25	0.0165	0.00294	0.00141	0.00012	-8.70	0.57	0.25
11/19/1994	16.17	11/19/1994	16.75	0.0060	0.00161	0.00069	0.00001	-7.31	1.36	0.44
12/1/1994	14.75	12/1/1994	15.25	0.1813	0.01543	0.01192	0.00308	-4.48	0.17	0.23
12/2/1994	11.25	12/2/1994	13.25	0.0627	0.02667	0.00031	0.01572	-4.03	0.21	0.10
2/25/1995	15.00	2/25/1995	16.00	0.0017	0.00098	0.00004	0.00368	-7.41	2.10	0.77
5/15/1995	18.00	5/15/1995	19.25	0.0044	0.00098	0.00612	0.00008	-8.62	1.07	0.53
6/10/1995	11.50	6/10/1995	13.00	0.0068	0.00126	0.00682	0.00000	-8.60	0.34	0.14
6/15/1995	11.50	6/15/1995	12.00	0.0100	0.00159	0.00015	0.00000	-8.35	0.14	0.06
6/16/1995	12.50	6/16/1995	13.50	0.0243	0.00393	0.00017	0.00000	-6.24	0.38	0.33
7/21/1995	17.50	7/21/1995	20.50	0.0013	0.00115	0.00412	0.00090	-9.25	0.34	0.10
9/6/1995	3.75	9/6/1995	7.00	0.0867	0.02493	0.00099	0.04273	-5.26	1.66	0.56

Reproduced with permission of the copyright owner. Further reproduction prohibited without permission.

Appendix 8.20. Continued.

Start Date	Start Time	End Date	End Time	BASE	L PK	L RULST	L L75OTI	L MXTMJPK	L SMLSPK	RNBTWTI
3/28/1992	15.25	3/28/1992	16.25	3.50	1800	1166	0.000002	29.94	0.11	17481
4/19/1992	12.00	4/19/1992	12.75	4.10	596	3192	0.000021	13.15	0.55	13951
4/29/1992	17.25	4/29/1992	21.00	2.10	844	18765	0.000057	3.74	3.09	17106
5/1/1992	16.75	5/1/1992	23.50	2.60	874	531977	0.000386	2.15	50.96	23125
5/16/1992	11.00	5/16/1992	12.25	2.80	919	2091	0.000023	12.22	0.44	11581
7/20/1992	10.75	7/20/1992	17.00	6.40	434	5968	0.000017	1.14	0.74	21798
8/5/1992	2.00	8/6/1992	2.5	8.00	1300	107047	0.000107	43.07	11.34	37774
9/6/1992	13.24	9/6/1992	14.75	6.97	593	22497	0.000096	6.46	4.02	27984
9/23/1992	10.50	9/23/1992	13.25	6.40	718	115694	0.000017	4.31	2.51	35138
6/9/1993	11.25	6/9/1993	13.00	7.60	420	154158	0.000360	3.93	19.04	32930
6/29/1993	17.00	6/29/1993	17.75	8.40	202	103219	0.000009	4.30	7.60	29401
9/6/1993	17.00	9/6/1993	17.75	8.90	1060	150616	0.000054	23.36	16.16	35694
1/11/1994	0.50	1/11/1994	3.75	4.25	214	706	0.000015	1.08	0.16	20509
1/23/1994	14.25	1/23/1994	15.50	5.97	269	47596	0.000068	3.50	5.93	22305
4/10/1994	7.50	4/10/1994	10.50	3.25	1292	15312	0.000073	7.16	3.45	12907
7/2/1994	8.83	7/2/1994	10.25	3.72	547	17574	0.000062	6.39	3.53	10887
11/19/1994	16.17	11/19/1994	16.75	6.22	1082	23295	0.000073	30.73	3.73	18243
12/1/1994	14.75	12/1/1994	15.25	9.93	249	812104	0.000104	7.96	81.14	41003
12/2/1994	11.25	12/2/1994	13.25	13.28	742	362386	0.000140	6.07	33.15	53485
2/25/1995	15.00	2/25/1995	16.00	2.82	2500	97647	0.000035	41.62	14.48	10540
5/15/1995	18.00	5/15/1995	19.25	2.82	767	4414	0.000045	10.19	0.90	10988
6/10/1995	11.50	6/10/1995	13.00	1.47	471	7619	0.000084	5.22	2.24	11249
6/15/1995	11.50	6/15/1995	12.00	1.40	388	31079	0.000046	12.88	4.32	7377
6/16/1995	12.50	6/16/1995	13.50	2.01	1134	133017	0.000262	18.87	39.17	9128
7/21/1995	17.50	7/21/1995	20.50	1.47	1039	8484	0.000015	5.76	1.91	6189
9/6/1995	3.75	9/6/1995	7.00	3.89	2965	182621	0.000560	16.45	20.99	16681

Appendix 8.21. Pearson correlation matrix to the the highest peak using runoff characteristics, Rio Piedras at El Senorial.

	LGSED	LGRU_SEDCONC	LGRUN	BASE
LGSED	1.000			
LGRU_SEDCONC	0.718	1.000		
LGRUN	0.838	0.221	1.000	
BASE	-0.191	-0.053	-0.226	1.000
LGMXTMJPK	0.274	0.324	0.130	-0.037
INT15	0.429	0.251	0.404	-0.137
LGRRISE	0.486	0.224	0.505	-0.162
RNBTWTI	-0.080	-0.017	-0.098	0.934
LGPPTBTW	-0.447	-0.410	-0.305	0.022
LGINTBET	0.446	0.330	0.367	0.453
LGSMLSPKTI	0.296	0.116	0.323	0.384
LGRULST	0.286	0.139	0.292	0.491
LGPPTLSTI	0.086	-0.054	0.163	0.395
LGLS75OTI	0.378	0.165	0.399	0.119
SUM3PPTI	0.128	0.009	0.172	0.312
RU3EVT	0.364	0.196	0.356	0.574
LGINTLST	0.272	0.012	0.371	0.388
LGPK	0.712	0.332	0.737	-0.277
LSPKTI	0.375	0.200	0.368	0.216

	LGMXTMJPK	INT15	LGRRISE	RNBTWTI	LGPPTBTW
LGMXTMJPK	1.000				
INT15	0.637	1.000			
LGRRISE	0.065	0.544	1.000		
RNBTWTI	-0.112	-0.123	-0.085	1.000	
LGPPTBTW	-0.061	0.034	0.133	-0.008	1.000
LGINTBET	-0.088	0.127	0.284	0.432	-0.010
LGSMLSPKTI	0.149	-0.053	-0.200	0.433	-0.279
LGRULST	0.121	-0.005	-0.125	0.567	-0.244
LGPPTLSTI	-0.139	-0.217	-0.073	0.476	0.034
LGLS75OTI	0.018	-0.091	-0.033	0.186	-0.267
SUM3PPTI	-0.050	-0.160	-0.085	0.363	0.080
RU3EVT	0.108	0.163	0.101	0.618	-0.075
LGINTLST	-0.081	-0.150	-0.038	0.481	-0.057
LGPK	0.658	0.779	0.484	-0.235	-0.122
LSPKTI	0.189	-0.059	-0.199	0.247	-0.398

Reproduced with permission of the copyright owner. Further reproduction prohibited without permission.

Appendix 8.21. Continued.

	LGINTBET	LGSMLSPKTI	LGRULST	LGPPTLSTI	LGLS75OTI
LGINTBET	1.000				
LGSMLSPKTI	0.295	1.000			
LGRULST	0.353	0.961	1.000		
LGPPTLSTI	0.247	0.827	0.836	1.000	
LGLS75OTI	0.177	0.768	0.653	0.751	1.000
SUM3PPTI	0.352	0.565	0.572	0.729	0.535
RU3EVT	0.584	0.615	0.630	0.455	0.486
LGINTLST	0.416	0.808	0.793	0.912	0.822
LGPK	0.171	0.081	0.062	-0.126	0.135
LSPKTI	0.155	0.942	0.874	0.711	0.742

	SUM3PPTI	RU3EVT	LGINTLST	LGPK	LSPKTI
SUM3PPTI	1.000				
RU3EVT	0.489	1.000			
LGINTLST	0.768	0.547	1.000		
LGPK	-0.019	0.190	0.074	1.000	
LSPKTI	0.470	0.480	0.687	0.138	1.000

Reproduced with permission of the copyright owner. Further reproduction prohibited without permission.

Appendix 8.22. Results of principal component analysis to the major peak using runoff characteristics.

=Component loadings

	1	2	3	4	5
LGRUN	0.366	0.749	-0.110	0.354	-0.248
BASE	0.540	-0.404	0.640	-0.264	-0.105
LGMXTMJPK	0.034	0.600	0.085	-0.649	0.343
INT15	-0.067	0.831	0.328	-0.187	0.194
LGRRISE	-0.042	0.821	0.185	0.312	-0.075
RNBTWTI	0.608	-0.362	0.595	-0.175	-0.130
LGPPTBTW	-0.201	-0.202	0.342	0.301	0.780
LGINTBET	0.481	0.149	0.561	0.372	-0.244
LGSMLSPKTI	0.933	0.037	-0.210	-0.199	0.004
LGRULST	0.933	0.011	-0.056	-0.201	-0.006
LGPPTLSTI	0.880	-0.200	-0.180	0.130	0.254
LGLS75OTI	0.788	0.105	-0.406	0.094	0.033
SUM3PPTI	0.722	-0.108	-0.010	0.291	0.325
RU3EVT	0.741	0.152	0.426	0.009	-0.102
LGINTLST	0.918	-0.048	-0.119	0.217	0.152
LGPK	0.080	0.942	0.062	-0.047	0.105
LSPKTI	0.827	0.125	-0.386	-0.246	-0.069

	6
LGRUN	0.027
BASE	0.030
LGMXTMJPK	-0.258
INT15	0.184
LGRRISE	0.264
RNBTWTI	0.140
LGPPTBTW	0.149
LGINTBET	-0.280
LGSMLSPKTI	0.062
LGRULST	0.145
LGPPTLSTI	0.176
LGLS75OTI	-0.000
SUM3PPTI	-0.325
RU3EVT	-0.021
LGINTLST	-0.054
LGPK	-0.118
LSPKTI	0.056

Reproduced with permission of the copyright owner. Further reproduction prohibited without permission.

Appendix 8.23. Results of principal component analysis to the major peak using runoff characteristics without the variable runoff..

Component loadings

	1	2	3	4	5	6
BASE	0.575	-0.300	0.641	0.317	0.124	0.023
LGMXTMJPK	0.009	0.710	0.002	0.323	0.537	-0.263
INT15	-0.117	0.882	0.265	0.003	0.146	0.191
LGRRISE	-0.105	0.781	0.162	-0.277	-0.345	0.283
RNBTWTI	0.636	-0.278	0.602	0.257	0.067	0.132
LGPPTBTW	-0.181	-0.176	0.347	-0.637	0.569	0.136
LGINTBET	0.464	0.156	0.576	-0.189	-0.425	-0.269
LGSMLSPKTI	0.930	0.111	-0.232	0.144	0.065	0.062
LGRULST	0.933	0.093	-0.076	0.158	0.071	0.145
LGPPTLSTI	0.891	-0.143	-0.178	-0.252	0.130	0.178
LGLS75OTI	0.776	0.129	-0.414	-0.132	-0.094	0.004
SUM3PPTI	0.727	-0.061	-0.006	-0.431	0.088	-0.316
RU3EVT	0.730	0.218	0.414	0.038	-0.114	-0.017
LGINTLST	0.915	-0.014	-0.114	-0.272	0.005	-0.056
LGPK	0.012	0.936	0.011	-0.062	0.030	-0.124
LSPKTI	0.817	0.180	-0.410	0.214	0.009	0.058

Reproduced with permission of the copyright owner. Further reproduction prohibited without permission.

Appendix 8.24. Results of principal component analysis to the major peak after varimax rotation using runoff characteristics.

Rotated Loading Matrix (VARIMAX, Gamma = 1.0000)

	1	2	3	4	5	6
BASE	0.175	-0.249	0.921	0.020	-0.033	0.057
LGMXTMJPK	0.036	0.183	-0.019	0.967	0.035	-0.050
INT15	-0.134	0.735	0.079	0.550	-0.126	-0.160
LGRRISE	-0.092	0.931	-0.061	0.044	-0.030	-0.009
RNBTWTI	0.262	-0.149	0.907	-0.078	-0.038	0.013
LGPPTBTW	-0.144	-0.064	0.013	-0.015	-0.945	0.029
LGINTBET	0.109	0.346	0.558	-0.131	0.047	0.618
LGSMLSPKTI	0.911	0.008	0.277	0.119	0.195	-0.011
LGRULST	0.852	0.042	0.422	0.091	0.138	-0.052
LGPPTLSTI	0.916	-0.073	0.218	-0.160	-0.197	0.034
LGLS75OTI	0.871	0.096	-0.038	-0.044	0.144	0.119
SUM3PPTI	0.671	-0.078	0.142	-0.006	-0.254	0.536
RU3EVT	0.446	0.277	0.647	0.077	0.049	0.250
LGINTLST	0.882	0.044	0.221	-0.103	-0.082	0.294
LGPK	0.062	0.756	-0.151	0.549	0.076	0.142
LSPKTI	0.878	0.031	0.097	0.147	0.330	-0.077
LGRUN	0.331	0.805	-0.111	-0.029	0.266	0.229

Reproduced with permission of the copyright owner. Further reproduction prohibited without permission.

Appendix 8.25. Results of principal component analysis to the major peak after varimax rotation using runoff characteristics without the variable runoff.

Rotated Loading Matrix (VARIMAX, Gamma = 1.0000)

	1	2	3	4	5	6
BASE	0.162	-0.206	0.929	-0.039	0.014	0.121
LGMXTMJPK	0.036	0.255	0.001	0.029	0.943	-0.092
INT15	-0.104	0.821	0.051	-0.074	0.471	-0.075
LGRRISE	-0.046	0.941	-0.135	0.038	-0.025	0.121
RNBTWTI	0.251	-0.126	0.915	-0.043	-0.079	0.089
LGPPTBTW	-0.153	-0.012	0.031	-0.953	-0.027	0.000
LGINTBET	0.134	0.279	0.454	0.066	-0.120	0.734
LGSMLSPKTI	0.910	-0.018	0.282	0.190	0.124	0.002
LGRULST	0.851	0.034	0.427	0.140	0.084	-0.016
LGPPTLSTI	0.914	-0.094	0.219	-0.197	-0.161	0.043
LGLS75OTI	0.879	0.036	-0.060	0.147	-0.032	0.125
SUM3PPTI	0.674	-0.141	0.094	-0.270	0.023	0.518
RU3EVT	0.460	0.260	0.598	0.064	0.068	0.348
LGINTLST	0.884	-0.037	0.193	-0.097	-0.068	0.305
LGPK	0.087	0.713	-0.192	0.084	0.553	0.174
LSPKTI	0.877	-0.001	0.108	0.326	0.153	-0.079

Reproduced with permission of the copyright owner. Further reproduction prohibited without permission.

Reproduced with permission of the copyright owner. Further reproduction prohibited without permission.

Appendix 8.26. Summary of dependent and inde
(A) Type 1 storms and (B) Type 3 storms.

(D indicates dependent variable; L indicates log transformed; LN indicates natural log transform

A.

Start Date	Start Time	End Date	End Time hour	Width of clockwise clockwise loop, mg/L D L	Discharge used in width analysis, ft3/s	Sediment load, tons SED	Discharge-weighted sediment concentration, mg/L CONC	Runoff ft3 2-RUN L	LN Sum of peak flows 9-SMPK	Maximum rate of hydrograph rise to the highest peak, cfs/min 6-MXTMJPK	Runoff of the previous event divided by the time since the previous event, fts/hour 25-RULST
9/6/1993	17.00	9/7/1993	6.00	1640	688	888	3935	7.23E+006	1060	23.36	150616
4/10/1994	7.50	4/10/1994	19.50	2270	162	244	1187	6.57E+006	1292	7.16	15312
12/2/1994	11.25	12/3/1994	15.25	1530	660	769	2721	9.06E+006	1268	6.07	362386
2/25/1995	15.00	2/26/1995	23.75	13810	1717	3358	5811	1.85E+007	2500	41.62	97647
7/21/1995	17.50	7/22/1995	4.25	2140	245	497	2959	5.38E+006	1165	5.76	8484
9/6/1995	3.75	9/7/1995	2.50	4910	2000	3721	4236	2.81E+007	4132	16.45	182621
			AVERAGE	**4383**	**912**	**1579**	**3475**	**1.25E+007**	**1903**	**17**	**136178**

Start Date	Start Time	End Date	End Time hour	Runoff of the 3 previous events divided by the time since the 3 events 31-RU3EVT	Sediment transport curve 'slope on falling limb, (ft3/s/mg/L) 32-RATE_FALL	Rainfall on the rising limb to the highest peak, 13-RRISE LG	Rainfall on the falling limb after the highest peak, in 14-RAINFOL	75% rainfall intensity of current event in/mim, 12-SFIVE	Runoff since the previous event over time since the previous event ft3/hour 17-RNBTWTI	Sediment transport curve 'slope on rising limb, (ft3/s/mg/L) 32-RATE_RISE	Time of peak sediment concentration relative to peak flow (minutes) 34-TIME_PKCON
9/6/1993	17.00	9/7/1993	6.00	13.88	2.67	0.57	0.721	0.0077	35694	-5.00	-20
4/10/1994	7.50	4/10/1994	19.50	9.38	-1.17	0.54	0.001	0.0092	12907	-3.07	-67
12/2/1994	11.25	12/3/1994	15.25	15.10	4.58	0.21	0.891	0.0007	53485	0.45	-8
2/25/1995	15.00	2/26/1995	23.75	14.18	-3.40	2.10	1.800	0.0005	10540	-13.03	-39
7/21/1995	17.50	7/22/1995	4.25	11.05	6.57	0.34	0.171	0.0015	6189	6.36	-5
9/6/1995	3.75	9/7/1995	2.50	14.24	4.52	1.66	1.254	0.0067	16681	1.33	7
			AVERAGE	**12.97**	**Average negative slop**	**0.85**	**0.41**	**0.0044**	**22583**	**Average negative slope = -7**	**-22**
					Average positive slope = 4.58					**Average positive slope = 2.71**	

Reproduced with permission of the copyright owner. Further reproduction prohibited without permission.

Appendix 8.26. (B) Type 3 storms.

Start Date	Start Time hour	End Date	End Time hour	Width of counter-clockwise loop. mg/L D L	Discharge used in width analysis, ft3/s	Sediment load tons	Discharge-weighted sediment concentration, mg/L	Runoff ft3 2-RUN L	Sum of peak flows 9-SMPK	Maximum rate of hydrograph rise to the highest peak, cfs/min 6-MXTMJPK L	Runoff of the previous event divided by the time since the previous event, fts/hour 25-RULST
3/28/1992	15.25	3/29/1992	4.00	43870	904	4302	18221	7.56E+006	1800	29.94	1166
4/19/1992	12.00	4/20/1992	6.00	45700	361	2051	15405	4.26E+006	703	13.15	3192
4/29/1992	17.25	4/30/1992	16.75	18700	562	3696	9273	1.28E+007	1223	3.74	18765
5/1/1992	16.75	5/3/1992	14.50	1770	772	4679	5807	2.58E+007	2082	2.15	531977
5/16/1992	11.00	5/17/1992	9.00	8800	602.6	2960	10495	9.04E+006	919	12.22	2091
8/5/1992	2.00	8/6/1992	10.50	13820	1047	3306	6931	1.53E+007	829	1.14	107047
9/6/1992	13.25	9/6/1992	21.50	490	325	398	3906	3.26E+006	1300	43.07	22497
9/23/1992	10.50	9/23/1992	21.00	1560	300	349	3507	3.19E+006	1083	6.46	115694
6/9/1993	11.25	6/9/1993	23.00	6000	327	1348	12974	3.33E+006	760	4.31	154158
6/29/1993	17.00	6/30/1993	2.50	7870	160	283	5140	1.76E+006	630	3.93	103219
7/2/1994	8.83	7/2/1994	23.25	3860	195	354	3930	2.89E+006	202	4.30	17574
11/19/1994	16.17	11/20/1994	2.50	1350	370	489	2635	5.94E+006	576	1.08	23295
12/1/1994	14.75	12/2/1994	3.75	2180	234	80	944	2.72E+006	469	3.50	812104
5/15/1995	18.00	5/16/1995	2.75	3655	500	453	5708	2.54E+006	875	6.39	4414
6/10/1995	11.50	6/10/1995	22.50	1100	350	198	1870	3.39E+006	1082	30.73	7619
6/15/1995	11.50	6/15/1995	21.25	2590	235	186	2942	2.03E+006	249	7.96	31079
6/16/1995	12.50	6/16/1995	23.75	3730	880	483	3611	4.29E+006	767	10.19	133017
			AVERAGE	**9826**	**478**	**1507**	**6665**	**6.47E+006**	**915**	**10.84**	**1.23E+005**

Start Date	Start Time hour	End Date	End Time hour	Runoff of the 3 previous events divided by the time since the 3 events 31-RU3EVT	Sediment transport curve 'slope on falling limb, (ft3/s/mg/L) 32-RATE_FALL	Rainfall on the rising limb to the highest peak, 13-RRISE	Rainfall on the falling limb after the highest peak, in 14-RAINFOL L	75% rainfall intensity of current event in/mim, 12-SFIVE	Runoff since the previous event over time since the previous event ft3/hour 17-RNBTWTI	Sediment transport curve 'slope on rising limb, (ft3/s/mg/L) 32-RATE_RISE	Time of peak sediment concentration relative to peak flow (minutes) 34-TIME_PKCON
3/28/1992	15.25	3/29/1992	4.00	8.77	-54.17	1.23	0.048	0.0206	17481	6.18	35
4/19/1992	12.00	4/20/1992	6.00	10.53	-162.73	0.62	0.498	0.0128	13951	2.28	35
4/29/1992	17.25	4/30/1992	16.75	11.45	-38.99	2.28	0.829	0.0093	17106	2.92	45
5/1/1992	16.75	5/3/1992	14.50	13.05	-27.27	1.98	0.284	0.0045	23125	7.39	-210
5/16/1992	11.00	5/17/1992	9.00	11.73	54.06	0.86	0.067	0.0127	11581	33.46	14
8/5/1992	2.00	8/6/1992	10.50	11.36	27.58	0.77	0.321	0.0244	37774	13.71	9
9/6/1992	13.25	9/6/1992	21.50	14.69	9.31	0.71	0.001	0.0128	27984	5.96	14
9/23/1992	10.50	9/23/1992	21.00	13.27	11.37	0.90	0.011	0.0054	35138	4.90	12
6/9/1993	11.25	6/9/1993	23.00	12.75	169.78	0.26	0.091	0.0024	32930	-24.54	-51
6/29/1993	17.00	6/30/1993	2.50	13.74	-93.14	0.26	0.058	0.0007	29401	32.64	42
7/2/1994	8.83	7/2/1994	23.25	11.84	-9.56	0.57	0.055	0.0060	10887	7.13	-61
11/19/1994	16.17	11/20/1994	2.50	9.81	3.98	1.36	0.169	0.0227	18243	0.94	31
12/1/1994	14.75	12/2/1994	3.75	12.29	43.87	0.26	0.211	0.0010	41003	136.23	7
5/15/1995	18.00	5/16/1995	2.75	10.13	6.39	1.07	0.225	0.0121	10988	9.05	5
6/10/1995	11.50	6/10/1995	22.50	12.35	5.26	0.34	0.751	0.0050	11249	5.97	11
6/15/1995	11.50	6/15/1995	21.25	14.79	10.09	0.14	0.601	0.0040	7377	14.75	20
6/16/1995	12.50	6/16/1995	23.75	9.60	6.90	0.14	0.295	0.0010	9128	-0.64	11
			AVERAGE	**12.24**	**Average negative slop**	**0.69**	**0.22**	**0.0082**	**21915**	**Average negative slope = -1**	**-10.3**
					Average positive slope = 31.69					**Average positive slope = 18.90**	

Reproduced with permission of the copyright owner. Further reproduction prohibited without permission.

Appendix 9.1. Summary of sediment trap data on total sediment (grams) and total runoff (grams).

Collection Date Trap	Total sediment, g A	Total sediment, g B	Total sediment, g C	Total sediment, g D	Total sediment, g E	Total runoff, g A	Total runoff, g B	Total runoff, g C	Total runoff, g D	Total runoff, g E
MU-P										
07/10/1991		84.0					16260			
08/08/1991		2.8					100			
08/19/1991	20.9	14.6	0.4			1118	7578	1616		
08/27/1991		13.9					15488			
09/09/1991	8.2	6.1		7.5	20.6	474	16853		5919	1665
10/01/1991	22.1	6.8	41.5	1.8	4.6	11980	16485	19528	90	2260
10/09/1991			10.2	5.1				7936	4767	
11/05/1991	2.1	1.8	2.8	1.9	10.3	4019	4944	1200	1008	186
11/27/1991	19.9	24.5	5.3	3.2	0.3	7311	706	692	815	466
01/08/1992	9.8	19.4	25.9	69.0	2.8	7562	17748	17457	10655	18017
04/21/1992	28.2	11.4	125.9			8375	24800	9714		
05/28/1992	27.9	7.3	4.6			7750	26054	18835		
06/15/1992	13.4		86.5	30.9	7.8	10575		19010	8450	6550
07/09/1992	69.9	243.9	64.4	191.5	73.2	12386	19712	7665	16255	7728
07/30/1992		0.1			3.3		6100			6825
09/02/1992	62.9	15.5	7.3	1.6	7.2	11200	16193	9737	4550	9035
09/21/1992	6.4	11.2	3.9		1.4	11194	20939	6796		10199
10/06/1992	5.7		2.4			10950		12350		
10/20/1992		0.4		0.1			225		600	
11/05/1992	0.2	0.1	0.2			600	625	4700		
11/17/1992		0.1	0.1	0.1	0.3	332	425	383	685	386
12/02/1992	0.3	10.9			21.1	7622	21075			7786

Reproduced with permission of the copyright owner. Further reproduction prohibited without permission.

Appendix 9.1. Summary of sediment trap data on total sediment (grams) and total runoff (grams).

Collection Date Trap	Total sediment, g A	Total sediment, g B	Total sediment, g C	Total sediment, g D	Total sediment, g E	Total runoff, g A	Total runoff, g B	Total runoff, g C	Total runoff, g D	Total runoff, g E
MU-P										
07/10/1991		84.0					16260			
08/08/1991		2.8					100			
08/19/1991	20.9	14.6	0.4			1118	7578	1616		
08/27/1991		13.9					15488			
09/09/1991	8.2	6.1		7.5	20.6	474	16853		5919	1665
10/01/1991	22.1	6.8	41.5	1.8	4.6	11980	16485	19528	90	2260
10/09/1991			10.2	5.1				7936	4767	
11/05/1991	2.1	1.8	2.8	1.9	10.3	4019	4944	1200	1008	186
11/27/1991	19.9	24.5	5.3	3.2	0.3	7311	706	692	815	466
01/08/1992	9.8	19.4	25.9	69.0	2.8	7562	17748	17457	10655	18017
04/21/1992	28.2	11.4	125.9			8375	24800	9714		
05/28/1992	27.9	7.3	4.6			7750	26054	18835		
06/15/1992	13.4		86.5	30.9	7.8	10575		19010	8450	6550
07/09/1992	69.9	243.9	64.4	191.5	73.2	12386	19712	7665	16255	7728
07/30/1992		0.1			3.3		6100			6825
09/02/1992	62.9	15.5	7.3	1.6	7.2	11200	16193	9737	4550	9035
09/21/1992	6.4	11.2	3.9		1.4	11194	20939	6796		10199
10/06/1992	5.7		2.4			10950		12350		
10/20/1992		0.4		0.1			225		600	
11/05/1992	0.2	0.1	0.2			600	625	4700		
11/17/1992		0.1	0.1	0.1	0.3	332	425	383	685	386
12/02/1992	0.3	10.9			21.1	7622	21075			7786

Reproduced with permission of the copyright owner. Further reproduction prohibited without permission.

Appendix 9.1. Continued.

Collection Date Trap	Total sediment, g A	Total sediment, g B	Total sediment, g C	Total sediment, g D	Total sediment, g E	Total runoff, g A	Total runoff, g B	Total runoff, g C
CE-C								
08/28/1991	15.5					4241		
09/04/1991	496.4	3796.7	82.7			3220	7167	1454
09/12/1991	94.3	62.6	3.7			14204	4389	641
10/08/1991	67.0	4029.3	37.1			5144	11448	15921
10/22/1991		469.2					5914	
10/29/1991	338.6		2.5			17812		846
11/13/1991	766.4	722.5	85.2			16644	12874	16724
11/21/1991	121.4	30.7				3541	1984	
11/30/1991			7.8					1126
12/12/1991	230.4	84.4	5.1			16709	8091	3976
01/14/1992	271.9	125.4	5.0			6988	1232	16262
07/02/1992	57.5	46.1	72.5			18004	6566	12110
07/28/1992	2.3	6.5				1150	3025	
08/27/1992		59.9	212.3			85	12177	6981
09/14/1992	3.8	5.5	4.5			2486	13645	10318
09/28/1992	0.1	0.2	9.5			2185	1100	1750
10/07/1992	0.5		0.1			985		772
10/22/1992	0.3		0.2			4400	2600	1500
11/25/1992	1.3		0.7			12500	3100	14000
12/03/1992	0.5	0.1	1.3			7150	7600	11850

Reproduced with permission of the copyright owner. Further reproduction prohibited without permission.

Appendix 9.1. Continued.

Collection Date / Trap	Total sediment, g A	Total sediment, g B	Total sediment, g C	Total sediment, g D	Total sediment, g E	Total runoff, g A	Total runoff, g B	Total runoff, g C	Total runoff, g D	Total runoff, g E
CH-C										
02/20/1991			2158.7					4743		
02/28/1991										
03/07/1991		1261.8					16561			
03/18/1991										
03/22/1991			1458.9					15133		
03/25/1991				0.1					403	
04/08/1991										
04/10/1991		2825.6					16298			
04/15/1991		1574.6					950			
04/29/1991										
05/13/1991				500.7	4388.6				2319	16533
05/20/1991			4727.8	6.5				15561	33	
05/28/1991			3354.3					4769		
06/17/1991										
06/24/1991				44.9					1287	
07/01/1991			3535.3	209.7				16684	4290	
07/09/1991			2532.4	81.2				7811	7997	
07/15/1991										
07/16/1991			1845.8	74.1	4205.0			2066	6650	16037
07/31/1991				4.5					3704	
08/09/1991			3990.4	24.4	966.4			6028	723	2872
08/20/1991										
09/03/1991	61.9	155.1	1439.1		413.5	7396	15389	13654		18796
09/10/1991	27.7	36.7	422.7	11.0	29.7	14641	4503	8779	2382	4729
10/08/1991	205.6	3205.1	4549.5		1692.4	14871	3011	18464		13477
10/30/1991					74.8					16132
11/06/1991	58.3	320.7	165.5			2198	11143	9150		
11/21/1991	6.2	455.8	64.8		55.7	5868	3492	15571		12877
12/12/1991	15.9	325.1	58.0	0.5	51.0	14934	16781	17774	665	19455
01/10/1992			97.9	18.7	29.8			10756	16689	12634
01/23/1992		78.1	21.2		9.3		8451	2524		15515
03/03/1992										
03/27/1992			145.2					12577		
06/09/1992										
07/06/1992			174.7	38.0	0.1			3305	347	525
08/18/1992			120.5	236.0	232.9			2907	1916	967
09/24/1992										5750
10/29/1992			33.2	27.4	2.1			10198	5729	6150
11/24/1992			5.1	0.1	2.8			11572	356	3325
12/02/1992			21.8	8.1	32.0			13422	8251	12722
12/21/1992			10.4	0.2	0.9			6922	656	2775

Reproduced with permission of the copyright owner. Further reproduction prohibited without permission.

Appendix 9.1. Continued.

Collection Date Trap	Total sediment, g A	Total sediment, g B	Total sediment, g C	Total sediment, g D	Total sediment, g E	Total runoff, g A	Total runoff, g B	Total runoff, g C
CH-F								
08/20/1991	2.2					7485		
09/03/1991			1.6					1526
09/10/1991								
10/17/1991		16.2	21.6				16532	4008
10/30/1991								
11/21/1991	8.8	3.3	2.9			16955	7457	4967
12/12/1991	9.3	9.8	3.0			15905	19561	3952
01/10/1992	25.1	3.9	6.6			18803	19525	17898
01/23/1992	1.3	0.8	13.1			13501	13700	8600
03/03/1992						725	224	1077
03/27/1992						750	1075	375
06/03/1992	28.7	9.1	10.8			16814	18317	18166
06/09/1992						4251	639	1333
07/06/1992	21.6	17.6	7.2			4321	2148	1843
07/20/1992	0.6	0.7	0.8			1350	680	1675
08/18/1992	1.8	15.8	16.5			8025	2769	4311
09/16/1992	9.5	1.7	3.9			12441	16498	5196
09/28/1992	18.7	2.2				12425	4324	1774
10/26/1992	6.7	31.8	0.2			11275	21024	5377
11/24/1992	40.9	27.6	1.8			9975	17832	14127
12/02/1992	55.8	23.1	13.1			11525	21024	19327
12/21/1992	6.3	4.9	1.1			16325	19274	12872

Reproduced with permission of the copyright owner. Further reproduction prohibited without permission.

Appendix 9.1. Continued.

Collection Date Trap	Total sediment, g A	Total sediment, g B	Total sediment, g C	Total sediment, g D	Total sediment, g E	Total runoff, g A	Total runoff, g B	Total runoff, g C	Total runoff, g D	Total runoff, g E
CO-C										
08/19/1991			35.7	72.1	564.4			6178	2042	7610
08/27/1991			58.9	91.4	120.0			2603	3505	266
09/09/1991			168.8	167.8	1088.5			7246	6469	4611
09/23/1991			49.7	554.4	205.7			7138	13324	17253
10/01/1991			30.8	49.7	65.2			18484	3220	3572
10/09/1991			51.6	7.2	42.2			3967	1960	6953
10/28/1991			50.6	6.4	26.5			4147	587	6674
11/05/1991			80.6	14.8	29.6			14255	5417	10413
12/04/1991			8.6	2.0	2.0			16182	15510	15410
01/09/1992			50.2	2.3	37.1			10558	6262	5115
03/19/1992								4600		1400
06/15/1992			0.4	3.3	1.2			4225	3750	14200
07/02/1992			12.3	0.6	41.0			3663	2650	1696
07/28/1992			1.2					4700	650	
09/08/1992			5.8	8.7				20683	3000	
09/22/1992			1.7	6.4				10698	13594	
11/05/1992			0.8	0.3				4533	13100	
12/03/1992			1.7	0.8				2833	13723	

Reproduced with permission of the copyright owner. Further reproduction prohibited without permission.

Appendix 9.1. Continued.

Collection Date Trap	Total sediment, g A	Total sediment, g B	Total sediment, g C	Total sediment, g D	Total sediment, g E	Total runoff, g A	Total runoff, g B	Total runoff, g C	Total runoff, g D	Total runoff, g E
DO-A										
04/08/1991				106.2					644	
04/10/1991				26.1					166	
05/09/1991	2043.3	195.2	1320.2			4327	10791	7947		
05/13/1991		1229.4		78.4			11961		370	
05/20/1991		2852.9		0.1			4003		1270	
05/28/1991		112.9		1126.8			2535		2401	
06/10/1991		11.8	16.0	54.2			7556	4163	234	
06/17/1991									274	
07/01/1991		179.3		9.0			9963		7513	
07/09/1991		490.6		14.4			7081		7345	
07/17/1991		25.1		164.0			7334		7135	
07/22/1991			248.3					14081		
07/31/1991		265.0					10126			
08/22/1991	46.4	583.4	297.0			8676	22867	9918		
08/29/1991	325.8	164.6	1295.1		184.3	13252	20533	14808		7879
09/05/1991			53.2					2371		
09/11/1991	10.4	23.9			83.5	1041	4671			1071
10/01/1991		37.6	6.2				9413	19197		
10/02/1991	22.7	412.2	491.0	8.4	323.4	17013	16506	15308	7614	4298
10/21/1991	2.7	548.2	103.9	150.6	17.9	4756	7756	7227	1359	1569
10/29/1991	3.1	362.0	5.0			1504	10685	932		
11/07/1991	43.7	592.2	22.8	16.5	99.3	13787	24072	3981	279	2134
11/25/1991	57.8	644.3	106.1	16.4	86.2	7555	25108	16325	7633	9653
01/14/1992	70.9	2195.9	1751.9	79.2	111.5	16485	19393	19356	5869	4671
01/22/1992	0.2	143.2	1250.9			5325	8903	4315		
03/12/1992	0.4	0.3	0.5			870	8137	525		223
07/01/1992	24.5	68.6	18.2	8.3	44.6	18289	10856	5110	892	12885
07/21/1992	0.7	282.3		331.1	108.6	975	7472		394	291
09/09/1992	10.3	93.1	68.4	27.7	11.2	5812	15344	12557	5233	15012
09/24/1992	39.8	163.8	422.1	0.7	218.9	12231	19050	17400	1261	14005
10/08/1992	0.8	354.5	49.0	14.8	28.5	3200	6937	8745	397	8058
10/21/1992	77.9	117.6	91.1	9.4	92.1	4030	13868	8250	758	7262
11/24/1992	35.3	95.9	91.6	6.1	19.5	6575	6474	7612	1006	5413
12/08/1992	31.8	165.9	72.7	3.5	100.9	8546	13816	12875	1962	7242
12/17/1992	107.3	147.3	61.3	29.5	1.9	965	13371	1565	934	881

Reproduced with permission of the copyright owner. Further reproduction prohibited without permission.

Appendix 9.1. Continued.

Collection Date Trap	Total sediment, g A	Total sediment, g B	Total sediment, g C	Total sediment, g D	Total sediment, g E	Total runoff, g A	Total runoff, g B	Total runoff, g C	Total runoff, g D	Total runoff, g E
ED-P										
10/01/1991		1.1					244			
10/15/1991		0.7					2847			
12/04/1991	7.9	1.3	1.5	0.5	0.9	10836	10653	13111	13192	8739
01/15/1992		1.2	4.0		0.1			12696		5243
02/04/1992	74.2					3024				
03/04/1992						10184				
07/07/1992	604.7	1.8	72.5	5.7	4.0	18302	10925	868	7435	8550
09/08/1992	41.3					8367				
09/30/1992	0.2				1.4	6100	2700			16899
11/02/1992	1.6					5600				
11/17/1992	0.3				0.1	3050				200
11/30/1992	0.2					2725				

Reproduced with permission of the copyright owner. Further reproduction prohibited without permission.

Appendix 9.1. Continued.

Collection Date Trap	Total sediment, g A	Total sediment, g B	Total sediment, g C	Total sediment, g D	Total sediment, g E	Total runoff, g A	Total runoff, g B	Total runoff, g C	Total runoff, g D	Total runoff, g E
IC-F										
1/10/1992	123.6	53.7	47.8	71.7	8.0	8608	9349	9480	2496	8752
1/27/1992	1.4	4.6	7.4	7.4	0.3	401	6486	7657	222	379
2/12/1992	1.6	6.3	0.1	12.5	1.7	3	11	122	750	78
2/25/1992	10.2	3.8	7.2	6.2	1.8	608	7	724	510	438
3/9/1992	93.3	28.9	31.0	26.3	4.9	7359	7781	8050	4790	8228
3/26/1992	41.7	4.7	23.4	18.0	5.5	4475	4513	9605	1831	2010
4/8/1992	51.1	3.3	27.4	17.3	3.5	6519	4791	21804	1831	1797
'4/22/1992	115.7	19.7	54.3	31.8	5.9	14873	22104	22104	5442	4436
5/5/1992	107.7	13.2	105.0	21.4	3.0	23000	22104	22104	1835	5621
5/18/1992	666.8	65.3	165.6	35.8	15.2	23684	21277	22124	4965	14941
6/4/1992	424.3	54.9	120.4	28.5	4.9	22200	22200	22200	13915	122
7/15/1992	324.0	19.3	79.6	-	4.8	21426	22200	22400		12231
8/6/1992	174.5	27.0	52.0	62.6	8.7	22250	22200	22700	6885	22200
8/20/1992	216.2	32.4	52.0	13.6	9.4	22500	22200	23000	3007	5917
9/9/1992	148.9	47.0	52.3	15.4	8.7	22200	22200	22200	2611	2280
9/30/1992	198.5	56.9	39.1	12.8	4.2	22200	22200	22200	3406	4444
10/16/1992	42.4	2.5	12.8	10.1	0.3	14800	800	5220	205	165
11/6/1992	162.0	48.8	26.9	13.5	9.0	23000	23000	23000	1070	8050
12/2/1992	267.2	180.3	85.3	26.9	11.2	22000	22000	22000	5320	14260
12/29/1992	162.9	185.1	71.5	38.4	10.8	22000	22000	22000	4444	22000
1/20/1993	96.3	73.6	104.3	16.9	13.6	22000	22000	22000	4733	22000
2/16/1993	63.9	37.9	41.1	6.6	4.7	28510	37700	34800	1900	10600
3/17/1993	53.3	19.0	12.4	13.3	3.1	37290	39043	21054	200	4151
4/12/1993	18.0	0.9	49.0	2.6	2.8	12231	1071	42900		250
5/7/1993	468.1	35.5	144.6	5.8	18.3	45300	38000	39000	3007	38000
6/9/1993	268.4	1.2	21.0	7.6	16.3	45000		3630	1071	7130
7/7/1993	42.4	2.5	12.8	10.1	0.3	36000	23000	36000	1900	1071
8/5/1993	292.5	3.8	33.4	7.2	105.1	22000	799	11250		15000
8/31/1993	40.3	5.4	33.6	7.1	6.9	18967	1100	6075		1341
10/12/1993	137.0	76.0	38.9	18.0	65.8	17356	21997	10265	3175	8009
12/21/1993	259.5	112.2	67.6	6.1	9.4	22000	22000	25091	500	7042
1/26/1994	82.6	25.9	68.6	9.4	1.3	27669	25091	5753	500	3300
2/25/1994	138.7	60.4	17.4		8.4	22000	22000	8300	532	11700
3/30/1994	44.0	3.7	8.2	3.7	1.8	15422	6200	300		2730
5/9/1994	24.2	23.9	16.3	1.6	3.5	5030	22000	4440	500	7440
6/9/1994	112.0	11.2	57.2	7.6	3.8	22000	14600	2700	500	7440
7/6/1994	69.6	9.3	10.3	2.8	1.3	29430	5030	3870		2730
8/11/1994	28.0	19.0	12.0	3.0	3.0	16690	16690	3870		1070
10/5/1994	35.3	31.8	7.3			22710	28790	9950		
12/6/1994	53.6	62.7	13.4			22000	24530	14600		
2/22/1995	134.1	5.1	25.0			22000	5030	10590		
3/6/1995	9.2	46.9	4.4			11240	30480	6220		
4/19/1995	10.2	8.2	7.2			3580	1100	3300		
5/31/1995	98.6	1.4	151.1			44000	2200	9630		
6/29/1995	437.9	4.9	17.9			44000	480	9950		
7/28/1995	266.7	11.2	32.7			44000	1620	3870		
8/23/1995	356.1	9.7	26.3			44000	5621	9948		
9/12/1995	407.6	41.9	14.5			44000	44000	4730		
9/20/1995	128.9	33.6	16.8			44000	44000	44000		

Reproduced with permission of the copyright owner. Further reproduction prohibited without permission.

Appendix 9.1. Continued.

Collection Date Trap	Total sediment, g A	Total sediment, g B	Total sediment, g C	Total sediment, g D	Total sediment, g E	Total runoff, g A	Total runoff, g B
IC-L							
1/10/1992	83.1	268.6				2166	8577
1/27/1992	108.5	73.0				7488	8076
2/12/1992	65.0	41.7				7194	5999
2/25/1992	29.9	23.3				6029	2162
3/9/1992	86.6	77.9				6442	10789
3/26/1992	76.5	56.3				4097	5156
4/8/1992	70.6	32.5				1287	5146
'4/22/1992	204.1	44.2				2445	9626
5/5/1992	215.9	93.6				3576	22104
5/18/1992	349.1	392.8				11700	22104
6/4/1992	90.1	141.3					22200
7/15/1992	140.7	113.3				2169	22200
8/6/1992	114.3	21.2				*na*	22200
8/20/1992	52.2	194.2				2728	12766
9/9/1992	57.6	79.8				3007	12566
9/30/1992	41.9	71.1				1071	17402
10/16/1992	17.5	81.3				25	4200
11/6/1992	3.2	53.3				300	23000
12/2/1992	73.8	136.3				3870	22000
12/29/1992	54.3	59.6				532	22000
1/20/1993	52.2	76.3				1620	22000
2/16/1993	30.4	17.1				530	34800
3/17/1993	22.4	22.9				270	20310
4/12/1993	48.4	42.7				2896	17970
5/7/1993	100.5	110.0				22000	37000
6/9/1993	27.3	29.7				3300	36000
7/7/1993	17.5	81.3				3300	30000
8/5/1993	15.5	37.7				3580	22000
8/31/1993	11.5	10.0				4464	6720
10/12/1993	67.7	13.8				21997	21997
12/21/1993	31.6	94.8				22000	22000
1/26/1994	12.9	28.4				15100	28636
2/25/1994	18.6	28.5				22000	21054
3/30/1994	9.8	5.5				11232	14777
5/9/1994	15.6	18.3				22000	22000
6/9/1994	4.2	26.7				22000	29200
7/6/1994	11.5	17.9				22000	25060
8/11/1994	8.0	28.0				18840	8050
10/5/1994	3.2	18.6				1070	13910
12/6/1994	5.2	28.2				22000	22000
2/22/1995	38.6	3.6				22000	28620
3/6/1995	4.5	6.2				10590	23000
4/19/1995	0.6	4.6				3580	1620
5/31/1995	4.3	6.1				22000	8300
6/29/1995	2.2	13.3				15300	7540
7/28/1995	3.5	6.2				25865	14600
8/23/1995	0.7	2.8				5621	6219
9/12/1995	2.1	23.2				14600	19940
9/20/1995	2.3	9.9				4444	18840

Reproduced with permission of the copyright owner. Further reproduction prohibited without permission.

Appendix 9.1. Continued.

Collection Date Trap	Total sediment, g A	Total sediment, g B	Total sediment, g C	Total sediment, g D	Total sediment, g E	Total runoff, g A	Total runoff, g B	Total runoff, g C	Total runoff, g D	Total runoff, g E
MO-P										
3/13/1991	0.8					4979				
4/10/1991			8.4			193		10899		
4/17/1991	0.4		1.8			1305		3853		
5/2/1991	0.1		4.1			33		4157		
5/9/1991						184				
5/15/1991			4.1			714		16135		
5/22/1991			0.3			204		1147		
5/30/1991	10.9					4183				
6/12/1991						791				
6/26/1991						231		3774		
7/11/1991	40.8	2.01				6154	12949	4125		
7/18/1991	0.4		0.1			2682		3475		
8/8/1991	1.4		2.1			198		8198		
8/21/1991	0.5		0.7			779		10799		
9/9/1991										
9/23/1991	7.1	1.00		1.2	1.5	5834	7460		12203	6410
10/1/1991	5.7	1.10	26.4	1.1		4215	2152	1074	1370	
10/15/1991	31.6	17.15	44.8	104.9	18.1	5553	12333	11033	13470	2124
10/28/1991	9.8		0.8	12.1		3356		6472	7074	
12/4/1991	52.9	4.03	0.1	278.9	163.3	3639	10365	673	16240	11099
1/7/1992	18.9	7.96		6.8	57.5	6106	15249		8785	3141
1/21/1992				51.3					12385	
1/27/1992					12.2					855
3/4/1992						1525	10025		9300	224
3/17/1992										
4/14/1992						9500	11872			
7/2/1992	0.2	11.92		5.3	2.8	5155	15508		17795	15697
8/25/1992	0.6	0.22				6099	722		14600	2950
9/21/1992	24.0	0.98		74.9	24.8	9526	15299		12625	18625
10/6/1992		3.36		2.9	0.4		13797		1121	2700
11/2/1992	269.5	3.38		6.3	4.3	3300	6150		7950	16800
11/18/1992	1.8	0.96		101.3	96.5	4633	11022		14224	10632
11/30/1992	41.7	23.98		70.2	145.0	4023	9872		10124	7582
12/11/1992	2.0	1.19		52.3	69.1	373	9122		9190	7301